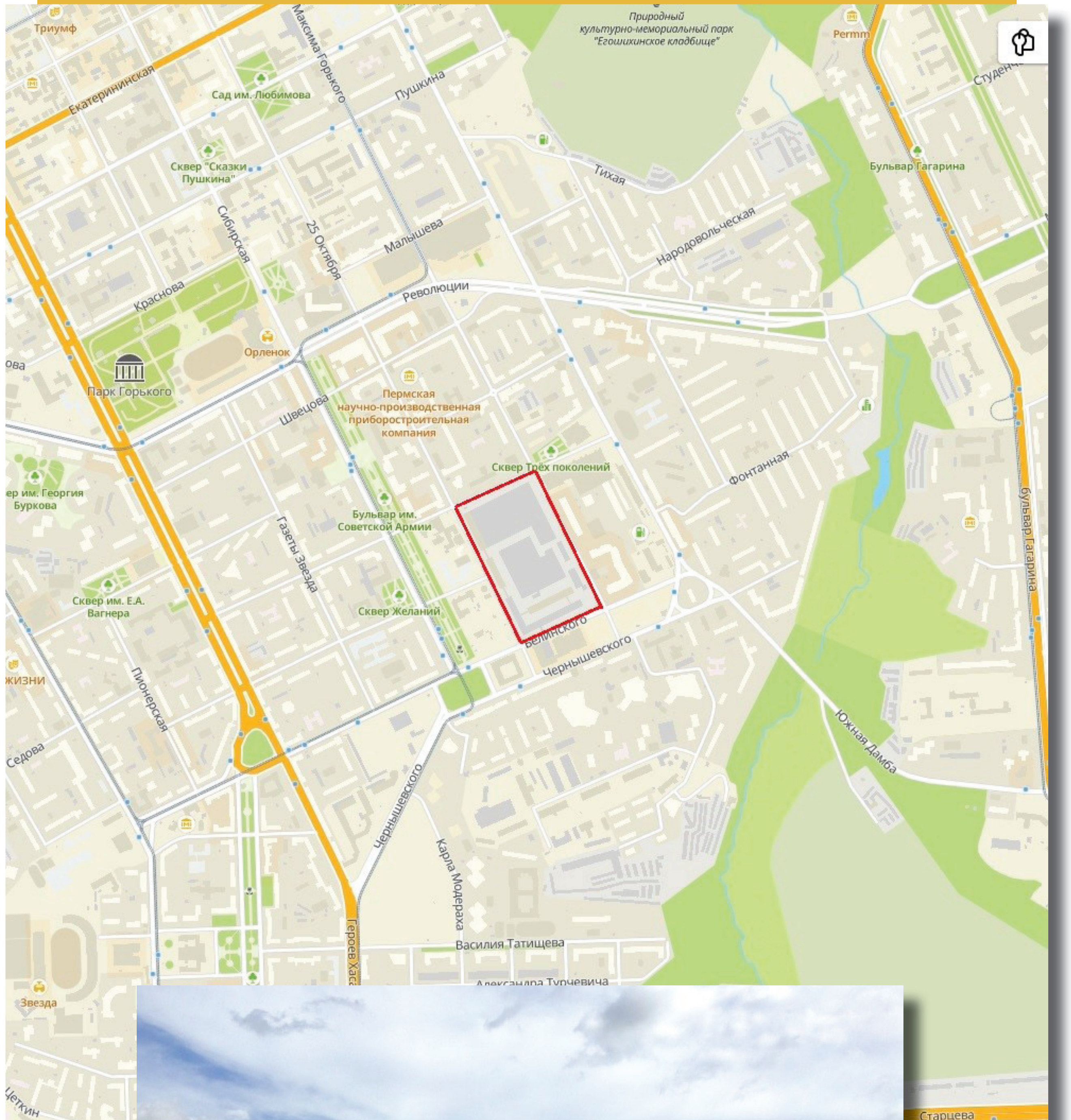

ISSN 1801-9064 (Print)
ISSN 2570-8775 (Online)
REGISTRACE MK ČR E 18950

AKUSTIKA

odborný časopis o akustice a vibracích

from content:

Studio D - akustika s.r.o.

VOLUME 41
November/Listopad 2021

This volume is contains the best selected papers of symposium "Acoustics and vibration" in frameworks of the Eighth international environmental congress (tenth international scientific-technical conference) "Ecology and life protection of industrial-transport complexes" ELPIT–2021 held in 22-26 September 2021 in Samara and Togliatti, Russia.

The ELPIT conferences project started in September 2003. Since that time in interval every two years conferences are arranging in Samara region of Russia and increasing the scale. In year of 2007 ELPIT conference has received the name of the international congress. Now ELPIT Congress became the largest event in the field of ecology and of environmental and life protection in Russia. ELPIT-2021 congress is continuing such successful tradition. Among of the congress organizers: Russian Academy of Science (Samara Federal Research Center, Institute of Ecology of Volga Basin), Ministry of Science and Higher Education of Russian Federation (Samara State Technical University, Baltic State Technical University „VOENMEH" named after D.F. Ustinov), Government of Samara Region of Russian Federation, International Academy of Ecology and Life Protection Science, Public Joint Stock Company «AVTOVAZ», Public Joint Stock Company "KuibyshevAzot", Russia, «Institute of Chemistry and Engineering Ecology» Limited Liability Company, Russia, etc.

CO-HEAD OF CONGRESS ORGANIZING COMMITTEE, CONGRESS SCIENTIFIC HEAD

Andrey V. Vasilyev, head of the Institute of Ecology of Volga Basin of Russian Academy of Science – branch of Samara Federal Research Center of Russian Academy of Science, professor of department of chemical technology and industrial ecology of Samara State Technical University, Doctor of Technical Sciences, Professor, Samara, Russia

CO-HEADS OF SYMPOSIUM "ACOUSTICS AND VIBRATION" IN FRAMEWORKS OF ELPIT-2021 CONGRESS

Nicolay I. Ivanov, professor of the Environmental studies and health and safety Department, Baltic State Technical University „VOENMEH" named after D.F. Ustinov, Doctor of Technical Sciences, Professor, St-Petersburg, Russia
Aleksander E. Shashurin, Dean of the Faculty, Baltic State Technical University „VoenMech", Doctor of Technical Sciences, Professor, St-Petersburg, Russia

ORGANIZING COMMITTEE OF SYMPOSIUM "ACOUSTICS AND VIBRATION"

Jana Dolejsi, The Editor-in-chief of Journal AKUSTIKA (Czech Republic)

Anna Nikitenko, Lecturer of the Environmental studies and health and safety Department, Baltic State Technical University „VOENMEH" named after D.F. Ustinov, Candidate of Technical Sciences, St-Petersburg, Russia

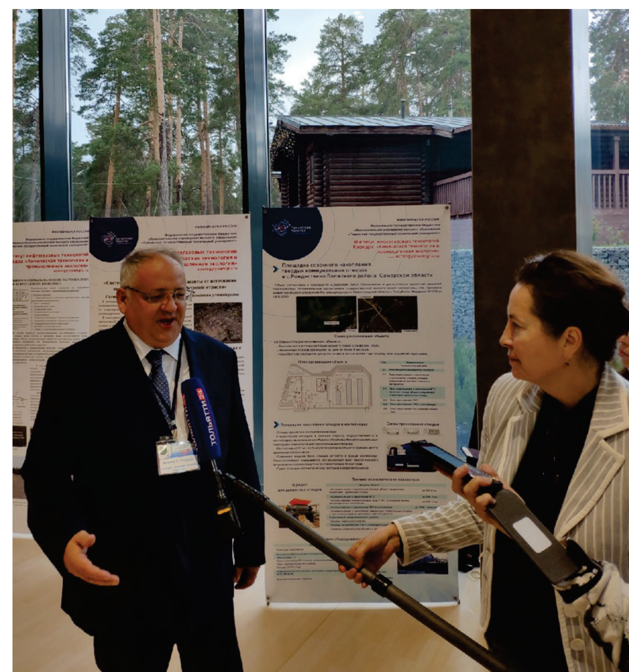

CONTENT / OBSAH

Paper No.343/2021

VIBRATIONS OF THE CLOSED FRAME STRUCTURES IN A STEADY-STATE CONDITION

Veronika Krutova, Besarion Meskhi

Don State Technical University, Rostov-on-Don, Russia, nikarostov@bk.ru

Abstract: *The load-bearing frames of the technological machinery of various functional purposes, such as bridge and gantry cranes, locomotives, motor locomotives, etc., are energetically closed rod systems [1-10].*

Keywords: *Overhead cranes, noise, vibration, rod systems, energy distribution.*

DOI: *: 10.36336/akustika/2021414*

1. INTRODUCTION

In the steady-state mode, the energy distribution in the rod system is carried out in accordance with the potential energy of each of the system elements. In other words, there are no energy flows through the boundaries of the elements in the system.

2. EQUIPMENT AND DEVICES USED IN THE RESEARCH

The boundaries of the elements in the system do not perform any work and, therefore, mechanical vibrations can be determined. Independent components that determine the potential energy distribution among the elements of the system can be reduced by some orthogonal transformation to the main (normal) axes. There is an orthogonal basis in $\{\overline{e_1}, \overline{e_2}, \dots, \overline{e_n}\}$, which $U^{i,II}$ is written as:

$$U^{i,II}(\overline{x}) = \frac{1}{2}\sum_{K=1}^{n} a_K^{I,II}\, x_K^2 \tag{1}$$

where

x is a vector of dimension n and when decomposed by basis vectors:

$$\overline{x} = x_1\overline{e_1} + x_2\overline{e_2} + \cdots + x_n\overline{e_n}$$

For each of the system rods.

Here

x_1, x_2...x_n are the coordinates of the vector x in the selected basis.

Thus, for example, when working with a rod system that corresponds to a differential equation.

$$\ddot{\overline{x}}^{(I,II)} = -\overline{grad}U^{I,II} \tag{2}$$

In the selected coordinate system, the latter equations will take the form:

$$\begin{matrix} \ddot{x}_1^I = -a_1^I x_1^I; & \ddot{x}_2^I = -a_2^I x_2^I; & \dots & \ddot{x}_n^I = -a_n^I x_n^I; \\ \ddot{x}_1^{II} = -a_1^{II} x_1^{II}; & \ddot{x}_2^{II} = -a_2^{II} x_2^{II}; & \dots & \ddot{x}_n^{II} = -a_n^{II} x_n^{II} \end{matrix} \tag{3}$$

3. RESULTS AND DISCUSSION

Thus, it is established that for longitudinal oscillations, the system splits into a number of separate invariant subspaces, which are independent solutions with eigenvalues ***ai(I,II)***, describing eigen-oscillations in each of them.

At the same time, if each of the forms $U^{(I,II)}(x)$ that determine the potential energies of the rods is positive definite, then all $a_k^{(I,II)}$ are positive. Then the considered point x (vector X), in each of the corresponding invariant subspaces, performs n independent oscillations along n mutually perpendicular directions in the corresponding bases selected in them: $e_1^{(I,II)}$; $e_2^{(I,II)}$; …, $e_n^{(I,II)}$. These oscillations are called the main or eigen-oscillations, and the numbers $\omega_k^{(I,II)}$ are the eigen-frequencies of vibrations for each individual element.

The eigen-frequencies can be found based on the equation of motion of a rod conjugated to another rod:

$$\frac{\partial^2 u}{\partial t^2} - c^2\frac{\partial^2 u}{\partial x^2} = -ku \quad or \quad c^2\frac{\partial^2 u}{\partial x^2} - ku = \frac{\partial^2 u}{\partial t^2}. \tag{4}$$

We are looking for a solution in the form of a product of two functions, one of which depends only on x, and the other depends only on t:

$$U(x,t) = X(x)T(t) \tag{4a}$$

Substituting (4a) into (4) gives:

$$c^2T(t)\cdot x^{II}(x) - k\cdot X(x)T(t) = X(x)\cdot T^{II}(t) \qquad or$$

$$\frac{c^2X^{II}(x) - k/X(x)}{X(x)} = \frac{T^{II}(t)}{T(t)} \qquad (4b)$$

The left part of this equality does not depend on ***t***, the right - on ***x***, therefore, their total value does not depend on either ***x*** or ***t***, and therefore reduces to a constant, which we take in the form **$-c^2\lambda^2$** (for **$\lambda>0$**). Then equation 4b decomposes into two ordinary differential equations:

$$T''(t) + c^2\lambda^2T(t) = 0 \qquad (a)$$

$$c^2x''(x) - kX(x) + c^2\lambda^2X(x) \qquad (b)$$

Their solution (general integrals) have the form:
for a)

$$T(t) = Acos(c\lambda t) + Bsin(c\lambda t).$$

To solve equation b), the boundary conditions on the left and right ends should be taken into account:

$$\frac{\partial u}{\partial x} = 0; \quad and \quad -k^I\frac{\partial u(x_2t)}{\partial x} = K_n^{II}(x_2,t)$$

$$c^2x''(x) + c^2\lambda^2X(x) = -K^Ix^I(x) = 0$$

Solution of the equation:

$$c^2x''(x) + c^2\lambda^2X(x) = 0$$

$$x''(x) + \lambda^2X(x) = 0$$

Is:

$$X(x) = Ccosx + Dsin\lambda x$$

Then, for the condition on the free boundary ***x=0***, we have:

$$X(x) = Ccos\lambda x + Dsin\lambda x$$

Or

$$Ccos\lambda x + Dsin\lambda x = 0; \quad Ccos\lambda 0 = 0; \quad C = 0$$

We consider the boundary condition for ***x_2=1*** , assuming that ***C=0***

$$k_2sin\lambda x = -k_1cos\lambda x$$

or from where

$$k_2sin\lambda l = -k_1cos\lambda l$$

$$tg\lambda l = -\frac{K_1}{K_2}\lambda = -\frac{K_1(\lambda l)}{K_2l} \qquad (5)$$

The graph shown in Fig. 1 provides information about the solutions of this equation. The positive roots ***λ_1, λ_2... λ_n*** give us eigenvalues with corresponding eigenfunctions ***sinλx, sinλ_2x,... sinλ_nx***.

In other words, a number of values is obtained for ***λ***

$$\lambda_n = -\frac{\xi}{l}$$

where
ξ (***n*** are integers) are the positive roots of the transcendental equation:

$$tg\xi = -\frac{k1}{k2l}\xi$$

$$y = -\frac{k1}{k2}\lambda$$

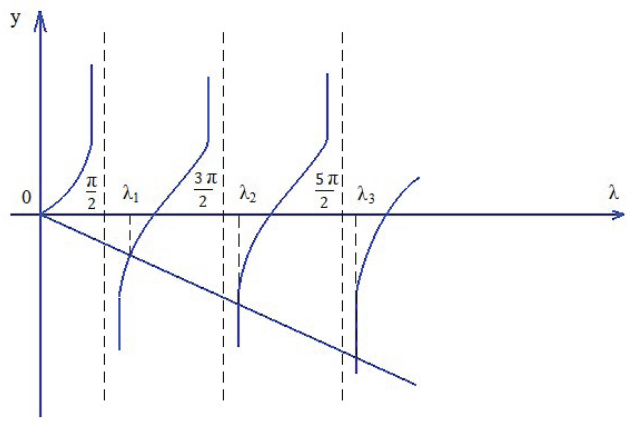

Fig. 1: Graphical definition of the positive roots of equation 5

For λ found in this way, in accordance with the superposition principle, we determine the general solution of the equation:

$$U(x,t) = \sum_{n=1}^{\infty}[Acos(c\lambda t) + Bsin(c\lambda t)]\,sin\lambda_n$$

Made up of a countable number of solutions.

Assuming here that ***c λω (ω>0)***.

We will get

$$U(x,t) = \sum_{n=1}^{\infty} C_n\,sin(\omega_nt + \alpha)sin\lambda_nx \qquad (6)$$

We determine the coefficients of this series from the initial condition

$$U = f(x), \qquad (0 \le x \le l)$$

Or

$$U = f(x) = \sum_{n=1}^{\infty}\overline{c_n}\,sin\lambda_nx = \sum_{n=1}^{\infty}\overline{c_n}\,sin\frac{\xi nX}{l}$$

4. CONCLUSION

The last equation can be considered as a generalized Fourier series in the interval (0, 1). Using the orthogonality of the found eigenfunctions

$$sin\frac{\xi nX}{l}$$

We determine the coefficients according to the known methods of normalization

$$C_n = \frac{\int_0^l f(x)\frac{\xi nX}{l}dx}{\int_0^l sin^2\frac{\xi nX}{l}dx}$$

For a known task ***f(x)***, these coefficients are uniquely found. The representation of the series in the form of 16 is an example of an anharmonic Fourier series (by the standing wave method). The components of this series do not have a common period, as in the harmonic Fourier series under normal conditions. The eigenvalues λn here have a bit more complex nature of their formation compared to those considerations when the boundary does not perform work, which is usually the case under other boundary conditions, starting from the initial moment of time ***(t=0)***.

Considering the expression 6, we see that the total oscillation of the rod ***u(x,t)*** is composed of a series of individual oscillations $u_n(x,t)$; where the points participating in such an elementary oscillation, determining the coordinates of the sections, oscillate with the same frequency. The amplitude of the oscillation of each point depends on its position. It is equal to:

$$\overline{C_n}\left|sin\frac{\xi nX}{l}\right|$$

The entire length of the rod is divided into not necessarily equal sections, and the point of the same section is always in the same phase, whereas the points of neighboring sections are in directly opposite phases. The points separating one section from another are at rest, these are the so-called 'nodes'. The midpoints of each of the sections ('antinodes') oscillate with the greatest amplitude, and, as can be seen from Fig. 1, the modes with a higher frequency of eigen-oscillations corresponding to the eigen-frequencies λ_i, 'fit" more closely to their corresponding vertical asymptotes.

Naturally, everything said about the rod I is exactly transferred to the rod II associated with it. When each of the rods vibrates at higher frequencies, there will be no multiplicity with respect to the main forms of vibrations, as it is easy to see in Fig. 1, for the boundary condition under consideration.

Since the steady-state energy mode of each of the rods is described by standing waves, as follows from the analysis of the solution, the average value of the energy flow for the period equals to zero, which allows us to conclude that there is no redistribution between neighboring antinodes in relation to kinetic and potential energy in a standing wave.

Taking further into account that at a steady energy state, a wave number is used as a characteristic of the description of the plane wave harmonicity, then with the known notation, on one side, we can write:

$$K = \frac{2\pi}{\lambda} = \frac{2\pi}{C\cdot T} = \frac{\omega}{C}$$

On the other side, based on the graphical construction for finding solutions, in accordance with Fig. 1, we establish that the roots of λ_n lie in the range:

$$\left(n-\frac{1}{2}\right)\pi < \lambda_n < \left(n+\frac{1}{2}\right)\pi$$
$$(2n-1)\frac{\pi}{2} < \lambda_n < (2n+1)\frac{\pi}{2}$$

Then for the eigen-frequencies we find the intervals of their changes taking into account

$$\lambda_n = \frac{\xi_n}{l} - \frac{\omega_n}{C}$$

We get the following:

$$\left(n-\frac{1}{2}\right)\pi < \frac{\omega_n l}{C} < \left(n+\frac{1}{2}\right)\pi$$

$$\frac{(2n-1)\frac{\pi}{2}C}{l} = \frac{(2n-1)\frac{\pi}{2}}{l}\left(\frac{E}{\rho}\right)^{\frac{1}{2}} < \omega_n < \frac{(2n+1)\frac{\pi}{2}}{l}\left(\frac{E}{\rho}\right)^{\frac{1}{2}}$$

where
n is integers,
c is propagation velocity.

The results obtained in this paper can be extended to a rod system (which, as it was noted, serves as a research model), consisting of a finite number of rods, and interconnected by various coupling conditions.

In this case, the energy distribution law for such a system is represented in a similar form for the time $t \gg t^*_{max}$, where t^*_i is the time required to establish an equilibrium state for each of the system rods, i.e.

$$A = \sum_i^n E_i$$

Since during the wave process, the kinetic (***T***) and potential (***U***) energy in the considered volume of the medium reach their experimental values simultaneously, therefore, when averaging them over time for each of the rods, there is

$$\langle E_i\rangle = \langle T_i + U_i\rangle = U_i$$

assuming that in the volume of each of the rods under consideration, the average value of the total energy coincides with the maximum value of the potential energy.

On this basis, the last relation is represented as:

$$A = \sum_{i=1}^n U_i(x); \qquad (t > t^*_{maxi})$$

where
n is the number of elements included in the core system.

Studying the influence of internal losses on the energy distribution of sound vibration has two goals. Firstly, it is necessary to find out how losses affect the speed of establishing a stationary process in the system, and secondly, whether the system has a general loss coefficient in a stationary mode.

REFERENCES

[1] Kolesnikov I.V., Podust S.F., Podust S.S., CHukarin A.N. Sposoby snizheniya shuma i vibracij pri proektirovanii, proizvodstve i ekspluatacii zheleznodorozhnogo podvizhnogo sostava // M.: VINITI RAN, 2015. – 216 s.
[2] Bondarenko V.A., Sposoby povysheniya vibrodempfirovaniya i zvukoizolyacii kolesnyh par mostovyh kranov // Vestnik Rybinskogo gosudarstvennogo aviacionnogo tekhnicheskogo universiteta im. P.A. Solov'eva. 2016. № 2 (37)
[3] Litvinov A.E., Novikov V.V., Noise Reduction for Multiblade Rip Saws // Russian Engineering Research, 2017, Vol. 37, No 9, pp. 807-808.
[4] Litvinov A.E., Novikov V.V., Reducing the Noise and Operator Injuries Associated with Circular Saws // Russian Engineering Research, 2017, Vol. 37, No 7, pp. 615-616.
[5] YAickov I.A., Finochenko T.A., Theoretical Research of Noise and Vibration Spectra in Cabins of Locomotive and Diesel Shunting Locomotive // International Journal of Applied Engineering Research, 2017, Vol. 12, No 21, pp. 10724-10730.
[6] I. A. YAickov, A. A. Fedenko, S.A. Razdorskij Opredelenie regressionnyh zavisimostej koefficientov peredachi energeticheskih potokov // Vestnik RGATU imeni P.A. Solov'eva. – Rybinsk:2018, 4(47). S.57-63.
[7] K.O. Kobzev, S.A. SHamshura, A.N. CHukarin, V.P. Bogdanovich, V.E. Kas'yanov, Method and description of dynamic vibration reduction in cabins of gantry cranes // 179 Method and description of dynamic vibration reduction in cabins of gantry cranes XIV International ScientifiTechnical Con-ference "Dynamics of Technical Systems". MATEC Web of Conferences, https://doi.org/ 10.1051/matecconf/201822601022
[8] K.O. Kobzev, S.A. Shamshura, A.N. Chukarin, V.P. Bogdanovich, V.E.Kasyanov. Method and description of dynamic vibration reduction in cabins of gantry cranes // XIV International Scientific-Technical Conference "Dynamics of Technical Systems". September 12-14, 2018.
[9] K.O. Kobzev, S.A. Shamshura, A.N. Chukarin, A.I. Buryanov, V.E. Kasyanov. Substantiation of the parameters of vibration system in the cab of the gantry crane at the workplace of crane operators // XIV International Scientific-Technical Conference "Dynamics of Technical Systems". September 12-14, 2018.
[10] Beskopylny A., Chukarin A., Isaev A. Noise Spectra of Ball-Rod Hardening of Welds of Rod Structures // International Scientific Conference Energy Management of Municipal Facilities and Sustainable Energy Technologies EMMFT 2018. Advances in Intelligent Systems and Computing, vol. 983. Sprinder, Cham.

Veronika Krutova *is a Candidate of Technical Sciences.*
Veronika Krutova is an expert in noise and vibration reduction of overhead cranes. Veronika Krutova is the author of 25 scientific articles and is the co-author of 1 monograph.

Besarion Meskhi *is a Russian scientist, Rector of the Don State Technical University (Rostov-on-Don, Russia), Doctor of Technical Sciences, Professor, Corresponding Member of the Russian Academy of Education.*
The area of scientific research is technology and industrial safety, theory and methods of comprehensive provision of occupational safety in machine-building industries and technological equipment during its design.
Prof. Meskhi has more than 30 monographs, 180 articles, 5 copyright certificates, diplomas, patents and licenses, 45 study guides approved by the Education and Methodics Association.
Besarion Meskhi actively participates in the training of academic teaching and research staff.

Paper No.344/2021

THEORETICAL STUDY OF THE CLOSED BAR SYSTEM LOSS FACTOR

Veronika Krutova, Besarion Meskhi

Don State Technical University, Rostov-on-Don, Russia, nikarostov@bk.ru

Abstract*: The coefficient of vibrational energy loss is a physical and mechanical characteristic, the accuracy of calculation of vibroacoustic characteristics of corresponding machines at the stage of their design to a great extent depends on its value.*

Keywords: *Overhead cranes, noise, vibration, rod systems, energy distribution.*

DOI: *: 10.36336/akustika/2021418*

1. INTRODUCTION

Currently, this value is studied for U-sections, angles and plates [1-11]. These data were obtained for some of the above-mentioned elements on a special stand. It should be mentioned that such studies have not been carried out for energetically closed systems (in this case, bars). Therefore, the purpose of studies, the results of which are given in this article, was to clarify the dissipative function of the bar system, which is a closed energy system itself.

2. EQUIPMENT AND DEVICES USED IN THE RESEARCH

The internal friction inherent in real materials causes the loss of energy in the current cycles of vibration of the system. To account for the total dissipation of energy, leading to a decrease in the specific energy per unit time, we introduce its evaluation, taking into account both internal and structural energy losses of the considered acoustic systems. A constant value called the loss factor (***η***) is taken as a quantitative characteristic of this estimation. The loss coefficient and the energy attenuation coefficient (***δ***) considered earlier are interrelated in harmonic motion as follows:

$$\delta = \frac{1}{2}\omega\eta = \frac{2\pi f\eta}{2} = \pi f\eta \tag{1}$$

where
f is the vibration frequency.

The loss coefficient shows what fraction of the total energy inherent in the element is lost during one complete period of oscillation and finds a relationship with the energy parameters by means of the ratios:

$$\frac{dE}{dt} = \pi E\eta$$
$$\frac{dU}{dt} = \pi U\eta \tag{2}$$

where
E and ***U***, respectively, are the total and potential energies of the element included in the system.

For the occurrence of flow under these conditions, the presence of an external force that would remove the bar from the state of equilibrium is necessary. A mere change in the internal energy state of the coupled bars due to losses will not lead to the emergence of such a force. Consequently, the elements of the bar system will oscillate in the mode corresponding to itself in the presence of internal losses. The time of this damping due to losses, during which the amplitude of oscillations will decrease "e" times, can be determined from the expression:

$$t_d = \frac{1}{\pi f\eta} \tag{3}$$

From where it is clear that the damping time depends on the frequency and the loss factor. This time, on the one hand, should be much longer than the time required for the energy flows through the adjacent boundary of the coupled rods to go to zero. At the same time, on the other hand, it should be longer, at least by an order of magnitude of time($t = \frac{10\ L_{tot}}{C}$, where L_{tot} is the total length of the system), necessary for the multiple origin of the elastic wave along the entire length of the system. Otherwise, the system we are considering will not satisfy the isolation conditions due to sufficiently large energy losses.

Further note that for each of the rods included in the system, we can write down the step-by-step (cycle-by-cycle) reduction of energy due to its internal losses

$$\mathbf{U\eta, U\eta^2, U\eta^3, \dots, U\eta^n}$$

where

U is the value of potential energy of the element under consideration in the system;

n is the number of full cycles of passage by the elastic wave at the time of observation.

3. RESULTS AND DISCUSSION

The above sequence can be used to estimate the amount of absorbed (***U***) (loss) energy for a finite period of time, for which we make an expression:

$$\mathbf{U_{le} = U\eta + U\eta^2 + \dots + U\eta^n = U\eta\frac{(1-\eta^n)}{1-\eta}} \tag{4}$$

Where the right (last) part is the result of summing the finite segment of a geometric progression series with denominator η less than unity. The limiting period at aspiration gives a finite amount of transverse energy, defined by the expression

$$\mathbf{U_{le} = U\frac{\eta}{1-\eta}} \tag{5}$$

Taking into account that the loss factor η for most engineering materials is, as a rule, much less than unity, the last expression will be written in the form

$$\mathbf{U_{le} = U\eta\frac{1}{1-\eta} = U\eta(1-\eta)^{-1} = U(\eta+\eta^2+\eta^3+\cdots)} \tag{6}$$

With sufficient estimation for practice, let us hold here only the decomposition term, the result being:

$$\mathbf{U_{le} = U\eta} \tag{7}$$

Analyzing the above relations, it is easy to see that the greatest amount of energy is lost during the first cycle of oscillations, which is also clear from the last equality, which is the result of the limiting operation, and this fact takes place for each element included in the system. At the same time, from the last relations we establish that the total energy of losses (resulting from the limiting operation) tends to its constant value.

The total energy of system losses will be added up from the losses of its individual elements, so for each first current cycle of elastic wave propagation through the system elements (its double stroke), we can write down the energy ratio taking into account the losses of the first main current cycle, i.e.

$$\mathbf{A\eta = U_1\eta_1 + U_2\eta_2 + \dots + U_n\eta_n = \sum_n U_n\eta_n} \tag{8}$$

From where, the total loss factor of the system will be represented by the formula

$$\mathbf{\eta_{tot} = \frac{U_1\eta_1}{A} + \frac{U_2\eta_2}{A} + \dots + \frac{U_n\eta_n}{A} = \frac{\sum_n U_n\eta_n}{A}} \tag{9}$$

If the loss factors of the individual elements that make up the system are equal to each other, then the total loss factor of the entire system will correspond to the loss factor of any element. If, however, the loss factor on the elements $\mathbf{\eta_i}$ $(\mathbf{i = \overline{1,n}})$ are not equal to each other, then the system loss factor ηcomm will be in the range

$$\mathbf{\eta_j < \eta_{tot} < \eta_i}$$

where

η_j<η_i

All the above, of course, carries over to a system with

$$\mathbf{U_1 = U_2 = U_3 = \cdots U_n}$$

If the potential energies are not equal to each other, then the loss factor of the system will depend on the condition which losses, by their values, belong to the corresponding energy element, for example, if the equation takes place:

$$\mathbf{U_1 > U_2 > U_3}$$
$$\mathbf{\eta_1 < \eta_2 < \eta_3}$$

Then the total loss coefficient will be close in value to the highest loss coefficient.

Provided that $\mathbf{U_1 > U_2 > U_3}$.
but $\mathbf{\eta_1 < \eta_2 < \eta_3}$

Then the total loss factor will lie between the boundaries

$$\mathbf{\eta_1 < \eta_{tot} < \eta_3} \tag{10}$$

However, its value will be closer to the lowest number.

To summarize, it should be mentioned that in a mechanical system, it is advisable to first impose conditions on the change of losses in the system elements having the greatest potential energy.

At the same time, the limiting total estimation of the value of energy losses in the mechanical system does not influence the character of energy distribution within the system and at the same time, as it is established in work, the presence of losses accelerates the process of approach in system of an energy stationary state at which energy exchange between its elements stops.

It is known that the loss factor, the inverse of the Q-value system, corresponds to the tangent of the phase angle (***φ***). For most materials used in engineering, the angle tangent can be replaced by the value of the total angle due to the smallness of its values, so that

$$\mathbf{\eta = tg\varphi \approx \varphi}$$

Since losses are caused by internal friction in the suppression elements of which the material is made, this makes it possible to consider them dependent on each other, at the same time, the stiffness factor (the value inverse of the suppression) is proportional to the elastic modulus, and therefore the elastic and dissipative properties of the suppression element can be characterized by the elasticity complex, which allows to write the equality

$$\mathbf{E^* = \bar{E} = E_0 + iE_0' \approx E_0(1 + i\eta)} \tag{11}$$

This equality is true to within an order of by virtue of the expansion, and since ***η«1***, the values ***E_0*** and $|\bar{E}| = E_0\sqrt{1+\eta^2} = E$, should be considered equal between themselves, so the zero index of ***E*** can be omitted to account for the real part.

In accordance with this complex modulus of elasticity let us write it in the form:

$$\mathbf{E^* = E(\alpha + i\beta) = E\left(\frac{1 + itg\varphi}{1 - itg\varphi}\right)} \tag{12}$$

where
φ is the phase angle when losses are taken into account.

By multiplying the numerator and denominator by the conjugate significant expression (***1+itg φ***) we successively obtain:

$$\mathbf{E(\alpha + i\beta) = E\left(\frac{1 + itg\varphi}{1 - itg\varphi}\cdot\frac{1 + itg\varphi}{1 + itg\varphi}\right) = E\frac{(1 + itg\varphi)^2}{1 + tg^2\varphi} = E\left(\frac{1 - tg^2\varphi}{1 + tg^2\varphi} + i\frac{2tg\varphi}{1 + tg^2\varphi}\right)} \tag{13}$$

Then for equality of complex quantities we must have:

$$(^*)\alpha = \frac{1 - tg^2\varphi}{1 + tg^2\varphi} = \cos 24$$

$$\beta = \frac{2tg\varphi}{1 + tg^2\varphi} = \sin 24$$

$$tg24 = \frac{2tg\varphi}{1 - tg^2\varphi} = \frac{\beta}{\alpha}$$

$$24 = arctg\frac{\beta}{\alpha}$$

Given that the tangent of the phase angle corresponds to the loss factor, we can write:

$$\alpha = \frac{1 - \varphi^2}{1 + \varphi^2}$$

$$\beta = \frac{24}{1 + \varphi^2}$$

and ***24 = arctg η = η***,
where : ***φ =η/2***

From this we obtain that ***φ*** is the coefficient of internal friction per half-period, corresponding to half of the loss coefficient per cycle.

Between α and β the conditions are fulfilled: modulus $|\mathbf{E^*}| = \mathbf{1}$; argument $\mathbf{E^*(arctE^* = 24)}$.

The transformations give:

$$\mathbf{|E^*| = \sqrt{\alpha^2 + \beta^2} = 1,\ \ arctE = arctg\frac{\beta}{\alpha} = 24 = \eta}$$

The limiting case, according to equality (*), we have when $\mathbf{tg\varphi = 1}$ or $\varphi = \frac{\pi}{4}$, at which ***α*** and ***β*** obtain values ***α=0, β=1***, corresponding to a perfectly plastic body. This result finds confirmation with the studies given in this paper, connected with the energy distribution in the presence of damping and without it, where the equality took place: ***η = arctg (1)***, by the example of considering the interaction of two identical rods. This condition was represented graphically as a sectorless line on the phase plane. Taking equality ***α+β=1*** as the basis, and also taking into account that by analogy with the complex modulus of elasticity the complex velocity of propagation ***c**** is connected with the loss factor by the following relation ***c* = c(1-i η/2)***, which gives the grounds for taking the energy conservation law as the second equality

$$\mathbf{\bar{Q} + \bar{R} = 1;\ \ (\bar{Q}, \bar{R} > 0)}$$

where
$\bar{\mathbf{Q}}$ and
$\bar{\mathbf{R}}$ are energy transition coefficients.

From these two equalities, one, and, putting additionally that $\mathbf{\bar{Q} = a^2;\ \bar{R} = b^2}$, we show that with these related parameters, the formula

$$\mathbf{f(Q, R, \eta) = |Q\alpha - R\beta|}$$

does not exceed unity element, i.e.$|\mathbf{Q\alpha - R\beta}| \le \mathbf{1}$, accounting for losses.

Indeed, multiplying the above equations term by term, we obtain

$$\mathbf{a^2\alpha^2 - a^2\beta^2 + b^2\alpha^2 + b^2\beta^2 = 1}$$

or

$$\mathbf{a^2\alpha^2 - a^2\beta^2 + b^2\alpha^2 + b^2\beta^2 + 2ab\alpha\beta = 1}$$

Whence $\mathbf{(a\alpha - b\beta)^2 + (b\alpha + a\beta)^2 = 1}$.

Since ***(bα-aβ right)² ≥0***, we have ***(aα-bβ right)² ≤1*** , hence we conclude that

$$\mathbf{\left|\sqrt{\bar{Q}}\cdot\alpha - \sqrt{\bar{R}}\cdot\beta\right| \le 1}$$

considering $\mathbf{\sqrt{\bar{Q}} = Q}$ and $\mathbf{\sqrt{\bar{R}} = R}$.

The obtained last equation establishes the relationship between the transition coefficients ***Q*** and ***R*** and the loss factor η.

It follows that taking into account the loss factor from the point of view of estimating energy absorption accelerates the process of establishing the stationary energy state by the system. Indeed, as shown earlier, the formula

$$\mathbf{W_0|Q - R|^n = f(n)}$$

represents the rate of change in the energy flux for each element of the system as a function of ***n = τ/T*** (the number of cycles at the moment of observation) in cases where energy losses were neglected.

When losses are taken into account for the values of Q and R under consideration, the analogue of the latter expression is the expression $\mathbf{W_0|Q\alpha - R\beta|^n}$, corresponding to the loss-aware flow for the current values of ***n***, which can only decrease as n passes. Let us show this by using the inequality:

$$\mathbf{f(Q, R, \eta) = |Q\alpha - R\beta| \leq |Q - R|}$$

Let us estimate the values of ***α*** and ***β***, whereby we present them as follows, given that ***η«1***

$$\frac{\mathbf{1-\eta^2}}{\mathbf{1+\eta^2}} = \frac{\mathbf{1+\eta^2-2\eta^2}}{\mathbf{1+\eta^2}} = \mathbf{1} - \frac{\mathbf{2\eta^2}}{\mathbf{1+\eta^2}} = \mathbf{1 - 2\eta^2(1+\eta^2)^{-1} \approx 1 - 2\eta^2}$$

Here in the expansion of the expression $\frac{1}{1+\eta^2} = (\mathbf{1+\eta^2})^{-1}$, the first two terms are taken into account due to the smallness of ***η***.

$$\boldsymbol{\beta} = \frac{\mathbf{2\eta}}{\mathbf{1+\eta^2}} = \frac{\mathbf{2}}{\boldsymbol{\eta} + \frac{\mathbf{1}}{\boldsymbol{\eta}}}$$

where we have ***β<1 since η+1/η>2 (η≠1)***.

Thus, we find that ***α*** and ***β*** for any values of the loss factor ***η<1*** are in the interval

$$\mathbf{0 < \alpha < 1}$$

and

$$\mathbf{0 < \beta < 1}$$

And hence we conclude that $\mathbf{|Q\alpha - R\beta| \leq |Q - R|}$,

wherefore

$$\mathbf{W_0|Q\alpha - R\beta|^n \leq W_0|Q - R|^n} \tag{14}$$

4. CONCLUSIONS

Physically, the last inequality means that for all possible cases of interaction of bars included in bar systems, the stationary energy equilibrium state for the system considering the internal energy losses will come earlier than without considering the latter, as it follows from the analysis of the energy direct image problems considered in the paper.

It was also presented that as a result of carried out an analysis of the bar elements system, each of them acquired a certain amount of energy in the time required for this purpose.

With further increase of time, as the results suggest the elements stop exchanging energy, which corresponds to the onset of the moment of stable oscillations of the system, corresponding to the eigenforms.

REFERENCES

[1] K.O. Kobzev, S.A. Shamshura, A.N. Chukarin, V.P. Bogdanovich, V.E.Kasyanov. Method and description of dynamic vibration reduction in cabins of gantry cranes // XIV International Scientific-Technical Conference “Dynamics of Technical Systems”. September 12-14, 2018.
[2] K.O. Kobzev, S.A. Shamshura, A.N. Chukarin, A.I. Buryanov, V.E. Kasyanov. Substantiation of the parameters of vibration system in the cab of the gantry crane at the workplace of crane operators // XIV International Scientific-Technical Conference “Dynamics of Technical Systems”. September 12-14, 2018.
[3] Beskopylny A., Chukarin A., Isaev A. Noise Spectra of Ball-Rod Hardening of Welds of Rod Structures // International Scientific Conference Energy Management of Municipal Facilities and Sustainable Energy Technologies EMMFT 2018. Advances in Intelligent Systems and Computing, vol. 983. Sprinder, Cham.
[4] Bondarenko V.A. Generation regularities of vibration and noise spectra of the gearboxes of overhead traveling crane // AKUSTIKA, ISSN 1801-9064, Studio D –Akustika s.r.o., České Budějovice, VOLUME 32, p. 120-122, 2019.
[5] Beskopylny A., Meskhi B., Isaev A. Spectral characteristics of noise during hardening of welds of rod structures // IOP Conf. Series: Materials Science and Engineering.709 (2020) p. 1-7.
[6] D.V. Ruslyakov Raschet vibroakusticheskikh kharakteristik korpusov sverlil'nykh babok //II Vserossijskaya nauchno-tekhnicheskaya konferentsiya «Otechestvennyj i zarubezhnyj opyt obespecheniya kachestva v mashinostroenii». October 8-9, 2020: collection of reports. Tula: TulSU Publishing House, 2020. pp. 161-163
[7] Balanova M.V., Finochenko T.A., YAitskov I.A. Obespechenie vibroakusticheskoj bezopasnosti operatorov putevykh dorozhno--stroitel'nykh gruzopod"emnykh mashin // FGBOU VO RGUPS. – Rostov-on-Don, 2020. – 103 s.
[8] Chukarin A.N., Isaev A.G., Shashurin A.E., Elkin Y.I., Theoretical studies of the processes of vibration excitation and noise generation during abrasive treatment of welds of frame structures// Noise Theory and Practice. 2020. T. 6. № 4 (22). pp. 71-80.
[9] Chukarin A.N., Isaev A.G., Abbakumov K.E., Lubianchenko A.A., Derivation of the dependences of the vibration rates of rod systems when strengthening welds to reduce noise levels at the operator's workplace// Noise Theory and Practice. 2020. T. 6. № 4 (22). pp. 60-70.

[10] A. Beskopyl'nyj, B. Meskhi, A. Isaev Modeling of Vibroacoustic Characteristics of Plate Structures of Vehicles during Abrasive Processing // Transportation Research Procedia Vol. 54 (2021) P. 39–46 doi: 10.1016/j.trpro.2021.02.045
[11] Nazaretov A.A., YAitskov I.A., The Derivation of the Noise Level Dependences and Vibration Velocities of Elements and Units of the Drive System of the Rail Grinding Machines // IOP Conference Series: Earth and Environmental Science: Earth and Environmental Science 720 (2021) 012014. IOP Publishing doi:10.1088/1755- 1315/720/1/012014

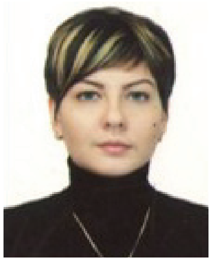

Veronika Krutova *is a Candidate of Technical Sciences.*
Veronika Krutova is an expert in noise and vibration reduction of overhead cranes. Veronika Krutova is the author of 25 scientific articles and is the co-author of 1 monograph.

Besarion Meskhi *is a Russian scientist, Rector of the Don State Technical University (Rostov-on-Don, Russia), Doctor of Technical Sciences, Professor, Corresponding Member of the Russian Academy of Education.*
The area of scientific research is technology and industrial safety, theory and methods of comprehensive provision of occupational safety in machine-building industries and technological equipment during its design.
Prof. Meskhi has more than 30 monographs, 180 articles, 5 copyright certificates, diplomas, patents and licenses, 45 study guides approved by the Education and Methodics Association.
Besarion Meskhi actively participates in the training of academic teaching and research staff.

Paper No.345/2021

DERIVING THE DEPENDENCIES FOR THE VIBRATING CAPACITY INTRODUCED INTO WHEELSET ASSEMBLIES

Veronika Krutova

FSBEI HE Rostov State Transport University, Rostov-on-Don, Russia, nikarostov@bk.ru

Abstract: *Despite the very large difference in lifting capacity, bridge cranes have an almost identical vibration control system layout, which predetermines the general approach to the theoretical assessment of vibration and noise spectra both in the production premises and at the crane operator's workplace. The bridge crane is characterized by potential danger for not only operators but also production personnel located in the crane area within the production workshop during its operation. The safe operating conditions of cranes are determined by not only their technical condition but also the crane operator fatigue, which, in turn, is caused mainly by the impact of increased noise and vibration.*

Keywords: *bridge cranes, noise levels, vibration, sanitary standards, wheelset assemblies*

DOI: *: 10.36336/akustika/20214113*

1. INTRODUCTION

An analysis of the layouts of all bridge crane types allows suggesting that wheelset assemblies are among the main sources of increased noise.

2. EQUIPMENT AND DEVICES USED IN THE RESEARCH

The wheels are actually emitters in the form of round plates with relevant inertia moments. For such sources, sound pressure and power levels are determined by the following equations:

$$L_{W_k} = 20lgV_k + 10\,lg(0.5\mathrm{D}_k + h_k)\,k + 174 \tag{1}$$

where
D_k is the wheel diameter, m;
h_k is the wheel rim thickness, m;
k is a coefficient determining the vibration eigenfrequency.

The vibration eigenmodes of the wheelset axles are defined considering their geometric configuration as follows:

$$f_k = 625\left(\frac{k}{l}\right)^2 \mathrm{D_0} \tag{2}$$

Then the following dependencies are obtained for the sound power levels:

- for two wheelset axles at : $0,02f_kD_0<1$

$$L_{w_0} = 40lgk\mathrm{D_0} - 30lgl + 10lgBV_kcos\beta + 183 \tag{3}$$

- or two wheelset axles at: $0,02f_kD_0\leq 1$

$$L_{w_0} = 40lg\frac{k}{l} + 20lg\mathrm{D_0} + 10lgBV_kcos\beta + 161 \tag{4}$$

- for four crane trolley wheels:

$$L_{w_k} = 20lgV_k + 10\,lg(0.5\mathrm{D}_k + h_k)\,k + 180 \tag{5}$$

3. RESULTS AND DISCUSSION

Thus, for the engineering calculation of the spectral component levels of the above sources, the amplitudes of vibration velocities in the eigenmode of each source should be determined.

The general approach to calculating the vibration velocities of wheels is based on energy techniques considering the wheelset assembly layout (as a system of two wheels and an axle) [1-11].

It should be noted that the actually introduced vibration capacity depends on both the force action in the wheel-rail system and the vibration speed of the rail itself. In this case, the force action is defined as:

$$P_\mathrm{i} = m_\mathrm{i} \cdot \left|R_e\{y''\}\right| \tag{6}$$

where
m_i is the mass reduced to each wheel, kg;
P_i is the acceleration of rail vibrations, m/s^2.

When the bridge crane moves, the force action on the wheelset assemblies is transmitted from the rails, the vibration acceleration of which is found as the time derivative of the vibration velocities at their eigenfrequencies, the equations for which are obtained in [1, 2]. Then, for the conditions of installing the rail as a rigidly fixed beam, the acceleration equations will be written as follows:

$$\left|\operatorname{Re}\left\{y_1''\right\}\right| = \left|\frac{2,6\cdot10^{-4}Ph_p^3}{F}\cdot\sum_{k=1}^{k^*}\left(\frac{7k-3}{l_1}\right)^4\cos1,3\cdot10^4\left(\frac{7k-3}{l_1}\right)^2\sqrt{\frac{I}{F}}t+\right.$$

$$+PVl_1^2\cdot10^{-2}\left\{\sum_{k=1}^{k^*}\frac{\frac{7k-3}{2l_1}\pi V\left[6,4\cdot10^7(7k-3)^2\frac{Y}{F}-(Vl_1)^2\right]\sin\frac{7k-3}{2l_1}\pi Vt\cdot\frac{1}{7k-3}}{\left[6,4\cdot10^7(7k-3)^2\frac{Y}{F}-(Vl_1)^2\right]^2+4\cdot10^{15}(7k-3)^4\left(\frac{Y}{F}\eta\right)^2}+\right.$$

$$+\frac{\frac{3-5k}{2l_1}\pi V\left[1,6\cdot10^8(7k-3)^4\cdot\frac{Y}{F}-(5k-3)^2(Vl_1)^2\right]}{\left[1,6\cdot10^8(7k-3)^4\cdot\frac{Y}{F}-(5k-3)^2(Vl_1)^2\right]^2+2,6\cdot10^{16}(7k-3)^8\left(\frac{Y}{F}\eta\right)^2}\times$$

$$\times(3-5k)\sin\frac{3-5k}{2l_1}\pi Vt+$$

$$+3,6\left(\sum\frac{\frac{3k-1}{2l_1}\pi V\left[1,6\cdot10^8(7k-3)^4\frac{Y}{F}-(3k-1)^2(Vl_1)^2\right]}{1,6\cdot10^8(7k-3)^4\frac{Y}{F}-(3k-1)^2(Vl_1)^2\ 2,6\cdot10^{16}(7k-3)^8\left(\frac{Y}{F}\eta\right)^2}\right)\times$$

$$\times(3k-1)\sin\frac{3k-1}{2l_1}\pi Vt+$$

$$+\frac{\frac{1-k}{2l_1}\pi V\left[1,6\cdot10^8(7k-3)^4\frac{Y}{F}-(1-k)^2(Vl_1)^2\right]}{1,6\cdot10^8(7k-3)^4\frac{Y}{F}-(1-k)^2(Vl_1)^2+2,6\cdot10^{16}(7k-3)^8\left(\frac{Y}{F}\eta\right)^2}\times$$

$$\left.\left.t\times(1-k)\sin\frac{1-k}{2l_1}\pi Vt\right)\right\}\sin\frac{7k-3}{2l_1}\pi x\Bigg|;$$

$$\left|\operatorname{Re}\left\{y''_2\right\}\right| = \left|\frac{2\cdot10^{-4}Ph_p^3}{F}\cdot\sum_{k=1}^{k^*}\left(\frac{3-5k}{l_1}\right)^4\cos1,3\cdot10^4\left(\frac{3-5k}{l_1}\right)^2\sqrt{\frac{I}{F}}t+\right.$$

$$+PVl_1^2\cdot10^{-2}\left\{\sum\frac{\frac{7k-3}{2l_1}\pi V\left[1,6\cdot10^8(3-5k)^4\frac{Y}{F}(7k-3)^2(Vl_1)^2\right]}{\left[1,6\cdot10^8(3-5k)^4\frac{Y}{F}-(7k-3)^2(Vl_1)^2\right]^2+2,6\cdot10^{16}(7k-3)^8\left(\frac{Y}{F}\eta\right)^2}\times\right.$$

$$\times(7k-3)\sin\frac{7k-3}{2l_1}\pi Vt+$$

$$+\frac{\frac{3-5k}{2l_1}\pi V\left[6,4\cdot10^7(3-5k)^2\frac{Y}{F}-(Vl_1)2\right]}{\left[6,4\cdot10^7(3-5k)^2\frac{Y}{F}-(Vl_1)^2\right]^2+4\cdot10^{15}(3-5k)^4\left(\frac{Y}{F}\eta\right)^2}\cdot\frac{\sin\frac{3-5k}{2l_1}\pi Vt}{3-5k}+$$

$$+3,6\sum\frac{\frac{3k-1}{2l_1}\pi V\left[1,6\cdot10^8(3-5k)^4\frac{Y}{F}-(3k-1)^2(Vl_1)^2\right]}{\left[1,6\cdot10^8(3-5k)^4\frac{Y}{F}-(3k-1)^2(Vl_1)^2\right]^2+2,6\cdot10^{16}(3k-1)^8\left(\frac{Y}{F}\eta\right)^2}\cdot(3k-1)\sin\frac{3k-1}{2l_1}\pi Vt+$$

$$+\sum\frac{\frac{1-k}{2l_1}\pi V\left|1,6\cdot10^8(3-5k)^4\frac{Y}{F}-(1-k)^2(Vl_1)^2\right|}{\left[1,6\cdot10^8(3-5k)^4\frac{Y}{F}-(1-k)^2(Vl_1)^2\right]^2+2,6\cdot10^{16}(3-5k)^8\left(\frac{Y}{F}\eta\right)^2}\times$$

$$\left.\left.\times(1-k)\sin\frac{1-k}{2l_1}\pi Vt\right)\right\}\sin\frac{3-5k}{2l_1}\pi x\Bigg|;$$

$$\left|\operatorname{Re}\left\{y''_3\right\}\right| = \left|-\frac{2\cdot10^{-4}Ph_p^3}{F}\cdot\sum_{k=1}^{k^*}\left(\frac{3k-1}{l_1}\right)^4\cos1,3\cdot10^4\left(\frac{3k-1}{l_1}\right)^2\sqrt{\frac{I}{F}}t+\right.$$

$$+PVl_1^2\cdot10^{-2}\left\{\sum\frac{\frac{7k-3}{2l_1}\pi V\left[1,6\cdot10^8(3k-1)^4\frac{Y}{F}-(7k-3)^2(Vl_1)^2\right]}{\left[1,6\cdot10^8(3k-1)^4\frac{Y}{F}-(7k-3)^2(Vl_1)^2\right]^2+2,6\cdot10^{16}(7k-3)^8\left(\frac{Y}{F}\eta\right)^2}\times\right.$$

$$\times(7k-3)\sin\frac{7k-3}{2l_1}\pi Vt+$$

$$+\frac{\frac{3-5k}{2l_1}\pi V\left[1,6\cdot10^8(3k-1)^4\frac{Y}{F}-(3-5k)^2(Vl_1)^2\right]\cdot(3-5k)\sin\frac{3-5k}{2l_1}\pi Vt}{\left[1,6\cdot10^8(3k-1)^4\frac{Y}{F}-(3-5k)^2(Vl_1)^2\right]^2+2,6\cdot10^{16}(3k-1)^8\left(\frac{Y}{F}\eta\right)^2}\cdot$$

$$+3,6\left(\sum\frac{\frac{3k-1}{2l_1}\pi V\left[6,4\cdot10^7(3k-1)^2\frac{Y}{F}-(Vl_1)^2\right]}{\left[6,4\cdot10^7(3k-1)^2\frac{Y}{F}-(Vl_1)^2\right]^2+4\cdot10^{15}(3k-1)^4\left(\frac{Y}{F}\eta\right)^2}\cdot\frac{\sin\frac{3k-1}{2l_1}\pi Vt}{3k-1}+\right.$$

$$\left.\left.+\frac{\frac{1-k}{2l_1}\pi V\left[1,6\cdot10^8(3k-1)^4\frac{Y}{F}-(1-k)^2(Vl_1)^2\right]\cdot\frac{\sin\frac{1-k}{2l_1}\pi Vt}{(1-k)}}{\left[1,6\cdot10^8(3k-1)^4\frac{Y}{F}-(1-k)^2(Vl_1)^2\right]^2+2,6\cdot10^{16}(3k-1)^8\left(\frac{Y}{F}\eta\right)^2}\right)\right\}\cdot\sin\frac{3k-1}{2l_1}\pi x\Bigg|;$$

$$\left|\operatorname{Re}\left\{y''_4\right\}\right| = \left|-\frac{2\cdot10^{-4}Ph_p^3}{F}\cdot\sum_{k=1}^{k^*}\left(\frac{1-k}{l_1}\right)^4 cos1,3\cdot10^4\left(\frac{1-k}{l_1}\right)^2\sqrt{\frac{I}{F}}t+\right.$$

$$+PVl_1^2\cdot10^{-2}\left\{\sum\frac{\frac{7k-3}{2l_1}\pi V\left[1,6\cdot10^8(1-k)^4\frac{Y}{F}-(7k-3)^2(Vl_1)^2\right](7k-3)\sin\frac{7k-3}{2l_1}\pi Vt}{\left[1,6\cdot10^8(1-k)^4\frac{Y}{F}-(7k-3)^2(Vl_1)^2\right]^2+2,6\cdot10^{16}(1-k)^8\left(\frac{Y}{F}\eta\right)^2}+\right.$$

$$+3,6\left(\sum\frac{\frac{3k-1}{2l_1}\pi V\left[1,6\cdot10^8(1-k)^4\frac{Y}{F}-(3k-1)^2(Vl_1)^2\right]\cdot(3k-1)\sin\frac{3k-1}{2l_1}\pi Vt}{\left[1,6\cdot10^8(1-k)^4\frac{Y}{F}-(3k-1)^2(Vl_1)^2\right]^2+2,6\cdot10^{16}(1-k)^8\left(\frac{Y}{F}\eta\right)^2}+\right.$$

$$\left.\left.+\sum\frac{\frac{1-k}{2l_1}\pi V\left[6,4\cdot10^7(1-k)^2\frac{Y}{F}-(Vl_1)^2\right]}{\left[6,4\cdot10^7(1-k)^2\frac{Y}{F}-(Vl_1)^2\right]^2+4\cdot10^{15}(1-k)^8\left(\frac{Y}{F}\eta\right)^2}\cdot\frac{\sin\frac{1-k}{2l_1}\pi Vt}{(1-k)}\right)\right\}\cdot\sin\frac{1-k}{2l_1}\pi x\Bigg|.$$

When the rail is installed on a damping pad, the acceleration equations will take the form:

$$\left|\operatorname{Re}\left\{y_1''\right\}\right| = \left|1,6\cdot10^{-12}\frac{Ph_p^3}{YF}\left[1,6\cdot10^8\left(\frac{7k-3}{l_1}\right)\cdot Y+1,3\cdot10^{-4}j_{np}\right]\times\right.$$

$$\cos\left[1,6\cdot10^8\left(\frac{7k-3}{l_1}\right)\frac{Y}{F}+1,3\cdot10^{-4}\frac{j_{np}}{F}\right]^{0,5}t+\frac{3\cdot P\cdot10^{-2}\cdot V}{l_1^2}\times$$

$$\times\left\{\sum\frac{-\frac{(7k-3)^2}{2l_1}\cdot\pi V\left\{\left[1,6\cdot10^8\left(\frac{7k-3}{l_1}\right)^4\cdot\frac{Y}{F}+1,3\cdot10^{-4}\frac{j_{np}}{F}\right]-\left(\frac{7k-3}{2l_1}\right)^2\cdot(\pi V)^2\right\}}{\left\{\left[1,6\cdot10^8\left(\frac{7k-3}{l_1}\right)^4\cdot\frac{Y}{F}+1,3\cdot10^{-4}\frac{j_{np}}{F}\right]-\left(\frac{7k-3}{2l_1}\right)^2\cdot(\pi V)^2\right\}^2+\left[1,6\cdot10^8\left(\frac{7k-3}{l_1}\right)^4\cdot\frac{Y}{F}\eta_1+1,3\cdot10^{-4}\frac{j_{np}}{F}\eta_2\right]^2}\times\right.$$

$$\times\sin\frac{(7k-3)}{2l_1}\cdot\pi Vt+$$

$$+\frac{-\frac{(3-5k)^2}{2l_1}\cdot\pi V\left\{\left[1,6\cdot10^8\left(\frac{7k-3}{l_1}\right)^4\cdot\frac{Y}{F}+1,3\cdot10^{-4}\frac{j_{np}}{F}\right]-\left(\frac{3-5k}{2l_1}\right)^2\cdot(\pi V)^2\right\}}{\left\{\left[1,6\cdot10^8\left(\frac{7k-3}{l_1}\right)^4\cdot\frac{Y}{F}+1,3\cdot10^{-4}\frac{j_{np}}{F}\right]-\left(\frac{7k-3}{2l_1}\right)^2\cdot(\pi V)^2\right\}^2+\left[1,6\cdot10^8\left(\frac{7k-3}{l_1}\right)^4\cdot\frac{Y}{F}\eta_1+1,3\cdot10^{-4}\frac{j_{np}}{F}\eta_2\right]^2}\times$$

$$\times\sin\frac{3-5k}{2l_1}\cdot\pi Vt+$$

$$+\frac{-\frac{(3k-1)^2}{2l_1}\cdot\pi V\left\{\left[1,6\cdot10^8\left(\frac{3k-1}{l_1}\right)^4\cdot\frac{Y}{F}+1,3\cdot10^{-4}\frac{j_{np}}{F}\right]-\left(\frac{3k-1}{2l_1}\right)^2\cdot(\pi V)^2\right\}}{\left\{\left[1,6\cdot10^8\left(\frac{7k-3}{l_1}\right)^4\cdot\frac{Y}{F}+1,3\cdot10^{-4}\frac{j_{np}}{F}\right]-\left(\frac{7k-3}{2l_1}\right)^2\cdot(\pi V)^2\right\}^2+\left[1,6\cdot10^8\left(\frac{7k-3}{l_1}\right)^4\cdot\frac{Y}{F}\eta_1+1,3\cdot10^{-4}\frac{j_{np}}{F}\eta_2\right]^2}\times$$

$$\times\sin\frac{3k-1}{2l_1}\cdot\pi Vt+$$

$$\left.+\frac{-\frac{(1-k)^2}{2l_1}\cdot\pi V\left\{\left[1,6\cdot10^8\left(\frac{1-k}{l_1}\right)^4\cdot\frac{Y}{F}+1,3\cdot10^{-4}\frac{j_{np}}{F}\right]-\left(\frac{1-k}{2l_1}\right)^2\cdot(\pi V)^2\right\}}{\left\{\left[1,6\cdot10^8\left(\frac{7k-3}{l_1}\right)^4\cdot\frac{Y}{F}+1,3\cdot10^{-4}\frac{j_{np}}{F}\right]-\left(\frac{7k-3}{2l_1}\right)^2\cdot(\pi V)^2\right\}^2+\left[1,6\cdot10^8\left(\frac{7k-3}{l_1}\right)^4\cdot\frac{Y}{F}\eta_1+1,3\cdot10^{-4}\frac{j_{np}}{F}\eta_2\right]^2}\times\sin\frac{1-k}{2l_1}\cdot\pi Vt\right\}\sin\frac{7k-3}{2l_1}\cdot\pi x\Bigg|,$$

$$\left|\operatorname{Re}\left\{y_2''\right\}\right| = \left|1,6\cdot10^{-12}\frac{Ph_p^3}{YF}\left[1,6\cdot10^8\left(\frac{3-5k}{l_1}\right)\cdot Y+1,3\cdot10^{-4}j_{np}\right]^{0,5}\times\right.$$

$$\times\sin\left[1,6\cdot10^8\left(\frac{3-5k}{l_1}\right)\frac{Y}{F}+1,3\cdot10^{-4}\frac{j_{np}}{F}\right]^{0,5}t+\frac{3\cdot P\cdot10^{-2}\cdot V}{l_1^2}\times$$

$$\times\left\{\sum\frac{-\frac{(7k-3)^2}{2l_1}\cdot\pi V\left\{\left[1,6\cdot10^8\left(\frac{3-5k}{l_1}\right)^4\cdot\frac{Y}{F}+1,3\cdot10^{-4}\frac{j_{np}}{F}\right]-\left(\frac{7k-3}{2l_1}\right)^2\cdot(\pi V)^2\right\}}{\left\{\left[1,6\cdot10^8\left(\frac{3-5k}{l_1}\right)^4\cdot\frac{Y}{F}+1,3\cdot10^{-4}\frac{j_{np}}{F}\right]-\left(\frac{7k-3}{2l_1}\right)^2\cdot(\pi V)^2\right\}^2+\left[1,6\cdot10^8\left(\frac{3-5k}{l_1}\right)^4\cdot\frac{Y}{F}\eta_1+1,3\cdot10^{-4}\frac{j_{np}}{F}\eta_2\right]^2}\times\right.$$

$$\times\sin\frac{7k-3}{2l_1}\cdot\pi Vt+$$

$$+\frac{-\frac{(3-5k)^2}{2l_1}\cdot\pi V\left\{\left[1,6\cdot10^8\left(\frac{3-5k}{l_1}\right)^4\cdot\frac{Y}{F}+1,3\cdot10^{-4}\frac{j_{np}}{F}\right]-\left(\frac{3-5k}{2l_1}\right)^2\cdot(\pi V)^2\right\}}{\left\{\left[1,6\cdot10^8\left(\frac{3-5k}{l_1}\right)^4\cdot\frac{Y}{F}+1,3\cdot10^{-4}\frac{j_{np}}{F}\right]-\left(\frac{3-5k}{2l_1}\right)^2\cdot(\pi V)^2\right\}^2+\left[1,6\cdot10^8\left(\frac{3-5k}{l_1}\right)^4\cdot\frac{Y}{F}\eta_1+1,3\cdot10^{-4}\frac{j_{np}}{F}\eta_2\right]^2}\times$$

$$\times\sin\frac{3-5k}{2l_1}\cdot\pi Vt+$$

$$+\frac{-\frac{(3k-1)^2}{2l_1}\cdot\pi V\left\{\left[1,6\cdot10^8\left(\frac{3-5k}{l_1}\right)^4\cdot\frac{Y}{F}+1,3\cdot10^{-4}\frac{j_{np}}{F}\right]-\left(\frac{3k-1}{2l_1}\right)^2\cdot(\pi V)^2\right\}}{\left\{\left[1,6\cdot10^8\left(\frac{3-5k}{l_1}\right)^4\cdot\frac{Y}{F}+1,3\cdot10^{-4}\frac{j_{np}}{F}\right]-\left(\frac{3-5k}{2l_1}\right)^2\cdot(\pi V)^2\right\}^2+\left[1,6\cdot10^8\left(\frac{3-5k}{l_1}\right)^4\cdot\frac{Y}{F}\eta_1+1,3\cdot10^{-4}\frac{j_{np}}{F}\eta_2\right]^2}\times$$

$$\times\sin\frac{3k-1}{2l_1}\cdot\pi Vt+$$

$$\left.+\frac{-\frac{(1-k)^2}{2l_1}\cdot\pi V\left\{\left[1,6\cdot10^8\left(\frac{3-5k}{l_1}\right)^4\cdot\frac{Y}{F}+1,3\cdot10^{-4}\frac{j_{np}}{F}\right]-\left(\frac{1-k}{2l_1}\right)^2\cdot(\pi V)^2\right\}}{\left\{\left[1,6\cdot10^8\left(\frac{3-5k}{l_1}\right)^4\cdot\frac{Y}{F}+1,3\cdot10^{-4}\frac{j_{np}}{F}\right]-\left(\frac{3-5k}{2l_1}\right)^2\cdot(\pi V)^2\right\}^2+\left[1,6\cdot10^8\left(\frac{3-5k}{l_1}\right)^4\cdot\frac{Y}{F}\eta_1+1,3\cdot10^{-4}\frac{j_{np}}{F}\eta_2\right]^2}\times\sin\frac{1-k}{2l_1}\cdot\pi Vt\right\}\sin\frac{3-5k}{2l_1}\cdot\pi x\Bigg|,$$

$$
\begin{aligned}
&\left|\mathrm{Re}\left\{y_3''\right\}\right| = \Bigg|1,6\cdot10^{-12}\frac{Ph_p^3}{YF}\left[1,6\cdot10^8\left(\frac{3k-1}{l_1}\right)\cdot Y+1,3\cdot10^{-4}j_{np}\right]^{0,5}\times\\
&\times\sin\left[,6\cdot10^8\left(\frac{3k-1}{l_1}\right)\frac{Y}{F}+1,3\cdot10^{-4}\frac{j_{np}}{F}\right]^{0,5}t+\frac{3\cdot P\cdot10^{-2}\cdot V}{l_1^2}\times\\
&\times\Bigg\{\sum\frac{-\frac{(7k-3)^2}{2l_1}\cdot\pi V\left\{\left[1,6\cdot10^8\left(\frac{3k-1}{l_1}\right)^4\cdot\frac{Y}{F}+1,3\cdot10^{-4}\frac{j_{np}}{F}\right]-\left(\frac{7k-3}{2l_1}\right)^2\cdot(\pi V)^2\right\}}{\left\{\left[1,6\cdot10^8\left(\frac{3k-1}{l_1}\right)^4\cdot\frac{Y}{F}+1,3\cdot10^{-4}\frac{j_{np}}{F}\right]-\left(\frac{7k-3}{2l_1}\right)^2\cdot(\pi V)^2\right\}^2+\left[1,6\cdot10^8\left(\frac{3k-1}{l_1}\right)^4\cdot\frac{Y}{F}\eta_1+1,3\cdot10^{-4}\frac{j_{np}}{F}\eta_2\right]^2}\times\\
&\times\sin\frac{7k-3}{2l_1}\cdot\pi Vt+\\
&+\frac{-\frac{(3-5k)^2}{2l_1}\cdot\pi V\left\{\left[1,6\cdot10^8\left(\frac{3k-1}{l_1}\right)^4\cdot\frac{Y}{F}+1,3\cdot10^{-4}\frac{j_{np}}{F}\right]-\left(\frac{3-5k}{2l_1}\right)^2\cdot(\pi V)^2\right\}}{\left\{\left[1,6\cdot10^8\left(\frac{3k-1}{l_1}\right)^4\cdot\frac{Y}{F}+1,3\cdot10^{-4}\frac{j_{np}}{F}\right]-\left(\frac{3k-1}{2l_1}\right)^2\cdot(\pi V)^2\right\}^2+\left[1,6\cdot10^8\left(\frac{3k-1}{l_1}\right)^4\cdot\frac{Y}{F}\eta_1+1,3\cdot10^{-4}\frac{j_{np}}{F}\eta_2\right]^2}\times\\
&\times\sin\frac{3-5k}{2l_1}\cdot\pi Vt+\\
&+\frac{-\frac{(3k-1)^2}{2l_1}\cdot\pi V\left\{\left[1,6\cdot10^8\left(\frac{3k-1}{l_1}\right)^4\cdot\frac{Y}{F}+1,3\cdot10^{-4}\frac{j_{np}}{F}\right]-\left(\frac{3k-1}{2l_1}\right)^2\cdot(\pi V)^2\right\}}{\left\{\left[1,6\cdot10^8\left(\frac{3k-1}{l_1}\right)^4\cdot\frac{Y}{F}+1,3\cdot10^{-4}\frac{j_{np}}{F}\right]-\left(\frac{3k-1}{2l_1}\right)^2\cdot(\pi V)^2\right\}^2+\left[1,6\cdot10^8\left(\frac{3k-1}{l_1}\right)^4\cdot\frac{Y}{F}\eta_1+1,3\cdot10^{-4}\frac{j_{np}}{F}\eta_2\right]^2}\times\\
&\times\sin\frac{3k-1}{2l_1}\cdot\pi Vt+\\
&+\frac{-\frac{(1-k)^2}{2l_1}\cdot\pi V\left\{\left[1,6\cdot10^8\left(\frac{3k-1}{l_1}\right)^4\cdot\frac{Y}{F}+1,3\cdot10^{-4}\frac{j_{np}}{F}\right]-\left(\frac{1-k}{2l_1}\right)^2\cdot(\pi V)^2\right\}}{\left\{\left[1,6\cdot10^8\left(\frac{3k-1}{l_1}\right)^4\cdot\frac{Y}{F}+1,3\cdot10^{-4}\frac{j_{np}}{F}\right]-\left(\frac{1-k}{2l_1}\right)^2\cdot(\pi V)^2\right\}^2+\left[1,6\cdot10^8\left(\frac{3k-1}{l_1}\right)^4\cdot\frac{Y}{F}\eta_1+1,3\cdot10^{-4}\frac{j_{np}}{F}\eta_2\right]^2}\times\sin\frac{1-k}{2l_1}\cdot\pi Vt\Bigg\}\sin\frac{3k-1}{2l_1}\cdot\pi x\Bigg|,
\end{aligned}
$$

$$
\begin{aligned}
&\left|\mathrm{Re}\left\{y_4''\right\}\right| = \Bigg|1,6\cdot10^{-12}\frac{Ph_p^3}{YF}\left[1,6\cdot10^8\left(\frac{1-k}{l_1}\right)\cdot Y+1,3\cdot10^{-4}j_{np}\right]^{0,5}\times\\
&\times\sin\left[1,6\cdot10^8\left(\frac{1-k}{l_1}\right)\frac{Y}{F}+1,3\cdot10^{-4}\frac{j_{np}}{F}\right]^{0,5}t+\frac{3\cdot P\cdot10^{-2}\cdot V}{l_1^2}\times\\
&\times\Bigg\{\sum\frac{-\frac{(7k-3)^2}{2l_1}\cdot\pi V\left\{\left[1,6\cdot10^8\left(\frac{1-k}{l_1}\right)^4\cdot\frac{Y}{F}+1,3\cdot10^{-4}\frac{j_{np}}{F}\right]-\left(\frac{7k-3}{2l_1}\right)^2\cdot(\pi V)^2\right\}}{\left\{\left[1,6\cdot10^8\left(\frac{1-k}{l_1}\right)^4\cdot\frac{Y}{F}+1,3\cdot10^{-4}\frac{j_{np}}{F}\right]-\left(\frac{7k-3}{2l_1}\right)^2\cdot(\pi V)^2\right\}^2+\left[1,6\cdot10^8\left(\frac{1-k}{l_1}\right)^4\cdot\frac{Y}{F}\eta_1+1,3\cdot10^{-4}\frac{j_{np}}{F}\eta_2\right]^2}\times\\
&\times\sin\frac{7k-3}{2l_1}\cdot\pi Vt+\\
&+\frac{-\frac{(3-5k)^2}{2l_1}\cdot\pi V\left\{\left[1,6\cdot10^8\left(\frac{1-k}{l_1}\right)^4\cdot\frac{Y}{F}+1,3\cdot10^{-4}\frac{j_{np}}{F}\right]-\left(\frac{3-5k}{2l_1}\right)^2\cdot(\pi V)^2\right\}}{\left\{\left[1,6\cdot10^8\left(\frac{1-k}{l_1}\right)^4\cdot\frac{Y}{F}+1,3\cdot10^{-4}\frac{j_{np}}{F}\right]-\left(\frac{7k-3}{2l_1}\right)^2\cdot(\pi V)^2\right\}^2+\left[1,6\cdot10^8\left(\frac{k-1}{l_1}\right)^4\cdot\frac{Y}{F}\eta_1+1,3\cdot10^{-4}\frac{j_{np}}{F}\eta_2\right]^2}\times\\
&\times\sin\frac{3-5k}{2l_1}\cdot\pi Vt+\\
&+\frac{-\frac{(3k-1)^2}{2l_1}\cdot\pi V\left\{\left[1,6\cdot10^8\left(\frac{k-1}{l_1}\right)^4\cdot\frac{Y}{F}+1,3\cdot10^{-4}\frac{j_{np}}{F}\right]-\left(\frac{3k-1}{2l_1}\right)^2\cdot(\pi V)^2\right\}}{\left\{\left[1,6\cdot10^8\left(\frac{k-1}{l_1}\right)^4\cdot\frac{Y}{F}+1,3\cdot10^{-4}\frac{j_{np}}{F}\right]-\left(\frac{3k-1}{2l_1}\right)^2\cdot(\pi V)^2\right\}^2+\left[1,6\cdot10^8\left(\frac{3k-1}{l_1}\right)^4\cdot\frac{Y}{F}\eta_1+1,3\cdot10^{-4}\frac{j_{np}}{F}\eta_2\right]^2}\times\\
&\times\sin\frac{3k-1}{2l_1}\cdot\pi Vt+\\
&+\frac{-\frac{(1-k)^2}{2l_1}\cdot\pi V\left\{\left[1,6\cdot10^8\left(\frac{1-k}{l_1}\right)^4\cdot\frac{Y}{F}+1,3\cdot10^{-4}\frac{j_{np}}{F}\right]-\left(\frac{1-k}{2l_1}\right)^2\cdot(\pi V)^2\right\}}{\left\{\left[1,6\cdot10^8\left(\frac{1-k}{l_1}\right)^4\cdot\frac{Y}{F}+1,3\cdot10^{-4}\frac{j_{np}}{F}\right]-\left(\frac{1-k}{2l_1}\right)^2\cdot(\pi V)^2\right\}^2+\left[1,6\cdot10^8\left(\frac{7k-3}{l_1}\right)^4\cdot\frac{Y}{F}\eta_1+1,3\cdot10^{-4}\frac{j_{np}}{F}\eta_2\right]^2}\times\sin\frac{1-k}{2l_1}\cdot\pi Vt\Bigg\}\sin\frac{1-k}{2l_1}\cdot\pi x\Bigg|,
\end{aligned}
$$

4. CONCLUSIONS

The obtained dependencies consider the structural, physical, and mechanical parameters of the 'wheel-rail' acoustic subsystem and the rail installation scheme. These dependencies allow performing an engineering calculation of the spectral composition of vibration and noise and justifying technical solutions for the required reduction in the levels of vibroacoustic characteristics.

REFERENCES

[1] Bondarenko, V.A. Theoretical Study of Vibration Spectra of Wheelset Assemblies of Bridge Cranes // NAUKOVEDENIE Internet Journal, Vol. 8, No. 4 (2016) http://naukovedenie.ru/PDF/04TVN416.pdf (free access). Title from the screen. Language: Russian, English

[2] Bondarenko, V.A. Theoretical Study of Vibration and Noise Spectra of the Rail During the Bridge Crane Movement // NAUKOVEDENIE Internet Journal, Vol. 8, No. 3 (2016) http://naukovedenie.ru/PDF/23TVN316.pdf (free access).

[3] Kolesnikov, I.V., Podust, S.F., Podust, S.S., Chukarin, A.N. Ways to Reduce Noise and Vibration in the Design, Manufacture, and Operation of Railway Rolling Stock. - M.: VINITI RAS, 2015. - 216 p. Il.

[4] Podust, S.F. Fundamentals of Vibroacoustic Calculations of Domestic Electric Locomotives: Monograph / S.F. Podust, A.N. Chukarin, I.V. Boguslavsky. – Rostov-on-Don: Publishing Center DSTU, 2013. - 150 p.

[5] Podust, S.F., Kuklin, D.A. Simulating Vibroacoustic Dynamics of a Rail on Sleepers. Bulletin of the Don State Technical University. 2013. Vol. 13, Nos. 1-2 (70-71). pp. 106-111.

[6] Podust, S.F. Impact of Corrugated Rail Wear on Vibroacoustic Characteristics During the Rolling Stock Movement. Bulletin of the Don State Technical University. 2013. Vol. 13, Nos. 5-6 (74). pp. 137-143.

[7] Podust, S.F. Simulating Vibroacoustic Dynamics of Sleepers During the Rolling Stock Movement. Bulletin of Rostov State Transport University. 2013. No. 1 (49). pp. 50-54.

[8] Podust, S.F. Experimental Studies of Noise and Vibration During the Movement of Passenger and High-Speed Trains. Bulletin of Rostov State Transport University. 2015. No. 2. pp. 30-35.

[9] Noise in Transport: trans. from English / ed. V.E. Tolsky, G.V. Butakov, B.N. Melnikov. - M.: Transport, 1995. - 368 p.

[10] Chukarin, A.N. Theory and Methods of Acoustic Calculations and Design of Mechanical Processing Machines. - Rostov-on--Don: Publishing Center DSTU, 2005. - 152 p.

[11] Ivanov, N.I., Nikiforov, A.S. Fundamentals of Vibroacoustic: Textbook for Universities. - SPb.: Polytechnic, 2000. - 482 p.

Veronika Krutova *is a Candidate of Technical Sciences.*
Veronika Krutova is an expert in noise and vibration reduction of overhead cranes. Veronika Krutova is the author of 25 scientific articles and is the co-author of 1 monograph.

Paper No.346/2021

AMBIENT NOISE: PROBLEM AND STUDY IN THE FRAMEWORK OF UAV AEROACOUSTICS

Petr Moshkov

Moscow Aviation Institute (National Research University), Moscow, Russia, moshkov89@bk.ru

Abstract*: The role of ambient noise in the problem of community noise of propeller-driven unmanned aerial vehicle is considered. The results of the author's measurements of the spectral characteristics of the background in open terrain, in the mountains, near the sea and the highway are presented. An expression is proposed for calculating the spectrum of background noise in open terrain (wind noise). It is shown that the ambient noise can be an effective noise masker of propeller-driven UAV in the low and medium frequencies.*

Keywords: *ambient noise, wind noise, background noise, UAV noise, sound scape*

DOI: *: 10.36336/akustika/20214116*

1. INTRODUCTION

The widespread development of unmanned aircraft systems poses the task of ensuring the highest possible characteristics of these systems at the current stage of the development of science and technology. At the same time, the noise indicators of military propeller-driven (UAVs) are one of the most important and priority at the present time, which is confirmed by numerous studies of the sources of UAV noise [1–3] and, in general, the problems of their audibility [4, 5] and acoustic signature [6, 7]. International standards regulating the maximum permissible community noise levels of civil UAVs are not currently developed, and low noise levels of general-purpose UAVs are, first of all, their competitive advantage.

The problem of determining ambient noise occupies a separate place within the framework of the topic of UAV aeroacoustics. Background noise acts as a masker of a useful signal and the task is to isolate the UAV noise against the ambient noise both by ear [8, 9] and with the help of special measuring systems. This leads to the need to establish objective criteria for assessing the degree of acoustic signature of different types of UAVs when they are used in various natural and weather conditions. The criteria of audibility and acoustic signature are objective noise parameters that allow us to assess the audibility and acoustic signature of various types of propeller-driven UAVs. These criteria generally depend on the spectral characteristics of the UAV sound field and ambient noise. The audibility criteria are also influenced by the peculiarities of human perception of moving sources.

Another aspect of the problem of background noise assessment is the wide application in the near future of aircraft in cities for the delivery of parcels, air taxis, etc. It is expected that by 2030-2035, air transport will be able to partially replace automobile transport, and in another five years, air taxi will be able to transfer to electric power supply schemes and an unmanned control system. The widespread use of UAVs in everyday life will lead to a significant transformation of the soundscape of cities. An important task will be to ensure the flight paths of the aircraft in urban conditions, so that the noise of the device is masked by background noise in the field of application and does not have an additional irritating effect on urban residents.

It should be noted that the transformation of urban soundscapes has already occurred around the world during the COVID-19 pandemic, and a significant number of studies have been devoted to this topic around the world [10–15].

This paper presents the results of ambient noise measurements performed in an open area at a local aerodrome [16]. Background measurements near the sea (surf noise) and in the mountains were carried out close to Gelendzhik (Krasnodar region, Russia) and in the forest near the highway close to Zvenigorod (Moscow region, Russia).

2. METHODOLOGY FOR MEASURING AMBIENT NOISE AND PROCESSING MEASUREMENT RESULTS

To measure the background noise levels, a single-channel measuring system based on a portable noise meter "Ecofizika-110A" was used. The measuring microphone with the installed wind protection was installed on a tripod at a height of 1.2 m relative to the ground surface. The main axis of the microphone was directed upwards. The audio signal was recorded at a sampling rate of 48 kHz. Post-processing of the signal within the framework of the purposes of this paper included obtaining in 5 s increments with exponential averaging of the 1/3-octave spectrum of sound pressure levels in the frequency range of 10–10000 Hz.

3. THE SPECTRAL CHARACTERISTICS OF AMBIENT NOISE

3.1. Open territory

The 1/3-octave spectrum of sound pressure levels measured in an open area with a step of 5 s at a wind speed of 3-6 m/s are shown in Fig. 1. Here and further to the left of the measured spectrum, the pictures show photos of the microphone location.

The spread of the spectrum in the studied frequency range is 20 dB, which is explained by a significant change in the wind speed during measurements. At the same time, three characteristic frequency ranges can be distinguished in the spectrum. The frequency range is 10-315 Hz, where the sound pressure levels decrease with frequency, which indicates the probable dominance of the turbulent atmosphere's self-noise in this frequency domain. The frequency range is 400-2000 Hz, where noise sources are present, apparently unrelated to atmospheric turbulence. The frequency range is 2500-10000 Hz, where noise levels decrease with frequency, but it is worth noting that the recorded background noise levels in this frequency range are commensurate with the natural noise of the measuring system.

In general, we note that background noise in an open area can be an effective marker of UAV noise in the frequency range up to 100 Hz for both the observer and the measuring microphone.

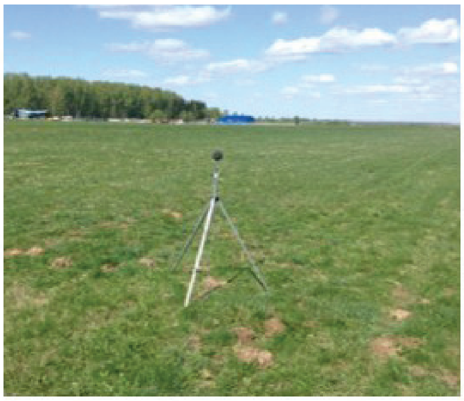

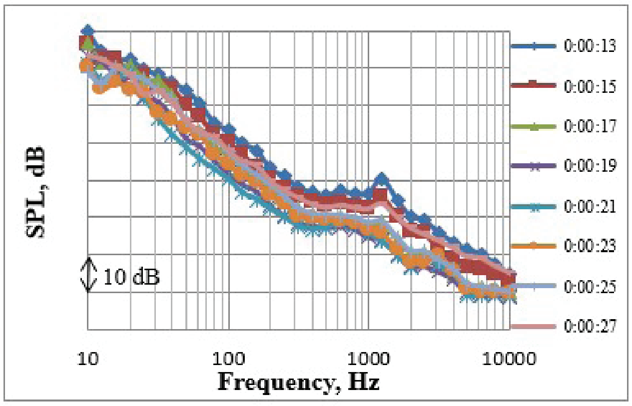

Fig. 1: 1/3-octave spectrums of ambient noise in open terrain conditions at a wind speed of 3–6 m/s

The influence of wind speed on the measured ambient noise levels is considered in Fig. 2. An increase in the wind speed by 2 m/s leads to an increase in the measured sound pressure levels in the entire studied frequency range by up to ~12 dB. At the same time, the A-weighted overall sound pressure level increases by 6 dBA. The increase in noise levels in the frequency range of 10–250 Hz is most likely due to an increase in the intrinsic noise of the turbulent atmosphere with an increase in wind speed. Since a change in wind speed also leads to an increase in noise levels in the range of 315-10000 Hz (Fig. 1, 2), therefore, it is most likely that the source of radiation in this frequency range is the noise of the flow around the grass cover. This hypothesis is confirmed by the expected size of the characteristic source, which, taking into account the maximum of vortex noise at a frequency of 1250 Hz at a wind speed of 6 m/s and the Strouhal number taken into account in the calculation of 0.2, is equal to 0.96 mm.

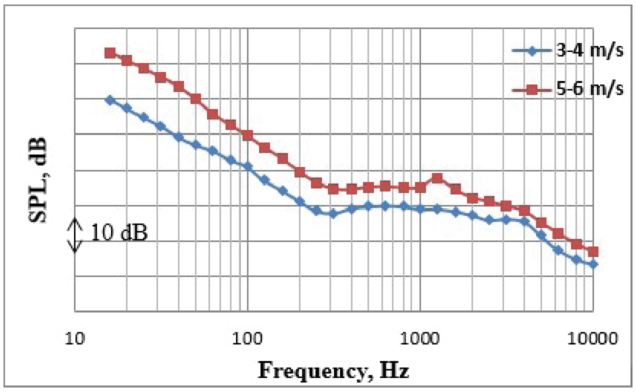

Fig. 2: Influence of wind speed on ambient noise levels in open terrain

In the spectral representation of atmospheric turbulence, it is customary to distinguish three characteristic intervals: energy, inertia and dissipation. The shape of the turbulence spectrum at the inertial interval, as a rule, agrees with the known Kolmogorov energy spectrum , where f – frequency in Hz [17].

The shape of the background noise spectrum with a frequency-decreasing intensity in the spectrum can be described by a functional dependence:

$$E(f) \propto f^{-\frac{5}{3}}$$

where
f – frequency in Hz [17].

Kraichnan [18, 19] suggested that two-dimensional turbulence can exhibit two types of inertial range: the range of energy transfer, for which the exponent is -5/3, and the range of entropy transfer, for which the exponent is -3.

The shape of the background noise spectrum with a frequency-decreasing intensity in the spectrum can be described by a functional dependence:

$$I(f) = c_1 f^{-\alpha} \qquad (1)$$

where

c_1 – empirical proportionality coefficient that depends on the wind speed and other parameters that determine the ambient noise levels of a turbulent atmosphere,

α – indicator of the decline in spectral intensity.

Expression (1) can be used to estimate background noise with a similar spectrum with a frequency-decreasing intensity in the presence of experimental constants α and c_1. According to the results of the author's research in an open area, the indicator of the decline curve α is 3. In accordance with the works of Kraichnan [18, 19], it can be concluded that the empirical constant corresponds to the range of entropy transfer in the inertial range of two-dimensional turbulence.

As an example, a comparison of the calculated and measured 1/3-octave spectrum of sound pressure levels at a wind speed of 5–6 m/s are shown in Fig. 3. One can see a good agreement between the calculated and experimental data up to the frequency of 315 Hz, where the ambient noise levels are determined by the self-noise of the turbulent atmosphere.

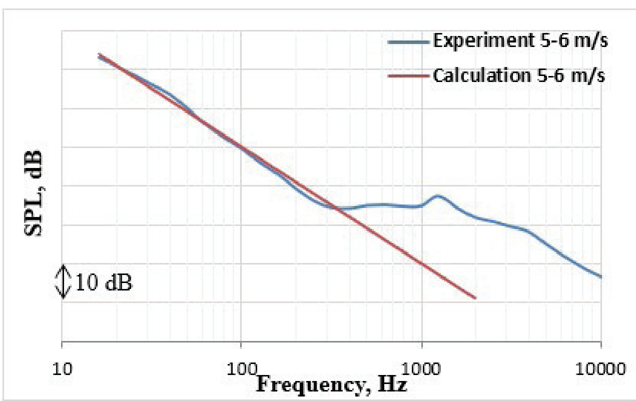

Fig. 3: Comparison of calculated and measured 1/3-octave spectrum of sound pressure levels

3.2. Near the sea

The 1/3-octave spectrum of sound pressure levels measured near the sea at low wind speed are shown in Fig. 4. The maximum levels are observed in the 1/3-octave bands with central frequencies of 50 and 400 Hz. The spread of the spectrum (up to ~20 dB) is most likely due to the different height and speed of the incoming waves. It can be seen that in this case, the ambient noise can be an effective masker of UAV noise in the range of ~250–2000 Hz, as well as tonal noise in the 50 Hz band.

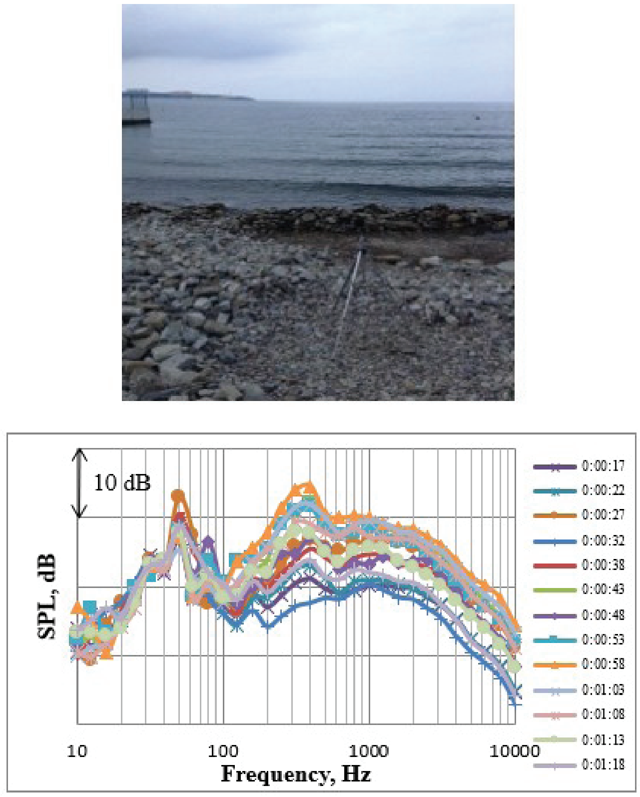

Fig. 4: 1/3-octave spectrum of sound pressure levels measured in 5 s increments near the sea (surf noise) at a wind speed of 0.5 m/s

3.3. In the mountains

The 1/3-octave spectra of sound pressure levels measured in the mountains at different control points at different wind speeds are shown in Fig. 5. You can see the decrease in the intensity of ambient noise with frequency, as well as when measuring the background in open terrain. At the same time, at a wind speed of 3.5–4.5 m/s (Fig. 5a), the spread of the measured sound pressure levels in the frequency range of 10–100 Hz is up to 10 dB, while in the frequency range of 100–100 Hz, the spread of sound pressure levels does not exceed 5 dB. The greatest spread of levels in the spectrum is observed at frequencies above 1000 Hz (up to 20 dB), which indicates that at high frequencies there are additional sources of noise of natural origin that are not associated with atmospheric turbulence.

At low wind speeds up to 1.5 m/s (Fig. 5b, c), the spread of the measured background levels reaches 35 dB in the low frequency range up to 100 Hz. At higher frequencies, the measured background levels are very low.

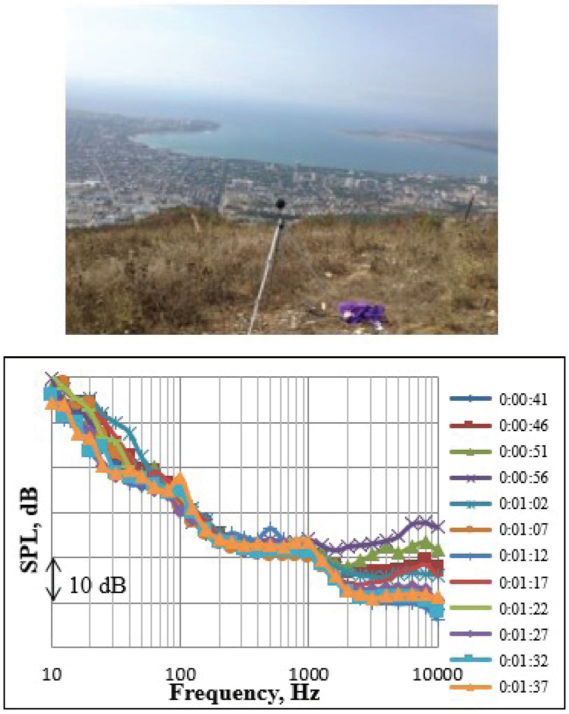

(a)

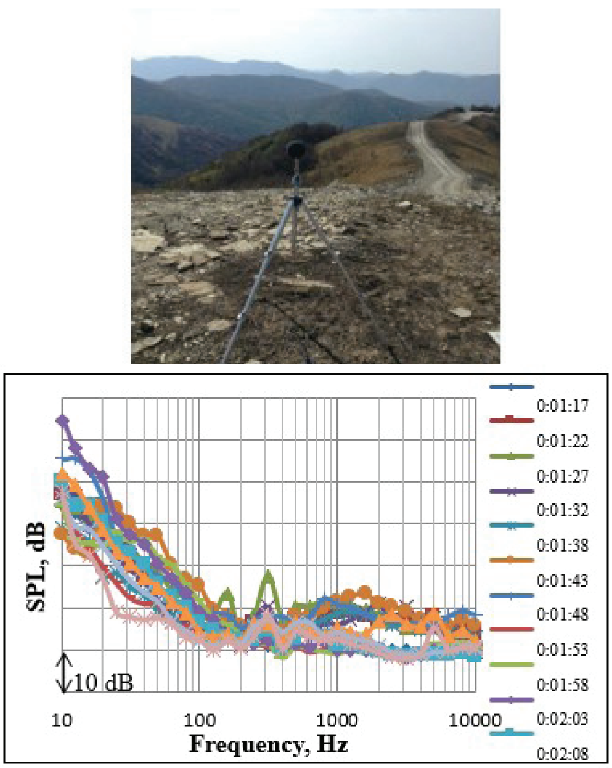

(b)

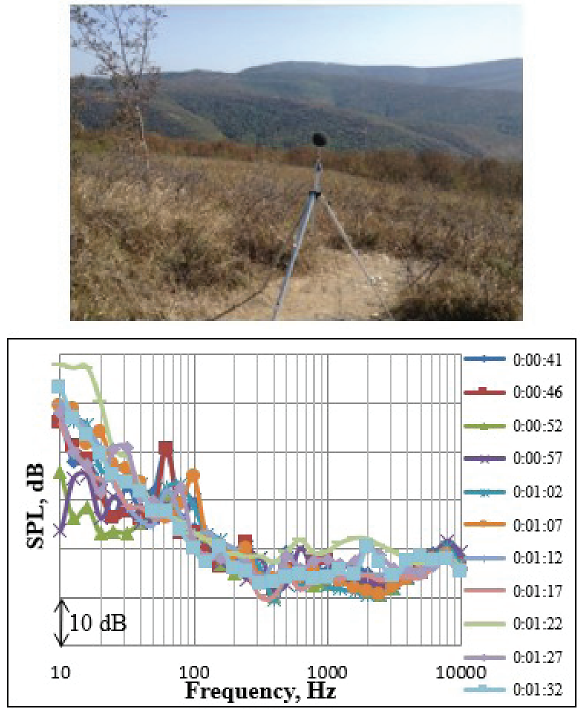

(c)

Fig. 5: 1/3-octave spectrum of sound pressure levels measured in 5 s increments at different control points in the mountains at different wind speeds

3.4. In a field

The 1/3-octave spectrum of sound pressure levels measured in a field near the city of Gelendzhik at a wind speed of 1 m/s are presented in Fig. 6. It can be seen that ambient noise levels in the frequency range of 200-1000 Hz are not related to the natural noise of the turbulent atmosphere. The measured levels above 2000 Hz are most likely related to the self-noise of the measuring system.

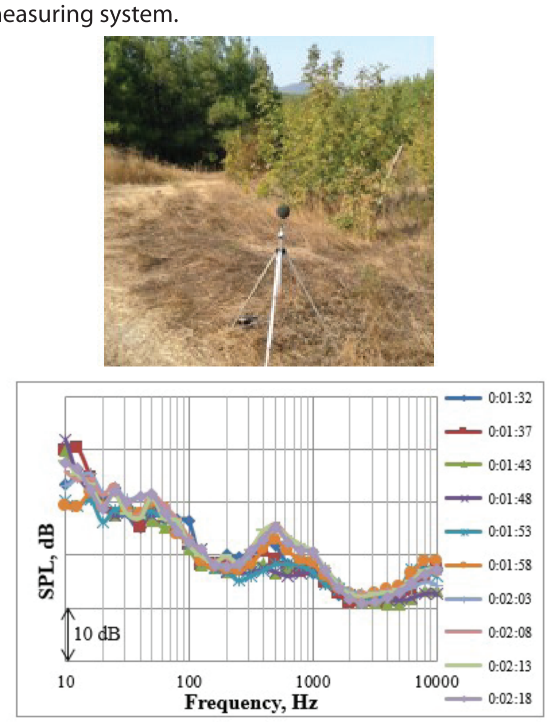

Fig. 6: 1/3-octave spectrum of sound pressure levels, measured in increments of 5 s, in the field at a wind speed of 1 m/s

3.5. In the forest near the highway

The 1/3-octave spectrum of the sound pressure levels of ambient noise measured in the forest at low wind speed with the audible noise of vehicles from the road are shown in Fig. 7. The greatest variation in the measured levels is observed in the frequency range 2000-10000 Hz, which, apparently, is due to the different power of car engines and their weight. In the frequency range of 10–2000 Hz, the spread of the measured sound pressure levels does not exceed 5 dB. Moreover, in the frequency range of 10-100 Hz, noise levels are almost constant, and some reduction in noise levels is observed at a frequency of 160 Hz. It can be seen that in this case, the noise of vehicles can be an effective masker of UAV noise in the frequency range of 10-1600 Hz. It should also be noted that in general, the noise level of the flow of vehicles is affected by many factors, such as traffic intensity, speed, the ratio between trucks and cars, road surface (type and condition), etc.

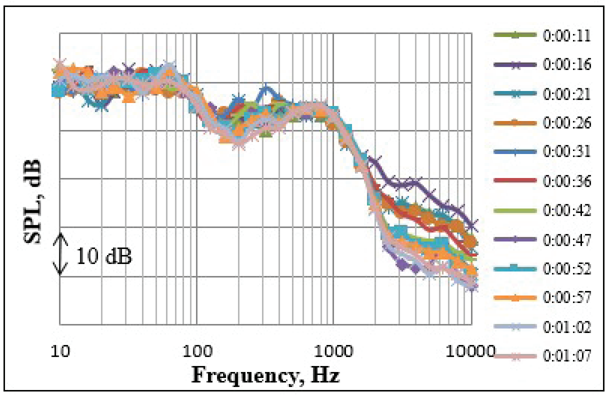

Fig.7: 1/3-octave spectrum of sound pressure levels measured in the forest near the highway at a wind speed of less than 1 m/s

4. CONCLUSION

The problem of ambient noise is considered in the context of the community noise problem of propeller-driven UAVs. The results of measurements of background noise in an open territory, near the sea, in the mountains and in the forest near the highway are presented. In the conditions of open terrain and in the mountains in the frequency range of 10-315 Hz in 1/3-octave frequency bands, the source of background noise is the self-noise of the turbulent atmosphere. It is shown that the ambient noise can be an effective masker of the UAV noise for both the observer and the measuring microphone. An expression for estimating the spectral characteristics of background noise in an open area is presented. The presented results of the author's studies of the spectral characteristics of ambient noise are consistent with the publications of other authors [20–26].

REFERENCES

[1] Moshkov, P., Ostrikov, N., Samokhin, V., Valiev, A.: Study of Ptero-G0 UAV Noise with Level Flight Conditions, 25th AIAA/CEAS Aeroacoustics Conference, AIAA Paper No. 2019-2514, 2019

[2] Luca, B.: Unmanned aircraft design with minimum acoustic footprint, 24th International Congress on Sound and Vibration, p. 1104-1109, 2017

[3] Moshkov, P.A., Samokhin, V.F., Yakovlev, A.A.: Study of the noise sources of an UAV with a two-stroke engine and shrouded propeller, Journal of Physics: Conference Series, ISSN: 1742-6588, IOP Publishing, VOLUME 1925, 2021

[4] Moshkov, P.A., Samokhin, V.F., Yakovlev, A.A.: Selection of an audibility criterion for propeller driven unmanned aerial vehicle, Russian Aeronautics, ISSN: 1068-7998, Allerton Press, Inc. (New York), VOLUME 61, p. 149-155, 2018

[5] Hoglund, E., Brungart, D., Iyer, N., Hamil, J., Mobley F., Hall J.: Auditory acuity for aircraft in real-world ambient environments, The Journal of the Acoustical Society of America, ISSN: 0001-4966, AIP Publishing on behalf of the Acoustical Society of America, VOLUME 128, p. 164-171, 2010

[6] Kloet, N., Watkins, S., Clothier, R.: Acoustic signature measurement of small multi-rotor unmanned aircraft systems, International Journal of Micro Air Vehicles, ISSN 1756-8293, Multi-Science Publishing, VOLUME 9, p. 3-14, 2017
[7] Feight, J.A., Donnel, G.W., Jacob, D.J., Gaeta, R.J.: Progress Towards Detection and Identification of sUAS via Acoustic Signature, 23th AIAA/CEAS Aeroacoustics Conference, AIAA Paper No. 2017-4052, 2017
[8] Moshkov, P.A.: Study of the audibility and masking of the propeller-driven unmanned aerial vehicle noise by ambient noise, Noise Theory and Practice, ISSN 2412-8627, JSC IAK, SPb, VOLUME 7, p. 28-38, 2021
[9] Moshkov, P.A., Samokhin, V.F.: Calculated estimation technique for audibility boundaries of propeller unmanned aerial vehicles, Aerospace MAI Journal, ISSN 0869-6101, Moscow Aviation institute, Moscow, VOLUME 28, p. 20-36, 2021
[10] Vasilyev, A.V.: Experimental research of environmental noise in urban conditions before and during Covid-19 period on the example of Samara Region of Russian Federation, AKUSTIKA, ISSN 1801-9064, Studio D – Akustika s.r.o., České Budějovice, VOLUME 39, p. 195-200, 2021
[11] Montano, W., Gushiken, E.: Covid-19 and soundscape changes due to the lockdown. The case of Lima, Peru, AKUSTIKA, ISSN 1801-9064, Studio D – Akustika s.r.o., České Budějovice, VOLUME 39, p. 48-55, 2021
[12] Hornberg, J, Haselhoff, T, Lawrence, BT, Fischer, J.L, Ahmed, S, Gruehn, D., Moebus, S.: Impact of the COVID-19 Lockdown Measures on Noise Levels in Urban Areas-A Pre/during Comparison of Long-Term Sound Pressure Measurements in the Ruhr Area, Germany, International Journal of Environmental Research and Public Health, ISSN 1660-4601, MPDI, VOLUME 18, p. 4653, 2021
[13] Steele, D, Guastavino, C.: Quieted City Sounds during the COVID-19 Pandemic in Montreal, International Journal of Environmental Research and Public Health, ISSN 1660-4601, MPDI, VOLUME 18, p. 5877, 2021
[14] Bonet-Solà D, Martínez-Suquía C, Alsina-Pagès RM, Bergadà P. The Soundscape of the COVID-19 Lockdown: Barcelona Noise Monitoring Network Case Study, International Journal of Environmental Research and Public Health, ISSN 1660-4601, MPDI, VOLUME 18, p. 5799, 2021
[15] Redel-Macías, M.D, Aparicio-Martinez, P., Pinzi, S, Arezes, P., Cubero-Atienza, A.J. Monitoring Sound and Its Perception during the Lockdown and De-Escalation of COVID-19 Pandemic: A Spanish Study, International Journal of Environmental Research and Public Health, ISSN 1660-4601, MPDI, VOLUME 18, p. 3392, 2021
[16] Kazhan, V.G., Moshkov, P.A., Samokhin, V.F.: Ambient Background Noise under Acoustic Tests of Aircrafts at the Local Aerodrome, Science and Education of the Bauman MSTU, ISSN 1994-0408, Moscow Aviation institute, Moscow, VOLUME 7, p. 146-170, 2015
[17] Kolmogorov, A. N. Local Structure of Turbulence in an Incompressible Fluid at Very High Reynolds Number, Dokl. Akad. Nauk SSSR, ISSN 0869-5652, NAUKA, Moscow, VOLUME 30, p. 299-303, 1941
[18] Kraichnan, R.H.: Pressure fluctuations in turbulent flow over a flat plate, The Journal of the Acoustical Society of America, ISSN: 0001-4966, AIP Publishing on behalf of the Acoustical Society of America, VOLUME 28, p. 378-390, 1956
[19] Kraichnan, R.H.: Inertial-range transfer in two- and three-dimensional turbulence, Journal of Fluid Mechanics, ISSN: 0022-1120, Cambridge University Press, VOLUME 47, p. 525-535, 1971
[20] Boersma H.F. Characterization of the natural ambient sound environment: Measurements in open agricultural grassland, The Journal of the Acoustical Society of America, ISSN: 0001-4966, AIP Publishing on behalf of the Acoustical Society of America, VOLUME 101, p. 2104-2110, 1997
[21] Raspet, R., Yu, J., Webster, J.: Low frequency wind noise contributions in measurement microphones, The Journal of the Acoustical Society of America, ISSN: 0001-4966, AIP Publishing on behalf of the Acoustical Society of America, VOLUME 123, p. 1260-1269, 2008
[22] Yu, J, Raspet, R, Webster, J., Abbott, J.: Wind noise measured at the ground surface, The Journal of the Acoustical Society of America, ISSN: 0001-4966, AIP Publishing on behalf of the Acoustical Society of America, VOLUME 129, p. 622-632, 2011
[23] Jackson, I.R., Kendrick, P., Cox, T.J., Fazenda, B.M., Li, F.F.: Perception and automatic detection of wind-induced microphone noise, The Journal of the Acoustical Society of America, ISSN: 0001-4966, AIP Publishing on behalf of the Acoustical Society of America, VOLUME 136, p. 1176-1186, 2014
[24] Raspet, R., Yu, J., Webster, J.: Wind noise under a pine tree canopy, The Journal of the Acoustical Society of America, ISSN: 0001-4966, AIP Publishing on behalf of the Acoustical Society of America, VOLUME 137, p. 651-659, 2015
[25] Bocharov, A.A., Kolesnik, A.G., Soloviev, A.V.: Two-parametric model of the spectrum of traffic noise in TOMSK, Acoustical Physics, ISSN: 1063-7710, Pleiades Publishing, Ltd., VOLUME 58, p. 718-724, 2012
[26] Butorina, M.V., Tyurina, N.V., Ivanov, N.I., Sannikov, V.A.: Classification of roads by noise levels, Noise Theory and Practice, ISSN 2412-8627, JSC IAK, SPb, VOLUME 6, p. 22-32, 2020

Petr Moshkov *is Ph.D. of Engineering Science, Leading engineer of the Moscow aviation institute (national research university) (Moscow, Russia).*
Petr Moshkov is a specialist in aeroacoustics. Petr Moshkov is the author of over 45 scientific papers. He presented the main results of scientific research at the international conferences in Moscow, Gelendzhik, Svetlogorsk, Delfts.

Paper No.347/2021

ANALYSIS OF THE AIRPORT NOISE IMPACT ON THE OCCURRENCE OF EMERGENCY SITUATIONS

[a)]Alexey Shvetsov, [b)]Viktor Gromov

[a)] North-Eastern Federal University, Yakutsk, Russia
[a)] Vladivostok State University of Economics and Service, Vladivostok, Russia, transport-safety@mail.ru
[b)] Peter the Great St.Petersburg Polytechnic University (SPbPU), St.Petersburg, vgromov2021@list.ru

***Abstract**: The high noise level in modern airports is one of the causes that affect the occurrence of accidents involving airliners and ground vehicles operating at the airport. In this study, an emergency prevention algorithm has been developed aiming at reducing the probability of an emergency collision of an airliner and a land vehicle by separating the noise generated during the airport operation into the noise that warns the pilot (operator) about the threat of an emergency collision and the noise that contributes to the accident initiation. The results of the study can be used in the development of new methods and technical means aimed at preventing accidents at airports.*

Keywords: *noise, airport, emergency*

***DOI:** : 10.36336/akustika20214122*

1. INTRODUCTION

According to the data [1-5], the high level of noise in modern airports, including generated in the process of the air (AV) and ground vehicles (GV) operation, is one of the main causes of airliners and GV emergency collisions during their interaction at the airport (Fig. 1).

Fig. 1. Accident at Gdansk airport (https://www.avianews.com/incidents/2021/01/08/wizzair_plane_car_collision_at_gdansk_airpor t/)

Due to the high traffic noise level at the airport at a time exceeding 140 dB, ground vehicle operators and airliner pilots are forced to use hearing protection devices (noise-absorbing headphones) and, as a result, they do not often hear approaching each other, as a result of which the probability of an airliner and a GV emergency collision increases [6].

Tab.1 contains the data on a number of such collisions in the period of 2000-2021.

Emergency situation	Year, airport	Consequences		
		AV damage	GV damage	Airport operations disruption
Collision of the water transporting vehicle and Airbus A320neo passenger plane	2021, Gdansk Airport (Poland)	√	√	√
Collision of the refueling vehicle and Airbus A321 passenger plane	2020, Sheremetyevo Airport (Russia)	√	√	
Collision of the airport service vehicle and Airbus A320 passenger plane	2017, Alicante Airport (Spain)	√	√	√
Collision of the airport service van and Airbus A330 passenger plane	2016, Hong Kong Airport (China)	√	√	√
Collision of an airport service van and an Airbus A330 passenger plane	2015, King Abdulaziz Airport (Saudi Arabia)	√	√	
Collision of the airport service vehicle and Boeing passenger plane	2007, Henri Coanda Airport (Romania)	√	√	√

Tab. 1: Emergency collisions at the airports

The necessity of analyzing the airport noise impact on the occurrence and development of emergency situations air and ground vehicles is primarily due to the need to preserve life and health of airline passengers, airliner pilots and GV operators who may suffer from such an accident.

2. ANALYSIS OF THE AIRPORT NOISE IMPACT ON THE EMERGENCY SITUATION DEVELOPMENT

The main noise in the airport operation first of all arises from the airliner engines operation [7-14].

In modern airliners the total sound pressure levels can reach 160-165 dB when the engines are operating in take-off mode, 160-168 dB when the flow is disrupted and 140-145 dB in the boundary layer [15].

The main sources of an airliner noise are: aero-and gas-dynamic flows in the power plant, air flow flowing around the aircraft and gas flows of on-board equipment systems [15].

The second main airport noise source is traffic noise that occurs during the operation of ground vehicles, which include tractors, tankers and other GV that ensure the airport operations. The main source of ground vehicle noise is the aerodynamic noise generated by the power plant.

Other noise sources during the airport operations that affect the development of an emergency situation include sound signals sent by vehicles to each other, as well as voice messages from pilots/operators and other airport traffic participants.

Analyzing the noise impact on the development of an emergency situation leading to a collision of an airliner and a ground vehicle, we can conclude that such an impact can be divided into two types (Fig. 2).

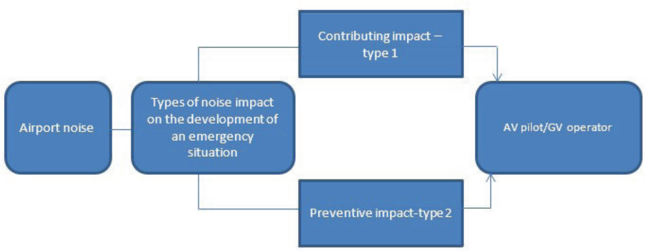

Fig. 2: The noise impact on the emergency situation development

Type 1 impact is the noise that reduces the probability of an audio contact between a pilot/operator and an approaching vehicle that is out of his sight, which contributes to the development of an emergency situation and a collision of vehicles.

The type 2 impact is the noise from an approaching vehicle that is out of pilot's/operator's sight, sound signals sent by vehicles to each other, as well as voice messages from pilots/operators and other airport traffic participants, allowing the pilot/operator to calculate and prevent the development of an emergency situation.

3. EMERGENCY PREVENTION ALGORITHM

As it can be seen from the presented scheme of the noise impact on the emergency situation development (Fig. 2), airport noise can contribute to both the occurrence and prevention of an emergency.

Based on this conclusion, it is possible to formulate an emergency prevention algorithm aimed at reducing the risk of an emergency collision of airliners and ground vehicles by separating and partially blocking the noise (Fig. 3).

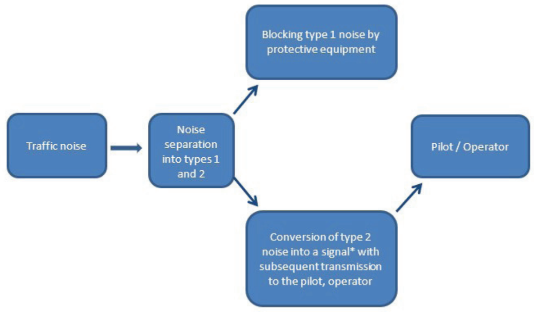

*Fig. 3: Emergency prevention algorithm (*audio and / or video signal)*

The practical implementation of the proposed algorithm can be carried out through the development and application of a hardware and software complex that implements the following functions: noise sources identification by type; analysis of the noise source and controlled vehicle (vehicle) approach; noise conversion into a signal transmitted to the vehicle pilot/operator.

To assess the effect of the emergency prevention algorithm on reducing the probability of emergency collisions of the airliners and ground vehicles, a survey of experts in the field of airport traffic management was conducted. The experts were asked three questions: how much will the probability of erroneous actions of the GV operator leading to a collision (Oo) decrease; how much will the probability of erroneous actions of the airliner pilot leading to a collision (Op) decrease; how much will the probability of erroneous actions of the dispatcher leading to a collision (Od) decrease.

The survey results are presented in Tab. 2.

Evaluated parameters	Expert assessment (according to the scale from 0 to 1)						
	1	2	3	4	5	6	7
O_o	0,5	0,4	0,6	0,6	0,5	0,6	0,4
O_p	0,3	0,2	0,2	0,2	0,3	0,4	0,3
O_d	0,1	0,3	0,3	0,3	0,1	0,1	0,2

Tab. 2: Expert assessment

The expert survey data was checked for consistency using the Kendal concordance coefficient (Tab.3, Formula 1).

Questions	Experts							Rank sum	Deviation from the average rank sum	Squares of deviations of the rank sums
	1	2	3	4	5	1	2			
O_o	3	3	3	3	3	3	3	21	7	49
O_p	2	1	2	1	2	2	2	12	-2	4
O_d	1	2	1	2	1	1	1	9	-5	25
Sum										78

Tab. 3: Rating ranks

$$W = \frac{12S}{m^2(n^3 - n)} = 0.796 \quad (1)$$

where
W is the concordance coefficient;
S is the sum of squares of the rank differences;
n is the number of questions,
m is the number of experts.

W = 0.796 indicates a high degree of consistency of experts, which allows us to consider the obtained evaluation result quite reliable.

4. CONCLUSION

The emergency prevention algorithm proposed in this study reduces the probability of an emergency collision of airliners and GV at the airport by reducing the risk of erroneous actions of the GV operator leading to a collision by 51,4%, reducing the risk of erroneous actions of the airliner pilot leading to a collision by 27,1%, reducing the risk of erroneous actions of the dispatcher leading to a collision by 20%.

REFERENCES

[1] ICAO Safety Report 2020. https://www.icao.int/safety/Documents/ICAO_SR_2020_final_web.pdf, (date of the application 01.09.2021)
[2] Boeing. Statistical summary of commercial jet airplane accidents: Worldwide operations 1959–2016. Technical Report. https://www.skybrary.aero/bookshelf/books/4239.pdf, (date of the application 01.07.2021)
[3] Shvetsova, S., Shvetsov, A.: Method for Managing the Route of an Unmanned Aerial Vehicle. Russian Aeronautics. VOLUME 64(1), pp. 142–145, 2021, doi: 10.3103/s1068799821010190
[4] The information from an investigation conducted by the Interstate Aviation Committee. https://www.mak-iac.org/rassledovaniya/, (date of the application 01.07.2021)
[5] Information on the state of safety of aircraft flights. Federal Air Transport Agency report. http://www.favt.ru/public/materials/6/8/8/6/1/688612206d6548462c1f2dac2aa1c161.pdf, (date of the application 01.09.2021).)
[6] Runway Safety Accident Analysis Report. Technical Report. International Air Transport Association. https://www.iata.org/en/publications/safety-report/, (date of the application 01.09.2021)
[7] Shvetsova, S., Shvetsov, A.: Ensuring safety and security in employing drones at airports, Journal of Transportation Security. VOLUME 14(1-2), pp. 41–53, 2021, doi: https://doi.org/10.1007/s12198-020-00225-z
[8] Blasch, E. et al.: Surveillance of ground vehicles for airport security. Proc. SPIE 9089, Geospatial InfoFusion and Video Analytics IV; and Motion Imagery for ISR and Situational Awareness II, 90890B (19 June 2014); 2014, doi: https://doi.org/10.1117/12.2053855
[9] Shvetsov, A.: Change in Fuel Consumption of a Hybrid Vehicle When Operating in the Far North. World Electric Vehicle Journal. VOLUME 12(3), p. 104, 2021, doi: 10.3390/wevj12030104
[10] Alomar, I., Tolujevs, J.: Optimization of ground vehicles movement on the aerodrome. Transportation Research Procedia. VOLUME 24, pp. 58–64, 2017, doi:10.1016/j.trpro.2017.05.068
[11] Shvetsov, A. et al.: Transportation safety in an urban condition, E3S Web of Conferences, VOLUME 135, Article Num. 02004, 2019, doi: https://doi.org/10.1051/e3sconf/201913502004
[12] Shvetsova, S., Shvetsov, A.: Safety when Flying Unmanned Aerial Vehicles at Transport Infrastructure Facilities. Transportation Research Procedia. VOLUME 54, pp. 397–403, 2021, doi: http://dx.doi.org/10.1016/j.trpro.2021.02.086
[13] Lyovin B. A., et al.: Method for Remote Rapid Response to Transportation Security Threats on High Speed Rail Systems. International Journal of Critical Infrastructures. VOLUME 15(4), pp. 324–335, 2019, doi: 10.1504 / IJCIS.2019.103015
[14] D'yachenkova, M., et al.: Aircraft and vehicle motion path registering and analyzing system for conflicts prediction at the aerodrome movement area. Aerospace MAI Journal. VOLUME 27(3), pp. 209-2018, 2020, doi: 10.34759/vst-2020-3-209-218
[15] AVIATION ACOUSTICS. https://bigenc.ru/technology_and_technique/text/4424361, (date of the application 03.09.2021)

Alexey Shvetsov *is Ph.D. of Engineering Science, Associate Professor of Department of Automotive Transport and Car Service of the North-Eastern Federal University (Yakutsk, Russia), and Associate Professor of Department of Transport Processes of the Technologies of the Vladivostok State University of Economics and Service (Vladivostok, Russia). He obtained his PhD in 2018 from the Russian University of Transport, in the field of transportation safety. He current research interests are in the fields of to protection transportation critical infrastructure. He has published more than 75 books, papers in journals and international conferences, on transportation safety and about the protection of critical infrastructures.*

Viktor Gromov *is a DSc, Professor of the Higher School of Cyber-Physical Systems and Management of Peter the Great St. Petersburg Polytechnic University (SPbPU), Honored Worker of the Higher School of the Russian Federation, Author of more than 280 publications of scientific works in the field of information technologies and automated control systems of metro systems, 4 monographs, 3 textbooks, 25 copyright certificates and 4 patents, 38 educational and methodological works. The leader of the scientific school of development of methodology, theory and practice of using the general logical-probabilistic method of modeling complex systems. The main results of scientific research were presented at international conferences in St. Petersburg, FarEastCon, Minzu University of China and other countries*

Paper No.348/2021

DETERMINATION OF THE IMPEDANCE OF A HONEYCOMB RESONATOR BY DEAN'S METHOD AND DIRECT METHOD IN A COMPUTATIONAL EXPERIMENT WITH GRAZING INCIDENCE OF WAVES

Igor Khramtsov, Vadim Palchikovskiy, Oleg Kustov

Perm National Research Polytechnic University (PNRPU), Perm, Russia, lmgsh@pstu.ru

Abstract: *The article considers the determination of the impedance of the acoustic liner sample on the basis of numerical simulation of physical processes in a honeycomb resonator with a grazing incidence of sound waves. The computational domain is the test section of a grazing incidence impedance tube with an acoustic liner sample. The liner sample is a single honeycomb resonator with a depth of 14 mm and an open area percent of 4.2%. Numerical simulation is performed based on the direct solution of the non-stationary compressible Navier-Stokes equations in a three-dimensional formulation. The pressure-time and velocity-time signals are recorded in the numerical simulation and processed by Dean's method and the direct method (from the ratio of acoustic pressure to normal acoustic velocity). The comparison of impedances obtained by the two methods demonstrates a good agreement with each other.*

Keywords: *Acoustic liner, acoustic impedance, grazing incidence impedance tube, Dean's method, direct method, numerical simulation*

DOI: *: 10.36336/akustika20214125*

1. INTRODUCTION

Acoustic liners are an effective means of reducing aircraft engine noise. The fundamental characteristic of the liners is the acoustic impedance, which is the ratio of the acoustic pressure to the acoustic normal velocity. This value depends on many parameters, which include: the sound pressure level, the presence of a grazing flow, the profile of the flow velocity, the signal spectrum, etc. Also, the impedance depends on the geometric characteristics (the size of the resonator cells, the thickness of the perforated sheets and their open area percent, the number of layers, etc.). The existing semi-empirical impedance models of the locally-reacting liners are based on a simplified description of physical processes and often lead to significant differences between the impedance predicted by these models from the experimental values [1].

In turn, the methods of experimental determination of the liner impedance also have some drawbacks. These methods are based on microphone measurements, while microphones are placed on the walls of experimental installations or test samples (in the case of multilayer liner sample, such placement of microphones is very problematic). At the same time, the results of the experimental determination of the liner impedance obtained by various methods at various installations differ not only from the results of impedance prediction but also among themselves [2-8]. This situation is partly due to insufficient information about the processes occurring inside the resonator cells, since measurements on the installation walls give an incomplete picture of the acoustic field inside the investigated area. The introduction of measuring probes into the channel of the installation or liner sample inevitably leads to a distortion of the values of the studied physical parameters.

In this regard, in recent years, much attention has been paid to the development of methods for predicting the impedance of the acoustic liners based on numerical simulation, which is able to more completely take into account the complex physical processes accompanying the liner operation. This approach allows both carrying out a direct simulation of a full-scale experiment and studying a number of physical quantities inside and on the surface of the sample, which can be used to refine the existing semi-empirical impedance models, as well as to correct the methods of experimental study of the acoustic characteristics of the liner.

Previously, the authors proposed a technique that, based on numerical simulation of processes in acoustic liner sample at normal incidence of waves, makes it possible to predict with good accuracy the acoustic characteristics of single-, double- and triple-layer honeycomb liners at high sound pressure levels [9-11]. In this case, the processing of the data obtained in the numerical simulation was carried out by the two-microphone transfer function method [12], which is easy to implement in a full-scale experiment and, accordingly, to verify the results of numerical simulation.

Another way to determine the acoustic characteristics of liner samples is Dean's method [13]. Its adaptation to numerical simulation was previously carried out by the authors for the case of normal [14] and grazing [15] incidence of waves.

The third way to determine impedance is the direct method. This method allows the impedance to be obtained directly from the ratio of acoustic pressure to normal acoustic velocity. The direct method is difficult to implement in a full-scale experiment, since it is required to measure the velocity variable in time and space inside the holes of the sample. However, this method can be relatively simple to implement in numerical simulation and thereby verify the existing computational and experimental methods for determining the impedance.

In the work [14], it was demonstrated that microphone measurements in the channel of a normal incidence impedance tube determine the impedance of the total front surface of the sample, and measurements by Dean's method determine the impedance of the resonator cell only. The present article is a continuation of the authors' work on determining the impedance of the samples of locally-reacting acoustic liners at a grazing incidence of a sound waves based on numerical simulation.

2. METHODS FOR DETERMINING THE IMPEDANCE OF ACOUSTIC LINER SAMPLE AT GRAZING INCIDENCE OF A SOUND WAVE

In ducts of the aircraft engines, sound propagates as grazing waves to the surface of the acoustic liners. To determine the impedance at the grazing incidence of sound waves, special installations are used – grazing incidence impedance tube (GIIT). These installations have a rather long narrow tube of the rectangular cross-section with flush-mounted microphones and liner sample. Acoustic drivers located outside the test section (distance between the first and last microphone) generate the sound waves. The transverse size of the duct is selected from the condition of single-mode sound propagation in the rigid-walled terminations of the test section. The use of a rectangular tube is dictated by the simplicity of the liner sample manufacture. In addition, GIIT allows the flow to be propagated in the duct, which is generated with compressors or fans (Fig. 1). It is also possible to supply the flow into the GIIT channel from the jet rig, as was done, for example, at the large-scale research facility "Anechoic Chamber with Flow AC-2" FSUE TsAGI [16].

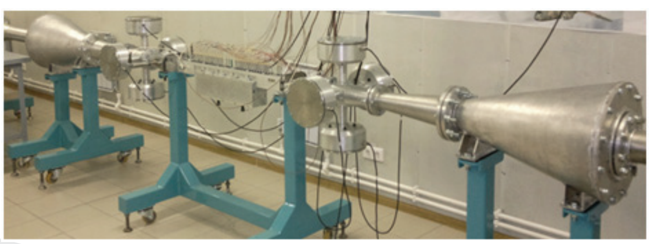

Fig. 1: Grazing incidence impedance tube with flow in PNRPU Acoustic Research Center

Various methods can be used to determine the impedance. Most of them are based on measurements of the acoustic pressure in the duct of GIIT [3, 6, 8]. Another method for determining the impedance of the acoustic liner samples is Dean's method. This method provides impedance determination on data obtained from microphones mounted into the acoustic liner sample. At the same time, when comparing the acoustic characteristics using different methods, a difference is observed. To better understand why it occurs, we can get useful information from computational experiments.

Determining the impedance by conducting a virtual experiment for a full-scale acoustic liner sample is extremely difficult, since such a sample consists of many honeycomb cells and holes in a perforated plate, which requires significant computational resources. In the work, we consider a model of a liner sample, which is a single honeycomb resonator with 5 holes. The parameters of the sample are presented in Table 1. Such a sample is too small to provide good absorption of sound energy in the duct, therefore, methods of impedance eduction based on minimizing the functional discrepancy between the calculated and measured acoustic pressure give large errors in impedance values. However, Dean's method and the direct method allow one to determine the impedance of a single resonator, so they are used to process the results of numerical simulations.

Parameter	Diameter of hole (mm)	Thickness of perforated plate (mm)	Height of honeycomb cell (mm)	Percent of open area (%)
Value	1.5	2	14	4.2

Tab. 1: Characteristics of honeycomb resonator

As is known, the normalized impedance is defined as the ratio of the acoustic pressure P at a point on the surface of the liner to the acoustic velocity Un at the same point, directed along the normal towards the liner surface:

$$\boldsymbol{Z = \frac{1}{\rho c}\frac{P}{U_n}} \tag{1}$$

where
$\boldsymbol{\rho}$ is a density of a medium; c is a velocity of sound. However, in practice, determining the impedance by formula (1) (hereinafter we call this the "direct method") is problematic due to the difficulties in simultaneous measurement of acoustic parameters at a point directly on the surface of the liner.

Dean proposed in [13] a method for determining the impedance, where the acoustic pressure on the front and rear wall of the resonator cell is measured. An important advantage of this method is that it can be used not only at the normal incidence of a sound wave but also at the grazing incidence. This allows one to determine the impedance of the acoustic liner directly on an aircraft engine [4]. The normalized impedance, in this case, is determined as:

$$\boldsymbol{Z = -i\frac{P_{face-sheet}}{P_{back-wall}} e^{i\varphi} sin^{-1}(kh)} \tag{2}$$

where
$\boldsymbol{h}$ is the liner depth and
$\boldsymbol{\varphi}$ is the phase angle between the two points of acoustic pressure measurement.

3. STATEMENT OF COMPUTATIONAL EXPERIMENT

Numerical simulation of acoustical processes at grazing incidence of waves is carried out using ANSYS Fluent software. It is used a system of nonlinear Navier-Stokes equations for a viscous heat-conducting gas. The computations are performed by under-resolved direct numerical simulation. The following features are used: Pressure Based Coupled Solver; implicit time-difference scheme of the second-order accuracy; second-order numerical schemes in spatial variables for approximation of convective terms in the equations.

The computational domain is the test section of the GIIT represented in Fig. 1 with liner sample. The test section of the GIIT has a cross section 0.04 x 0.04 m and length 0.76 m. The liner sample is a single honeycomb resonator with 5 holes (Fig. 2) located in the center of the GIIT's test section. The characteristics of the honeycomb resonator are given in Tab. 1.

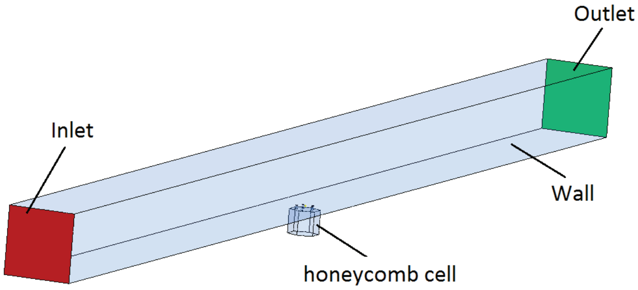

Fig. 2: Geometry of the computational domain

To reduce computational time, the CutCell meshing [17] was applied. The mesh was thickened in the orifices so that there were 12 cells along the orifice height. With distance from the orifice, the linear dimensions of the element increased until the average linear dimension was 4 mm. Additionally, it was used a thickening on the wall of 15 layers with a growth factor of 1.2. The size of the wall cell is 0.002 mm. As a result, a computational mesh of 541 019 elements was obtained. Examples of the computational mesh are shown in Fig. 3.

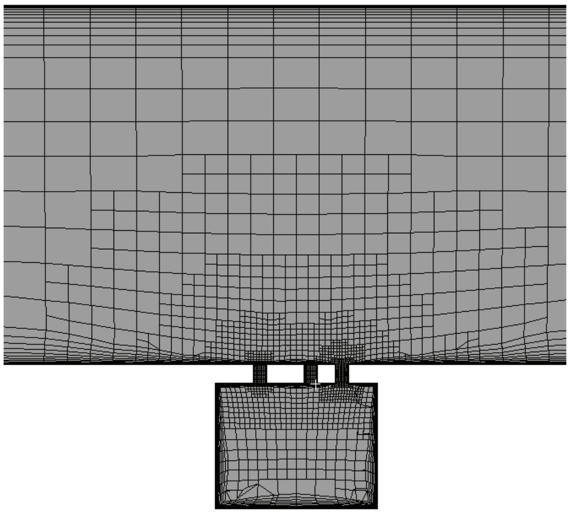

Fig. 3: View of the computational mesh near the honeycomb resonator

At the entrance to the computational domain, the "Inlet" boundary condition was used. The acoustic signal at this boundary was imported from the text file, in which instantaneous pressure values were recorded with a time step of 1/65536 s. This time signal is a time function with a flat frequency spectrum in the frequency range 500-3600 Hz with a total sound pressure level of 140 dB. During the computation, at each time step, the values at the inlet boundary were updated. As a result, a piston wave propagated inside the computational domain, similar in spectral composition to the text file. At the exit from the computational domain, the "Outlet" boundary condition was set with the non-reflecting boundary condition and zero excess pressure to exclude reflections of the acoustic wave from the output boundary. The "Wall" with adhesion boundary condition was used on the walls of the duct, perforated plate, and honeycomb. The computations were carried out under normal environmental conditions. The working medium was air, the properties of which changed according to the law of an ideal gas.

To record the pressure-time signal for Dean's method, one probe was set on the perforated plate and the other on the bottom of the resonator (Fig. 4). In the direct method, the probe for recording the pressure-time signal was set on the perforated plate, and the probes for recording the velocity-time signals were set on the orifices. The recorded signals were divided into segments and processed using the fast Fourier transform. The obtained spectra were averaged over the number of segments. The averaging was carried out taking into account the overlap of adjacent segments; when calculating the spectra, the Hanning window function was used. The computations were carried out with a time step of 1/65536 s for 32768 time steps.

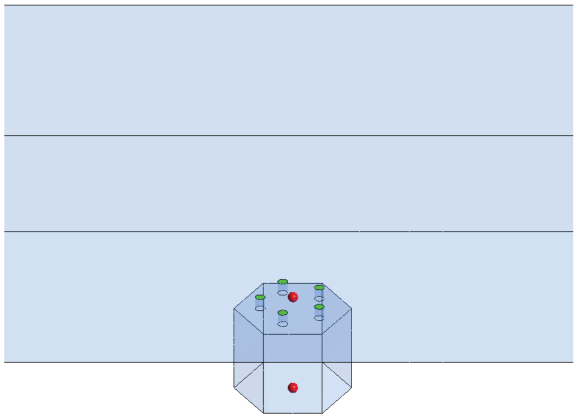

Fig. 4: Location of probes for recording pressure (red dots) and velocity (green dots) signals over time

To determine the impedance of the honeycomb resonator by Dean's method, the obtained pressure spectra can be substituted into the formula (2). However, in the direct method, the pressure and velocity spectra cannot be substituted directly into expression (1) for the following reasons. As the normal velocity on the face wall of the liner sample is zero, only the normal velocity in the orifices contributes to the velocity averaged over the face wall. The mass flow rate is a constant, therefore only porosity of the face wall is required to be taken into account for the correction of the velocity. The mass flow generated by the acoustic driver in GIIT propagates through the duct and then passes through the orifices of the liner sample. The flow that has passed through the orifices continues to propagate inside the cell of the honeycomb resonator. Therefore, it is possible to determine the porosity F through the ratio of the total area of the orifices $\Sigma S_{orifice}$ to the total cross-sectional area of the honeycomb cavity ΣS_i in the sample. In this case, expression (1) is transformed to the form:

$$Z = \frac{P}{\rho c U_{aver} F} \tag{3}$$

The velocity at the orifice varies: it equals zero on the walls and then increases with the distance from the wall. The velocity profile across the orifice depends on the direction of the vortex movement and the stage of its formation or destruction. In this case, the velocity in each orifice is different, which is associated with a delay in the phase of the sound wave arriving at the every orifice. In this regard, in formula (3), we used the velocity averaged over all orifices of the honeycomb resonator at each moment of time:

$$u_{aver} = \frac{1}{A}\int u\, dA \tag{4}$$

where
A is a total area of the orifices. In our computations, the average velocity varies within wide limits: from -24.55 m/s to 24.76 m/s. The modulus of the average velocity is 6.34 m/s, which corresponds to the Reynolds number 650.

4. RESULTS OF COMPUTATIONS

Fig. 5 shows the acoustic characteristics obtained by processing the results of numerical simulation by the direct method (3) and by Dean's method (2). As can be seen, the obtained acoustic characteristics are in good agreement with each other. Thus, Dean's method is well verified by the direct method and can be used in numerical simulation for sound propagation in GIIT with acoustic liner samples installed in it. This approach is relevant in the sense that the implementation of the full-scale determination of impedance based on Dean's method requires measurements at many points, since Dean's method determines the impedance of only one resonator, therefore, a full-scale experiment turns out to be very laborious. In addition, the mounting microphones in a sample is in itself a delicate work and takes a lot of time, and also violates the integrity of the sample, while the implementation of Dean's method in numerical simulation is free of the listed disadvantages.

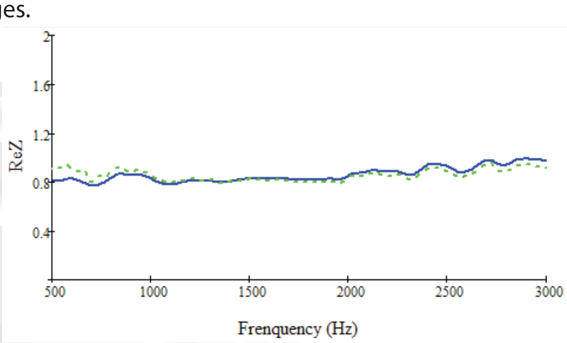

(a)

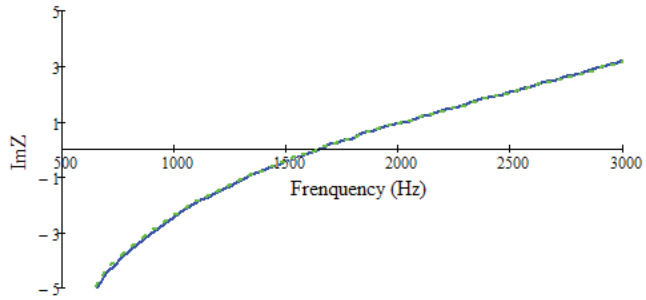

(b)

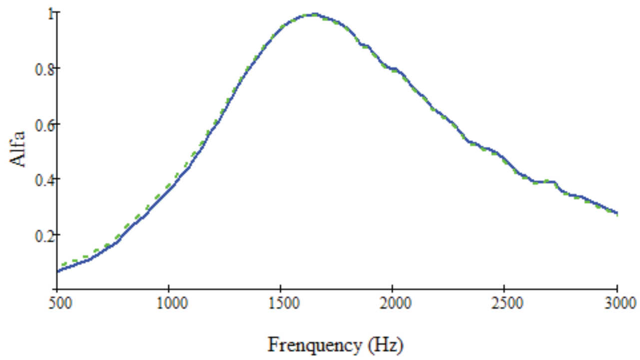

(c)

Fig. 5: Comparison of the acoustic characteristics obtained by numerical simulation: green dot line is direct method; blue solid line is Dean's method; a) real part of impedance; b) imaginary part of impedance; c) sound absorption coefficient

5. CONCLUSION

The article presents the results of determining the acoustic characteristics of the liner sample based on the solution of the nonstationary gas-dynamic problem. The acoustic characteristics determined using Dean's method and the direct method agree well with each other. In this regard, it can be concluded that Dean's method allows one to qualitatively determine the acoustic characteristics of acoustic liner samples at a grazing incidence of a sound wave and can be successfully used both in a full-scale experiment and in computational methods.

ACKNOWLEDGEMENT

The work was funded by a grant from the President of the Russian Federation for young scientists - candidates of science MK-541.2021.1.2. The work was carried out on the basis of the large-scale research facility "Anechoic Chamber with Flow AC-2" FSUE TsAGI.

REFERENCES

[1] Khramtsov, I.V., Kustov, O.Yu., Palchikovskiy, V.V., Bulbovich, R.V.: Comparison of acoustic characteristics of resonant liner samples at normal incidence of waves based on semiempirical model, Natural Experiment and Numerical Simulation, AIP Conference Proceeding, Vol. 2351, No. 030036, 2021
[2] Motsinger, R.E., Kraft, R.E.: Design and performance of duct acoustic treatment, Aeroacoustics of flight vehicles. Theory and practice. Acoustical Society of America, New York, 1995
[3] Auregan, Y., Leroux, M., Pagneux, V.: Measurement of liner impedance with flow by an inverse method, AIAA Paper, No. 2838, 2004
[4] Gaeta, R.J., Mendoza, J.M., Jones, M.G.: Implementation of in-situ impedance techniques on a full scale aero-engine system, AIAA Paper, No. 2007-3441, 2007
[5] Schuster B.: A comparison of ensemble averaging methods using Dean's method for in-situ impedance measurements, AIAA Paper, No. 2012-2244, 2012
[6] Watson, W.R., Jones, M.G.: A comparative study of four impedance eduction methodologies using several test liners, AIAA Paper, No. 2274, 2013
[7] Bodén, H., Cordioli, J.A., Spillere, A., Serrano P.: Comparison of the effect of flow direction on liner impedance using different measurement methods, AIAA Paper, No. 2017-3184, 2017
[8] Sobolev, A.F., Ostrikov, N.N., Anoshkin, A.N., Palchikovskiy, V.V., Burdakov, R.V., Ipatov, M.S., Ostroumov, M.N., Yakovets, M.A.: Comparison of liner impedance derived from the results of measurements at two different setups using a small number of microphones, PNRPU Aerospace Engineering Bulletin, No. 45, p. 59-113, 2016
[9] Khramtsov, I.V., Kustov, O.Yu., Fedotov, E.S., Siner, A.A.: On numerical simulation of sound damping mechanisms in the cell of a sound-absorbing structure, Acoustical Physics, Vol. 64, No. 4, p. 511-517, 2018
[10] Khramtsov, I.V., Kustov, O.Yu., Palchikovskiy, V.V.: Determination of acoustic characteristics of full-scale sample of single-layered honeycomb liner based on numerical simulation, Akustika, Vol. 32, p. 182-188, 2019
[11] Khramtsov, I.V., Kustov, O.Yu., Palchikovskiy, V.V.: Determination of acoustic characteristics of the double-layer honeycomb liner based on numerical simulation, Akustika, Vol. 34, p. 32-36, 2019.
[12] Chung, J.Y., Blaser, D.A.: Transfer function method of measuring in-duct acoustic properties. I. Theory. II. Experiment, Journal of the Acoustical Society of America, Vol. 68, No. 3, p. 907-921, 1980
[13] Dean, P.D.: An in-situ method of wall acoustic impedance measurement in flow duct, Journal of Sound and Vibration, vol. 34, No. 1, p. 97-103, 1974
[14] Khramtsov, I.V., Kustov, O.Yu., Palchikovskiy, V.V.: Investigation of the reason for the difference in the acoustic liner impedance determined by the transfer function method and Dean´s method, Akustika, Vol. 39, p. 226-230, 2021
[15] Khramtsov, I.V., Kustov, O.Y., Palchikovskiy, V.V.: Technique for evaluating the acoustic properties of a liner at grazing incidence of wave based on numerical simulation, AIP Conference Proceedings, Vol. 2351, No. 030038, 2021
[16] Kopiev, V.F., Ostrikov, N.N., Yakovets, M.A., Ipatov, M.S., Kruglyaeva, A.E., Sidorov, S.Yu.: Radiation of sound from the open end of a duct simulating an air inlet under static conditions and in a flow, Acoustical Physics, Vol. 65, p. 76-89, 2019
[17] Ansys User's guide. Ansys Release 17.0. Ansys Inc., 2016

__Igor Khramtsov__ is Ph.D. of Engineering Science, researcher of the Laboratory of Noise Generation Mechanisms and Modal Analysis, and Assistant Professor of the Perm National Research Polytechnic University. His research area includes aeroacoustics, investigation of characteristics of sound-absorbing structures and materials, and acoustic measurements. He presented the main results of scientific research at the international conferences in Moscow, St. Petersburg, Novosibirsk, and Perm.

__Vadim Palchikovskiy__ is Ph.D. of Engineering Science, researcher of the Laboratory of Noise Generation Mechanisms and Modal Analysis, and Associate Professor of the Perm National Research Polytechnic University. His research area includes acoustic measurements, investigation of characteristics of sound-absorbing structures and materials, numerical methods and programming, numerical simulation of acoustic processes. He presented the main results of scientific research at the international conferences in Moscow, St. Petersburg, Kazan, and Perm.

__Oleg Kustov__ is junior researcher of the Laboratory of Noise Generation Mechanisms and Modal Analysis, and postgraduate student of the Perm National Research Polytechnic University. His research area includes acoustic measurements, and investigation of characteristics of sound-absorbing structures and materials. He presented the main results of scientific research at the international conferences in Moscow, Kazan, Novosibirsk, and Perm.

Paper No.349/2021

CONTRIBUTION OF NON-ISOTHERMAL JETS TO THE PROCESSES OF NOISE GENERATION OF ENERGY MACHINES WHEN INSTALLING SILENCERS

[a)]Aleksandr Shashurin, [b)]Nickolay Ivanov, [c)]Andrey Vasilyev, [d)] Yuri Elkin, [e)] Zhenish Razakov

[a,b,c)]Samara State Technical University, Samara, Russia
[a)] 7596890@mail.ru
[d)] Moscow Automobile and Road Construction State Technical University (MADI), Moscow, Russia, elkiny@mail.ru
[e)] Baltic State Technical University 'VOENMEH' named after D.F. Ustinov, St. Petersburg, Russia

***Abstract**: The method of James Lighthill is known and widely used, which allows determining the acoustic power of isothermal jets. A mathematical model for calculating the acoustic parameters (sound power, radiation pattern) of non-isothermal sound jets is proposed, taking into account the noise silencer installed in the gas exhaust tract. At the output, the equations of continuity, the amount of motion, energy, as well as the Lighthill wave equation are used. A statistical model is used as a turbulence model for calculations. A physical mechanism of noise generation by turbulent flows is proposed, which consists in considering "own" and "shear" noise. The " own " noise is caused by turbulent pulsations of the gas-dynamic flow, the "shift" noise is caused by the presence of a flow velocity gradient. Analytical dependences of the components of "own" and "shift" noise are obtained.*

***Keywords:** non-isothermal jet, acoustic power, the continuity equation, equation of the amount of motion, the energy equation, the Lighthill wave equation, "own" noise, "shift" noise*

***DOI:** : 10.36336/akustika20214130*

1. INTRODUCTION

Noise silencers are a device for reducing noise in gases released into the atmosphere. The principle of operation of such devices is based on a gradual decrease in this pressure or a corresponding decrease in the exhaust gas velocity to a value less than the speed of sound. A muffler is a complex structural element, for the calculation of which it is necessary to take into account the features of its own and shear noise, turbulent features, and so on.

2. CALCULATION OF GAS-DYNAMIC PARAMETERS OF TURBULENT JETS

This section presents a mathematical model for calculating the gas-dynamic parameters of non-isothermal turbulent jets of combustion products and the parameters of acoustic fields generated by these jets. A detailed description of the physical and mathematical model is given in the monograph [1].

The basic equations for describing processes in a turbulent jet are given below [2]:
- the continuity equation:

$$\frac{\partial \rho}{\partial t} + \frac{\partial}{\partial x_j}(\rho V_j) = 0 \qquad (1)$$

- equation of the amount of motion:

$$\frac{\partial(\rho V_j)}{\partial t} + \frac{\partial}{\partial x_j}(\rho V_j V_k) = -\frac{\partial p}{\partial x_k} + \frac{\partial}{\partial x_j}\tau_{jk} \qquad (2)$$

- the energy equation:

$$\frac{\partial}{\partial t}(\rho h) + \frac{\partial}{\partial x_j}(\rho V_j h) = \frac{\partial p}{\partial t} + V_k\frac{\partial p}{\partial x_k} + \tau_{jk}\frac{\partial V_k}{\partial x_j} + \frac{\partial q_j}{\partial x_j} \qquad (3)$$

where:

$\tau_{jk} = -\delta_{jk}\frac{2}{3}\mu\frac{\partial V_j}{\partial x_j} + \mu(\frac{\partial V_j}{\partial x_k} + \frac{\partial V_k}{\partial x_j})$ – components of the viscous tangential stress tensor;

$\delta_{jk} = \begin{cases} 1 \text{ by } j = k \\ 0 \text{ by } j \neq k \end{cases}$ Kronecker symbol;

where: μ dynamic viscosity coefficient, Pa·s;
$j, k=1,2,3$ indexes that determine the direction of the axes;
V_j, V_k speed components;
p, ρ, t pressure, density, time;
q_j components of the heat flow vector.

According to the Reynolds model, the instantaneous values of any gas-dynamic parameters $(V_j, p, \rho, \tau_{jk}, q_j)$ can be represented as the sum of the time-averaged $(\overline{V}_j, \overline{p}, \overline{\rho}, \overline{\tau}_{jk}, \overline{q}_j)$ and the pulsation component $(V_{pj}, p_p, \rho_p, \tau_{pjk}, q_{pj})$:

$$V_j = \overline{V}_j + V_{pj};$$
$$p = \overline{p} + p_p;$$
$$\rho = \overline{\rho} + \rho_p;$$
$$\tau_{jk} = \overline{\tau}_{jk} + \tau_{pjk};$$
$$q_j = \overline{q}_j + q_{pj},$$

where
(**–**) means averaging over time.

We use the assumptions made for the equations 1-3

$$\frac{\partial \overline{\rho}}{\partial t} + \frac{\partial}{\partial x_j}(\overline{\rho}\overline{V}_j) + \frac{\partial}{\partial x_j}(\rho_p V_{pj}) = 0 \qquad (4)$$

$$\overline{\rho}\frac{\partial \overline{V}_k}{\partial t} + \overline{\rho}\overline{V}_j \frac{\partial \overline{V}_k}{\partial x_j} = 0 \qquad (5)$$

$$\overline{\rho}\frac{\partial \overline{h}}{\partial t} + \overline{\rho}\overline{V}_j \frac{\partial \overline{h}}{\partial x_j} = \frac{\partial \overline{p}}{\partial t} + \frac{\partial \overline{q}_j}{\partial x_j} + \overline{V}_k \frac{\partial \overline{p}}{\partial x_k} + \overline{V}_{pk}\frac{\partial \overline{p_p}}{\partial x_k} + \overline{\tau}_{jk}\frac{\partial \overline{V}_k}{\partial t} \qquad (6)$$

$$+ \overline{\tau}_{pjk}\frac{\partial \overline{V}_{pk}}{\partial t} - \frac{\partial}{\partial t}\overline{\rho_p h_p} - \frac{\partial}{\partial x_j}\overline{\rho_p V_{jp} h_p} - \overline{\rho_p V_{pj}}\frac{\partial h}{\partial x_j}$$

$$\overline{p} = \overline{\rho}\overline{R}T \qquad (7)$$

$$\frac{\partial}{\partial t}\overline{\rho V_{pi} V_{pk}} + \frac{\partial}{\partial x_j}\left(\overline{V_j \rho V_{pi} V_{pk}}\right) + \frac{\partial}{\partial x_j}\left(\overline{\rho V_{pi} V_{pj} V_{pk}}\right) = -\overline{V_{pj}\frac{\partial p_p}{\partial x_k}} - \overline{V_{pk}\frac{\partial p_p}{\partial x_i}}$$
$$+ \overline{V_{pi}\frac{\partial \tau_{pjk}}{\partial x_j}} + \overline{V_{pk}\frac{\partial \tau_{pij}}{\partial x_j}} + \overline{V}_i \frac{\partial}{\partial x_j}\left(V_j \rho_p V_{pk}\right) + \overline{V}_k \frac{\partial}{\partial x_j}\overline{\left(V_j \rho_p V_{pi}\right)} + \overline{V}_i \frac{\partial}{\partial t}\overline{\rho_p V_{pk}}$$
$$+ \overline{V}_k \frac{\partial}{\partial t}\overline{\rho_p V_{pi}} + \overline{\rho_p V_{pj}}\frac{\partial}{\partial x_j}\overline{V_i V_k} - \overline{\rho V_{pj} V_{pk}}\frac{\partial \overline{V}_i}{\partial x_j} - \overline{\rho V_{pi} V_{pj}}\frac{\partial \overline{V}_k}{\partial x_j} \qquad (8)$$

A statistical model is used as a turbulence model for calculating gas-dynamic parameters. The physical model is formulated as follows. In the initial section, the flow under consideration is a set of point formations – quasiparticles. The movement of such a particle downstream is random, while the particle retains all its individual properties. To describe the probabilistic trajectory of a particle, it is generally necessary to set a multi-dimensional probability density, which is the joint probability density of a particle hitting from point A of the initial section sequentially to random points B, C, D, etc.

Without going into details, we can say that the above system of equations allows us to determine all the gas-dynamic parameters and the scale of turbulence in the jet flow field.

Lighthill proposed approximate formulas for calculating the acoustic power emitted by a gas stream, having the form [3-6]:

$$N_{ac} = k\frac{\rho_a^2 V_a^8 d_a^2}{\rho_0 a_0^5}, by\ V_a \geq 150\frac{m}{s} \qquad (9)$$

$$N_{ac} = k\frac{\rho_a^2 V_a^6 d_a^2}{\rho_0 a_0^3}, by\ V_a \geq 150\frac{m}{s} \qquad (10)$$

where:
***K=(2,5÷4,5)•10**$^{-5}$* – dimensionless coefficient;
ρ_a, V_a – density and speed on the exhaust pipe cut;
ρ_0, a_0 – density and speed of sound in an undisturbed medium;
d_a – diameter of the output section [m].

To calculate the vibroacoustic parameters of non-isothermal jets, we supplement the system of equations (9-10) with the wave equation (the Lighthill wave equation):

$$\frac{\partial^2 \rho}{\partial t^2} - a_0^2\frac{\partial^2 \rho}{\partial x_i^2} = \frac{\partial^2}{\partial x_i \partial x_j}\left[\rho V_i V_j - \delta_{ij}(\rho a_0^2 + p) - \mu\left(\frac{\partial V_i}{\partial x_j} + \frac{\partial V_j}{\partial x_i} - \frac{2}{3}\frac{\partial V_k}{\partial x_k}\delta_{ij}\right)\right] \qquad (11)$$

where
ρ, p – density, static pressure,
a_0 – the speed of sound in an undisturbed environment,
V – speed,
t – time,
x_i, x_j – coordinates, $i, j, k, l = 1,2,3$.

If the right part of equation (11) is known to us, i.e. the distribution of gas-dynamic parameters in the flow is known, the solution for the energy ***N(θ,Ø)*** radiated by the flow per unit time to a point with coordinates ***x, θ, Ø***, is constructed by classical acoustics methods in the following form [7]:

$$N(\theta, \phi) = \int N(\theta, \phi, y)d^3y$$
$$N(\theta, \phi, x) = \frac{x_i x_j x_k' x_l'}{16\pi^2 \rho_0 a_0^5 |x|^4}\int \frac{\partial^4}{\partial \tau^4}\overline{T_{ij}T_{kl}'}\,d^3y \qquad (12)$$

where:
N – radiated acoustic power;

$$T_{ij} = \rho V_i V_j - \delta_{ij}(\rho a_0^2 + p) - \mu\left(\frac{\partial V_i}{\partial x_j} + \frac{\partial V_j}{\partial x_i} - \frac{2}{3}\frac{\partial V_k}{\partial x_k}\delta_{ij}\right) \qquad (13)$$

T_{ij}, T'_{kl} – voltage tensors related to various sound sources in the flow (13)

After simple transformations, taking into account the decomposition of gas-dynamic parameters into the average and pulsation components of noise and neglecting the viscous stress tensor in (13), the integrand in (12) has the form [1]:

$$\overline{T_{ij}T_{kl}'} = \overline{[\overline{\rho}V_i V_j - \delta_{ij}(\rho a_0^2 - p)][\rho V_k' V_l' - \delta_{kl}(\rho' a_0^2 - p')]} = \overline{\rho\rho' V_i V_j V_k' V_l'}$$
$$- \delta_{ij}a_0^2\overline{\rho\rho' V_k' V_l'} - \delta_{kl}a_0^2\overline{\rho\rho' V_i V_j} + \delta_{kl}\overline{\rho\rho' V_i V_j} + \delta_{ij}\overline{\rho\rho' V_k' V_l'}$$
$$+ \delta_{ijkl}\left(a_0^4\overline{\rho\rho'} - a_0^2\overline{\rho\rho'} - a_0^2\rho' p + pp'\right) \qquad (14)$$

3. SPATIAL-TEMPORAL CORRELATIONS OF PULSATION PARAMETERS

In order to fully describe the radiation sources, it is necessary to have information about the mutual space-time correlations and autocorrelations of the average and pulsation components of gas dynamic quantities.

To date, the question of the types and forms of correlation relationships in turbulent flows has not been fully studied. This method is based on the data of [2, 8-10], taking into account the uniformity, isotropy and compressibility of the flow. All space-time correlations of the pulsation parameters can be represented as:

$$\overline{S_\iota S_k'}(x_p, z, \tau) = f(x_p, z) g(x_p, \tau) \sqrt{\overline{S_\iota^2}} \sqrt{\overline{S_k^2}} \quad (15)$$

where:

$f = e^{-\frac{\pi z^2}{L^2}}$	spatial factor,
$g = e^{-\omega\tau}$	time factor,
$r^2 = r_1^2 + r_2^2 + r_3^2$-	the distance between the correlated points,
$\omega = \frac{1}{T_E}$	characteristic frequency of turbulent pulsations,
$L,\ T_E$	typical turbulence scales.

Tab. 1 shows the analytical dependences obtained taking into account the space-time correlation between the gas-dynamic parameters for 9 summand included in the product of tensors (15), reflecting the contribution of various gas-dynamic parameters (pulsation, average), each elementary volume of the jet to acoustic radiation.

Tab. 1 uses the terminology of the physical mechanisms of noise generation by turbulent flows accepted in modern aero-acoustics: "own" and "shear" noise. The "own " noise is caused by turbulent pulsations of gas-dynamic parameters. The "shift" noise is caused by the presence of a flow velocity gradient [1].

The presented mathematical model allows performing calculations of acoustic parameters (sound pressure, acoustic power, intensity, radiation pattern, etc.) generated by gas flows.

		Own noise	Shift noise
1	$\overline{\rho\rho' V_\iota' V_J' V_k' V_l'}$	$\frac{1}{2}\omega^4 L^3 V_P^4 [(-23cos^4\theta + (30 + 72\sqrt{3})cos^2\theta + 11 + 36\sqrt{3})\rho_p^2 + 8\sqrt{2}]$	$\omega^4 L^3 \tilde{V} cos^2\theta (4\tilde{V}\tilde{\rho} V_p^2 \rho_p cos^2\theta + 4(3 + 8\sqrt{2})\tilde{\rho} V_p^3 \rho_p + \tilde{V}^3 \rho_p^2 cos^2\theta + 4\tilde{V}\tilde{\rho}^{2\cdot} V_p^2 + 2\tilde{V} V_p^2 \rho^2 \times [(2 + + 8\sqrt{2})cos^2\theta + 1 + 8\sqrt{2}])$
2	$\overline{\delta_{kl}^* V_\iota V_J \rho\rho'}$	$\omega^4 L^3 V_p^2 \rho_p p_p$	$\omega^4 L^3 \tilde{V} p_p (\tilde{V}\rho_p + 2V_p\tilde{\rho}) cos^2\theta \times (2 - cos^2\theta)$
3	$\overline{\delta_{\iota J}^* V_k' V_l' \rho' \rho}$	$\omega^4 L^3 V_p^2 \rho_p p_p \times (2cos^4\theta + 1)$	$\omega^4 L^3 \tilde{V} p_p (\tilde{V}\rho_p + 2V_p\tilde{\rho}) cos^4\theta$
4	$\overline{\delta_{\iota J}^* \delta_{kl}^* p p'}$	$\omega^4 L^3 p_p^2$	$-$
5	$\overline{-a_0^2 \delta_{kl}^* \rho V_\iota V_J \rho'}$	$-\omega^4 L^3 a_0^2 V_p^2 (2cos^4\theta - 4cos^2\theta - 1)\rho_p^{2\prime}$	$-\omega^4 L^3 a_0^2 \tilde{V} \rho_p (\tilde{V}\rho_p + 2V_p\tilde{\rho}) cos^2\theta \times (2 - cos^2\theta)$
6	$\overline{-a_0^2 \delta_{\iota J}^* \rho V_k' V_l' \rho'}$	$\omega^4 L^3 a_0^2 V_p^2 \rho_p^2 (2cos^4\theta + 1)$	$-\omega^4 L^3 a_0^2 \tilde{V} \rho_p (\tilde{V}\rho_p + 2V_p\tilde{\rho}) cos^2\theta$
7	$\overline{a_0^4 \delta_{\iota J}^* \delta_{kl}^* \rho\rho'}$	$\omega^4 L^3 a_0^4 \rho_p^2$	$-$
8	$\overline{-a_0^2 \delta_{\iota J}^* \delta_{kl}^* \rho p'}$	$-\omega^4 L^3 a_0^2 \rho_p p_p$	$-$
9	$\overline{-a_0^2 \delta_{\iota J}^* \delta_{kl}^* \rho' p}$	$-\omega^4 L^3 a_0^2 \rho_p p_p$	$-$

Tab. 1: Analytical dependences of the components of "own" and "shift" noise

4. CONCLUSION

A mathematical model for calculating the acoustic parameters of non-isothermal jets flowing from a silencer is developed. The equations of continuity, the amount of motion, energy, as well as the wave equation of James Lighthill are used. Analytical expressions for determining the "shift" noise and "intrinsic" noise are obtained.

ACKNOWLEDGEMENT

The research described in this paper was supported by the grant of Russian Scientific Foundation, project number: 20-19-00222.

REFERENCES

[1] Glaznev V.N.. Zapryagayev V.I.. Erofeyev V.K. i dr. Struynyye i nestatsionarnyye techeniya v gazovoy dinamike. Novosibirsk. Izd. SO RAN. 2000. – 200 p.
[2] Reynolds A. Dzh. Turbulentnyye techeniya v inzhenernykh prilozheniyakh. – M.: Energetika, 1979. – 405 p.
[3] Goldsteyn M.E. Aeroakustika: Per.s angl./Pod red. A.G. Munina. - M.: Mashinostroyeniye, 1981. – 294 p
[4] Munin A.G.. Kuznetsov V.M.. Leontyev E.A. Aerodinamicheskiye istochniki shuma. – M.: Mashinostroyeniye, 1981. – 248 p.
[5] Lighthill M.J. On sound generated aerodynamically. Part 2: Turbulence as a source of sound // Proc. Roy. Soc. (London), 1954, v.222A, 51148, p.1-32
[6] Lighthill M.J. On sound generated aerodynamically. Part 1: General theory. // Proc. Roy. Soc. Lond., 1952. – P. 564-587.
[7] GOST 24346-80. «Vibratsiya. Terminy i opredeleniya». – M.: Standartinform, 2010. – 28 p
[8] Berdshou P. Vvedeniye v turbulentnost i eye izmereniye. M.: Mir 1974 – 278 p.
[9] Khintse I.O. Turbulentnost. eye mekhanizm i teoriya. – M.: FIZMALIT, 1963. – 680 p.
[10] Ribner H.S. Quadropole correlations governing the pattern of jet noise // J. Fluid Mech., 1969, v.38, 51, p. 1-24.

Nickolay Ivanov *is Doctor of Engineering Science, Professor of Department of Ecology and Industrial Safety of the Baltic State Technical University 'VOENMEH' named after D.F. Ustinov (Saint-Petersburg, Russia), Honored Scientist of the Russian Federation.*
Nickolay Ivanov is the creator of the transport acoustics scientific school. He developed the theory of the transportation vehicles acoustics, proposed the solution to the problems of generating the sound field in low volume, diffraction on complex obstacles, methods of calculation of the sound fields of spatial emitters. Nickolay Ivanov has published over 400 scientific papers, including about 10 textbooks, manuals and monographs. He presented the main results of scientific research on the international conferences in Australia, Austria, Hungary, Germany, Denmark, Italy, Canada, China, the Netherlands, Poland, Portugal, the USA, Finland, Switzerland, Sweden and other countries.

Aleksandr Shashurin *is Doctor of Engineering Science, Professor, Head of Department of Environment and Safety of the Baltic State Technical University 'VOENMEH' named after D.F. Ustinov (Saint-Petersburg, Russia), CEO of the LLC (OOO) 'Acoustic Design Institute'.*
Aleksandr Shashurin is a specialist in calculation and design of noise barriers, noise reduction at production facilities, soundproof booths design and others. He is a member of the organizing committees of conferences and seminars in the field of acoustics and ecology held in St. Petersburg and Moscow. Aleksandr Shashurin is the author of over 40 scientific publications and the co-author of textbooks and teaching aids, the author of 6 patents for noise control devices. He presented the main results of scientific research at the international conferences in St. Petersburg, Moscow, Samara, Hiroshima (Japan).

Andrey Vasilyev *is Doctor of Technical Science, Professor, honorary worker of higher education of Russia. Presently he is director of the Institute of Ecology of Volga Basin of Russian Academy of Science – Branch of Samara Federal Research Center of Russian Academy of Science and professor of Department of Chemical Technology and Industrial Ecology of Samara State Technical University, head of Povolzhsky Resources Center of Industrial Ecology and Chemical Technology of Samara State Technical University. Author of over 15 books (ecology, environmental protection, acoustics), over 900 scientific papers. Main organizer and scientific manager of ELPIT congresses since 2003 (http://elpit-congress.ru). Editorial and scientific member of a number of famous Russian and foreign scientific journals and editions. Expert of Russian Academy of Science, of Russian scientific fund, of scientific-technical field of Ministry of education and science of Russia etc., grant-holder of DAAD (Germany), Open world program (USA) etc.*

Yuri Elkin *is Doctor of Technical Sciences, Professor, Department of Technosphere Safety, Moscow Automobile and Road Construction State Technical University (MADI), (Moscow, Russian Federation), Academician of the International Academy of Ecology and Life Protection Sciences (IAELPS).*
Yuri Elkin - a specialist in the calculation and design of noise absorption, noise reduction on industrial premises and roads, sound insulation structures, silencing installations, etc.
Yuri Elkin is the author of more than 70 scientific publications, the author of 2 patents and co-author of textbooks and teaching aids. He presented the main results research at international conferences in in St. Petersburg, Moscow, Samara.

Zhenish Razakov *is Post-graduate student of the Baltic State Technical University "VOENMEH" named after D. F. Ustinov (St. Petersburg, Russia). After graduating from the Baltic State Technical University "VOENMEH" named after D. F. Ustinov he worked in various positions from an engineer of a defense enterprise to a senior manager. Deals with issues of noise and vibration during the final processing of metal products. Labor protection specialist. He has a number of conference presentations and scientific articles.*

Paper No.350/2021

DESIGNING OF RRJ-95NEW-100 AIRCRAFT WITH REGARD TO CABIN NOISE REQUIREMENTS

Kirill Kuznetsov, Vladimir Lavrov, Petr Moshkov, Victor Rubanovsky

IRKUT Corporation Regional Aircraft, Moscow, Russia, moshkov89@bk.ru

***Abstract**: The work is devoted to the problem of designing aircraft according to the specified parameters of acoustic comfort of passengers and crew members. The initial data for the design of the aircraft are presented. The concept of acoustic design of the RRJ-95NEW-100 aircraft based on the RRJ-95 prototype aircraft is considered. The issues of verification and validation of the calculation software used in the development of "digital twins" (acoustic simulation models) are considered, the main methods of visualization of the sound field in the aircraft cabin are presented.*

***Keywords:** acoustic designing, civil aircraft, cabin noise, "digital twin", acoustic simulation model, RRJ-95-NEW-100.*

***DOI:** : 10.36336/akustika20214134*

1. INTRODUCTION

Currently, providing increased acoustic comfort is one of the priority tasks of aircraft construction companies. Providing the concept of aircraft acoustic design, i.e. according to the acoustic comfort parameters set by the Customer, is an important task, the successful solution of which ensures the competitiveness of aircraft, especially in the business jet segment [1, 2].

The importance of this topic is confirmed by the currently being developed national standard of the Russian Federation "Requirements for cabin acoustic design of transport aircraft", which will reflect the main research and development work (R&D) within the life cycle, the implementation of which is necessary to ensure the concept of aircraft acoustic design.

The aim of the work is to form the concept of RRJ-95 NEW-100 acoustic design. The features of the concept under consideration are related to the fact that the aircraft is designed on the basis of the successfully operated RRJ-95 aircraft, subject to maximum import substitution of components and systems, as well as taking into account more stringent requirements for acoustic comfort parameters of passengers and crew members.

2. ABOUT THE PROBLEM OF AIRCRAFT ACOUSTIC DESIGN

As the initial data for the acoustic design of the aircraft, we note the following normative documents:

- GOST 20296-2014 (with addition) [2], according to which noise levels in aircraft cabins are normalized. And also the requirements from the Customers of the aircraft are formed.
- Certification specifications and acceptable means of compliance for large aeroplanes paragraph (CS-25) [4] 25.771 (e), Vibration and noise characteristics of cockpit equipment may not interfere with safe operation of the aeroplane.
- Within the framework of the problem of cockpit noise, ISO 9921:2003 [5] formulates an objective criterion for evaluating the quality of recording audio information on the non-directional microphone of the solid-state cockpit voice recorder (SSCVR). Such an objective criterion is the Speech transmission index (STI). The speech intelligibility score "excellent" is provided when STI>0.75. In addition to background noise in the area where the non-directional microphone is located, the reverberation time significantly affects the speech transmission index, which in turn depends on the geometry of the cockpit and the sound-absorbing properties of the interior.
- Acoustic design of a modern civil aircraft in the Russian Federation should be carried out in accordance with GOST R 58849-2020 [6], taking into account the following criteria. The created aeronautical engineering must meet the requirements of the Customer, the requirements for airworthiness and environmental protection from the effects of aviation and ensure the possibility of its effective and safe use. When creating aeronautical engineering, it is necessary to be guided by modern principles of its design and development on the basis of advanced scientific and technical reserve.

When designing aircraft salons with a VIP-interior, the initial data is data on sound pressure levels in the salons of operated and promising business jets. At the same time, the Customer of the business version of the aircraft can independently formulate the required parameters of acoustic comfort in various areas of the cabin. The design solution of this problem is a separate area of work in the aircraft design.

The calculation mode for aircraft designing taking into account the requirements for cabin noise is the cruise straight-line flight mode, which normalizes the noise levels in the aircraft cabin, and for which the placement of acoustic materials in the on-board structure is optimized.

Acoustic materials in the framework of this work are understood as heat-and sound-insulating, sound-absorbing, vibro-absorbing and vibro-insulating materials, metamaterials [7], as well as materials that implement the principles of active noise and vibration suppression used in the aircraft design to ensure the required parameters of acoustic comfort [8].

The content of R&D complex when performing acoustic design of an aircraft depends on the ratio between noise sources in different control sections along the length of the aircraft cabin.

For aircraft with a classical configuration of the power plant – two turbofan engines, located on pylons under the wing, the main noise sources in the cabin are:

- field of pressure pulsations on the fuselage surface (turbulent boundary layer) [9, 10],
- air conditioning system (ACS) [11, 12],
- vibration effect of the power plant (structural-borne noise) [13],
- acoustic loads on the fuselage surface (jet noise [14] and fan noise [15]), etc.

The aircraft developer does not design the aircraft systems, but formulates requirements for system Suppliers and ensures a rational layout of noisy units on the aircraft.

For the power plant (PP), the main problem is community noise, i.e. ensuring the sound pressure levels required for successful certification of the aircraft as a whole in the EPNdB metric in the far field in the sum of three control certification points. The problem of cabin noise is secondary and consists in obtaining data on the sound field structure of engines on the surface of the fuselage, taking into account the use of noise-muffling devices and the real configuration of PP on the aircraft for further modeling of the sound field in the cabin from this source.

3. THE DESIGN CONCEPT OF RRJ-95NEW-100 TAKING INTO ACCOUNT THE REQUIREMENTS FOR CABIN NOISE

The general concept of acoustic design of RRJ-95 NEW-100 aircraft is shown in Fig 1. The list of necessary R&D is formulated in this case on the basis of a in-flight experiment on identification, localization and ranking by intensity of the main noise sources in the cabin of RRJ-95 prototype aircraft [16, 17].

The overall sound field in the RRJ-95 cabin is dominated by the turbulent boundary layer noise and air conditioning system noise, the ratio between which varies along the length of the cabin. The ACS noise can dominate in different areas of the passenger cabin. The main units of the ACS that generate noise include exhaust valves, an air cooling unit, pressure and exhaust fans, recirculation fans, ejectors, air ducts and other elements that supply air to the passenger cabin. If we evaluate the contribution of the jet to the overall sound intensity, calculated through the overall sound pressure levels in dBA, then in the tail section of the cabin it does not exceed 1.5 %. The contribution of structural-borne noise from vibrations of the engine fan shaft does not exceed 4 % in the tail section of the cabin and 10% in the wing section.

The initial data for modeling the turbulent boundary layer noise is information about the structure of pressure pulsation fields on the fuselage surface. To calculate the noise from the acoustic impact of the power plant, it is necessary to have data on the sound field structure of the power plant in the conditions of its real configuration on the aircraft.

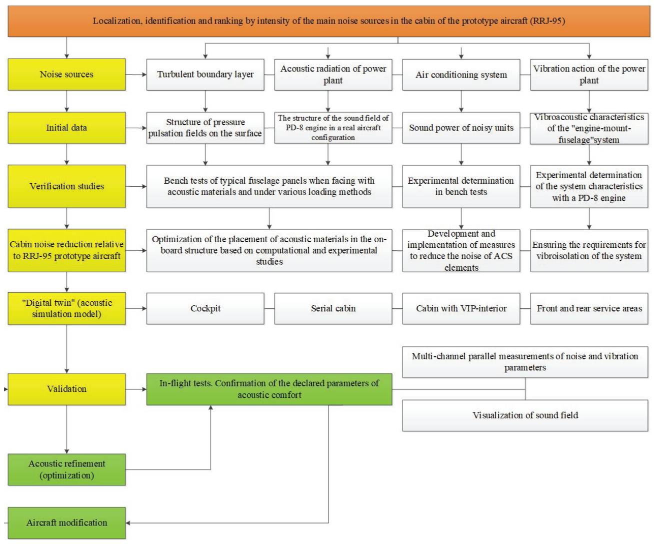

Fig. 1: General strategy of RRJ-95 NEW-100 acoustic design

In order to verify the simulation software and select acoustic materials for use on the RRJ-95NEW-100, studies of typical curved fuselage panels (side and ceiling) with different types of facing with acoustic materials and different types of loading were performed. In model experiments, the field of pressure pulsations is modeled by vibration loading of the panel under study, and the sound field of the power plant is modeled by a diffuse sound field in the reverberation chamber.

To simulate the structural-borne noise from the vibration effect of a power plant, data on the vibroacoustic characteristics of the "engine-mount-airframe" system are needed. Since the PD-8 engine will be installed on the RRJ-95NEW-100, and the SaM-146 engine is installed on the RRJ-95, a complex of additional studies is needed to ensure vibration isolation in the "engine-mount-airframe" system, which guarantees low levels of structural-borne noise in the aircraft cabin.

To simulate the ACS noise and the optimal placement of noisy units, data on the sound power of the main noise sources are needed. Bench tests to determine the sound power of ACS units are performed in accordance with the requirements of ISO 3745:2012 [18].

A separate place in the problem of ACS noise is occupied by the use of noise reduction technologies, both in the source and on the way of sound propagation to the cabin. Suppliers of ACS elements should provide the concept of acoustic design of the system units [19], including providing, if necessary, the installation of sound-proofing housings and vibration-proofing fasteners of the units, as well as the development and installation of mufflers for exhaust valves. Also, to improve the acoustic characteristics of the cabin, it is possible to install dissipative mufflers in the air supply channels to cabin [20]. This method of reducing the ACS noise is provided for on all business jets of RRJ-95NEW-100.

When developing a "digital twin" (acoustic simulation model) of RRJ-95NEW-100, the cockpit, the passenger cabin in serial and VIP configurations, as well as the front and rear service areas are considered separately. At the same time, the methods used for numerical modeling of interior noise are limited by the frequency range and to cover the problem range of the aircraft cabin under study, it is necessary to develop computational models using different numerical methods. For RRJ-95NEW-100 aircraft, the expected problematic frequency range corresponds to the range of 1/3-octave frequency bands of 100-4000 Hz [17].

The main calculation methods and the frequency range of their applicability are considered in Fig. 2. This is Finite Element Method (FEM), Boundary Element Method (BEM), Statistical Energy Analysis (SEA), Hybrid Method (FEM-SEA), and Ray Tracing method, etc. Generally, FEM and BEM are adopted for the low-frequency range, FEM-SEA is adopted for middle-frequency range, and SEA and Ray Tracing Method are adopted for high-frequency range.

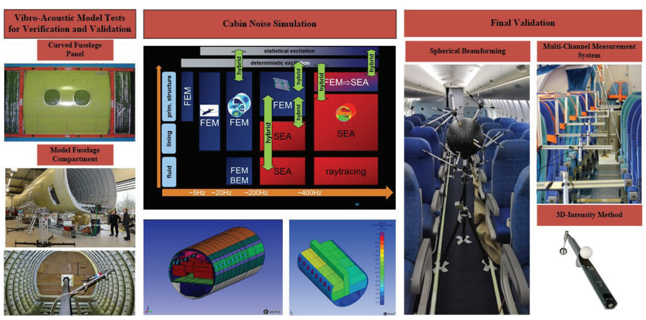

Fig. 2: Verification and validation of the simulation software during the development of the "digital twin" (acoustic simulation model) of the cabin

To verify the simulation software, vibroacoustic tests of typical fuselage panels with different types of facing with acoustic materials are performed, as well as tests of fuselage compartments.

As part of the validation of numerical models [21], it is necessary to perform research using sound field visualization technologies, as well as multi-channel parallel measurements of noise and vibration parameters.

The acoustic refinement (optimization) of the operated aircraft is based on the acoustic simulation model of the cabin. The in-flight experiment is performed before the introduction of design changes in the series to confirm the required level of increase in acoustic comfort.

4. MODERN METHODS OF SOUND FIELD VISUALIZATION IN AIRCRAFT CABINS

Technologies for visualizing sound fields in aircraft cabins are used to solve the following tasks:

- Localization and ranking by intensity of the main noise sources;
- Determination of sections of the aircraft structure where it is necessary to increase sound insulation or possibly reduce it by reducing the mass of acoustic materials without compromising the acoustic parameters of the cabin;
- Obtaining initial data for verification and validation of calculation methods, especially when developing "digital twines" of the passenger cabin and cockpit;
- Performing acoustic diagnostics of aircraft interiors and searching for the reasons for the difference in the noise characteristics of the cabin of separate aircraft from the acoustic portrait of the series.

Currently, three main technologies are used to visualize the sound field in aircraft cabins:

- Spherical beamforming;
- 3D-intensity method;
- Multi-channel parallel measurements of sound signals with the subsequent construction of noise maps using specially developed algorithms.

When performing acoustic measurements using spherical microphone arrays [22, 23], signal post-processing can be performed by different methods. These are the methods of standard spherical beamforming, acoustic holography, equivalent source and deconvolution method, etc.

As an example, the localization maps of noise sources in the RRJ-95 cabin in 1/3-octave band of 400 Hz with a contrast of 8 dBA for cases of ACS on and off are shown in Fig. 3. The characteristic frequency of operation of the system fans is 380 Hz into the frequency band under consideration, and, as expected, the sources of increased noise in this frequency band are located on the side of the air supply pipelines to the cabin. When the ACS is turned off, the intensity level of this source decreases by 2–3 dBA.

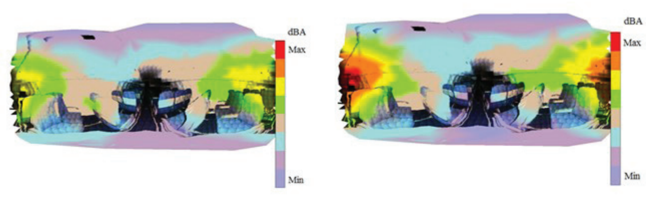

a) ACS off *b) ACS on*

Fig. 3: Localization maps of noise sources in the area of the 14th row of economy class seats for 1/3-octave frequency band of 400 Hz (in dBA)

The 3D-intensity method [24] is a development of the classical method of intensity [25], and in fact consists in scanning the sound field using an acoustic (intensimetric) probe when it moves along the enclosing surface. The acoustic probe of such a system can include from 1 to 4 microphones, depending on the signal post-processing algorithm. If several microphones are included in the acoustic probe, then in this case it becomes possible to build 3D sound intensity maps in vector form. Such maps can help determine the location of noise sources. When using a single microphone as part of an acoustic probe, it is possible to build acoustic maps of only scalar values along the measured surfaces.

As an example, a sound intensity map obtained in a vertical plane (marked in blue on the left side of the figure) parallel to the main axis of the aircraft is shown in Fig. 4. The measurements were performed under static conditions when ACS is operated from an auxiliary power plant.

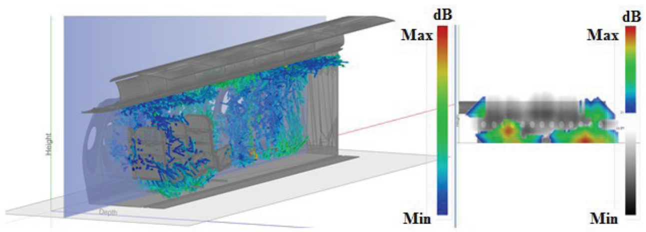

Fig. 4: The sound intensity field in vector form (graph on the left) and the sound intensity map in the vertical plane (graph on the right), marked in blue on the left graph, for the overall radiation in the range of 1/3-octave frequency bands 100-4000 Hz

When building noise maps based on multi-channel parallel measurements in the cabin using microphones distributed along the length of the cabin, the algorithms for visualizing the sound field are based on correlation functions and interpolation of measurement results. An example of building noise maps based on the results of multi-channel measurements on an Airbus A350 is shown in Fig. 5 [26]. Note that in this case, the microphones are located in one plane parallel to the floor plane, and multi-channel measurements of noise signals are performed in accordance with the requirements of ISO 5129:2001 [27].

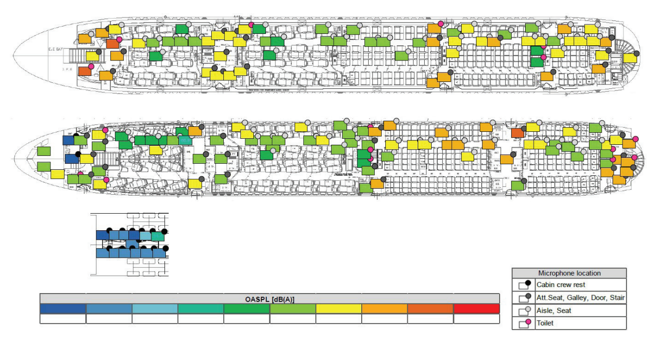

Fig. 5: Example of a noise map based on the results of measurements in the Airbus A350 cabin (the results are presented in dimensionless form) [26]

5. CONCLUSION

The problem of designing civil aircraft taking into account the requirements to cabin noise is considered. The paper presents the concept of acoustic design of the RRJ-95NEW-100. The peculiarity of the concept is that the aircraft is designed on the basis of the successfully operated RRJ-95, taking into account the requirements of import substitution of the main components and systems, as well as the need to ensure promising acoustic comfort requirements. Modern technologies for visualizing the sound field in aircraft cabins and the tasks for which they are used are considered.

ACKNOWLEDGEMENT

The authors thank IRKUT Corporation Regional Aircraft for the financial help and organization of the in-flight tests. The author also expresses gratitude to the employees of the Siemens Industries Software (Moscow branch) for their help in processing the measurement results using spherical beamforming technology.

REFERENCES

[1] Moshkov, P.A.: Problems of civil aircraft design with regard to cabin noise requirements, Aerospace MAI Journal, ISSN 0869-6101, Moscow Aviation institute, Moscow, VOLUME 26, p. 28-41, 2019
[2] Pennig, S., Quehl, J., Rolny, V.: Effects of aircraft cabin noise on passenger comfort, Ergonomics, ISSN 0014-0139, Taylor & Francis Ltd, VOLUME 55, p. 1252-1265, 2012
[3] GOST 20296-2014: Aircraft and helicopter of civil aviation. Acceptable noise levels in flight decks and in salons and methods of noise measurement, 12 p, 2014
[4] CS-25. Certification Specification and acceptable means of compliance for large aeroplanes, 1126 p, 2018
[5] ISO 9921:2003: Ergonomics. Assessment of speech communication, 36 p, 2003
[6] GOST R 58849-2020: Commercial aeronautical engineering. Degree creation. Fundamentals, 61 p, 2020
[7] Bobrovnitskii, Y.I., Tomilina, T.M.: Sound absorption and metamaterials: A review, Acoustical Physics, ISSN: 1063-7710, Pleiades Publishing, Ltd., VOLUME 64, p. 519-526, 2018
[8] Zverev, A.Y.: Noise control mechanisms of inside aircraft, Acoustical Physics, ISSN: 1063-7710, Pleiades Publishing, Ltd., VOLUME 62, p. 478-482, 2016
[9] Hu, N., Appel, C., Haxter, S., Callsen, S., Klabes, A.: Simulation of wall pressure fluctuations on an Airbus-A320 fuselage in cruise flight condition, 25th AIAA/CEAS Aeroacoustics Conference, AIAA Paper No. 2019-2728, 2019
[10] Abdrashitov, R., Golubev, A.: Identification of sources of noise in the cabin and the definition of the local passage of sound energy through fuselage based on the results of in-flight measurements of the Superjet, 21th AIAA/CEAS Aeroacoustics Conference, AIAA Paper No. 2015-3114, 2015
[11] Hu, N., Buchholz, H., Herr, M., Spehr, C. Haxter, S.: Contributions of Different Aeroacoustic Sources to Aircraft Cabin Noise, 19th AIAA/CEAS Aeroacoustics Conference, AIAA Paper No. 2013-2030, 2013
[12] Bodén, H, Efraimsson, G.: Aeroacoustics research in Europe: The CEAS-ASC report on 2012 highlights, Journal of Sound and Vibration, ISSN: 0022-460X, Academic Press, VOLUME 332, p. 6617-6636, 2013
[13] Baklanov, V.S.: Role of structural noise in aircraft pressure cockpit from vibration action of new generation engines, Acoustical Physics, ISSN: 1063-7710, Pleiades Publishing, Ltd., VOLUME 62, p. 456-461, 2016
[14] Bassetti, A., Guerin, S.: Semi Empirical Jet Noise Modelling for Cabin Noise Predictions – Acoustic Loads in the Geometric Near Field, 17th AIAA/CEAS Aeroacoustics Conference, AIAA Paper No. 2011-2925, 2011
[15] Samokhin, V., Moshkov, P., Yakovlev, A.: Analytical model of engine fan noise, AKUSTIKA, ISSN 1801-9064, Studio D – Akustikas.r.o., ČeskéBudějovice, VOLUME 32, p. 168-173, 2019
[16] Lavrov, V., Moshkov, P., Popov, V., Rubanovskiy, V.: Study of the Sound Field Structure in the Cockpit of a Superjet 100, 25th AIAA/CEAS Aeroacoustics Conference, AIAA Paper No. 2019-2726, 2019
[17] Moshkov, P.: Contributions of Different Sources to Cabin Noise of a Superjet 100 in Cruise Flight Condition, 2021 AIAA AVIATION FORUM, AIAA Paper No. 2021-2272, 2021
[18] ISO 3745:2012: Acoustics –Determination of sound power levels and sound energy levels of noise sources using sound pressure – Precision methods foranechoic rooms and hemi-anechoic rooms, 63 p, 2012
[19] SAE AIR 1826: Acoustical considerations for aircraft environmental control system design, 44 p, 2016 https://www.sae.org/standards/content/air1826/
[20] Yan, X.: Acoustics analysis and experimental study on silencer for commercial airplane air conditioning system, ICASSE 2021, Lecture Notes in Electrical Engineering, ISBN 978-981-33-6060-0, 2021
[21] Guruprasad, S., Ram, P.R.M., Blech, C., Langer, S.: Aircraft Cabin Noise Prediction Under Uncertainty, Fundamentals of High Lift for Future Civil Aircraft, ISBN 978-3-030-52429-6, Braunschweig, Germany, VOLUME 27, p. 247-261, 2021
[22] Moshkov, P.A., Vasilenkov, D.A., Rubanovskii, V.V., Stroganov, A.I.: Noise sources localization in the RRJ-95 aircraft pressure cabin by spherical microphone array. Part 1. Cockpit, Aerospace MAI Journal, ISSN 0869-6101, Moscow Aviation institute, Moscow, VOLUME 27, p. 37-51, 2020
[23] Moshkov, P.A., Vasilenkov, D.A., Rubanovskii, V.V., Stroganov, A.I.: Noise sources localization in the RRJ-95 aircraft pressure cabin by spherical microphone array. Part 2. Passenger cabin, Aerospace MAI Journal, ISSN 0869-6101, Moscow Aviation institute, Moscow, VOLUME 27, p. 60-72, 2020
[24] Miah, K.H., Hixon, E.L.: Design and performance evaluation of a broadband three dimensional acoustic intensity measuring system, The Journal of the Acoustical Society of America, ISSN: 0001-4966, AIP Publishing on behalf of the Acoustical Society of America, VOLUME 127, p. 2338-2347, 2010
[25] Golubev, A.Y., Potokin, G.A.: Features of the Use of Intensimetry to Determine the Power of Acoustic Radiation of a Panel in the Field of Aerodynamic Pressure Pulsations, Measurement Techniques, ISSN: 0543-1972, Springer New York Consultants Bureau, VOLUME 61, p. 1228-1233, 2019
[26] Helffer, E., Deille, O., Briand, J., Delverdier, O.: Fast and Light Acoustic Flight Test Measurements in Aircraft, AIAA Flight Testing Conference, AIAA Paper No. 2014-2581, 2014
[27] ISO 5129:2001: Acoustics. Measurement of sound pressure levels in the interior of aircraft during flight, 10 p, 2001

Kirill Kuznetsov *is Chief Designer of SSJ-NEW of the IRKUT Corporation Regional Aircraft (Moscow, Russia).*
Kirill Kuznetsov is an expert in the design of modern civil aircraft.

Vladimir Lavrov *is Chief Designer of SSJ program of the IRKUT Corporation Regional Aircraft (Moscow, Russia).*
Vladimir Lavrov is an expert in the design of modern civil aircraft.

Petr Moshkov *is Ph.D. of Engineering Science, Leading designer of the IRKUT Corporation Regional Aircraft (Moscow, Russia).*
Petr Moshkov is a specialist in aeroacoustics. Petr Moshkov is the author of over 40 scientific papers. He presented the main results of scientific research at the international conferences in Moscow, Gelendzhik, Svetlogorsk, Delfts.

Victor Rubanovsky *is Head of the SBJ Development Integration Department of the IRKUT Corporation Regional Aircraft (Moscow, Russia).*
Victor Rubanovsky is a specialist in the design of high-comfort cabins for business jets.

Paper No.351/2021

COMPREHENSIVE ASSESSMENT OF THE IMPACT OF AIR NOISE AND DUST ON FOUNDRY OPERATORS

[a)]Lyudmila Drozdova, [b)]Vyacheslav Manokhin, [c)]Elena Golovina, [d)]Alexander Kudaev

[a, d)] Baltic State Technical University 'VOENMEH' named after D.F. Ustinov, St. Petersburg, Russia
[b, c)] Voronezh State Technical University, Voronezh, Russia
[a)] drozdovalf@yandex.ru, [b)] manohinprof@mail.ru, [c)] u00111@vgasu.vrn.ru, [d)] ksiombarg1@yandex.ru

***Abstract**: The main goal of the work is a comprehensive assessment of the impact of noise and dust in the foundry. Based on the results of the analysis, the main disadvantage areas with exceeding the permissible noise and dust level are presented – areas of knockout grates and casting cleaning areas.*
Recommendations are proposed for the selection of technical measures, including the rational placement of equipment, their mode of operation, the installation of acoustic screens and sound-insulating partitions near unprotected workplaces, as well as a rational selection of the equivalent sound absorption area of the workshop premises, which will create safe production conditions. Ways of improving the working conditions of operators of sand and shot blasting installations by reducing noise at their workplaces are considered: increasing sound absorption in the body of the shot blasting chamber and installing noise-protective shielding structures to fence off areas with the most intense noise.

***Keywords:** noise, vibration, dust, foundry, shot blasting section, noise-reducing shielding structures, sound absorption*

***DOI:** : 10.36336/akustika20214140*

1. INTRODUCTION

The article is devoted to a comprehensive assessment of the impact of dust, noise and vibration on the operating personnel of the foundry. The complexity of technological processes, the presence of harmful factors in the working area of the operators of the foundry affect the quality of the air environment of the foundry, which usually does not meet sanitary and hygienic standards. Special equipment located in the foundry additionally releases a large amount of heat into the air of the working areas, the surplus of which can also lead to changes in climatic conditions inside the production premises of the foundries.

Improving the quality of production products, increasing their reliability and durability to a greater extent depend on the cleanliness of the surfaces. Processing by shot blasting reels and chambers is the most common method in industrial sphere. This equipment belongs to the group of the most environmentally unfriendly: a large amount of emitted dust, the presence of shot supplied under pressure, which are accompanied by high levels of noise and an increase in vibration activity. Increased noise and vibration are considered those environmental criteria for which it is technically most difficult to achieve their compliance with regulatory values. The harmful effects of noise and vibration on the human body are manifested in various forms, for example, noise (neuritis of the auditory nerve) and vibration diseases, increased fatigue, decreased productivity and the quality of work. And at present, noise and vibration diseases in foundry occupy the second and third places in the list of occupational diseases [1].

In the shops of mass foundry production, the largest number of occupational diseases associated with exposure to excessive noise from the equipment on workers are of a longer duration.

The highest incidence rate of auditory neuritis in foundries is found among the professions such as cutters, molders, shapers, smelters, and cast cleaners working with shot blasting equipment.

2. NOISE ASSESSMENT IN FOUNDRY AREAS

The objective of this study is to analyze the experimental characteristics of noise in the working area of the foundry when performing various operations.

The research results showed that the noise parameters of the main types of foundries exceed the permissible noise standards at workplaces. At the same time, the greatest excess of the permissible sound levels [2] is noted at work places (by sound pressure levels) at rod and molding shaking machines by 12-23 dB, at knock-out grates by 17-26 dB, at cutting and cleaning equipment by 16-27 dB [3].

The noise spectra from the main casting machines are broadband, and at the same time the sound field in the working areas of the shop is non-uniform due to the fact that the main noise sources have different powers and different patterns of the spectrum. Equipment with shock operating mode emits intermittent noise with the maximum sound power level in the medium and high frequencies, which are most sensitive and dangerous to humans.

Index for the noise factor Ksh obtained by calculation based on empirical data for various sections of the foundries. As can be seen from the table, the greatest impact, increased noise, is observed in the areas of molders, cutters and cast cleaners 1,43-2,67 [3].

A specific feature of batch production foundries is that, despite a large number of technological processes, a lower level of automation and mechanization of these processes allows choosing a more rational and, as a rule, isolated arrangement of equipment that creates increased noise levels. It should be noted that in these workshops the operation of the equipment occurs cyclically and, accordingly, the equivalent noise levels will have lower values. This is especially evident when foundry production in a stepped mode. Knock-out grates work in the third shift, when only the knock-out of castings from the mold takes place. Therefore, the development of recommendations for reducing noise in the foundry through a reasonable choice of technical measures, including the rational placement of equipment, the mode of their operation, the installation of acoustic screens and sound-insulating partitions at unprotected workplaces, as well as the rational selection of the equivalent sound absorption area of the workshop room by increasing the area of the sound-absorbing the wall cladding of the workshop and the use of piece sound absorbers [4].

3. REDUCING NOISE FROM MAJOR SOURCES

One of the main objectives of this study was to identify the main sources of radiated noise and dust in the cutting-cleaning areas with the highest pollution index by the noise factor Ksh, in particular in the shot blasting chamber.

The most common surface processing for metal parts is sandblasting or shot blasting. This technological operation allows high-quality grinding of the casting, it is carried out in a shot blasting chamber.

An integrated approach to reduce the level of noise and dust emitted during the shot-blasting process, including: determining the main sources emitting noise, assessing the sound field in the chamber, accounting the sound insulation of the chamber walls, choosing materials that reduce noise and installing noise-protective structures allows you to consistently solve the issue of creating safe production conditions [5].

Figure 1 shows a diagram of the drone-blown area.

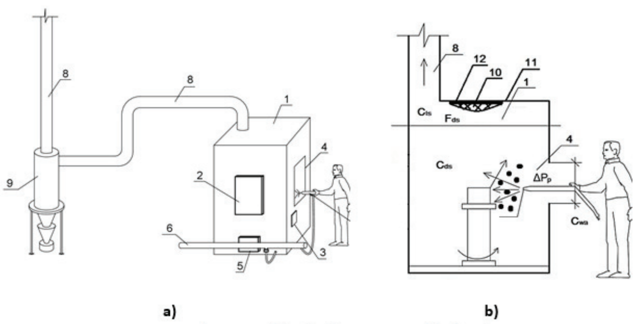

Fig. 1: The system of the shotblasting section of the foundry: a – shot blasting chamber scheme; b – section of the shot blasting chamber; 1 - shot blasting chamber; 2 - boot sector of the parts to be cleaned with a sealed door; 3 - control panel; 4 - shot blasting machine supply window; 5 - technological hole with a sealed cover for shot removal; 6 - compressed air line; 7 - air supply to the nozzle; 8 - air duct; 9 - conical cyclone for air purification 10 - VDM (vibration damping material); 11 - construction material; 12 - ZPM (sound-absorbing material)
Legend: $C_w a$ - concentration in the working area, C_{dc} - concentration in the dust chamber, C_{ls} - concentration in the local suction, F_{dc} is the area of the dust chamber, ΔP_p is the pressure drop during control

The shot blasting process operates in a one-shift mode with insignificant technological breaks. Shot-blasting of castings is carried out in chambers, which are a closed metal structure measuring 2000 x 2000 x 2500 mm, the inner lining of the chamber is made of steel sheet 3 mm thick and covered with rubber 10 mm thick. In the upper part, the chamber is connected via a 630 mm diameter branch pipe to the local exhaust ventilation, which contains a TsN-11 cyclone for dust removal [6].

As studies have shown, shot with an average diameter of up to 2 mm is directed by a compressed air flow at a speed of 30 m/s through the feed window to the surface of the product. The principle of operation of a simple injection shot blasting machine is based on the operation of a hermetically sealed tank, in which shot is located under the pressure of compressed air. Under the action of gravity and compressed air pressure, the shot is fed into the chamber. In this case, noise emission of increased intensity occurs.

The main effect on the formation of the sound field in the shot blasting chamber is provided by the noise emission of the jet supplied under pressure of compressed air, that is, aerodynamic noise. To reduce aerodynamic noise, various sound-absorbing elements with curved channels are used. Reducing aerodynamic noise is also possible by improving the aerodynamic characteristics of vehicles.

The authors have proposed technical measures to reduce noise levels due to the optimal selection of sound-insulating and sound-absorbing elements of the blast machine housings, which make it possible to reduce the noise levels inside the plant and to reduce the noise outside the shot blasting machine body.

Experimental studies of the absorption coefficients of a large number of facing materials in the octave bands of the audio frequency spectrum, presented in [7], made it possible to choose the most effective combination of structural, sound-absorbing and vibration-damping materials. The method of engineering calculation of the acoustic characteristics of foundry equipment made it possible to create a computer-aided design system for shot and sandblasting installations, minimized in noise level by selecting the optimal combination of wall thickness and grades of facing material.

The authors proposed to keep the thickness of the structural material equal to 3 mm in the shot blasting chamber, and leave the existing layer of glued rubber 10 mm thick as additional sound insulation of the chamber walls. What is more, the rubber layer will be useful for vibration damping. Additionally, on the inner surface of the chamber, it was proposed to apply a sound-absorbing material 30 mm thick, which are products made from a loose layer of canvases of super-thin basalt fibers in a glass fabric sheath. The sound absorption coefficient of such materials in the mid-high frequency range ranges from 0.5 to 0.9.

The preliminary calculation of noise reduction at the operator's workplace when using the proposed measures showed that it is impossible to achieve the expected noise requirements of sanitary standards.

As a result of the above measures, the noise level at the workplace of the operator of shot blasting processing outside the chamber can be reduced by no more than 8-10 dB in the normalized frequency range.

To minimize the noise level, correct technological measures are required for the introduction of remote control and work on the sealing and isolation of equipment, which makes it possible to reduce noise pollution immediately at the source of its formation [8].

The authors also propose to install noise-protective shielding structures and shield areas with the most intense noise, which will increase dissipation and form sound protection for a more favorable acoustic field in the foundry, and in particular at the workplace of the operator of the blast chamber. [9].

The recommended measures do not allow achieving the required standard values of the existing noise characteristics. Since making changes to the design of the blasting chamber is technically unfeasible, the use of personal protective equipment - a helmet with headphones is considered [11].

4. REDUCING DUSTINESS IN THE FOUNDRY SHOT BLASTING AREA

The second task of the study was to ensure the reduction of dustiness and create a safe environment for the operators of the shot blasting section of the foundry, since a large content of dust was found precisely in the shot blasting section of the foundry.

The shot-blasting process allows for high-quality grinding of casting products of various shapes, however, this technological process is accompanied by the generation of a large amount of dust, which poses a threat to the health of workers. An integrated approach to reduce dust content and prevent occupational diseases allows consistently solving the problem of creating safe production conditions [5].

Special technological measures for the introduction of continuous production technology remove dust immediately from the places of its formation, and also prevent the formation and spread of dust; mechanization and automation of processes; introduction of remote control; work on sealing and insulation of equipment; creation of devices for local ventilation suction, exhaust or supply and exhaust ventilation [8].

In the foundry, polluted air is filtered using a variety of dust collectors and then released into the atmosphere. However, the effectiveness is not sufficient [1].

At the same time, the concentration of dust in the aspiration system before the dust collecting equipment, as shown by measurements, is 5.6 gm3, in the operator's working area - 8.7 mg/m^3 [6]. The degree of air pollution in the working area of production depends on many factors, for example: the quality and consistency of maintenance, effective operating modes of aspiration systems, the state of dust collection equipment [10].

Dust after processing the surface of metal parts with shot is converted into a multicomponent, therefore, to search for highly effective means of cleaning gas dust, the study of the elemental and dispersed composition of dust particles is considered relevant. Granulometric analysis was used to evaluate dust particles by size [3]. Particle size and particle density affect the properties of pulverized materials. The particle size distribution of the dust was determined on a Fritsch Analisette-22 NanoTec laser particle analyzer using the Fritsch Mas control software.

It was found that a significant amount of fine and medium-dispersed dust with a particle size of less than 100 microns, which amounted to about 90%, Particles, whose size is less than 100 microns, pose the greatest threat to human health, since, lingering in the lungs, provoke the onset of pneumoconiosis, and in the presence of a SiO2 film - silicosis.

The second stage of the experiment was aimed at detailing the dispersed composition of dust and determining the elemental composition, which were carried out using X-ray spectral microanalysis [6].

X-ray phase analysis is characterized by high reliability and expressiveness, it is direct (that is, it is based not on indirect comparison with any samples, but on the determination of the crystal structure of a substance). It is insensitive to the volume of the investigated product, can be carried out without disturbing the sample or part, and estimate the number of phases in the mixture. All of the above refers to the advantages of this type of analysis.

The dust, studied by means of X-ray spectral microanalysis, caught in the shot-blasting section and the section for removing molds, had a shape that allows it to be conventionally considered spherical. As a rule, when settling, dust particles rotate, occupying the position that provides the greatest resistance to air. The spherical shape promotes settling in the atmosphere and inertial dust collectors. Particles less than 10 microns in size settle for a rather long time, their presence indicates the need for highly efficient air purification systems.

X-ray spectral analysis on a wave X-ray fluorescence spectrometer "Bruker S8 Tiger" at the Center for Collective Use of Voronezh State University made it possible to obtain a more accurate percentage of elements in the sample. For the purpose of additional treatment of the emission to standard concentrations equal to MPCr.z., it is proposed to supplement the existing dust collection system with a "wet" stage.

5. CONCLUSION

The article presents an analysis of the effect of noise on foundry operators and considers ways to improve the working conditions of operators of sand and shot blasting plants by reducing noise at their workplaces, which is an important socio--economic, environmental, scientific and technical problem. The results are presented in the following key findings:

1. Unfavorable areas for exceeding the permissible noise level were identified - areas of knock-out gratings and areas for cleaning casting.
2. It was found that the noise levels at the workplaces of operators of sand and shot blasting chambers exceed the standard values by 4-18 dB. The greatest excess of actual noise levels over the normative ones is observed at the workplaces of operators of shot blasting machines.
3. Disperse (granulometric) analysis of dust generated in shot blasting areas showed that a fraction of less than 100 microns in size accounts for 90%.
4. The authors offer recommendations for reducing noise and dust at the operator's workplace.

REFERENCES

[1] Orekhova L.I. Ecological problems of foundry production / A.I. Orekhova // Ecology of production. - 2005. - No. 1. - p. 2-3.
[2] 2.2.4.3359-16 "Sanitary and Epidemiological Requirements for Physical Factors at Workplaces", Section III "Noise at Workplaces".
[3] Lazarenko A.M., Khoreva S.A., Melnichenko V.V. Assessment of the impact of noise on workers in the foundry / Casting and metallurgy. No. 3 (62), 201. p.194-195.
[4] Kapustyansky A.M. Methods for noise reduction in the design and operation of shot blasting and sandblasting installations, dis. ... candidate of technical sciences: 05.26.01 / Kapustyanskiy A.M. Rostov-on-Don, 2001 .-- 181 p.
[5] Pachurin G.V. Influence of the complex impact of harmful factors of foundry production on the level of professional risk / G.V. Pachurin, A.A. Filippov // XXI century. Technosphere safety. - 2017. - No. 2 - p. 10-17.
[6] Golovina E.I .: dissertation by the Candidate of Technical Sciences: 05.26.01 / E.I. Golovin. Rostov-on-Don, 2020 .-- 111 p.
[7] Drozdova L.F., Chebotareva E.Yu., Kudaev A.V. An overview of modern compressor units and materials to reduce their noise. NOISE Theory and Practice. Vol. 4, No. 2, 2018. p. 11-20.
[8] Novikov VP Automation of foundry production: in 2 hours / VP Novikov. - M.: MGIU, 2006. - Part 1: Management of foundry processes. - 292 p.
[9] Trukhov Yu. A. Technology of foundry production: casting in sand molds / A. P. Trukhov, Yu. A. Sorokin, M. Yu. Ershov; ed. A.P. Trukhova. - M.: Academy, 2005 .-- 524 p.
[10] Solovieva O.S., Elkin Yu.I. Protecting residential buildings from construction site noise NOISE Theory and Practice. Vol. 6, No. 3, 2020. c. 7-15.
[11] J. Haider Health and Environmental Impacts in Metal Machining Processes / J. M. Haider, S. J. Hashmi // Comprehensive Materials Processing. - (2014). - Vol. 8. - p. 7-33.
[12] Patent No. 2702554 Russian Federation, IPC B01D 47/06 (2006.01) / Device for wet gas cleaning / E.I. Golovina, T.V. Shchukin, Yu.V. Sychev, [and others]. - No. 2702554; app. 07/16/2018; publ. 08.10.2019. - 7 p.

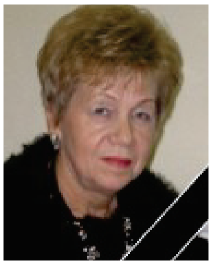

Lyudmila Drozdova *is the Ph.D. of Engineering Science, Professor of Environment and Safety chair of the Baltic State Technical University 'VOENMEH' named after D.F. Ustinov (St.Petersburg, Russia). She is the author of over 135 scientific papers, also the co-author of 11 textbooks and manuals, 3 handbooks (2 of them are in English), 10 patents. She presented the main results of research at international conferences in Australia, Austria, Denmark, Germany, China, Lithuania, Poland, Portugal, USA Sweden and other. Lyudmila Drozdova is the Deputy Chairman and member of organizing committees of more than 20 congresses, conferences, workshops in the field of acoustics and ecology which were conducted in St. Petersburg, including the International Conference "NOISE-93", 4th International Congress of sound and vibration (1996) and 9th International Congress of sound and vibration (2004). She was one of the founders (1996) and the associate editor of the "International Journal of Acoustics and Vibration" (IJAV). She is a specialist in calculation and design of soundproof enclosures, development of mobile compressor stations with noise-protection performance, vibration and sound energy propagation, acoustoelectronics and other.*

Vyacheslav Manokhin *is a Doctor of Technical Sciences, Professor, Professor of the Department of Technosphere and Fire Safety, Voronezh State Technical University (Voronezh, Russia). Specialist in the field of environmental safety and labor protection at work. He is the author of over 100 scientific publications and co-author of textbooks and patents. Presented the main results of scientific research at international conferences in Voronezh, Rostov-on-Don, St. Petersburg, Moscow.*

Elena Golovina *is the Candidate of Technical Sciences, Senior Lecturer at the Department of Technosphere and Fire Safety, Voronezh State Technical University (Voronezh, Russia), Deputy Dean for Academic Affairs of the Faculty of Engineering Systems and Structures. Elena Golovina, specialist in the field of air dust reduction in the foundry industry. Elena Golovina is the author of over 50 scientific publications and co-author of textbooks and patents. She presented the main results of scientific research at international conferences in Voronezh, Rostov--on-Don, St. Petersburg, Sevastopol.*

Kudaev Alexander *is the Candidate of Technical Sciences, Associate Professor of the Department of Ecology and Industrial Safety of the Baltic State Technical University "VOENMEKH"*
D. F. Ustinova (St. Petersburg, Russia). She is the author of over 35 scientific publications. Presented the main results of scientific research at international conferences in Samara, Sevastopol, St. Petersburg.

Paper No.352/2021

CALCULATIONS FOR EVALUATING THE ACOUSTIC EFFICIENCY OF MEASURES TO REDUCE PULSE NOISE IN INDUSTRIAL PREMISES

[a] Alexander Antonov, [b]Irina Matveeva, [c]Igor Shubin, [d]Ilya Tsukernikov

[a, b] Tambov State Technical University, Tambov, Russia
[a, c, d] Research Institute of Building Physics, Moscow, Russia

***Abstract**: At modern manufacturing enterprises, machines and mechanisms that emit pulsed noise are widely used. Pulse noise has a more harmful effect on workers than time-constant, time fluctuating and intermittent noises. Pulse noise reduction is possible through the application of design changes in the pulse noise source and the development of organizational, technological, construction and acoustic measures. The choice of specific events is made on the basis of their acoustic efficiency assessment. For this purpose, it is necessary to have a method for calculating pulse noise that takes into account its space-time characteristics and their possible changes with structural changes of the source, as well as with changes in the space-planning and acoustic parameters of premises. In the article, to assess the acoustic efficiency of pulse noise, it is proposed to use a combined calculation method developed by the authors, taking into account the real mirror-diffuse nature of sound reflection from the room fences. On its basis, it is analyzed the possibilities of using various methods and means to reduce the impact of noise on the workers in rooms with pulsed sound sources.*

***Keywords:** pulse noise, noise calculation methods, sound reflection from fences, industrial buildings, noise protection.*

***DOI:** : 10.36336/akustika20214145*

1. INTRODUCTION

Studies of noise effects on the human body show that pulse noise has the most adverse effect on the cardiovascular system and hearing organs [1]. According to GOST 23337-2014 "Noise. Methods of noise measurement in residential areas and in the rooms of residential, public and community buildings", pulse noises consist of one or a number of sound signals (pulses) with a duration of less than 1 second. Currently, at many enterprises, for example, at railway repair enterprises, due to the peculiarities of their technological processes, pulse noise is the determining factor of noise pollution [2]. For this reason, the development of measures to reduce pulse noise is of great socio-economic importance. To reduce it, it is required the implementation of complex and expensive design solutions to reduce the radiation of sound energy by a source and the design of organizational, technological, construction and acoustic measures in rooms with these sources.

The choice of specific measures and the assessment of their acoustic and economic efficiency depends on the accuracy of calculations of pulse noise levels before and after performing noise protection measures. This is possible if there are noise calculation methods that provide objective information about the processes of formation and propagation of pulsed sound energy in the premises. The methods should take into account the design and technological features of sound sources, acoustic and geometric parameters of premises and adequately respond to their changes in the process of developing noise reduction measures.

Pulse noise refers to non-constant noise, the magnitude of which varies in space and time. This circumstance should be taken into account when developing methods for calculating pulse noise used in assessing the acoustic efficiency of noise protection measures.

The impact of pulsed noise on workers is determined by the time-variable sound coming to the calculated point directly from the source of pulsed sound energy and the reflected energy components of the pulses which occur in the room when direct sound is reflected from fences. Reflected energy depends on the characteristics of the direct sound source, as well as on the geometric and acoustic parameters of the premises, the position of the sound source relative to the calculated point and the surfaces of fences with different sound-absorbing and sound-reflecting properties. Therefore, the process of occurrence, propagation in the space of the room and changes in time of the reflected sound energy of the pulse is a multifactorial process. For this reason, methods for calculating pulse noise in rooms should take into account all the factors listed above and their mutual influence on each other.

The methods of pulse noise calculation developed by the authors are analyzed in the article and the results of their use in assessing the acoustic efficiency of methods and means of reducing the effects of pulse noise on workers are presented.

2. METHODS

Reducing the effects of pulse noise on a person can be provided in a sufficiently large number of ways. The first of them include measures related to structural changes in machines and mechanisms that emit pulsed sound energy. The second group of methods includes organizational, technological, construction and acoustic measures to reduce pulse noise in the volume of the room. The choice of one or another type of methods depends on the parameters of the emitted sound energy by the source, as well as on the space-planning and acoustic characteristics of the premises. The noise mode at workplaces in the premises is determined by the direct sound coming from the source directly, and the reflected sound energy that occurs when the direct sound is reflected from the fences of the room. As mentioned earlier, the formation of reflected energy depends on the characteristics of the energy emitted by the source and the parameters of the room that affect the formation of reflected noise. For this reason, when reducing pulse noise, it is necessary to use both groups of noise reduction measures, using their various combinations.

At the stage of technological design of enterprises, the selection of machines and mechanisms is made taking into account the parameters of the pulsed sound energy emitted. These parameters include the sound power level, pulse duration, pulse emission frequency, and the frequency bandwidth of the emitted noise. These indicators depend on the design features of machines and mechanisms and are determined in the process of their design. During the operation of the object, in order to reduce the harmful effects of pulse noise, measures can be taken to reduce the pulse levels, change its duration, the frequency of pulse radiation in time and the frequency band of the emitted noise. These changes in the source parameters also affect the change in the processes of formation of reflected noise. For this reason, to assess the acoustic efficiency of the listed design measures, a method for calculating pulse noise should be used, which allows determining changes not only in direct sound, but also changes in the energy characteristics of reflected noise over time, taking into account the space-planning and acoustic parameters of the premises. For example, the method should evaluate the change in the depth of pulse noise modulations with an increase in the frequency of pulse radiation in rooms with different conditions for the formation and change in time of the reflected component of pulse noise.

For this purpose, computational models should be used, including methods for calculating direct sound and reflected noise.

The magnitude of the direct sound levels depends on the shape of the emitted pulse. In the article [3], possible variants of time radiation of energy pulses are considered and formulas for determining their sound power are given.

The formation of reflected noise depends on a large number of factors. For this reason, its calculation is more complicated than the estimation of direct sound. In numerous studies, it has been established that one of the most significant factors affecting the distribution of reflected energy is the nature of sound reflection from fences. According to [4], the reflection of sound from fences can be represented in the form of several characteristic schemes: mirror; randomly directed; directional-scattered; scattered according to Lambert's law (diffuse); mirror-scattered. The adoption of a particular reflection scheme significantly affects the choice of a computational model of reflected noise and methods for its implementation [4].

Among the listed schemes, the most widespread in practice are mirror, diffuse and combined (mirror-scattered) schemes.

In the case of a mirror reflection of sound, calculation models based on the principles of geometric acoustics are used. In this case, the methods of imaginary sources and sound ray tracing are used to calculate the pulse noise [4]. The method of imaginary sources is used for calculating in rooms of a regular rectangular shape, and the method of ray tracing allows calculations to be made in rooms of complex shape.

Diffuse reflection of sound implies the complete scattering of the reflected energy in accordance with the radiation pattern, which is approximated by the cosine dependence according to Lambert's law. When using a diffuse reflection scheme, several methods for calculating the reflected energy have been developed. Some of them are based on the ideas of the diffuse nature of the distribution of reflected energy in the room volume, in which the conditions of uniformity of the energy distribution over the volume and isotropy of the arrival of reflected sound rays at any point of the room are observed [5]. Others proceed from the fact that quasi-diffuse reflected sound fields are formed in the room, in which the condition of isotropy in the angular direction of sound rays is provided, but the uniformity of the distribution of reflected energy over the volume of the room is not observed [6]. In this case, methods based on statistical energy principles for estimating reflected sound fields can be used for calculation [4].

Based on the statistical theory of room acoustics, we have developed methods for calculating pulse noise that implement a diffuse sound reflection scheme. The methods are currently used to assess the noise regime in rooms with pulsed sound sources and to develop measures to reduce the harmful effects of pulsed noise on workers [7].

Our comparisons of the calculation results by methods using mirror or diffuse sound reflection schemes with experimental data in many cases show a significant discrepancy between them. Figure 1 shows as an example the results of comparing calculated and experimental data in long and flat rooms.

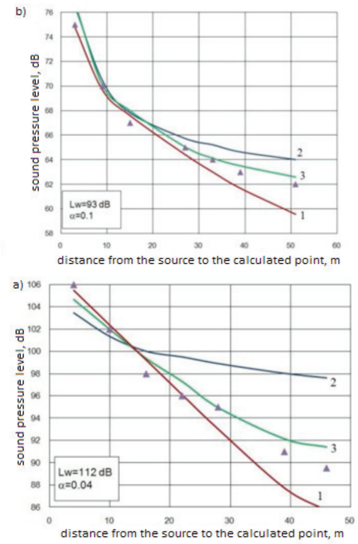

Fig. 1: Experimental and calculated sound pressure levels in a long room (a) with dimensions of 49. 6x2.5x3.5 m and a flat room (b) with dimensions of 72x36x6 m in the octave frequency band with $\boldsymbol{f}_{mid}$=4000 Hz:
***Δ** – experimental data; 1 - calculation for completely diffuse reflection; 2 - calculation for completely mirror reflection; 3 - calculation for a mirror-diffuse reflection scheme*

It is established that the real reflection of sound simultaneously has the signs of mirror and diffuse reflection. For this reason, we proposed to use the combined mirror-scattered scheme of sound reflection from fences as the main one in the calculation methods. With such a reflection scheme, part of the energy that falls on the fence in a mirror is reflected in a mirror, and the other part of it is scattered diffusely. In Figure 1, line 3 indicates the calculation results for a mirror-diffuse reflection scheme, when 20% of the incident mirror energy is diffusely scattered.

Thus, with a mirror-diffuse reflection, a reflected sound field is formed in the room, including the mirror and diffuse components. The processes of the origin and propagation of the energy of these components in the volume of the room differ significantly. For this reason, their calculation should be carried out separately within the framework of a single combined calculation model, which provides for a sequential transition of mirror-reflected energy into diffusely scattered energy [8,9]. In the articles [8,9], a similar combined model was developed for calculating time-constant noise. In this case, the direct sound energy and the mirror component of the reflected noise are calculated by the ray tracing method [10], and the diffusely scattered component of the reflected noise is determined by the numerical statistical energy method [4].

Pulse noise refers to non-constant noise in time and we have proposed another combined calculation model for its calculation. The calculation model and methods of its implementation are considered in the articles [11].

In this case, the sound pressure levels at the calculated points of the premises at any current time ***t*** is determined by the equation

$$L_t = 10\,lg\left[\left(\varepsilon_t^{dir} + \varepsilon_t^{mir} + \varepsilon_t^{dif}\right)c/I_0\right] \qquad (1)$$

where
$I_0 = 10^{-12}$ W/m² is the intensity at the threshold of audibility;
$\varepsilon_t^{dir}, \varepsilon_t^{mir}, \varepsilon_t^{dif}$ are the densities of the sound energy of the direct sound, the mirror and scattered components of the reflected sound at the calculated point of the room at the time t, J/m³;
c is the speed of sound in the air, m/s.

In the most general case, in rooms of complex shape, calculations of direct sound and mirror-reflected energy can be performed using the ray tracing method, and diffusely scattered energy using the Kuttruf equation [12].

When using these calculation methods in the combined model, the sound pressure levels at the i-th calculated point of the room at the time of observation t will be determined by the expression

$$L_{(t)i} = 10\,lg\left\{\frac{1}{I_0 N S_{red}}\left[W_{p(t-r_{dir.i}/c)} K_{dir}\,exp(-m_a r_{dir.i}) + \sum_{k=1}^{K_{mir}} W_{p(t-R_{k.i}/c)}\,exp(-m_a R_{k.i}) \prod_{p=1}^{P} (1-\alpha'_p)^{D_p}\right] + \int_S \frac{I_{(dS,t-\frac{r_S}{c})}(1-\alpha_{dS})\cos\theta\, dS\, exp(-m_a r_S)}{\pi (r_S)^2 I_0}\right\} \qquad (2)$$

In the Eq. (2)
N is the number of rays coming from the source;
S_{red} is the reduced area of the section of an elementary sound energy receiver with the center at the calculated point, m², [8];
$W_{p(t)}$ is the time-varying acoustic power of the pulse emitted, W;
$r_{dir,i}$ is the distance from the source to the calculated point, m;
K_{dir} is the number of direct rays falling into the receiver area;
m_a is the spatial coefficient of sound attenuation in the air, m⁻¹;
$R_{k,i}$ is the distance traveled by the ***k-th*** ray from the sound source to the ***i-th*** calculated point, m;
$\alpha'_p=(1-\alpha_p)(1-\beta_p)$ is the coefficient of sound energy loss by a mirror beam on the ***p-th*** surface as a result of its absorption and partial scattering;
α_p is the coefficient of sound absorption of the ***p-th*** surface of the fence, on which the traced beam fell;
β_p is the fraction of the mirror diffusely scattered energy of the ***k-th*** ray after its reflection from the ***p-th*** surface of the fence;
D_p is the number of acts of incident of the ***k-th*** ray on the ***p-th*** surface in the process of its propagation over a distance $R_{k,i}$;
P is the total number of acts of reflection of the ***k-th*** ray from all surfaces encountered over its path during propagation over a distance $R_{k,i}$ to the ***i-th*** calculated point;
K_{mir} is the number of mirror rays passing through the ***i-th*** elementary volume with the reduced area S_{red};
$I_{(dS,t-r_S/c)}$ is the intensity of the scattered sound energy radiated to the calculated point from the surface ***S, W/m²***;
r_S is the distance from the platform ***dS*** of the surface ***S*** up to the calculated point, m;
θ is the angle of direction from the platform ***dS*** of the surface ***S*** to the calculated point, grad;
α_{dS} is the sound absorption coefficient of the platform ***dS*** of the surface ***S***.

3.RESULTS AND DISCUSSION

The study of the influence of various noise reduction measures in all cases was performed for a room with a size of 60x60x6m in an octave band with f = 2000 Hz with an average sound absorption coefficient of fences α = 0.10. Coordinates of the position of the noise source are 10x30x1.2 (h) m. The scattering coefficient of the reflected sound energy for all cases is assumed to be equal β_p=0.10.

The influence of the shape of the emitted sound energy on the value of the sound pressure levels in the room for the calculated point with coordinates 26x30x1.5(h)m is estimated. The forms of the considered energy pulses are shown in Tab. 1.

Pulse form number	Scheme	Expression for W_t
1	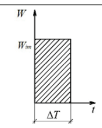	$W_t=W_{im}$ by $0 \le t \le \Delta T$
2	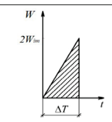	$W_t=\frac{2W_{im}t}{\Delta T}$ by $0 \le t \le \Delta T$
3	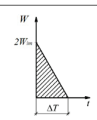	$W_{ti}=2W_m\left(1-\frac{t}{\Delta T}\right)$ by $0 \le t \le \Delta T$
4	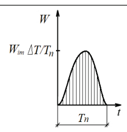	$W_t=W_{im}\,\Delta T/T_n[1-\cos(2\pi t/T_n)]/2$ by $0 \le t \le T_n$
5	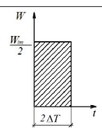	$W_t=W_{im}/2$ by $0 \le t \le 2\Delta T$
ΔT, T_n are the duration and period of the reference pulse (form 1).		

Tab. 1: Emission forms of sound energy pulses

In the calculations, the pulse duration and acoustic power of the radiation were selected from the condition that the radiated energy for all the studied pulse forms should be the same. In this case, for forms 1-3, the pulse duration was equal to ΔT = 0.5 s, for form 4 to ΔT = 1.5 s, and for form 5 to ΔT = 1.0 s. The acoustic power of the reference pulse (form 1 of Tab. 1) was used equal to $W_{im}=W_0 10^{0,1L_{Wp}}$ at L_{wp} = 100 dB, $W_0 = 10^{-12}$ W. The period of action of the source when emitting pulses of different forms was equal to T_p = 1.5 s.

The calculation results are shown in Fig. 2. It can be seen that by changing the shape of the pulse, noise reduction can be achieved. In this case, this decrease does not exceed 3 dB.

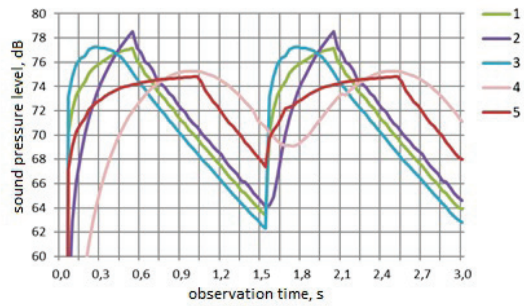

Fig. 2: Changes in the sound pressure levels in the room with different pulse forms (see Tab. 1)

The effect of changing the periodicity of pulse emission on the ratio of the minimum and maximum levels is studied. Fig. 3 shows the results of calculations of sound pressure levels with a change in the periodicity of pulse emission by a rectangular pulse with a duration of 0.10 s. The situations are considered with T_n = 0.60 s и 1.20 s. The studies were performed in the room considered earlier.

It is established that when the pulse periodicity changes, the time averaged (equivalent) sound pressure levels change also: at T_n = 0.60 s – L_{eq} = 63.5 dB; at T_p = 1.20 s – L_{eq} = 61.1 dB. When the periodicity changes, there is a significant change in the difference between the maximum L_{max} and minimum L_{min} levels. The level difference at the periodicity T_n = 0.60 s was 9.1 dB, and at T_n = 1.20 s – 15.8 dB.

The minimum sound pressure level can be considered as a constant background noise, which can significantly depend on the periodicity of pulse emission. The corresponding data are shown in Fig. 3.

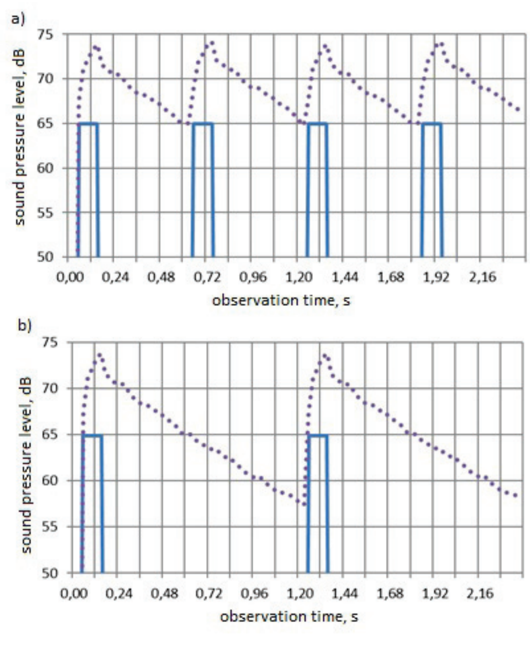

Fig. 3: Change in sound pressure levels at the calculated point at a distance of 16 m from the sound source with a rectangular pulse duration of 0.1 s: a) with the periodicity of a source of 0.6 s; b) with the periodicity of the source of 1.2 s: ________ - direct sound level; ………… - total level of direct and reflected sound

The influence of the position of the calculated points relative to the sound source on the value of the pulse noise is estimated. The calculation results are shown in Fig. 4.

It is established, that equivalent noise levels are equal to: at the distance of $\boldsymbol{r}$ = 5 m – $\boldsymbol{L_{eq}}$ = 64.8 dB; at the distance $\boldsymbol{r}$ = 30 m – $\boldsymbol{L_{eq}}$ = 58.6 dB. The difference between the maximum and minimum noise levels was:
at $\boldsymbol{r}$ = 5 m – $\boldsymbol{L_{max}} - \boldsymbol{L_{min}}$ = 80.0 – 58.1 = 21.9 dB;
at $\boldsymbol{r}$ = 30 m – $\boldsymbol{L_{max}} - \boldsymbol{L_{min}}$ = 69.4 – 57.0 = 12.4 dB.

The minimum noise level as a constant background noise is almost the same at all points of the room. It can be seen that the removal of workplaces from the sound source significantly reduces the difference $\boldsymbol{L_{max}} - \boldsymbol{L_{min}}$, that is, it reduces the harmful effect of pulse noise (see also the article [13]).

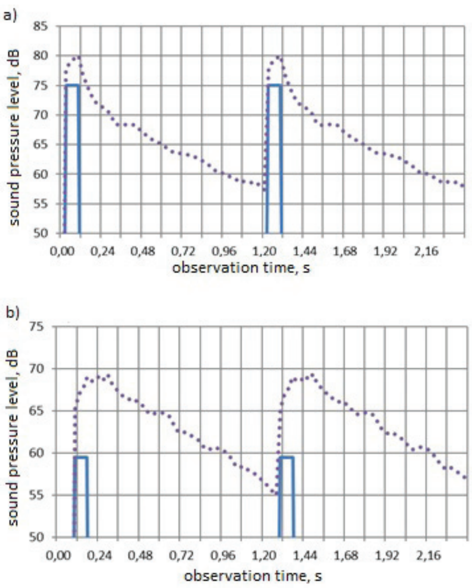

Fig. 4: The change in the sound pressure levels at the calculated point with the periodicity of the sound source 1.2 s and the duration of the rectangular pulse 0.1 s: a) at a distance from the sound source r=5 m (top); b) at a distance from the sound source r=30 m (bottom):______ - direct sound level; ……… - total level of direct and reflected sound

Influence of sound absorption of the room on the characteristics of pulse noise is estimated. Calculation results are shown in Fig. 5.

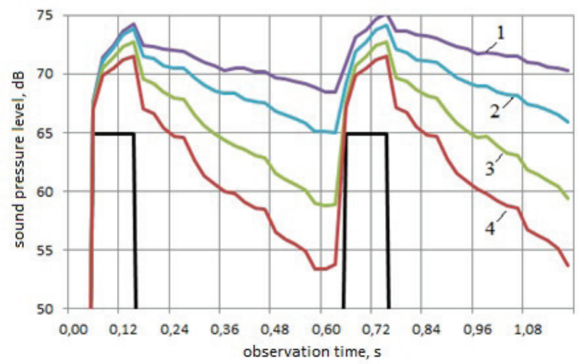

Fig. 5: The change in the sound pressure levels at the calculated point at the distance of r = 16 m from the sound source with the periodicity of 0.6 s and the rectangular pulse duration of 0.1 s at average sound absorption coefficients: 1 - α = 0.05; 2 - α = 0.1; 3 - α = 0.2; 4 - α = 0.3

When calculating, the following results are established. The equivalent sound pressure levels are equal: at $\boldsymbol{\alpha}$ = 0.05 – $\boldsymbol{L_{eq}}$ = 65.6 dB, at $\boldsymbol{\alpha}$ = 0.1 – $\boldsymbol{L_{eq}}$ = 63.5 dB, at $\boldsymbol{\alpha}$ = 0.2 – $\boldsymbol{L_{eq}}$ = 61.3 dB, at $\boldsymbol{\alpha}$ = 0.3 – $\boldsymbol{L_{eq}}$ = 59.2 dB. The difference between the maximum and minimum sound pressure levels was: at $\boldsymbol{\alpha}$ = 0.05 - $\boldsymbol{L_{max}}$–$\boldsymbol{L_{min}}$ = 75.1 – 67.7 = 7.4 dB; at $\boldsymbol{\alpha}$ = 0.1 – $\boldsymbol{L_{max}} - \boldsymbol{L_{min}}$ = 74.1 – 65.0 = 9.1 dB, at $\boldsymbol{\alpha}$ = 0.2 – $\boldsymbol{L_{max}}$–$\boldsymbol{L_{min}}$ =72.8 – 58.8 = 14.0 dB, at $\boldsymbol{\alpha}$ = 0.3 – $\boldsymbol{L_{max}}$–$\boldsymbol{L_{min}}$ = 71.5 – 53.4 = 18.1 dB. It can be seen that with the increase in sound absorption, the difference $\boldsymbol{L_{max}}$–$\boldsymbol{L_{min}}$ increases also, that is, the harmfulness of pulse noise increases (see also the article [13]).

Influence of background noise on the change in pulse noise at the calculated point is estimated. Results are shown in Fig. 6.

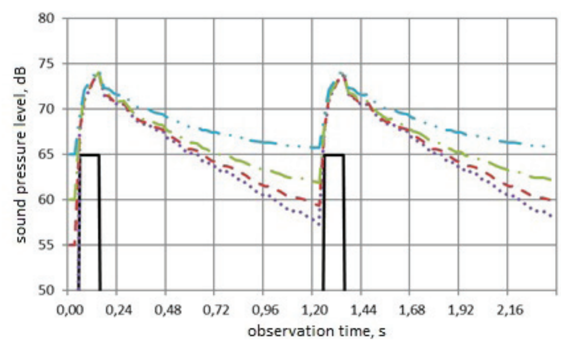

Fig. 6: The change in the sound pressure levels at the calculated point at the distance of r = 16 m from the sound source with the periodicity of 0.6 s of the source and the duration of a rectangular pulse of 0.1 s at different values of background noise: ……. - there is no background noise from other noise sources; - - - - - L_b = 55 dB; _._._._. L_b = 60 dB; __..__..__..__.. L_b = 65 dB

It was found that with an increase in background noise, the difference $\boldsymbol{L_{max}}$–$\boldsymbol{L_{min}}$ decreases. Due to this, the harmfulness of pulse noise is partially reduced (see also the article [13]).

4. CONCLUSIONS

1. The proposed combined method for calculating pulse noise in industrial premises allows us to solve a wide range of tasks for assessing the acoustic effectiveness of measures to reduce harmful effects on workers. The results obtained in solving the problems are consistent with the provisions indicated in the article [13].
2. The computer implementation of the method makes it possible to estimate the space-temporal distribution of pulse noise over the volume of the room and thereby establish the zones of the room where the pulse noise exceeds the normative levels.
3. Reliable information about the size of the pulse noise zone and its characteristics within the zone allows to make a purposeful choice of structural and construction--acoustic means of pulse noise reducing.

REFERENCES

[1] Suvorov G.A., Likhnitsky A.M. Impulse noise and its effect on the human body - L .: Medicine, 1975. – 207 p.
[2] Golovko A., Ledenev V., Antonov A. Measurement method of non-continuous noise in industrial buildings of railway enterprises // Advances in Intelligent Systems and Computing (look in the books). 2020. T. 1116 AISC. Pp. 237-248.
[3] Batsunova A.V. Calculation of noise fields of industrial premises during the operation of periodic noise sources / Questions of modern science and practice. V. I. Vernadsky University. 2015. No. 3 (57). Pp. 46-52.
[4] Antonov A. I., Ledenev V. I., Matveeva I. V., Shubin I. L. Noise calculations in the design of noise protection in industrial buildings // Moscow-Berlin: Direct-Media, 2020. 274 p.
[5] Furduev V. V. Electroacoustics. - Moscow: Gostekhteorizdat, 1948 – - 515 p.
[6] Ledenev V. I. Statistical energy methods for calculating noise fields in the design of industrial buildings. - Tambov, 2000. - 156 p.
[7] Antonov A. I., Batsunova A.V., Kryshov S. I. Noise assessment in rooms with sources of pulsed sound of periodic action // Bulletin of the MGSU. 2011. No. 3-1. Pp. 48-53.
[8] Giyasov B.I. Method for noise calculation under specular and diffuse reflection of sound / Giyasov B.I., Ledenev V.I., Matveeva I.V. // Magazine of Civil Engineering. 2018. No. 1 (77). Pp. 13-22.
[9] Tsukernikov I., Shubin I., Antonov A., Ledenev V., Nevenchannaya T. Noise calculation method for industrial premises with bulky equipment at mirror-diffuse sound reflection // Procedia Engineering. 2017. No. 176. Pp. 218-225.
[10] Ondet A.M., Barbry J.L. Modeling of sound propagation in fitted workshops using ray tracing // Journal of the Acoustical Society of America. 1989. Vol.85. No.2. Pp.787-796.
[11] Antonov A., Matveeva I., Shubin I., Tsukernikov I. Calculation of impulse noise with mirror-diffuse reflection of sound from fences // Akustika. 2019. Vol. 34. Pp. 90-105.
[12] Kuttruff H. Stationare Schallausbreitung in Flachraumen // Acustica.1985. Vol.57. № 2. Pp. 62-70.
[13] Kanshin V. B. Investigation of the impact and consideration of methods for reducing pulse-type noise on the human body // III All-Union Conference on combating noise and vibration: materials of the theses of the reports of the section «The effect of noise and vibrations on the body». Chelyabinsk. 1980. Pp. 24-27.

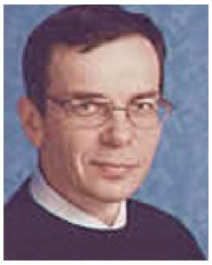

Alexander Antonov *is Doctor of Engineering Science, Head of the Department of Architecture and Building Construction at Tambov State Technical University (Tambov, Russia). Alexander Antonov has been researching sound fields based on the statistical theory of acoustics, developing methods for calculating permanent and intermittent sound fields taking into account various models of sound reflection from fences. Alexander Antonov is the author of more than 50 scientific publications, co-author of textbooks, the author of 14 computers Tertiary programs for the calculation of noise fields and the design of noise protection means. He presented the main results of research at international conferences in Moscow, Samara, Tambov, Vienna (Austria).*

Irina Matveeva *is Ph.D. of Engineering Science, Assistant Professor at the Department of Urban Construction and Highways of Tambov State Technical University (Tambov, Russia). Irina Matveeva is engaged in the study of sound fields based on the statistical theory of acoustics, the development of methods for calculating permanent and non-constant in time sound fields of premises, taking into account various models of reflection of sound from fences. Irina Matveeva is the author of more than 40 scientific publications, co-author of textbooks, monographs, patents, computer programs for the calculation of noise fields. She presented the main results of research at international conferences in Moscow, Saratov, Krasnoyarsk, Tambov.*

Igor Shubin *is Doctor of Engineering Science, Professor, Civil engineer, Director of the Research Institute of Building Physics (Moscow, Russia), Corresponding Member of the Russian Academy of Architecture and Construction Science.*
Igor Shubin is a specialist in the field of building acoustics. He is the author more than 260 scientific publications, including five mographies, five manuals for students of High schools, more than 40 standard documents, 12 author's inventions and patents. Igor Shubin presented the main research results on the international conferences in Australia, Austria, Brazil, Canada, China, Denmark, Germany, Italy, Portugal, Spain, the USA, Finland,, Sweden and other countries.

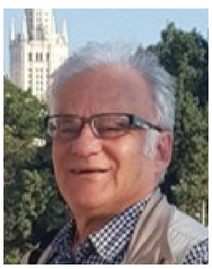

Ilya Tsukernikov *is Doctor of Engineering Science, Professor, Chief Scientific Officer of the Research Institute of Building Physics (Moscow, Russia), Corresponding Member 0f the Metrological Academy.*
Ilya Tsukernikov is a specialist in the field of vibroacoustics, building acoustics, machinery noise and vibration characteristics measurement, calculation and reduction. Ilya Tsukernikov has published over 260 scientific papers, is the co-author of a monograph, tutorial, encyclopedia "Ecometry" and nine copyright certificates for inventions, the developer of more than 30 regulatory and technical documents. He presented the main research results on the international conferences in Australia, Austria, Brazil, Canada, China, Denmark, France, Germany, Italy, Japan, Portugal, Spain, Sweden, USA, and other countries.

Paper No.353/2021

APPROACHES TO CLASSIFICATION OF REDUCTION METHODS OF LOW FREQUENCY NOISE AND VIBRATION OF POWER PLANTS

Andrey Vasilyev

Samara State Technical University, Samara, Russia, avassi62@mail.ru

***Abstract**: The importance of the problem of low-frequency noise and vibration reduction now may be considered as urgent. Increased influence of low-frequency noise and vibration may cause both human health problems and equipment damage. Power plants (internal combustion engines, compressors, heat-exchanges etc.) are one of the main low-frequency noise and vibration sources. The principles of classification of methods of power plants low-frequency noise and vibration reduction are suggested. Author is proposing energetic approach, according of which all the methods and arrangements of reduction may be classified as passive (adaptive and non-adaptive), active and hybrid passive-active. The classification is illustrated by the different examples, including constructions of mufflers and dampers, some of which are developed by author.*

***Keywords:** industrial low frequency, noise, vibration, classification, reduction*

***DOI:** : 10.36336/akustika20214152*

1. INTRODUCTION

Presently noise and vibration impact to the population and to equipment operation in industrial and domestic conditions is increasing every year [10, 14, 16 etc.]. Inadmissible noise levels affection to the housing estates leads to cities population disease growth. It is well known, that the strongest impact produced by noise effects on man is in frequency range from 1000 to 4000 Hz (middle- and high frequencies). But for industrial town environment the most strong noise impact to the city population is first of all caused by low frequency noise (from 20 to 300 Hz). Analysis of population complaints confirms it [16 etc.]. Low frequency noise is spreading for a long distances without significant absorption. Low frequency vibration may cause professional illnesses of workers and workers disease, negative impact to environment and to the health of inhabitant on the territory near to industrial enterprises. Intensive vibration during exploitation of power plants and mechanical noise may cause reduction of attention and increasing of number of mistakes during work.

Among of the main low-frequency noise and vibration sources in conditions of urban territories are:

- Transport (especially automobile internal combustion engine intake and exhaust systems);
- Industrial enterprises and equipment (compressors, ventilators, pumps, mechanical noise etc.);
- Urban and domestic noise sources (noise from offices, shops, stadiums etc; noise generated by office and domestic ventilation systems, TV, broadcasting, musical equipment, human speech etc.).

Analysis of scientific research is showing that power plants of different kinds (compressors, automobile internal combustion engines, pumps, ventilators, heat-exchanges, stationary engines etc.) are one of the main low-frequency noise and vibration sources in conditions of urban territories.

This paper is devoted to developing approaches and principles of classification of methods of power plants low-frequency noise and vibration reduction.

2. DISCUSSION OF THE APPROACHES TO CLASSIFICATION OF REDUCTION OF POWER PLANTS LOW FREQUENCY NOISE AND VIBRATION REDUCTION METHODS

Generally, the classification of low-frequency transport noise and vibration reduction may be based on the variety principles. In Tab. 1 approach to systematization of criteria and types of classification of methods of power plants low-frequency noise and vibration reduction is shown, proposed by the author of this paper.

N	Criteria of classification	Types of classification	Examples
1.	The general way of power plants low-frequency noise & vibration reduction	Reduction in the source of generation	Noise mufflers
		Reduction on the ways of propagation	Acoustic barriers
		Individual means of protection	Electrodynamics anti-noise headphones
2.	The spatial kind of low-frequency noise & vibration source reduction	One-dimensional (ducts)	Gas pressure pulsations compensator in compressor pipeline
		Two-dimensional (plane surfaces)	Compensation of low-frequency noise spreading through the windows inside of buildings
		Three - dimensional	Reduction of low frequency noise and vibration from industrial equipment in working place
		Reduction inside of enclosed volume	Compensation of low-frequency noise inside of automobile passenger compartment
		Reduction in open space	Compensation of low-frequency transport noise in open space of living territory
3.	Periodicity of low-frequency noise & vibration generation	Periodical	Internal combustion engines (ICE) intake & exhaust mufflers
		Non-periodical	Traffic noise barriers
4.	Completeness of low-frequency noise & vibration sources reduction	Reduction of single source	Automobile ICE exhaust noise muffling
		Reduction of several sources	Automobile ICE intake & exhaust noise muffling
		Complex reduction	Complex automobile low-frequency noise & vibration reduction
5.	The kind of noise & vibration source spectrum	Broadband noise	Noise inside of building
		Narrowband (tonal) noise	ICE intake & exhaust noise active mufflers
		Broadband vibration	Vibration dampers
		Narrowband (tonal) vibration	Resonators
6.	The kind of transport	Aircraft low-frequency noise and vibration Separate automobiles, motorcycles	Reduction of noise and vibration by mufflers, vibration isolation etc.
		Noise of automobile transport flows	Noise mufflers, vibration mounts Noise reducing road surfaces
		Trolleybuses	Acoustic barriers
		Railway transport, trams	Acoustic barriers
		Metro transport	Underground vibration isolation
		Water transport	Ship diesel engines noise muffling
		Submarines	Vibration dampers inside of submarine
		Pipeline transport	Pipeline vibration reduction mounts
		Military transport	Active noise & vibration reduction inside of tank
		Space transport	Active vibration reduction

Tab. 1: Systematization of criteria and types of classification of methods of power plants low-frequency noise and vibration reduction

Let us consider more detailed the criteria of classification.

For the **general way of low frequency noise and vibration reduction** the classical approach is to subdivide the methods and means of noise and vibration reduction on the general way (in the source of generation and on the ways of propagation) and on the meaning of reduction methods (collective and individual protection). As collective methods of protection acoustic barriers may be considered, as individual – electronic headphones.

The spatial distribution of low-frequency noise & vibration sources has a great significance when choosing the way of reduction. Low-frequency noise in ventilation ducts (one-dimensional spatial distribution) may be efficiently cancelled by active noise control. Two-dimensional vibration e.g. we may find in the case of vibrating surface. Three-dimensional noise & vibration sources are in automobile passenger compartment (the case of enclosed space) or transport noise from the several highways (the case of open space). The most complicated case is three-dimensional broadband noise & vibration cancellation.

According to **periodicity of low-frequency noise & vibration generation** it should be noted that mainly low-frequency noise and vibration source radiate periodical sound. E.g., intake or exhaust noise of automobile internal combustion engine is caused by piston periodic operation and acoustic waves propagating in intake or exhaust ducts due to flow pulsations, so it has the periodical mechanism of generation. One of the main vibration sources of piston compressors pipelines are low-frequency gas pressure oscillations (pulsations) [8, 9].

Completeness **of low-frequency noise & vibration sources reduction** here is meaning how many low frequency noise or vibration sources have been cancelled. The simplest case is reduction of single source. For example, it may be reduction of automobile internal combustion engine intake low frequency noise by the active system [13, 15].

Reduction of several sources may be illustrated as following. Automobile internal combustion engine radiate both intake and exhaust noise. If reduced it separately by active mufflers strong coherent low-frequency sound radiation near to the air-suctioning pipe and exhaust pipe may appear. Combined control of ICE intake & exhaust noise is suggested in some General Motors patents [17 et al].

The kind of **low-frequency noise & vibration** spectrum may be very differs for different kind of transport or transport systems. E.g., for some cases in order to reduce significantly external engine noise it is enough often to reduce noise only for one or two harmonics [11, 15].

The kind of **transport** presently may be widely subdivided, e.g. aircrafts, automobiles, motorcycles, railway transport, trams, pipeline transport etc. Of course, every different kind of transport requires the separate approach when choosing the method of cancellation.

Sure, the described above systematization of criteria and types of classification of methods of power plants low-frequency noise and vibration reduction is not complete and we may add further some new suggestions for classification.

3. ENERGETIC APPROACH TO CLASSIFICATION OF REDUCTION OF POWER PLANTS LOW FREQUENCY NOISE AND VIBRATION REDUCTION METHODS

According to energetic approach it is suggested to classify power plants low frequency noise and vibration reduction methods as passive, adaptive-passive, active and hybrid active-passive.

Passive methods are traditional and admit that passive elements do not add energy to the system. They may absorb energy or change the impedance of the source such that undesirable energy is not created. Classical passive noise control example – sound absorption and sound isolation. Presently there are significant efforts to increase efficiency of passive control elements. We may either use new materials, or use existing materials in more effective ways (e. g. to absorb energy more effectively). But the negative feature is that passive methods are not sufficiently reduces noise and vibration in low frequency range.

In general passive methods may be subdivided to completely passive and adaptive-passive [1, 5, 14]. Completely passive methods are the most oldest and traditional. E.g., it could be using of absorbing materials or noise barriers. Adaptive-passive methods utilize passive elements which can be tuned such that performance can be optimized over some specified range of conditions. But in this case passive elements again cannot add energy to the system. Adaptive-passive solutions are the most efficient for narrowband applications. For example, the adaptive Helmholtz resonators described by Lamancusa [5] would be used for control of narrowband sound at several running speeds.

Dampers with pliable walls may be considered as adaptive-passive constructions, for example, intake manifold oscillations damper of internal combustion engine [2]. However this construction cannot provide maximal efficiency of oscillations attenuation. Adaptive-passive low-frequency pulsations damper in piston machine pipeline is described in [9]. At least one of the damper walls is pliable. Oscillatory gas movement will extend the walls and all variable flow consumption through the compressor pipeline will be locked within the damper. Another damper construction with pliable capacity is membrane-spring damper [12], where connection between the main and the damper is achieved through the light movable hermetically suspended membrane jointed with elastic high-pliable element, for example, soft spring. Effective pressure impulses attenuation in abutting pipeline occurs due to membrane and spring oscillation and by means of resilient characteristics of spring.

As subclass of adaptive-passive schemes the so-called semi-active control systems may be considered [1, 5]. These systems are built up of passive components with adaptive parameters. However, for semi-active systems the parameters are changed at the same rate as the excitation.

Active noise control systems are capable of putting energy into a system. Classically, these systems use loudspeakers to generate an acoustic wave interfering with the disturbance wave and are making stable system unstable. Active systems are generally relatively complicated compared to passive methods and require a source of power.

Active vibration control (AVC) presently is well developed, especially for transport. For cars AVC may be used for vibrations reduction of engine body, pan, steering wheel, seats etc., see e.g. developments of "Lotus Engineering", "Carl Freudenberg" etc.

Hybrid (active-passive) methods are very promising. It is not the most efficient to implement purely active noise and vibration control systems. In fact most so called active systems are a combination of an active system and passive system, so called active-passive hybrid [4, 6, 7, 14].

4. CONCLUSIONS

The principles of classification of methods of power plants low-frequency noise and vibration reduction are suggested. Author is proposing energetic approach, according of which all the methods and arrangements of reduction may be classified as passive (adaptive and non-adaptive), active and hybrid passive-active. The classification is illustrated by the different examples, including constructions of mufflers and dampers, some of which are developed by author. The classification proposed in this paper is not complete and further we may add some new suggestions for classification. Using of results of this paper may be useful for analyzing and selecting optimal decisions for power plants low-frequency noise and vibration reduction and for further development and application of constructions of pumps plants with reduced vibration levels.

ACKNOWLEDGEMENT

The research described in this paper was supported by the grant of Russian Scientific Foundation, project number: 20-19-00222.

REFERENCES

[1] Bernhard R.J., Hall H.R., Jones J.D. Adaptive-Passive Noise Control. Proc. of "Inter-Noise 92" Congress, 1992, pp.427-430.
[2] Cortemiglio C., Piron M. Absorbeur de pulsations pour le collecteur d'alimentation d'un moteur a combustion interne. Appl. Patent France N 2579667, 1986.
[3] Hansen C.H., Snyder S. D. Active Control of Noise and Vibration. 1997, Cambridge University Press UK. P:1267.
[4] King S.P., Staple A.E. Minimization of Helicopter Vibration Through Active Control of Structural Response. Technical Report, Westland Helicopter Ltd.
[5] Lamancusa J.S. An Actively Tuned, Passive Muffler System For Engine Silencing. "Noise-Con 87" Conference, 1987, pp.313-318.
[6] Mechel F.P. Hybrider Schalldämpfer. German Patent Application No. 40 27 511 C1. Filed: August 30, 1990. Patented: October 2, 1991.
[7] Möser M. Aktive Kontrolle einfacher, selbsterregter Resonatoren. Acustica, Vol. 69, pp.175-184, 1989.
[8] Ogarkov A.A., Vassiliev A.V., Voltchonkov V.I. About the experience of low-rotated piston compressor units vibration reduction. Proc. of the 29 International Congress on Noise Control Engineering "Inter-noise 2000", Nice, France, 2000 August 27-30, Volume 6, pp.3932-3936.
[9] Starobinsky R.N., Vassiliev A.V., Krokhin V.N., Voltchonkov V.I., Desyatkin A.M. Pressure oscillations damper for the suction system of piston machine. Invention certificate 1789748, Russia, 1993.
[10] Tan Y., Guan R., Zhang Z. Performance of accelerated oscillator dampers under seismic loading. Advances in Mechanical Engineering, 2018, 10 (4).
[11] Vassiliev A.V. Compact active noise control units for automobile intake low-frequency noise attenuation. Proc. of "ACTIVE 97" International Symp., Budapest, Hungary, August 21-23 1997, p.587-594.
[12] Vassiliev A.V. Membrane-spring damper of low-frequency gas dynamic pulsation - Proc. of "Transport noise and vibration" International EAA/EEAA Symposium, Tallinn, 1998, pp.43-46.
[13] Vassiliev A.V. Automobile engine low frequency noise reduction by complex using of active noise control method: Proc. of "ISMA 25" the International Noise and Vibration Conference, Leuven, Belgium, September 13-15 2000, Vol.1, pp.37-44.
[14] Vasilyev A.V. Development and approbation of methods and technical solutions of reduction of vibration of power plants and joining mechanical systems. Procedia Engineering. 2015. Vol. 106. pp. 354-362.
[15] Vasilyev A.V. Automobile internal combustion engine low frequency noise reduction using active noise control solutions. Journal "Akustika", Czech Republic, Volume 34, November 2019, pp. 113-117.
[16] Vasilyev A.V., Approaches to the estimation of ecological risk during the impact of acoustical pollutions. "Ecology and Industry of Russia", Moscow, 2018, Vol. 22, N3, pp. 25-27.
[17] Yuan Y. (General Motors, USA): Active Noise Control System for Attenuating Engine Generated Noise. US Patent No. 5,222,148. Filed: April 29, 1992. Patented: June 22, 1993. and: US Patent No. 5,321,759. Filed: April 29, 1992. Patented: June 14, 1994.

Andrey Vasilyev *is Doctor of Technical Science, Professor, honorary worker of higher education of Russia. Presently he is director of the Institute of Ecology of Volga Basin of Russian Academy of Science – Branch of Samara Federal Research Center of Russian Academy of Science and professor of Department of Chemical Technology and Industrial Ecology of Samara State Technical University, head of Povolzhsky Resources Center of Industrial Ecology and Chemical Technology of Samara State Technical University. Author of over 15 books (ecology, environmental protection, acoustics), over 900 scientific papers. Main organizer and scientific manager of ELPIT congresses since 2003 (http://elpit-congress.ru). Editorial and scientific member of a number of famous Russian and foreign scientific journals and editions. Expert of Russian Academy of Science, of Russian scientific fund, of scientific-technical field of Ministry of education and science of Russia etc., grant-holder of DAAD (Germany), Open world program (USA) etc.*

Paper No.354/2021

ASSESSING EXPOSURE TO NOISE IN HIGH DENSITY URBAN AREAS

Irina May, Dmitrii Koshurnikov

Federal Budget Scientific Institution 'Federal Scientific Center for Medical and Preventive Health Risk Management Technologies', Perm, Russia, kdn@fcrisk.ru

***Abstract**: The present research dwells on existing methodical approaches to modeling and noise assessment involving mapping procedures in high density urban areas by the example of urbanized territories in a big city. The suggested approach is based on results obtained via multiple acoustic computations that were performed using specialized software packages. Computed data are interfaced with geoinformation systems for further visualization and quantitative assessment of obtained results. As regards hygienic standardization, hardware and software that are used within the approach allow accomplishing it in high density urban areas. The research concentrates on basic approaches to creating a calculated model as well as parameters of all accomplished computations. The research was performed as per a regular grid within a calculated rectangle sized 0.8*0.8 km and with a step being equal to 25 meters. This calculated rectangle contained 1,122 points. Overall, computed exposure was determined at 486,246 points located in 43 planes. A separate calculated grid corresponded to each of them in order to build a 3D model. This 3D model was made up of 43 planes including one built at 1.5 meter height in a residential area. This 3D model was created for assessing living conditions depending on a height of living (a floor in a residential building). A square of acoustic discomfort was assessed depending on a height as per such a hygienic criterion as noise exceeding 55 dBA and it allowed establishing effects produced by motor transport on noise levels. This research is an initial stage in substantiating violations of citizens' rights for a favorable living environment and human well-being; in future it is planned to perform instrumental measurements and assess health risks.*

***Keywords:** Acoustic computation, geoinformation systems, transport noise, noise exposure*

***DOI:** : 10.36336/akustika20214156*

1. INTRODUCTION

As big cities are being developed at present, fewer industrial objects remain within their boundaries. However, industrial objects are being moved away from cities rather slowly and there are still zones with elevated adverse exposure influenced by them. Rospotrebnadzor organs are responsible for control over living conditions provided for population; results obtained via control activities are annually collected and presented in the State Report "On sanitary-epidemiologic welfare of the population in the Russian Federation". This report contains complete data on the situation with providing sanitary-epidemiologic welfare of the population in the RF in all relevant spheres [1].

Acoustic exposure that is primarily caused by rapidly growing numbers of private vehicles is, together with chemical contamination, among vital aspects of economic activities in dense urban environment. High density in urban areas leads to deteriorating acoustic situation and creates elevated noise levels. Actually industrial objects located in big cities are predominantly objects with 3-5 hazard categories as per sanitary classification [2] and they do not cause significant noise exposure. Noise is produced at such objects mostly due to ventilation and air-conditioning systems that create an overall acoustic picture.

Unfortunately it is not always possible to assess noise exposure levels taking into account a height at which people live via hygienic assessments performed only at bottom layers. Data taken from the State Report "On sanitary-epidemiologic welfare of the population in the Russian Federation in 2020" confirm that the issue is truly vital since there are a lot of people's complaints about exposure to physical factors with noise being a prevailing one (62%) [1].

This research is vital due to a necessity to build a 3D picture showing acoustic exposure and to assess actual noise levels depending on a height exposed people live at.

Our research goal was to test approaches to creating a 3D-picture of exposure in high density urban areas taking into account space-and-planning solutions and architectural aspects of existing and future buildings that can act as screening elements.

2. DATA AND METHODS

Hygienic assessment that took into account a 3D-picture of acoustic exposure was performed at a site where an economic entity was located; this entity belonged to the 4th hazard category as per sanitary classification and operated in radio-electronic industry. The assessment was performed basing on the existing situation and taking into account planned residential building on sites adjoining the examined industrial one. Exposure levels obtained via acoustic modeling are of practical importance both for an economic entity regarding conformity with sanitary legislation and for executive authorities that perform control over living conditions provided for population.

A central micro-district located in Sverdlovsky district in Perm was chosen as an examined territory. This micro-district is a territory with residential blocks consisting of housing with a different number of floors (from 1 to 25). The examined industrial object is located in an area with its square being equal to 10 hectares within a block bounded by 1st Krasnoarmeiskaya street, Sergeya Sukhanova street, Belinskogo street, and 25th October street. There are several buildings on the enterprise territory with a number of floors varying from 1 to 8 (from 5 to 25 meters high) and with noise sources located on them. There are no other outdoor noise sources on the enterprise territory, service transport excluded.

There are existing and planned high residential buildings (up to 25 floors) located on adjoining territories to the east, south-east, and south from the examined site.

All the streets in the area are city motorways with intense traffic loads; they were taken into account as sources of background noise exposure. Fig. 1 is a scheme showing location of the examined enterprise within the selected high density urban area.

The present research involved using databases on linear noise exposure sources (city motorways) and stationary sources belonging to the examined enterprise stating their parameters and noise properties. Databases on noise sources contained data on 74 stationary noise sources belonging to the enterprise (ventilation and air-conditioning systems), and 281 mobile noise sources (linear sections in traffic networks) in Perm. A set of all aforementioned sources is a base for a noise map in any city [3].

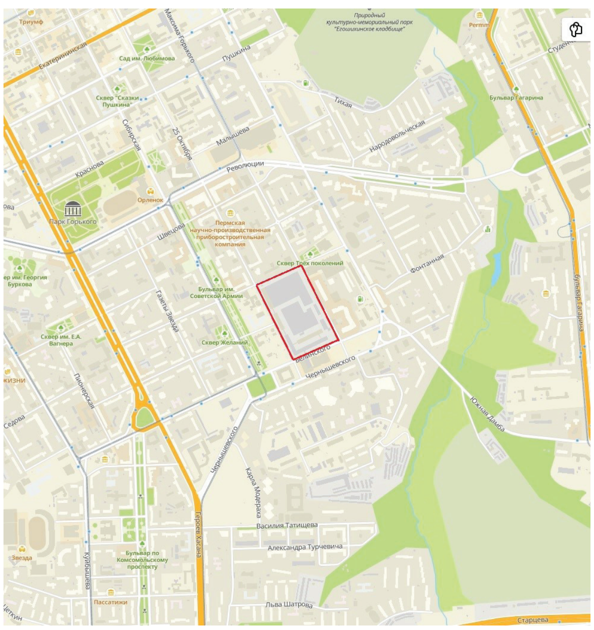

Fig. 1: Location of the examined enterprise within high density urban area

Noise properties for stationary noise sources belonging to the enterprise were determined basing on their profiles and instrumental observations. Noise properties for mobile noise sources were determined as per data on actual traffic loads on the examined motorways obtained from Perm city administration; they were as follows: 1st Krasnoarmeiskaya street, 200 vehicles per hour; Sergeya Sukhanova street, 143 vehicles per hour; Belinskogo street, 495 vehicles per hour; and 25th October street, 246 vehicles per hour. Besides, further studies on traffic flow intensity in greater detail (provided there are relevant data) will allow performing spatial-time analysis and prediction of an acoustic situation [4].

Hygienic assessment was performed basing on results obtained via acoustic computations; these computations were accomplished with a specialized software package aimed at estimating noise propagation over an area. In this research "Ekolog-SHUM" software package was applied; this package is approved on by the Federal Service for Surveillance over Consumer Rights Protection and Human Well-being. The package implements the following regulatory documents: CR 51.13330.2011 Protection from noise. The latest edition of construction rules and regulations SNiP 23-03-2003 (with Alteration No. 1) [5], State Standard GOST 31295.1-2005 (ISO 9613-1:1993) Noise. Sound damping during propagation over a territory. Part 1. Calculation of acoustic absorption in the atmosphere [6].

The research was performed as per a regular grid within a calculated rectangle sized 0.8*0.8 km and with a step being equal to 25 meters. This calculated rectangle contained 1,122 points at 1.5 meter height (a height at which a regular person breathes) in a residential area. Overall, computed exposure was determined at 486,246 points located in 43 planes that corresponded to each calculated grid; it was done to build a 3D model [7, 8, 9].

Overall, to make the model well-planned and visually efficient, it was built with a step being equal to 2 meters as per height.

Hygienic assessment was based on an electronic vector map of Perm made up of electronic layers in *.shp format. These applied layers contain spatial data on used objects in electronic format with all necessary attributive information.

In this research attributive data were taken into account for each type of noise exposure sources, screening objects, and other elements that participated in acoustic modeling. Attributive data on objects participating in acoustic computations contain information on parametric and acoustic properties of a noise source, heights of buildings and constructions included into computations, and other parameters relevant for assessment [10, 11].

ArcGIS 9.3, a specialized GIS software product, was applied to perform hygienic assessment taking into account a height at which noise propagated with subsequent visualization. Attributive data on fields in GIS were prepared in accordance with fields that were to be filled in "Ekolog-SHUM" program an tables with obtained results.

A 3D-picture showing noise exposure was created via combining data from modules built into two applied programs, namely GIS-Ekograf in Ekolog-SHUM and ArcScene in ArcGIS 9.3. These modules allowed transforming computed data for modeling and visualizing results obtained via acoustic computations for further analysis. Results were transformed twice, in a two-dimensional (2D) model and a three-dimensional (3D) one. Zoning in models was accomplished as per hygienic criteria regarding exposure to noise.

Hygienic assessment involved preparing maps of the examined territory with data on estimated existing noise exposure including estimated degree of acoustic exposure and a zone influenced by it.

Results obtained via acoustic modeling were visualized and mapped; it allowed estimating zones with acoustic discomfort and quantitatively assessing noise exposure at reference points located in residential areas where exposed people lived. This model provides an opportunity to perform further research and assess possible health disorders among population living in zones with acoustic discomfort [12].

3. HYGIENIC ASSESSMENT OF RESULTS OBTAINED VIA ACOUSTIC COMPUTATIONS WITH GIS APPLICATION

3.1. Analysis of results obtained via acoustic computations

The initial stage in the research involved performing acoustic computation in bottom layers at 1.5 meters height to assess occurring exposure as well as to visualize transport noise on the territory.

Results obtained via acoustic computations indicate that noise levels within the boundaries of the calculated rectangle in bottom layers exceed hygienic standards (they are higher than 55 dBA in daytime and higher than 45 dBA at night). These noise levels are caused by neighboring motorways. Maximum equivalent noise value was detected near the motorways, predominantly at crossroads, and was up to 72.2 dBA (Fig. 2).

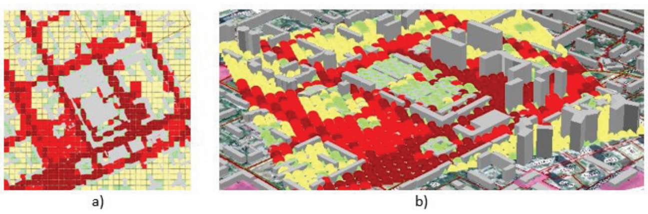

Fig. 2: Zoning of the examined territory as per equivalent noise levels (a is 2D-model, b is 3D-model)

Zones with acoustic discomfort that are shown in Fig. 2 are caused by 55 dBA and 60 dBA isolines that occur along the motorways and yard passages.

Analysis of the obtained results allows revealing regularity in occurrence of zones with acoustic discomfort in bottom layers around high buildings (up to 25 floors), primarily due to multiple acoustic reflections within yard territories.

Fig. 3 shows results obtained via several acoustic computations performed at different heights that are typical for residential buildings: 15 meters for 5-floor buildings; 27 meters, 9-floor ones; 43 meters, 14-floor ones; 61 meters, 20-floor ones; and 75 meters, for 25-floor ones.

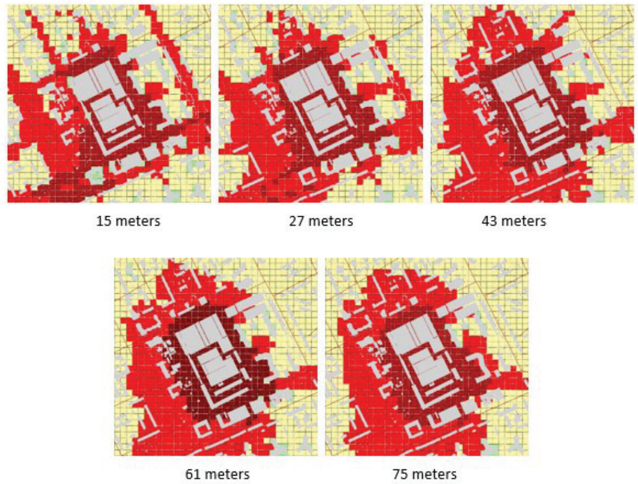

Fig. 3: Zoning of the examined territory as per equivalent noise levels at different heights

It is obvious from schemes shown in Fig. 3 that as a building becomes higher, a contribution made by motor transport into noise exposure goes down and exposure levels occur only due to operations performed at the examined economic entity. Results obtained via several acoustic computations allowed obtaining the following areas with acoustic discomfort (higher than 55 dBA) at different heights: at 1.5 m, 0.29 km^2; at 15 m, 0.38 km^2; at 27 m, 0.40 km^2; at 43 m, 0.43 km^2; at 61 m, 0.41 km^2; at 75 m, 0.41 km^2.

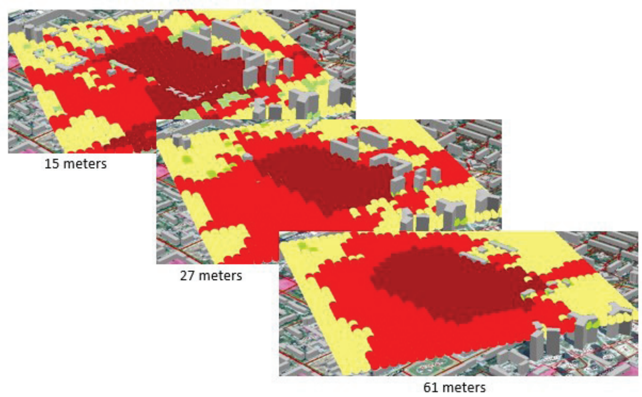

Fig. 4: 3D pictures showing noise exposure at different heights

3D pictures of noise exposure show that a zone with acoustic discomfort (55 dBA and higher) that occurs at heights greater than 1.5 meters predominantly influences high residential buildings located to the east and south-east.

First of all, all the obtained results provide new evidence substantiating that citizens' rights to live in a favorable urban environment are violated.

Research results, taking modeling into account, allowed determining zones and heights at which established hygienic standards were violated as per noise levels. Such a situation is simply impermissible when new residential areas are planned since citizens' rights to live in a favorable environment are not ensured.

Using 3D models allows comprehensive assessment of the existing situation and prediction of a future one taking into account development plans for residential areas in the city. Obtained results and suggested approaches are promising bearing in mind growing traffic on city motorways and urban environment becoming denser [7].

4. CONCLUSION

Hygienic assessment results revealed that hygienic standards were violated as per noise levels at certain points within the examined territory where these levels exceeded 72.2 dBA. This is due to the calculated area being close to neighboring motorways that produce a lot of traffic noise.

Results obtained via hygienic assessment of acoustic exposure indicate that it is necessary to develop short-term and long-term activities aimed at managing noise in dense urban environment. The following activities seem to be optimal in the existing situation:

- traffic schemes need improving; there should be a reduction in a number of vehicles allowed to pass through the city center; public transport routes need optimizing; junctions, crossing, and parking places need modernizing;
- traffic should be allowed to move non-stop due to "green time" and adhering to speed regimes fixed for vehicles;
- noise-insulating glazing should be provided for residential buildings at lower floors (the effect reaches 25-27 dBA).

These results obtained via modeling play a significant role in developing an architectural outline of the city and determining functional zoning of its territory owing to noise factor being truly important for population health.

Modeling results are recommended to be used for:

- submitting them to specifically authorized bodies that are responsible for monitoring and control over the environment;
- informing people about noise contamination on a territory where they live;
- managerial decision-making and developing action plans aimed at health risks reduction.

To apply methodical approaches that involve computing and mapping noise exposure levels via building up and visualizing (3D) an acoustic situation is a unique and promising assessment tool. These approaches, together with risk assessment methodology, allow making long-term predictions of an acoustic situation and providing sanitary-epidemiologic welfare of urban population as per health risk criteria taking chronic exposure into account.

This research is only an initial stage in substantiating violations of citizens' rights for favorable environment. This modeling is a component in a whole set of approaches to identifying noise exposure sources and establishing actual noise exposure levels.

The next stages in the complex research are planned to involve instrumental measurements aimed at verifying the calculated model and establishing actual acoustic exposure. The determined exposure will subsequently be applied to calculate population health risks taking into account living on the model territory under combined exposure to background traffic noise and noise effects produced by the industrial object located there.

REFERENCES

[1] The State Report "On sanitary-epidemiologic welfare of the population in the Russian Federation in 2020"» - URL: https://www.rospotrebnadzor.ru/documents/ details.php?ELEMENT_ID=18266 (September 06, 2021).
[2] SanPiN 2.2.1/2.1.1.1200-03 "Sanitary protection zones and sanitary classification of enterprises, constructions, and other objects".
[3] Bogolepov I.I., Lapteva N.A. Noise map of cities and agglomerations // Engineering and construction journal. – 2010. – P. 5–11.
[4] May I.V., Koshurnikov D.N., Galkina O.A. Space-time analysis of risk to public health under the exposure to urban noise (on the example of Perm) Hygiene and sanitary. 2017. Vol. 96. No. 1. P. 35-39.
[5] CR 51.13330.2011 Protection from noise. The latest edition of construction rules and regulations SNiP 23-03-2003 (with Alteration No. 1).
[6] State Standard GOST 31295.1-2005 (ISO 9613-1:1993) Noise. Sound damping during propagation over a territory. Part 1. Calculation of acoustic absorption in the atmosphere.
[7] Sagdeeva S.N., Chabotaryova E.V. Computer modeling of a three-dimensional map showing noise level in a residential area neighboring to a railway // Collection of articles submitted to the distant International theoretical and practical conference. Voronezh branch of the Russian University of Transport (RUT), "Technosphere safety" department. – 2013. – P. 193–196.
[8] Nikiforov A.V., Ivanov A.V. 3D-modeling and visualization of environmental noise contamination // Housing construction. 2013. No. 6. P. 16-18.
[9] Alekseev V.A., Gorodilov M.A., Korobeynikov A.V., Kuchuganov A.V. The program complex for simulation and analysis of noise propagation on urbanized territories // Intellectual systems in production. 2012. Vol. 2 (20). P. 140-143.
[10] Levanchuk A.V., Kurepin D.E. Hygienic assessment of noise road transport depending on the distance and height from the noise source // Naukobedenye Internet journal. 2014. No. 6 (25). P. 21.
[11] Shubin I.L., Antonov A.I., Ledenyov V.I. Estimation of influence of reflected sound energy on the noise regimeof residential development // Housing construction. 2018. No. 8. P. 18-21.
[12] Yu Semeykin A. Risk assessment for public health from transportation noise (on the example of the city of Belgorod) // In the collection: IOP Conference Series: Earth and Environmental Science. Current Problems and Solutions. 2018. P. 012019.

__Irina May__ is Doctor of Biological Sciences, Professor, Deputy Director for Scientific Work of the Federal Research Center of Medical Preventive Technologies for Managing Public Health Risks (Perm, Russia).
Irina May is the founder of the scientific school of methodology for assessing the risk to public health from the effects of environmental factors. Under the leadership of Irina May, methodological approaches have been developed for hygienic assessment and risk assessment from exposure to physical factors of influence, in particular noise. The developments are based on the optimization of computational and instrumental assessment methods in order to improve the quality of the resulting exposure. Irina May's works are devoted to improving the efficiency of the Rospotrebnadzor service to ensure the sanitary and epidemiological population of Russia.
Irina May is the author of over 250 scientific papers, including about 8 textbooks, teaching aids and 26 patents for inventions. She presented the main results of scientific research at international conferences in Germany, UK, France, Vietnam and other countries.

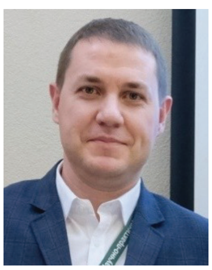

__Dmitrii Koshurnikov__ is senior research fellow of the Department of the system methods for sanitary analysis and monitoring of the Federal Budget Scientific Institution "Federal Scientific Center for Medical and Preventive Health Risk Management Technologies" (Perm, Russia).
Dmitriy Koshurnikov is an expert in the field of acoustic modeling of noise propagation using special programs and visualization using GIS technologies. Dmitriy Koshurnikov is the author of methodological recommendations, research works, databases and patents. Dmitriy Koshurnikov is the author of more than 30 scientific publications. He presented the main results of scientific research at the international conferences in St. Petersburg, Moscow, Krakow (Poland), Minsk (Belarus).

Paper No.355/2021

DEVELOPMENT AND ANALYSIS OF NEW THEORETICAL MODELS OF GAS DYNAMIC PARAMETERS OF LOW-FREQUENCY PRESSURE PULSATIONS IN EXHAUST TRACTS

[a] **Anna Lubyanchenko,** [b] **Aleksandr Shashurin,** [c] **Nickolay Ivanov**

[a] *Baltic State Technical University 'VOENMEH' named after D.F. Ustinov, St. Petersburg, Russia*
[b] *7596890@mail.ru*
[b, c] *Samara State Technical University, Samara, Russia*

Abstract: *The exhaust tract with a silencer installed in it is represented by a design scheme consisting of a set of separate volumes connected to each other by holes or pipes. The following assumptions were made during the calculations: working fluid (combustion products), ideal gas, gas – dynamic parameters are averaged by volume, thermodynamic parameters are constant, the walls of the structure are rigid, the turbulent jet behind the exhaust tract is non-isothermal. The basic equations of the gas-dynamic mathematical model are used: the equation of conservation of matter, the equations of conservation of energy, the equations of state. After the transformations, dependences are obtained that allow us to determine the flow rate at the gas outlet of the dynamic path, pressure, and temperature in various sections of the path.*

Keywords: *gas-dynamic path, gas-dynamic parameters, non-isothermal jet, accepted assumptions, equation of conservation of matter, equations of conservation of energy, equation of state, transformations, flow velocity, flow temperature, pressure*

DOI: *: 10.36336/akustika20214161*

1. INTRODUCTION

Non-muffled exhaust noise is the main and prevailing source of internal combustion engines. Analysis of the noise spectrum of the non-muffled exhaust noise shows that it has a pronounced low-frequency character [1, 7, 8]. The main low-frequency component in the noise spectrum is a multiple of the rotation frequency of the crankshaft of the internal combustion engine. Noise generation processes occur in the engine cylinders. The fuel combustion products located in the engine cylinder, from the moment the exhaust valve moves, begin to flow through the annular gap, first under the influence of a pressure drop, and then under the action of the ejecting movement of the piston. When the exhaust valve moves, the area of the flow section constantly changes. Pressure pulsations occur in the gas outlet tract. To solve the issues related to noise reduction in the gas outlet tract, it is necessary to determine its gas-dynamic parameters: speed, pressure, temperature. It is especially important to determine the listed parameters when installing a silencer in the gas outlet path.

2. CALCULATION SCHEME AND ASSUMPTIONS FOR CALCULATIONS

Depending on the design of the muffler, there may be several volumes in it, through which gas flows and flows into the atmosphere through the exhaust hole.

Fig. 1 shows a scheme for approximate calculations of gas-dynamic parameters in a gas path. This design scheme fundamentally reflects the geometry of the silencers, i.e. a set of individual volumes ($\boldsymbol{W_1,......,W_N}$) , connected to each other by holes ($\boldsymbol{d_1,......,d_N}$) or different pipes.

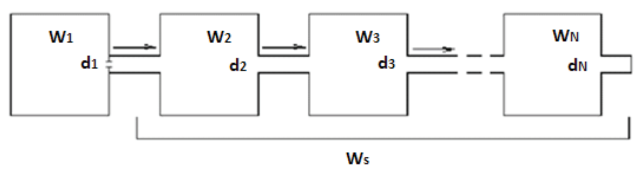

Fig. 1: Design scheme of the silencer: W1 – engine cylinder capacity; W_2 ,W_3,......,W_N – volumes that simulate the design of a silencer; d_1,......,d_N– exit hole diameters, where N – number of volumes

The following assumptions were made during the calculations:

- working fluid (combustion products) - ideal gas;
- gas-dynamic parameters are averaged by volume;
- the thermodynamic parameters are constant;
- the walls of the structure are rigid.

At the first stage, for approximate calculations, the area of the valve bore was assumed to be constant, the processes were considered quasi-stationary and calculations were carried out for several values of pressure in the engine cylinder.

3. MODEL FOR CALCULATING THE GAS DYNAMIC PARAMETERS OF THE SILENCER

The main equations of the gas-dynamic mathematical model are given below [2-6]:

The equation of conservation of matter:

$$m_{01}+m_{02}+\cdots+m_{0i}+\cdots+m_{0N}=m_1+m_2+\cdots+m_i+\cdots+m_N \quad (1)$$

where:

$$\left.\begin{array}{c} m_1=m_{01}-m_{12} \\ m_2=m_{02}+m_{12}-m_{23} \\ \dots \\ m_i=m_{0i}+m_{i-1,i}-m_{i,i+1} \\ \dots \\ m_N=m_{0N}+m_{N-1,N}-m_{N,N+1} \end{array}\right\}$$ the current mass of gas in the ***i-th*** volume;

0 – index of initial values;

i =1....N – the number of volumes in the design scheme of the exhaust tract (Fig. 1).

Energy conservation equations for all volumes:

$$\begin{array}{l} m_{01}c_vT_{01}-\int c_vT_1\,dm_{12}=m_1c_vT_1 \\ m_{02}c_vT_{02}+\int c_pT_1\,dm_{12}-\int c_pT_2\,dm_{23}=m_2c_vT_2 \\ \dots \\ m_{0i}c_vT_{0i}+\int c_pT_{i-1}\,dm_{i-1,i}-\int c_pT_i\,dm_{i,i+1}=m_ic_vT_i \\ \dots \\ m_{0N}c_vT_{0N}+\int c_pT_{N-1}\,dm_{N-1,N}-\int c_pT_N\,dm_{N,N+1}=m_Nc_vT_N \end{array}$$

In the differential form, the energy conservation equations have the form:

$$\begin{array}{c} c_pT_1\,dm_{12}=d(m_1c_vT_1) \\ c_pT_1\,dm_{12}-c_pT_2\,dm_{23}=d(m_2c_vT_2) \\ c_pT_{i-1}\,dm_{i-1,i}-c_pT_i\,dm_{i,i+1}=d(m_ic_vT_i) \\ \dots \\ c_pT_{N-1}\,dm_{N-1,N}-c_pT_N\,dm_{N,N+1}=d(m_Nc_vT_N) \end{array} \quad (2)$$

where:

C_p, C_v – isobaric, isochoric heat capacity, kJ/(kg·K);

T_i – the current temperature in the ***i-th*** volume [°K];

$$\left.\begin{array}{l} m_{12}=\int_0^t g_{12}\,dt \\ m_{23}=\int_0^t g_{23}\,dt \end{array}\right\}$$ the mass of the gas coming from the ***i*** volume to the (***i+1***) volume;

g – consumption of combustion products, kg/s.

Equation of state for the i-th volume:

$$P_iW_i=m_iRT_i \quad (3)$$

where:

R - gas constant, kJ/(kg·K);

P - pressure in the ***i-th*** volume [Pa];

W - i^{th} volume [m^3].

When developing the solution algorithm, a number of transformations of the original system were made, so from equations (2), (3) for the first volume, we obtain:

$$\frac{dT_1}{dt}=\frac{T_1(k-1)g_{12}}{m_1} \quad (4)$$

$$P_1=\frac{m_1RT_1}{W_1} \quad (5)$$

where:

$$m_{12}=\int_0^t g_{12}\,dt \quad (6)$$

$$g_{12}=\begin{cases} c_QF_1\sqrt{\dfrac{2k}{k+1}\dfrac{P_1}{RT_{01}}\left[\left(\dfrac{P_2}{P_1}\right)^{\frac{2}{k}}-\left(\dfrac{P_2}{P_1}\right)^{\frac{k+1}{k}}\right]}, & \left(\dfrac{2}{k+1}\right)^{\frac{k}{k-1}}\le\dfrac{P_2}{P_1}\le 1 \\ c_QF_1\left(\dfrac{2}{k+1}\right)^{\frac{k+1}{2(k-1)}}\dfrac{k}{R}\dfrac{P_1}{\sqrt{T_{01}}}, & 0\le\dfrac{P_2}{P_1}\le\left(\dfrac{2}{k+1}\right)^{\frac{k}{k-1}} \end{cases} \quad (7)$$

where:

$k=\frac{c_p}{c_v}$ adiabatic index.

For any ***i-th*** volume, the analogous equations have the form:

$$m_{01}c_vT_{01}-\int c_vT_1\,dm_{12}=m_1c_vT_1$$

$$\frac{dT_i}{dt}=\frac{k\left(T_{i-1}g_{i-1,i}-T_ig_{i,i+1}\right)-T_i\left(g_{i-1,i}-g_{i,i+1}\right)}{m_i}$$

$$m_i=m_{0i}+m_{i-1,i}-m_{i,i+1}$$

$$P_i=\frac{m_iRT_i}{W_i}$$

For (***N***) volume, the equations have the form:

$$\frac{dT_N}{dt}=\frac{kT_{N-1}g_{N-1,N}-T_Ng_{N-1,N}}{m_N}$$

where:

$$m_N=m_{ON}+m_{N-1,N}$$

$$P_N=\frac{m_NRT_N}{W_N}$$

The consumption of combustion products from volume to volume is determined by the following dependencies:

$$g_{i,i+1}=\begin{cases} c_QF_i\sqrt{\dfrac{2k}{k+1}\dfrac{P_i}{RT_{0i}}\left[\left(\dfrac{P_{i+1}}{P_i}\right)^{\frac{2}{k}}-\left(\dfrac{P_{i+1}}{P_i}\right)^{\frac{k+1}{k}}\right]}, & \left(\dfrac{2}{k+1}\right)^{\frac{k}{k-1}}\le\dfrac{P_{i+1}}{P_i}\le 1 \\ c_QF_i\left(\dfrac{2}{k+1}\right)^{\frac{k+1}{2(k-1)}}\dfrac{k}{R}\dfrac{P_i}{\sqrt{T_{0i}}}, & 0\le\dfrac{P_{i+1}}{P_i}\le\left(\dfrac{2}{k+1}\right)^{\frac{k}{k-1}} \end{cases} \quad (8)$$

The system of equations (4-8), implemented for ***N*** volumes, allows us to determine: ***V***-velocity, ***P***-pressure, ***T***-temperature in various sections of the path, averaged and pulsating gas-dynamic parameters of non-isothermal turbulent jets behind the exhaust path section. Accepted assumptions: the working fluid is an ideal gas, the gas-dynamic parameters are averaged by volume.

4. CONCLUSION

Under the assumptions of non-isothermal turbulent jets, a method is proposed for calculating the following gas-dynamic parameters of a gas pipeline tract when considering low-frequency dynamic pressure pulsations: flow velocity and pressure, temperature in various sections of the tract. The calculations were confirmed by:

- the gas flow rate at the inlet to the muffler of internal combustion engines (ICE) ranged from 50 to 80 m/s, at the outlet about 15-20 m/s, the inlet temperature is 400-500˚C, at the outlet from 200 to 350˚C;
- the speed of the cold jet at the suction of compressors and internal combustion engines was from 10 to 50 m/s, the ambient temperature;
- the speeds of the hot jet of turbojet engines reach 300 m/s, the temperature reaches 1200-1500˚C, the temperature and speed in the mufflers decrease by about an order of magnitude.

ACKNOWLEDGEMENT

The research described in this paper was supported by the grant of Russian Scientific Foundation, project number: 20-19-00222.

REFERENCES

[1] Ivanov N.I.. Shashurin A.E.- Zashchita ot shuma i vibratsii. Pechatnyy tsekh 2019 – 284 p.
[2] Ginzburg. I.P. «Prikladnaya gidrogazodinamika». – Izdatelstvo Leningradskogo universiteta, 1958. – 360 p.
[3] Komkin. A.I. Osobennosti izlucheniya shuma sistemoy vypuska avtotransportnykh sredstv / A. I. Komkin. G. G. Nadareyshvili. S. I. Yudin // Bezopasnost zhiznedeyatelnosti. – 2005. – № 11. – P. 45-49.
[4] Komkin A.I. Tupov V.V. K raschetu akusticheskikh kharakteristik glushiteley shuma // Vestnik MGTU. Ser. Mashinostroyeniye. – 1994. – № 3. – P. 118-124.
[5] Komkin. A.I. Osnovy proyektirovaniya glushiteley shuma transportnykh sredstv / A. I. Komkin. V. V Tupov // Bezopasnost zhiznedeyatelnosti. – 2003. – №1. – P. 15-20.
[6] Lukanin. V.N. Shum avtotraktornykh dvigateley vnutrennego sgoraniya. Metody issledovaniya. puti snizheniya. – M.: Izd. Mashinostroyeniya, 1971. – 267 p.
[7] Vasilyev A.V. Development and approbation of methods and technical solutions of reduction of vibration of power plants and joining mechanical systems. Procedia Engineering. 2015. Vol. 106. pp. 354-362.
[8] Vasilyev. A.V. Automobile internal combustion engine low frequency noise reduction using active noise control solutions. Journal "Akustika", Czech Republic, Volume 34, November 2019, pp. 113-117.

Anna Lubianchenko *is Ph.D. of Engineering Science, Assistant Professor of Department 'Ecology and Industrial Safety' of the Baltic State Technical University 'VOENMEH' named after D.F. Ustinov (Saint-Petersburg, Russia), Acoustics Expert of the LLC (OOO) 'ExpertProject', Director of the LLC (OOO) 'StroyCenter'.*

A. Lubianchenko is a specialist in calculation of architectural and construction acoustics, noise reduction at production and construction facilities. She is a member of the organizing committees of conferences and seminars in the field of acoustics and ecology held in St. Petersburg. A. Lubianchenko is the author of over 15 scientific publications and the co-author of textbooks.

Aleksandr Shashurin *is Doctor of Engineering Science, Professor, Head of Department of Environment and Safety of the Baltic State Technical University 'VOENMEH' named after D.F. Ustinov (Saint-Petersburg, Russia), CEO of the LLC (OOO) 'Acoustic Design Institute'.*

Aleksandr Shashurin is a specialist in calculation and design of noise barriers, noise reduction at production facilities, soundproof booths design and others. He is a member of the organizing committees of conferences and seminars in the field of acoustics and ecology held in St. Petersburg and Moscow. Aleksandr Shashurin is the author of over 40 scientific publications and the co-author of textbooks and teaching aids, the author of 6 patents for noise control devices. He presented the main results of scientific research at the international conferences in St. Petersburg, Moscow, Samara, Hiroshima (Japan).

Nickolay Ivanov *is Doctor of Engineering Science, Professor of Department of Ecology and Industrial Safety of the Baltic State Technical University 'VOENMEH' named after D.F. Ustinov (Saint-Petersburg, Russia), Honored Scientist of the Russian Federation.*

Nickolay Ivanov is the creator of the transport acoustics scientific school. He developed the theory of the transportation vehicles acoustics, proposed the solution to the problems of generating the sound field in low volume, diffraction on complex obstacles, methods of calculation of the sound fields of spatial emitters. Nickolay Ivanov has published over 400 scientific papers, including about 10 textbooks, manuals and monographs. He presented the main results of scientific research on the international conferences in Australia, Austria, Hungary, Germany, Denmark, Italy, Canada, China, the Netherlands, Poland, Portugal, the USA, Finland, Switzerland, Sweden and other countries.

Paper No.356/2021

EXPERIMENTAL STUDY OF DYNAMIC PARAMETERS OF COMPLEX PIPELINE SYSTEM

[a)] Antonina Sekacheva, [b)] Lilia Pastukhova, [c)] Alexander Noskov

[a)] *Hydraulics Department, Ural Federal University, Yekaterinburg, Russia, tonechka_marakulina@mail.ru*
[b)] *Hydraulics Department, Ural Federal University, Yekaterinburg, Russia, l.g.pastuhova@urfu.ru*
[c)] *Hydraulics Department, Ural Federal University, Yekaterinburg, Russia, noskovurfu@yandex.ru*

Abstract: *The article discusses the results of studies of the dynamic parameters of a pipeline connected to a pump, carried out in order to obtain data in full-scale conditions. At this stage of the study, the stationary process of the pump operation, which forms a turbulent flow in the pipeline, was studied. A computational and experimental technique for studying natural frequencies and vibration modes of pipelines of complex spatial configuration has been developed. The adequacy of the developed methods of finite element modeling of dynamic processes in pipeline systems in the frequency range up to 400 Hz has been confirmed.*

Keywords: *noise, vibration, pipeline system, vibroacoustic loads, dynamic parameters*

DOI: *: 10.36336/akustika20214165*

1. INTRODUCTION

A comfortable acoustic environment is one of the most important components of human health and life support in the conditions of modern buildings in large cities. Pipeline systems are mandatory elements of any hydromechanical systems, including water supply, heat supply and fire extinguishing systems in modern high-rise residential buildings (17 or more floors). In individual heating points and roof-top boiler rooms of such buildings, pumping units of large capacities are widely used, the pipeline systems of which are designed to transport working fluid in the range of high flow rates (up to 16 m3/h in vertical main pipelines of multi-storey buildings with roof-top boiler rooms) and pressures (up to 25 atm.). In addition, they are long and are usually laid in utility mines.

During the operation of such pumping units, a number of significant shortcomings in their operation are revealed due to the presence of pulsations of the liquid (water), vibrations of pipelines and injection units.

The main source of vibrations for internal vertical pipelines is mainly the pulsating flow of the medium. Simultaneous and asynchronous operation of several pumps often results in high instantaneous discharge pressures. In addition, high pressures arise in pipelines with pulsating flow in the presence of tight bends. Also, due to fluctuations in the pressure of the medium, the throughput of the pipeline decreases and, accordingly, the productivity of the pumping units decreases.

In construction design, the modal analysis method has been widely used to study the vibrations of building structures. Nevertheless, to solve vibration problems of hydraulic systems, only the methods of experimental and analytical modal analysis were used, described in the works of G. Mikota, A. F. D'Souza, D. J. Ewins, J. C. Wachel, J. D. Tison, X. Li, J. J. Nieter, G. M. Makaryants, T.B. Mironova, A.B. Prokofiev, E.V. Shakhmatova, and many others [1-15].

The results of G. Mikota's work [5-8] provide a theoretical basis for experimental modal analysis of hydraulic pipelines. They demonstrate how standard experimental modal analysis techniques can be adopted for hydraulic pipelines.

G.M. Makaryants, A.B. Prokofiev, E.V. Shakhmatov [14-15] proposed to supplement the analysis of the vibroacoustic response with the calculation of the modal parameters of the pipeline. Instead of experimentally observing modal frequencies and shapes, scientists performed a mathematical calculation to eliminate interference introduced by attached mechanical equipment. In addition, the mathematical calculation of the modal parameters of the pipeline made it possible to derive the modal frequencies of the pipeline from the frequency range of the water hammer due to the displacement of additional supports.

In the works of J.C. Wachel, J.D. Tison [9], estimates of the acceptability of vibrations and troubleshooting methods for reciprocating compressors, pumps and / or pipelines are presented to determine the nature of the causes of their occurrence (pulsation or mechanical resonances). The basic principles of generation and control of pulsation are presented. The authors believe that the key to the design and operation of safe piping systems is to control the pulsation levels, and to separate the mechanical natural frequencies and the pulsation excitation frequencies.

In the works of many of these authors, fluctuations in the pressure of the working fluid are considered as the main cause of high dynamic loads in pipelines. Such fluctuations are caused by pressure pulsations created by the supercharger and hydropercussion phenomena that arise as a result of the operation of the automation equipment. An increased level of fluctuations in the pressure of the working fluid leads to vibration and noise of the hydraulic systems and their possible destruction.

In the works of G.M. Makaryants, devoted to the study of the knee-like shape of the pipeline section, also adopted a large set of design assumptions, such as the absence of viscosity in the liquid, low flow rate, and the lack of consideration of the wave properties of the working fluid. The calculation was carried out for small diameters, low flow rates and working fluids of technological pipelines of aircraft (AMG-10), which is irrelevant for solving vibroacoustic problems in the construction industry.

2. METHOD

The well-known analytical expression for the natural frequencies of the hydraulic subsystem of the pipeline can be written in the form [16]:

$$f_n = \frac{c_{red} \cdot (2n-1)}{4 \cdot l_{pipe}} \tag{1}$$

where
n – the number of the natural frequency;
l_{pipe} – the total pipeline length;
c_{red} – the sound speed in the working fluid, taking into account the ductility of the pipeline walls.

Traditionally, an isolated approach is used to determine the dynamic characteristics of the hydraulic and mechanical parts of the system. For example, when calculating fluid pressure pulsations along the length of a pipeline, only the boundary conditions of the hydraulic subsystem are taken into account in the form of impedances of the connected circuits. The influence of the pipeline itself on the flow of the working medium is assessed indirectly, for example, from the point of view of the change in the velocity of propagation of waves of the working fluid in the pipeline in comparison with the speed in an open medium. Consideration of the physical properties of the pipeline material, which consists in a decrease in the speed of sound in the pipeline due to the ductility of the pipeline wall, is made according to the formula:

$$C = \frac{c_0}{\sqrt{1+\frac{d_{in} \cdot E_{water}}{\delta_{pw} \cdot E_{pipe}}}}, \tag{2}$$

where
c_0 – the velocity of propagation of pressure waves in a liquid enclosed in a pipeline with absolutely rigid walls (for water at 22 °C c_0 =1486,2 м/с);
d_{in} – the inner diameter of the pipeline;
δ_{pw} – the pipeline wall thickness;
E_{water} – the modulus of elasticity of the working fluid (water);
E_{pipe} – the elastic modulus of pipeline material.

2.1. The main results of the previous stage of the study

The previous part of the study was devoted to the study of the intrinsic dynamic characteristics of the elements of pipeline systems, as well as the study of the influence of the geometric parameters of the straight section of the pipeline (length, diameter, wall thickness) on its own vibroacoustic characteristics [1-4].

To determine the required characteristics (frequencies and modes of natural vibrations), the calculation of the vibrations of a straight section of the pipeline by the method of modal analysis was used. As a modeling tool, the ANSYS software package was chosen, which implements the finite element method for solving a wide range of problems, including the problems of studying coupled vibrations of an elastic structure and fluid.

Based on the results of a computational experiment, analysis of the influence of the geometry of the pipeline on its own vibration parameters and multiple regression analysis, the following conclusions were made:

1. The functional relationship between the value of the first frequency of natural vibrations and the length, diameter, wall thickness of the pipeline section is nonlinear (power-law).
2. The regression model of the dependence of the first natural frequency on two parameters (length l and outside diameter d of the pipeline section) has the form:

$$F_1 = 80.592 \cdot l^{-1.688} \cdot d^{0.468} \tag{3}$$

The coefficient of determination in this case is $R^2 = 0.879$.

3. The regression model of the dependence of the first natural frequency on three parameters (length l, outside diameter d and wall thickness of the pipeline section δ) has the form:

$$F_1 = 27.569 \cdot l^{-1.658} \cdot d^{1.093} \cdot \delta^{-1.25} \tag{4}$$

The coefficient of determination in this case is $R^2 = 0.893$.

4. The value of the coefficient of determination (the quality of the correspondence of the regression model to the experimental data) is the higher, the greater the number of factor signs.

2.2. Initial data and formulation of a physical experiment

In this experiment, the dynamic parameters of a pipeline connected to a centrifugal pump were investigated. At this stage of the study, the stationary process of operation of the pump, which forms a turbulent flow in the pipeline, was studied.

Fig. 1 shows a schematic diagram of the structure of the pipeline system under study. To study the vibration parameters of long pipelines, commensurate with the real engineering networks of residential buildings, the complex pipeline system (D_{out} = 114 mm) in the laboratory of the Department of Hydraulics was adapted, the axonometric diagram of which is shown in Fig. 2. This pipeline system is complex, consisting of many straight and elbow-shaped sections. The pipeline material is steel. The working fluid is water, t = 12 ° C, density

$\boldsymbol{\rho}$ = 1000 kg / m^3, the speed of sound in the working medium $\boldsymbol{c}$ = 1453.8 m / s.

The experimental setup includes a 4NDV type I pump with a rotational speed of n = 1490 rpm, which sucks in water from underground pool 2 and supplies it to the pipeline system (network). From the network, the water is drained into the measuring tank 3 and from it through the trays it returns to the pool. The installation is equipped with a pressure gauge 4 on the discharge line 5, a vacuum gauge 6 on the suction line 7, electrical measuring instruments 8. The flow can be measured using a diaphragm 9 with a differential pressure gauge and a secondary device. The flow rate was measured using a measuring tank 3 by the volumetric method. The flow rate is regulated by a valve 10 installed on the discharge pipeline.

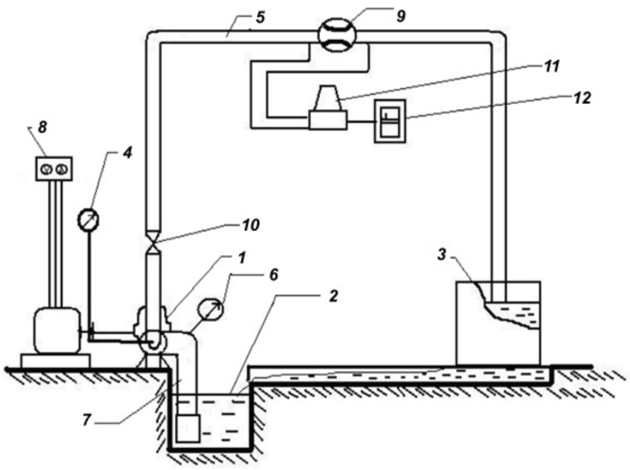

Fig. 1: Schematic diagram of the installation: 1 - pump; 2 - underground reservoir; 3 - measuring tank; 4 - manometer; 5 - discharge line; 6 - vacuum gauge; 7 - suction line; 8 - electrical measuring instruments (voltmeter, ammeter); 9 - diaphragm; 10 - gate valve; 11 - differential pressure gauge DM; 12 - secondary device

At this stage, the total vibrations of the pipelines were determined when they were loaded by pressure pulsations of the working fluid (water) and structural vibrations transmitted through the pipeline structure from the pump.

Fig. 2: Axonometric diagram of the investigated pipeline system

The amplitude and frequency of forced vibrations in many cases are of decisive importance for assessing the strength and stability of pipelines and injection installations; in general, vibrations can occur simultaneously in all directions. A fairly complete characteristic of the vibration state of a structure can be obtained by measuring the amplitude and frequency of vibrations in three mutually perpendicular directions.

The measurements were carried out using a vibration analyzer (Fig. 3) and a data collector for vibration monitoring SD 12-M (with the AR28I accelerometer, shown in Fig. 3, and standard equipment), which passed state tests and entered into the State Register of Measuring Instruments (No. 21953-01) as a device for measuring, collecting and analyzing vibration parameters.

a) *b)*

Fig. 3: Experimental measurement equipment:
a) the vibration analyzer VAST SD-12M; b) the accelerometer AR28I

The studies were carried out at three flow rates. The flow rate was set by the position of the valve on the discharge pipe of the pipeline ($\boldsymbol{Q}$ is the volumetric flow rate; $\boldsymbol{P_{man}}$ is the pressure in the manometer located on the discharge pipe of the pump). Performance characteristics of system (Pump type I 4NDV):

$\boldsymbol{Q}$ = 103,3 m3 / h; $\boldsymbol{P_{man}}$ = 2,05 atm.;
$\boldsymbol{Q}$ = 99,1 m3 / h; $\boldsymbol{P_{man}}$ = 2,20 atm.;
$\boldsymbol{Q}$ = 76,1 m3 / h; $\boldsymbol{P_{man}}$ = 2,35 atm.

2.3. Control point selection

The measurement points (accelerometer settings) were chosen so that the relative distance from the point to the support (equal to the ratio of the distance from the point to the support to the distance between the supports) varied from 0 to 0.5, and characteristic points were also determined (before the bend, at the bend, after the bend). A total of 62 control points were selected (Fig. 4-9).

a) *b)*

Fig. 4: Scheme of drawing control points. First floor plan

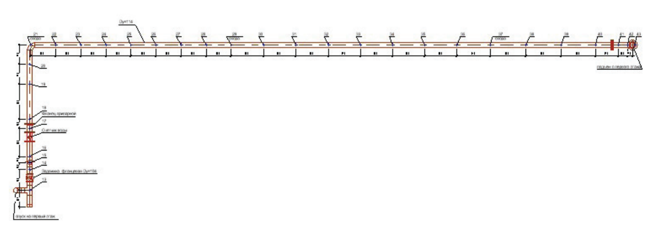

Fig. 5: Scheme of drawing control points. Second floor plan

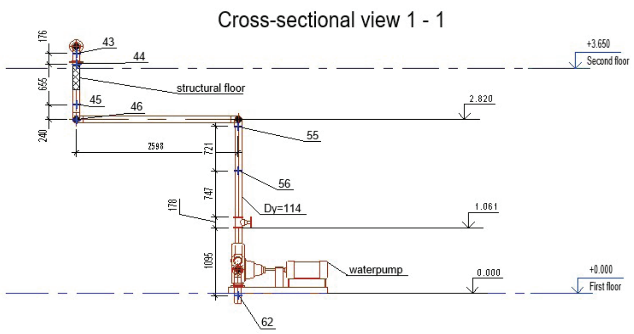

Fig. 6: Cross-sectional view 1 - 1

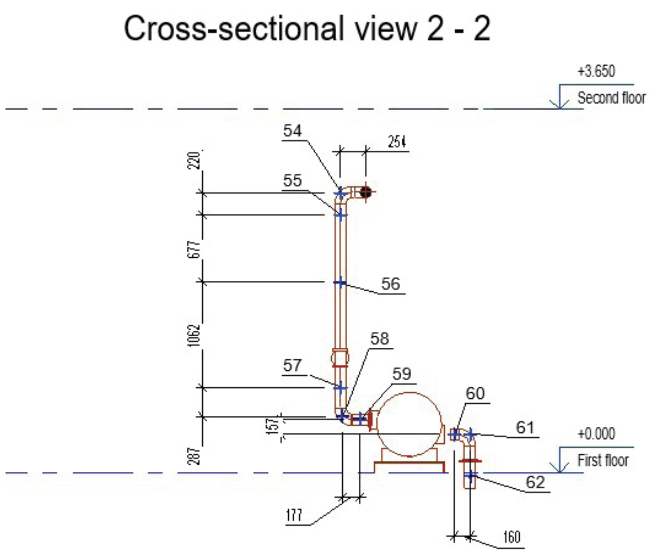

Fig. 7: Cross-sectional view 2 - 2

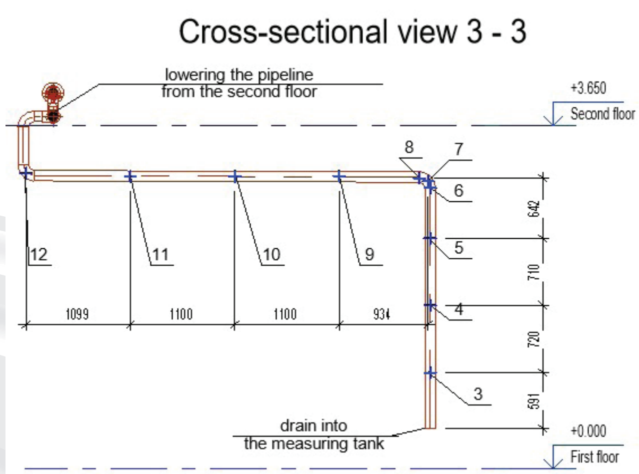

Fig. 8: Cross-sectional view 3 - 3

When studying the vibration of this complex pipeline, a straight-line section 5.78 m long with two supports at the ends at points 37 and 29 was selected for detailed study, and vibration acceleration spectra were plotted at the points under study numbered 37, 35, 33, 31, 29. Point 35 lies at a distance ¼ of the span length (1.46 m from the support at point 37), point 33 lies at a distance ½ of the span length (2.9 m from the supports at points 37 and 29), point 31 lies at a distance ¾ of the span length (4, 34 m from the support at point 37). The choice of these points was determined by the fact that they are characteristic and most fully describe the behavior of the system under vibration load conditions. Geometrical parameters of the pipeline section: outer diameter $\boldsymbol{d_{out}}$ = 114 mm; inner diameter $\boldsymbol{d_{in}}$ = 104 mm; section length l = 5.78 m; wall thickness $\boldsymbol{\delta}$ = 5 mm.

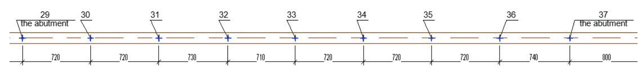

Fig. 9: Scheme of the calculated straight-line section

3. RESULTS

3.1. Analysis of spectrograms of vibration accelerations in the middle of a straight section of the pipeline for three estimated flow rates

The resulting accelerograms at point 33 (1/2 span length) in three directions for three different flow rates in the system are shown in Fig. 10 - 12.

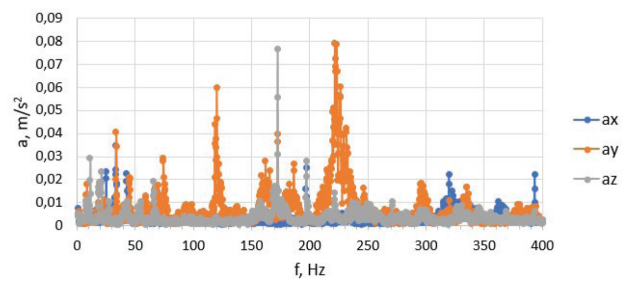

Fig. 10: Spectrogram of vibration acceleration of the pipeline system at point 33 at the maximum design flow rate $\boldsymbol{Q_{max}}$

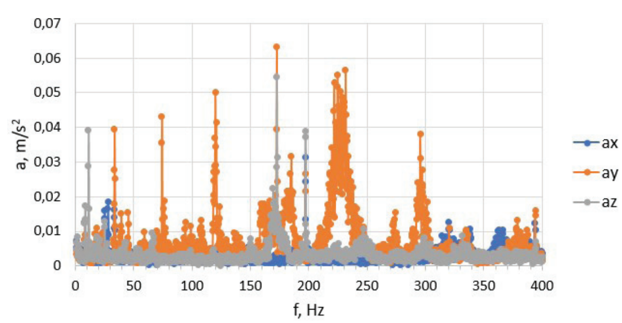

Fig. 11: Spectrogram of vibration acceleration of the pipeline system at point 33 at the average design flow rate **Q**

Stable peaks for all three flows are observed at frequencies of 10, 32, 45, 120, 170, 185, 198, 225, 295, 335, 395 Hz, and peaks at frequencies of 10, 32, 75, 120, 175, 185, 198, 225, 235, 295 Hz have the greatest amplitudes. In addition, spectral analysis showed the presence of one clearly expressed resonance zone in the studied frequency range located from 205 to 250 Hz with maxima at frequency 225 and 235 Hz. At the same time, in all cases, the largest value of spectral density (that is, the fundamental tone of the oscillations) falls on the frequency of 225 Hz.

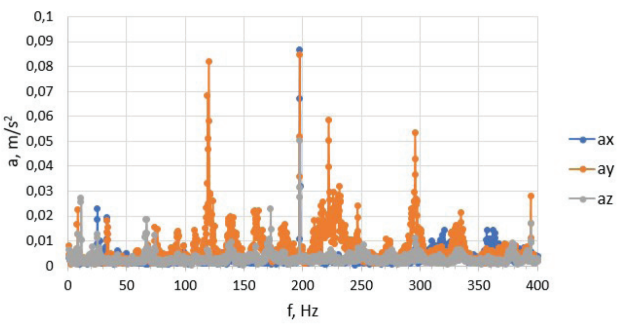

Fig. 12: Spectrogram of vibration acceleration of the pipeline system at point 33 at the minimum design flow rate $\mathbf{Q}_{min}$

Based on the analysis of the obtained spectrograms, the following conclusions were made:

1. At the minimum liquid flow rate in the system, the highest vibration accelerations are observed in those points of the section that are not fixed. As the flow rate in the pipeline increases, the maximum vibration accelerations move to the reference points. This may be due to the fact that a higher flow rate increases the rigidity of the pipeline and thereby reduces vibrations at unsecured points of the investigated area. However, increased vibrations in the first support in the direction of fluid movement (point 37) on the investigated straight section can occur due to turbulent phenomena that arise in the adjacent knee section (point 42-43). Therefore, it is also important to model and study the turbulence phenomena occurring in the sections of the pipeline with elbow-like shape.

2. Vibration accelerations in the X direction (longitudinal vibrations) are much less than vibration accelerations in the Y and Z directions (lateral vibrations) at different flow rates, but have the same order. This suggests that lateral vibrations are more significant in this case. However, in the works of Yu. A. Demyanov [17, 18] on the vibrations of strings, ropes, membranes, thin rods and thin-walled pipes, taking into account the dynamic effects on them, it is shown that, under certain circumstances, resonance phenomena between longitudinal and transverse vibrations are possible, which can cause the destruction of structures.

3. The largest peak of vibration acceleration, equal to 0.38 m / s², is observed in the Z direction at point 37 (support) at an average flow rate. This means that the values of vibration accelerations do not depend on the values of flow rates. However, the flow rate is a concomitant factor that must be taken into account and taken into account, since it can affect the parameters of the structure (for example, stiffness) and the hydrodynamic processes that occur when the fluid moves through the pipeline. Figs. 13-15 show the graphs of changes in the relative vibration displacement along the length of the investigated straight section. The value of the relative vibration displacement

$$\bar{A} = \frac{A}{x}, \tag{5}$$

equal to the ratio of the vibration displacement at the design point A to the amplitude of the support oscillations x (point 29), which has the minimum values of vibration acceleration, was recorded at all calculated points of the investigated area (point 29 - point 37).

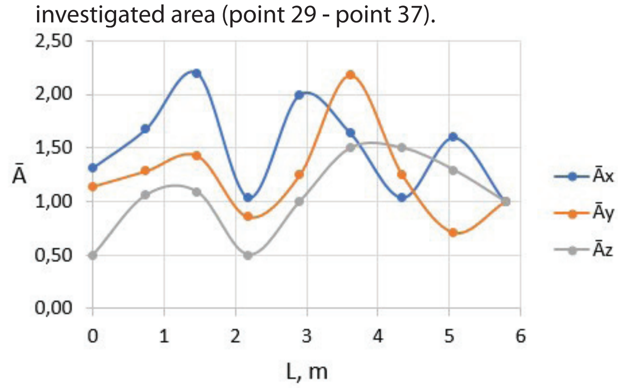

Fig. 13: The graph of the change in the relative vibration displacement along the length of the investigated straight section at the maximum flow rate

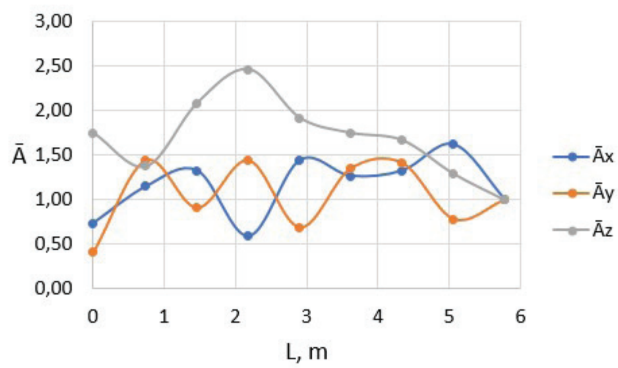

Fig. 14: Graph of changes in the relative vibration displacement along the length of the investigated straight section at an average flow rate

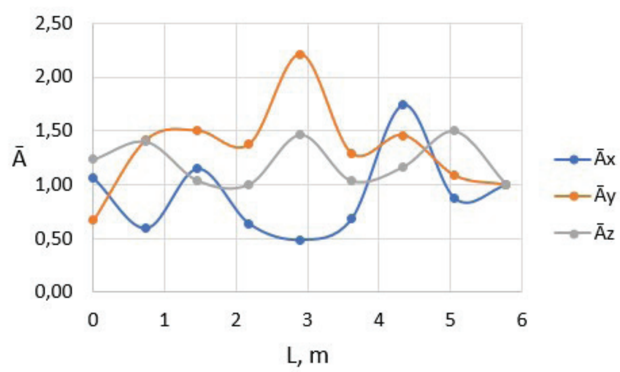

Fig. 15: Graph of changes in the relative vibration displacement along the length of the investigated straight section at a minimum flow rate

From the graphs of the change in the relative vibration displacement along the length of the section, it can be seen that with an increase in the flow rate, the relative vibration displacement in the X direction also increases and its oscillations become clearly pronounced. It can be assumed that at high flow rates, the greatest vibration load is created by the pressure pulsations of the working fluid, which means that the pipeline system for the most part should be considered at high flow rates as hydraulic.

3.2. Comparison of the analytical model with the experimental results

To determine the adequacy of the developed analytical model, the first frequencies of natural vibrations were calculated for straight sections of the pipeline with randomly selected geometric parameters (104 cases) in three ways: using the existing technique, using the developed analytical model, using modal analysis in the ANSYS software package.

Then the relative errors of the known and developed analytical models were calculated in relation to the values calculated using the specified software package. It was found that in 78 cases out of 104 (75%), the developed analytical model describes the values of the first frequencies of natural vibrations, which are closer to the experimental ones, in comparison with the known analytical model. Based on the results of the analysis, it was concluded that the formula for calculating the natural frequencies of the existing technique works with greater accuracy at small diameters and small lengths of sections. The developed analytical model provides high accuracy over a wide range of diameters and lengths of pipeline sections.

The natural frequencies of the section were also calculated using the formula (4) of the developed analytical model, since it showed greater accuracy than that of the known one when calculating a straight section with a diameter of 114 mm. It was found that the first and subsequent natural frequencies, calculated by multiplying the first frequency by a factor (2n-1), where n is the number of the natural frequency, are equal to: $\boldsymbol{f_1}$ = 36 Hz; $\boldsymbol{f_2}$ = 107 Hz; $\boldsymbol{f_3}$ = 178 Hz; $\boldsymbol{f_4}$ = 249 Hz; $\boldsymbol{f_5}$ = 321 Hz; $\boldsymbol{f_6}$ = 392 Hz. The obtained natural frequencies are very close to the peaks of the forced load, which allows us to speak about possible resonance phenomena at the following frequencies 32, 120, 175, 245, 320, 395 Hz.

Experiment	Developed analytical model $F_1 = 27.569 \cdot l^{-1.658} \cdot d^{1.093} \cdot \delta^{-1.25}$	Well-known analytical model $f_n = \frac{c_{red} \cdot (2n-1)}{4 \cdot l_{pipe}}$
32	36	57
120	107	-
175	178	172
245	249	286
320	321	-
395	392	400

Tab. 1: Comparison table of natural frequencies (Hz)

4. CONCLUSION

Experimental development of methods for studying the dynamic characteristics of pipelines has been carried out.

1. An experimental study of the vibroacoustic characteristics of a complex pipeline system of spatial configuration was carried out, vibroacoustic spectra were constructed.
2. A computational and experimental technique for studying natural frequencies and vibration modes of pipelines of complex spatial configuration has been developed.
3. The adequacy of the developed methods of finite element modeling of dynamic processes in pipeline systems in the frequency range up to 400 Hz was confirmed.
4. It was concluded that with an increase in the diameter, there is a high probability of occurrence of radial resonant oscillations in the range of operating frequencies. Therefore, the calculation of such operating modes is impossible using only the theory of vibrations of strings, ropes, membranes, thin rods and thin-walled pipes, and the distribution of hydrodynamic parameters over the diameter cannot be neglected.

The adequacy and effectiveness of the developed analytical model is assessed by comparing it with the known analytical model and the data of a computational experiment.

The created methods, in comparison with the existing ones, allow:

- to reduce the complexity of the calculation;
- to expand the range of geometric characteristics (lengths, diameters, wall thicknesses of the pipeline section) for calculating your own design parameters;
- to increase the accuracy of calculating the natural frequencies of vibrations by an analytical method and to reduce the relative error of calculations of this kind from 0.8 ± 0.6 to 0.3 ± 0.2 in 75% of cases;
- to apply the developed analytical model in the practice of engineering design of vibration resistance of pipeline systems.

ACKNOWLEDGEMENTS

The reported study was funded by RFBR, project number 19-38-90284.

REFERENCES

[1] Sekacheva, A., Noskov, A. and Pastukhova, L.: Investigation of natural frequencies of complex water pipelines, AKUSTIKA, VOLUME 38, p. 3-8., 2021
[2] Nazzal, A. S. E., Sekacheva, A. A. and Noskov, A. S.: Method for vibration measurement in pipelines of residential buildings, IOP Conference Series: Materials Science and Engineering, VOLUME 972(1), 2020, [012070]
[3] Sekacheva, A., Pastukhova, L., and Noskov, A.: NUMERIC ANALYSIS OF VERTICAL PIPELINE ELEMENT NATURAL FREQUENCIES, AKUSTIKA, VOLUME 32, p. 272-278, 2019
[4] Pastukhova, L.G. & Sekacheva, A. A.: CHISLENNYY ANALIZ DINAMICHESKIKH KHARAKTERISTIK ELEMENTA TRUBOPROVODNOY SISTEMY MNOGOETAZHNOGO ZHILOGO DOMA [NUMERICAL ANALYSIS OF DYNAMIC CHARACTERISTICS OF THE ELEMENT OF THE PIPELINE SYSTEM OF A MULTI-STOREY RESIDENTIAL BUILDING], International Journal for Computational Civil and Structural Engineering, VOLUME 4, p. 137-146, 2016
[5] Mikota, G, Manhartsgruber, B, Kogler, H and Hammerle, F.: Modal testing of hydraulic pipeline systems, Journal of Sound and Vibration, VOLUME 409, p. 256–273, 2017
[6] Mikota, G.: Modal analysis of hydraulic pipelines, Journal of Sound and Vibration, VOLUME 332, p. 3794–3805, 2013
[7] Mikota, G.: Experimentelle modal analyse hydraulischer netzwerke (Experimental modal analysis of hydraulic networks), Proceedings of the VDI-Schwingungstagung (Wiesloch), VOLUME 1, p. 15–26, 2004
[8] Mikota, G.: Duality applied to experimental modal analysis, Proceedings of the Bath Workshop on Power Transmission and Motion Control (Bath), VOLUME 1, p. 111–122, 2004
[9] Wachel, J. C. and Tison, J. D.: Vibrations in reciprocating machinery and piping systems, Proceedings of 23rd Turbomachinery Symposium (College Station), VOLUME 1, p. 242–272, 1994
[10] D'Souza, A. F. and Oldenburger, R.: Dynamic response of fluid lines, Journal of Basic Engineering, VOLUME 86, p. 589-598, 1964
[11] Li, X., Wang, S. and Liang, R.: Modal analysis of two typical fluid-filled pipes in aircraft, Proceedings of the International Conference on Fluid Power and Mechatronics (Beijing), VOLUME 1, p. 468–472, 2011
[12] Nieter, J. J. and Singh, R.: Acoustic modal analysis experiment, The Journal of the Acoustical Society of America, VOLUME 72 (2), p. 319–326, 1982
[13] Ewins, D. J.: Modal Testing: Theory, Practice and Application (Baldock: Research Studies Press Ltd.), 2000
[14] Makaryants, G. M., Prokofiev, A. B. and Shakhmatov, E. V.: Vibroacoustics analysis of punching machine hydraulic piping, Procedia Engineering, VOLUME 106, p. 17–26, 2015
[15] Mironova, T. B., Prokofiev, A. B. and Sverbilov, V. Y.: The finite element technique for modelling of pipe system vibroacoustical characteristics, Procedia Engineering, VOLUME 176, p. 681–688, 2017
[16] Sapozhnikov, V.M., Lagosyuk, G.S.: Strength and testing of pipelines for hydraulic systems of airplanes and helicopters, Moscow, Mashinostroenie, 243 p, 1973
[17] Demyanov, Yu. A.: Influence of stiffness on the transverse-longitudinal movements of musical strings, Applied Mathematics and Mechanics, VOLUME 75(1), p. 95-100, 2011
[18] Demyanov, Yu. A.: On the theory of transverse-longitudinal vibrations of prestressed beams and rods, Reports of the Academy of Sciences, VOLUME 401(4), p. 476-478, 2005

Antonina Sekacheva *is a Postgraduate Student and Assistant of the Hydraulics Department of the Ural Federal University named after the first President of Russia B.N. Yeltsin (Yekaterinburg, Russia).*
Antonina Sekacheva is the author of over 10 scientific publications. She presented the main results of scientific research at the international conferences in Bath (UK), Moscow, St. Petersburg, Yekaterinburg. She created a master's thesis on the topic: "Numerical analysis of the length and shape of an element of a pipeline system, made with the aim of predicting and eliminating the possibility of the occurrence of resonant modes." The topic of work is directly related to the solution of one of the tasks related to noise and vibrations in pipeline systems.

Lilia Pastukhova *is Ph.D. of Engineering Science, Assistant Professor of Hydraulics Department of the Ural Federal University named after the first President of Russia B.N. Yeltsin (Yekaterinburg, Russia).*
Lilia Pastukhova is a specialist in noise protection, numeric analysis of vibration impact and others. She is a member of the organizing committees of conferences and seminars in the field of safety problems of civil engineering and ecology held in UrFU. Lilia Pastukhova is the author of over 60 scientific publications and the co-author of textbooks and teaching aids. She presented the main results of scientific research at the international conferences in Cambridge (UK), Cheske-Budievice (Czech Republic), Yekaterinburg.

Alexander Noskov *is Doctor of Engineering Science, Professor, Head of the Hydraulics Department of the Ural Federal University named after the first President of Russia B.N. Yeltsin (Yekaterinburg, Russia), RAASN adviser.*
Alexander Noskov is known as a leading expert in the field of developing the fundamentals of the theory and methods of mathematical modeling of various tasks of civil engineering, as well as energy-saving hydraulic devices for various purposes. He is author of 150 scientific and methodical works, several monographs and textbooks, in particular, "Fluid and Gas Mechanics", 7 inventions. Inventions are implemented at the enterprises of the Sverdlovsk region and other regions. Under his leadership, an educational program has been developed in postgraduate studies in the specialty "Hydraulic machines and hydropneumatic assemblies", he is also a member of the Council for the protection of dissertations for the degree of Doctor of Science in this specialty. Alexander Noskov is participant of scientific and methodological international programs implemented in cooperation with educational institutions of the United Kingdom, the Netherlands, Italy and others. He is a member of the organizing committee of all-Russian and international conferences in the field of energy saving and safety of civil engineering, and the chief editor of the «Russian Journal of Construction Science and Technology».

Paper No.357/2021

HIGHWAY RECREATION AREAS NOISE PROTECTION AS A ROAD SAFETY IMPROVING FACTOR

[a)]Danil Bazarov, [b)]Yuri Elkin, [c)]Alexey Abramov, [d)]Oleg Gogiberidze

[a, b, c, d)] Moscow Automobile and Road Construction State Technical University (MADI), Moscow, Russia
[a)] dan.cartel@mail.ru [b)] elkiny@mail.ru, [c)] abramov-54@yandex.ru, [d)] kristyfire@mail.ru

***Abstract**: The article discusses the problem of noise pollution on the territory of driver's recreation areas on roads of various categories. Recreation areas can be both a separate element of roadside infrastructure and an integral part of multifunctional road service areas (MRSA). Recreation areas are not equipped with means of protection against traffic noise, the increased level of which makes it difficult for drivers to have a good rest. Obviously, this circumstance increases driver overwork while driving, thereby increasing the likelihood of road traffic accidents (RTA). The article proposes to protect recreation areas and MRSA with the help of noise protection screens (NPS), the installation of which will improve the quality of rest (including short-term) of drivers. At the same time, for the noise protection of a specific MRSA (M-4 Don highway), a screen with a height of 3 m was proposed, and its acoustic efficiency was calculated. Also, in the article, as a first approximation, an assessment of reducing the risk of road accidents by reducing the level of traffic noise at the rest areas of drivers is given.*

***Keywords:** traffic noise level, multifunctional roadside service area, driver's rest area, noise protection screen, driver overwork, traffic safety, road traffic accident.*

***DOI:** : 10.36336/akustika20214173*

1. INTRODUCTION

The acoustic impact of traffic flows is one of the most important problems of protecting the human environment, which are solved in the design of transport construction facilities.

In areas where major highways pass, as a rule, transport is the main source of noise, which in most cases requires the development of noise protection measures not only for places of permanent residence of a person, that is, residential buildings [1, 2], but also, apparently, for places of his temporary being in the process of life. The temporary locations of a person, obviously, can be attributed to both multifunctional road service areas (MRSA) with places for rest and parking, and separate recreation areas on motorways of various categories.

At these facilities, a high-quality recreational potential for recreation of various durations should be provided for drivers of both trucks and buses (professionals) and personal cars (amateurs).

Unfortunately, the increased level of traffic noise makes it difficult for drivers to have a good rest, which increases the neuropsychic (psychoemotional) load on the human body, thereby increasing the likelihood of an accident while driving.

2. MULTIFUNCTIONAL ROAD SERVICE AREAS

Multifunctional areas of road service of motor roads are buildings, structures, structures, other objects intended for servicing road users along the route (gas stations, bus stations, bus stations, hotels, campings, motels, catering points, service stations, similar objects), as well as the places of rest and parking of vehicles necessary for their functioning.

Currently, 126 MRSA are open on toll roads of Rosavtodor, 7 MRSA operate on free federal highways of Rosavtodor, 41 areas are being designed, 271 areas are planned for construction in the coming years [3]. The plans until 2030 include the placement of additional 744 similar objects, including 222 multifunctional road service areas and 426 recreation areas, 50 food outlets, 166 service stations.

MRSA are subdivided into types (A, B, C) - depending on the functional purpose and into categories (1-4) - depending on the capacity or performance of the facility [4]. The current classification of multifunctional road service areas is shown in Tab. 1.

TYPE A (petrol station, recreation area)	TYPE B (gas station, recreation area, catering, service station)	TYPE B (gas station, recreation area, catering, service station, motel)
Type «A»	Type «B»	Type «C»
A-1	B-1	C-1
A-2	B-2	C-2
A-3	B-3	C-3
A-4	B-4	C-4

Tab. 1: Classification of multifunctional road service areas

The division of the MRSA into categories is adopted depending on the capacity of the road service facilities that are part of the areas, namely:

- First category – *«large»*, high capacity of road service facilities, traffic intensity over 35 thousand transport units per day;
- Second category – *«medium-large»*., the capacity of road service facilities is above average, the traffic intensity is from 15 to 35 thousand transport units per day;
- Third category – *«medium-small»*., the capacity of road service facilities is below average, the traffic intensity is from 5 to 15 thousand transport units per day;
- Fourth category – *«small»*., low capacity of road service facilities, traffic intensity less than 5 thousand transport units per day.

3. HUMAN OVERWORK IMPACT ON ROAD SAFETY

3.1. Cars

The American Automobile Association («AAA») has investigated the effect of driver overwork on the likelihood of being involved in a road traffic accident [5]. Over the course of several months, more than 3,500 volunteer drivers, whose cars were equipped with video cameras, participated in the research.

Tired drivers have been found to be responsible for one in 10 road accidents. At the same time, it is noted that sleepy drivers are an «underestimated problem», as they endanger not only their own lives, but also the lives and health of other traffic participants.

During the observation period, 3,500 volunteer drivers were involved in road accidents about 700 times. Driver overwork was a contributing factor in 9,5 % of these accidents, which is much higher than previously thought in studies (no more than 1 to 2%).

According to the AAA survey (January 2018), 29 % of drivers admitted that they often had to drive in a state of extreme overwork, when their eyes «just stick together». It should be noted that almost 70 % of «sleepy» accidents took place during the day, and half of them involved drivers aged 16 to 28 years.
It has been found that just two or three hours of lack of sleep more than quadruples the risk of an accident, and a sleepy driver is almost indistinguishable from a drunk driver [5,12].

3.2. Trucks

Research carried out by a group of experts from the International Road Transport Union (IRU) identified the causes of accidents involving trucks and other road users in the European Union [6].

In total, the experts investigated 624 road accidents. The analysis of these accidents showed that the cause of 85,2 % of all accidents is the human factor (the fault of the truck driver, the fault of the driver of the car, the fault of the pedestrian, etc.). Among other causes of road accidents (with corresponding weight coefficients, %), the following were identified: weather conditions is 4,4 %, infrastructure is 5,1 %, technical malfunction of vehicles is 5,3 % (Fig. 1).

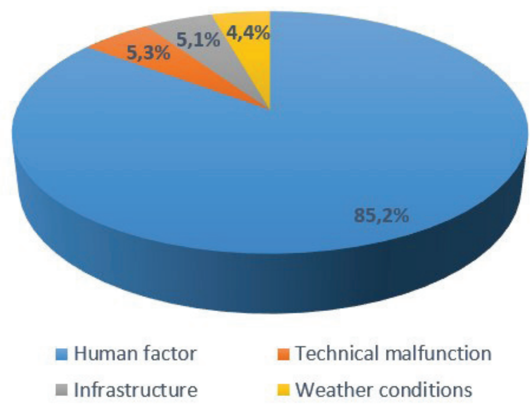

Fig. 1: Main causes of road traffic accidents involving trucks in the European Union

It should be noted that here the term «truck involvement» is not identical to «truck fault» in an accident. For example, truck drivers are responsible for the above accidents due to human factors (85,2 % of all accidents) in only 25 % of cases.

Further, all types of accidents were divided into 5 configurations, namely [6]:
1-st configuration of the accident: accident at an intersection;
2-nd configuration of road accident: accident in traffic jam;
3-rd configuration of the accident: accident due to departure to another lane;
4-th configuration of the accident: accident due to violation of the maneuver during overtaking;
5-th accident configuration: accident involving one truck.

For each configuration, experts identified the causes of road accidents with appropriate weighting factors.

For the purpose of this work, of all the possible causes of accidents in all five configurations, the most interesting are «overwork» causes, namely:
– inattention of drivers;
– overwork/drowsiness of drivers.

In the article authors opinion, it is these causes of road accidents that can be caused by the difficulty of full rest for drivers during long journeys due to the effect of an increased level of traffic noise on the MRSA.

At the same time, if such a cause (factor) of an accident as «overwork/drowsiness» is unambiguously caused by impaired rest (sleep) of drivers, then the factor «inattention» requires, in our opinion, the use of a lowering weight coefficient equal to 80 %.

Indeed, the factor of «inattention» as a cause of an accident can be determined not only by the nervous and mental state of tired drivers, but also, for example, by talking on a mobile phone, working with a navigator, smoking, etc. while driving.

Considering the assumptions proposed by the authors of the article and the results of studies by experts from the European Union [6], the weight coefficients of the causes of road accidents (for all five configurations) were determined for two selected factors: «overwork/drowsiness» and «inattention» (Tab. 2).

Causes (factors)	Configuration / Weight coefficients (%)					
	1-st	2-nd	3-rd	4-th	5-th	Average value
Inattention (considering 80%)	2,6	12,8	3	0	8,4	5,36
Overwork/sleepiness	0	2,3	1,5	8,8	18,6	6,24

Tab. 2: Weight coefficients of the causes of road accidents by the factor's «inattention» and «overwork/drowsiness»

Analyzing the data from the report of the IRU experts [6], it is possible to determine the total values of the weight coefficients of the «overwork» causes of road accidents (factors «inattention» + «overwork/drowsiness»), which are presented in Fig. 2 (also for all five configurations).

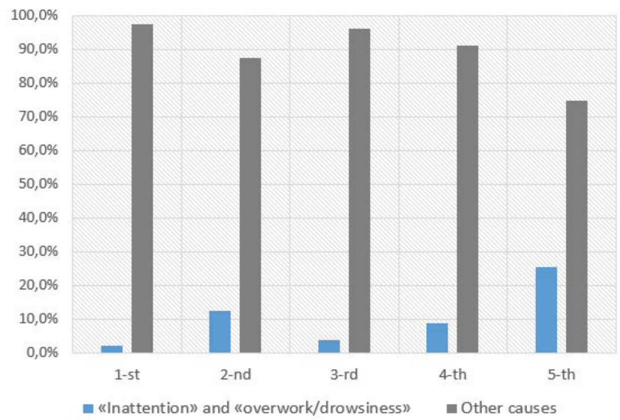

Fig. 2: Weight coefficients (%) of «overwork» and other causes of road accidents with trucks in the European Union

It should be noted that of 624 investigated accidents, only in 9,4 % of cases the main cause of the accident was overwork or drowsiness of the driver, of which 37 % were fatal.

In 68 % of cases when overwork is the main cause of an accident, a truck and another vehicle (a car, two-wheeled vehicle, two-wheeled vehicle with an engine, etc.) were involved in the accident; and in 29 % of cases, only one truck was involved in an accident. Most accidents occurred between 2:00 and 2:59 a.m. (most likely, at the time when the driver's biorhythms were at their lowest point), as well as between 3:00 and 3:59 p.m. (almost at the end of the working day). Almost 90 % of all accidents due to driver overwork occurred on highways or roads between cities; in the cities themselves, accidents due to such reasons are extremely rare [6,12].

At the same time, it is very difficult to prove that the main cause of a road traffic accident is driver overwork. There are various stages of overwork - from slight overwork to falling asleep [12]; in addition, experts can often make decisions only on the basis of an accident seen at the scene or on the basis of information received from drivers and witnesses of the accident [6].

Thus, summarizing and analyzing the above data, the following conclusions were made:

– it can be assumed that the main reason for the occurrence of «overwork» factors that cause road accidents are disturbances in proper rest/sleep of drivers (both professionals and amateurs) due to the increased level of traffic noise at the MRSA and individual recreation areas;

– it is accepted that the «overwork» factor is a generalized indicator of the sum of two factors of road accidents – «inattention» and «overwork/drowsiness», while, if the weighting factor of the factor «overwork/drowsiness» is taken as 100 % according to the statistical data of reports [5, 6], then for the weighting factor of the factor «inattention», a decreasing factor of 80 % (0,8) is additionally used;

– it was found that the weight coefficients of the causes of road accidents by the factor of «carelessness» are in the range from 0 % to 10,2 % (with an average value of 4,28 % for all five configurations, with a maximum of 10,2 % in the 2-nd configuration) , according to the factor «overwork/drowsiness» is from 0 % to 18,6 % (average value is 6,24 % with a maximum of 18,6 % in the 5-th configuration), and the sum of the weight coefficients of these factors, that is, the value of «overwork» factor will be from 2,1 % to 25,3 % (average value is 10,52 %);

– therefore, to reduce the likelihood (risk) of road accidents due to «overwork» factors, it is necessary to reduce the level of traffic noise at MRSA and recreation areas by installing noise protection screens (NPS).

4. TRAFFIC NOISE REDUCTION ASSESSMENT IN MULTIFUNCTIONAL ROAD SERVICE AREAS WHEN INSTALLING A NOISE PROTECTION SCREEN

To assess the reduction of traffic noise in the MRSA, it is necessary to calculate the noise characteristic of the traffic flow (NCTF), NPS parameters and equivalent sound levels (SL) at design points (DP) at recreation areas of multifunctional areas. As an object of research, a section of the M-4 Don highway (from 777 km to 933 km) was selected, on which 10 multifunctional road service areas will be located; for calculations, the right (from Moscow) part of the MRSA at 863 km was chosen for the calculations (Figure 3). The developed recommendations will be similar for the left side of this MRSA.

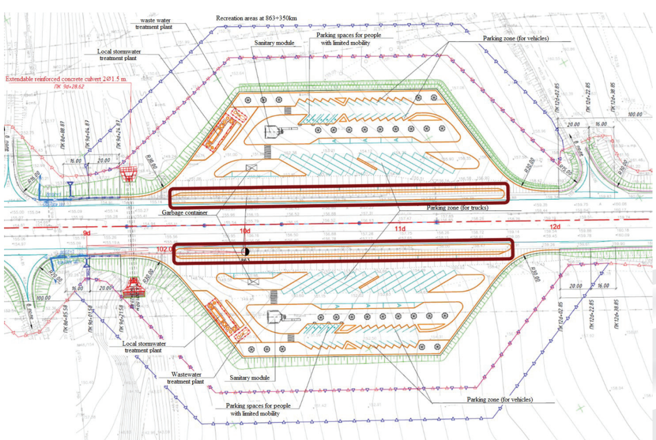

Fig. 3: Plan of the projected MRSA at 863 km of the M-4 Don highway.

The specified calculation will be carried out in accordance with the approaches and provisions set forth in Rules set (RS) 276.1325800.2016 [7] and in Industry road methodology document (IRMD) 218.2.013 - 2011 [8].

According to the forecasted data for 2021 and 2031, the traffic intensity on this section of the M-4 highway will be [9]:
– 2021 is 62 thousand red. units/day
– 2031 is 79 thousand red. units/day

The composition of the movement with a free travel system:
– cargo cars – 37 %
– passenger cars – 63 %.

The composition of the movement with a toll travel system:
– freight cars – 42 %
– passenger cars – 58 %.

As can be seen from the above results, the traffic intensity of vehicles is high, while the composition of the traffic flow is dominated by cars (from 58 to 63 %).

NCTF in the form of an equivalent sound level (LAeq7,5) at 7.5 m from the axis of the near strip for roads to be reconstructed is calculated by the formula [7, 8]:

$$L_{Atr\ 7,5} = 50+8{,}8*lg\ N,\ \text{dBA},$$

where
N is the estimated traffic intensity, vechicles/h, in the day or night periods of time, determined by:
$N_D = 0{,}076\ N_{day}$, vehicles/h,
$N_N = 0{,}039\ N_{day}$, vehicles/h,

where
$N_{D,N}$ is average annual daily traffic intensity, vehicles/day.

$N_D = 0{,}076*62000 = 4712$, vehicles/h,

$N_N = 0{,}039*62000 = 2418$, vehicles/h.

$L_{Atr7,5d} = 50+8{,}8*\lg 4712 = 82{,}3$ dBA

$L_{Atr7,5n} = 50+8{,}8*\lg 2418 = 79{,}8$ dBA

$L_{Atr7,5average} = \frac{82{,}3+79{,}8}{2} = 81{,}1$ dBA

The decrease in SL, dBA, by a noise shield on the path of sound beams from the road to the DP is calculated by the formula:
where
ΔL_{screen} is screen noise reduction, dBA.

The acoustic efficiency of the NPS depends on the difference in the lengths of the sound beam paths ***δ***:

$$\delta = a+b-c$$

where
δ is the difference in the lengths of the paths of the sound beam, m;
a is the shortest distance between the acoustic center of the traffic flow and the upper edge of the screen, m;
b is the shortest distance from the upper edge of the screen to DP, m;
c is shortest distance from the acoustic center of the traffic flow to the DP, m.

The height of the DP and the height of the acoustic center of the traffic flow are taken equal to 1 m.

The height of the NPS proposed in the article is h_{screen} = 3 m, and its length l_{screen} = 210 m according to the dimensions of the projected MRSA.

Consequently, the calculated [7, 8] acoustic efficiency of NPS is:

$$\Delta_{Lscreen} = 18{,}2+7{,}8\ \log\ (0{,}43+0{,}02) = 15{,}5\ \text{dBA}.$$

Thus, this screen will reduce the level of traffic noise in the DP MRSA on 863 km of the M-4 highway to 66,8 dBA in the daytime and up to 64,3 dBA at night.

5. HEALTH RISK ASSESSMENT OF DRIVERS AT RECREATION AREAS FROM TRAFFIC NOISE

At present, the only normative document that makes it possible to assess the health risks of the population (human) from the impact of traffic noise is, perhaps, Methodological Recommendations (guidelines) 2.1.10.0059-12 [10] with the same name.

These recommendations determine the types of health disorders (nervous system, circulatory system, diseases of the ear and mastoid) of the population (that is, people living in any residential area) from the effects of traffic noise in the daytime (from 7:00 a.m. to 11:00 p.m.) and night (from 11:00 p.m. to 7:00 a.m.) time.

The population in [10], obviously, means people who are not at their workplaces. Taking into account the purpose of this article, drivers (both amateurs and professionals) who do not participate in road traffic, that is, those who rest in the recreational areas of the MRSA, can also be attributed to such categories.

Regarding daytime and nighttime, it can be assumed that the concept of «rest for drivers» (regardless of the time of day) will, in fact, be identical to the concept of «nighttime» for the population, since these time intervals are intended for good rest/sleep. Indeed, according to the norms of the time for driving and resting [11], the driving time should not exceed 9 hours during a period not exceeding 24 hours from the moment of the start of driving; at the same time, no later than 4,5 hours from the moment of starting to drive the vehicle, the driver must take a break for not less than for 45 minute rest.

Therefore, for our purpose, it is permissible to use the approaches outlined in [10] only for the nervous system, that is, for disturbances in proper rest/sleep of drivers on the MRSA due to an increased level of traffic noise.

Threshold values of the harmful effects of traffic noise are presented in Tab. 3.

Effect	Threshold, dB	Evidence degree
Restlessness in sleep (sleep fidgeting)	32	High *
Disruption of the course of various stages of sleep, «fragmentation» of sleep	35	High
Complaints	35	Average *
Waking up at night and / or very early in the morning	42	High
Prolonged falling asleep (difficult falling asleep)	*	High
Sleep fragmentation, reduced sleep time	*	High
Growing up average	42	High
Restless movements during sleep	42	High
Disturbed sleep feeling	40	High
Using sedatives or other medications	42	High

** Effects for which, according to WHO experts, sufficiently reliable data have been accumulated, are attributed to a high degree of evidence; effects for which data are limited are attributed to a medium degree.*

Tab. 3: Public health effects of nighttime noise exposure found in epidemiological studies (extract) [10]

The calculation of the risk of disturbances in the functioning of the nervous system is carried out for average (between day and night noise) values:

– before installation of NPS – 81,1 dBA;
– after installation of NPS – 65,6 dBA.

Calculations of the reduced health risk index associated with the level of exposure to traffic noise are shown in Fig. 4 and Tab. 4. This indicator characterizes the likelihood of health disorders (including the nervous system) when exposed to a noise factor, considering the increase in the overall health risk with increasing age.

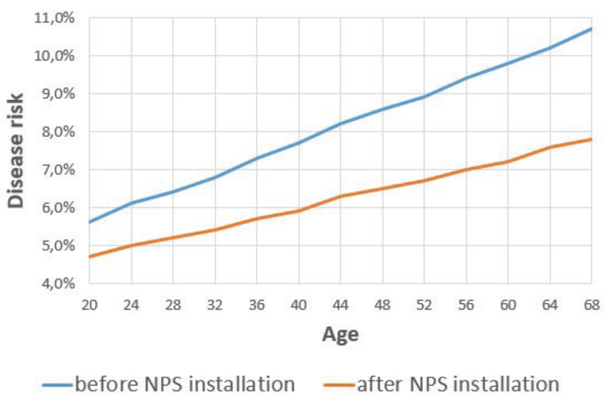

Fig. 4: Reduced risk index for diseases of the nervous system when exposed to traffic noise

Age	Nervous system disease risk	
	At 81,1 dBA	At 65,6 dBA
20	0,056	0,047
24	0,061	0,050
28	0,064	0,052
32	0,068	0,054
36	0,073	0,057
40	0,077	0,059
44	0,082	0,063
48	0,086	0,065
52	0,089	0,067
56	0,094	0,070
60	0,098	0,072
64	0,102	0,076
68	0,107	0,078

Tab. 4: Reduced risk index of nervous system diseases depending on age

According to the presented data the decrease in the reduced risk index for diseases of the nervous system associated with sleep disorders, with a decrease in the level of traffic noise at recreation sites from 81,1 dBA to 65,6 dBA will be 0.009 - 0.029 (depending on the drivers age).

6. CONCLUSION

Analyzing the data presented in the article, it can be noted that the installation of a noise protection screen (with a noise protection efficiency of 15,5 dBA) along the MRSA will reduce the risk of an accident due to «overwork» («inattention» + «overwork/drowsiness») reasons for the following quantities:

– young drivers (from 20 to 32 years old) – 18,35 %;
– middle-aged drivers (from 32 to 52 years old) – 22,65 %;
– elderly drivers (from 52 to 68 years old) – 25,9 %.

REFERENCES

[1] Solovieva O., Elkin Y. «Noise reduction measures development of construction sites in residential building area»/Akustika. 04.2021. Vol. 39. P. 269-273.
[2] Kutyrin B., Elkin Y. «Assessment of noise and electromagnetic effects of traffic flow on residential buildings at the design, construction and exploitation of acoustic screens» / Akustika. 11.2019. Vol. 34. P. 107-112.
[3] Buranov I. «The GOST will for the first time write down the requirements for roadside gas stations, hotels and parking lots» / Kommersant. 03.11.2018 URL: https://www.kommersant.ru/doc/3791364 (treatment date 09.06.2021).
[4] Methods for determining the capacity of road service facilities and the distance between them, depending on the intensity of the traffic flow on the road section. / Rosavtodor. - M., 2016. – 12 p. Application N2 to Rosavtodor order N2124 (12.12.2016).
[5] Alekseeva E. «Sleepy drivers are responsible for every tenth accident» / Za rulem. 02.11.2018, URL: https://www.zr.ru/content/news/910717-sonlivost-voditelya-stanovitsya (treatment date 09.08.2021)
[6] Scientific research. Causes of Truck Accidents in Europe / IRU. - European Union., 2016. – 19 p.
[7] Rules Set 276.1325800.2016 Design rules for protection against traffic noise / Rosavtodor. – M., 2016. – 146 p.
[8] Industry road methodology document (IRMD) 218.2.013-2011. Guidelines for the protection of areas adjacent to highways from traffic noise / Rosavtodor. – M., 2011. – 164 p.
[9] V. Nepogodina «Route M-4" Don ": road works on the highway to the sea» / Dorinfo 15.01.2021. URL: https://dorinfo.ru/99_detail.php?ELEMENT_ID=88784 treatment date 10.09.2021)
[10] Guidelines 2.1.10.0059-12 Assessment of public health risk from traffic noise. / Federal Service for Supervision of Consumer Rights Protection and Human Welfare. – M., 2012. – 40 p.
[11] Resolution of the Government of the Russian Federation. No. 1733 "On Amendments to the Traffic Rules of the Russian Federation", treatment date 12.20.2019.
[12] Yu. V. Trofimenko, V.I. Komkov, T. Yu. Grigoryeva. Influence of rest sites of highways to the safety of traffic movement and to environmental pollution. Proceedings of the Samara Scientific Center of the Russian Academy of Sciences, vol. 14, №1(3), 2012, pp. 918 – 922.

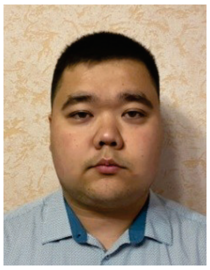

Danil Bazarov *is Master student, engineer, Department of Technosphere Safety, Moscow Automobile and Road Construction State Technical University (MADI), (Moscow, Russian Federation).*
Bazarov Danil, specialist in environmental engineering.
Bazarov Danil is the author of 2 scientific publications. He presented the main results of scientific research at international conferences in Moscow.

Yuri Elkin *is Doctor of Technical Sciences, Professor, Department of Technosphere Safety, Moscow Automobile and Road Construction State Technical University (MADI), (Moscow, Russian Federation), Academician of the International Academy of Ecology and Life Protection Sciences (IAELPS).*
Yuri Elkin - a specialist in the calculation and design of noise absorption, noise reduction on industrial premises and roads, sound insulation structures, silencing installations, etc.
Yuri Elkin is the author of more than 70 scientific publications, the author of 2 patents and co-author of textbooks and teaching aids. He presented the main results research at international conferences in in St. Petersburg, Moscow, Samara.

Alexey Abramov *is Candidate of Technical Sciences, Docent, Department of Technosphere Safety, Moscow Automobile and Road Construction State Technical University (MADI), (Moscow, Russian Federation).*
Alexey Abramov - a specialist in technosphere safety and ecology.
Alexey Abramov is the author of 117 scientific publications, the author of 45 patents and co-author of textbooks and teaching aids.

Oleg Gogiberidze *is Candidate of Technical Sciences, Docent, Department of Technosphere Safety, Moscow Automobile and Road Construction State Technical University (MADI), (Moscow, Russian Federation), Correspondending member of the International Academy of Ecology and Life Protection Sciences (IAELPS).*
Oleg Gogiberidze - a specialist in technosphere safety and ecology.
Oleg Gogiberidze is the author of more than 30 scientific publications and co-author of textbooks and teaching aids.

Paper No.358/2021

IMPORTANT FACTOR IN GENERATING ACOUSTIC ENVIRONMENT WITHIN THE TERRITORIES ADJACENT TO HIGHWAYS

Tatyana Germanova

Industrial University of Tyumen, Tyumen, Russia, ecogtv@mail.ru

Abstract: *As things stand today, most of acoustic studies have been focused on predicting the pattern of noise and analyzing the related factors such as various types of noise protection installations, noise transmission, housing density, building position and landscaping. At the same time, the acoustic environment studies are directly linked to the main urban structures (the so-called urban morphology) comprising the coordinated open spaces, buildings and residential areas. An important element of assessing the expected level of the environment acoustic pollution appears to be the experience of implementing planned and project documents. The given article deals with the problem of street lines [1] (red lines). These lines became widely used at designing residential and public buildings in areas adjacent to highways, urban and city-wide roads. Due to this fact the legal and technical aspects in transforming the area introduce certain difficulties. The presented article is concerned with the circumstances of applying street (red) lines in urban transportation area from the viewpoint of its acoustic impact on adjacent territories.*

Keywords: *acoustic impact, sound pressure level, main urban arteries with regulated traffic, red lines, street width, building line.*

DOI: *: 10.36336/akustika20214179*

1. INTRODUCTION

Urbanization that over the past few decades takes place at a very rapid pace causes an increasingly strong impact on the natural and human environment [1-5]. At the same time, anthropogenic sounds being accompanied by an accelerated process of urbanization, turned out to dominate the urban acoustic environment. Noise as a form of physical pollution occurs when the sound pressure level exceeds the permissible value. In case of short exposure duration it causes anxiety but if the exposure time is rather long it provokes damage in the body [6, 7]. A large number of studies on the assessment of environmental pollution, especially in the field of engineering, are presented in corresponding literature. Part of this information remains to be fragmentary, mostly specific in one peculiar aspect and appears to be rather technical, scarcely applicable to urban planning [8-12]. Nowadays a number of acoustic studies mostly deal with predicting the noise model and analyzing the associated factors such as a variety of different types of noise protection installations; built-up density, empty spaces, building position and even outdoor vegetation [11, 13]. Therefore, examination of the acoustic environment cannot be distinguished from the main urban structures (the so-called urban morphology). More specifically, it is important to study those urban structures that include coordinated open spaces, buildings, and neighborhoods. Urban planning should be an important tool for determining the expected level of pollution from noise sources. The given article deals with the problem of street lines that affect the conditions of use and development of cities. Red lines (street lines) indicate the boundaries of public areas [1]. An important aspect in red lines use is known to be their legal application at laying out residential and public buildings on territories adjacent to highways, roads of urban and citywide roads. Red lines are determined based on the norms of the Russian Federation Urban Planning Code and on the instruction for designing and establishing street (red) lines procedure that does not contradict this Code. The presented article discusses inconsistencies in preserving and improving the acoustic environment based on the criteria of planning. Street lines are aimed at protecting the citizens' right to friendly urban environment, so they are extremely important for providing comfortable living conditions.

2. MATERIALS AND METHODS

The current process of urbanization is accompanied by an increase in city territories, the enlargement of motor transport pool and, as a result, by degradation of the urban environment quality as well as the widespread loss of historically valuable urban spaces. The evolution of settlement planning shows that this activity is greatly influenced by the scale of urban planning transformations due to social-economic aspects, technical capabilities and the state economic potential. Transition to regular urban planning in Russia began only with the reforms of Peter the Great. To analyze the spatial differentiation of planning elements in the city of Tyumen layout we used traditional research methods: mapping and geodesy, comparative-descriptive legislative acts, regulatory and engineering requirements as well as basic project designs. Sound pressure level detection was implemented using the method of calculation according to approved procedures.

At present practicable flexibility in making decisions concerning territory planning projects (TPP) makes possible to insert necessary changes into the development of territories. TPPs are aimed at establishing certain boundaries for planning elements. Red lines are regarded to be assigned to these boundaries.

The Town-Planning Code of Russia in section 11 of Article 1 defines red lines as lines that indicate the existing, planned (changeable, newly formed) boundaries of public territories and (or) the boundaries of territories covered with linear objects and (or) intended for siting linear objects. Previously in section 10.1 of the same Article 1 we saw the following definition: linear objects - power lines, communication lines (including linear cable structures), pipelines, highways, railway lines and other similar structures. Thus, the development and approval of these red lines turn out to carry the sense of the whole planning project of today. Information concerning the location of land plot boundaries is determined with consideration to red lines of the adjacent land plots boundaries location (if any) and natural boundaries of the land plot [4]. Red lines specify the configuration of various land object boundaries. These land plots comprise a unified system of street and road network. The network throughput is determined by the level of motorization according to regional standards of urban planning design. Approved street-road network should necessarily make allowance for the pattern of the territory development in the given settlement. According to Construction Regulations (SR) 42.13330.2016 the categories of streets and roads in the cities are distinguished paying due consideration to their functional purpose: i.e. streets and roads of main and local significance. Parameters of streets and roads in a city should be specified according to clause 11.4 in SR 369.1325800.2018. The width of streets and roads in red lines is adopted pursuant to the notes under Table 11.2 in SR 42.13330.2016. The territory for permanent pass of urban motor vehicle traffic regarded as a mobile source of impact on the adjacent area (permanent acoustic source) is dimensioned due to the above procedures.

Fig. 1 schematically shows a planning concept of street width determination within cross direction profile via use of red lines determining street boundaries. The concepts of arrangement employ side dividing strips to separate various constituents of cross direction profile. Planted lands are sited within the side and central dividing strips.

The situation is especially critical at the intersections of the main streets during the hours of maximum traffic intensity and on the main highways of the city. The analysis of generated noise maps for urban centres shows a high noise level in the adjacent areas [15-19]. The maps are drawn based on the data of full-scale observations over composition and intensity of traffic flows.

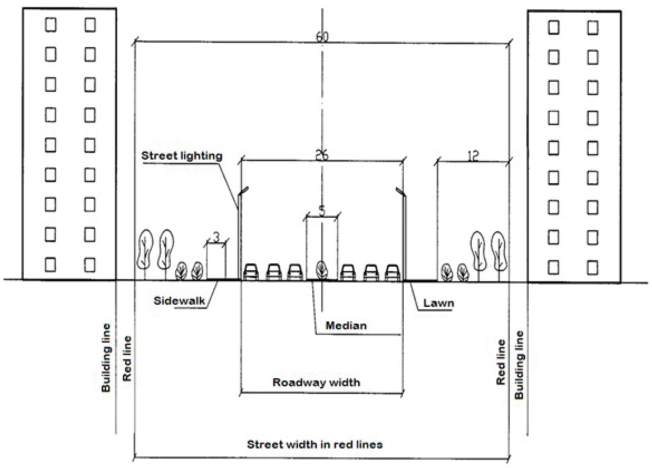

Fig. 1: Street in red lines

A set of measures aimed at improving fuel and environmental friendliness of the car, pollutional load reduction, road network development [4], activities on protecting territories from noise pursuant to sanitary and hygienic requirements will undoubtedly contribute to sound control.

Permissible equivalent sound levels according to Sanitary Standards for areas near residential buildings make 55 dBA during the day (from 7 to 23) and 45 dBA at night (from 23 to 7). At present a number of regulatory and technical documents have been developed and applied for noise protection measures planning and development. The authors [20] have developed and proposed classification of noise for highways. This classification is based on such constituents as traffic intensity, speed, construction of traffic stream and the number of a road or highway lanes. Certain noise levels and distances tom roadside clear zone will facilitate the timely and correct managerial decision-making concerning territorial planning and urban developing. Implementation of up-to-date technological means for noise reduction, noise maps generating and use will definitely promote the excessive road noise control.

To identify the features of traffic stream in the city of Tyumen students and postgraduates of the Tyumen Industrial University have implemented a visual survey of road network segments and interchanges. They have also carried out the analysis of long-term research programs in Tyumen. The traffic streams in Tyumen are mainly concentrated in the central city zone. And the situation is particularly critical at the intersection of the main streets loaded with cargo during the hours of maximum traffic intensity and on the main highways of the city: Republic Street, Lenin Street, Melnikaite Street, Pervomaiskaya Street, Trade Union Street, 50 let Oktyabrya Street.

3. RESULTS

The site boundaries are set at arranging buildings, structures, objects with an offset from the red line or the building line. Subparagraph 3 of paragraph 6 in Article 43 of the Town-Planning Code of Russia states that lines of setback or the boundaries of the site are used to determine the places of permissible arrangement of buildings, structures and objects. These lines are drawn parallel to the red lines with the setback of at least 3 m to the boundaries of the land plot. The territory between the building line and the red line is a zone where construction is not allowed according to the provisions stated in the Russian Federation Town-Planning Code. And the distance will be varied with consideration to current practice of designing setback to the first buildings along highways and streets. So , urban planning regulations for the city of Tyumen are determined.

Previously in the practice of urban planning red lines formed blocks and microdistricts. The obtained setback zones and adjacent territories were given favorable conditions in the context of sanitation and hygiene what made possible to secure favourable environment for the planning border-the red line as well. And atmospheric air quality in the residential area (within red lines) was considered to be quite satisfactory. Nowadays this setback procedure is still put into practice. Main and local street territories of the city in view of sanitation and hygiene are not secured favourable environment so, the planning border of the street in the red lines can also be characterized as unfavorable.

The ubiquity of red lines enforcement is of paramount importance at arranging residential zones and changing the existing planning structures what appears to be rather problematic in view of legal and technical mechanism in territory transformation implementing. The main singularity lies in the fact that red lines are used for zoning territories i.e. they "work" with them but not with land plots. Moreover, information concerning red lines application is currently not included into the State Real Estate Cadastre. Red lines are not regarded as an object of land management.

In the context of peculiarities existing in urban planning practice noise impact upon residential buildings adjacent to city highway in the area of junction Trade Union Street – 50 years of October Street has been analyzed. The initial planning data are shown in Fig. 2.

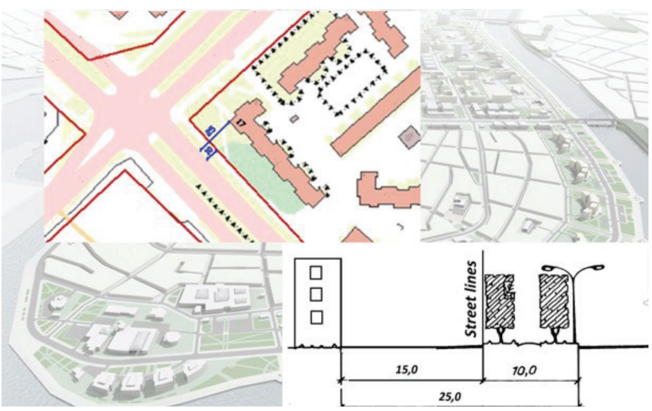

Fig. 2: A layout drawing of Street lines and a transversal profile on the examined lot Tyumen - 50 Jears of October str, 17

The sound pressure level was estimated by the method of calculation for house 17 located in 50 Years of October Street. The minimum distance from the roadway border to the facade of a residential building makes 25 m. The distance from the roadway border to red line is 10 m and the length from red line to the facade makes 15 m. The result of noise level calculation showed that noise level on highway located at the distance of 7.5 m from the outer lane at traffic intensity of 1500 units per hour makes 80 dBA, noise reduction at the distance will be 4 dBA, the addition due to the reflection of sound between the facades is 1.9 dBA. At the distance of 2 m from the facade the level of sound will be 77.5 dBA. This value exceeds the sanitary and hygienic norm making 50 dBA by 22.5 dBA . Therefore, this calculation revealed significant traffic stream noise impact on the adjacent territory and the facade of building located at frontage line. Accordingly, it is necessary to assess urban planning decisions in view of the risk to public health.

4. DISCUSSION

The authors of the article Classification of Highways by Noise Levels have completely analysed the sound impact of traffic streams on the levels of noise in the residential development territories adjacent to highways. The article states the obtained levels of noise and the required figure of noise reduction for residential areas as well as the measures to reduce the roadside clear zone. The noise level at setting out points on the 1st and 2nd class city-wide highways will be 81-83 dBA, the required figure of reduction makes 27-29 dBA. The size of the road side clear zone recommended by the authors for main urban roads depending on their class makes900 and 1300 m.

The existing practice of territory planning by means of red lines gave rise to a conflict in territory developing. This contrariety rendered impossible to create an acoustically comfortable living environment in the territories adjacent to highways. Thus, at evaluating urban planning decisions it is necessary to take into account the level of traffic stream acoustic pollution and risk thereof for public health.

By way of combining acoustic pollution maps and maps with territory zoning according to risk level will make possible to justify the authorized application of red lines for city highways. Timely arrangement of residential territories due to competent fixing the lines in urban planning regulation will contribute to forming the safe level of acoustic impact employing special noise protection measures.

5. CONCLUSION

The author has conducted the analysis of planning urban streets and adjacent residential buildings. The novelty of the study lies in the analysis of territories in view of its impact on the adjacent buildings. The analysis of red lines as the boundaries of the city highways showed that in accordance with the current legislation urban planning regulations can not be applied to land plots intended for arranging linear objects.

REFERENCES

[1] Wang B., Kang J. Effects of urban morphology on the traffic noise distribution through noise mapping: A comparative study between UK and China// Applied Acoustics, 72 , pp. 556–568, 2011
[2] Vasil`ev A.V. Shum kak faktor e`kologicheskogo riska v usloviyax urbanizirovanny`x territorij // Noise Theory and Practice, VOLUME 1, Issue 2, p. 27-40, 2015
[3] Volkodaeva M.B., Levkin A.V., Demina K.V. The use of noise maps of the city for selection of management decisions about the regulation of road traffic// Noise Theory and Practice, Volume 1, Issue 2, p. 22-31, 2015
[4] Germanova, T., Kernozhitskaya, A. To a question of ecological assessment of a condition of inhabited territories near traffic flows // Akustika, 32, pp. 312-315, 2017
[5] Pijanowski, B.C., Villanueva-Rivera, L.J., Dumyahn, S.L., Farina, A., Krause, B.L., Napoletano, B.M., Gage, S.H., Pieretti, N.,. Soundscape ecology: the science of sound in the landscape. BioScience 61, 203e216, 2011
[6] Towards a Comprehensive Noise Strategy, Policy Department Economic and Scientific Policy. Environment, Public, Health and Food Safety. - 2012. –82 p.
[7] Zhang X., Li H. Cities. 72, 141-148, 2018.
[8] Sharifi A. Resilient urban forms: A review of literature on streets and street networks // Building and Environment, 147, 171–187, 2019
[9] Han X., Huang X., Liang H., Ma S., Gong J. Analysis of the relationships between environmental noise and urban morphology// Environmental Pollution, 233, p. 755-763 21, 2018
[10] Drozdova L.F., Butorina M.V., Kuklin D.A. Ocenka snizheniya urovnej shuma zdaniyami razlichnoj formy`// Noise Theory and Practice, VOLUME 6, Issue 4, p. 95-103, 2020.
[11] Vasil`ev A.V. Issledovanie infrazvukovogo izlucheniya v usloviyax urbanizirovanny`x territorij na primere Samarskoj oblasti // Noise Theory and Practice, Volume 6, Issue 4, p. 155-162,2020.
[12] Nagaeva O.S., Peshkicheva N.S., Germanova T.V. Insolyaciya kak odin iz kriteriev, opredelyayushhij minimal`noe hasstoyanie mezhdu zdaniyami // Uspexi sovremennogo estestvoznaniya. - 2012. - № 6. - S. 189-190.
[13] Germanova, T., Kernozhitskaya, A. Emissions of exhaust gases and health of the person/IOP Conference Series: Earth and Environmental Science, 90(1),012036, 2017.
[14] Grimm, N.B., Faeth, S.H., Golubiewski, N.E., Redman, C.L., Wu, J., Bai, X., Briggs, J.M. Global change and the ecology of cities. Science 319, 756e760, 2008
[15] Zhang, Q., Seto, K.C., 2011. Mapping urbanization dynamics at regional and global scales using multi-temporal DMSP/OLS nighttime light data. Remote Sens. Environ. 115, 2320e2329, 2011.
[16] Fang, C., Li, G., Wang, S. Changing and differentiated urban landscape in China: spatio-temporal patterns and driving forces. Environ. Sci. Technol. 50 (5), 2217e2227, 2016.
[17] Pham, T.T.H., Apparicio, P., Landry, S., Lewnard, J. Disentangling the effects of urban form and socio-demographic context on street tree cover: a multi-level analysis from Montreal. Landsc. Urban Plan. 157, 422e433, 2017.
[18] Votsi,N.-E.P., Kallimanis, A.S., Pantis,I.D., 2017. An environmental indexof noise and light pollution at EU by spatial correlation of quiet and unlit areas. Environ. Pollut. 221, 459e469, 2017.
[19] Germanova, T., Kernozhitskaya, A., Davydova, I. On the concept "street lines" in urban planning practice /MATEC Web of Conferences, 106, 01021, 2017.
[20] Butorina M.V., Tyurina M.V., Ivanov N.I., Sannikov V.A. Klassifikaciya avtomobil`ny`x dorog po urovnyam shuma// Noise Theory and Practice, VOLUME 6, Issue 4, p. 22-32, 2020.
[21] Voordeckers D., Lauriks T., Denys S., Billen P., Tytgat T., M.Van Acker. Guidelines for passive control of traffic-related air pollution in street canyons: An overview for urban planning // Landscape and Urban Planning, Volume 207, March 2021, 103980
[22] Lebedev O.A., E`l`kin Yu.I. Vliyanie na uroven` transportnogo shuma i vy`brosov meropriyatij po povy`sheniyu e`ffektivnosti nazemnogo transporta v g. Moskovskij // // Noise Theory and Practice, VOLUME 6, Issue 2, p. 69-76, 2020

Tatyana Germanova, *is candidate of technical Sciences, associate Professor of the Department "Industrial heat power engineering" of Tyumen industrial University. Tatyana Germanova has been dealing with issues of urban ecology for many years. Her interests include physical and chemical impacts on the built-up area. Tatyana Germanova is the author of more than 20 scientific publications. She presented the main results of scientific research at international conferences in St. Petersburg, Moscow, Samara.*

Paper No.359/2021

METHOD FOR ESTABLISHING THE SEVENTH SUBZONE OF THE AERODROME AREA

[a)] Dmitrii Koshurnikov, [b)] Mikhail Kartyshev

[a)] *Federal Budget Scientific Institution 'Federal Scientific Center for Medical and Preventive Health Risk Management Technologies', Perm, Russia, kdn@fcrisk.ru*
[b)] *LLC 'Civil aviation environmental safety center', Moscow, Russia, eco@ecoflight.ru*

Abstract: *The existing regulatory and methodical base does not provide for establishing airport zones (AZs). There are no unified approaches to establishing relevant boundaries, control over them, and substantiating limitations on use of land spots.*
The developed procedure for establishing the sanitary (seventh) subzone in an AZ creates a universal algorithm for determining boundaries of this subzone in any AZ. Methodical approaches contain requirements to creating boundaries of the sanitary (seventh) subzone including relevant computations, computed boundaries being verified with instrumental observations (measurements), zoning the sanitary (seventh) subzone as per health risk criteria, and subsequent production control. Airports used in civil aviation have been differentiated for the first time within the procedure; it was done in order to separate requirements to accomplishing both verifying measurements and production control. Besides, approaches to zoning the sanitary (seventh) subzone in an AZ as per health risk criteria have been implemented for the first time; these criteria are applied to determine limitations on use of land spots. Averaged daily noise level (LAd) was used as a noise exposure indictor. Four zones with different risk levels were determined with different types of economic activities to be performed in them depending on functions of capital construction objects located there.

Keywords: *the sanitary (seventh) subzone, airport zone, noise computation, verification, risk assessment, production control.*

DOI: *: 10.36336/akustika20214183*

1. INTRODUCTION

The Russian Federation has been a member of the International Civil Aviation Organization (ICAO) since 1970; this organization performs its activities, among other things, within a well-balanced approach to managing aircraft noise aiming at relevant planning regarding use of land spots exposed to aircraft noise in zones close to airports. To implement activities aimed at aircraft noise management, ICAO experts believe it is necessary to establish zones with different levels of noise exposure.

In the Russian Federation civil aviation airports, as well as state and experimental aviation airports are obliged to develop a draft of an airport zone (hereinafter called AZ) substantiating its borders for its subsequent establishment; this obligation arises in conformity with the Federal Law No,. 135 issued on July 01, 2017 [1] and the Federal Law No. 191 issued on July 02, 2020 [2], as well as with the RF Government Order dated December 02, 2017 No. 1460 [3]. An AZ is created for providing safe flights of aircrafts (hereinafter called ACs), future development of an airport, and eliminating adverse effects produced by ACs flights on human health and the environment.

The existing valid regulatory documents stipulate the following prohibitions or limitations in subzones established within an airport zone:

- a prohibition to place any objects that are not meant for organizing and maintaining air traffic (the first subzone);
- a prohibition to place any objects that are not part of an airport (air field) infrastructure (the second subzone);
- a limitation on placing any objects with their height exceeding bounding surfaces installed for ensuing ACs flights safety (the third subzone);
- a prohibition to place capital construction objects that can create disturbances when radiotechnical equipment is operated at an airport (the fourth subzone);
- a prohibition to place hazardous industrial objects (the fifth subzone);
- a prohibition to place objects that could attract mass gathering of birds (the sixth subzone).

The sanitary (seventh) subzone is established as a territory where hygienic standards might be violated; however, it can be used for civil construction only when health risk criteria are taken into account (risk factors include chemical exposure, noise [4], and electromagnetic radiation). All this results in a specific status assigned to the sanitary (seventh) subzone as a zone with specific conditions for the use of territory (ZSCUT).

An airport zone is a zone close to an airport with its boundaries being external boundaries of subzones created within it.

We should note that the sanitary (seventh) subzone has a square which is significantly greater than squares of all other subzones. It is predominantly due to acoustic exposure occurring due to aircraft noise (AN) from aircrafts moving during the whole ICAO landing and takeoff cycle (Fig. 1).

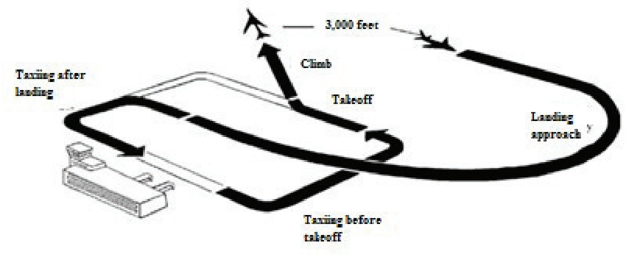

Fig. 1: ICAO standard landing and takeoff cycle

Issues related to use of land spots within AZs close to airports call for relevant improvements in the existing regulatory-methodical base as regards determining limitations that should be imposed on use of land spots as per such a health risk factor as aircraft noise and make these improvements much more vital at the moment.

At present the existing regulatory-methodical base in the RF is not sufficiently ready for implementing procedures developed by ICAO with the balanced approach to AN management.

There are no unified algorithms for designing subzones and software packages that implement regulatory documents existing in foreign countries (for example such programs as INM or AEDT) that gave grounds for establishing boundaries of the sanitary (seventh) subzone. In particular, in different years different developers created boundaries for the same objects that were significantly different from each other as per their square and configuration and it made legitimacy of any limitations imposed on use of land spots and removal of substantial territories from land tenure rather questionable [10, 11, 12, 13].

Besides, experience gained in using methodical approaches adopted in other countries that are based on balanced approach to aircraft noise management stipulated by ICAO revealed that boundaries of the sanitary (seventh) subzone have significant differences in outlines of their design and it influences the whole city development in areas close to airports.

The present paper dwells on basic methodical approaches that are suggested to be implemented in the Russian Federation and are aimed at regulating issues related to establishing the sanitary (seventh) subzone for providing sanitary-epidemiologic well-being of the population and creating a favorable urban environment.

The paper concentrates on the basic stages included into the developed procedure for establishing boundaries of the sanitary (seventh) subzone in an airport zone as a unified algorithm. The suggested approaches will allow establishing an AZ as a zone with specific conditions for the use of territory (hereinafter ZSCUT); it will help provide sanitary-epidemiologic well-being of the population both beyond boundaries of the sanitary (seventh) subzone and within them as per health risk criteria [14, 15].

2. REGULATORY AND LEGAL GROUNDS FOR ESTABLISHING AZ (REVIEW)

2.1. Regulatory and legal instruments for hygienic assessment

The sanitary (seventh) subzone in an AZ should be established basing on federal laws on sanitary-epidemiologic welfare of the population (The Federal Law issued on March 30, 1999 No. 52-FZ), on establishing and using an airport zone, a sanitary protection zone (the Federal Law issued on July 01, 2017 No. 135-FZ, the RF Air Code issued on March 19, 1997 No. 60-FZ, the Federal Law issued on August 03, 2018 No. 342-FZ, the Federal Law issued on June 11, 2021 No. 191-FZ), as well as RF Government Orders (the RF Government Order issued on December 02, 2017 No. 1460, the RF Government Order issued on March 03, 2018 No. 222).

Boundaries of the sanitary (seventh) subzone in an AZ should be established in conformity with the renewed requirements and criteria fixed for territories that are subject to standardization (SRS 2.1.3684-21, SRS 1.2.3685-21).

Besides, when developing methodical approaches, the authors have analyzed other legislative acts that are valid in the RF and regulate issues related to assessing impacts on the environment and human health exerted by air transport and ACs flights.

Verification and planned production control over levels of exposure to aircraft noise are based on the existing procedures for measuring and controlling noise levels in residential areas (MUK (methodical guidelines) 4.3.2194-07, GOST (State Standard) 23337-2014, GOST (State Standard)P 53187-2008).

3. METHODICAL APPROACHES TO ESTABLISHING THE SANITARY (SEVENTH) SUBZONE IN AN AZ, COMPUTING AND ASSESSING HEALTH RISKS

3.1. General provisions

In accordance with ICAO standards aircraft noise is estimated basing on objective and measurable criteria. An outline of equivalent noise level is a calculated line showing a constant value of aircraft noise exposure averaged over a certain period of time that occurs due to air traffic created by different aircrafts during their normal operation.

Estimation of an actual acoustic situation existing on a given territory in order to confirm calculated data is an integral part in aircraft noise management. To do this, short-term and long-term activities for AN monitoring can be recommended; such activities are aimed at confirming that a calculated model is correct or dispute its correctness. Measuring plays an extremely significant role in actual or planned use of land spots and imposing limitations on such use as per aircraft noise factor. Additionally, monitoring programs that are being developed at the moment are intended to provide an evidence base for research, inspections, and expertise, including those conducted owing to people’s complaints about unfavorable environment in case there is acoustic discomfort.

These methodical approaches to establishing (changing) the sanitary (seventh) subzone in an AZ are developed and recommended exclusively for civil aviation airfields. The suggested algorithm is made up of the following stages:

1. a procedure for collecting data about airport operations that should be accounted for proper determination of computed AN outline using a software package intended for computing AN outline;
2. making acoustic computation and establishing calculated outlines of equivalent noise level (LAeq);
3. verifying boundaries of the sanitary (seventh) subzone and noise zones determined within them as per results obtained via instrumental observations (measurements). Making adjustments if necessary;
4. assessing health risks within boundaries of the sanitary (seventh) subzone as per computed averaged daily noise levels (LAd) and preset risk indexes;
5. substantiating a list of limitations imposed on use of land spots and real estate objects within boundaries of the sanitary (seventh) subzone;
6. accomplishing instrumental observations (measurements) of noise levels within production control after boundaries of the sanitary (seventh) subzone have been established.

According to the existing regulatory documents the following criteria are to be used when boundaries of the sanitary (seventh) subzone in an AZ are established: there should be no violation of the existing hygienic standards regarding equivalent noise levels at day (55 dBA) for airports that operate in daytime, or at night (45 dBA) for airports that operate round the clock; and providing permissible health risks caused by exposure to AN as per averaged daily equivalent noise level (LAd) that characterizes chronic long-term exposure.

3.2. Collecting data on airport operations

When the sanitary (seventh) subzone in an AZ is established, an airport should be identified completely and collected data that in future can be used for establishing AZ boundaries should cover basic parameters of operations performed there. General data on any airport include the following:

- basic data on an airport in conformity with the State Register of airports and heliports used in the civil aviation in the Russian Federation (ICAO code, runaway and airport reference point coordinates, types of allowed ACs, data on an airport operator, operating conditions, takeoff and landing routes, etc);
- documents on future development of an airport designed as documents on territorial planning in the RF and documents on territorial development (construction and reconstruction of objects at an airport), as well as data on possible future takeoff and landing routes provided by an airport operator;
- geographical parameters of an airport within a system of coordinates used for keeping the Unified State Real Estate Register (USRER) given as a map (scheme);
- data on actual ACs takeoff/landing routes that are kept when an airport is in operation and established routes according to air-navigation profile of an airport (hereinafter called ANPA) or flight instruction (hereinafter called FI);

Existing schemes for territorial planning and urban development zoning are recommended to be used as cartographic grounds.

All the above mentioned data are to be collected and provided by an airport operator who bears the full responsibility for their completeness and validity.

3.3. Performing an acoustic computation of the sanitary (seventh) subzone outline and noise zones within it

Computed determination of the sanitary (seventh) subzone is a significant stage in establishing its boundaries; if necessary, this determination should be verified and adjusted. Boundaries of outlines are determined via computations using algorithms and mathematical apparatus as well as specialized software packages recommended by ICAO.

Computed AN outlines for airports should be built using certified software than implements ICAO Doc 9911 Recommended Method for Computing Noise Contours Around Airports [7] or (in case there are any available) domestic methods and software packages certified as per established procedure.

At present only one software package developed in the Russian Federation implements provisions fixed in ICAO Doc 9911 since it was verified by CAEP ICAO in 2016 as conforming to required standards; it is AcousticLab software package developed by "The Civil aviation environmental safety center" LLC [8].

Acoustic computations primarily aim to give a preliminary, operative, tentative, and quantitative estimation of expected equivalent AN levels on a given territory as a whole and at control points in particular. Computed values are used for:

- selecting places where filed observations (measurements) are to be performed for verifying calculated outlines;
- selecting places where production control is to be performed in future at boundaries of noise zones caused by exposure to ACs flights.

Model acoustic computations in the suggested procedure are recommended to be based on data on airport operation conditions, flight intensity (as per an average annual flight day), and ACs flying routes.

Acoustic computations allow determining equivalent noise levels that create an outline of the sanitary (seventh) subzone in an AZ taken into account in accordance with airport operation conditions ($L_{Aeq.d}$ for operations at day, $L_{Aeq.n}$ for round the clock operations). Aggregated exposure value used for health risk assessment is characterized with averaged daily noise level ($L_{Aeq.d}$).

Computed design of noise levels outlines is suggested to be accomplished taking into account actual distribution of ACs flight routes over the last calendar year as well as TLOs distribution as per these routes over an average flight day in a given year. An external boundary of the sanitary (seventh) subzone in an AZ is an external boundary of an outline of equivalent noise level L_{Weq} that corresponds to time-averaged annual airport operation conditions as per the greatest exposure to noise at day or at night. In an ordinary situation, a boundary is set as per an outline of AN value at night for round the clock airports, $L_{Aeq.n}$ (45 dBA); for airports that are operated only in daytime, as per an outline of AN value at day, $L_{Aeq.d.}$(55 dBA).

Additionally, according to results obtained via acoustic computations, boundaries of noise zones are determined within the sanitary (seventh) subzone in an AZ as per L_{Ad} that is used in calculating relevant risk indices for risk assessment.

3.4. Verifying computed boundaries of the sanitary (seventh) subzone in an AZ with instrumental (field) measurements

A built mathematical model should be verified basing on instrumental research (measurements) performed at control points that characterize a computed boundary of aircraft noise outlines with takeoff/landing routes or takeoff/landing operations (hereinafter called TLO); this verification provides objective evidence that aircraft noise distribution was computed correctly. It is suggested within the present procedure to verify data obtained for airports with more than 2,000 TLO per year with instrumental measurements in order to confirm validity of computed models within boundaries of aircraft noise levels established according to airport operations scenario.

For the first time, basing on practical experience in collecting, analyzing, and processing data on air traffic objects, it is suggested within the present procedure to differentiate civil aviation airports as per a number of accomplished takeoff/landing operations (hereinafter called TLO) per year (Tab. 1).

	I Group	II Group	III Group	IV Group
TLO number per year *	More than 40,000	More than 11,000 and less than 40,000	More than 2,000 and less than 11,000	Less than 2,000

** determined as a sum of all TLO accomplished at an airport In case flight intensity is planned to increase in future, a group for an airport is to be determined as per future flight intensity*

Tab. 1: Civil aviation airports differentiated as per TLO number

It seems advisable to omit instrumental verification for airports from Group IV within the present procedure and to establish outlines for boundaries of the sanitary (seventh) subzone only as per computed data; it is done in order to simplify procedures for establishing the sanitary (seventh) subzone in an AZ and to avoid creating barriers for development of small regional airports and airports in areas beyond the Polar circle.

To verify boundaries of the sanitary (seventh) subzone it is suggested to quantitatively differentiate the conditions for accounting a number of ACs that are to be fixed without losing reliability of estimates as per observation results:

- monitoring over AN should be performed at each point and all types of ACs that perform not less than 90% TLO are to be fixed to verify boundaries of the sanitary (seventh) subzone at airports from Group I.
- monitoring over AN should be performed at each point and all types of ACs that perform not less than 80% TLO are to be fixed to verify boundaries of the sanitary (seventh) subzone at airports from Groups II and III.

An overall scope of accomplished observations is determined in such a way so that the results would be sufficient for verifying boundaries of the sanitary (seventh) subzone in an AZ and noise zones detected within these boundaries with precision not exceeding 2 dBA (for airports from Group III) and not exceeding 1.5 dBA and 1 dBA for airports from Group II and I accordingly.

Verification involves determining equivalent noise level L_{Aeq} during the whole period of estimation and maximum noise level L_{Amax} determined for each noise event caused by ACs flights.

Verification results are then compared with data computed for a boundary of the sanitary (seventh) subzone in an AZ at points corresponding to those selected for verifying ACs routes. Verification results are to be documented.

Boundaries of AN outlines are adjusted taking into account data on actual ACs flight trajectories that were obtained via field observations with future flight intensity also borne in mind. Boundaries of the sanitary (seventh) subzone that were adjusted as per instrumental measurement results are to be submitted for establishing.

3.5. Production control over established boundaries of the sanitary (seventh) subzone in an airport zone performed via field observations (measurements)

Production control over established boundaries of the sanitary (seventh) subzone in an AZ is to be accomplished in order to ensure that these boundaries are observed. In case any discrepancy in boundaries of the sanitary (seventh) subzone in an AZ is detected via production control activities, the sanitary (seventh) subzone in an AZ is to be adjusted with subsequent approval of its new boundaries as per the established procedure.

It is suggested to perform production control during 1 year since boundaries of the sanitary (seventh) subzone in an AZ have been established at operating airports and during 1 year since a new airport, either built or reconstructed, has been put into operation. Instrumental observations (measurements) of noise levels are accomplished at a boundary of the sanitary (seventh) subzone and noise zones within it. Data obtained via production control are to be submitted to territorial bodies of a relevant federal executive authority that is responsible for performing federal state sanitary-epidemiologic surveillance. To assess whether established boundaries of the sanitary (seventh) subzone in an AZ and noise zones within it are objective according to airport operation scenario, observations (measurements) of noise levels are performed to establish whether equivalent and averaged equivalent noise levels correspond to calculated ones.

Scopes of field observations (measurements) depend on a number of TLO performed at an airport during one calendar year and are determined similarly to a procedure outlined in Item 3.4 "Verifying calculated boundaries of the sanitary (seventh) subzone in an AZ with instrumental (field) measurements". AN is measured when ACs perform ordinary flight operations (rolling, taking off, climbing, flying, approaching, and landing).

It is suggested to not perform production control over established boundaries of the sanitary (seventh) subzone in an airport zone at airports with TLO number being less than 2,000 per year.

A number of places (points) where observations are accomplished is determined basing on computed boundaries of a zone exposed to noise and ACs routes that cause exposure to noise when taking off, landing, or taxiing in an AZ.

When it comes down to substantiating selected points where field observations are to be performed, it is advisable to select points in residential areas and places where socially significant objects are located.

3.6. Health risk assessment

Health risk assessment is performed within the present procedure in order to correctly zone the sanitary (seventh) subzone in an AZ and to make up a list of limitations imposed on use of land spots including ban on construction and reconstruction of specific objects; another goal is to substantiate managerial decisions on minimizing adverse medical-demographic and social consequences caused by exposure to noise within established boundaries of the sanitary (seventh) subzone.

Health risk assessment methodology stipulated by the Methodical guidelines 2.1.10.0059-12 "Assessing health risks caused by exposure to transport noise" [9] is used as methodical grounds for providing evidence of adverse impacts produced by noise factor on health.

Risk assessment is performed using computed and/or instrumental data on noise exposure levels and criteria recommended by international methodical documents.

Bearing in mind that there are no instant health disorders caused by exposure to external environmental aircraft noise with its level being estimated with value L_{Ad} and that such disorders develop gradually over time, it is recommended to assess health risks occurring within boundaries of the sanitary (seventh) subzone in an AZ as lifetime ones caused by noise contamination on a territory.

To calculate exposure for residential areas, it is necessary to take into account results obtained via acoustic calculations and/or data obtained via instrumental observations (measurements) accomplished at a stage when computed data were being verified. It doesn't seem advisable to create a section in health risk assessment for airports with TLO number not exceeding 2,000 a year.

3.7. Substantiating limitations imposed on use of land spots within the sanitary (seventh) subzone in an AZ

Limitations are imposed on use of land spots within the sanitary (seventh) subzone basing on health risks levels and an opportunity to implement noise protection aimed at preventing and (or) eliminating adverse impacts on human health when objects are constructed and reconstructed.

It is suggested to spot out the following zones as per health risks:

– *a zone with permissible (low) lifetime risk* for population with no limitations imposed on use of land spots within it. But still, any construction or reconstruction should be performed involving obligatory activities aimed at preventing and (or) eliminating adverse physical impacts inside buildings.
– *a zone with impermissible (average, high, or extreme) health risk* for population and there are limitations imposed on use of land spots within such zones; it is also prohibited to build residential buildings or social objects there. And in case any allowed objects are constructed or reconstructed in these zones and there are sanitary-epidemiologic requirements regarding maximum permissible noise levels inside such objects, ordinary activities aimed at noise protection are to be developed and implemented (for a zone with average risks) or specific enhanced activities (for zones with high or extreme risks) that can provide conformity with maximum permissible noise levels inside premises.

It should be noted that acoustic computations are required for assessing whether it is possible to conform to maximum permissible noise levels inside constructed and reconstructed objects and for estimating whether activities aimed at noise protection are efficient.

Acoustic computations of expected noise levels inside premises should give grounds for making a decision whether it is possible or impossible to conform to established standards regarding noise. Computations are recommended to be performed taking into account insulating capacities of building envelopes regarding noise (bearing in mind variety of applied walls and façade systems, roofs, window and door blocks, a possibility to use specific engineering ventilation systems in protected premises etc.).

Assessing and analyzing existing noise levels as well as those expected in future and, subsequently, making a decision whether it is possible or impossible to place relevant capital construction objects close to ACs routes require convincing conclusions and recommendations based on acoustic computations performed as per established procedures. It should be noted that, assessment of noise levels inside buildings aimed at determining their conformity with the valid sanitary legislation after all activities aimed at protection from noise have been accomplished will be accomplished both as per maximum (L_{Amax}), and equivalent (L_{Aeq}) noise levels.

4. CONCLUSION

The developed procedure for establishing the sanitary (seventh) subzone in an AZ with territory zoning depending on health risk levels allows reaching a compromise between the valid legislation as regards sanitary-epidemiologic requirements being violated within boundaries of the sanitary (seventh) subzone and minimization of health risks for population who live near airports or will live in residential areas that are being developed on such territories (are planned to be constructed or reconstructed).

The suggested methodical approaches fully correspond to European experience gained in establishing noise zones in conformity with ICAO requirements. Thus balanced approach to aircraft noise management is ensured. Besides, risk assessment methodology is implemented within these approaches; this methodology allows avoiding ungrounded complaints from people about their deteriorating health caused by airport operations, namely ACs flights, at any stage in decision making.

It should be noted that the domestic approach has certain peculiarities; they are use of instrumental measurements at an early stage in establishing the sanitary (seventh) subzone, namely, at a stage when verification is performed, and zoning of a territory as per health risk criteria.

It is extremely important to use results obtained via instrumental measurements since it provides an opportunity to eliminate any inaccuracies and errors in creating an outline of the sanitary (seventh) subzone that is to be established.

Zoning of the sanitary (seventh) subzone as per risk rates will allow differentiating a list of capital construction objects that are permitted to be reconstructed or placed there given the existing impacts exerted by aircraft noise on population health.

Violation of established boundaries and zones within the seventh subzone in an airport zone as per AN factor will allow using legislative mechanisms for compensating for damages due to violated sanitary-epidemiologic welfare of the population or reconsidering the established boundaries with subsequent compensation for damages to population.

REFERENCES

[1] The Federal Law issued on July 1, 2017 No. 135-FZ "On making alterations into certain legislative acts of the Russian Federation as regards improving the procedure for establishing and using an airport zone and sanitary protection zone".
[2] The Federal Law issued on June 11, 2021 No. 191-FZ "On making alterations into certain legislative acts of the Russian Federation".
[3] The RF Government Order issued on December 2, 2017 No. 1460 "On approval of the Rules for establishing an airport zone, the Rules for determining subzones in an airport zone, and the Rules for resolving disagreements between the supreme state executive authorities in the RF regions and federal executive authorities authorized by the RF Government when reaching an approval on a draft decision on establishing an airport zone"
[4] Sanitary rules and standards 2.1.3684-21 "Sanitary-epidemiologic requirements to maintenance on urban and rural territories, to water objects, drinking water and drinking water supply, ambient air, soils, residential premises, operation of industrial and public buildings, organization and implementation of sanitary-anti-epidemic (prevention) activities".
[5] The Land Code of the Russian Federationissued on October 25, 2001 NO. 136-FZ (last edited on July 02, 2021) (with alterations and addenda that came into forceon September 01, 2021).
[6] ICAO Doc 9829. The balanced approach to aircraft noise management, 2008 [web-source]. URL: http://www.aviadocs.net/icaodocs/docs/9829_cons_ru.pdf (August 26, 2021).
[7] Doc 9911Recommended Method for ComputingNoise Contours Around Airports, Second Edition, 2018 [web-source]. URL: http://icscc.org.cn/upload/file/20190102/Doc.9911-EN%20Recommended%20Method%20for%20Computing%20Noise%20Contours%20Around%20Airports.pdf (August 26, 2021).
[8] ICAO Doc 10069 - Report of CAEP/10 «Committee on aviation environmental protection», 2016[web-source].URL: https://www.icao.int/environmental-protection/Pages/environment-publications.aspx (August 26, 2021).
[9] The Methodical guidelines 2.1.10.0059-12 "Assessing health risks caused by exposure to transport noise"». – M.:The Federal Center for Hygiene and Epidemiology ofRospotrebnadzor, 2012[web-source]. URL: https://www.rospotrebnadzor.ru/documents/details.php?ELEMENT_ID=4649 (August 26, 2021).
[10] May I.V., Koshurnikov D.N., Sedusova E.V. Issues related to accomplishing an examination of a draft decision on airport zone establishing // In the collection: Health risk analysis- 2020 together with the international meeting on the environment and health Rise-2020 the round table on nutrition safety. Materials of the X All-Russian scientific and practical conference with international participation. In 2 volumes. Edited by A.Yu. Popova, N.V. Zaitseva. 2020. P. 148-152.
[11] Koshurnikov D.N. Risk assessment as a criterion for establishing the sanitary (seventh) subzone in an airport zone // In the collection: Fundamental and applied aspects of health risk analysis. Materials of the All-Russian scientific and practical online conference with international participation for young researchers and experts of Rospotrebnadzor. Edited by A.Yu. Popova, N.V. Zaitseva. 2019. P. 29-33.
[12] KleinS.V., KoshurnikovD.N., ChigvintsevV.M. Experience of urban territory zoning on risk level of possible violation of the population health as a result of environmental technogenic noise // proceedings of the Samara Scientific Center,the Russian Academy of Sciences. 2015. Vol. 17. No. 5-2.P. 469-476.
[13] Kartyshev O.A.., Dmovskiy I.G., Averkiveev A.A., Koshurnikov D.N. Features of estimation of adverse impact on the environment during the operation of airports of local air lines // Scientific bulleting of the State Scientific Research Institute of Civil Aviation. 2021. No. 34. P. 59-67.
[14] Koshurnikov D.N. Risk assessment as a criterion for establishing the sanitary (seventh) subzone in an airport zone // In the collection: Fundamental and applied aspects of health risk analysis. Materials of the All-Russian scientific and practical online conference with international participation for young researchers and experts of Rospotrebnadzor. Edited by A.Yu. Popova, N.V. Zaitseva. 2019. P. 29-33.
[15] Klein S.V., Koshurnikov D.N., Chigvintsev V.M. Experience of urban territory zoning on risk level of possible violation of the population health as a result of environmental technogenic noise // proceedings of the Samara Scientific Center, the Russian Academy of Sciences. 2015. Vol. 17. No. 5-2.P. 469-476.
[16] Kartyshev O.A., Nikolaykin N.I. Criteria of the aviation noise assessment for aerodrome environs zoning of the airports and protective measures justification // Scientific bulletin of the Moscow State Technical Civil Aviation University. 2017. Vol. 20. No. 3. P. 30-40.

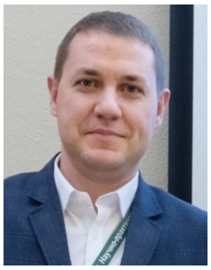

Dmitrii Koshurnikov *is senior research fellow of the Department of the system methods for sanitary analysis and monitoring of the Federal Budget Scientific Institution "Federal Scientific Center for Medical and Preventive Health Risk Management Technologies" (Perm, Russia).*
Dmitriy Koshurnikov is an expert in the field of acoustic modeling of noise propagation using special programs and visualization using GIS technologies. Dmitriy Koshurnikov is the author of methodological recommendations, research works, databases and patents. Dmitriy Koshurnikov is the author of more than 30 scientific publications. He presented the main results of scientific research at the international conferences in St. Petersburg, Moscow, Krakow (Poland), Minsk (Belarus).

Mikhail Kartyshev *is the employee of Civil aviation environmental safety center.*
Aircraft noise research. Development and design of aircraft noise monitoring systems.
Mikhail is the author of a number of methods and measurement techniquesin the field of aviation acoustics.
Mikhail is the author of a number of aircraft noise measurement techniques and methods for computing noise contours around airports.

Paper No.360/2021

MODEL VALIDATION OF THE ACOUSTIC SYSTEMS "TOOTH WHEELS-MANDRELS" OF THE VERTICAL GEAR GENERATOR AND GEAR SHAPING MACHINES

Sergey Ryzhov, Tatiana Finochenko, Alexander Chukarin, Ivan Yaitskov

Rostov State Transport University, Rostov-on-Don, Russia, fta09@bk.ru

***Abstract**: The research paper is devoted to one of the engineering characteristics of the machine tool equipment, which largely determines the safe working conditions for machine operators and competitiveness that is the sound pressure levels at workplaces. The problem of reducing noise levels to sanitary standards at the workplaces of the machine operators is relevant for mechanical engineering and has an important scientific, engineering and socio-economic significance and it corresponds to the priority and advanced scientific directions of the Strategy for scientific and technological development of the Russian Federation (part 20 g "the possibility of an effective response of the Russian society to grand challenge with the interaction of man and technology ... "It should be noted that in this direction a number of theoretical and practical works have been carried out to reduce the noise of the universal turning, milling, and abrasive wheel grinder machines.*

***Keywords:** vertical gear generator, gear sharping machine, tooth-wheel, sound pressure, noise, vibration, cutting tool, vibroacoustic characteristics, mandrel*

***DOI:** : 10.36336/akustika20214190*

1. INTRODUCTION

The most important characteristics of the machine tools are productivity, adaptability, reliability, durability, ergonomics and environmental friendliness during operation as well as engineering and economic efficiency [1,2]. Moreover, during the operation of the machine-tool equipment, a mandatory requirement is the safety labor process. A large scope of scientific research have been devoted to the issues of the vibroacoustic dynamics and reduction of noise discomfort at the machine operators` workplaces of the metalworking machines, however, the vibroacoustic characteristics of the vertical gear generator and gear sharping machines haven`t been practically studied yet.

2. ANALYSIS OF MACHINE LAYOUTS

The vibroacoustic characteristics of the vertical gear generator and gear shaping machines are practically not studied. Among this machine group influenced the machine operators working in increased noise level, it should be highlighted the vertical gear generator and gear shaping machines which implement the technological process with the cutting tool. The sound levels of these machines reach 96 dBA for edge cutting machining. It is processed the tooth-wheels with a significantly different in diameters in Tables 1, 2, 3 and tooth length in such machine group.

The analysis of the machine tool assembly assume that in the general oscillatory system, the most intense radiation of sound energy is created by two subsystems such as the cutting tool and the workpieces under cut as open noise sources and having the maximum values of the flexural stiffness.

Parameter	5С263	527В	5С27П	5С280П
Maximum diameter	320	500	500	800
Maximum module	8	12	12	12
The maximum length of the generatrix of the initial cone (with an already inclined tooth of 30%)	150	265	220	400
Gear-shaping cutter head diameter	60;80;100; 125;160;200; 250	160; 200; 250; 315; 400	160; 200; 250; 315; 400	160; 200; 250; 315; 400; 500
Rotation frequency of the gear-shaping cutter head	20-155	20-155	20-155	20-155
Electric motor power	3	4	4	7,5

Tab. 1: Technological characteristics of the gear shaping machines for a spur wheel

Parameter	5236П	5Т23В	5С268	5С277П	5С286П
Maximum diameter	125	125	320	500	800
Maximum module	1,5	1,5	8	12	16
Maximum width of face	20	16	16	80	125
Strokes per min	160-800	210-820	210-820	210-820	34-167
Rotational speed of disk cutters			10,5-20	20-80	
Electric motor power	1,1	1,1	10	5,5	7,5

Tab. 2: Technological characteristics of the gear shaping machines for a spiral-bevel-gear cutting

Parameter	5111	5122	5122Б	5122В	5140	5М150	5М161
Maximum workpiece diameter	80	200	200	200	500	800	1250
Maximum face width	20	50	30	50	100	160	160
Maximum module	1	5	4,5	4,5	8	12	12
Cutter diameter	40	100	100	100	100	200	200
Strokes per min	250-1600	200-850	280-1200	200-850	65-450	33-188	33-212
Rotary feed mm/strokes	0,016-0,4	0,003-0,286	0,051-0,55	0,14-0,75	0,14-0,75	0,2-1,5	0,2-1,5
Rated power of the electric motor	1,1	2,1;3	3,7	2,1;3	4;4,5	4,8; 5,7	4,8;5,7; 7,5

Tab. 3: Technological characteristics of the vertical gear generator

Despite the difference in the technological processes of the vertical gear and gear shaping processing, as well as the rotation and copying methods, the theoretical study of the vibration, radiation and sound energy processes can be carried out by a unified methodological approach.

3. NATURAL VIBRATION FREQUENCIES

The automated tooth-wheels are mounted on cylindrical mandrels. Regardless of any centering method, the automated tooth-wheels are circular plates rigidly fixed in the center [3,4]. Using data of theoretical studies for tooth-wheels, the dependence for calculating the natural vibration frequencies is reduced to the form

$$\boldsymbol{f_k = \frac{kh}{D}\sqrt{\frac{E}{3\rho(1-\mu^2)'}}}$$

where
k is a coefficient that determines the natural vibration frequencies;
h is the length of the tooth, m;
D is the diameter of the point circle, mm;
E is the modulus of elasticity, Pa;
ρ is the density of the wheel material, kg / m^3;
μ is Poisson's ratio.

In machine building enterprises, in the overwhelming majority of cases, the steel and cast iron wheels are processed. Then, substituting the values of the mechanical parameters, the following dependences are obtained for the natural vibration frequencies

Steel $\boldsymbol{f_k = 3 \cdot 10^3 \frac{kh}{D}}$

Cast iron $\boldsymbol{f_k = 2,4 \cdot 10^3 \frac{kh}{D}}$

It depends on the ratio of the radius and wavelength in the air at the natural vibration frequencies. According to data works, the following dependences were obtained for sound pressure (***P***) and sound power (***N***):

It is point source (steel)

$$\boldsymbol{P = 6 \cdot 10^3 \frac{DkhV_k}{r}} \qquad \boldsymbol{N = 6 \cdot 10^5 D^4 (hkV_k)^2}$$

It is round plate (steel)

$$\boldsymbol{P = 3 \cdot 10^3 \frac{DkhV_k}{r}} \qquad \boldsymbol{N = 1,4 \cdot 10^5 D^4 (hkV_k)^2}$$

Point source (cast iron)

$$\boldsymbol{P = 4,5 \cdot 10^3 \frac{DkhV_k}{z}} \qquad \boldsymbol{N = 4,6 \cdot 10^5 D^4 (hkV_k)^2}$$

Round plate (cast iron)

$$\boldsymbol{P = 2,3 \cdot 10^3 \frac{DkhV_k}{z}} \qquad \boldsymbol{N = 1,1 \cdot 10^5 D^4 (hkV_k)^2}$$

where
$\boldsymbol{V_k}$ is the vibration velocities at natural frequencies, m/s;
r is the distance from the tooth-wheel to the machine operator's workplace, m.

The results of calculating the natural oscillation frequencies of the tooth-wheels are presented in Tabs. 4 and 5.

	Natural vibration frequencies										
Geometric parameters of a tooth-wheel, $D \times h$ (mm)	f_1	f_2	f_3	f_4	f_5	f_6	f_7	f_8	f_9	f_{10}	f_{11}
20 x 50	6000	12000									
50 x 50	2400	4800	7200	9600	12000						
80 x 100	3000	6000	7200	9000	12000						
125 x 100	1900	3300	5700	7600	9500	11400					
200 x 200	2400	4800	7200	9600							
200 x 160	1900	3800	5700	7600	9500	11400					
320 x 220	1650	3300	4950	6600	9500	3250	9900	11500			
320 x 180	1350	2700	4050	5400	6750	8100	9450	10800	12150		
500 x 300	1440	2880	4320	5760	7200	8640	10080	11520			
500 x 350	1680	3360	50400	6720	8400	10080	11760				
800 x 350	1000	2000	3000	4000	5000	6000	7000	8000	9000	10000	11000
1250 x 560	1100	2200	3300	4400	5500	6600	7700	8800	9900	11000	
3200 x 1350	1000	2000	3000	4000	5000	6000	7000	8000	9000	10000	11000

Tab. 4: Natural vibration frequencies of the cast iron wheels

Geometric parameters of a tooth-wheel, $D \times h$ (mm)	Its vibration frequencies							
	f_1	f_2	f_3	f_4	f_5	f_6	f_7	f_8
20 x 50	7500							
50 x 50	5000	10000						
80 x 100	3750	7500	11250					
125 x 100	2400	4800	7200	9600	12000			
200 x 200	3000	6000	9000					
200 x 160	2400	4800	7200	9600				
320 x 220	2000	4000	6000	8000	10000			
320 x 180	1688	3376	5064	6752	8440	10128		
500 x 300	1800	3600	5400	7200	9000	10800		
500 x 350	2100	4200	6300	8400	10500			
800 x 350	1300	2600	3900	4200	6500	7800	9100	10400
1250 x 560	1344	2688	4032	6720	8064	9408		
3200 x 1350	1266	2532	3798	5064	6330	7596	8862	10128

Tab. 5: Natural vibration frequencies of the steel tooth-wheel

The calculation results showed that the tooth-wheels have significant differences in the number of the natural vibration frequencies in the normalized frequency range. Moreover, almost all tooth-wheels fall into the medium and high frequency range of 100-11200 Hz [5,6].

The mandrels which are centered on machined tooth-wheels differ in the ways of fixing on machines. In particular, with machining on vertical gear generator and gear shaping machines using the rotation method, the mandrels are cantilevered fixed rods [7]. During machining on gear grinding and hobbing machines using the rotation method, the mandrels are round steel rods on two supports, which also should be considered as hinged-supported and rigidly fixed.

A cylinder of limited length is adopted as an acoustic model of any mandrel. Sound pressure and sound power for the three mounting options are given as follows [8,9]:

for hinged-supported mandrel

$$\boldsymbol{P = \frac{2,5 \cdot 10^2 D^3 V_k}{r}\left(\frac{k}{l}\right)^2} \qquad \boldsymbol{N = \frac{3 \cdot 10^5 D^4 {V_k}^2 k^6}{l^5}}$$

for cantilever-mounted mandrel

$$\boldsymbol{P = \frac{2,5 \cdot 10^2 D^3 V_k}{r}\left(\frac{2k-1}{l}\right)^2} \qquad \boldsymbol{N = \frac{3 \cdot 10^5 D^4 {V_k}^2 (2k-1)^6}{l^5}}$$

for rigidly fixed mandrel

$$\boldsymbol{P = \frac{2,5 \cdot 10^2 D^3 V_k}{r}\left(\frac{2k+3}{l}\right)^2} \qquad \boldsymbol{N = \frac{3 \cdot 10^5 D^4 {V_k}^2 (2k+3)^6}{l^5}}$$

Sound pressure and sound power levels generated by the technological subsystem at the workplaces of machine operators` workplaces are determined as follows:

$$\boldsymbol{L_{p(N)}} = \mathbf{10}\ \boldsymbol{lg}(\mathbf{10}^{\mathbf{0,1}\boldsymbol{L_1}} + \mathbf{10}^{\mathbf{0,1}\boldsymbol{L_2}})$$

where
$\boldsymbol{L_1}$ and $\boldsymbol{L_2}$ are the sound pressure (sound power) levels of the tooth-wheel and mandrel, dB.

4. CONCLUSION

In the above dependences, the parameters of the technological processes implemented on vertical gear generator and gear shaping machines will be taken into consideration the dependences of the vibration speeds at natural frequencies [9,10].

The obtained data make it possible to calculate theoretically the spectral sound pressure levels of the above sources at the design stage and to identify frequency intervals and values of excess over sanitary standards. In fact, such calculations make it possible to determine the acoustic efficiency of the noise protection systems with designing such machines.

REFERENCES

[1] Chukarin A.N.: Experimental studies of the noise levels of the range of woodworking drilling machines/ A.N. Chukarin, D.V. Ruslyakov // Izvestiya TulGU, Technical science, Issue. 2, pp. 622-626, 2021
[2] Life safety: textbook / I.G. Pereverzev, T.A. Finchenko, I.A. Yaitskov [and others]; FSBEI VO RSTU. –2nd ed., Rev. and add., Rostov n / a, 308 p., 2019
[3] Goguadze M.G.: Experimental studies on the noise and vibration of a special boring machine due to the formation of the operator`s workplace sound field / M. Goguadze, A. Shashurin, A. Lubianchenko // AKUSTIKA, Vol. 34, pp. 100-104, 2019
[4] Litvinov A.E.: Research of cutting modes on band saw machines / A.E. Litvinov, V.G. Kornienko, N.I. Sukhonosov // Machine Tools Tool (STIN), № 10, pp. 5-8, 2010
[5] Motrenko D.V.: Modeling of vibroacoustic dynamics of the cutting tool of chain-slotting woodworking machines / D.V. Motrenko, I.A. Yaitskov // Bulletin of the Rostov State Transport University, Rostov n / a, № 2 (74), pp. 37-42, 2019
[6] The design of the support mechanism for the faceted rod / A.N. Chukarin, T.A. Finochenko // Patent for invention RU 2718511 C1, 04/08/2020. Application No. 2019123512 dated 07.19.2019.
[7] Chukarin A. N.: Theoretical studies of centrifugal-ball processing of steels / A. N. Chukarin, Yu.A. Proskoryakova, A.A. Fedenko // Bulletin of the Rybinsk State Aviation Technological Academy. P. A. Solovyova, № 4 (51), pp. 56-60, 2020
[8] Sound absorbing materials and structures. Book of reference. Moscow: Communication, 124 p., 1970
[9] Ivanov N.I.: Fundamentals of vibroacoustics / N.I. Ivanov, A.S. Nikiforov // St. Petersburg: Polytechnic, 482 p., 2020
[10] Chukarin A.N.: Theory and methods of acoustic calculations and design of technological machines for mechanical processing / Rostov n / a: Publishing center of DSTU, 152 p., 2004

Sergey Ryzhov *the applicant of the Department of Life Safety, Rostov State University of Railways (RGUPS), (Rostov-on-Don, Russia)*
The direction of scientific research is the processes of vibroacoustic dynamics. Participant of international and national scientific and practical conferences.

Tatiana Finochenko *candidate of Technical Sciences, Associate Professor, Head of the Department of Life Safety, Head of the Research and Production Center "Labor Protection" of the Research Unit of the Rostov State University of Railways (RGUPS), (Rostov-on-Don, Russia)*
Author of over 160 scientific works, educational and methodological works, including 7 monographs, as well as 3 patents for noise reduction devices.
Finochenko T. conducts active research work in the field of labor protection and vibroacoustic dynamics of technological machines. Participant of international and all-Russian exhibitions.
Has received awards from the Ministry of Transport of the Russian Federation, the Central Committee of the Russian Trade Union of Railway Workers and Transport Builders and Russian Railways.

Alexander Chukarin *is Doctor of Engineering Sciences, Professor, Head of the Chair «Fundamentals of Machine Design», Rostov State Transport University (RSTU) (Rostov-on-Don, Russia).*
The direction of the scientific research is the process of vibro acoustic dynamics of the technological machines in various functional purposes.
In 1985 he defended his thesis on the topic «Improving vibro acoustic characteristics of the bearing assemblies of the machine tools». In 1996 he defended his doctoral thesis in the specialty «Vibro acoustic bases for calculating machine tools at the design stage».
Under the leadership of Professor A.N. Chukarin, 3 doctoral and 19 master's theses were defended.
A.N. Chukarin published more than 220 scientific and educational works: 6 monographs.
He is the Deputy Chairman of the Doctoral Dissertation Council on the specialties «Labor Protection» (mechanical engineering) and «Machine engineering, Drive Systems and Machine Parts». He is a member of the editorial boards of a number of the abstract journals.

Ivan Yaitskov *is Doctor of Engineering Sciences, Professor, Dean of the Electromechanical Faculty of the Rostov State Transport University (RSTU), Leading Researcher at the Scientific and Production Center "Labor Protection" of the RSTU (Rostov-on-Don, Russia).*
He is the author of over 90 scientific papers, monographs, educational and methodical works for patent of reducing noise device. Yaitskov I.A. conducts the research work and made a significant contribution in the field of vibro acoustic safety of the railway transport and transport workers, engineering, improving the design of noise and vibration protection, automatic brakes of the railway rolling stock, ensuring the safety of train traffic and labor protection. He is the participant of the international and all-Russian exhibitions. He is a winner of an increased candidate grant from the Russian Ministry of Railways, a grant within the framework of the Federal Targeted Program "Scientific and Scientific-Pedagogical Personnel of Innovative Russia" and a number of others. Under the leadership of Yaitskov I.A. Research grants of the Russian Railways company are performed.He is a participant and organizer of the international conferences, exhibitions, forums and symposia held by the Transport Ministry of the Russian Federation, Russian Railways and the University in the field of transport, industry and life safety.He passed a foreign internship at the Berlin Technical University, Faculty of Transport and Machine Systems of the Institute of Land and Water Transport, Department of Railways and Operation of Railways "Functioning of Innovative Infrastructure Objects Based on the University" and a course in innovative management. Yaitskov I.A. has awards from the Transport Ministry of the Russian Federation, the Central Committee of the Russian Trade Union of Railway Workers and Transport Builders and Russian Railways.

Paper No.361/2021

NOISE REDUCTION AT WORKPLACE IN CONSTRUCTION

[a)] Marina Butorina, [b)] Nickolay Ivanov, [c)] Alisa Troshchinina

[a, b, c)] *Baltic State Technical University 'VOENMEH' named after D.F. Ustinov, St. Petersburg, Russia*
[a)] *butorina_mv@voenmeh.ru* [b)] *ivanov_ni@voenmeh.ru*

Abstract: *Construction machinery is one of the most common noise sources in the environment and at the workplace. In Russia about 40% of all occupational injuries and 40% of the loss of working capacity are recorded at the construction sites. The noise levels at the operator's position exceeds noise limits up to 40 dBA. However, personal hearing protection recommended in Russia can not provide sufficient noise reduction. To reduce construction noise administrative and engineering controls, substitution of noise with the standardization of noise emissions and replacing of noisier equipment with quieter items can be recommended. Administrative measures of noise reduction include reduction of work time, training and audiometric testing. To elaborate engineering controls a method of separation of noise sources with mathematical modelling was proposed. Basing on this method the most effective noise reduction measures were proposed that helped to reduce noise in the cabin of a backhoe by 6-7 dBA.*

Keywords: *noise, construction, noise limits, sound isolation, muffler, hood.*

DOI: *: 10.36336/akustika20214194*

1. INTRODUCTION

Construction machinery is one of the most common noise sources in the environment and at the workplace. Given the rapidly growing infrastructure of cities, various noises from construction machines are increasingly interfering in human life. According to statistical data, about 56% of the total number of occupational diseases falls on the operators of construction machines, while the construction industry is one of the most unfavorable ones in terms of working conditions. In Russia about 40% of all occupational injuries and 40% of the loss of working capacity are recorded here. Noise-induced hearing loss is one of the most common work-related illnesses that is observed at construction.

The noise at construction sites is emitted by heavy-equipment and power tools. Noise levels of power tools reaches 117 dBA, heavy-equipment noise is ranged as 80-125 dBA [1-3]. Noise exposure varies depending on the type of equipment and operation executed. Operators of cranes and bulldozers are influenced by noise levels of 103-106 dBA, operators of handy appliances such as chainsaws, jackhammers and sand blasting nozzles are exposed to noise levels of 115-117 dBA [1,4]. On the other hand, the U.S. National Institute for Occupational Safety and Health (NIOSH) recommends the limit noise value at the workplace of 85 dBA [5]. Russian provisions according to SanPiN 1.2.3685-21 [6] are even more serious since they recommend that noise levels at the workplace should not exceed 80 dBA.

Reducing noise levels in construction industry can be achieved using different measures. According to NIOSH [7] they include personal protection, administrative and engineering controls, substitution and elimination of noise (Fig. 1). Since it's absolutely impossible to physically remove the noise hazard at the workplace, let us focus on the other measures of noise reduction.

Individual protection devices are considered to be the least effective measure. Ministry of Labour, Training and Skills Development of Ontario [8] reported that operator average noise exposure reaches up to 125 dBA. Comparing to Russian limit value the noise reduction should reach up to 45 dBA, although the most effective headphones can reduce noise only up to 35 dBA according to the data of the manufacturers [9]. Also hearing protection are ineffective in reducing noise influence due to low or irregular usage [10]. To avoid excess exposure American health care institutions recommend to use administrative controls [11] or substitute noisier equipment with less noisy items. NIOSH recommends to purchase newer and quieter equipment [12]. However, replacing older heavy-construction equipment sometimes is not financially feasible.

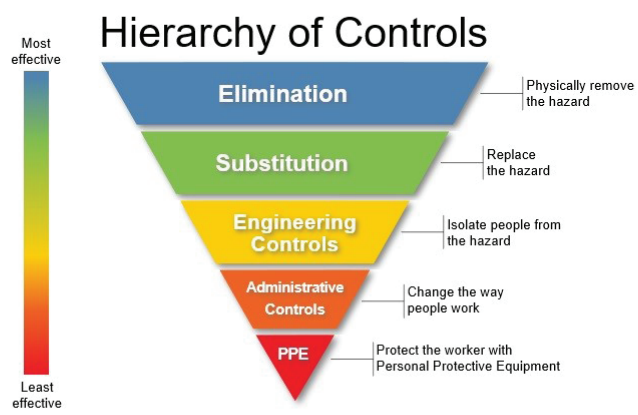

Fig. 1: Noise control measures [7]

The most widespread measure of construction noise reduction is implementation of engineering noise control. The first step of implementation of such controls is to define which sources of noise contribute the noise levels at the workplace. The main sources of noise emitted by construction machines include the hydraulic systems, the exhaust and intake of the combustion engine and the engine itself. The easiest ways to reduce noise are replacing of defective parts, proper maintenance and repair of equipment but usually they are not enough. The difficulty in reducing the total noise level of the construction machinery lies in the difficulty of evaluation of the contributions of various sources to the total noise level. Russian researchers in cooperation with American practitioners have proposed [13] and improved [1] a method of separation of noise sources basing on which the most effective noise reduction measures are proposed.

2. NOISE EXPOSURE, HEALTH STANDARDS AND ADMINISTRATIVE CONTROLS

The main sources of noise in construction include: impacting tools (such as concrete breakers); use of explosives (such as blasting, cartridge tools); pneumatically powered equipment and internal combustion engines. The noise levels associated with the operation of equipment found on construction sites is provided in Tab. 1 according to [8].

Equipment	Noise Level (dBA) at Operator's Position
Cranes	78 – 103
Backhoes	85 – 104
Loaders	77 – 106
Dozers	86 – 106
Scrapers	97 – 112
Trenchers	95 – 99
Pile drivers	119 – 125
Compactors	90 – 112
Grinders	106 – 110
Chainsaws	100 – 115
Concrete saw	97 – 103
Sand blasting nozzle	111 – 117
Jackhammers	100 – 115
Compressors	85 – 104

Tab. 1: Typical Noise Levels for Construction Equipment

If we compare the noise levels given in Table 1 to the provision of NIOSH we can see that the excess of noise limits is the greatest for the operator of a pile driver (40 dBA), sand blasting nozzle (32 dBA) and jackhammers (30 dBA). At the same moment all those types of equipment are not used for the duration of the whole working day. So, it is not feasible to compare these levels to the limit of equivalent sound level.

According to Russian sanitary norms [6] we should evaluate equivalent, maximum and peak sound levels at the workplace, the limit values for which make 80 dBA, 110 dBA and 137 dBC accordingly. Some samples of maximum and peak noise levels of construction equipment measured at a distance of 50 feet (15 meters) and calculated at the operator's position are given in Tab. 2 [3].

Equipment	Acoustical Usage Factor (% / hours)	Maximum Noise level, dBA	Peak Noise Level, dBA
Cranes	16 / 1,5	112	125
Backhoes	40 / 3	109	123
Front Loaders	40 / 3	110	127
Dozers	40 / 3	113	124
Graders	40 / 3	116	122
Scrapers	40 / 3	115	129

Tab. 2: Maximum and peak noise levels of construction equipment

So, we can see that the peak levels comply to Russian noise limit and maximum noise levels normally exceeds it by 2-6 dBA. Taking into account that construction machinery often operates together with other types of equipment, the excess of noise limit will be even higher.

To reduce noise levels at the workplace located at the construction site Washington Industrial Safety and Health Act (WISHA) [11] recommends the noise evaluation criteria and administrative measures that for Russian sanitary norms can be transformed as it is shown in Tab. 3.

Criteria	Description	Requirements	Allowable exposure times for unprotected workers
80 dBA	Full-day noise exposure dose, protection for employees exposed to higher levels	Hearing protection Training Audiometric testing	8 hours
85 dBA	Full-day noise exposure dose, reduction of noise exposure	Noise controls Hearing protection Training Audiometric testing	4 hours
90 dBA			2 hours
95 dBA			1 hour
100 dBA			30 min
105 dBA			15 min
110 dBA	Extreme noise level (greater than 1 second in duration)	Hearing protection Signs posted in work areas warning of exposure	0 min
137 dBC	Extreme impulse or impact noise (less than one second in duration)	Hearing protection	0 min

Tab. 3: Noise criteria evaluation and exposure times

If we consider the noise levels and times of acoustical operation of equipment given in Tabs. 1 and 2, we can see that most types of construction equipment require noise controls the most efficient of which are engineering methods of noise reduction.

3. ENGINEERING CONTROLS

Any technology that uses internal combustion engines as a source of energy generates high sound levels, and the sound intensity generated is higher the higher the power of the engine. Noise in construction machines' cabins, as a rule, has a low--frequency character. Since external noise is of a medium and high frequency nature, it can be stated that the cabins have pretty high sound insulating properties.

We should also note that in the stationary mode (idling position), the noise in the cabins of the construction machines is lower than in the dynamic (full-throttle) mode. Such, for wheeled and tracked vehicles the noise in the stationary mode is 1-3 dBA lower than in the dynamic mode, for vibratory rollers it is 10 dBA lower in the static mode than in the dynamic mode.

One of the main sources of noise in the cabin is the internal combustion engine or vibratory drum. Also, the type of drive and design affect the noise level in the cabs. This is especially noticeable for the example of a cargo crane, the power plant of which can be located both under the hood and in the engine room. In the cabins of cranes with a diesel drive, the noise is 10-11 dBA higher than in the cabs with an electric drive, and the noise in bonnet-type cranes is 8-12 dBA higher than in cranes with an engine room, and 5-10 dBA higher than in mobile cranes.

So, the main sources of noise that should be taken into account are ventilation system; internal combustion engine; parts located in the engine compartment near the cab; intake and exhaust of the internal combustion engine.

Exhaust and intake noise penetrates the cabin both directly through the glazed panel behind which these sources are located, and as a result of sound diffraction over other panels of the cab (except for the partition and the floor). Noise from the internal combustion engine passes from the engine compartment into the cab through the floor directly or through the lower openings in the hood and further through the cabin floor, taking into account the reflection from the surface. The noise from the cooling system fan enters the cab in two ways: first, through the lower openings in the hood and then through the cabin floor, taking into account the reflection from the surface, and second, through the hood rails, and then through the cab panels, with the exception of the floor.

For the evaluation of noise penetrating the cabin a mathematical modelling was executed and formulae provided. The formulae account the sound isolating properties of the cabin walls and floor, their areas, acoustical properties of the cabin, the presence and geometrical parameters of openings. For example, engine noise penetrating the workplace through the cab floor is determined by the formula, dB(A):

$$L_{eng.floor}^{cab} = L_{w_{eng}} + 10\lg\left(\frac{\chi_{hood}}{S_{hood}} + \frac{4\psi_{hood}}{B_{hood}}\right) + 10\lg\frac{S_{ch}}{S_{pen.hood}} - R_{floor} + 10\lg\frac{S_{floor}}{A_{cab}} + 1$$

where

- L_{weng} is the sound power emitted by the engine, dB(A);
- X_{hood} is the coefficient taking into account the influence of the near sound field of the engine;
- ψ_{hood} if the coefficient taking into account the violation of the diffuseness of the sound field under the engine hood;
- S_{hood} is the total area of the internal fencing of the engine hood panels, m^2;
- B_{hood} is the acoustical constant of the hood, m^2;
- S_{ch} is the cross-sectional area of the channel through which the sound passes from the engine under the cabin floor, m^2;
- $S_{pen.hood}$ is the area of the engine hood fencing through which sound penetrates, m^2;
- S_{floor} is the area of the cabin floor through which sound penetrates, m^2;
- A_{cab} is the equivalent area of sound absorption of the cab, m^2;
- R_{floor} is the sound insulation of the cabin floor, dB(A).

Similar formulae are provided for the other passes of sound penetrating into cabin. The summary noise level in the cabin is added up by the contributions of noise penetrating from different sources.

The results of calculation performed for the backhoe show that in the static mode of operation, the noise level in the cabin was 84.8 dBA with the main contributions of the engine (82.9 dBA), exhaust (77.2 dBA), cooling fans (73.3 dBA) and intake (72.6 dBA). In dynamic mode of operation, the noise level in cabin was 87.5 dBA, coming from the main sources such as engine (85.6 dBA), exhaust (81.5 dBA), cooling fans (75.7 dBA) and intake (73.6 dBA). The contribution of engine noise exceeds all other emitting sources; the exhaust noise is the second influencing source. The noise of the fan system is comparable to the noise of the intake, while neither noise of the fans, nor intake noise is comparable to the noise of the internal combustion engine.

Since the main sources of noise in the cab are the internal combustion engine and the exhaust system, it is necessary to propose measures to reduce the noise of these particular sources. To reduce exhaust noise, it is advisable to use noise mufflers. However, installing a silencer in the gas path introduces losses into it, which contribute to an increase in its back pressure. This leads to a decrease in engine power, therefore, when designing a muffler, it is necessary to find a balance between achieving the required noise reduction and the requirements for minimum back pressure [14]. Silencers are a mandatory tool that is installed in the gas exhaust ducts, as well as on the intake of the internal combustion engine. It is recommended to use a combined muffler that construction is presented in Fig. 2.

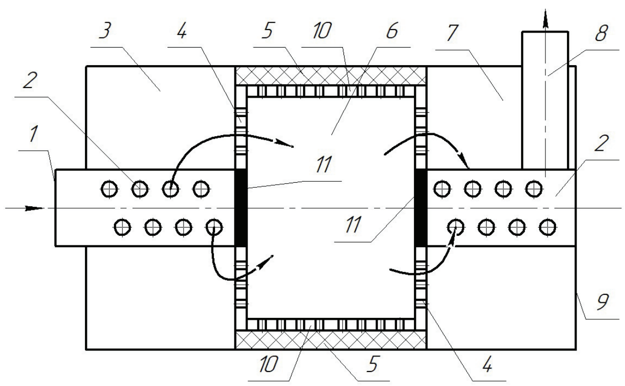

Fig. 2: Muffler's construction

This muffler is mounted in a housing (9) with a turn of gas flows by 90 ° at the outlet. It has three chambers (3, 6, 7), separated by special perforated partitions (4). Two perforated nozzles (2) are located in the first and third chambers, the nozzles are closed at the ends with plugs (11). The perforated shell (10) is made in the form of a cylinder, where the perforation is made in the form of two large holes with a diameter of 33 mm and 58 holes with a diameter of 5 mm, perforation of the branch pipes is presented with 48 holes with a diameter of 8 mm. Sound-absorbing material is applied around the shell (5). Gases through the nozzle (2) enter the expansion chamber (3), where the flow expands, then through the holes they flow into the second expansion chamber (6), lined with sound-absorbing material (5), then through the perforated partition (4) they enter the chamber (7) with a perforated nozzle, where the stream turns 90 ° and exits. The efficiency of such a muffler makes 15 dBA.

To reduce noise from the internal combustion engine, we will use a sound-insulating hood, that is a closed structure installed on the internal combustion engine so that there is an air gap between the hood and the source. In such a hood, holes, openings and slots must be provided, which serve for normal heat exchange with the engine compartment. The main performance indicators of the hood are acoustic efficiency and the degree of sealing. To increase the sound insulations properties of the hood the inside of the hood must be lined with sound insulating material [15].

To reduce engine noise a special insulation for the hood is proposed in [2]. These sound dampening mats (SDMats) are made of two layers of open-cell polyurethane foam separated by high-density polyvinyl chloride vinyl flexible sheet. The inner side of the mats is coated with an adhesive layer that could be attached to a metal surface. The exterior layer is covered with thin film of Mylar reinforced with elastomer-coated fiberglass providing additional surface heat protection, resulting in the material being fire retardant. SDMats are used to insulate not only engine but the cabin itself (Fig. 3). The measurements show that efficiency of SDMats makes 5-12 dBA.

Fig. 3: Cabin and engine compartments with sound dampening mats installed

In the result of application of the described above complex of noise reduction measures the reduction of noise in cabin made 6-7 dBA, that is the compliance to the noise limits at the workplace is observed.

4. SUBSTITUTION – NOISE LIMITATION

One more important measure that should be wider implemented in Russia is the limitation of noise of construction equipment. In Russia the state standard named GOST 12.2.011-2012 [16] acts. However, the exact figures of noise emissions for the construction machinery are not stated there. The standard says only that the noise limits for the workplace (80 dBA) should be observed. The operational documentation for machines of specific models must indicate the actual sound level at the operator's workplace and the external noise of the machine. If the limit values are exceeded, prescriptive signs must be applied on the machine, and the operational documentation must contain recommendations for the use of personal protective equipment for hearing organs.

Such an approach does not lead to the reduction of the construction noise focusing on the application of personal hearing protection that is sometimes not efficient enough to provide sufficient noise reduction.

A much better approach is provided by European legislation, i.e. Directive 2000/14/EC [17]. It states the permissible sound power levels for different types of construction machines that the manufacturer should ensure (Table 4). These values are a subject of revision, thus, starting from 2002 the limits were reduced by 2-3 dBA up to now. This approach encourages the manufacturers of construction equipment to reduce noise levels of machinery providing reduction of noise both at the workplace and in the vicinity of construction site.

Type of equipment	Net installed power P, kW Electric power P el, kW Mass m, kg	Permissible sound power level, dB/1 pW
Compaction vibrating machines	P ≤ 8 8 ≤ P ≤ 70 P > 70	105 106 86 + 11 lg P
Tracked machines	P ≤ 55 P > 55	103 84 + 11 lg P
Wheeled machines	P ≤ 55 P > 55	101 82 + 11 lg P
Compressors	P ≤ 15 P > 15	97 95 + 2 lg P
Excavators, builders' hoists for the transport of goods	P ≤ 15 P > 15	93 80 + 11 lg P
Tower cranes	-	96 + lg P
Hand-held concrete-breakers and picks	m≤ 15 15 ≤ m ≤ 30 m> 30	105 92 + 11 lgm 94 + 11 lg m
Welding and power generators	P el≤ 2 2≤ P el ≤ 10 P el > 10	95 + lg P el 96 + lg P el 95 + lg Pel

Tab. 4: Permissible noise emission of construction machinery

One more way of noise reduction that should be mentioned here, is Buy Quiet program implemented by NIOSH to create a more healthful workplace [12]. Buy Quiet is a prevention initiative which encourages companies to purchase or rent quieter machinery and tools to reduce worker noise exposure. NIOSH provides information on equipment noise levels, so companies can buy quieter products that make the workplace safer and encourages manufacturers to design quieter equipment by creating a demand for quieter products.

Quieting equipment during design and manufacture process is more effective and economically-efficient than implementing noise controls after manufacture. Buy Quiet assigns the engineering decisions to the equipment designers and manufacturers and removes the complexity of noise control from the purchaser, renter or end user whose core business is not noise control. Concurrent with protecting worker's hearing health, the Buy Quiet initiative aims to remove workers from legally mandated hearing conservation programs by reducing noise exposures to below 85 decibels (dBA) for 8 hours. Any company whose workers are subjected to hazardous noise exposures can benefit from Buy Quiet. Such a program initiated at the state level could be of a benefit for Russian companies as well at the same time it could help to provide better and quieter situation at the construction sites.

5. CONCLUSION

According to statistical data, about 56% of the total amount of occupational diseases falls on the operators of construction machines, while the construction industry is one of the most unfavorable ones in terms of working conditions.

Noise exposure varies depending on the type of equipment and operation executed. Operators of cranes and bulldozers are influenced by noise levels of 103-106 dBA, operators of handy appliances such as chainsaws, jackhammers and sand blasting nozzles are exposed to noise levels of 115-117 dBA.

The U.S. National Institute for Occupational Safety and Health recommends the limit noise value at the workplace of 85 dBA. According to Russian sanitary norms one should evaluate equivalent, maximum and peak sound levels at the workplace, the limit values for which make 80 dBA, 110 dBA and 137 dBC accordingly. The peak levels of construction equipment comply to Russian noise limit, while equivalent and maximum noise levels are normally exceeded.

To reduce noise levels at the workplace located at the construction site the administrative measures including reduction of work time, hearing protection, training, audiometric testing and warning signs can be implemented. The most widespread measure of construction noise reduction is implementation of engineering noise control.

First, one should define which sources of noise contribute the noise levels at the workplace. A method of separation of noise sources was proposed. For the evaluation of noise penetrating the cabin from the main sources such as engine, intake, exhaust and ventilation, a mathematical modelling was executed and formulae provided. The formulae account for the sound isolating properties of the cabin walls and floor, their areas, acoustical properties of the cabin, the presence and geometrical parameters of openings.

The main sources of noise in the cab are the internal combustion engine and the exhaust system. To reduce exhaust noise, it is advisable to use noise mufflers. To reduce engine noise a special insulation for the hood with sound dampening mats is proposed. In the result of application of the complex of noise reduction measures the reduction of noise in cabin made 6-7 dBA, that is the compliance to the noise limits at the workplace is observed.

One more important measure that should be implemented in Russia is the limitation of noise of construction equipment. Russian state standard does not provide the exact figures of noise emissions for the construction machinery stating only unreachable level of 80 dBA complying the sanitary norm. Such an approach should be substituted with European way of limitation of the permissible sound power levels for different types of construction machines.

Also construction companies should be stimulated to buy quieter machines that makes the workplace safer and encourages manufacturers to design quieter equipment by creating a demand for quieter products.

REFERENCES

[1] N.I. Ivanov. Zashchita ot shuma i vibratsii / N. I. Ivanov. – SPb: NITS ART, 2017. – 267 p.
[2] Saleh S, Woskie S, Bello A. The Use of Noise Dampening Mats to Reduce Heavy-Equipment Noise Exposures in Construction. Saf Health Work. 2017;8(2):226-230. doi:10.1016/j.shaw.2016.09.006
[3] Construction Noise Handbook / U.S. Department of Transportation, Federal Highway Administration, Office of Natural and Human Environment. – 2006. https://www.fhwa.dot.gov/environment/noise/construction_noise/handbook/handbook09.cfm
[4] Kerr M.J., Brosseau L., Johnson C.S. Noise levels of selected construction tasks. Am Ind Hyg Assoc J. 2002;63:334–339.
[5] National Institute for Occupational Safety and Health. Preventing hazardous noise and hearing loss during project design and operation [Internet]. 2015 [cited 2016 Sep 20]. Available from: https://www.cdc.gov/niosh/docs/2016-101/.
[6] SanPiN 1.2.3685-21 "Hygienic standards and requirements for ensuring the safety and (or) harmlessness to humans of environmental factors"
[7] By Original version: NIOSHVector version: Michael Pittman - Original version: JPEG file by NIOSH:, CC0, https://commons.wikimedia.org/w/index.php?curid=90190143
[8] Ministry of Labour, Training and Skills Development Ontario https://www.labour.gov.on.ca/english/hs/
[9] https://spb.technoavia.ru/katalog/siz/sluch
[10] Edelson J., Neitzel R., Meischke H., Daniell W., Sheppard L., Stover B., Seixas N. Predictors of hearing protection use in construction workers. Ann Occup Hyg. 2009;53:605–615.
[11] Chapter 296-817 WAC. Hearing Loss Prevention (Noise) / WISHA hearing conservation web site: https://lni.wa.gov/safety--health/safety-rules/chapter-pdfs/WAC296-817.pdf
[12] National Institute for Occupational Safety and Health. Buy Quiet [Internet]. December 5, 2014 [cited 2016 Feb 22]. Available from: http://www.cdc.gov/niosh/topics/buyquiet.
[13] Ivanov N., Kurtsev G., Copley D., Elkin Y. Cab noise generation and noise control in construction machinery / 12th International Congress on Sound and Vibration 2005, ICSV 2005. 2005. C. 3268-3275.
[14] Sakhapov R., Makhmutov M. Analysis of noise reduction methods for construction / Modern mechanical engineering: science and education – 2017. – No. 6. – p. 774-783. – DOI 10.1872/MMF-2017-69.
[15] Drozdova L., Kudaev A., Matveev P. Investigation of the effectiveness of noise protection elements of the hood / Noise Theory and Practice. – 2017. – Vol. 3. – No 3(9). – p. 39-45.
[16] GOST 12.2.011-2012 Occupational safety standards system. Building, road and earth-moving machinery. General safety requirements
[17] DIRECTIVE 2000/14/EC OF THE EUROPEAN PARLIAMENT AND OF THE COUNCIL of 8 May 2000 on the approximation of the laws of the Member States relating to the noise emission in the environment by equipment for use outdoors (amended in 2005, 2009, 2019) http://data.europa.eu/eli/dir/2000/14/oj/eng

Marina Butorina *is Ph.D. in Engineering Science, Assistant Professor of 'Ecology and industrial safety' Department of the Baltic State Technical University 'VOENMEH' named after D.F. Ustinov (Saint-Petersburg, Russia), Chief Engineer of the LLC 'Institute of Vibroacoustic Systems'.*
Marina Butorina is a specialist in noise mapping, calculation and design of noise protection for roads, railroads and industrial enterprises. She has presented her Post-Doctorate thesis in this field in 2021. She is a specialist in noise calculation programs representing SoundPLAN, a world-wide leader in this field. Marina Butorina has served as an author of a list of national regulation in the field of noise reduction. Marina Butorina has published over 150 scientific papers, including about 6 textbooks. She presented the main results of her scientific research at the international conferences in Austria, Germany, England and in Russia.

Nickolay Ivanov *is Doctor of Engineering Science, Professor of Department of Ecology and Industrial Safety of the Baltic State Technical University 'VOENMEH' named after D.F. Ustinov (Saint-Petersburg, Russia), Honored Scientist of the Russian Federation.*
Nickolay Ivanov is the creator of the transport acoustics scientific school. He developed the theory of the transportation vehicles acoustics, proposed the solution to the problems of generating the sound field in low volume, diffraction on complex obstacles, methods of calculation of the sound fields of spatial emitters. Nickolay Ivanov has published over 400 scientific papers, including about 10 textbooks, manuals and monographs. He presented the main results of scientific research on the international conferences in Australia, Austria, Hungary, Germany, Denmark, Italy, Canada, China, the Netherlands, Poland, Portugal, the USA, Finland, Switzerland, Sweden and other countries.

Alisa Troshchinina *is PhD student, engineer of the research laboratory of the Baltic State Technical University 'VOENMEH' named after D.F. Ustinov (St. Petersburg, Russia), performer of a number of applied scientific research within the framework of the federal target program "Research and Development in Priority Areas of Development of the Scientific and Technological Complex of Russia for 2014-2021" commissioned by the Ministry of Science and higher education. Alisa Troshchinina was a member of the organizing committees of scientific and technical conferences, seminars and competitions held at BSTU "VOENMEH" named after D.F. Ustinov, including the All-Russian Youth Scientific and Practical Conference "The Orbit of Youth-2019 Prospects for the Development of Russian Cosmonautics". Alisa Troshchinina was awarded the medal of the Russian Federation of Cosmonautics. Research interests include research in the field of labor protection, industrial safety and safety in construction.*

Paper No.362/2021

NUMERICAL SIMULATION OF THE LIGHT AIRCRAFT PROPELLER NOISE UNDER STATIC CONDITION

Sergey Timushev, Alexey Yakovlev, Petr Moshkov

Moscow Aviation Institute (National Research University), Moscow, Russia, tempero.m@gmail.com

***Abstract**: The problem of simulation the noise generated during the operation of the propeller is considered. Calculation methods are described and numerical simulation of the noise of a light aircraft propeller by the acoustic-vortex method is performed. The results of numerical modeling of the tonal components of the propeller noise when operating under static conditions are compared with experimental data and calculation results based on a semiempirical model.*

***Keywords:** propeller noise, community noise, UAV noise, aeroacoustics, noise simulation*

***DOI:** : 10.36336/akustika202141100*

1. INTRODUCTION

The first successful model describing the mechanisms of noise generation during the operation of an air propeller has proposed by Gutin L.Ya. in 1936 [1]. Since then, a significant number of methods for estimating the noise of various types of propellers has proposed. However, at present, the problem of calculating the noise of the propeller is again becoming more and more urgent due to the following circumstances:

- Wide application of civil and special propeller-driven unmanned aircrafts (UAV) [2, 3],
- In the short term (10-15 years old) in small and unmanned aircraft is expected to transition to electric [4-6], hybrid and distributed [7] power plant (PP) [8], for which the propeller noise is expected to dominate the overall community noise of the aircraft (a/c).

Modern trends in the development of aircraft industry pose the task of developing "digital twins" of the main components and systems. Within the framework of the problem of propeller noise, the "digital twin" is an aeroacoustic simulation model that reliably describes the aerodynamic and acoustic characteristics of the propeller both isolated and in the configuration of a real aircraft [9, 10].

The aim of the work is a preliminary validation of the acoustic-vortex method [9, 10] by the example of solving the problem of numerical modeling of the tonal components of the propeller noise.

The following tasks have solved in the work:

- A numerical analysis of the sound field of a low-load propeller of light aircraft was performed;
- The results of numerical modeling are compared with experimental data [11], as well as with the calculation of propeller noise by the semiempirical method [12].
-

2. ABOUT THE PROBLEM OF CALCULATING THE PROPELLER NOISE

The paper [13] presents a comparison of the sound pressure levels of the first tone of noise for different propellers under different experimental conditions with calculations based on the well–known early propeller noise theories (Gutin L.Ya. [1], Barry and Magliozzi [14], Hanson [15]) and numerical calculations based on the Ffowcs Williams-Hawkings integral method (FW-H) implemented in the SmartRotor and STAR-CCM+ commercial software packages.

It was found that the best calculation results with an average error of 7.2 dB relative to the experimental data are provided by the Hanson model. At the same time, the Gutin's model shows good agreement with the experiment at Mach numbers of the incoming flow less than 0.3, and the Barry and Magliozzi model at Mach numbers less than 0.6. And the results of calculating the tonal noise of the propeller in commercial products (SmartRotor, STAR-CCM+) cannot be used to support the design of propeller aircraft due to the high error of the calculation results. Therefore, interested organizations are developing their own software for modeling the propeller noise [16-18].

The different methods for calculating the propeller noise in the context of taking into account the most important parameters in the models, such as airspeed, the shape of the blade in the plan and sweep, the non-compactness of the source, the angle of attack (pitch) of the aircraft are presented in Tab. 1.

The Barry and Magliozzi model [14] is a development of the Gutin's model [1] in terms of taking into account the airspeed in the calculated ratio. Hanson's analytical model allows us to take into account the non-compactness of the source, the angle of attack (pitch) of the aircraft and the detailed propeller geometry. At the same time, although the model takes into account the influence of the angle of attack of the propeller, but computational studies [13] have shown that this influence is insignificant within the framework of this model.

The semiempirical method proposed by Samokhin V.F. [12] does not explicitly take into account the shape of the blade in the plan and sweep, but these parameters can be taken into account by introducing additional corrective functions. In contrast to the other methods considered, the calculation of propeller noise using a semiempirical model is impossible without experimentally obtained proportionality coefficients for propellers that are similar in geometric and aerodynamic characteristics to the one under study. At the same time, the error of calculation by the semiempirical method in the presence of appropriate empirical coefficients is significantly less than in the case of the above methods.

Method of analysis	Airspeed	Blade sweep and shape in the plan	Non-compactness	Angle of attack (non-axial flow)
Gutin L. Ya. [1]	No	No	No	No
Barry and Magliozzi [14]	Yes	No	No	No
Hanson [15]	Yes	Yes	Yes	Yes
Simiempirical method (Samokhin V.F.) [12]	Yes	No	No	No
Numerical simulation	Yes			

Tab. 1: Possibilities of taking into account the influence of parameters on the propeller noise in different methods

3. THE OBJECT OF THE STUDY

The object of the study is a low-loaded 4-bladed variable-pitch propeller with a diameter of 3.6 m, installed on an AN-2 light propeller-driven aircraft (Fig. 1). The maximum take-off weight of the aircraft is 5500 kg, and the maximum airspeed is 236 km/h. The aircraft's power plant also includes an ASH-62IR 9-cylinder 4-stroke piston engine with a maximum available power of 735.4 kW.

Fig. 1: General view of AN-2 aircraft

The geometric characteristics of the propeller in a dimensionless form are considered in Fig. 2. The laws of variation in radius $\bar{r} = r / R$ (where R is propeller radius, r is distance from the axis of rotation to the considered section of the profile of the propeller blade) of the relative width of the propeller blade $\bar{b} = b / d$ (where b is the blade width, d is propeller diameter) and the relative thickness of the blade profile $\bar{c} = c / b$ (where c is thickness of the profile) are shown in Fig. 2a.

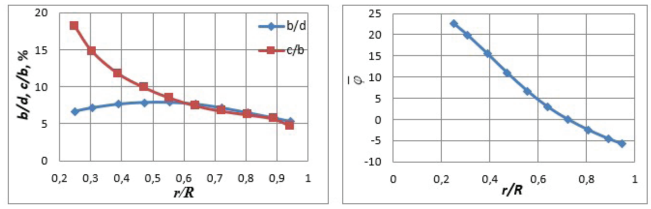

a) Relative width and thickness of the blade

b) The twist angle of the blade relative to the cross section at a relative radius of 0.75

Fig. 2: Geometric characteristics of the propeller

The change in the length of the blade of the twist angle $\bar{\varphi} = \varphi_{\bar{r}} - \varphi_{0.75}$ relative to the section located at a relative radius $\bar{r} = 0.75$ (where $\varphi_{\bar{r}}$ is the angle of installation of the section of the propeller blade at a relative radius , $\bar{r}$ $\varphi_{0.75}$ is angle of section installation of the propeller blade at a relative radius of 0.75 ($\bar{r} = 0.75$)are shown in Fig. 2b.

In the framework of this work, the nominal power condition of a power plant with an available power of 603.1 kW at propeller speed (***n***) 1446.6 rpm is considered. This mode was chosen for the analysis of aeroacoustics due to the fact that the angle of installation of the studied automatic propeller varies in the range of 15°. At the same time, it is known that when the propeller is operating under static conditions at the maximum power condition, the angle of installation of the blade will be the minimum possible. The selected mode is the maximum for the operation of the propeller in static conditions and the blade in the study was set to the minimum angle (17° at a radius of 1 m).

4. EXPERIMENTAL RESULTS

At the first stage of the work, the study of the acoustic characteristics of the propeller as part of the power plant of AN-2 aircraft when operating under static conditions was carried out [14]. The propeller sound field was supposed to be symmetrical relative to its axis. Measuring microphones of a free field with a diameter of 1/2" from GRAS (Denmark) were located at the level of the earth's surface on a circular arc (***R***) of 30 m with a step of 15° in the range of azimuthal angles of 0-165°. The direction of 0°corresponded to the radiation into the front hemisphere along the axis of the propeller, and the direction of 90° corresponded to the radiation in the plane of rotation of the propeller. The measurements were performed in parallel with 12 measuring channels with a sampling frequency of 51200 Hz for 40 seconds. Further post-processing of the signal for the purposes of this work included obtaining narrow-band spectra of sound pressure levels with a bandwidth (Δf) of 1.56 Hz.

Narrow-band spectrum of sound pressure levels measured during the operation of AN-2 PP in the direction(ϑ) 120° is presented in Fig. 3. On the graph, the first 10 tones are marked with numbers with "p" indices at frequencies that are multiples of the frequency of the propeller blades. In the noise spectrum in the low and medium frequencies, there are tonal components at frequencies that are multiples of the frequency of flashes in the engine cylinders. The presented spectrum of sound pressure levels also includes a broadband component that passes through the entire spectrum. Its sources are the vortex component of the propeller noise [19] and the broadband component of the piston engine noise [20].

In the framework of solving the problems of this work, only the tonal components of the propeller noise are considered further. At the same time, we note that the sound pressure levels of the tonal components of the piston engine noise and the broadband noise of PP are 10-20 dB lower than the noise levels of the tonal components of the propeller noise (Fig. 3) and cannot affect the overall noise level of the PP when operating under static conditions.

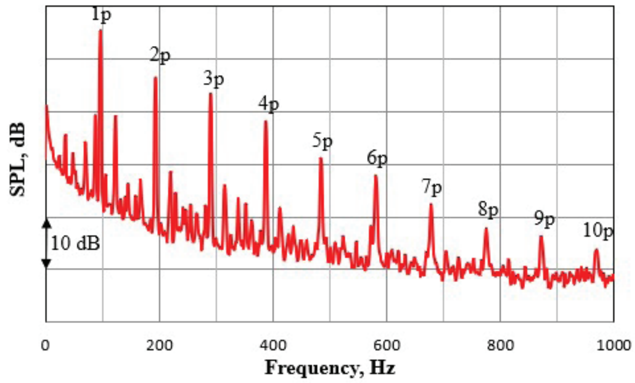

*Fig. 3: Narrow-band spectrum of sound pressure levels measured during the operation of AN-2 power plant under static conditions (**n**=1446.6 rpm, **ϑ** =120°,**R**=30 m, **Δf**=1.56 Hz)*

The directivity patterns of the first six tones of the propeller noise and their overall radiation are considered in Fig. 4. It can be seen that the direction of the overall tonal radiation of the propeller in the direction of azimuthal angles of 45-165° is determined by radiation at the frequency of the 1st tone of the propeller noise, and in the range of angles of 0-30° by radiation at the frequency of the 2nd tone of the propeller noise. The maximum of the directional characteristics of the first tone and the overall tonal radiation of the propeller occur in the rear hemisphere in the direction of 105°, which is consistent with the results of studies by other authors [13].

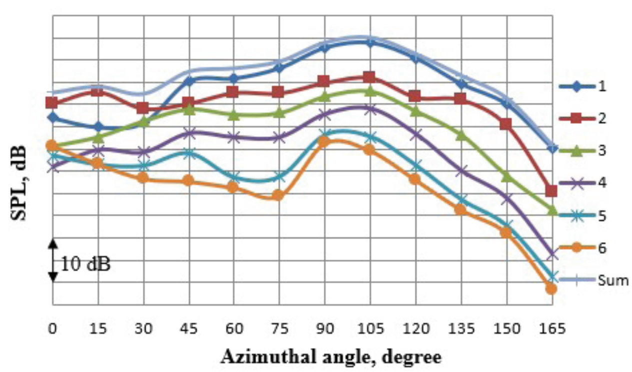

Fig. 4: Directivity patterns of the first six tones of the propeller noise and their sum

5. RESULTS OF AEROACOUSTIC SIMULATION

5.1. Main equations

Aeroacoustics modeling is based on the equations of decomposition of the motion of a compressible medium into vortex (vortex motion of an incompressible medium) and acoustic modes [12, 13]. The velocity is represented as the sum of the velocity of the vortex flow and the velocity of acoustic motion, which gives an acoustic-vortex equation with respect to the fluctuations of the enthalpy (i) in the isentropic flow of the compressible medium:

$$\frac{1}{\boldsymbol{a}^2}\frac{\partial^2 \boldsymbol{i}}{\partial \boldsymbol{t}^2} - \Delta \boldsymbol{i} = \nabla(\nabla(\tfrac{1}{2}\boldsymbol{U}^2) - \mathbf{U}\times(\nabla\times\mathbf{U})) \tag{1}$$

where
a – mean sound speed,
U – the velocity field of the vortex mode (pseudo-sound).

The equations of moments are used to model the vortex mode:

$$\frac{\partial \rho \mathbf{U}}{\partial \boldsymbol{t}} + \nabla\cdot(\rho\mathbf{U}\otimes\mathbf{U}) = -\nabla \boldsymbol{P} + \nabla\cdot((\mu+\mu_t)(2\hat{\mathbf{S}} - \tfrac{2}{3}(\nabla\cdot\mathbf{U})\hat{\mathbf{I}}) \tag{2}$$

and continuity:

$$\frac{\partial \rho}{\partial \boldsymbol{t}} + \nabla(\rho\cdot\mathbf{U}) = 0 \tag{3}$$

where
ρ – air density,
P – pressure in the vortex flow,
μ – molecular coefficient of dynamic viscosity,
$\boldsymbol{\mu_t}$ – turbulent coefficient of dynamic viscosity,
$\hat{\mathbf{S}}$ – strain rate tensor,
$\hat{\mathbf{I}}$ – unit tensor.

To determine the turbulent viscosity, a standard ***k-ε*** turbulence model is used with the setting of boundary conditions on a solid boundary in the form of wall functions that model the logarithmic law of change for the velocity component tangent to the wall.

5.2. Calculated area and grid

The initial data for aeroacoustic modeling is the geometry of the propeller blades operating under static conditions at a rotation speed of 1446.6 rpm. The rotor, which is the working surfaces of the propeller blades, is placed in the geometric center of the calculated area in the form of a hemisphere with a radius of 10 m, at a height of 3 m from the lower flat wall modeling the earth (Fig. 5a). In the calculation area, a rectangular initial grid with a cell size of 0.333 m is determined. In the rotor area, the grid cells are thickened four times, so that more than 20 cells fit on the propeller diameter (Fig. 5b).

The FlowVision method also implements the so-called "subgrid adaptation". Where the rotating blade intersects a rectangular cell, the latter is divided into a number of cells of arbitrary geometry, in which the discretization and solution of hydrodynamic equations are performed. Thus, an increase in the accuracy of the approximation is provided without a strong thickening of the grid. The calculations were carried out on a grid with more than 150,000 calculation cells.

On the boundary surfaces of the rotor, the adhesion condition with zero surface roughness is set, on the earth's surface, the boundary condition of adhesion with a roughness of 1000 microns is set. A constant pressure of 101000 Pa is assumed at the outer boundary of the region.

The solution of finite-difference equations (2-3) is carried out by the "rotating body method". The propeller rotates in the calculated area in an absolute coordinate system, while at each step of the calculation, the rotor is rotated and the grid is rebuilt near the blades that intersect the grid cells.

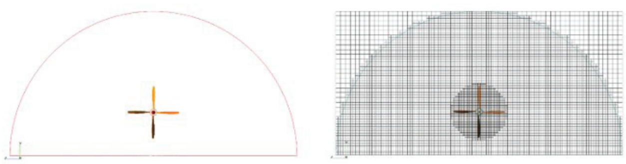

a) Propeller position *b) Calculation grid with adaptation*

Fig. 5: Geometry of the computational domain and the computational grid

5.3. Aerodynamic results

The establishment of a numerical solution to a quasi-stationary periodic one is achieved approximately within 20 full revolutions of the propeller. On the i7 – 2.8 GHz processor, the calculation time of one rotation of the propeller is approximately 700 s. The features of the unsteady flow around the rotor are revealed, in particular, by the instantaneous velocity vector field in the plane of the propeller (Fig. 6a) and in the meridional plane perpendicular to the plane of the earth (Fig. 6b). In all the figures, the positive direction of the x-axis corresponds to the positive direction of the propeller thrust.

A periodic spatial structure of the velocity field is formed in the plane of the propeller, which rotates in the coverage area of the blades together with the rotor. Outside the propeller, there is also a spatial structure of the velocity field associated with the recirculation flow. The nature of this flow is revealed in the meridional plane. An intense vortex flow is recorded at a distance of more than a radius, both on the periphery of the propeller and behind it. It is obvious that the recirculation flow affects the instantaneous values of the aerodynamic characteristics of the propeller and the generation of acoustic fluctuations. Integrating the pressure field over the propeller surface gives the value of the propeller thrust.

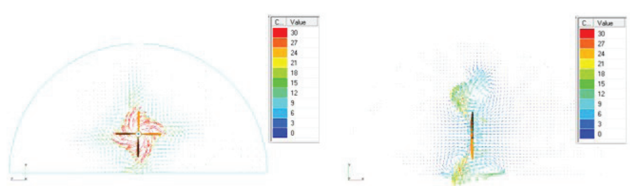

a) In the plane of the propeller *b) In the meridional plane*

Fig. 6: Instantaneous velocity field (m/s) in two planes

Dependences of the propeller thrust and torque on time are shown in Fig. 7. The average value of the propeller thrust according to the graph (Fig. 7a) is 2130 N. The average torque according to the graph (Fig. 7b) is 3550 Nm, which corresponds to the power on the propeller shaft of 540 kW.

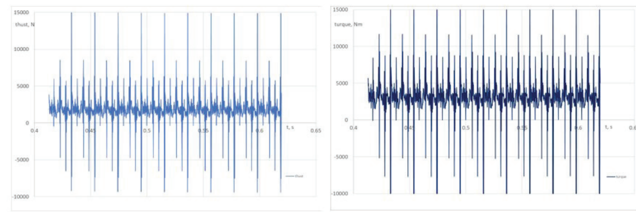

a) Propeller thrust *b) Propeller torque*

Fig. 7: Thrust and torque of the propeller

The instantaneous pressure field (in Pa) in two planes is shown in Fig. 8. Data on the instantaneous pressure field in the propeller plane (Fig. 8a) show that the source of acoustic disturbances is associated with the circular symmetry of the flow field rotating together with the blades and generating vibrations at the repetition frequency of the propeller blades and its tones.

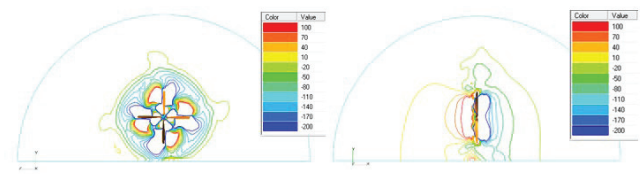

a) In the plane of the propeller *b) In the meridional plane*

Fig. 8: Instantaneous pressure field (Pa) in two planes

5.4. Acoustic results

The solution of the inhomogeneous wave equation (1) is carried out separately for each tones of the propeller noise. At the outer boundary of the spherical region, the specific acoustic impedance for all tones is assumed to be one. On the earth's surface, the impedance is assumed to be equal to infinity.

Below are some results on the first tone of the propeller noise. The wavelength of the first tone of the propeller noise is 3.5 m. Therefore, these results correspond to the near acoustic field and clearly reflect the features of the generation of acoustic vibrations.

The instantaneous acoustic pressure field in the propeller plane and the meridional plane is shown in Fig. 9. In the plane of the propeller (Fig. 9a), one can see the appearance of quasi-spiral modes near the propeller , which are transformed into "petal" modes that provide radiation directivity in five directions, which are well detected in the distribution of the amplitude of the first tone of the propeller noise (Fig. 10). The resulting amplitude distribution is established after about 20 oscillation periods and remains stable when the calculation continues. On the i7 – 2.8 GHz processor, the calculation time for one BPF (blade passing frequency) period is approximately 750 s.

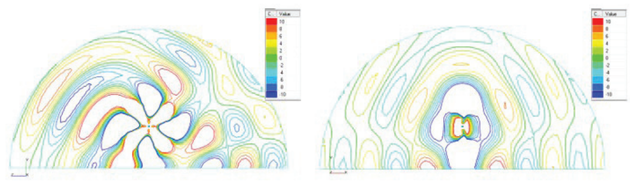

a) In the plane of the propeller b) In the meridional plane

Fig. 9: Instantaneous sound pressure field (Pa) in two planes

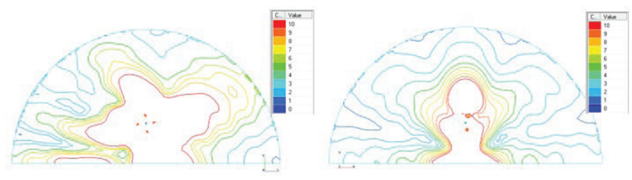

a) In the plane of the propeller b) In the meridional plane

Fig. 10: The amplitude of the 1st tone of the propeller noise (Pa) in two planes

The analysis of the acoustic pressure field and the amplitude distribution in the plane passing through the propeller axis and parallel to the ground (Fig. 11) indicates the dipole nature of the radiation, but also reveals a certain asymmetry of the dipole source, apparently associated with the influence of the recirculation flow and the relative proximity of the solid surface.

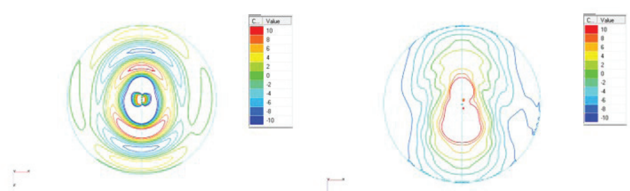

a) Acoustic pressure field b) Sound pressure amplitude

Fig. 11: The field of acoustic pressure and the amplitude of the 1st tone of the propeller noise (Pa) in the meridional plane parallel to the ground

6. COMPARISON OF CALCULATED AND EXPERIMENTAL DATA

A comparison of the sound pressure levels of the tonal components of the propeller noise obtained in the experiment and during the computational study based on numerical and semiempirical methods are shown in the Fig. 12. The sound pressure level of 1st tone was overestimated by 7.3 dB during numerical modeling. The sound pressure levels of the 2nd, 3rd and 4th tones for the radiation direction considered in the Fig. are in good agreement with the experimental data. The calculated sound pressure levels of 5th and 6th tones of the propeller noise were 20 dB lower than the experimental values. This result of the loss of accuracy is probably due to the insufficient density of the finite-difference grid when determining the amplitude of the source function.

The calculation by the semiempirical method showed a good agreement with the experiment for the first six tones of the propeller noise. For tones from 7 to 10, the calculated values are significantly overestimated to 10 dB.

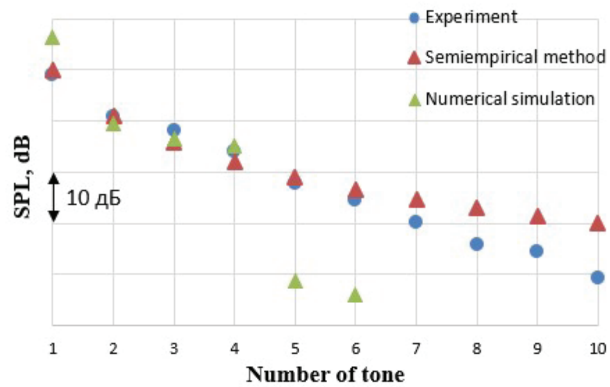

*Fig. 12: Comparison of the sound pressure levels of the tonal components of the propeller noise obtained in the experiment, with numerical and semiempirical modelling (**n**=1446.6 rpm, **ϑ** =105°, **R**=30 m)*

A comparison of the directional characteristics of the first four tones of the propeller noise obtained during numerical modeling and in the experiment is shown in Fig. 13 . The obtained radiation patterns of the first three tones of the propeller noise are qualitatively consistent with experimental data in the range of azimuthal angles of 45-120°. For the 4th tone, the coincidence of the calculated sound pressure level with the experimental value in the direction of 105° is random.

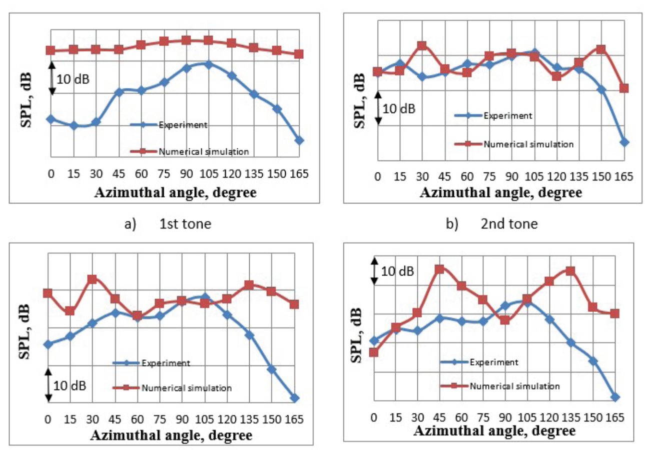

Fig. 13: Comparison of the directivity patterns of the first four tones of the propeller noise obtained in the experiment and in numerical modelling

7. CONCLUSION

The paper presents the results of numerical simulation of the noise of a low-loaded 4-bladed propeller of AN-2 aircraft. The calculation is performed for the case of an isolated propeller operating under static condition at the nominal power condition of the power plant. The results of numerical simulation are compared with the data of a previously performed experiment and with the results of calculation using a semiempirical model. For the direction of the maximum radiation of the studied propeller (105°), the sound pressure level of the first tone of the propeller noise was overestimated by 7.3 dB during numerical modeling.

The presented results indicate the possibility of using the acoustic-vortex method for evaluating the propeller noise within the framework of the methodology for assessing the overall sound field of propeller-driven a/c at various design stages.

The work will be continued in terms of studying the influence of the calculation grid parameters, the influence of recirculation flow and other factors on the simulation results, as well as the influence of in-flight conditions and installation effects [21] on the propeller noise of a light aircraft.

ACKNOWLEDGEMENT

The authors of the paper expresses gratitude to the head of the local aerodrome of the Moscow Aviation Institute, Yevgeny Kozhevnikov, for his help in organizing and conducting acoustic tests of light propeller-driven aircraft.

REFERENCES

[1] Gutin, L.Ya.: About the sound field of a rotating propeller, Technical Physics, ISSN: 0044-4642, Springer, VOLUME 6, p. 899-909, 1936

[2] Moshkov, P., Ostrikov, N., Samokhin, V., Valiev, A.: Study of Ptero-G0 UAV Noise with Level Flight Conditions, 25th AIAA/CEAS Aeroacoustics Conference, AIAA Paper No. 2019-2514, 2019

[3] Moshkov, P.A., Samokhin, V.F., Yakovlev, A.A.: Study of the noise sources of an UAV with a two-stroke engine and shrouded propeller, Journal of Physics: Conference Series, ISSN: 1742-6588, IOP Publishing, VOLUME 1925, 2021

[4] Ovdienko, M.A., Varyukhin, A.N., Zakharchenko, V.S., Vlasov, A.V.: A review of electrified propulsion system concepts for advanced aircraft, Journal of Physics: Conference Series, ISSN: 1742-6588, IOP Publishing, VOLUME 1891, 2021

[5] Varyukhin, A.N., Zakharchenko, V.S., Geliev, A.V., Zhuravlev, D.I.: Development of an electric propulsion system demonstrator for an ultralight manned aircraft, Journal of Physics: Conference Series, ISSN: 1742-6588, IOP Publishing, VOLUME 1891, 2021

[6] Hallez, R., Colangeli, C., Cuenca, J., Ryck, L.D.: Impact of electric propulsion on aircraft noise – all-electric light aircrafts case study, 2018 AIAA/IEEE Electric Aircraft Technologies Symposium, AIAA Paper No. 2018-4982, 2018

[8] Riboldi, C.E.D., Trainelli, L., Mariani, L., Rolando, A., Salucci, F.: Predicting the effect of electric and hybrid-electric aviation on acoustic pollution, Noise mapping, ISSN: 2084-879X, De Gruyter Open Access, VOLUME 7, p. 35-56, 2020

[7] Chen, B., Yakovlev, A.A., Moshkov, P.A.: Fast prediction method of aircraft noise with distributed propulsion in the far field, Journal of Physics: Conference Series, ISSN: 1742-6588, IOP Publishing, VOLUME 1925, 2021

[8] Moshkov, P., Samokhin, V., Yakovlev, A., Bolun, C.: The problems of selecting the power plant for light propeller-driven aircraft and unmanned aerial vehicle taking into account the requirements for community noise, AKUSTIKA, ISSN 1801-9064, Studio D – Akustika s.r.o., České Budějovice, VOLUME 39, p. 164-169, 2021

[9] Timushev, S., Klimenko, D., Aksenov, A., Gavrilyuk, V., Li, J.: On a new approach for numerical modeling of the quadcopter rotor sound generation and propagation, Proceedings of 2020 International Congress on Noise Control Engineering, INTER--NOISE, 2020

[10] Aksenov, A.A., Gavrilyuk, V.N., Timushev, S.F.: Numerical simulation of tonal fan noise of computers and air conditioning systems, Acoustical Physics, ISSN: 1063-7710, Pleiades Publishing, Ltd., VOLUME 62, p. 447-455, 2016

[11] Samokhin, V., Moshkov, P.: Experimental research of acoustical characteristics by power plant of An-2 aircraft in static conditions, Trudy MAI, ISSN 1727-6942, Moscow aviation institute, Moscow, VOLUME 82, p. 1-26, 2015

[12] Samokhin, V.F.: Semiempirical method for estimating the noise of a propeller, Journal of Engineering Physics and Thermophysics, ISSN: 1062-0125, Springer New York Consultants Bureau, VOLUME 85, p. 1157-1166, 2012

[13] Herniczek, M.T.K., Feszty, D., Meslioui, S., Park, J.: Applicability of Early Acoustic Theory for Modern Propeller Design, 23rd AIAA/CEAS Aeroacoustics Conference, AIAA Paper No. 2017-3865, 2017

[14] Barry, F.W., Magliozzi, B.: Noise Detectability Prediction Method for Low Tip Speed Propellers,AFAPL-TR-71-37, Hamilton Standard, Wright-Patterson Air Force Base, OH, 1971

[15] Hanson, D.B., Parzych, D. J.: Theory for Noise of Propellers in Angular Inflow with Parametric Studies and Experimental Verication, NASA-CR-4499, Hamilton Standard, Windsor Locks, CT, 1993

[16] Mankbadi, R.R., Afari, S.O., Golubev, V.V.: High-fidelity simulations of noise generation in a propeller-driven unmanned aerial vehicle, AIAA Journal: devoted to aerospace research and development, ISSN 0001-1452, American Institute of Aeronautics and Astronautics, VOLUME 59, p. 1020-1039, 2021

[17] Titarev, V.A., Faranosov, G.A., Chernyshev, S.A., Batrakov, A.S.: Numerical modeling of the influence of the relative positions of a propeller and pylon on turboprop aircraft noise, Acoustical Physics, ISSN: 1063-7710, Pleiades Publishing, Ltd., VOLUME 64, p. 760-773, 2018

[18] Abalakin, I.V., Bakhvalov, P.A., Bobkov, V.G., Kozubskaya, T.K., Anikin, V.A.: Numerical investigation of the aerodynamic and acoustical properties of a shrouded rotor, Fluid Dynamics, ISSN: 0015-4628, Pleiades Publishing, Ltd., VOLUME 51, p. 419-433, 2016
[19] Moshkov, P.A.: Study of vortex noise of rotating blades, Herald of the Bauman Moscow State Technical University, Series Natural Science, ISSN: 1812-3368, VOLUME 89, p. 85-98, 2020
[20] Moshkov, P.A.: Acoustic characteristics of aircraft piston engines, Russian Aeronautics, ISSN: 1068-7998, Allerton Press, Inc. (New York), VOLUME 63, p. 568-574, 2020
[21] Drofelnik, J. et al.: Measurement and modelling of aero-acoustic installation effects in tractor and pusher propeller architectures, 2021 AIAA AVIATION Forum, AIAA Paper No. 2021-2301, 2021

Sergey Timushev *is Dr.Tech.Sc, Professor of the Moscow aviation institute (national research university) (Moscow, Russia), senior researcher of 'Theory and Calculation of Turbomachines' in Rocket Engines Department.*
The last decade Sergey Timushev works on the problem of computational prediction of pressure pulsations in centrifugal pumps and ventilators and reduction of vibration and noise in such machines. He is author and co-author of more than 100 scientific journal and conference papers and is a member of the INCE/Europe, ASME, reviewer of IJAV.

Alexey Yakovlev *is Ph.D. of Engineering Science, Assistant Professor of the Moscow aviation institute (national research university) (Moscow, Russia), senior researcher 'Theory of air-jet engines' Department.*
Alexey Yakovlev is a specialist in gasdynamics and aeroacoustics. Alexey Yakovlev is the author of over 30 scientific papers. He presented the main results of scientific research at the international conferences.

Petr Moshkov *is Ph.D. of Engineering Science, Leading engineer of the Moscow aviation institute (national research university) (Moscow, Russia).*
Petr Moshkov is a specialist in aeroacoustics. Petr Moshkov is the author of over 45 scientific papers. He presented the main results of scientific research at the international conferences in Moscow, Gelendzhik, Svetlogorsk, Delfts.

PRACTICAL METHODS OF ACOUSTIC MATERIALS PATTERNING FOR INCREASE OF THEIR EFFECTIVENESS

Paper No.363/2021

[a] **Aleksandr Krasnov,** [b] **Igor Deryabin**

[a] *Togliatti State University, Togliatti, Russia, kaw@yandex.ru*
[b] *Togliatti State University, Togliatti, Russia, iglen19@yandex.ru*

Abstract*: This article includes the results of experimental investigations of patterned noise-reducing materials and components, carried out using special-purpose laboratory-scale bench plants (Alpha Cabin, Torre di Pisa, RTC-3, Oberst). Illustrative examples of constructive-technological structurization of the components (gaskets, panels and upholstery) providing noise reduction of passenger cars are given.*

Keywords: *noise-reducing, material, structurization, patterning.*

DOI: *: 10.36336/akustika202141107*

1. INTRODUCTION

It is known that while designing a car there are actual problems of minimization of weight, size and cost parameters of its components within the noise insulation set, when obtaining acceptable high acoustical comfort in passenger compartment and providing low external noise levels meeting law requirements. Carried out by the authors research shows that complex solution of above-listed technical problems is reached to a great extent by using various methods of constructive-technological patterning of acoustic (sound absorbing, sound-insulating, vibrodamping) materials and components.

2. STRUCTURED SOUND ABSORBING MATERIALS

Carried out experimental investigations show that the increase of level of acoustic energy absorption by small-size panels (upholstery) can be reached, in particular, by performing appropriate effective perforation of sound absorbing material porous layer, applying through cuts within the protective facing layer, purposive partition (size reduction) of integrated noise absorbing component into several component parts (of the same or smaller total area of surface), shaping of limit geometric contour of noise absorbing component, which imparts to this component the enlarged outer contour perimeter while keeping its face area changeless (or reduced) [1]. Experimental investigations of patterned specimens of sound absorbing materials and full-sized noise absorbing components were carried out using laboratory-scale bench plant «Alpha Cabin», «reverberation sound absorption coefficient» $\boldsymbol{\alpha_r}$) was the evaluating parameter [2, 3].

Perforation of monolithic sound absorbing material porous layer allows to increase dynamic compliance and resilient (bumping) frame of perforated structure deformations in the areas directly adjoining to the contours (free edges) of perforation holes, as well as by additional introduction of perforation holes into the process of absorption of open surfaces of porous end areas. It causes, accordingly, the increase of effect of impinging sound wave energy absorption by indicated local perforated zones. The perforation degree of noise absorbing material porous structure is characterized by the parameter «perforation coefficient» ($\boldsymbol{k_{per}}$) – as the relation of the total area of perforation holes projection $\boldsymbol{S_{per}}$ to the area of face of continuous nonperforated layer of sound absorbing material $\boldsymbol{S_{face}}$:

$$\boldsymbol{k}_{per} = \boldsymbol{S}_{per} \; / \; \boldsymbol{S}_{face} \tag{1}$$

The results of the experiments carried out with the specimens of noise absorbing components like flat-leaf panels with the leaf thickness of 12,5 and 25 mm, made of open-porous foamed polyurethane, with the studied diameter of perforation holes of 6 mm, in pitch variations (12,5 mm, 25,0 mm, 50,0 mm), indicate the growth of values of reverberation sound absorption coefficient $\boldsymbol{\alpha_r}$ by 0,3 (See Fig.1a). Maximum growth of parameter αr reached when the values of perforation holes center-to-center distance are equal to the sound absorbing panel thickness, where the perforation holes diameter is $\boldsymbol{d \approx 1/4h}$. Perforation coefficient value $\boldsymbol{k_{per}=0,04}$ ensures maximum growth of reverberation sound absorption coefficient $\boldsymbol{\alpha_r}$, with the studied range of variations of perforation coefficient $\boldsymbol{k_{per}=0,01...0,20}$.

The effectiveness of this constructive-technological method of purposive applying of through damaging cuts within the monolithic surface of "cross-linked" structure of conjugate protective and porous sound absorbing layers is illustrated with the results of determination of reverberation sound absorption coefficient αr of flat-leaf panels with the leaf thickness of 25 mm. The results (See Fig.1b) show that the partition of monolithic flat-leaf noise absorbing panel with outer protective film into 100 independent small-size panels and their subsequent gapless mosaic conjugation can cause the additional growth of reverberation sound absorption coefficient $\boldsymbol{\alpha_r}$ by the value up to 0,3.

The applying of separate, spaced into prescribed intervals, small-size noise absorbing panels made in the form of 100 identical rectangles with the size of 200x50 mm, spaced from each other with the formation of air clearances (gaps) with width equal 25 mm, relative to monolithic square flat-leaf specimen of the same face area equal 1000x1000 mm causes the considerable growth of the reverberation sound absorption coefficient $\boldsymbol{\alpha}_r$. In particular, $\boldsymbol{\alpha}_r$ increases in more than 2 times within the octave band with the center of 2000 Hz.

The increase of perimeter of monolithic flat-leaf panel outer contour with the forming of additional area of open end surfaces, when the area of its face projection is constant, can be reached by putting it into a certain geometric shape (See Fig.1c). The experimental estimates showed that the use of rectangular flat-leaf noise absorbing panel with the outer contour total perimeter ***P*** four times much, in comparison with the base square monolithic noise absorbing panel of the same surface area, allowed to increase reverberation sound absorption coefficient αr by the value up to 0,36. It is necessary to note that the effect of increased sound absorption effect of non-square by shape panels with increased contour perimeter caused also by intensification of effect of diffracting sound absorption by more stretched free rim zones [4, 5].

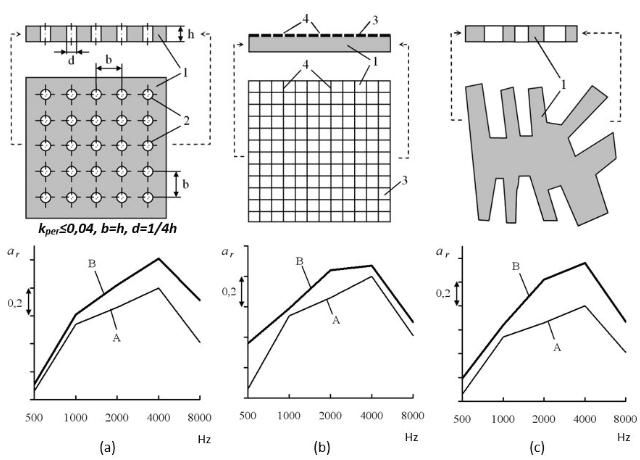

Fig. 1: The examples of patterning of flat-leaf noise absorbing panels and the achieved effect of growth of parameter «reverberation sound absorption coefficient» $\boldsymbol{\alpha}_r$
1 – porous layer of sound-absorbing material; 2 – perforation holes; 3 – sound-transparent face decorative or protective layer; 4 – holes in face sound-transparent decorative or protective layer; 5 – air spaces between separated small-size panels; $\boldsymbol{k}_{per}$ *- perforation coefficient;* ***b*** *– center-to-center distance of perforation holes;* ***h*** *– thickness of sound-absorbing panels;* ***d*** *– diameter of perforation holes;* ***t*** *– width of air clearance between detached small-size panels; curve* ***A*** *– value of parameter* $\boldsymbol{\alpha}_r$ *of non-patterned noise absorbing panel; curve* ***B*** *– value of parameter* $\boldsymbol{\alpha}_r$ *of noise absorbing panel structured according to the scheme illustrated on the upper figure*

3. PATTERNED SOUND-INSULATING MATERIALS

The process of typical two-layer soundproof materials patterning means, in particular, the technological methods of nonthrough blind perforation of three-dimensional structure of porous layer contained in continuous dense acoustical reflecting layer. Such type of patterning allows to increase sound-proofing effectiveness of the material (estimating parameter «soundproofing capacity» r) within the frequency range with the less consumption (and the less cost) of the material of sound absorbing layer.

The effect of sound-proofing effectiveness increase is caused by the formed family of numerous closed sound absorbing cavities which allow to intensify the process of dynamic deformation of more pliable resilient porous frame with the concomitant dynamic (oscillatory) shift of air from the cavities of perforation holes into adjoining communicating cavities of porous structure of the material. Mentioned dynamic processes accompanied by the intensification of the processes of sound energy absorption.

Constructive-technological patterning of typical two-layer soundproof material, contained in dense sound-reflecting and porous sound absorbing layers, using respective perforation of its porous sound absorbing layer by the blind holes, can be characterized by the parameter «structuring coefficient» $\boldsymbol{k}_{str}$.

Structuring coefficient $\boldsymbol{k}_{str}$ in that case is determined in the following way:

$$k_{str} = S_{\Sigma}\, n \,/\, S \qquad (2)$$

where
$\boldsymbol{S}_{\Sigma}$ is the total surface area of blind perforation hole;
n is the number of perforation holes;
S is the face area of porous sound absorbing layer.

Experimental investigations of patterned sound-insulating materials carried out on laboratory-scale bench plants «Torre di Pisa» and «RTC-3» using the estimating parameter «soundproofing capacity» r [6]. The effectiveness of suggested constructive-technological method illustrated with the results of experimental research shown on Fig. 2.

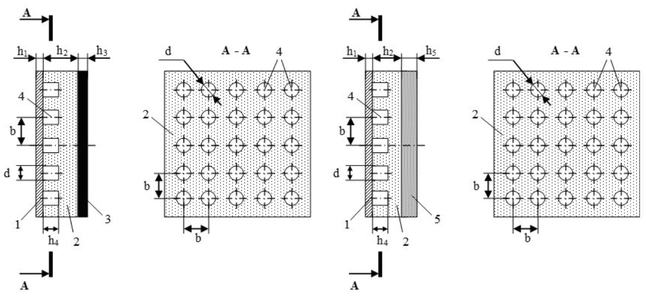

Fig. 2: The variant of patterning of sound-insulating material sample mounted on the lifting body panel
1 – lifting thin sheet metal body panel; 2 – porous sound-absorbing layer; 3 – dense sound-reflecting layer; 4 – blind perforation holes; 5 – porous sound-insulating layer high density; ***k_{str}*** *– structuring coefficient of porous sound-absorbing layers;* ***h_1*** *– thickness of sheet metal body panel;* ***h_2*** *– thickness of porous sound-absorbing layer;* ***h_3*** *– thickness of dense sound-reflecting layer;* ***h_4*** *– depth of patterning (height of blind perforation holes);* ***d*** *– diameter of blind perforation holes;* ***b*** *– center-to-center distance of blind perforation holes*

The results of the experiments with flat-leaf samples of sound-insulating materials containing sound absorbing fibrous layer (thickness ***h_2***=20 mm, relative surface density 1,2 kg/m^2) and bitumen-based gravimetric sound-reflecting layer of «septum» type (thickness ***h_3***=4 mm, relative surface density 5,0 kg/m^2), while patterning them with blind holes, show the increase of parameter «soundproofing capacity» ***r*** within the frequency range of 400...6300 Hz by the value of 3...12 decibel. The results of experimental investigations show the porous layer patterning effectiveness with ***k_{str}*** =0,85 which allows to reduce material consumption of porous fibrous layer of upholstery ***Δm*** by 13% and increase considerably the value of the parameter «soundproofing capacity» ***r*** (See Fig. 3).

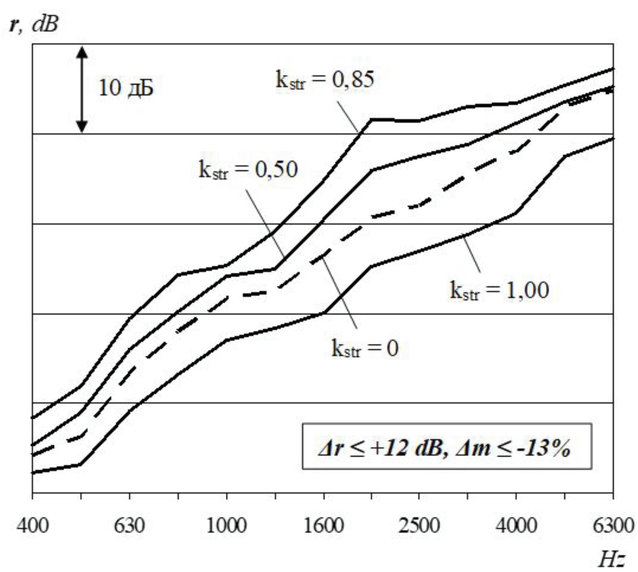

Fig. 3: Parameter r of patterned and non-patterned of sound-insulating material samples
k_{str} *– structuring coefficient of porous sound-absorbing layers;* ***r*** *– parameter «soundproofing capacity»;* ***Δr*** *– value of parameter* ***r*** *change in result of patterning,* ***Δm*** *– value of change of relative surface density of patterned material*

4. PATTERNED VIBRODAMPING MATERIALS

To damp bending vibrations of body panels and weaken radiated by them structural noise they use flat-leaf vibrodamping gaskets conjugate adhesively (by sticky glue or thermosetting layer) with counter surfaces of body panels forming laminated vibrodamping coverings.

Under patterned vibrodamping materials we consider flat-leaf materials contained in perforated structure of viscoelastic layer – for one-layer hard and two-layer reinforced with the continuous reinforcing layer vibrodamping materials, and also with through perforation of viscoelastic and reinforcing layers – for two-layer types of reinforced vibrodamping materials. One-layer hard vibrodamping materials consist of viscoelastic layer only (modulus of elasticity ***E_2***≥1,5x10^9 N/m^2). Two-layer reinforced vibrodamping materials consist of viscoelastic material layer (modulus of elasticity ***E_2***≤0,5x10^9 N/m^2) and outer reinforcing layer (modulus of elasticity ***E_3***≥(68...70)x10^9).

Experimental investigations of patterned vibrodamping materials characteristics were carried out on laboratory-scale bench plant of RTC-3 type used for study of vibrating and sound-emitting properties of hard lamellate structures (estimating parameter – transfer function «force-vibration» N) [4]. Composite structures consisting of lifting thin-sheet metal plate (thickness of 1 mm) laminated with different variants of nonperforated (non-patterned) and perforated (patterned) flat-leaf vibrodamping materials were used as test specimens. Formed composite structure was induced by electrodynamic vibration generator rod within the frequency range of 60...350 Hz. Perforation of structure of one-layer vibrodamping material (***k_{per}*** =0,2) contained in indicated composite structure causes the growth of resonance oscillation frequencies values by 8...27 Hz and the decay of amplitudes of test transfer function within the bending vibrations resonance frequencies 1,1...2,0 times less. Through perforation (***k_{per}*** =0,2) of two-layer reinforced vibrodamping material (See Fig. 4) contained in composite structure also increased bending vibrations resonance frequencies values (by 10...30 Hz). At the same time, the amplitudes of test transfer function within the bending resonances frequencies reduced in 1,2...1,6 times. During researches (their results shown on Fig. 4), reinforced vibrodamping material of DF-5AL type were used, with relative density of 5,0 kg/m^2, viscoelastic layer thickness of 3,3 mm, reinforced layer thickness of 0,2 mm.

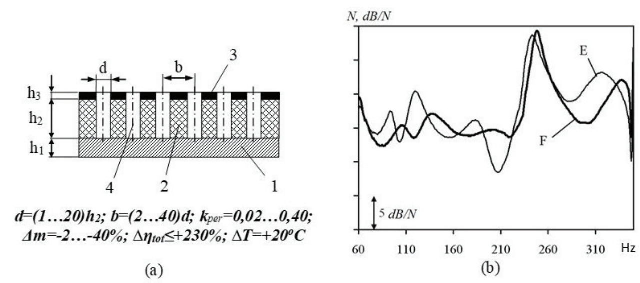

Fig. 4: Structural diagram (a) and transfer function «force-vibration» N (b) of composite structure, contained in steel thin-leaf plate laminated with flat-leaf two-layer reinforced vibrodamping material
1 – lifting flat-leaf body panel; 2 – viscoelastic layer; 3 – reinforcing layer; 4 – perforation holes; $\boldsymbol{k_{per}}$ *– perforation coefficient;* $\boldsymbol{\Delta m}$ *– value of material relative density change;* $\boldsymbol{\eta_{tot}}$ *– reduced composite loss factor;* $\boldsymbol{\Delta T}$ *– value of material effectiveness temperature span;* $\boldsymbol{h_1}$ *– thickness of sheet metal body panel;* $\boldsymbol{h_2}$ *– viscoelastic layer thickness;* $\boldsymbol{h_3}$ *– reinforcing layer thickness;* ***d*** *– perforation holes diameter;* ***b*** *– center-to-center distance of perforation holes*
Curves ***E*** *and* ***F*** *– transfer function «force-vibration» of composite structure with nonperforated (E) and perforated (F) flat-leaf vibrodamping materials*

The increase of vibrodamping effectiveness (growth of loss factor) of perforated vibrodamping materials is determined by the intensification of dynamic processes of increase of amplitudes of viscoelastic layer shift deformations and deflections «tension-compression» in localised perimetritic zones of perforation holes. In particular, through perforation of vibrodamping material reinforced structure causes the increase of reduced composite loss factor upto 25% within the temperature span +20...+40°C, and more than in 2 times – within the temperature span +60...+80°C (See Fig.5). Thus, test material perforated specimen ($\boldsymbol{k_{per}}$ =0,25) has by 25% less relative density with reached higher vibrodamping effectiveness within wider (≈20 °C) temperature span of effective vibrodamping, and having improved technological properties.

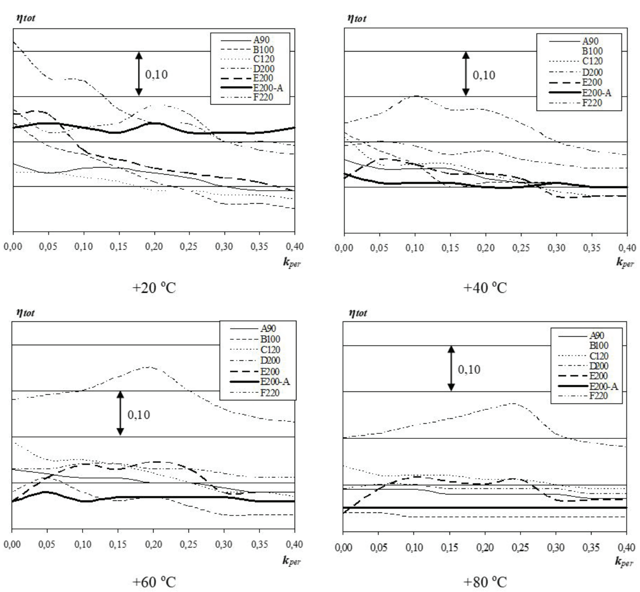

Fig. 5: Parameter ηtot of reinforced vibrodamping material samples A90, B100, C120, D200, E200, F200-A, F-220 – shorthand of marks reinforced vibrodamping material

Perforation of viscoelastic layer structure contained in reinforced vibrodamping material doesn't cause any noticeable change of reduced composite loss factor $\boldsymbol{\eta_{tot}}$. It's necessary to note that the relative density of reinforced vibrodamping material specimen with the perforated structure of viscoelastic layer with $\boldsymbol{k_{per}}$ =0,40 is 40% less. The effects of increase of reduced composite loss factor $\boldsymbol{\eta_{tot}}$ of two-layer reinforced vibrodamping materials is observed within definite relations of physical properties of composite layers. In particular, the value of «reduced loss module» parameter ***M*** of viscoelastic layer lies within the range of ***M***=(0,5...1,8)·10^8 N/m^2, and the value of «reduced hardness module» ***K*** of reinforcing layer is ***K***≥6,8·10^7 N/m. Reduced loss module ***M*** of viscoelastic layer and reduced hardness module ***K*** of reinforcing layer are determined by the following expressions:

$$M=\beta\text{-}E_2 \tag{3}$$

$$K=h_3\text{-}E_3 \tag{4}$$

where
$\boldsymbol{\beta}$ and $\boldsymbol{E_2}$ are respectively reduced coefficient of inner loss and reduced modulus of elasticity of viscoelastic layer;
$\boldsymbol{h_3}$ and $\boldsymbol{E_3}$ are respectively thickness and reduced modulus of elasticity of reinforcing layer.

5. CONCLUSION

The results of experimental researches of patterned noise--lowering materials and components testify the considerable potential of increase of their acoustic effectiveness. Presented types of patterned noise-lowering materials and components can be used effectively not only in passenger cars but also in the designs of other transport machinery (overland, water, air), and also be used to reduce the noise of energy equipment, domestic equipment and so on.

REFERENCES

[1] M. Fesina, I. Deryabin, L. Gorina. On the porous sound-absorbing panels with the end low-frequency resonant cavities. AKUSTIKA, V. 32, March 2019, p. 10-16.
[2] H.V. Fuchs «Alternative fibereless absorbers – new tools and materials for noise control and acoustic comfort», Acta Acustica – ACUSTICA 87 (4), 2001, p. 414-422.
[3] Acoustics: Measurement of sound absorption in a reverberation room, International Standart ISO 354 Second edition, Switzerland: 2003, p. 21.
[4] H.V. Fuchs «From advanced acoustic research to novel silencing procedures and innovative sound treatments», Acta Acustica – ACUSTICA 87 (4), 2001, p. 407-413.
[5] Ary Deddy Putranto, Oryza Ardiansyah. Origami Tessellation Ceiling Panels to Improve the Room Acoustic Quality (Case Study: Lecture Hall of the Department of Architecture, Universitas Brawijaya). Proceedings of the International Conference of Heritage & Culture in Integrated Rural-Urban Context (HUNIAN 2019). Advances in Engineering Research, volume 195, p. 179-183.
[6] A.V.Krasnov. Methods of experimental test of acoustic characteristics of passenger car body parts and soundproof materials // «Car Engineers Magazine». - №4. – 2007. – P. 34...39.

***Aleksandr Krasnov** is a candidate of technical Sciences, an associate professor of "Industrial and Environmental Safety Management" department of Togliatti State University. Studying and research interests are in studying and development of an innovative technical equipment to improve vibroacoustic characteristics of the wheeled transport and power generating systems and also studying and development of an innovative technical equipment to reduce an acoustic environmental pollution. The author of more than 130 scientific articles, including 2 research monographs, 72 articles in a periodic scientific and technical journals and academic conference papers, workshops and congresses. The author of 43 inventions and utility models.*

***Igor Deryabin** is a postgraduate of Togliatti State University.*
Igor Deryabin –an expert in a field of automobile vibroacoustics, studies the problems of the reduction of low frequency noise emissions of noise-generating technical objects. The author of more than 100 patents of Russian Federation on inventions and utility models, 50 of which are implemented into production as functional devices for acoustic properties improving in technical rooms. Igor Deryabin is the author of 18 scientific papers, presented his research results at international conferences in Dmitrov, Kazan, Samara, Saint Petersburg.

Paper No.364/2021

REDUCING THE NOISE LOAD ON WILDLIFE DURING SCIENTIFIC EXPEDITIONS

[a, b]**Alexey Shvetsov**

[a)] *North-Eastern Federal University, Yakutsk, Russia*
[b)] *Vladivostok State University of Economics and Service, Vladivostok, Russia, transport-safety@mail.ru*

***Abstract**: Scientific expeditions to the wild are usually carried out by cars that create a negative noise load on the inhabitants of the wild. This study suggests a way to reduce such a noise load by replacing cars with internal combustion engines with electric vehicles. The measurements made it possible to specify the quantitative indicators of reducing the noise load achieved as a result of replacing cars with internal combustion engines with electric vehicles. The article specifies the limitations in the use of electric vehicles during scientific expeditions into the wild, resulting from special conditions, such as impassability and lack of service infrastructure, such as battery charging stations. The data presented in this paper may be of interest both for scientific and environmental organizations, and for government regulatory institutions in the fields of ecology, nature protection and scientific activity.*

***Keywords:** expeditions, wildlife, noise, car, electric car.*

***DOI:** : 10.36336/akustika202141112*

1. INTRODUCTION

Scientific expeditions to the wild are regularly conducted on all continents of the planet, including Antarctica. Currently, in land expeditions, cars with an internal combustion engine are most commonly used as vehicles. The level of traffic noise generated by such cars is in the range of 75-85 dB [1].

The main component of the traffic noise generated by the car occurs as a result of the operation of the internal combustion engine. The hearing distance of such noise reaches several hundred meters, depending on the terrain.

For most inhabitants of the wild, hearing is the main tool for perceiving the surrounding reality, by means of which, in particular, animals learn about potential danger.

Traffic noise is 'alien' to the inhabitants of the wild, and therefore it is a source of concern, which is especially dangerous during the breeding season, as it can lead to a violation of this process.

Also, the negative consequences of traffic noise generated by the expedition cars can be attributed to a decrease in the effectiveness of the expedition itself. So, the noise can make the animals (birds) that are the subject of the study leave their location or change the usual order of their life, which in turn will lead to distortion of the results of the study.

According to the data (Fig. 1), more than 2 thousand scientific expeditions are conducted annually in the world [2-4]. Reducing the noise load during their implementation is an important factor in preserving the ecology in the few regions of the planet with preserved wildlife.

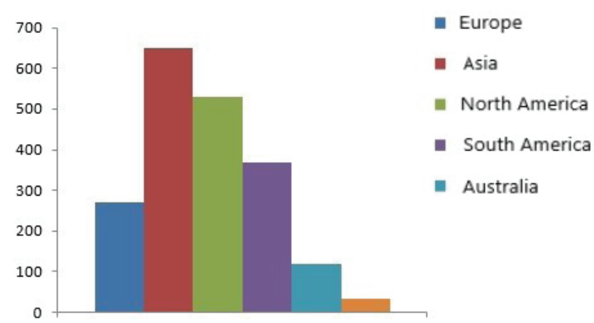

Fig. 1: Statistics on the number of scientific expeditions.

2. USING ELECTRIC VEHICLES AS A WAY TO REDUCE THE NOISE LOAD ON WILDLIFE DURING A SCIENTIFIC EXPEDITION

A promising way to reduce the noise load on wildlife during scientific expeditions is to replace cars with an internal combustion engine used for transporting employees and equipment of the expedition with electric vehicles. Such a change requires specification of quantitative indicators of noise load reduction to justify the effectiveness of this method. In addition, it is necessary to specify the existing restrictions on the use of electric vehicles during scientific expeditions.

The following factors can be attributed to the special conditions of conducting expeditions into the wild that affect the restrictions in the use of electric vehicles:

- impassability, on a significant part of the way;
- lack of stations for charging electric vehicle batteries, on a significant part of the way.

The factors of off-road driving and the lack of charging stations allow us to formulate two requirements that an electric car must meet in order to be able to use it in an expedition.

The off-road factor determines the requirement for the electric vehicle used in terms of increased cross-country ability. Increased cross-country ability is achieved through the use of all-wheel drive and increased ground clearance (the distance between the ground and the lower suspension point of the electric vehicle). Most common, such features are possessed by vehicles of the SUV category.

The factor of the absence of stations for charging the batteries of an electric vehicle determines the requirement for the electric vehicle used, in terms of having the necessary power reserve to reach the destination and return back.

Until recently, the electric vehicles produced were represented by passenger cars with a small ground clearance and a fairly small power reserve of 200-300 km [5-7], which limited the possibility of their use in scientific expeditions into the wild, in off-road conditions and the lack of service infrastructure.

The increase in the capacity of electric car batteries achieved in recent years has led to the appearance on the market of a number of electric car models belonging to the SUV category, i.e. meeting the requirement for the presence of an all-terrain function [7-10].

Considering the power reserve of electric vehicles of the SUV category, we see that now in some models it has already reached 500-800 km (Tab. 1). From the data in Tab. 2, it follows that electric vehicles from points 1-3 of the table are applicable in expeditions which destination is located at a distance of up to 220-400 km from the last station of the stations for charging electric vehicle batteries. The power reserve of such electric vehicles will allow you to reach your destination and return back.

Points	Vehicles	Power reserve (km)
1	Tesla Model X	545
2	Rivian R1T	640
3	Tesla Cybertruck	800

Tab. 1: Power reserve of electric vehicles of the SUV category

3. SPECIFICATION OF THE QUANTITATIVE INDICATORS OF THE NOISE LOAD REDUCTION WHEN USING ELECTRIC VEHICLES

To specify the quantitative indicators of reducing the noise load as a result of replacing cars with internal combustion engines with electric vehicles, it is firstly necessary to analyze the noise level generated by electric vehicles in the open air. Next, it is necessary to compare the results obtained with the noise level generated by cars with an internal combustion engine. The resulting difference will be an indicator of reducing the noise load when using electric vehicles.

To determine the noise range generated by a moving electric vehicle, portable noise meters were used for measuring (in accordance with the regulatory methodology – 'Regulation No. 51' of the UNECE [15]) the level of the acoustic radiation intensity adjusted according to 'A' scale (Fig. 2).

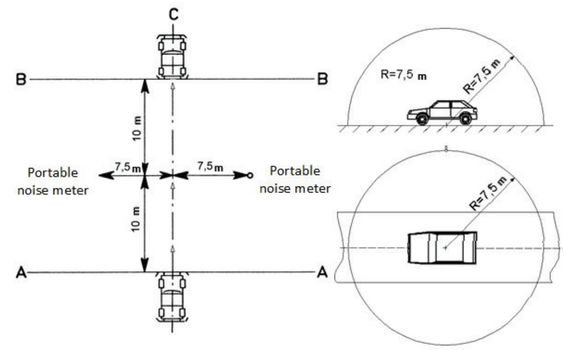

Fig. 2: Electric vehicle noise detection scheme
** When preparing the drawing, the elements of the scheme for measuring the noise from the source were used [1]*

At the same time, the following conditions for determining were set: tests for evaluating are carried out on a measuring section of the road A-B with a length of 20 m; the vehicle in front of the measuring section (up to the A-A line) moves uniformly at a speed of ~30 km/h; the measurement is made when the vehicle passes the middle of the measuring section with noise meters [14, 15] installed at a distance of 7.5 m from its axis; two measurements are made on each side of the vehicle. The maximum sound level, expressed in decibels (dB), is measured at the moment when the vehicle passes between lines A-A and B-B. The resulting value is the measurement result [1].

The experimental measurement was performed using an electric car of the SUV category-Tesla Model X 2018 (without using the function of creating artificial noise).

The obtained measurement results are shown in Tab. 2.

Vehicle	Generated noise level (dB)
Tesla Model X	58

Tab. 2: Noise generated by an electric vehicle

Comparing the obtained data (Tab. 2) with the noise level generated by cars with an internal combustion engine, we see the following difference (Tab. 3). The resulting difference is an indicator of reducing the noise load when using electric vehicles.

Electric vehicle (Tesla Model X)	A car with an internal combustion engine (average indicator)	The difference in the noise level
58	80 dB	22

Tab. 3: Comparison of the noise generation indicators

4. CONCLUSION

In this study, a method for reducing the noise load on wildlife during scientific expeditions is proposed. The method provides the replacement of cars used for transportation of the employees and equipment of the expedition with electric vehicles. Replacing one car with an internal combustion engine of the SUV category with an electric car of the same category allows reducing the noise load by 22 dB at a speed of 30 km/h. The paper specifies the existing restrictions in using electric vehicles in expeditions, including the maximum distance from the destination of the expedition. According to the presented data, the existing electric vehicles of the SUV category are applicable in expeditions with a destination point of up to 400 km (the distance is measured from the last charging station located on the way of the expedition). Reducing the noise load is also a factor in increasing the effectiveness of scientific expeditions. As a result of reducing the noise load, the probability of wild nature inhabitants (objects of research) leaving their location or changing their usual routine of life is reduced, which reduces the likelihood of distortion of the scientific results obtained by the expedition.

REFERENCES

[1] M.G. Shatrov, A.L. Yakovenko, T.Y. Krichevskaya: The noise of automobile internal combustion engines [Shum avtomobil'nykh dvigateley vnutrennego sgoraniya : ucheb. Posobiye], MADI, p. 68, 2014
[2] https://www.researchgate.net, (date of the application 01.09.2021)
[3] https://www.nature.com/, (date of the application 01.07.2021)
[4] Shvetsov, A.: Change in Fuel Consumption of a Hybrid Vehicle When Operating in the Far North. World Electric Vehicle Journal. VOLUME 12(3), p. 104, 2021, doi: 10.3390/wevj12030104
[5] https://insideevs.com/reviews/445868/electric-suv-truck-coming-2021/, (date of the application 01.07.2021)
[6] Shvetsov, A. et al.: Transportation safety in an urban condition, E3S Web of Conferences, VOLUME 135, Article Num. 02004, 2019, doi: https://doi.org/10.1051/e3sconf/201913502004
[7] https://www.truecar.com/best-cars-trucks/fuel-electric/all-wheel-drive/, (date of the application 01.09.2021)
[8] Shvetsova, S., Shvetsov, A.: Safety when Flying Unmanned Aerial Vehicles at Transport Infrastructure Facilities. Transportation Research Procedia. VOLUME 54, pp. 397–403, 2021, doi: http://dx.doi.org/10.1016/j.trpro.2021.02.086
[9] Lyovin B. A., et al.: Method for Remote Rapid Response to Transportation Security Threats on High Speed Rail Systems. International Journal of Critical Infrastructures. VOLUME 15(4), pp. 324–335, 2019, doi: 10.1504 / IJCIS.2019.103015
[10] Shvetsov, A.: ASPECTS OF TRAFFIC NOISE REDUCTION. Akustika. VOLUME 39, p.25, 2021, doi: 10.36336/akustika20213925

Alexey Shvetsov *is Ph.D. of Engineering Science, Associate Professor of Department of Automotive Transport and Car Service of the North-Eastern Federal University (Yakutsk, Russia), and Associate Professor of Department of Transport Processes of the Technologies of the Vladivostok State University of Economics and Service (Vladivostok, Russia). He obtained his PhD in 2018 from the Russian University of Transport, in the field of transportation safety. He current research interests are in the fields of to protection transportation critical infrastructure. He has published more than 75 books, papers in journals and international conferences, on transportation safety and about the protection of critical infrastructures.*

Paper No.365/2021

REGRESSION ANALYSIS OF THE COEFFICIENTS OF VIBRATION ENERGY LOSSES IN GAS-DISCHARGE SYSTEMS OF POWER PLANTS

[a)]Aleksandr Chukarin, [b)]Alexey Fedenko, [c)]Aleksandr Shashurin, [d)] Viktoriia Vasilyeva

[a,b)]Rostov State Transport University, Rostov-on-Don, Russia
[c)]Samara State Technical University, Samara, Russia, 7596890@mail.ru
[d)] Baltic State Technical University 'VOENMEH' named after D.F. Ustinov, St. Petersburg, Russia

***Abstract**: Within the framework of this article, an experiment was conducted to determine the coefficient of energy loss of oscillatory motion. The analysis of the behavior of the frequency dependence of the coefficient showed that the approximation by a polynomial of degree 7 gives the most approximate result to the experimental values. The standard deviation of the experimental data from the polynomial is consistent with the error of the experimental data.*

***Keywords:** regression analysis, vibration energy, pipeline, analysis.*

***DOI:** : 10.36336/akustika202141115*

1. INTRODUCTION

Vibration of power plants is a serious problem [1, 2, 6-8]. The coefficients of vibration energy losses have quite interesting features [1]. Their values depend not only on the frequency of vibrations, but also on the physical and mechanical characteristics of the material and, as it turned out, on the configuration of the section of the part or structure. The gas-discharge systems of power plants (pipelines) are somewhat different in design from other elements of the system. The wall thickness of the pipelines is much smaller than the diameter and length, i.e. the density of the flow of vibration energy passing along the pipe is much higher than that of the beams. In addition, the pipeline is experiencing excessive pressure from the inside, so the values of the vibration energy loss coefficients of the pipelines do not coincide with the values of these coefficients of other load-bearing elements.

2. DESCRIPTION OF THE EXPERIMENTAL SETUP AND THE PROCEDURE FOR CONDUCTING THE EXPERIMENT

To determine the reliable values of the frequency-dependent loss coefficients of the vibration energy of pipelines, a special stand was created using modern measurement technology (fig. 1).

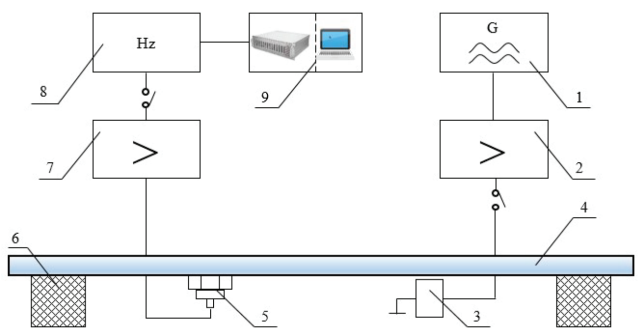

Fig. 1: Scheme of the experimental stand for determining the loss coefficient: 1 – generator; 2 – excitation signal amplifier; 3 – vibration exciter; 4 – the object under study; 5 – accelerometer; 6 – vibration isolators; 7 – accelerometer signal amplifier; 8 – analyzer; 9 – computing complex.

The hardware system of the stand has two lines: one is designed to excite vibrations in the pipeline under study, the second is for recording and processing vibroacoustic emission signals.

Fig. 1 shows the scheme of excitation of vibrations in the pipeline. A sinusoidal sound signal excited in the generator 1 is fed to the power amplifier 2. Next, the amplified signal gets to the electromagnet 3, which excites the part at forced and natural frequencies. The natural frequencies are recorded by an oscilloscope (analyzer 8). With the help of vibration isolators 6, on which the pipeline rests, the influence of external vibrations is reduced. The need for the formation of sinusoidal oscillations is explained by the requirements of the applied research methods.

The second line of the stand, which performs the functions of signal recording and processing, includes an accelerometer 5, a signal amplifier 7, a computing complex 9 for digitizing and registering signals based on a personal computer and a multi-channel input-output unit with an analog-to-digital converter (ADC).

At the research object, a piezoaccelerometer of the DN-4-M1 type is used to register vibration accelerations. The sensor characteristics can be seen in Tab. 1.

The coefficient of conversion of acceleration to voltage	$k_C = 1{,}00\, mV \cdot s^2/m$
Transverse resonance frequency	$f_T = 14{,}0\, kHz$
Installation resonance frequency	$f_I = 43{,}0\, kHz$

Tab. 1:Characteristics of the piezoaccelerometer sensor type DN-4-M1

To amplify and match the sensor with the ADC, a 4-channel vibration amplifier I 1002 (RTF) is used, which has a wide frequency range and a large selection of gain factors, both in voltage and charge. Based on the conditions of analog-to-digital conversion, the signal coming from the accelerometer, in addition to pre-amplification, should be subjected to Antialiasing filtration to prevent the phenomenon of frequency substitution of high-frequency information. Further, to prepare for conversion to digital form with an ADC, the processed signal is fed to the normalizing amplifiers.

The digitized signal is centered to eliminate the zero error of the measuring path, digital filtering is performed that compensates for the accelerometer's own amplitude-frequency characteristics (frequency response).

This signal is "weighed" using the Nuttall function to suppress the effects caused by the presence of side lobes in the spectral estimates due to the finiteness of the sample size. The processed signal is converted to the frequency domain using fast Fourier transform algorithms. Signal processing of this kind can be performed using Mathcad, other applied mathematical packages, or using the original application software package.

The loss coefficients are determined by the formula [2]:

$$\eta = \frac{1}{\pi n} \ln \frac{A_1}{An} \qquad (1)$$

where

n – the number of vibrations at the measuring distance;

A1 and ***An*** – the amplitude of the first and last oscillations at the measuring distance.

Experimental studies of the vibrational energy loss coefficients of the pipeline made it possible to determine their values at the average geometric frequencies of the octave spectrum, which makes it possible to use them for vibroacoustic calculations. However, quite often vibroacoustic calculations must be performed for natural oscillation frequencies other than the average geometric ones. Therefore, based on experimental data, it is necessary to determine analytical dependencies that allow calculating the coefficient of loss of vibrational energy at any intermediate oscillation frequency. We will conduct a regression analysis of the values of the vibrational energy loss coefficients of the pipeline obtained as a result of experiments on the above-described stand.

3. REGRESSION ANALYSIS

One of the most common methods of regression analysis for estimating the parameters of regression models from sample data is the least squares method (OLS) [3]. This method allows us to solve a fairly wide range of problems, including the approximation of experimental data, determining initially unknown coefficients of the analytical dependence of a certain function. At the same time, it is possible to determine not one, but several analytical dependencies and evaluate their adequacy using the sum of the squares of deviations from the experimental values. As a rule, the analytical dependencies obtained using OLS are linear or polynomial in nature. However, there are a number of nonlinear functions that can be reduced to a linear form (linearized) with the help of simple mathematical transformations and the coefficients of regression models can be determined using OLS. Since the analytical dependences found can be linear, nonlinear functions, as well as polynomials of various degrees, it is necessary to evaluate the adequacy of the model using a more strict parameter-the standard deviation (RMS) [4,5]:

$$\sigma = \sqrt{\frac{1}{(n-m)-1} \sum_{i=1}^{n} \left(y_{ex_i} - y_i\right)^2} \qquad (2)$$

where

n – number of experiments;

m – the degree of the polynomial;

y_{ex} – the value of the function in the experiment;

y_i – calculated value according to the model.

The values of the experimental loss coefficients of the vibrational energy of the pipeline are shown in Fig.2.

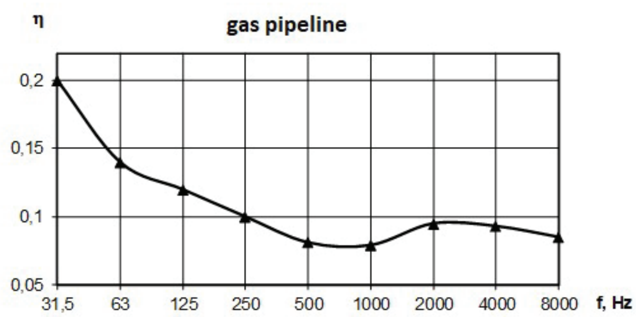

Fig. 2: The coefficient of loss of vibrational energy of the pipeline

The results of regression analysis by nonlinear functions are presented in Tab.. 2 and in Fig. 3.

Name of the curve	The equation	RMS
Exponential	$\eta = 0{,}115e^{-4{,}9\cdot10^{-5}f}$	$3{,}56\cdot10^{-2}$
Power-law	$\eta = 0{,}235f^{-0.13}$	$2{,}22\cdot10^{-2}$
Hyperbolic of type 1	$\eta = 0{,}085 + \frac{3{,}62}{f}$	$6{,}88\cdot10^{-3}$
Hyperbolic of type 2	$\eta = \frac{1}{9{,}09 + 0{,}0004f}$	$3{,}65\cdot10^{-2}$
Hyperbolic of type 3	$\eta = \frac{f}{-221{,}79 + 11{,}4f}$	$1{,}42\cdot10^{-2}$
Logarithmic	$\eta = 0{,}21 - 0{,}016 \cdot ln\, f$	$2{,}41\cdot10^{-2}$
S-shaped	$\eta = e^{-2{,}44+\frac{27{,}54}{f}}$	$8{,}29\cdot10^{-3}$
Inversely logarithmic	$\eta = \frac{1}{3{,}11 + 1{,}08 \cdot lnf}$	$2{,}22\cdot10^{-2}$

Tab. 2: Results of regression analysis by nonlinear functions

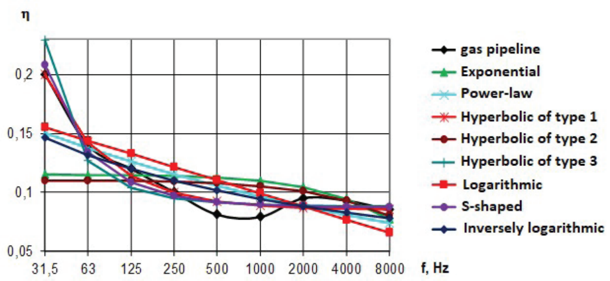

Fig. 3: Approximation by nonlinear functions for the pipeline

Fig. 3 shows that nonlinear functions do not approximate the experimental data well.

The approximation by a polynomial forms an adequate mathematical model under the condition of uniformity of the initial data. In our case, the frequency series has a geometric progression, so the maximum and minimum values of ***f*** differ from each other by two orders of magnitude. To align the source data, we will make a replacement ***-x=lgf***. Since the measurements of the vibrational energy loss coefficient were carried out at 9 frequencies, the maximum degree of the approximating polynomial will be 7. The results of regression analysis by polynomials are presented in Tab.. 3 and in Fig. 4.

Degree	The equation	RMS
1	$\eta=0{,}21-0{,}037(lg f)$	$2{,}57 \cdot 10^{-2}$
2	$\eta=0{,}47-0{,}246(lg f)+0{,}038(lg f)^2$	$1{,}19 \cdot 10^{-2}$
3	$\eta=0{,}872-0{,}744(lg f)+0{,}232(lg f)^2-0{,}024(lg f)^3$	$7{,}16 \cdot 10^{-3}$
4	$\eta=0{,}567-0{,}237(lg f)-0{,}07(lg f)^2+0{,}053(lg f)^3-0{,}0072(lg f)^4$	$7{,}68 \cdot 10^{-3}$
5	$\eta=3{,}816-6{,}984(lg f)+5{,}361(lg f)^2-2{,}069(lg f)^3+0{,}396(lg f)^4-0{,}0299(lg f$	$6{,}44 \cdot 10^{-3}$
6	$\eta=20{,}23-47{,}76(lg f)+46{,}56(lg f)^2-23{,}75(lg f)^3+6{,}67(lg f)^4-0{,}978(lg f)^5+$	$2{,}73 \cdot 10^{-3}$
7	$\eta=-16{,}008+56{,}78(lg f)-80{,}2(lg f)^2+60{,}04(lg f)^3-25{,}96(lg f)^4+6{,}51(lg f)^5$	$8{,}23 \cdot 10^{-4}$

Tab. 3: Results of regression analysis by polynomials

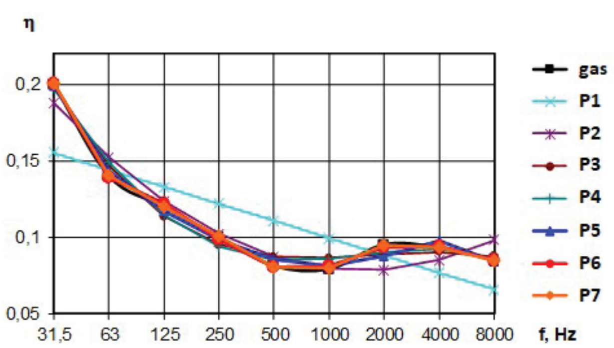

Fig. 4: Approximation by polynomials for a pipeline.

Since the smallest standard deviation of all functions has a polynomial of the seventh degree, the regression dependence has the following form:

$$\boldsymbol{\eta = -16{,}008 + 56{,}78(lg\, f) - 80{,}2(lg\, f)^2 + 60{,}04(lg\, f)^3 - 25{,}96(lg\, f)^4 + 6{,}51(lg\, f)^5 - 0{,}88(lg\, f)^6 + 0{,}05(lg\, f)^7} \quad (3)$$

The approximation of the experimental data by a polynomial of degree 7 is consistent with the measurement error and is sufficient to estimate the change in the vibration energy coefficient as a function of frequency.

ACKNOWLEDGEMENTS

The third author thanks the Russian Scientific Foundation for support the research described in this paper by grant, project number: 20-19-00222.

4. CONCLUSION

In conclusion, it should be noted that, despite the complexity and high degree of the polynomial, the obtained analytical dependence is quite accurately approximated to the experimental curve (see Fig. 4) and with modern resources and computing power, it can be used to calculate the loss coefficients of the vibrational energy of the pipeline at any intermediate oscillation frequency.

REFERENCES

[1] Chukarin A. N. Teoriya i metody akusticheskikh raschetov i proyektirovaniya tekhnologicheskikh mashin dlya mekhanicheskoy obrabotki: monografiya. Izdatelskiy tsentr DGTU. Rostov n/D. 2005. – 152 p.
[2] Vibratsii v tekhnike: Spravochnik. T. 1 pod redaktsiyey V. V. Bolotina. Kolebaniya lineynykh sistem. – M.: Mashinostroyeniye, 1999. – 328 p.
[3] Dubrov A. M.. Mkhitaryan V. S.. Troshin L. I. Mnogomernyye statisticheskiye metody: uchebnik. – M.: Finansy i statistika, 2003. – 352 p.
[4] Kokhanovskiy V. A. Planirovaniye eksperimentalnykh issledovaniy / V. A. Kokhanovskiy. M. Kh. Sergeyeva. – Rostov n/D: Izdatelskiy tsentr DGTU, 2014. – 256 p.
[5] Shashurin A.E. Analysis of the experimental study of the axle lathe machine vibroacoustic characteristics for workplace noise reduction. AKUSTIKA, Volume 34, 2019, p. 104-107 - ISSN 1801-9064.
[6]. Vasilyev A.V. Russian experience of transport noise estimation and mapping. Journal “Akustika”, Czech Republic, Volume 32, March 2019, pp. 105-109.
[7]. Vasilyev A.V. Development and approbation of methods and technical solutions of reduction of vibration of power plants and joining mechanical systems. Procedia Engineering. 2015. Vol. 106. pp. 354-362.
[8]. Vasilyev. A.V. Automobile internal combustion engine low frequency noise reduction using active noise control solutions. Journal “Akustika”, Czech Republic, Volume 34, November 2019, pp. 113-117.

__Alexander Chukarin__ is Doctor of Engineering Sciences, Professor, Head of the Chair «Fundamentals of Machine Design», Rostov State Transport University (RSTU) (Rostov-on-Don, Russia).
The direction of the scientific research is the process of vibro acoustic dynamics of the technological machines in various functional purposes.
In 1985 he defended his thesis on the topic «Improving vibro acoustic characteristics of the bearing assemblies of the machine tools». In 1996 he defended his doctoral thesis in the specialty «Vibro acoustic bases for calculating machine tools at the design stage».
Under the leadership of Professor A.N. Chukarin, 3 doctoral and 19 master's theses were defended.
A.N. Chukarin published more than 220 scientific and educational works: 6 monographs.
He is the Deputy Chairman of the Doctoral Dissertation Council on the specialties «Labor Protection» (mechanical engineering) and «Machine engineering, Drive Systems and Machine Parts». He is a member of the editorial boards of a number of the abstract journals.

__Aleksey Fedenko__ is Candidate of Technical Sciences, Associate Professor of the Department of Fundamentals of Mechanical Engineering, Rostov State Transport University.
Alexey Fedenko is a specialist in vibroacoustic dynamics of technological equipment of various functional values. Alexey Fedenko is the author of 50 scientific articles and co-author of 2 monographs.

__Aleksandr Shashurin__ is Doctor of Engineering Science, Professor, Head of Department of Environment and Safety of the Baltic State Technical University ‘VOENMEH’ named after D.F. Ustinov (Saint-Petersburg, Russia), CEO of the LLC (OOO) ‘Acoustic Design Institute’.
Aleksandr Shashurin is a specialist in calculation and design of noise barriers, noise reduction at production facilities, soundproof booths design and others. He is a member of the organizing committees of conferences and seminars in the field of acoustics and ecology held in St. Petersburg and Moscow. Aleksandr Shashurin is the author of over 40 scientific publications and the co-author of textbooks and teaching aids, the author of 6 patents for noise control devices. He presented the main results of scientific research at the international conferences in St. Petersburg, Moscow, Samara, Hiroshima (Japan).

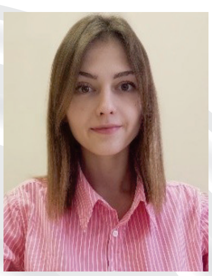

__Viktoriia Vasilyeva__ is Assistant of the Department of Ecology and Industrial Safety of the Baltic State Technical University "VOENMEH" named after D.F. Ustinov (St. Petersburg, Russia), Viktoriia Vasilyeva is engaged in research on the effects of noise on the human body. Development of methods for determining the individual body's response to noise with prevailing high and low frequencies. Author of scientific publications. Participant of scientific conferences on noise protection in St. Petersburg and Moscow.

Paper No.366/2021

RESEARCH TO IMPROVE POWERTRAIN NOISE, VIBRATION AND HARSHNESS CHARACTERISTICS

[a,*]Rakhmatdzhon Rakhmatov, [a]Vitaliy Krutolapov, [a]Vladimir Galevko, [a]Sergey Gaslov,
[a] Aleksandr Bokarev, a)Dmitriy Butuzov

[a]*Russian State Scientific Research Center FSUE 'NAMI', Moscow, Russia*
[*]e-mail: rakhmatjon.rakhmatov@nami.ru

***Abstract**: The paper presents a research algorithm consisting of: a developed methodology for selection of target values for natural frequencies and localization of vibration-loaded area of the powertrain based on calculation (simulation) and experimental research of resonant frequencies of the powertrain in operating modes and disturbances from two types of roads, calculation and experimental methodology for research of natural frequencies and oscillation modes of the powertrain, developed methodology for powertrain design refinement in terms of natural frequencies up to compliance with the target values and reduction of structural noise. Results of calculation and experimental research of resonant frequencies of the powertrain in operating modes and in case of disturbance from two types of roads are provided. There is also a justification given for selection of the target value for the powertrain natural frequency. Calculation of powertrain natural frequencies and oscillation modes was performed using the finite element method; experimental verification of the calculation was carried out as well. Using the verified calculation (simulation) model, design changes were introduced to reach the target values for natural frequencies and to reduce structural noise. Comparative calculation studies of the frequency response confirming the efficiency of the design changes are carried out.*

***Keywords:** powertrain, target values, 1D simulation, finite element modeling, natural frequencies and modes calculation, modal analysis, experimental verification, parametric optimization, frequency response, vibration speed, NVH characteristics improvement.*

***DOI:** : 10.36336/akustika202141119*

1. INTRODUCTION

Today, the task of vehicle noise and vibration reduction has become even more relevant not only because of legislative control, but also due to consumer properties, on the satisfaction of which the competitiveness of the vehicle in the sales market depends. With the emergence of hybrid power units and the rise in their power and agility, there is a trend towards increasing vehicle vibration loading caused by the implementation of an additional power energy source, namely an e-machine. One of the main ways to reduce hybrid powertrain oscillation intensity and the loads transmitted from the powertrain to the vehicle body is choosing the correct position and characteristics of the powertrain mounts [1-35] as well as eliminating resonances of the system in operating modes and thus excluding coalescence of natural frequencies of the design with the dynamic (load) disturbing frequencies. A huge amount of work related to the powertrain noise, vibration and harshness characteristics (NVH) has been performed by Tolskiy V.E., Zhang T., Guo R., Govindswamy K., Abe T., Rahnejat H., Van Der Auweraer H., Cheng M.T., Shangguan W.B., Theodossiades S. Eisele G., Fang Y., Lim T.C., Yu P., Albers A., Janssens K., Jen M.U., Lu M.H., Galvagno E., Robinette D., Shi W., Singh R., Stoffels H., Vigliani A., Wellmann T., Chen Z., Lee M.R., Qatu M.S., Rust A., Tousignant T., Warth M., Yu H., Behrendt M., Lee S.K., Li M., Ravaglioli V., Steffens C., Wu J., Zhang Y., Bassett M., Chauvicourt F., De Oliveira L.P.R., Duan J., Graf B., Orzechowski J., Ponti F., Prokop A., Raghavendran P., Stout J.L., Tota A., Wolff K., Wu G., Zheng X., Allman-Ward M., Brandl S., Canova M., Ciceo S., De Cesare M., Du L., Hao Z., Hazra S., Jung I., Kelly P., Ma Z.D., Meng D., Mohammadpour M., Resch T., Ruotolo R., Sbarbati F., Shangguan W., Sottek R., Tomazic D., Vanhaaften W., Vecchio A., Velardocchia M., Xu P., Yang F., Yu S., Zhang N., Anthonis J., Armentani E. and others, whose scientific research results analysis showed that there is no unified approach to the research of the powertrain NVH characteristics for improvement purposes, which shall consist of:

1. Justified calculation and experimental selection of target natural frequencies at the component (powertrain) level;
2. Identification of the vibration-loaded area of the powertrain;
3. Methodological approach for achieving target natural frequencies at the component (powertrain) level;
4. Methodological approach for reduction of the powertrain structural noise.

The objective of this work is to develop a research algorithm to improve the powertrain NVH characteristics that shall include:

1. Methodology for selection of target natural frequencies and localization of the powertrain vibration-loaded area based on:
   1.1. Calculation and experimental definition of the powertrain resonant frequencies in operating modes;
   1.2. Calculation and experimental research of the powertrain resonant oscillations in case of disturbance from two types of roads;
2. Study of the powertrain natural frequencies and oscillation modes:
   2.1. Calculation study through the finite element method;

2.2. Experimental research;
2.3. Calculation model verification.

3. Methodology for improvement of the powertrain NVH characteristics (in terms of natural frequencies up to compliance with the target values and reduction of structural noise).

2. METHODOLOGY FOR SELECTION OF TARGET VALUES

2.1. Calculation and experimental definition of powertrain resonant frequencies in operating modes

The methodology for selection of target natural frequencies is based on definition of the powertrain resonant frequencies in operating modes. For these purposes, a calculation model consisting of the internal combustion engine (ICE), transmission and powertrain mount models was formed in the Simcenter Amesim software. Each component part of the calculation model is a system of bodies having mass and inertial characteristics and united with elastic and damping, linear and non-linear links and connections. The ICE is represented by the elements included in the crank train and the cylinder and piston group. The rigidity of the cranks is determined by the numerical simulation. The indicator charts for the cylinders are obtained by indication of the engine combustion chamber on the engine test bench with the characteristics of the engine as given in Tab. 1.

Type	gasoline
Cylinder block configuration and V-angle	V(90°)
Number of cylinders, pcs	8
Displacement, l	4.4
Rated power at 5500 rpm, hp	600
Maximum torque, N*m	880
Fuel supply system	direct injection

Tab.1: ICE main characteristics

The engine multi-mass system diagram is shown in Fig. 1.

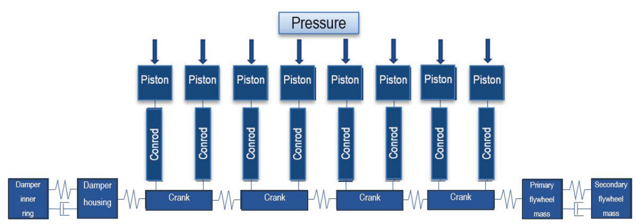

Fig. 1: ICE multi-mass system diagram

The model, the basic diagram of which is shown in Fig. 1, considers rigidity characteristics of the crankshaft that were determined according to the calculation and experimental research results. Also, the characteristics of the torsional vibration damper and dual mass flywheel are taken into account. The ICE virtual model made in the Simcenter Amesim software is shown in Fig. 2.

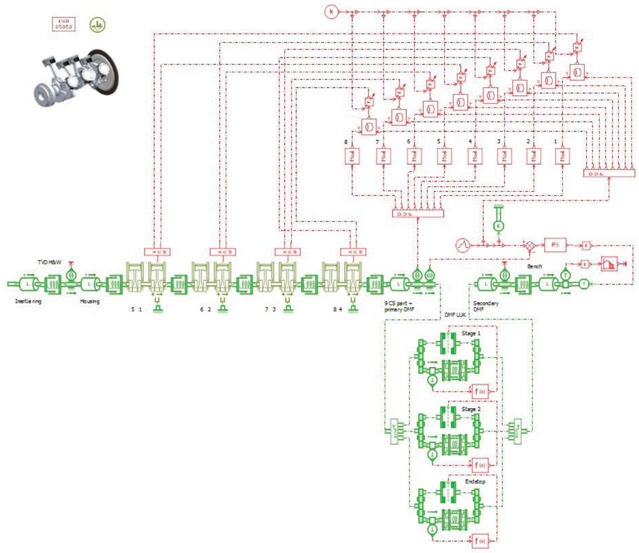

Fig. 2: Diagram of ICE virtual model made in Simcenter Amesim software

For the calculation model verification, the ICE was tested on the engine test bench running in the full-load curve within the crankshaft rpm range of 1000-6000 min-1. In the process of the tests, the torsional vibrations of the ICE crank train elements were measured in two places: in the front end of the crankshaft, where the torsional vibration damper is installed, and on the primary disk (mass) of the dual mass flywheel. The sensors positions are shown in Fig.3.

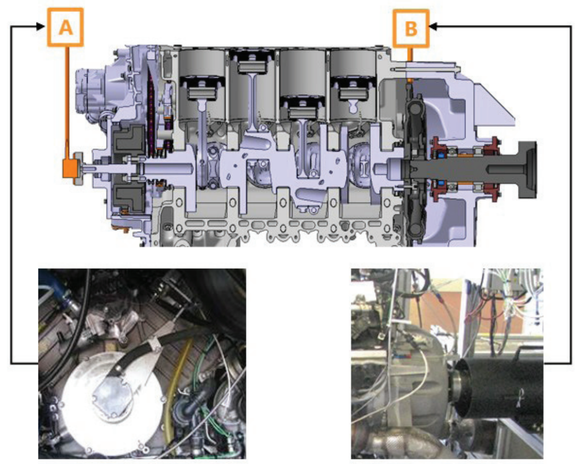

Fig. 3: Sensors positions: A – encoder, B – speed sensor

Fig. 4 shows the results of the comparative study of the calculation and experiment. The 4^{th} harmonic of the torsional vibrations of the ICE elements: a – angular displacements and b – angular accelerations measured by the encoder.

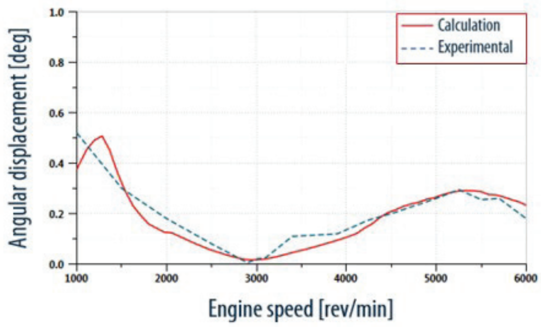

a

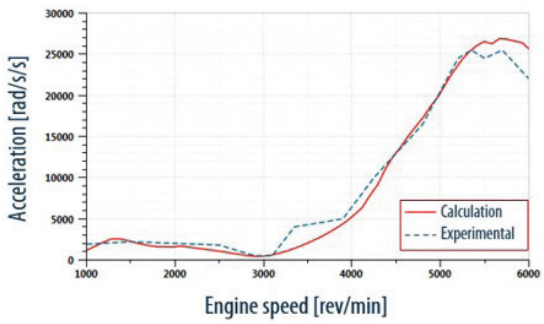

b

Fig. 4: Comparison of virtual simulation and experimental study results

Fig. 5 shows the results of the comparative study of the calculation and experiment. The 4th harmonic of the torsional vibrations of the ICE elements: a – angular displacements and b – angular accelerations measured by the radially installed sensor.

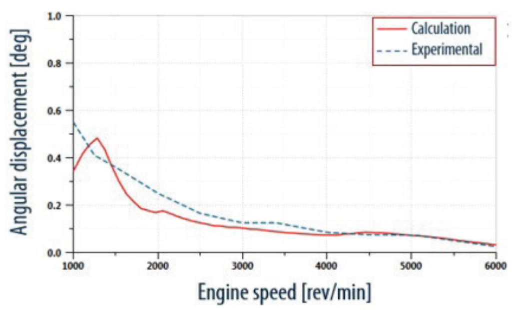

a

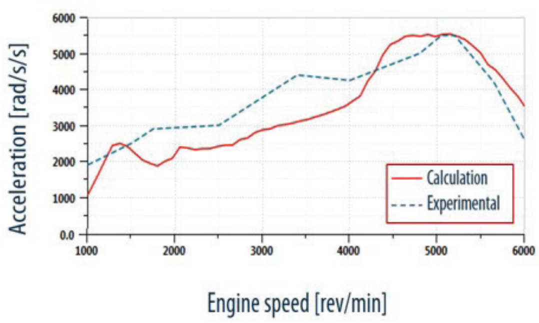

b

Fig. 5: Comparison of virtual simulation and experimental study results

The ICE calculation and experimental results correlate well with each other, therefore, the calculation model can be considered verified. In order to take into account the influence of not only the engine inertial mass, but also transmission components inertial mass on the powertrain torsional vibrations, a transmission multibody model has been developed that has 10 degrees of freedom. The transmission model diagram is shown in Fig. 6.

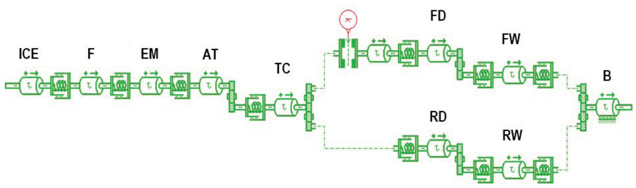

Fig. 6: Calculation model of transmission designed for analysis of torsional vibrations of unit shafts made in Simcenter Amesim software: ICE – internal combustion engine, F – flywheel, EM – e--machine, AT – automatic transmission, TC – transfer case, FD – front differential, RD – rear differential, FW – front wheels, RW – rear wheels and B – body

As an example, the calculation results for the spectra of the angular accelerations of the e-machine shaft in gear 5 are shown in Fig. 7.

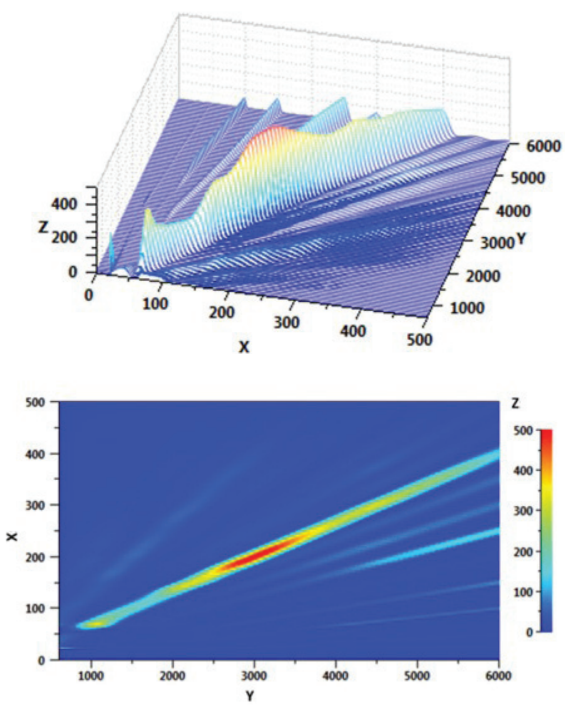

Fig. 7: Calculation results for spectra of torsional vibration angular accelerations on e-machine shaft in gear 5: X-axis – vibration frequency [Hz]; Y-axis – engine crankshaft rotation rate [min-1]; Z-axis – angular accelerations amplitude [rad/s2]

Based on the analysis of the amplitudes of the powertrain torsional vibration angular accelerations, Tab. No. 2 was drawn up, in which the frequency range of the maximum amplitudes of the angular accelerations caused by torsional vibrations is determined.

Unit denomination	AT gears								
	1	2	3	4	5	6	7	8	9
	Frequency, Hz								
E-machine	170-250	180-240	180-230	75-80 180-220	75-80 180-230	55-60 180-230	55-60 180-230	55-60 180-230	55-60 180-230
AT	100-105	75-80	80	75	60-65	50-55	50-55	50-55	50-55
Transfer case	105-115	70-75	80	75	60-65	50-55	50-55	50-55	50-55
Rear suspension axle drive	200-205	195-200	80 200-205	80 200-205	60-65 200-205	50-55 195-200	55-60 200	55-60 200	55-60 200
Front suspension axle drive	100 275-280	80-85 280-285	85-90 275-280	80-85 280	65-80 280	50-55	55-60	50-55	50

Tab. 2: Frequency range of maximum amplitudes of transmission components' angular accelerations

And in order to define the linear and angular accelerations spectra for the powertrain mass center, an additional calculation model has been developed that includes the ICE multibody model, transmission multibody model and powertrain mount model. The powertrain installed on the mounts is shown in Fig. 8. The illustration of the model structure is given in Fig. 9.

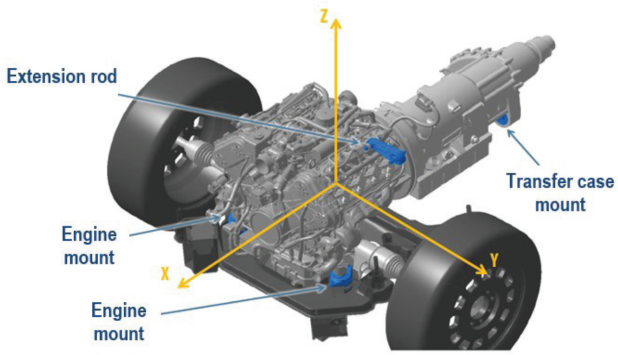

Fig. 8: Powertrain installed on mounts

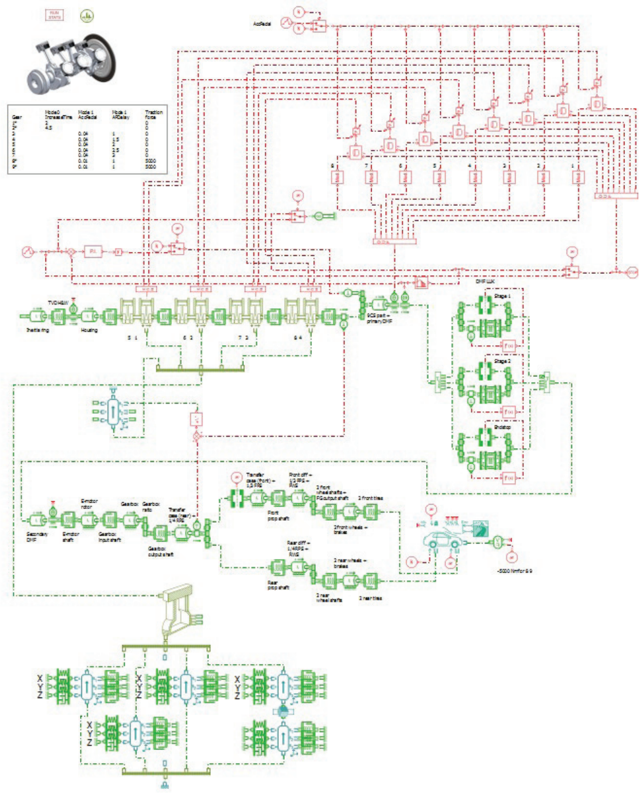

Fig. 9: Structure of powertrain and transmission model made in Simcenter Amesim software

As an example, the calculation results for the spectra of the powertrain linear accelerations along the vertical axis in gear 5 are shown in Fig. 10.

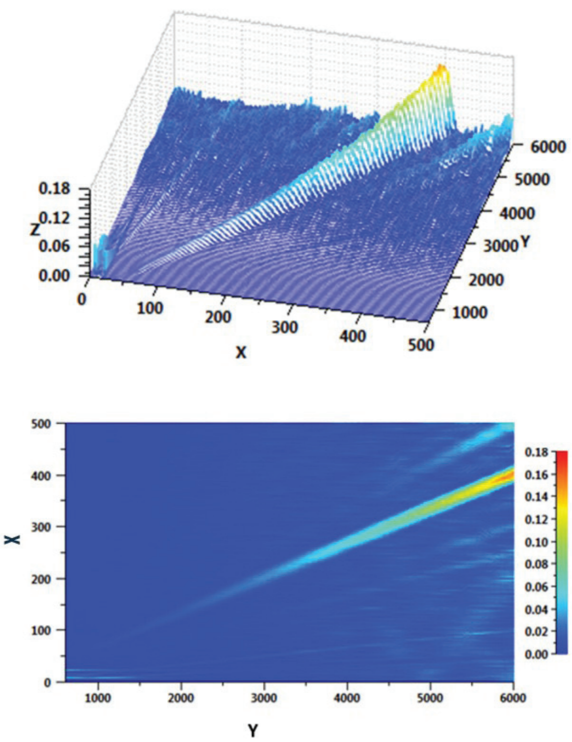

Fig. 10: Calculation results for spectra of powertrain mass center linear accelerations along the vertical axis and in gear 5: X-axis – vibration frequency [Hz]; Y-axis – engine crankshaft rotation rate [min-1]; Z-axis – angular accelerations amplitude [rad/s^2]

Based on the analysis of the linear and angular acceleration amplitudes of the powertrain mass center in all three directions X, Y and Z in all gears, Tab. No. 3 was drawn up that gives the frequency range for the maximum amplitudes of the linear and angular accelerations of the powertrain mass center.

Accelerations		AT gears 1	2	3	4	5	6	7	8	9
		Frequency, Hz								
Linear	X	10-100	10-100	10-110	10	10-110	10-110	10-110	10-110	10-110
	Y	430-500	430-500	430-500	10	10	10, 20	10, 20	10, 20	10, 20
	Z	330-430	330-430	330-430	330-430	330-400	330-410	350-410	350-410	300-410
Angular	X	105, 200-430	75-80 200-400	75-80 190-400	75-80 180-400	70-80 180-400	60-70 180-400	60-70 180-400	55-65 180-400	55-65 180-400
	Y	10-110	60-100	60-100	60-100	60-100	70-100	75-100	50-90	75-100
	Z	350-450	350-440	350-440	330-440	330-400	330-400	350-400	350-400	330-400

Tab. 3: Frequency range of maximum amplitudes of powertrain mass center linear and angular accelerations in three directions

Thus, based on the three developed models, the resonance frequency range was determined for the powertrain in operating modes [110-180 Hz]. And based on the frequency response function analysis for the maximum amplitudes of both linear and angular accelerations, the target value of the powertrain lowest global mode was determined, which shall correspond to 145 Hz. Furthermore, it follows from the frequency response function analysis for the linear accelerations of the powertrain mass center that the most vibration-loaded area is the mounting seat of the automatic transmission main shaft.

2.2. Calculation and experimental research of powertrain resonant oscillations in case of disturbance from two types of roads

The next stage of the research is the analysis of the influence of the road frequency disturbance on the powertrain within the vehicle. For the calculation, a mathematical model is used, which is a non-linear dynamic vehicle model in the form of a mass-elastic system with more than 94 degrees of freedom, including the mathematical description of vehicle systems and components in the form of a set of bodies with linear and non-linear connections as well as the mathematical description of vehicle interaction with the environment. The mathematical description of the typical models is given in reference [36]. The mathematical multilink models were developed in the MSC Adams/Car environment; the suspension guide apparatus and load-bearing structure are deformable bodies with linear properties. The component nodal points are implemented as the RBE2 elements equivalent to rigid fixation of the finite element mesh nodes. The standard settings of compliant bodies damping are taken for the calculations [37].

The characteristics of the elastic and damping suspension components are set according to the specification of the luxury class vehicle for driving on uneven roads. All the main damping sources, stiffness of all elastic elements along with their non-linear characteristics are taken into account. In the mathematical model, the weight-inertial and geometric parameters of the front and rear suspension, weight-inertial and geometric parameters of the steering equipment together with the power steering unit characteristic, wheel and tyre models, as well as weight-inertial and geometric parameters of the body and running gear systems are taken into account. For confidentiality reasons, the minimum allowed information on the mathematical models and objects of research is provided. The main vehicle parameters are given in Tab. 4.

Parameter denomination	Front suspension	Rear suspension
Vehicle fully loaded weight (GVW), kg	3490	
Vehicle weight distribution between the axles, F/R, %	50.2	49.8
Height of center of mass, mm	665	
Suspension vertical stiffness normalized to wheel center, N/mm	36.39	34.12
Front suspension roll stiffness normalized to wheel center, Nm/deg	2096.7	1505.8

Tab. 4: Main parameters of vehicle being researched

The following assumptions are taken into account in the mathematical model:

1. The body elasticity is not considered (solid model);
2. The transmission mathematical model describes motion of the engine and transmission parts considering inertial and dissipative properties of the engine-transmission system;
3. For investigation of the vehicle model behavior on uneven roads, an improved mathematical model Pacejka with a 3D contact is used (assumption of necessity due to absence of frequency-dependent tyre models, such as F-Tire and MF-Swift). [38]

The illustration of the mathematical model and markers for vibration acceleration measurement on the powertrain mounts is shown in Fig. 11. The vibration accelerations are measured on the left and right powertrain mounts and in the X, Y and Z directions of the vehicle respectively.

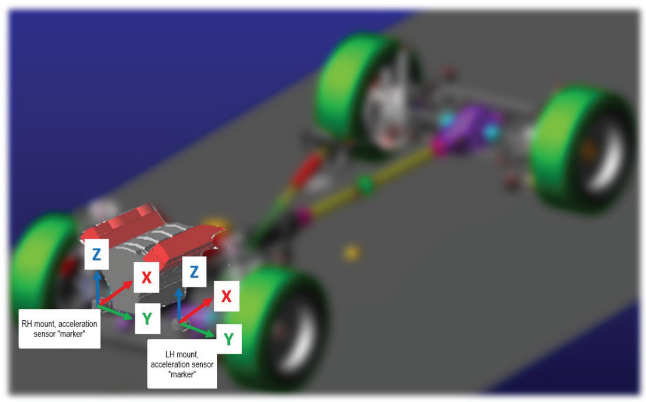

Fig. 11: Illustration of vehicle mathematical model and positions for vibration acceleration measurement

Based on literary sources [38] and [39], several special cases of the virtual vehicle motion are taken into account for analysis of the powertrain behavior and determination of the resonant disturbing frequencies:

1. Acceleration from 10 km/h to 100 km/h with the steady acceleration of 0.5 g on a scanned horizontal straight road with the following parameters:
   - Total length of the road: 5.4 km;
   - Width: 10 m;
   - Road pavement: sandy asphalt concrete on cement concrete bed;
   - Purpose: for tests for fuel efficiency, traction, speed and brake properties of all vehicle types.

The road illustration is given in Fig. 12.

Fig. 12: Illustration of the horizontal straight road of FSUE "NAMI" NICIAMT proving ground

2. Acceleration from 10 km/h to 100 km/h with the steady acceleration of 0.5 g on a scanned noise generating surface road with the following parameters:
   - Total length of the road: 0.75 km;
   - Width: 5 m;
   - Road pavement: granite stacked stone (cobblestone), even pavement, on sand-cement bed;
   - Purpose: for tests on detection of driving noise sources and definition of noise characteristics.

The road illustration is given in Fig. 13.

Fig. 13: Illustration of the noise generating surface road of FSUE "NAMI" NICIAMT proving ground

As an example, the results of the simulation of motion on the horizontal straight road are shown in Fig. 14 in the form of waterfall charts. The frequency response functions of the engine mounts in the vertical direction were calculated for each 0.1 s within the whole range of the motion cases simulation.

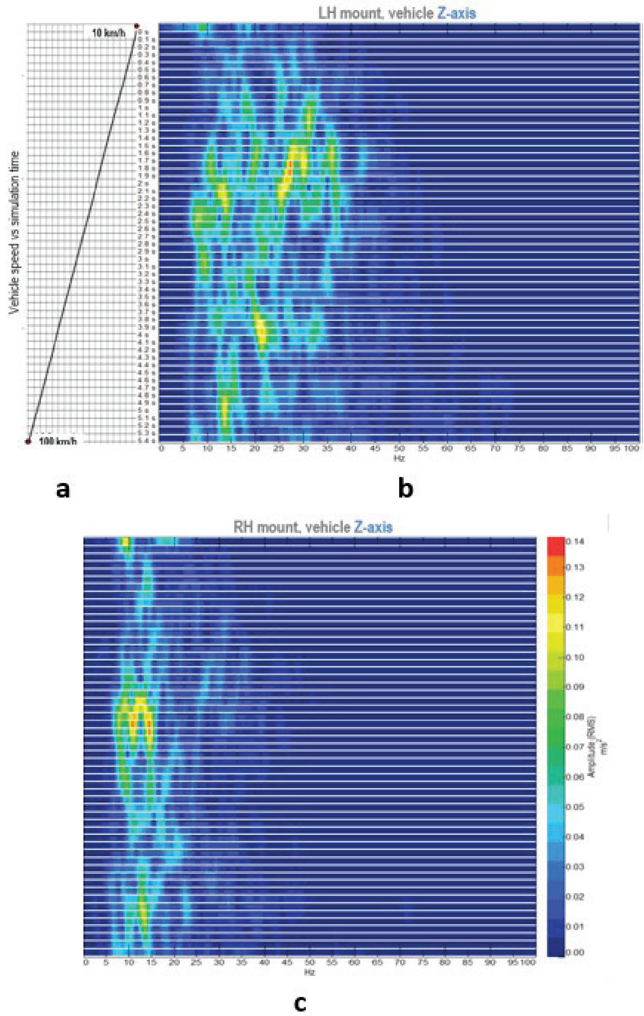

Fig. 14: Dependence of vehicle speed on time (a), acceleration spectra of the front left (b) and right (c) powertrain mounts in the vertical direction on the horizontal straight road

Based on the analysis of the acceleration amplitudes of the results of the simulation of motion on horizontal straight and noise generating surface roads in all the directions, the frequency range of disturbance from the road is defined, that amounted to 5-45 Hz.

Based on the abovementioned research and investigations, it can be concluded that the powertrain natural frequencies shall be within the frequency range of 110-180 Hz, outside of disturbance from the road surface (5-45 Hz) as well as gas and inertial forces (10-110 and 180-400 Hz) arising in the course of powertrain operation, thus the choice of the target values for the natural frequencies at the component level is substantiated. Moreover, the research analysis shows that the maximum amplitudes of the angular accelerations fall to the automatic transmission main shaft.

The next stage of the research is the calculation of the powertrain natural frequencies and oscillation modes, and upon that the first lowest global frequency shall be outside of the disturbance from the road surface as well as gas and inertial forces arising in the course of the powertrain operation.

3. RESEARCH OF NATURAL FREQUENCIES AND OSCILLATION MODES

3.1. Calculation studies

A finite element model (FEM) was developed for calculation of the natural frequencies and oscillation modes of the powertrain. The FEM consists of 2,629,032 volume elements (tetrahedral ones of the second order), 11,567 shell elements (triangles and squares of the first order), 7,257 – RBE3 elements, 3,902 – RBE2 elements, 1,764 – CBEAM elements, 188 CONM2 elements (224.3 kg of concentrated weight in total) and 4,740,735 nodes. The powertrain finite element model is shown in Fig. 15.

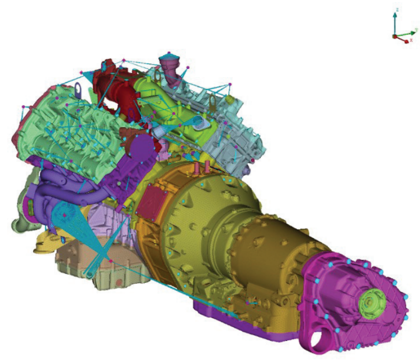

Fig. 15: Powertrain finite element model

The calculations were performed within the MSC Nastran software, Sol 103 EIGRL solution type, free-free boundary conditions. As an example, Figure 16 shows the results of the calculations of the first global modes.

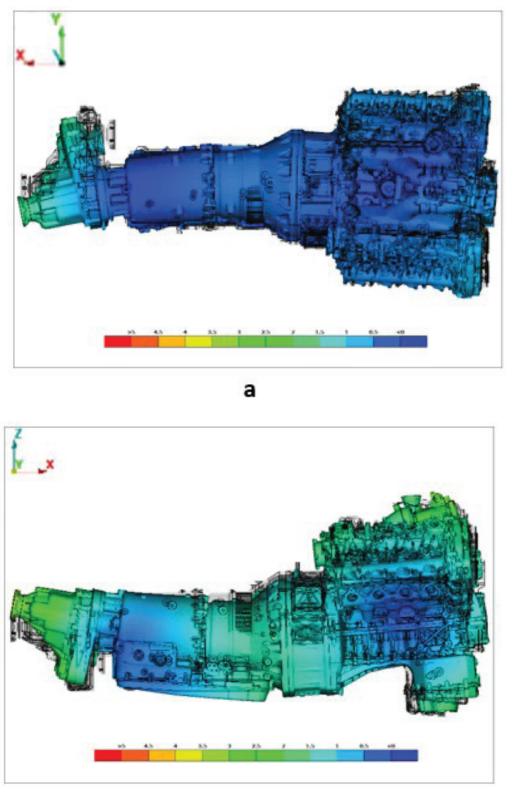

a

b

Fig. 16: Horizontal bend at 129.4 Hz frequency (a) and vertical bend at 139.9 Hz frequency (b), displacements displayed

The maximum displacements in case of the horizontal bend of the powertrain at the frequency of 129.4 Hz fall to the transfer case output shaft. The maximum displacements in case of the vertical bend at the frequency of 139.9 Hz fall to the transfer case output shaft and engine water cooling pipe.

The natural modes at the frequencies of 129.4 and 139.9 Hz with strain energy extraction are shown in Fig. 17:

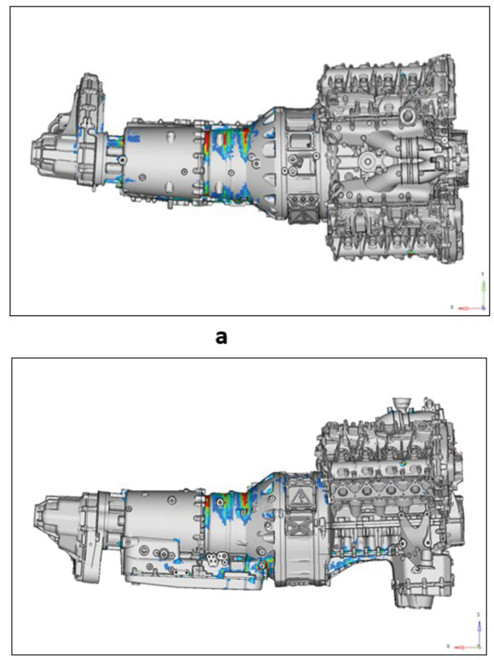

a

b

Fig. 17: Horizontal bend at 129.4 Hz frequency (a) and vertical bend at 139.9 Hz frequency (b), strain energy displayed

The strain energy in case of horizontal and vertical bends at the frequencies of 129.4 and 139.9 Hz concentrates in the AT front housing. In order to assess the adequacy of the calculation studies, experimental studies and validation were performed.

3.2. Experimental studies

The experimental studies were performed in the semi-anechoic chamber. When defining the natural frequencies and modes of the powertrain, it was hung up on flexible cables attached to the eye bolts, Fig. 18 (a). As an example, 4 of 20 mounting positions of the powertrain accelerometers are shown in Fig. 18 (b). The measured data were analyzed using the LMS Modal Analysis software in order to create the modal shapes of the powertrain and to calculate its natural frequencies. The coherence of the input and output signals was checked in the course of measurement. For calculation of oscillation modes, the range of 50-500 Hz was chosen in the Polymax Plus menu.

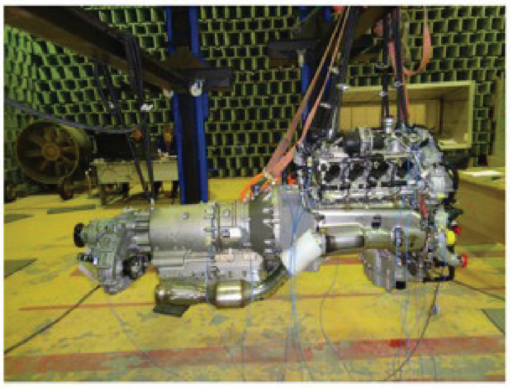

a

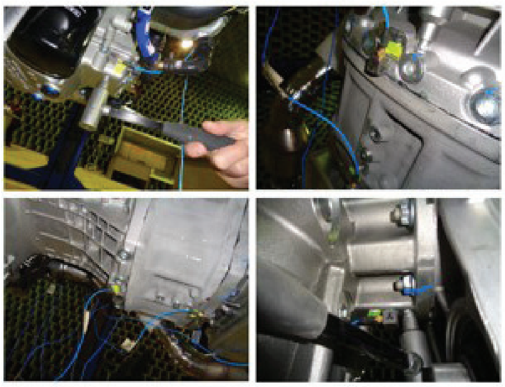

b

Fig. 18: Powertrain hung up on flexible cables (a) and accelerometer mounting positions

A stabilization diagram was generated in the Polymax Plus Stabilization menu (Fig. 19 a). Taking into account the generated diagram, constant polylines were selected and analyzed to create modal shapes for each frequency (Polymax Plus Shapes menu). For the selected modes, a correlation matrix was created (Fig. 19 b).

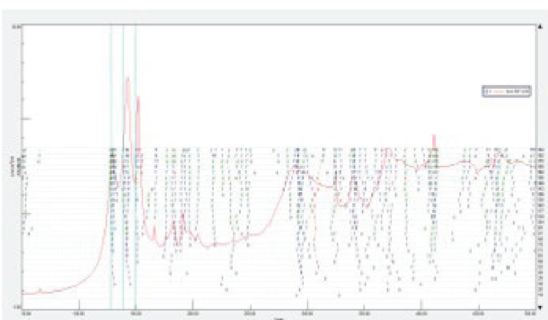

a

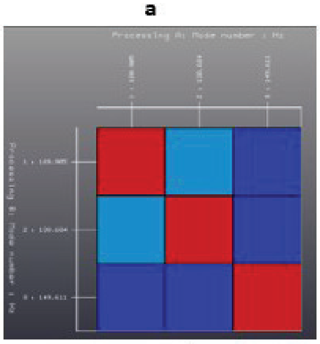

b

Fig. 19: Stabilization diagram (a) and correlation matrix (b)

3.3. Calculation model verification

The calculation model verification is performed using the correlation matrix constituting a set of calculated and experimentally obtained natural modes at the same frequencies. The compliance of the oscillation modes is estimated by the MAC (Modal Assurance Criterion) correlation coefficient calculated for each couple of modes (both calculated and experimental) and comprises the information on compliance of the frequency response function (FRF) in the control points of the FEM and experimental models (spatial position of accelerometers). At MAC=1, a complete coincidence of the FEM and experiment natural modes is achieved. The FEM verification is considered complete upon observance of the following requirements:

1. The MAC coefficients of the lowest global modes are within the range from 0.8 to 1;
2. The difference in frequencies of the calculated and experimental values for a couple of modes shall not exceed 3%.

The correlation matrix is built according to the procedure described in the Correlation module of the Siemens NX CAE software and shown in Fig. 20.

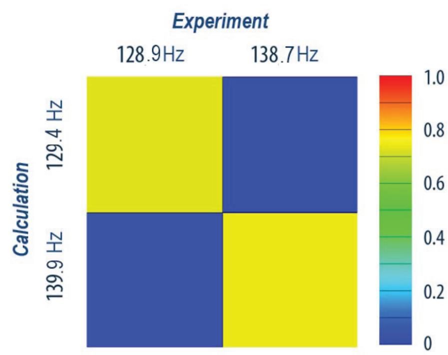

Fig. 20: Calculation/experiment correlation matrix

To meet the requirements for the correlation matrix and natural frequencies, the powertrain FEM parametric optimization was performed in the Siemens NX CAE software, Sol 200 solution type, criterion (target) function, minimization:

1. Divergences of the frequency response function (FRF) in 20 points (corresponding to the spatial position of the accelerometers in experimental studies);
2. Divergences of the first three frequencies.

The modulus of elasticity of the powertrain part materials shown in Fig. 21 is selected as a design variable.

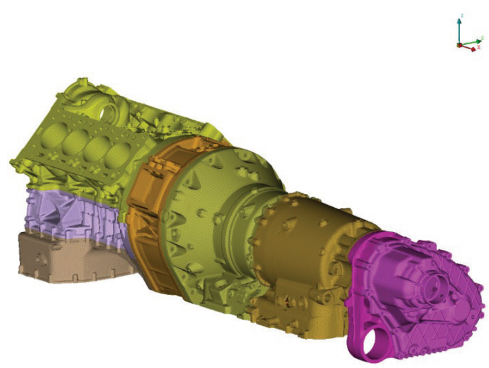

Fig. 21: Parts included in parametric optimization as project variable

Figure 22 shows the sensitivity analysis results.

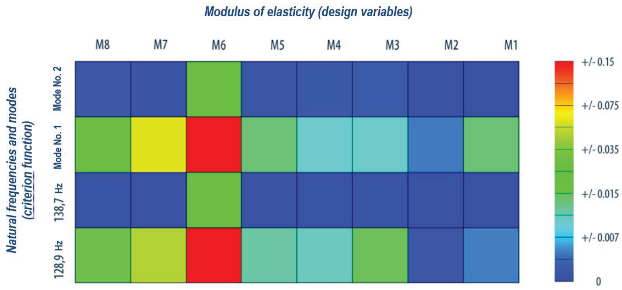

Fig. 22: Sensitivity matrix

Fig. 23 shows verification results for the powertrain calculation model. For the horizontal bend, the difference in frequencies amounts to 0.1 Hz and MAC=0.95. In case of the vertical bend, the difference in frequencies amounts to 0.2 Hz and MAC=0.97.

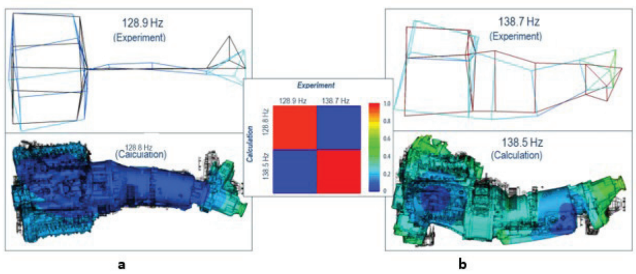

Fig. 23: Results of verification activities

The lowest global oscillation modes of the powertrain amount to 128.9 (Fig. 23a) and 138.7 Hz (Fig 23b). Based on the validation activities results, we managed to develop the powertrain FEM with an error of less than 1% for the oscillation modes and frequencies. Based on the analysis of the frequency response function (FRF) of disturbances, the target value of the powertrain lowest global mode shall be 145 Hz, for which reason it is necessary to increase the frequency of the lowest global bend. Changing the powertrain design in order to achieve the natural frequencies target values will lead to changes in the FRF of the powertrain radiating surfaces noise. Therefore, it is necessary to conduct design optimization not only in terms of natural frequencies, but also in terms of radiating surfaces structural noise.

4. METHODOLOGY FOR IMPROVEMENT OF POWERTRAIN NVH CHARACTERISTICS

It follows from the analysis of Fig. 16 and 17 that the high values of the energy of elastic deformations are located on the front housing of the automatic transmission (AT) (due to its location in the middle of the powertrain), accordingly, the increase in stiffness of the elements in this area will raise the powertrain vibration frequency. After the design elaboration taking into account the packaging and technological constraints, longitudinal stiffening ribs were introduced on the front part of the housing. The longitudinal stiffening ribs are also connected by the tangential ribs and the stiffened flange in order to prevent bending of the ribs themselves shown in Fig. 24b. In order to reduce the powertrain structural noise, longitudinal stiffening ribs adjacent to the stiffening ribs introduced to increase the global bend were introduced into the transmission design, and also stamped reinforcements were introduced into the automatic transmission sump based on the results of the analysis of the oscillation modes and concentration of the elastic deformations. The initial model of the automatic transmission (a) and the modified transmission (b) are shown in Fig. 24.

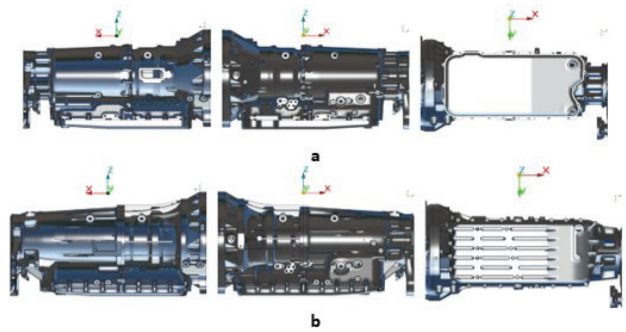

Fig. 24: Transmission designs: a - initial, b - modified

The FEM of the modified powertrain is shown in Fig. 25.

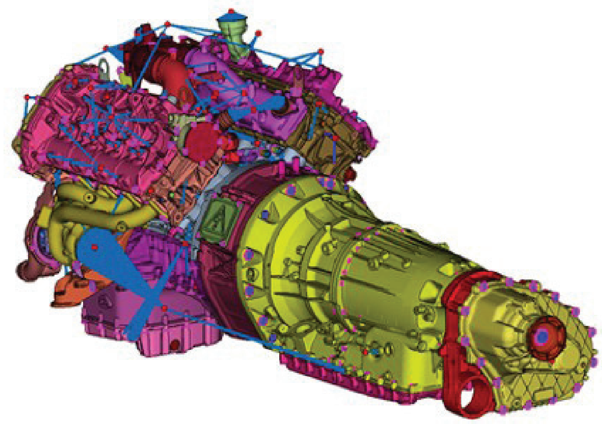

Fig. 25: Modified powertrain design

The FEM of the modified powertrain design consists of 2,937,314 volume elements (tetrahedral ones of the second order), 11,344 shell elements (triangles and squares of the first order), 6,917 – RBE3 elements, 3,653 – RBE2 elements, 1,903 – CBEAM elements, 184 CONM2 elements (222.4 kg of concentrated weight in total) and 5,367,450 nodes. Calculations in the MSC Nastran software, Sol 103 EIGRL solution type, free-free boundary conditions, were conducted to assess the efficiency of the measures aimed at increasing the frequency of the lowest global bend. The first 10 modes were exposed to deriving of natural frequencies and modes. As an example, the calculation results for the first global modes are shown (Figure 26).

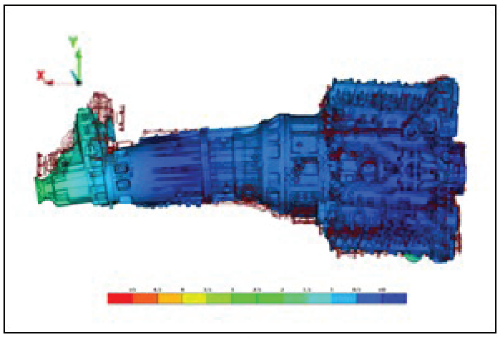

a

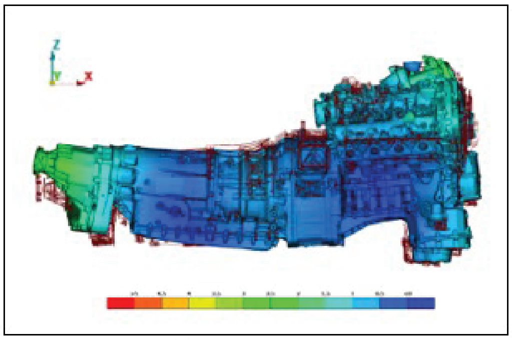

b

Fig. 26: Horizontal bend at 145.9 Hz frequency (a) and vertical bend at 160.7 Hz frequency (b), displacements displayed

The maximum displacements in case of the horizontal bend of the powertrain at the frequency of 145.9 fall to the transfer case output shaft. And the maximum displacements in case of the vertical bend at the frequency of 160.7 Hz fall to the transfer case output shaft and engine water cooling pipe. The comparative results of the modal analysis of the initial and modified powertrain designs are given in Tab. 5.

Oscillation mode	Frequency, Hz		
	Initial	Modified	Difference
Horizontal bend	129.4	145.9	+16.5
Vertical bend	139.9	160.7	+20.8

Tab. 5: Comparison table of modal analysis results

The developed modified powertrain design allows increasing the natural frequencies in case of the horizontal bend by 16.5 Hz, and in case of the vertical bend by 20.8 Hz, which complies with the target values.

To assess the efficiency of the measures to reduce structural noise, calculations were made in the MSC Nastran software, solution type Sol 111. The positions of the response points of the AT housing are shown in Fig. 27.

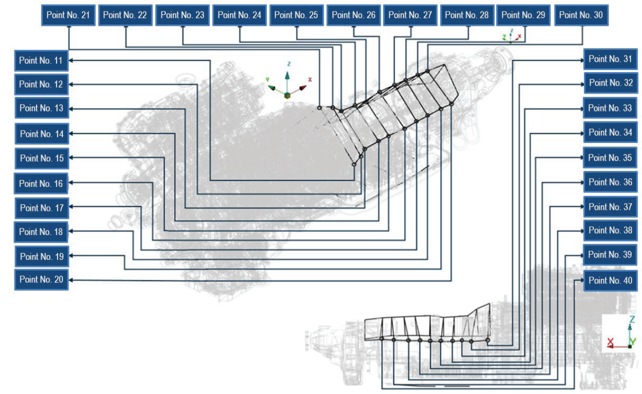

Fig. 27: AT housing response points position

The positions of the response points of the AT sump are shown in Fig. 28.

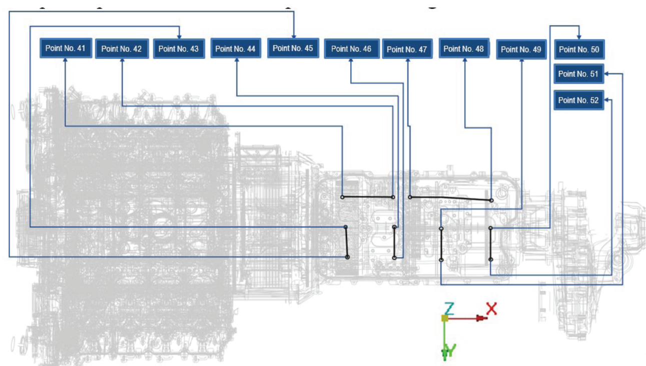

Fig. 28: AT sump response points position

At frequencies over 1000 Hz, the oscillations of the AT structure within the powertrain occur as in a distributed parameters system - certain AT external surfaces having boundaries of sharp change of the shape, stiffness, mass or damping characteristics have their own natural and forced oscillation frequencies and modes. Based on the above, the transmission housing and sump were divided into zones as shown in Fig. 29.

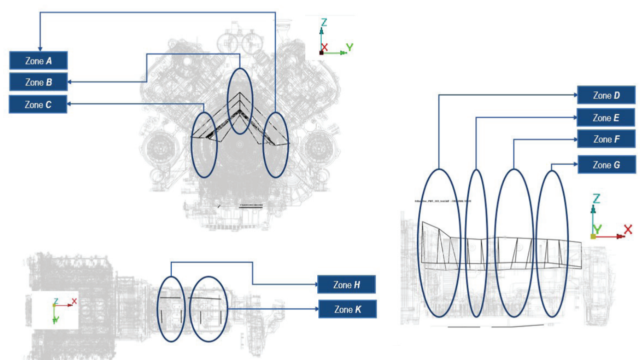

Fig. 29: AT sump response points position

It is known that the sound power radiated by a certain external surface can be defined as follows [40]:

$$W(f) = \sigma(f) \cdot \rho \cdot c \cdot S \cdot \tilde{V}^2(f) \tag{1}$$

where:
$\sigma(f)$ – source radiation coefficient,
$(\rho \cdot c)$ – acoustic resistance of the medium,
S – radiator area,
$\tilde{V}^2(f)$ – radiating surface vibration speed mean-square value.

It follows from the expression that in order to reduce the acoustic radiation from a certain external surface, it is necessary to reduce the squared vibration speed values in the considered frequency range. It is expedient to assess the efficiency of two designs based on the results of reduction of the mean-square vibration speed for certain considered areas.

As the maximum amplitudes of the angular accelerations fall to the automatic transmission main shaft, it is expedient to apply load in this area. As a load, a single load in all three directions is used, the excitation point falls to an independent node (RBE2 element) located on the AT main shaft mounting seat (see Fig. 30).

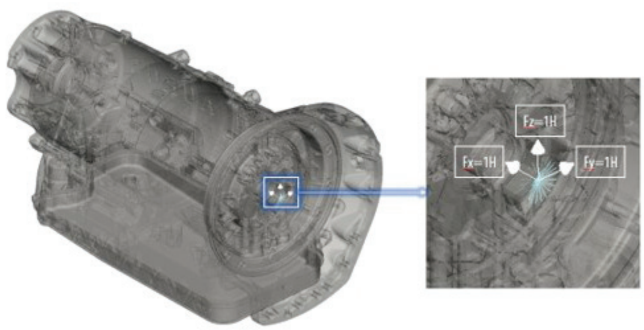

Fig. 30: AT sump response points position

As an example, in order to assess the efficiency of the considered design changes in area A, the spectra or ranges of the mean-square vibration speed values from a single load applied along the vertical axis (Z) are shown (Fig. 31).

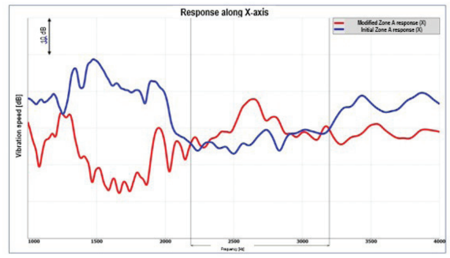

a

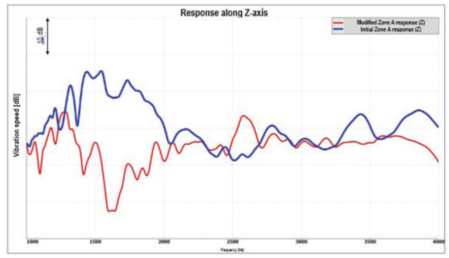

b

Fig. 31: Results of vibration speed calculation in area A (a - response along X-axis, b - response along Z-axis): blue - initial variant; red – modified variant

It follows from the analysis of the results of the mean-square vibration speed values that in case of single loads along axes X and Y, there is a decrease in amplitudes in the frequency range of 1,000-2,200 Hz and from ~ 3,200 Hz in all the areas, and in case of a single load along the Z-axis, there are partial decreases and occasional increases in certain frequency ranges. Therefore, the analysis of the calculation results for the frequency response in three directions and for all the areas or zones of the AT within the powertrain shows that in order to reduce the noise from the surfaces, the modified AT design can be recommended.

Strain energy distributions of both the initial and the modified design (Fig. 32) are shown as an example for visualization of forced oscillations of the vibration speed amplitude maximum (peak) level (Fig. 30b – frequency of 1,640 Hz).

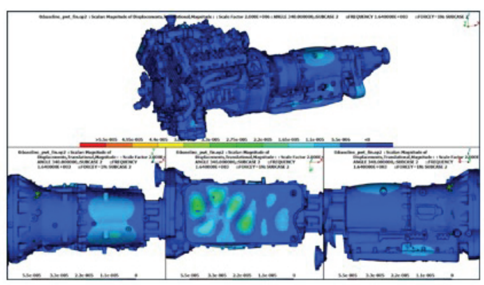

a

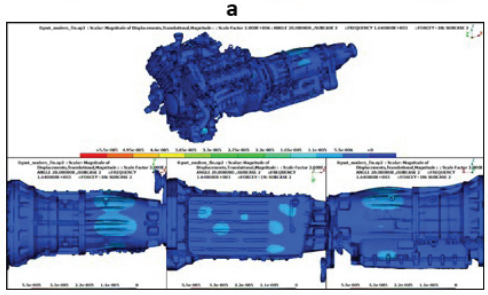

b

Fig. 32: Strain energy at the frequency of 1,640 Hz, single excitation along Z-axis: a – initial design, b – modified design of the powertrain

It follows from the analysis of Fig. 32 that the strain energy field of the modified powertrain design is less distinct in all the zones considered, which proves the efficiency of the developed modified powertrain design.

Based on the results of the comprehensive comparative analysis of the frequency response from local areas of the AT within the powertrain, the modified powertrain design is recommended by the criteria of reducing noise from the AT surfaces.

5. CONCLUSION

1. The methodology for selection of the target values has been developed and the vibration-loaded area of the powertrain has been localized based on the calculation and experimental research of the resonant frequencies in operating modes and disturbance from two types of roads.
2. Based on the research, a frequency range of 110-180 Hz is defined as the one in which the first lowest natural frequency shall be located. Based on analysis of the FRF of the powertrain resonant frequencies, the most favorable and optimal value of the first lowest frequency should be 145 Hz. The vibration-loaded area is found to be the mounting seat of the automatic transmission main shaft.
3. The finite element model was developed, calculation and experimental research of the powertrain natural frequencies and oscillation modes were conducted, experimental verification of the calculation was performed, which allowed error reduction not only for the natural frequencies but also for the oscillation modes of the powertrain. According to the verification work results, the error amounted to less than 1%.
4. The methodology for powertrain design refinement in terms of natural frequencies was developed as well as the modified powertrain design based on the verified model of the powertrain, the first lowest mode of the global bend of which corresponds to the target value of 145 Hz.
5. The methodology for powertrain design refinement in terms of structural noise reduction was developed. The refinement criterion is the radiating surfaces vibration speed mean-square value.

REFERENCES

[1] Ahn Y.K., Kim Y.C., Yang B.S. Optimal design of an engine mount using an enhanced genetic algorithm with simplex method // Vehicle System Dynamics 43(1): 57–81.
[2] Troth, C., An Alternative Mounting System Concept for Improved NVH for a 3-Cylinder Power Train // Published February 24, 2021 by SAE International in US
[3] Aoues Y. Benchmark study of numerical methods for reliability-based design optimization // Structural and Multidisciplinary Optimization 41(2): 277–294.
[4] Azadi M., Behzadipour S., Faulkner G. Introducing a new semi-active engine mount using force controlled variable stiffness // Vehicle System Dynamics 51(5): 721–736.
[5] Chen P., Zhang Y., Qin G., Wu J. Interval analysis method of a powertrain mounting system with uncertain parameters. SAE technical paper no. In: 2010-01-0905
[6] Courteille E., Mortier F., Leotoing L. Multi-objective robust design optimization of an engine mounting system // SAE 2005 Noise and Vibration Conference and Exhibition, USA, Technical paper 2005-01-2412.
[7] Cunrui Sh., Chihua Lu A refined torsional-lateral-longitude coupled vehicular driveline model for driveline boom problems // Applied Mathematical Modelling Volume 90, February 2021, Pages 1009-1034.
[8] Cai B., Shangguan W.B., Lü H. An efficient analysis and optimization method for powertrain mounting systems involving interval uncertainty // Proc Instit Mech Eng Part D: J Autom Eng 234(5):1318–1329
[9] Farjoud A., Taylor R. Advanced semiactive engine and transmission mounts: tools for modelling, analysis, design, and tuning // Vehicle System Dynamics 52(2): 218–243.
[10] Foumani M.S., Khajepour A. Optimization of engine mount characteristics using experimental/numerical analysis // Journal of Vibration and Control 9(10): 1121–1139.

[11] Han J., Papalambros P.Y. An SLP filter algorithm for probabilistic analytical target cascading // Structural and Multidisciplinary Optimization 41(6): 935–945.
[12] Hasofer A.M., Lind N.C. Exact and invariant secondmoment code format // Journal of the Engineering Mechanics Division 100(1): 111–121.
[13] Hui L.,Zebin Z., Xiaoting H., Hui Y.,Wen-Bin Sh. A methodology for design optimization of powertrain mounting systems involving hybrid interval-random uncertainties // Structural and Multidisciplinary Optimization volume 63, pages 1265–1285.
[14] Kim H.M., Kokkolaras M., Louca L.S. Target cascading in vehicle redesign: a class VI truck study // International Journal of Vehicle Design 29(3): 199–225.
[15] Kim H.M., Michelena N.F., Papalambros P.Y. Target cascading in optimal system design // Journal of Mechanical Design 125(3): 474–480.
[16] Kim J.S. Engine mounting system optimization for improve NVH // Journal of the Korea Academia-Industrial Cooperation Society 14(10): 4665–4671.
[17] Lee J.Y., Kim C.M. An experimental study of engine mounting optimization to improve noise and vibration quality of F.R. vehicle // Transactions of the Korean Society for Noise and Vibration Engineering 7(4): 681–688.
[18] Liu H., Chen W., Kokkolaras M. Probabilistic analytical target cascading: a moment matching formulation for multilevel optimization under uncertainty // Journal of Mechanical Design 128(4): 991–1000.
[19] Michelena N., Park H., Papalambros P.Y. Convergence properties of analytical target cascading // AIAA Journal 41(5): 897–905.
[20] Ooi L.E., Ripin Z.M. Optimization of an engine mounting system with consideration of frequency-dependent stiffness and loss factor // Journal of Vibration and Control 22(10): 2406–2419.
[21] Ouyang Q., Chen X. Yao W. Sequential probabilistic analytical target cascading method for hierarchical multilevel optimization under uncertainty // Structural and Multidisciplinary Optimization 49(2): 267–280.
[22] Qin W., Shangguan W.B., Luo G., Xie Z. A method for estimating mount isolations of powertrain mounting systems // J Sound Vib 426:278–295.
[23] Shangguan W.B. Engine mounts and powertrain mounting systems: a review // Int J Veh Des 49(4):237–258.
[24] Shin J. Lee I. (2014) Reliability-based vehicle safety assessment and design optimization of roadway radius and speed limit in windy environment // Journal of Mechanical Design 136(8): 081006.
[25] Sues R., Ceasare M., Pageau S. Reliability based MDO for aerospace systems. In: Proceeding of the symposium on multidisciplinary analysis and optimization // Long Beach, CA, 6–8 September 2000. Reston, VA: American Institute of Aeronautics and Astronautics. 14 Journal of Vibration and Control 0(0)
[26] Tao J.S., Liu G.R., Lam K.Y. Design optimization of marine engine-mount system. Journal of Sound and Vibration 235(3): 477–494.
[27] Wang F., Xiao M., Gao L. Probabilistic analytical target cascading combined with Kriging metamodel for multidisciplinary robust design optimization // Proceeding of the 2015 IEEE international conference on industrial engineering and engineering management, Singapore, 6–9 December 2015, pp. 1407–1411.
[28] Wu J., Shangguan W.B. Dynamic optimization for vibration systems including hydraulic engine mounts // Journal of Vibration and Control 16(11): 1577–1590.
[29] Wu Y.T. Computational methods for efficient structural reliability and reliability sensitivity analysis // AIAA Journal 32(8): 1717–1723.
[30] Wu J., Shangguan W.B. Robust optimization design method for powertrain mounting systems based on six sigma quality control criteria / Int. J Automot Technol 11(5):651–658.
[31] Xiong F. Liu Y., Yang S. A new probabilistic distribution matching PATC formulation using polynomial chaos expansion // Engineering Optimization 44(7): 843–858.
[32] Xu X., Su C., Dong P. Optimization design of powertrain mounting system considering vibration analysis of multi-excitation // Advances in Mechanical Engineering 10(9): 1012.
[33] Youn B.D., Choi K.K. A new response surface methodology for reliability-based design optimization // Computers & Structures 82: 241–256.
[34] Youngjun K., Jongsoo L. Probabilistic optimization of engine mount to enhance vibration characteristics using first-order reliability-based target cascading // Journal of Vibration and Control 2020, Vol. 0(0) 1–15.
[35] Yu Y., Naganathan N.G., Dukkipati R.V. A literature review of automotive vehicle engine mounting systems. Mech Mach Theory 36(1):123–142.
[36] Blundell M., Harty D., The Multibody System Approach to Vehicle Dynamics // Ox.: Elsevier, 2015 – 756 p.
[37] Kulagin V.A. Studying the effect of compliance of vehicle suspension guiding elements on damageability accumulation in simulation of endurance test load cycle // Cand.Sc. (Eng.) A.I. Bokarev, V.A. Kulagin // IASF 2020.
[38] Shelginskikh I.N. Development of comprehensive methodology for testing and evaluating algorithms for vehicle suspension control system // Cand.Sc. (Eng.) A.I. Bokarev, I.N. Shelginskikh // Trudy NAMI. – 2020. - No. 4 (283).
[39] Belousov B.N. Heavy-Duty Wheeled Vehicles: Design, Theory, Calculations // B.N. Belousov, S.D. Popov; Under general editorship of B.N. Belousov. - M.: Bauman Moscow State University Publ., 2006. - 728 p.
[40] Rakhmatov R.I. Improvement methods of research and design exhaust system vehicles on NVH parameters: PhD dissertation: 05.05.02 / Rakhmatov R.I. -M.: FSUE NAMI, 2018. -174 p.

Rakhmatdzon Rakhmatov *is Ph.D. of Engineering Science, Lead of NVH department, State Research Center "NAMI". Rakhmatov Rakhmatjon is a specialist in calculation and experimental research NVH vehicle: Research on vehicle analogs in NVH, compiling target values from the level of components and systems to the level of the car assembly. Making tests program for vehicle. Compiling catalogs of target values. Drawing up plans for design and physical tests, etc. Planning, coordinating and control NVH testing and CAE analysis of vehicle (from components to systems). Calculations and experimental validation calculations: Modal analysis components, units, systems & BIW. Design optimization to remove from resonant frequencies; Vibration and noise transfer function analysis & local dynamic stiffness. Design optimization to improve vibration & acoustic isolation; Noise sources research: exhaust and intake systems, turbocharger (including noise when the bypass valve is open), cooling Fan. Design optimization to reduce sound pressure level (using active, constructive and passive methods). Radiation noise research: engine, automatic gearbox housing, air filter housing and etc. Design optimization to reduce radiation noise. Selection of noise absorbing and vibration-insulating material for vehicle panels. Aeroacoustics, including HVAC. Participation in tests, processing of experimental results, preparation of reports on results of computational and experimental research.*

Vitaliy Krutolapov *is Ph.D. of Engineering Science, Head of FEM modelling department, State Research Center "NAMI". Krutolapov Vitaliy is a specialist in calculation and experimental research NVH vehicle. Planning, coordinating and control NVH testing and CAE analysis of vehicle (from components to systems). Calculations and experimental validation calculations. Modal analysis components, units, systems & BIW. Vibration and noise transfer function analysis & local dynamic stiffness. Design optimization to improve vibration & acoustic isolation. Noise sources research: exhaust and intake systems, turbocharger (including noise when the bypass valve is open), cooling Fan. Design optimization to reduce sound pressure level (using active, constructive and passive methods). Research a new approach of modelling vibro-damping composires. Selection of noise absorbing and vibration-insulating material for vehicle panels.).*

Vladimir Galevko *is Ph.D. of Engineering Science, Head NVH department, State Research Center "NAMI". Galevko Vladimir is a specialist in calculation and experimental research NVH vehicle. Planning, coordinating and control NVH testing and CAE analysis of vehicle (from components to systems). Calculations and experimental validation calculations. Modal analysis components, units, systems & BIW. Vibration and noise transfer function analysis & local dynamic stiffness. Design optimization to improve vibration & acoustic isolation. Noise sources research: exhaust and intake systems, turbocharger (including noise when the bypass valve is open), cooling Fan. Design optimization to reduce sound pressure level (using active, constructive and passive methods). Research a new approach of modelling vibro-damping composires. Selection of noise absorbing and vibration--insulating material for vehicle panels.).*

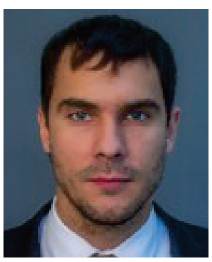

Sergey Gaslov *is a CAE engineer of 1D Modeling Department, State Research Center "NAMI". Sergey Gaslov is a specialist in a multidisciplinary full vehicle level modeling for estimation of vehicle performance, drivability and energy efficiency.*

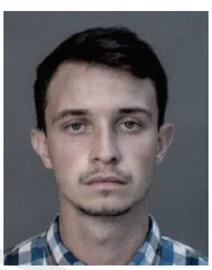

Aleksandr Bokarev *is Ph.D. of Engineering Science, Lead engineer of MBS (Multi Body Simulation) department of State Research Center "NAMI".*

Dmitriy Butuzov *is M. of Engineering Science, Gearbox Department Expert, State Research Center "NAMI". Dmitry Butuzov is a specialist in the design, calculations and experimental research of vehicle transmissions. Design of AT, DCT, AMT, research of transmissions analogs, engineering verification calculations, preparation of test programs on the stand and car, preparation of technical specifications for the development of transmissions and their components. Development and analysis of kinematic transmission schemes, design and engineering calculations of friction elements, dog chlutchs, gears, shafts and bearings. Preparation of the test program of the investigated unit. Participation in tests, processing of experimental results, preparation of reports on results of computational and experimental research. Research of the features of the hydraulic clutches working and brakes and shift strategy without interrupting the power flow. Calculations and experimental verification of transmission NVH. Optimization of the transmission design based on the results of research and testing.*

Paper No.367/2021

SANITARY PROTECTION ZONES BY NOISE FACTOR FROM GAS DISTRIBUTION POINTS

[a)]Vladimir Tupov, [b)] Vitaliy Skvortsov

[a)] National Research University 'Moscow Power Engineering institute', Moscow, Russia, TupovVB@mpei.ru
[b)] National Research University 'Moscow Power Engineering institute', Moscow, Russia, skvor.vitalya@yandex.ru

***Abstract**: The power equipment of thermal power plants is a source of noise to the surrounding area. One of the sources of noise for the surrounding area are gas distribution points (GDP) of thermal power plants (TPP) and district thermal power plants. Noise from gas distribution points may exceed sanitary standards at the border of the sanitary protection zone. The article shows that the radiated noise from gas distribution points depends on the power of the thermal power plant (natural gas consumption) and the type of valves. Three types of valves used in gas distribution points are considered. Formulas are obtained for calculating the width of the sanitary protection zone for gas distribution points for thermal stations, depending on the consumption of natural gas (electric power of the thermal power plant) and the type of valve. It is shown that, depending on the valve used, the noise level at the border of the sanitary protection zone can either meet sanitary standards or exceed them. This allows at the design stage to select the required type of valve or to determine mitigation measures from hydraulic fracturing.*

***Keywords:** noise, gas distribution point, sanitary protection zone.*

***DOI:** : 10.36336/akustika202141133*

1. INTRODUCTION

The power equipment of thermal power plants is a source of noise for the surrounding area [1]. One of the sources of noise for the surrounding area are gas distribution points (GDP) of thermal power plants [2]. In Russia, more than 60% of the fuel consumed at thermal power plants is gas. Natural gas is supplied to TPPs from a gas station. On the territory of the station at the gas distribution point, the gas pressure decreases from 1-1.2 MPa to 0.05-0.12 MPa. The decrease in pressure in gas distribution points is associated with significant sound emission, which can become a source of exceeding sanitary standards [3] at the border of the sanitary protection zone.

Sanitary protection zones (SPZ) in Russia are determined in accordance with regulatory documents [9]. Thermal power plants using natural gas as a fuel with a capacity of more than 600 MW belong to the second hazard class of the enterprise, and thermal power plants and district boilers with a thermal capacity of more than 200 Gcal, also running on natural gas, belong to the third hazard class of the enterprise. In accordance with [9], a sanitary protection zone of 500 m is introduced for the second hazard class, and 300 m for the third hazard class.

2. RESULTS OF CALCULATIONS OF SANITARY PROTECTION ZONES

The actual dimensions of the sanitary protection zones, depending on the type of valve and natural gas flow rate (Fig. 1) and plant capacity (Fig. 2), were determined as a result of acoustic calculations in accordance with [10].

When performing acoustic calculations, we use the following data.

The level of the total sound power, dB, of the reducing valve depends on the design characteristics of the valves, natural gas flow rate, sound speed in the channel and gas density [4-6]:

$$L_W = L_{WT} + 101gq + 201gc + 10lg\ \rho - 30 \tag{1}$$

where
L_{WT} — a correction that depends on the valve design and the pressure drop across it, dB
q — the flow rate of the medium, m^3/h;
c — the speed of sound in the valve, m/s.

The amount of consumed natural gas q, m^3/s, which passes through the gas distribution point, depends on the capacity of the TPP N, MW.

$$q = N\ \eta / Q \tag{2}$$

where
η — the efficiency of the station;
Q — calorific value of fuel, MJ / m^3.

Considering (1) and (2), we obtain

$$L_W = L_{WT} + 10lg(N\ \eta\ c^2\ \rho\ /Q\ 10^3) \tag{3}$$

In [7], a classification of various valves of GDP is given depending on the radiated noise. The valve type has been shown to strongly influence the sound power level emitted by the valves. When natural gas consumption changes from 30 to 800 thousand m^3/h, the maximum difference in sound power levels is about 14 dB. At the same time, the difference in sound power levels at the same flow rate for the valves under consideration can reach 40 dB. In [8], the features of noise emission from the building of GDP and gas pipelines after it are shown.

The obtained values of the sound power levels were used to calculate the sanitary protection zone. The distance of the corresponding sanitary protection zone is taken as the distance at which the sound level from the building of GDP is equal to 45 dBA [3].

Fig. 1 shows the dependence of the size of the sanitary protection zone on the natural gas consumption for three types of valves to comply with the norm for the border of the sanitary protection zone of 45 dBA.

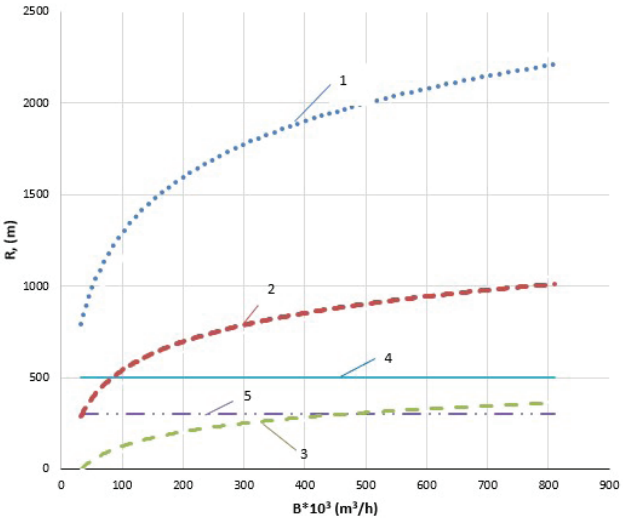

Fig. 1: The width of the sanitary protection zone for a residential area, depending on the fuel consumption and the type of valve to comply with the norm for the boundaries of the sanitary protection zone of 45 dBA: 1, 2, 3 —types of valves; 5—SPZ at 500 m; 6 — SPZ at 300 m

The calculation results in Fig. 1 can be approximated by the formula for calculating the size of the sanitary protection zone R, m, from the natural gas consumption B, thousand m^3/h:

$$R(B)=A\ ln(B)-C \tag{4}$$

where
B — the fuel consumption, thousand m^3/h;
A and **C** — are empirical coefficients, which are presented in Tab. 1.

Valve type	Coefficient a	Coefficient c	Confidence value R^2
1	441	742,65	0.98
2	225	497,38	0.97
3	114	398,19	0.99

Tab. 1: Empirical coefficients characterizing the dependence of the SPZ size on fuel consumption for different types of control valves

The confidence value R^2 for the obtained values according to the formula (4) is in the range from 0.97 to 0.99.

Formula (4) characterizes the size of the SPZ from the noise factor for stations do not produce electrical power.

From Fig. 1 the SPZ of 300 meters will not be exceeded with a gas flow rate of less than 500 thousand m3 / h when installing a type 3 valve, an SPZ of 500 meters will not be exceeded with a gas consumption of about 120 thousand m^3 / h when installing the valve type 2. The use of type 1 valve is possible only with the implementation of measures for noise suppression.

Fig. 2 shows the dependence of the size of the sanitary protection zone on the plant capacity for three types of valves to comply with the norm for the border of the sanitary protection zone of 45 dBA.

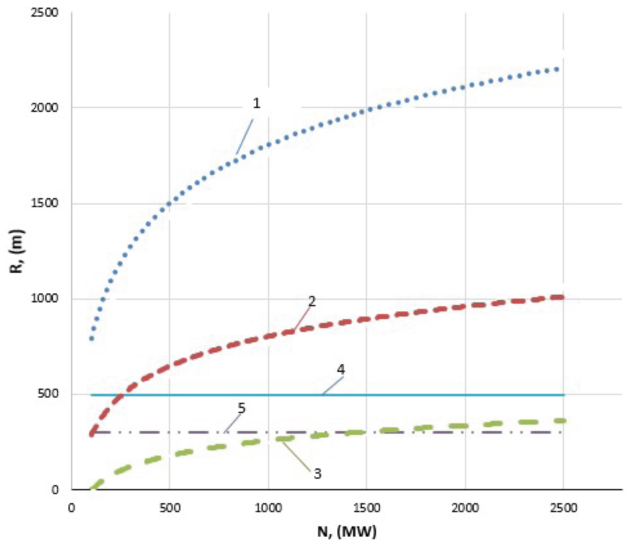

Fig. 2: The width of the sanitary protection zone for a residential area, depending on the power of the station and the type of valve to comply with the norm for the boundaries of the sanitary protection zone of 45 dBA: 1, 2, 3 — types of valves; 5-SPZ at 500 m; 6 — SPZ at 300 m

The calculation results in Fig. 2 can be approximated by the formula for calculating the size of the sanitary protection zone ***R***, m, from the electric power of the station ***N***, MW:

$$R(N)=a\ ln(N)-c \tag{5}$$

where
N — the electric power of the station, MW;
a and **c** — are empirical coefficients, which are presented in Tab. 2.

The confidence value R^2 for the obtained values according to the formula (5) is in the range from 0.97 to 0.99.

Valve type	Coefficient a	Coefficient c	Confidence value R^2
1	441	1240,2	0.98
2	225	751,46	0.97
3	113,7	526,47	0.99

Tab. 2: Empirical coefficients characterizing the dependence of the size of the SPZ on the electrical power for different types of control valves

From Fig. 2, the SPZ of 300 m will not be exceeded by the electric power of the station less than 1500 MW when installing a type 3 valve, less than 106 MW when installing a type 2 valve. The sanitary protection zone of 500 m will not be exceeded when the electric power of the plant is less than 8300 MW when installing a type 3 valve, less than 260 MW when installing a type 2 valve. Sound attenuation measures are required when using a type 1 valve.

These formulas (4) and (5) can be recommended for calculating the SPZ from gas distribution points with different valves. The use of formulas (4-5) makes it possible to determine the need to develop additional measures to reduce noise from gas distribution points [11].

3. CONCLUSION

1. According to the noise factor, the sanitary protection zones of gas distribution points depend on the natural gas consumption (station capacity) and the type of valve. At the same time, the type of valve has the greatest influence on the size of the sanitary protection zone in terms of the noise factor.
2. Formulas have been obtained for calculating the required width of the SPZ of gas distribution points by the noise factor to comply with the norm for the border of the sanitary protection zone of 45 dBA, depending on the type of valve and natural gas consumption (4) and the power of the station (5).
3. The data obtained allow at the design stage to assess the need to take measures for noise suppression.

REFERENCES

[1] Tupov, V.B., Taratorin, A.A. Influence of thermal power equipment structure on the size of sanitary protection zone by noise factor (2020) Proceedings of the 2st IEEE 2020 International Youth Conference on Radio Electronics, Electrical and Power Engineering, REEPE 2020, article № 9059202 , DOI: 10.1109 / REEPE49198.2020.9059202
[2] Tupov, V.B. Increasing safety of thermal and nuclear power stations energy equipment by reducing noise// IOP Conf. Series: Journal of Physics: Conf. Series 891 (2017) 012186 doi :10.1088/1742-6596/891/1/012186
[3] Sanitary rules and norms SanPiN 1.2.3865-21 "Hygienic standards and requirements for ensuring the safety and (or) harmlessness to humans of environmental factors", Moscow, 2021
[4] Yudin, E. Yu.: Control of noise in the workplace, Moscow, Mashinostroenie, 1985
[5] Golovanov V. I., Slavyaninov V. N., Fedorov V. K. Noise silencer for gas jets with large flow rate. Electronic Journal "Technical Acoustics", http://www.ejta.org, 2002, 9 . [In Russian]
[6] Floyd D. Jury Fundamentals of aerodynamic noise in control valves/ Marshalltown, IA, Fisher Controls International Inc., 1999
[7] Skvortsov, V.S., Tupov, V. B. Classification of gas reduction valve silencers at TPP gas distribution points. MATEC Web of Conferences 320, 00020 (2020), DOI: 10.1051/ matecconf/202032000020
[8] Tupov, V.B., Tupov, B. V., Skvortsov, V. S.: Features of the noise emission of gas distribution stations and gas pipelines, ISSN 1570-1468, Power Technol Eng, 52 (4), pp. 448-450, 2018
[9] SanPiN 2.2.1 / 2.1.1.1200-03 "Sanitary protection zones and sanitary classification of enterprises, structures and other facilities", Moscow, 2003
[10] ISO 9613-2: 1996, Acoustics-Sound attenuation during outdoor propagation-Part 2: General method of calculation, Geneva: International Organization for Standardization, 1996
[11] Tupov, V.B. A package of measures to reduce the noise from thermal power plants. Power Technology and Engineering, 47 (3), p. 217-221, 2013

Vladimir Tupov *is Doctor of Engineering Science, Professor, Department of Heat Power Stations of National Research University "Moscow Power Engineering Institute" (Moscow, Russia). He is Laureate of Government of Russian Federation in the field of science and technology.*
Vladimir Tupov is the creator a theory of sound propagation in the channels of large power gas and air ducts, as well as a theory for calculating emissions of high parameters from energy objects. Vladimir Tupov has published over 290 scientific papers, including about 26 textbooks, manuals and monographs, 18 patents. Several hundred of his original silencers were introduced at large and small power facilities. He presented the main results of scientific research on the international conferences in Australia, Brazil, Germany, Denmark, Italy, China, Poland, Portugal, USA, Russia, South Korea, Sweden and other countries.

Vitaliy Skvortsov *is a graduate student*
of Department "Thermal Power Plants" and an engineer of the testing laboratory of the Scientific and Educational Center "Reducing the noise of power equipment" in Moscow Power Engineering Institute (MPEI).
Vitaliy Skvortsov is a specialist in noise reduction of Thermal power plants and industrial facilities. Scientific interests are also including problems of noise reduction at gas control points of TPPs. Research work is studies of noise emission from gas control points of thermal power plants.
He presented the main results of scientific research at the international conferences in Moscow.

Paper No.368/2021

SELECTION OF TURBULENCE MODEL IN ANSYS CFX FOR INVESTIGATION OF TURBULENT NOISE AND VIBRATION OCCURRING IN INTERSCAPULAR SPACE OF THE CENTRIFUGAL TURBINE

Antonina Sekacheva, [b] Anatoly Khait, [c] Alexander Noskov, [d] Lilia Pastukhova

[a] Hydraulics Department, Ural Federal University, Yekaterinburg, Russia, tonechka_marakulina@mail.ru
[b] School of Mechanical Engineering and Mechatronics, Faculty of Engineering, Ariel University, Israel, hait@mail.ru
[c] Hydraulics Department, Ural Federal University, Yekaterinburg, Russia, noskovurfu@yandex.ru
[d] Hydraulics Department, Ural Federal University, Yekaterinburg, Russia, l.g.pastuhova@urfu.ru

Abstract: *The article is devoted to issues related to the occurrence of noise and vibration in the centrifugal turbine of ventilation equipment of residential buildings. Airflow in the rotating radial-axial channel representing a simplified configuration of the inter-blade channel of a centrifugal turbine is studied. Numerical simulation of the airflow in the considered geometrical domain is performed using ANSYS CFX solver. A particular attention is given to different turbulence closures used in the model. Accuracy of the simulation results was estimated with respect to the laboratory measurements by J. Moore [9]. The comparison was carried out for velocity profiles measured at three different cross-sections of the channel under different mass flow rates.*

Keywords: *noise, vibration, microturbine, inter-blade channel, turbulence models, interscapular space, ANSYS CFX.*

DOI: *: 10.36336/akustika202141137*

1. INTRODUCTION

Noise inside residential buildings in some cases is caused by the influence of sources of external noise, such as road and rail transport, engineering and technological equipment of industrial enterprises, etc. A comparative share falls on sources located directly inside the building. These sources include elevator equipment, ventilation and air conditioning systems, engineering and technological equipment of individual heating points (IHP).

The relevance of this research topic is confirmed by a large number of complaints from apartment owners located above individual heating points of multi-storey apartment buildings. A number of works are devoted to the issues of reducing this negative impact in the premises of residential and office buildings [1-4].

Within the framework of this article, the ventilation equipment of multi-storey residential buildings is considered, the vibration of which generates noise in the living quarters of apartments in multi-storey buildings. The movement of the air flow through the ventilation ducts can be accompanied by the formation of turbulent noise both on homogeneous surfaces and on various inhomogeneous ones, leading to a sudden change in pressure. Valves, throttling devices and similar structures play a special role in the formation of this kind.

This study is aimed at creating a model of flow movement in a radial-axial channel, which, in further research, will help to investigate the mechanism of formation of turbulent noise and vibration from elements of a centrifugal turbine and, therefore, reduce noise from ventilation equipment of residential buildings.

The main attention is paid to the study of the flow movement in the channel, which is a simplified configuration of the inter-blade space of a centrifugal turbomachine.

In this regard, the article discusses methods for numerical analysis of the interspace of a centrifugal turbine using various turbulence models in the ANSYS CFX software package to determine the most effective turbulence model and the possibility of its further use in modeling hydrodynamic models for acoustic calculations. The adequacy of the results and the effectiveness of the turbulence models were evaluated by comparison with the data obtained empirically during the actual test described in J. Moore's article "A Wake and an Eddy in a Rotating, Radial-Flow Passage". The comparison was carried out for three profiles of the flow rate of the medium in different sections of the channel and at three mass flow rates.

One of the most complex and important problems not only in recent years, but also in previous decades in hydrodynamics is the calculation of turbulent flows. Despite the growth in computer performance and great advances in the construction of efficient numerical algorithms, correct and accurate mathematical prediction of turbulent flows is still more the exception than the rule. This can be explained by physical complexity, namely, at the same time a chaotic and weakly periodic structure, three-dimensional nature, nonstationarity, and a large scatter of spatial and temporal scales.

2. METHOD

The development of turbulent flow modeling begins with semi-empirical models based on the Reynolds Averaged Navier-Stokes (RANS) system of equations averaged over Reynolds.

Now, a large number of computational software systems based on RANS models are used to solve complex gas-dynamic problems. RANS methods can be based on k – ε, k – ω or SST – model.

The turbulence model ***k - ε***, using the equations for the transfer of the kinetic energy of turbulence (k) and the rate of its dissipation (***ε***), is used and gives good results in most cases [5]. The turbulence model ***k - ω*** solves two transport equations - one for the turbulent kinetic energy ***k***, the second for the specific rate of its dissipation ***ω***. The biggest disadvantage of this model is its strong sensitivity to boundary conditions. And also to obtain the correct solution requires a large number of cells in the wall layers [5].

The SST (Shear Stress Transport) turbulence model is one of the varieties of ***k - ω*** turbulence models. SST is used when a good wall solution is required. It combines the advantages of the basic ***k - ω*** and ***k - ε*** models, but like ***k - ω***, it places high demands on the mesh resolution near the walls. The model was proposed in 1993 and thus has more than 20 years of experience. This experience indicates that the model, in terms of the totality of its qualities, is one of the best, if not the best, among the existing RANS turbulence models [6].

In recent years, approaches to modeling turbulent flows based on the initial principles of hydrodynamics have found wide application, namely, the Direct Numerical Simulation (DNS) method and the Large Eddy Simulation (LES) method for modeling large eddies, as well as the increasingly widely used , Detached-Eddy Simulation (DES) method. The widespread practical application of these methods even with today's computing power is extremely limited. Some studies suggest that, according to the most optimistic forecasts, the use of the listed turbulence models in practice is possible only by the end of this century.

The DNS model approach is based on only one simplification, the essence of which is the absolute reliability of the description of both laminar and turbulent flows by the system of Navier-Stokes equations. In this model, the flow is calculated by direct numerical solution of the system of Navier-Stokes equations. And since turbulence is three-dimensional and unsteady, the equations automatically become three-dimensional unsteady. When modeling real processes, we are talking about flows with sufficiently large Re values, a fine scale grid, due to the geometric complexity of bodies, as well as a large number of time steps.

Considering the above, now the DNS model is used only for calculations with relatively low Re values and mainly only for basic research. However, this approach is very important, it is especially worth noting that in the future DNS will become a leading direction of development not only in hydrodynamics, but also in related fields.

The next of the existing models in terms of the volume of computational costs is the large eddy simulation method (LES), formulated at the end of the twentieth century [7]. The main idea of this approach lies in the spatial "filtration" of the characteristics of a real turbulent flow, that is, information about small inhomogeneities with sizes smaller than the filter size is not taken into account.

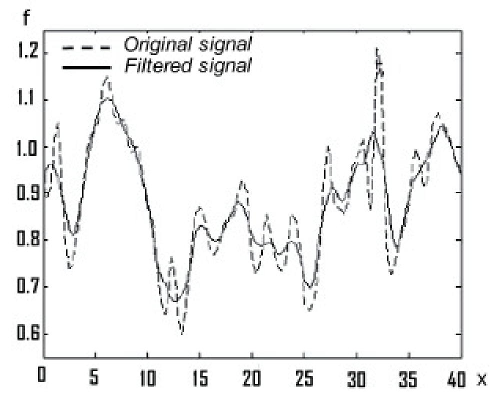

Fig. 1: Comparison of the original and average signals

When comparing the real turbulent flow and its LES model, it becomes obvious that small eddies are not taken into account in the simulation. Comparison of the filtered and original signals is shown in Fig.1.

In the system of Navier-Stokes equations, the variables ***f*** are represented as the sum of "filtered" and small-scale variables. The LES system of equations after all transformations has the following form:

$$\begin{cases} \dfrac{\partial \rho}{\partial t} + \nabla \cdot (\rho \vec{u}) = 0 \\ \dfrac{\partial (\rho \vec{u})}{\partial t} + \nabla \cdot (\rho \vec{u} \vec{u}) = -\nabla p + \nabla \cdot (\tau_m + \tau_{SGS}) \end{cases} \quad (1)$$

The LES system is very similar in form to the system of equations of the model, RANS. The only formal difference between them is in the indices of additional members. The fundamental difference is that within the LES framework, vortex structures with dimensions exceeding the filter dimensions are resolved "exactly", and only vortex structures of smaller dimensions are modeled, while in RANS, all vortices must be modeled, despite the fact that large vortices are not subject to any universal laws.

The natural price to be paid for the described advantages of LES is that it requires incomparably more computational resources than RANS. On the other hand, because the small--scale portion of the spectrum is modeled rather than "accurately" calculated, the resources required to implement the LES are much smaller than for the DNS. It is this circumstance that stimulated the creation of hybrid RANS-LES approaches, the most developed of which is the DES method.

The lion's share of the computational costs of LES is associated with the calculation of the near-wall part containing small vortices, and the calculation of just such flows using RANS is quite reliable and economical.

The DES method was proposed as an alternative to the RANS and LES methods for calculating near-wall flows with large separation zones, for which the RANS models are not capable of providing acceptable accuracy, and the LES requires excessively large computational resources.

In the framework of DES, not all vortices are calculated "exactly", but only "disconnected" ones, that is, those that are present in separation zones, while the rest are described by conventional semi-empirical RANS models [7].

When using DES, almost all parameters can be calculated with a sufficiently high accuracy even on relatively coarse grids; moreover, when the grid is refined, the calculation error decreases and tends to zero in the limit (DES becomes DNS). However, it should be emphasized that, even with a total number of cells of about 400,000, which is very modest by modern standards, the calculations take several tens of hours.

Based on the limited computing power and time constraints, in this work, we used two semiempirical RANS models based on ***k - ε*** and SST, a detailed mathematical description of which is given in the next section.

2.1. Description of the used turbulence models

Consider the standard two-equation ***k - ε*** model, which is now regarded as the standard model for describing turbulence and solving engineering problems. In this model, two important concepts are introduced - generation ***P*** and dissipation ***ε***.

The physical meaning of the generation of turbulence P lies in the generation of new vortices and pulsations, which form the turbulence [8]. Dissipation ε, on the contrary, is the scattering of large eddies into smaller ones, leading to averaging of the flow and a decrease in turbulence. Two transport equations allow us to consider turbulence in space and time. This model is semi-empirical and is based on a phenomenological approach and empirical results.

The kinetic energy of turbulence is defined as $k = 0,5\,\overline{u_i u_j}$.

Equation for kinetic energy:

$$\frac{\partial}{\partial t}(\rho k) + \frac{\partial}{\partial x_i}(\rho k \overline{u_i}) = \frac{\partial}{\partial x_i}\left[\left(\mu + \frac{\mu_t}{\sigma_k}\right)\frac{\partial k}{\partial x_j}\right] + G_k - \rho\varepsilon + S_k \tag{2}$$

where

G_k represents the turbulent kinetic energy generated from the mean velocity gradients:

$$G_k = \mu_t S^2 \tag{3}$$

μ_t – turbulent dynamic viscosity;
S – strain tensor invariant.

The equation for dissipation is not derived analytically and is written by analogy with the equation of kinetic energy:

$$\frac{\partial}{\partial t}(\rho\varepsilon) + \frac{\partial}{\partial x_i}(\rho\varepsilon\overline{u_i}) = \frac{\partial}{\partial x_i}\left[\left(\mu + \frac{\mu_t}{\sigma_\varepsilon}\right)\frac{\partial \varepsilon}{\partial x_j}\right] + C_{1\varepsilon}\frac{\varepsilon}{k}G_k - C_{2\varepsilon}\rho\frac{\varepsilon^2}{k} + S_\varepsilon \tag{4}$$

The rest of the constants are determined from experiments for turbulent fluids.

Thus, the ***k-ε*** model has proven itself well in calculating free and jet shear flows, and the ***k-ω*** model provides a much more accurate description of the near-wall boundary layers [8]. Taking these circumstances into account, it was proposed to combine these models in SST using a specially designed empirical function F_1, which ensures that the summary model is close to the ***k-ε*** model far from solid walls and to the ***k-ω*** model in the near-wall part of the flow.

The equations of this "hybrid" model, written in terms of k (kinetic energy of turbulence) and ω (specific rate of its dissipation) are as follows:

$$\frac{\partial}{\partial t}(\rho k) = \frac{\partial}{\partial x_i}\left[(\mu + \sigma_k\mu_t)\frac{\partial k}{\partial x_i}\right] + P_k - \beta^*\rho\omega k \tag{5}$$

$$\frac{\partial}{\partial t}(\rho\omega) = \frac{\partial}{\partial x_i}\left[(\mu + \sigma_\varepsilon\mu_t)\frac{\partial \omega}{\partial x_i}\right] + \gamma\frac{\rho}{\mu_t}P_k + -\beta\rho\omega^2 + (1 - F_1)D_{k\omega} \tag{6}$$

The generation term is calculated according to the formula:

$$P_k = min(\mu_t S^2, 20\beta k\omega) \tag{7}$$

The last term on the right side of the transfer equation ***ω*** is determined by the relation:

$$D_{k\omega} = \frac{2\rho\sigma_{\omega 2}}{\omega}\frac{\partial k}{\partial x_i}\frac{\partial \omega}{\partial x_i} \tag{8}$$

Turbulent viscosity in this model is determined

$$\mu_t = \frac{\rho a_1 k}{max(a_1\omega, \Omega F_2)} \tag{9}$$

Functions F_2 and F_1 are empirical, like the rest of the constants.

2.2. Description of the design model

At present, it is becoming difficult to imagine carrying out calculations without the use of software systems for three-dimensional gas-dynamic modeling.

ANSYS CFX is a high-performance computational fluid dynamics (CFD) tool that reliably and quickly solves a wide range of fluid and gas flow problems for over 20 years. CFX, due to its accuracy, reliability and speed, finds the most frequent application in turbomachinery. Ease of work with it provides a modern, flexible, intuitive graphical interface that provides the ability to customize and automate the modeling process.

Most importantly, ANSYS CFX offers a wide range of models to accurately account for turbulence effects.

ANSYS CFX uses numeric grid points to solve equations, a so-called finite element grid. Particular emphasis is placed on solving the basic equations of motion (conjugate algebraic mesh).

With this approach, it becomes extremely important to analyze the degree of adequacy of the modeling results.

The main task of the study is to build a model of air movement in a rotating radial-axial channel. To evaluate the simulation results, a comparison was made with the data obtained empirically during the real test described in the article by J. Moore [9].

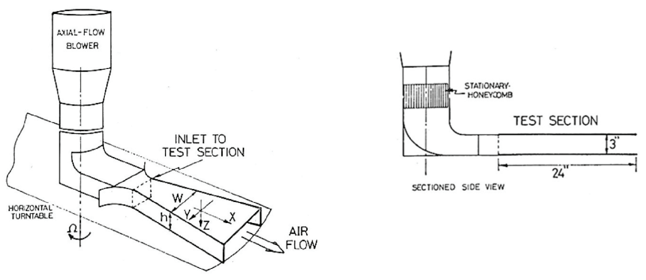

Fig. 2: Interscapular canal model

The experimental setup described in [9] is shown in Fig. 2 and represents a simplified configuration of a centrifugal turbine blade channel placed on a rotating table with a constant rotation speed of 206 rpm. The axis of rotation of the channel coincides with the axis of the cylindrical inlet section. The air flow enters the channel along the axis of its rotation, after which it turns at right angles in the radial direction and expands, falling into the directly modeled part ("interscapular" channel). The flow enters the channel through a stationary stabilizing device in the form of an equalizing grid with a mesh size of 4.8 mm, which ensures a constant flow rate across the section. A fan is located in front of the stabilizing device, which makes it possible to forcibly supply air with different flow rates into the channel. The outlet section of the channel is open to the atmosphere. The working medium is air with a temperature of 25 ° C and atmospheric pressure.

Here are the geometrical parameters of the directly investigated part (Fig. 3) [9]. In section a, the model has a square with a side of 76 mm. Section b - a rectangle with a height of 76 mm and a width of 236 mm. The distance between the indicated sections is 610 mm. Rotation occurs around the Z axis, located 305 mm from the section a.

The study used three geometric configurations of the channel:

1. Geometry 1 is shown in Fig. 3, without turning the stream by ninety degrees.
2. Geometry 2 is shown in Fig. 4, a flow turn has been added, where the transition of the horizontal flow to the vertical one is carried out.
3. Geometry 3 is shown in Fig. 5. The main difference from Geometry 2 is a rounded flow turn and a change in the inlet section.

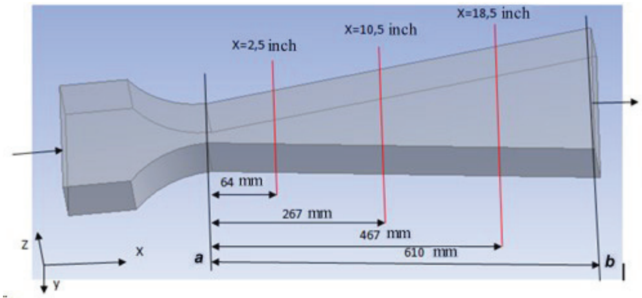

Fig. 3: The investigated part of the channel for configuration № 1

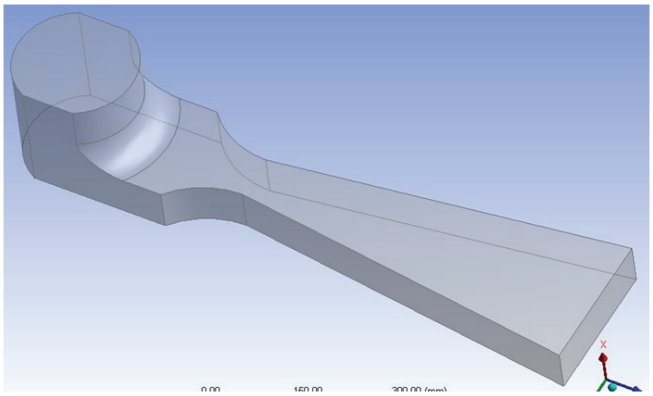

Fig. 4: Channel configuration № 2

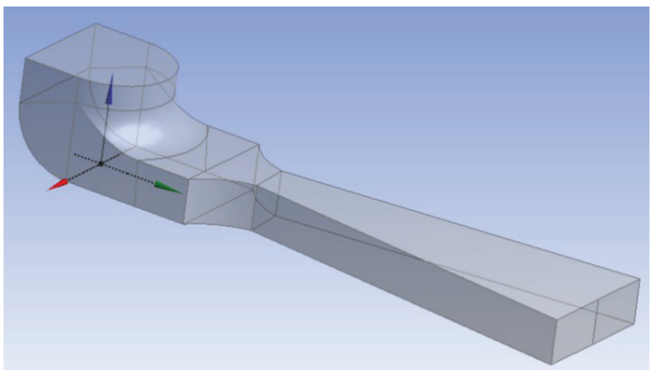

Fig. 5: Channel configuration № 3

One of the stages of numerical modeling is the division of the computational domain into elements (cells), the so-called mesh generation process. It is at the grid nodes that the values of the sought variables are determined and the boundary conditions of the problem are imposed. The quality of the mesh, as well as the number of cells, strongly depends on the result of the calculations. A detailed description of the selection of the grid and the number of its elements is given in the next section.

Another important component of the successful obtaining of the calculated data is the correct setting of the boundary conditions. Three types of boundary conditions were used in the work - input (INLET), output (OUTLET), impenetrable wall (WALL).

When setting the boundary conditions on an impenetrable wall (WALL), all components of the velocity vector were set equal to zero (no slip wall).

Inlet boundary conditions (INLET) were specified using mass flow. The flow is investigated at three air flow rates [9]:

S - small - small 0.062 kg/s,

M - medium - average 0.116 kg/s,

L - large - large 0.240 kg/s.

The use of equations describing turbulence leads to the fact that additional parameters for the simulation must be set for the mass flow rate. For calculations in the CFX package, one parameter was used - the intensity of turbulence - information on the numerical values of which is absent. As a rule, the intensity of turbulence does not exceed 20%, but in most cases it is in the range from 1 to 10%. The selected average intensity of turbulence is 5%.

Outlet boundary conditions (OUTLET) were set using overpressure. Since the outlet section of the channel is open to the atmosphere, the overpressure is zero. As well as for the input boundary conditions, the parameter - turbulence intensity (5%) was used to simulate turbulence in the CFX package.

3. RESULTS

3.1. Description of the design model

When developing a numerical model of air movement in a radial-axial channel, which represents a simplified configuration of an inter-blade channel of a centrifugal turbine, the first stage is to develop a geometric configuration of the computational model. The closest results of calculations carried out with the help of the ANSYS CFX software package to the experimental data will speak about the correctness of the construction. For the study, three geometric configurations of the channel were used, a detailed description is presented in the previous section.

The data given in the article by Moore J. [9] were obtained empirically only for the experimental section, therefore, the first configuration of the Geometry 1 channel was created, completely repeating the geometry with the indicated dimensions in the article [9].

The ANSYS ICEM CFD package was used to construct the computational grid. The computational grid is shown in Fig. 6, in this case hexahedral cells are used. The number of cells in this case is 11568, and the maximum size is 1×10^{-2} m.

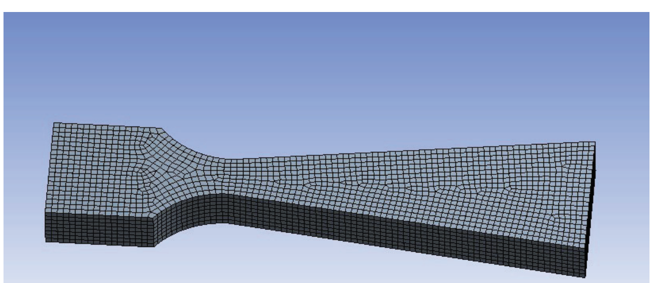

Fig. 6: Computational mesh for Geometry 1

To set the boundary conditions at the inlet and outlet, the mass flow rate of the medium was used. The flow is investigated at three air flow rates at which the data were obtained during the experiment detailed in the previous section.

To determine the nature of the turbulence at the inlet, an average intensity of 5% (Medium) was set.

In this work, when creating calculations in the CFX package, two turbulence models were used: k-ε and SST.

The article [9] shows the results obtained experimentally for three sections shown in Fig. 3:

- at a distance of 2.5 inches (64 mm) from the section a along the X axis,
- at a distance of 10.5 inches (267 mm) from the section a along the X axis,
- at a distance of 18.5 inches (467 mm) from section a along the X-axis.

We will call the indicated cross-sections control, in which a comparison is made between the air flow rates obtained by the experimental [9] and calculated using the ANSYS software package.

For a qualitative assessment of the data obtained, graphs of the distribution of the flow velocity over the section for each air flow rate were constructed. For a quantitative assessment, the value of the cross-section average of the relative error of the data obtained as a result of the calculation is given in relation to those given in [9]. In this case, the relative error is determined in accordance with formula (10).

$$E = \frac{\sum \frac{v_i - v_{exp}}{v_{exp}}}{n} \cdot 100\% \qquad (10)$$

where

V_{exp} – the value of the air flow velocity at the point belonging to the control section, from the experimental data [9], m/s;

V_i – the value of the air flow velocity at a point belonging to the control section, obtained by calculation using the ANSYS software package, m/s;

n – total number of points.

The average relative errors for the air flow rates of Geometry 1 and two turbulence models (k-ε and SST) are presented in Tab.1.

Consumption	Model	Cross-sectional error, %		
		X=2,5	X=10,5	X=18,5
S	k-e	13,61	27,72	69,10
	SST	12,50	23,30	59,20
M	k-e	9,89	18,66	52,58
	SST	9,27	12,43	30,67
L	k-e	12,61	15,56	39,75
	SST	11,34	9,03	38,13

Tab. 1: Average relative errors for the case "Geometry 1"

The results obtained show that the calculated data more accurately describe the flow closer to the center of rotation. In the first section, the relative error does not exceed 14%, while in the latter it is more than 69%.

It should be noted that the SST turbulence model in all calculations describes the flow better than ***k-ε***. The relative error of the SST model in the first section is less than the relative error ***k-ε*** by only 0.62 - 1.27%, and in the last - by 1.62 - 21.91%.

The relative error of 69% is due to the fact that the geometric configuration was chosen incorrectly and is unacceptable for further research. To improve the results, the calculations were performed again with Geometry 2, which is more suitable for the description of the article containing experimental data [9]. The main difference from Geometry 1 is the addition of a 90-degree rotation in which the flow goes from vertical to horizontal. The Geometry 2 configuration shown in Fig. 4.

The computational grid is shown in Fig. 7, in this case, tetrahedral cells are used. The number of cells in this case is 140519, and the maximum size is 1×10^{-2} m.

To form the wall layer, two layers of flat cells were added at the solid walls. The height of the first wall cell was 2×10^{-3} m. The next cells increase by 1.2 times in comparison with the previous cell.

The average relative error for Geometry 2 is shown in Tab. 2.

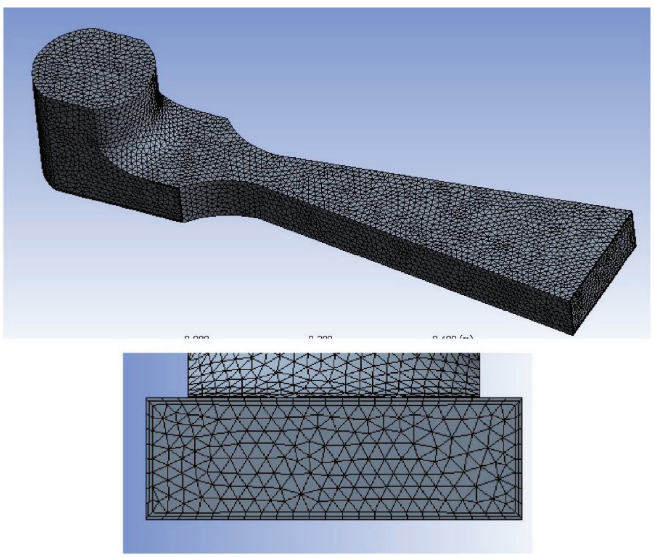

Fig. 7: Computational mesh for Geometry 2

Consumption	Model	Cross-sectional error, %		
		X=2,5	X=10,5	X=18,5
S	k-ε	13,19	14,57	50,47
	SST	11,83	11,16	20,5
M	k-ε	7,02	18,44	61,0
	SST	5,33	11,63	32,03
L	k-ε	9,86	12,05	48,78
	SST	9,13	7,32	25,15

Tab. 2: Average relative errors for the case "Geometry 2"

The results obtained show that the calculated data more accurately describe the flow closer to the center of rotation, as in Geometry 1. In the first section, the relative error does not exceed 14%, while in the latter it is more than 60%.

It should be noted that the SST turbulence model in all calculations describes the flow better than ***k-ε***. In the first (X = 2.5) and second sections (X = 10.5), the results of calculations with the configuration of the Geometry 2 channel are closer to the experimental data in comparison with the calculations of Geometry 1. The relative error decreased by 0.42 - 18.63% ... In the last section (X = 18.5), it was possible to approach the experimental data only in calculations at a flow rate S, at flow rates M and L, the relative error increased.

The relative error of 61% is caused by the fact that some features of the geometric configuration were not taken into account. To improve the results, the previous channel configuration was modified, the calculations were performed again with Geometry 3, shown in Fig. 8.

The main difference is the rounded transition of the vertical flow to the horizontal one and the change in the inlet section.

The computational grid is shown in Fig. 9. The number of cells in this case is 156599, and the maximum size is 1×10^{-2} m.

To form the wall layer, two layers of flat cells were added at the solid walls. The height of the first wall cell was 2×10^{-3} m. The next cells increase by 1.2 times in comparison with the previous cell.

The average relative error for Geometry 3 is presented in Tab. 3.

The calculated data show that in the first section the relative error does not exceed 11%, while in the latter it is more than 46%.

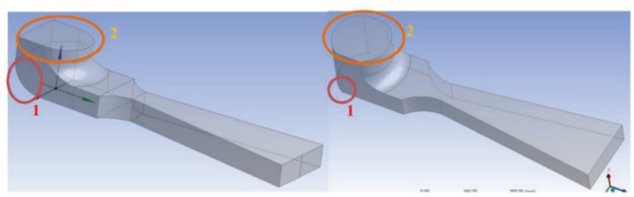

a) b)

Fig. 8: The main differences between Geometry 3 (a) and Geometry 2 (b)

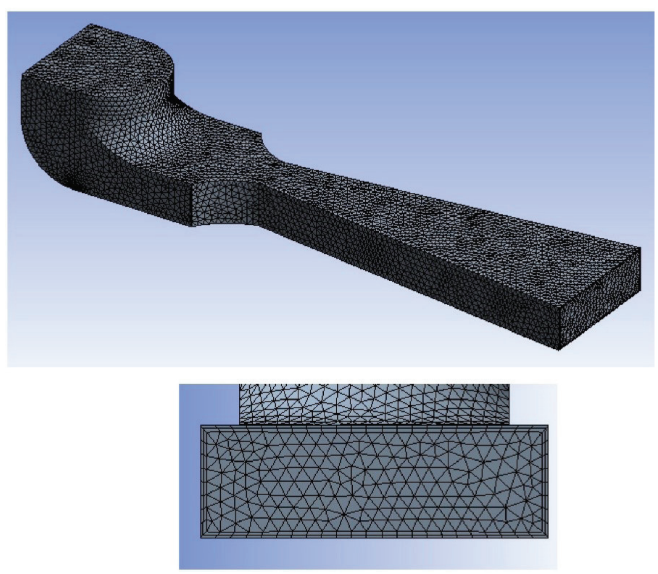

Fig. 9: Computational mesh for Geometry 3

It should be noted that the SST turbulence model in all calculations describes the flow better than ***k-ε***. By changing the geometric configuration of the channel, it was possible to reduce the value of the relative error in all sections and at all flow rates compared with Geometry 1 - by 0.44 - 42.65%, compared with Geometry 2 - by 0.22 - 19.78%.

Of the presented flow configurations, the smallest relative errors were obtained in calculations in the CFX package with Geometry 3, therefore, for further research, only the specified channel configuration was used.

Consumption	Model	Cross-sectional error, %		
		X=2,5	X=10,5	X=18,5
S	k-e	10,22	6,74	46,76
	SST	9,67	6,53	16,55
M	k-e	6,18	18,22	41,22
	SST	4,31	11,09	22,72
L	k-e	9,82	9,28	33,22
	SST	8,92	7,02	13,80

Tab. 3: Average relative errors for the case "Geometry 3"

3.2. Grid Sensitivity Analysis

One of the stages of numerical modeling is the division of the computational domain into elements (cells), the so-called mesh generation process. It is at the grid nodes that the values of the sought variables are determined; in this work, the values of the air flow velocity. The quality of the grid, as well as the number of cells, strongly depends on the result of the calculations.

To assess the effect of the number of cells on the calculated data, the size of the elements of the computational grid was reduced several times. To reduce the number of calculations, the grid analysis was carried out only for the smallest (S) and largest (L) air flow rates.

Three series of calculations were carried out with the number of cells 291, 608 and 1156 thousand without a wall layer. The relative error is shown in Table 4. The calculation results are shown in Fig.10-Fig.13.

Consumption	Model	Relative error, %							
		X=2,5				X=18,5			
		Number of cells, thousand pcs.				Number of cells, thousand pcs.			
		156	291	610	1156	156	291	610	1156
S	k-e	13,95	12,05	10,97	8,97	18,97	23,84	35,03	80,09
	SST	11,57	11,34	10,29	8,87	14,45	12,83	23,3	27,96
L	k-e	15,58	15,41	14,02	13,12	27,46	15,40	32,81	31,63
	SST	14,26	14,13	12,53	11,03	14,85	12,98	25,69	30,11

Tab. 4: Average relative errors for different values of the number of cells

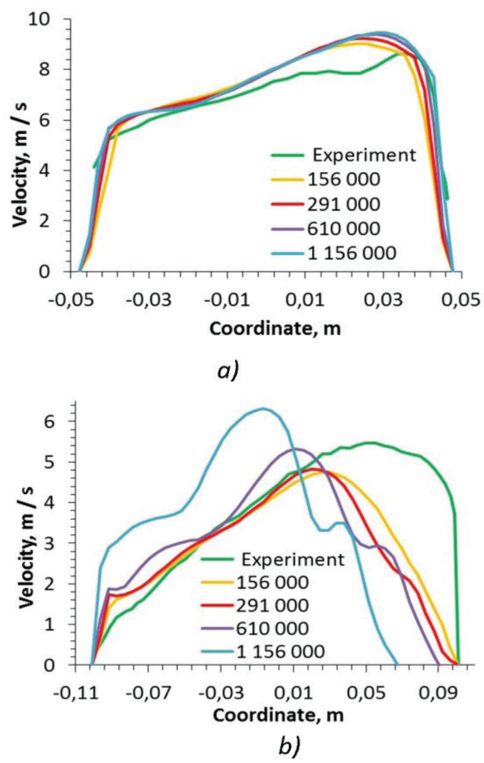

Fig. 10: Graphs of air flow velocity distribution when using the k-ε turbulence model and S for the cross-sections: a) X=2,5; b) X=18,5

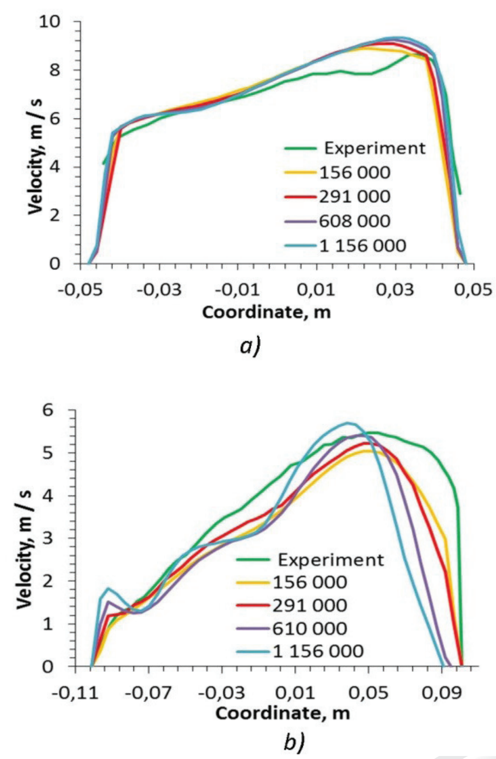

Fig. 11: Graphs of air flow velocity distribution when using the k-ε turbulence model and S for the cross-sections: a) X=2,5; b) X=18,5

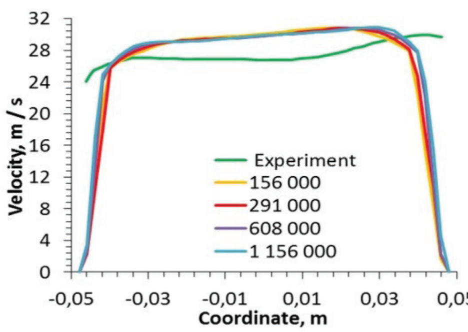

a)

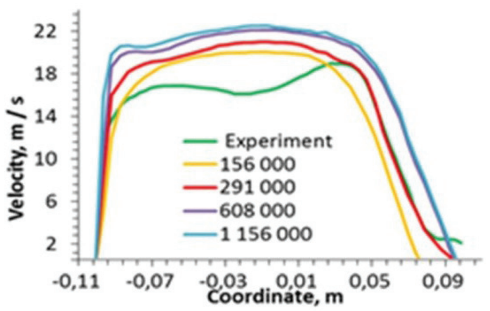

b)

Fig. 12: Graphs of air flow velocity distribution when using the k-ε turbulence model and flow rate L for cross-sections: a) X=2,5; b) X=18,5

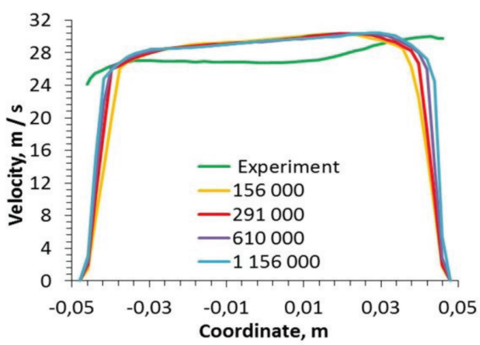

a)

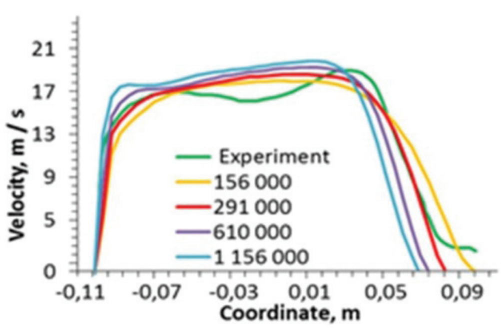

b)

Fig. 13: Graphs of air flow velocity distribution when using the k-ε turbulence model and flow rate L for cross-sections: a) X=2,5; b) X=18,5

Analysis of the data obtained showed that the simulation results behave ambiguously.

When using the k-ε model in the control section closest to the rotation axis (X = 2.5), the results behave predictably, that is, with an increase in the number of cells, the relative error decreases. However, in the section X = 18.5 at the lowest flow rate S, an increase in the deviation is observed, and at a flow rate L, when the number of mesh elements changes from 156 to 291 thousand, it decreases almost 2 times, and increases with further refinement. This can be explained by the fact that flow separation from the walls begins to appear in the section X = 18.5, and the turbulence model used cannot fully take into account this phenomenon.

When using the SST model in the control section X = 2.5, with an increase in the number of cells, the relative error decreases. However, in the section X = 18.5, a situation is observed similar to the flow rate L when using the k-ε model. In this case, this situation is explained by the absence of a distinguished near-wall layer, where the flow is separated from the channel wall; its influence is shown in the next section.

For further research, we select a grid with 291 thousand cells, since it shows the smallest relative error in most calculations.

When comparing the data obtained in the calculations in the CFX package, we can unequivocally say that SST is more suitable for this problem of the two turbulence models used. The relative SST error in almost all the calculations performed turned out to be less than that of k-ε, therefore, further study of the air movement was carried out only using the SST model.

3.3. Analysis of the Influence of the Size of the Wall Cells of the Computational Mesh on the Simulation Results

The flow of the medium can be divided into two principal zones: the boundary layer and the core of the flow [10]. The boundary layer can be laminar or turbulent. The turbulent boundary layer, in turn, consists of a laminar sublayer, a turbulent layer and a transition zone (Fig. 14).

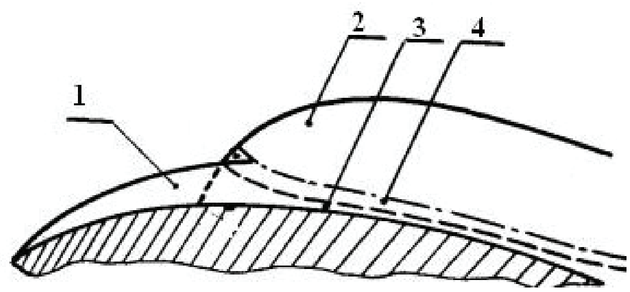

Fig. 14: Boundary layer structure: 1 – laminar flow; 2 – turbulent boundary layer; 3 – laminar sublayer, 4 – transition zone

The SST model is able to describe well the phenomena near the walls, since different dependences are used for different regions of the boundary layer, but only with a high quality of the computational grids there. Therefore, to increase the accuracy of simulation calculations, it is required to evaluate the effect of the number of layers and their thickness in the boundary region near solid walls.

The following results are presented in calculations with the number of near-wall layers from 2 to 5 and the thickness varied from 2×10^{-3} m to 5×10^{-5} m. The outlet section of the channel for different parameters of the near-wall layers of the computational grids is shown in Fig. 15.

As well as when choosing the number of cells, the calculations were carried out for the flow rates S and L, using the SST turbulence model. The air flow velocity distribution graphs are shown in Fig. 16, Fig. 17. The relative error results are shown in Tab. 5.

Of the data obtained, the smallest relative error was shown by calculations with a near-wall layer of 5x0.002m. When an attempt was made to increase the number of layers, the calculations stopped converging, that is, it was not possible to obtain a numerical solution with acceptable accuracy for the variables of the system of equations.

An increase in the relative error with a decrease in the thickness of the peri-wall layer of the grid cells indicates that the numerical model used does not take into account the significant physical features of the problem under consideration. Consequently, to increase the accuracy of the results of numerical modeling, it is necessary to amend the equations of the numerical model, which will take into account all the physical features of the studied air movement.

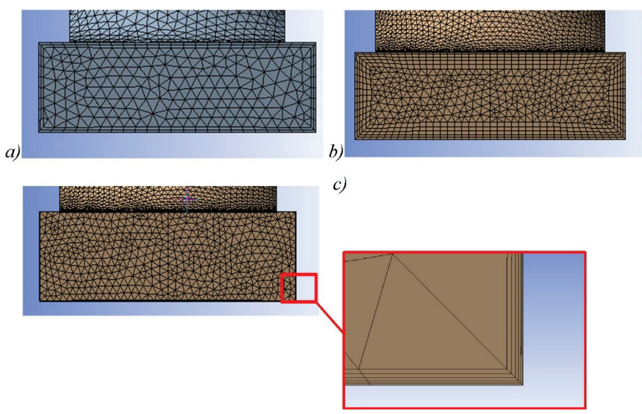

Fig. 15: The outlet section of the channel with the parameters of the near-wall layer
a)2x0,002m b) 5x0,002m c)5x0,0001m

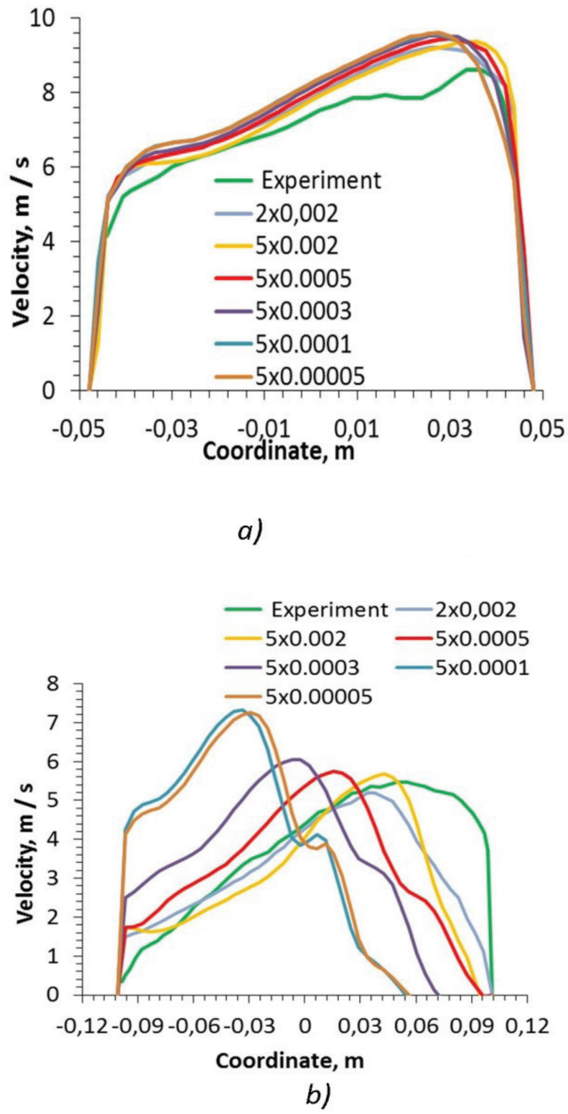

Fig. 16: Air velocity distribution graphs at a flow rate S for cross--sections:
a) X=2,5 b) X=18,5

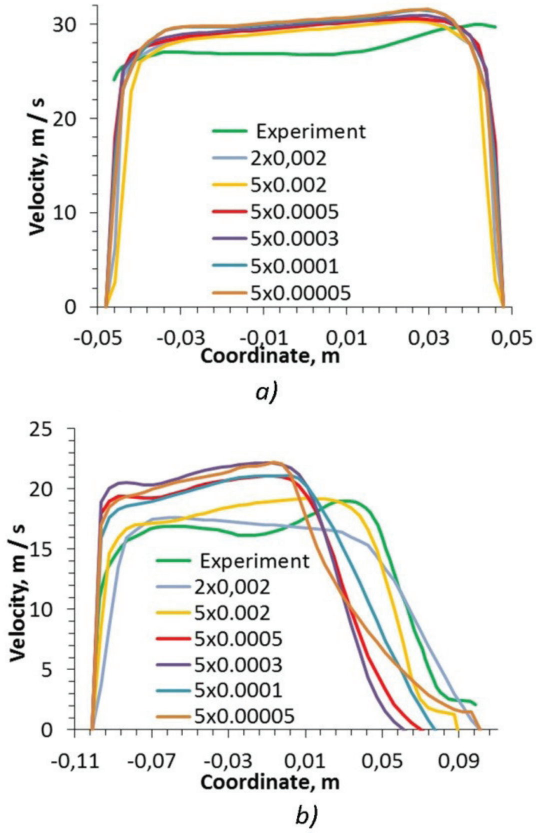

Fig. 17: Air velocity distribution graphs at a flow rate L for cross--sections:
a) X=2,5 b) X=18,5

An increase in the relative error with a decrease in the thickness of the peri-wall layer of the grid cells indicates that the numerical model used does not take into account the significant physical features of the problem under consideration. Consequently, in order to increase the accuracy of the results of numerical modeling, it is necessary to amend the equations of the numerical model, which will take into account all the physical features of the studied air movement.

Consumption	Relative error, %											
	X=2,5						X=18,5					
	Characteristics of the parietal layer						Characteristics of the parietal layer					
	2x0,002 m	5x0,002 m	5x0,0005 m	5x0,0003 m	5x0,0001 m	5x0,00005 m	2x0,002 m	5x0,002 m	5x0,0005 m	5x0,0003 m	5x0,0001 m	5x0,00005 m
S	9,67	8,29	9,85	11,56	12,93	12,98	16,55	15,12	36,89	67,45	121,22	117,38
L	8,92	7,88	8,99	9,83	11,74	12,54	13,8	12,46	44,79	53,73	37,49	33,46

Tab. 5: Average relative errors when changing the characteristics of the near-wall layer

3.4. Generalization of calculation results in the CFX package

As a result of calculations in the CFX package, and comparison of the results with experimental data, for further studies, the geometric configuration of the channel (Geometry 3), the turbulence model that most accurately describes the flow of the flow - SST, the number of cells for calculations (291 thousand pieces) were selected. and the number of near-wall layers (5 pcs.), as well as their thickness 0.002 m. The values of the relative error obtained by comparing the calculated data with the experimental are presented in Tab. 6. The graphs of the velocity distribution are shown in Fig. 18 - Fig. 20.

Consumption	Model	Cross-sectional error, %		
		X=2,5	X=10,5	X=18,5
S	SST	8,29	5,60	15,12
M	SST	4,01	10,34	22,23
L	SST	7,88	6,94	12,46

Tab. 6: Average relative errors when calculating in the CFX package

The results of calculations in the ANSYS CFX package turned out to be ambiguous. On the one hand, a fairly good match at the closest section (X = 2.5), where the relative error does not exceed 9%, and on the other hand, a poor match in the last section (X = 18.5), the relative error exceeds 22%.

These results indicate that the used model does not fully take into account the phenomena characteristic of a developed turbulent flow, such as flow separation and the possibility of back flow of the medium in the outlet section.

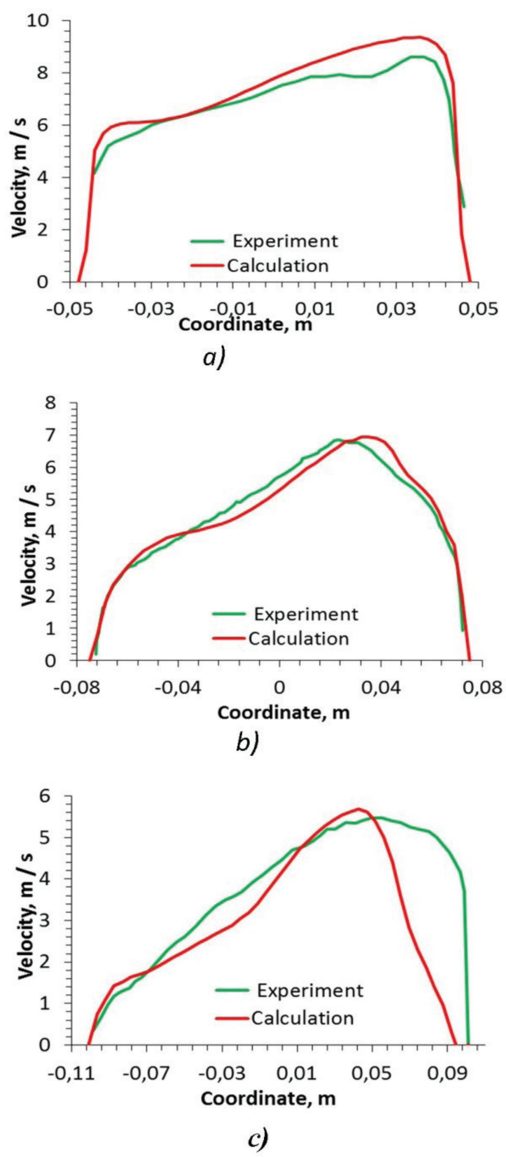

Fig. 18: Air flow velocity distribution graphs at flow rate S for cross-sections:
a) X=2,5; b) X=10,5; c) X=18,5.

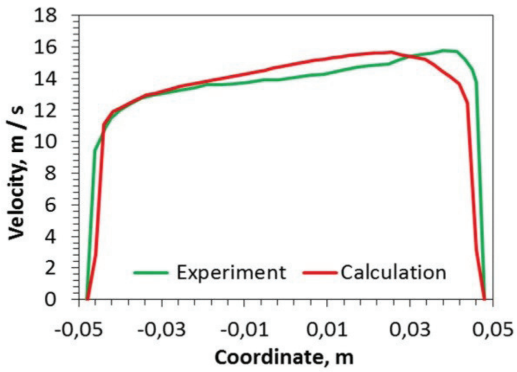

a)

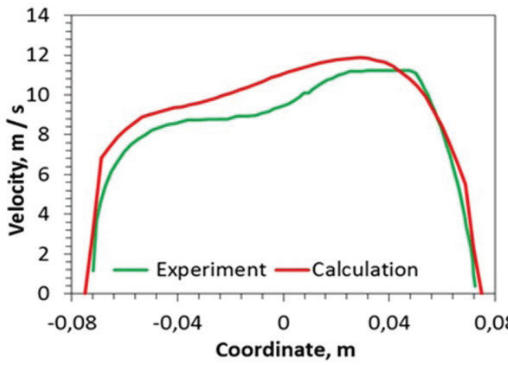

b)

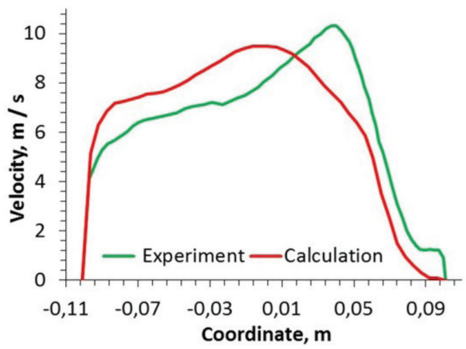

c)

Fig. 19: Air flow velocity distribution graphs at flow rate M for cross-sections:
a) X=2,5; b) X=10,5; c) X=18,5.

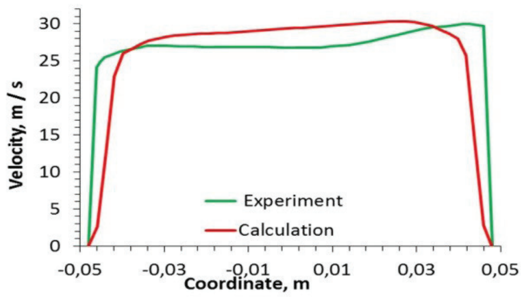

a)

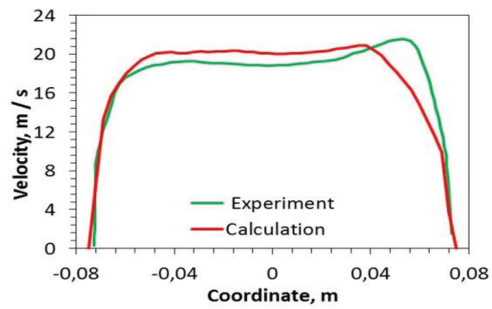

b)

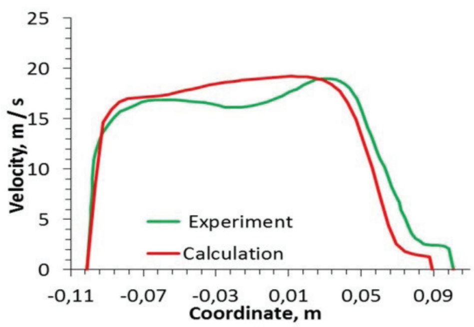

c)

Fig. 20: Air flow velocity distribution graphs at flow rate L for cross-sections:
a) X=2,5; b) X=10,5; c) X=18,5.

4. CONCLUSION

This study is aimed at creating a model of air movement in the radial-axial channel, which, with further research, will help improve the efficiency of microturbines. The main attention is paid to the study of air movement in the channel, which is a simplified configuration of the interscapular space of a centrifugal turbomachine.

The adequacy of the simulation results, namely the air velocity profile in various sections of the channel, was assessed by comparison with the empirical data described in detail in the article by J. Moore [9].

In the course of the work, the following main results were obtained:

1. Found the geometric configuration of the channel for modeling, which provides the greatest approximation of the calculated data to the experimental.
2. It was found that the best correspondence of the calculated velocity profiles to the experimental data is achieved for the following configuration of the computational grid:

the number of cells is 291 thousand, the wall layer with parameters 5x 0.002 m.

3. It was revealed that the smallest relative error when comparing the data obtained experimentally and the simulation results is observed when using the turbulence model - SST corrected for the curvature of streamlines.

As a result of the calculations performed in the CFX package, the relative error of the data obtained during the simulation to the experimental ones was from 4.01 to 22.23%.

The analysis of the results of modeling the air movement showed that to reduce the error, further research is required, in which the main attention will be paid to performing calculations in a non-stationary mode, as well as the use of other turbulence models, which require significant time costs and large computer power.

ACKNOWLEDGEMENTS

The reported study was funded by RFBR, project number 19-38-90284.

REFERENCES

[1] Sekacheva, A., Noskov, A. and Pastukhova, L.: Investigation of natural frequencies of complex water pipelines. AKUSTIKA, VOLUME 38, p. 3-8., 2021
[2] Nazzal, A. S. E., Sekacheva, A. A. and Noskov, A. S.: Method for vibration measurement in pipelines of residential buildings. IOP Conference Series: Materials Science and Engineering, VOLUME 972(1), 2020, [012070]
[3] Sekacheva, A., Pastukhova, L., and Noskov, A.: NUMERIC ANALYSIS OF VERTICAL PIPELINE ELEMENT NATURAL FREQUENCIES. AKUSTIKA, VOLUME 32, p. 272-278, 2019
[4] Pastukhova, L.G. & Sekacheva, A. A.: CHISLENNYY ANALIZ DINAMICHESKIKH KHARAKTERISTIK ELEMENTA TRUBOPROVODNOY SISTEMY MNOGOETAZHNOGO ZHILOGO DOMA [NUMERICAL ANALYSIS OF DYNAMIC CHARACTERISTICS OF THE ELEMENT OF THE PIPELINE SYSTEM OF A MULTI-STOREY RESIDENTIAL BUILDING]. International Journal for Computational Civil and Structural Engineering, VOLUME 4, p. 137-146, 2016
[5] Travin, A., Shur, M., Strelets, M., Spalart, P. R.: LES of complex transitional and turbulent flows. Fluid Mechanics and Its Applications, VOLUME 65, p. 239-254, 2002
[6] Description of cogeneration plants [Electronic resource]. URL: http://www.suet-holding.ru/.
[7] Ferziger, J. H.: Recent Advances in Large Eddy Simulation. Elsevier. VOLUME 3, p.163-176, 1996
[8] Belov, I.A., Isaev, S.A.: Modelirovaniye turbulentnykh techeniy [Modeling turbulent flows], Textbook. SPb, Balt. state tech. unt., 108 p., 2001
[9] Moore, J. A.: Wake and an Eddy in a Rotating, Radial-Flow Passage. Part 1: Experimental Observations. Journal of Engineering for Power. July 1973, p. 205-212
[10] Frost, W., Moodlen, T. and others.: Turbulentnost'. Printsipy i primeneniye. [Turbulence. Principles and Applications.] Moscow, Mir, 220 p., 1980

Antonina Sekacheva *is a Postgraduate Student and Assistant of the Hydraulics Department of the Ural Federal University named after the first President of Russia B.N. Yeltsin (Yekaterinburg, Russia).*
Antonina Sekacheva is the author of over 10 scientific publications. She presented the main results of scientific research at the international conferences in Bath (UK), Moscow, St. Petersburg, Yekaterinburg. She created a master's thesis on the topic: "Numerical analysis of the length and shape of an element of a pipeline system, made with the aim of predicting and eliminating the possibility of the occurrence of resonant modes." The topic of work is directly related to the solution of one of the tasks related to noise and vibrations in pipeline systems.

Anatoly Khait *is Ph.D. of Engineering Science, Assistant Professor of School of Mechanical Engineering and Mechatronics of the Faculty of Engineering of the Ariel University (Ariel, Israel).*
Anatoly Khait is an expert in hydraulics, aerohydromechanics, hydraulic and pneumatic systems and others. He worked as a research associate at leading universities in England (Manchester Metropolitan University) and Israel (Tel Aviv University, Ariel University) in fields of mechanical and ocean engineering. Anatoly Khait is the author of over 40 scientific publications and the co-author of textbooks and teaching aids. Most of his work is devoted to unsolved fundamental problems of wave generation and absorption.

Lilia Pastukhova *is Ph.D. of Engineering Science, Assistant Professor of Hydraulics Department of the Ural Federal University named after the first President of Russia B.N. Yeltsin (Yekaterinburg, Russia).*
Lilia Pastukhova is a specialist in noise protection, numeric analysis of vibration impact and others. She is a member of the organizing committees of conferences and seminars in the field of safety problems of civil engineering and ecology held in UrFU. Lilia Pastukhova is the author of over 60 scientific publications and the co-author of textbooks and teaching aids. She presented the main results of scientific research at the international conferences in Cambridge (UK), Cheske-Budievice (Czech Republic), Yekaterinburg.

Alexander Noskov *is Doctor of Engineering Science, Professor, Head of the Hydraulics Department of the Ural Federal University named after the first President of Russia B.N. Yeltsin (Yekaterinburg, Russia), RAASN adviser.*
Alexander Noskov is known as a leading expert in the field of developing the fundamentals of the theory and methods of mathematical modeling of various tasks of civil engineering, as well as energy-saving hydraulic devices for various purposes. He is author of 150 scientific and methodical works, several monographs and textbooks, in particular, "Fluid and Gas Mechanics", 7 inventions. Inventions are implemented at the enterprises of the Sverdlovsk region and other regions. Under his leadership, an educational program has been developed in postgraduate studies in the specialty "Hydraulic machines and hydropneumatic assemblies", he is also a member of the Council for the protection of dissertations for the degree of Doctor of Science in this specialty. Alexander Noskov is participant of scientific and methodological international programs implemented in cooperation with educational institutions of the United Kingdom, the Netherlands, Italy and others. He is a member of the organizing committee of all-Russian and international conferences in the field of energy saving and safety of civil engineering, and the chief editor of the «Russian Journal of Construction Science and Technology».

Paper No.369/2021

SEPARATION OF THE CONTRIBUTIONS OF "OWN" AND "SHIFT" NOISE AND DETERMINATION OF GAS-DYNAMIC AND ACOUSTIC PARAMETERS OF SILENCERS

a)Aleksandr Shashurin, b)Nickolay Ivanov, c)Anna Lubyanchenko, d) Viktoriia Vasilyeva

a) 7596890@mail.ru
a, b) Samara State Technical University, Samara, Russia
c, d) Baltic State Technical University 'VOENMEH' named after D.F. Ustinov, St. Petersburg, Russia

***Abstract**: This article presents the results of calculations of acoustic and gas-dynamic parameters of silencers of various design designs. The calculations are based on the developed methods [1, 2]. 8 types of exhaust noise mufflers of various design designs were selected for the calculations. The article contains calculated values of the following parameters: the range of gas flow velocities at the muffler outlet pipe, m/s; pressure range, Pa; temperature range, K and acoustic power values, dB. Radiation patterns with the values of the "own" and "shift" noise parameters are presented. The separation of "own" and "shift" noise is performed. The data of comparative results of experimental and numerical parametric studies are presented; satisfactory comparative results are obtained. The influence of individual design parameters (the volume of the silencer, the presence of perforation) on the acoustic efficiency of silencers is analyzed. The mechanisms of noise reduction and ways to improve their designs are shown.*

***Keywords:** "own" noise, "shift" noise, silencers, gas-dynamic path, flow rate, volume pressure, temperatures in the volume, acoustic power, directional patterns, design of silencers.*

***DOI:** : 10.36336/akustika202141150*

1. INTRODUCTION

Noise and vibration reduction of power plants presently is a serious problem [1, 5-8]. The developed calculation methods [1, 2] were used to determine the numerical values of the gas--dynamic and acoustic parameters of silencers of various design versions (Tab. 1).

№	Theschemeofsilencers	Theirdesignation
1	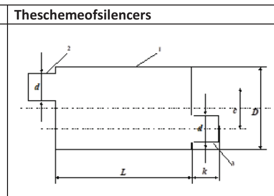	***L**$_1$*= 500 mm ***D**$_1$* = 300 mm **V$_1$** = 0,035 m^3 (**V$_6$** = 0,063 m^3 **V$_7$** = 0,098 m^3 **V$_8$** = 0,0141 m^3 **V$_9$** = 0,049 m^3) 1 – silencer housing, 2 – inlet pipe, 3 – outlet pipe, 4 – perforated pipe or partition, ***c*** = 150 mm, ***k*** = 150 mm, ***d*** = 100 mm
2	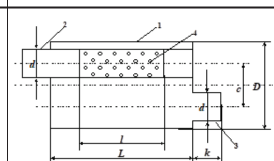	***L***= 500 mm ***D*** = 300 mm ***l*** = 300 mm **V** = 0,035 m^3 **S** perforations 15% ∅ perforations 10 mm 1 – silencer housing, 2 – inlet pipe, 3 – outlet pipe, 4 – perforated pipe or partition, ***c*** = 150 mm, ***k*** = 150 mm, ***d*** = 100 mm
3	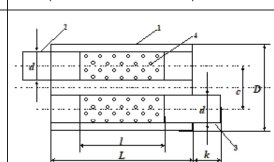	***L***= 500 mm ***D*** = 300 mm ***l***= 300 mm **V** = 0,035 m^3 **S** perforations 15%, ∅ perforations 10 mm 1 – silencer housing, 2 – inlet pipe, 3 – outlet pipe, 4 – perforated pipe or partition, ***c*** = 150 mm, ***k*** = 150 mm, ***d*** = 100 mm
4	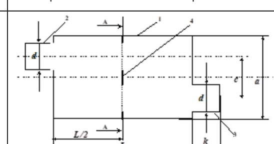	***L*** = 500 mm ***D*** = 300 mm **V** = 0,035 m^3 2 holes ∅ 100 mm 1 – silencer housing, 2 – inlet pipe, 3 – outlet pipe, 4 – perforated pipe or partition, ***c*** = 150 mm, ***k*** = 150 mm, ***d*** = 100 mm
5	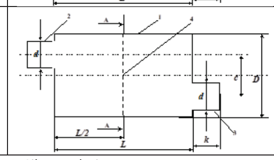	***L*** = 500 mm ***D*** = 300 mm **V** = 0,035 m^3 **S** perforations 10%, ∅ perforations 5 mm 1 – silencer housing, 2 – inlet pipe, 3 – outlet pipe, 4 – perforated pipe or partition, ***c*** = 150 mm, ***k*** = 150 mm, ***d*** = 100 mm

Tab. 1: Silencer designs

The main task of our research was the need to study and show the processes of noise generation and compare theoretical and experimental data with each other. In this method of determining the gas-dynamic characteristics in this track of operation, the pulse nature of the outflow was not taken into account.

The values were calculated:
pressure range in volume, Pa;

- temperature range in volume, ˚C;
- the intensity of the total noise, including the intensity of "own" and "shift" noise;
- acoustic power, dB.

The radiation patterns of the gas outlet path noise for various silencers were also obtained.

2. NUMERICAL PARAMETRIC STUDIES OF SILENCERS

The data obtained is shown below. So, for the silencer №1, according to the calculations, we received:

- the speed varies in the range $\boldsymbol{V}$ = 50 % 125 m/s;
- pressure range in volume $\boldsymbol{P_0}$ = 103000 % 109623 Pa;
- temperature range in volume $\boldsymbol{T_0}$ = 290 % 466 ˚C.

For the study of silencers, directional diagrams are constructed: the intensity of the total noise $\boldsymbol{J_{sum}}$[W/m²], the intensity of "own" noise – $\boldsymbol{J_{pulse}}$[W/m²], intensity of "shift" noise – $\boldsymbol{J_{sh}}$[W/m²] and sound pressure – PPB [Pa].

The radiation patterns were plotted using 16 points on a sphere with an angular pitch Δ22,5˚. Calculations of acoustic power and distribution of sound pressure levels of the silencer №1, performed for the conditions - $\boldsymbol{T_0}$ = 359 ˚C, $\boldsymbol{P_0}$ = 109316 Pa, $\boldsymbol{V}$ = 124,44 m/s, shown in the Fig.1. The radiation patterns are given for a sphere with a radius of 12 m. Such removal makes it possible to take into account as much as possible the contribution of various components along the entire length of the gas flow to the acoustic characteristics.

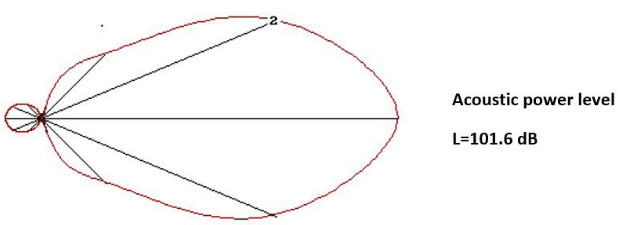

Fig. 1: Directional pattern of acoustic characteristics of the muffler №. 1: 1 – «Own» noise, 2 – «Shift» noise

Consider the materials on the silencer № 6 ($\boldsymbol{V}$ = 0,063 m³).

The results of determining the gas dynamic characteristics are listed below for different silencers, where:SVR – the speed varies in the range; PRV – the pressure range in the volume; TRV – the temperature range in the volume.

- SVR$\boldsymbol{V}$ = 30 ÷ 140 m/s
- PRV$\boldsymbol{P_0}$ = 102388 ÷ 109385 Pa
- TRV$\boldsymbol{T_0}$ = 290 ÷ 400°C.

The following parameters were used to calculate the acoustic fields: $\boldsymbol{V}$ = 124 m/s; $\boldsymbol{T_0}$ = 352°C; P_0 = 109385 Pa. The results of calculations of acoustic parameters and the radiation pattern are shown in the Fig.2.

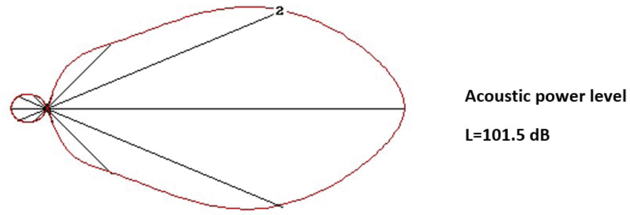

Fig. 2: Directional pattern of acoustic characteristics of the muffler №. 6: 1 – "Own" noise, 2 – "Shift" noise

Consider the materials on the silencer № 7 ($\boldsymbol{V}$=0,093 m³).

The results of calculations of gas dynamic parameters are given below:

- SVR$\boldsymbol{V}$ = 25 ÷ 145 m/s
- PRV$\boldsymbol{P_0}$ = 101708 ÷ 109420 Pa
- TRV$\boldsymbol{T_0}$ = 290 ÷ 390°C

To determine the sound pressure, the following characteristics were taken: $\boldsymbol{V}$ = 123 m/s; $\boldsymbol{T_0}$ = 348°C; $\boldsymbol{P_0}$ = 109414 Pa. The results of calculations of acoustic parameters and the radiation pattern are shown in the Fig.3.

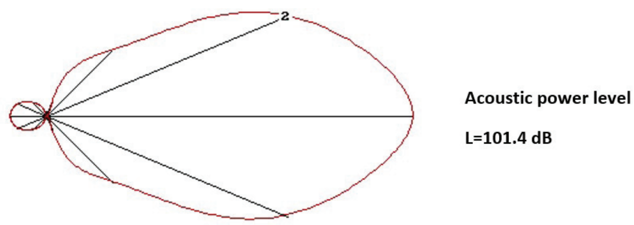

Fig. 3: Directional pattern of acoustic characteristics of the muffler № 7: 1 – "Own" noise, 2 – "Shift" noise

Consider the materials on the silencer № 8 (V= 0,141 m³).

The results of calculations of gas dynamic parameters are given below:

- SVR$\boldsymbol{V}$ = 25 ÷ 140 m/s
- PRV$\boldsymbol{P_0}$ = 101650 ÷ 109240 Pa
- TRV$\boldsymbol{T_0}$ = 290 ÷ 400°C

The following parameters were used to calculate the acoustic fields: $\boldsymbol{V}$ = 123,5 m/s; $\boldsymbol{T_0}$ = 355°C; $\boldsymbol{P_0}$= 109240 Pa. The results of calculations of acoustic parameters and the radiation pattern are shown in the figure 4.

Consider the following group of silencers № 2, 3 ($\boldsymbol{V}$= 0,035 m³). These models have perforated pipes for gas supply and discharge.Silencer № 2 is equipped with one perforated pipe for gas input. The results of calculations of gas dynamic parameters are given below:

- SVR$\boldsymbol{V}$ = 20 ÷ 120 m/s
- PRV$\boldsymbol{P_0}$= 101578 ÷ 109600 Pa
- TRV$\boldsymbol{T_0}$= 290 ÷ 500°C
-

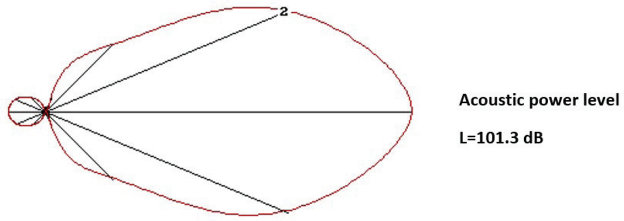

Fig. 4: Directional pattern of acoustic characteristics of the muffler № 8: 1 – "Own" noise, 2 – "Shift" noise

The following parameters were used to calculate the acoustic fields: $\boldsymbol{V}$ = 97 m/s; $\boldsymbol{T_0}$ = 302°C; $\boldsymbol{P_0}$ = 107009 Pa.

The results of calculations of acoustic parameters and the radiation pattern are shown in the Fig. 5.

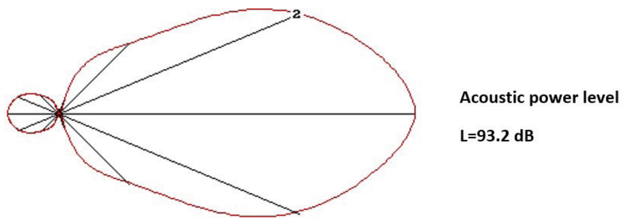

Fig. 5: Directional pattern of acoustic characteristics of the muffler № 2: 1 – "Own" noise, 2 – "Shift" noise

Consider the materials on the silencer № 3 (V = 0,035 m^3 with two perforated pipes).

The results of calculations of gas dynamic parameters are given below:

- SVR$\boldsymbol{V}$ = 20 ÷ 140 m/s
- PRV$\boldsymbol{P_0}$ = 103049 ÷ 109000 Pa
- TRV$\boldsymbol{T_0}$ = 280 ÷ 480°C

The following parameters were used to calculate the acoustic fields: $\boldsymbol{V}$ = 108 m/s; $\boldsymbol{T_0}$ = 310°C; $\boldsymbol{P_0}$ = 108279 Pa.

The results of calculations of acoustic parameters and the radiation pattern are shown in the Fig. 6.

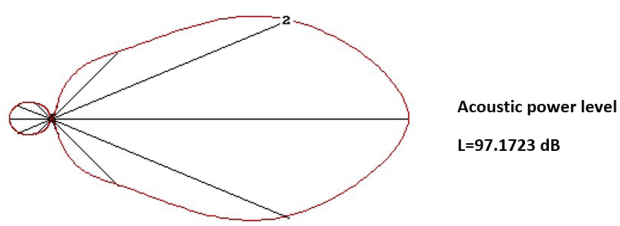

Fig. 6: Directional pattern of acoustic characteristics of the muffler № 3: 1 – "Own" noise, 2 – "Shift" noise

Consider a group of silencers № 4, 5 (two-chamber, $\boldsymbol{V}$=0,035 m^3).

The presence of two chambers in the silencer cavity required the determination of the natural frequencies for each of them and the natural frequencies for the associated flow cavities [3, 4].

The results of calculations of the gas dynamic parameters of the silencer № 4 are given below:

- SVR$\boldsymbol{V}$ = 18 ÷ 140 m/s
- PRV$\boldsymbol{P_0}$= 101799 ÷ 108600 Pa
- TRV$\boldsymbol{T_0}$ = 310 ÷ 510°C

The following parameters were used to calculate the acoustic fields: $\boldsymbol{V}$ = 124 m/s; $\boldsymbol{T_0}$ = 340°C; $\boldsymbol{P_0}$ = 109768 Pa.

The results of calculations of acoustic parameters and the radiation pattern are shown in the Fig. 7.

Results of calculations of acoustic parameters and radiation pattern for a silencer № 5 (two chambers with a perforated partition) shown in the Fig. 8.

The results of calculations of gas dynamic parameters are given below:

- SVR$\boldsymbol{V}$ = 30 ÷ 150 m/s
- PRV$\boldsymbol{P_0}$ = 101493 ÷ 107100 Pa
- TRV$\boldsymbol{T_0}$ = 280 ÷ 550°C

The following parameters were used to calculate the acoustic fields: $\boldsymbol{V}$ = 125 m/s; $\boldsymbol{T_0}$= 498°C; $\boldsymbol{P_0}$= 107116 Pa.

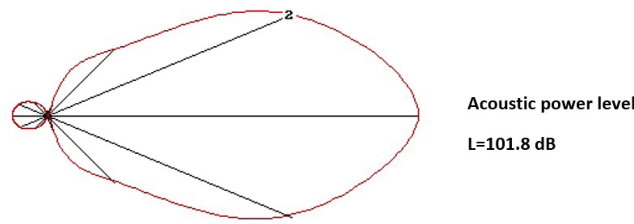

Fig. 7: Directional pattern of acoustic characteristics of the muffler № 4: 1 – "Own" noise, 2 – "Shift" noise

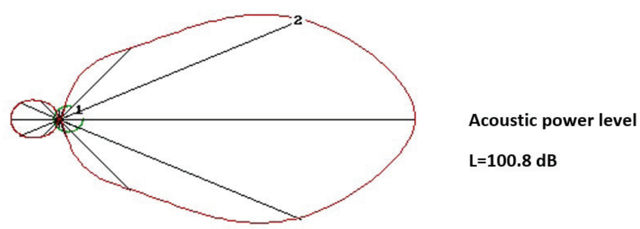

Fig. 8: Directional pattern of acoustic characteristics of the muffler № 5 (12 m): 1 – "Own" noise, 2 – "Shift" noise

Fig. 9 shows the calculations of the acoustic power level and the radiated acoustic power for the muffler № 5, the reference distance for measurements is 7 m. With a decrease in the length of recording parameters in the flow, the radiated acoustic power decreases.

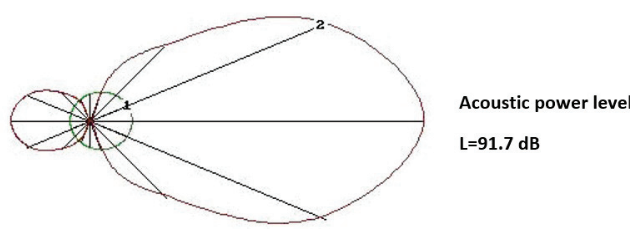

Fig. 9: Directional pattern of acoustic characteristics of the muffler № 5 (7 m): 1 – "Own" noise, 2 – "Shift" noise

3. COMPARATIVE ANALYSIS OF THE RESULTS OF EXPERIMENTAL AND NUMERICAL PARAMETRIC STUDIES

In the comparative analysis, the experimental data of testing models of silencers from the work [5] were used. The sound levels at a distance of 0.5 m from the exhaust pipe section, measured during experimental studies of muffler models, were converted into equivalent sound power levels and, along with the calculated values of acoustic power levels for a group of muffler models, are presented in Tab. 2.

	Model numbers of silencers							
	1	**2**	**3**	**4**	**5**	**6**	**7**	**8**
Equivalent sound power levels (experimental)	110,9	104,2	104,6	107,6	108,6	108,9	106,9	105,4
Acoustic power levels (calculated)	101,6	93,2	97,1	101,8	100,8	101,5	101,4	101,

Tab. 2: Research results for silencer models № 1-8

A comparative analysis of the results of experimental and numerical studies of the acoustic parameters of turbulent gas flow noise for muffler models № 1-8 shows that the discrepancies between the values of the aeroacoustic parameters of sound fields obtained experimentally and by calculation vary in the range from 4 to 12 %, which can be considered satisfactory.

Thus, it can be stated that the results of numerical studies of the gas-dynamic and aeroacoustic parameters of sound fields (Tab. 2) showed a satisfactory agreement with the experimental data. The obtained radiation patterns of the gas flow indicate a significant unevenness in the distribution of acoustic energy.

The analysis of the results for a group of silencers (models №. 1, 6-8), which differ in the volume of the hollow chamber, allows us to make a number of generalizations:

- the processes of sound wave formation at a frequency of 250 Hz are caused by the operation of the internal combustion engine. We can say that the hypothesis describing the high quality of the muffler is due to the coincidence of the frequencies from the internal combustion engine and the natural frequencies of the muffler.
- calculations and estimates of the turbulent flow noise for these silencers showed a decrease in acoustic power levels with an increase in the volume of the silencer.

Consider the following group of silencers № 1-3 with a constant volume ($\boldsymbol{V} = 0.035$ m^3) and characterized by the presence of perforated pipes (1-without pipes, 2-one pipe, 3-two pipes). The analysis of this group of silencers showed that the use of perforated pipes in the silencer gives a shift in the natural frequencies of the silencer, and this simply changes the efficiency of the entire system in different octaves.

Consider a group of two two-chamber silencers with a volume of 0.035 m^3: № 4 with a partition with two holes Ø100 mm and №. 5 with a perforated partition. An analysis of the functioning of this group of silencers showed that in the case of multi-chamber silencers № 4, 5, the radiation levels in the lower octaves decrease slightly, and the radiation levels in the high-frequency octaves remain at the same levels.

4. CONCLUSION

Numerical parameters of gas-dynamic paths with installed silencers were determined. For 8 silencers of various design versions, the following were determined:

- gas flow rate, m/s;
- pressure range in the silencer volume, Pa;
- temperature range in the volume, ˚C;
- values of the intensity of "own" and "shift" noise, W/m^2;
- acoustic power values, dB.

For the tested silencers, directional diagrams were constructed, where the separation of "own" and "shift" noise is shown. Depending on the design of the silencer, the flow rate varies between 20-140 m/s, the pressure range in the volume is from 101000 to 109000 Pa, the temperature range is from 290 to 540˚C.

The speed characteristics of the expiration affects the noise parameters, including the own and shift noise. When the flow rate changes in the range of 50-200 m/s, the radiated power levels increase by 15-20 dB. At low speeds, the "own" noise has the greatest influence, and with increasing speed, the contribution of "shift" noise also increases.

Features of changes in thermal parameters that affect the sound pressure less noticeably: a difference of 100-200°C increases the acoustic power level by 3-6 dB. At low temperatures, the main contribution to the acoustic power is made by "shift" noise, with an increase in temperature, the role of "own" noise becomes decisive.

There are two independent noise reduction mechanisms in the silencer. The first is related to the impact on the noise generated in the exhaust tract, it works mainly at low and medium frequencies in the range up to an octave band with an average geometric frequency of 500 Hz. The design of silencers for operation in this range involves tuning them to the engine noise frequencies.

The operation of the muffler at high frequencies (above the octave band with an average geometric frequency of 500 Hz) is determined by the effect of its elements on the gas-dynamic parameters of the outgoing working gas flow (speed, pressure and temperature). There is a decrease in speed (in the range of 25-140 m/s), pressure (8000-10000 Pa) and temperature (100—200°C). To achieve these effects, perforation in tubes and partitions, a change in the number of chambers, the use of sound absorption, a change in the flow direction, etc. are used. At the same time, the conditions of minimum back pressure must be met.

ACKNOWLEDGEMENT

The research described in this paper was supported by the grant of Russian Scientific Foundation, project number: 20-19-00222.

REFERENCES

[1] Agrafonova A.A.. Smirnov S.G.. Tupov V.V. Issledovaniye akusticheskoy effektivnosti glushiteley shuma // Izvestiya vysshikh uchebnykh zavedeniy. Mashinostroyeniye. №9 [666] 2015, p. 75-82
[2] Balter I.I.. Berezovskiy A.M.. Butakov G.V. i dr. Sposoby zashchity ot shuma i vibratsii zheleznodorozhnogo podvizhnogo sostava. Pod red. G.V. Butakova. M.. «Transport», 1978, 231p.
[3] Goldsteyn M.E. Aeroakustika: Per.s angl./Pod red. A.G. Munina. - M.: Mashinostroyeniye, 1981. – 294 p.
[4] GOST 12.1.003-83*. «SSBT. Shum. Obshchiye trebovaniya bezopasnosti»
[5] Drobakha M.N. Snizheniye shuma transportnykh mashin glushitelyami (na primere traktora MTZ 82). Dissertatsiya. Sankt--Peterburg, 2004.
[6] Vasilyev A.V. Experience and perspectives of using active noise and vibration control for reduction of low frequency noise and vibration in gas guide systems of power plants. 46th International JVE Conference in St. Petersburg, Russia, June 29 - July 1, 2020. Vibroengineering PROCEDIA, Vol. 32, June 2020, pp. 123-128.
[7] Vasilyev A.V. Approaches and technical solutions of reduction of low frequency vibration caused by gas pressure oscillations in pipelines of piston compressors during suction process. Proceedings of the 2020 IEEE International Conference on Dynamics and Vibroacoustics of Machines (DVM), September, 16-18, 2020, Samara. Samara, Samara University. IEEE Xplore edition, 2020, paper 137.
[8] Vasilyev A.V. Research of industrial noise impact to the urban environment on the example of enterprises of north industrial unit of Togliatti city of Russia. IOP Conference Series: Earth and Environmental Science, Volume 607, 4th Conference on actual problems of specially protected natural areas. 17-18 September 2020, Togliatti, Samara region, Russian Federation. Published under licence by IOP Publishing Ltd. Paper No. 012015. Published online: 30 November 2020.

Aleksandr Shashurin *is Doctor of Engineering Science, Professor, Head of Department of Environment and Safety of the Baltic State Technical University 'VOENMEH' named after D.F. Ustinov (Saint-Petersburg, Russia), CEO of the LLC (OOO) 'Acoustic Design Institute'.*
Aleksandr Shashurin is a specialist in calculation and design of noise barriers, noise reduction at production facilities, soundproof booths design and others. He is a member of the organizing committees of conferences and seminars in the field of acoustics and ecology held in St. Petersburg and Moscow. Aleksandr Shashurin is the author of over 40 scientific publications and the co-author of textbooks and teaching aids, the author of 6 patents for noise control devices. He presented the main results of scientific research at the international conferences in St. Petersburg, Moscow, Samara, Hiroshima (Japan).

Nickolay Ivanov *is Doctor of Engineering Science, Professor of Department of Ecology and Industrial Safety of the Baltic State Technical University 'VOENMEH' named after D.F. Ustinov (Saint-Petersburg, Russia), Honored Scientist of the Russian Federation.*
Nickolay Ivanov is the creator of the transport acoustics scientific school. He developed the theory of the transportation vehicles acoustics, proposed the solution to the problems of generating the sound field in low volume, diffraction on complex obstacles, methods of calculation of the sound fields of spatial emitters. Nickolay Ivanov has published over 400 scientific papers, including about 10 textbooks, manuals and monographs. He presented the main results of scientific research on the international conferences in Australia, Austria, Hungary, Germany, Denmark, Italy, Canada, China, the Netherlands, Poland, Portugal, the USA, Finland, Switzerland, Sweden and other countries.

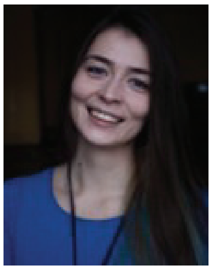

Anna Lubianchenko *is Ph.D. of Engineering Science, Assistant Professor of Department 'Ecology and Industrial Safety' of the Baltic State Technical University 'VOENMEH' named after D.F. Ustinov (Saint-Petersburg, Russia), Acoustics Expert of the LLC (OOO) 'ExpertProject', Director of the LLC (OOO) 'StroyCenter'.*
A. Lubianchenko is a specialist in calculation of architectural and construction acoustics, noise reduction at production and construction facilities. She is a member of the organizing committees of conferences and seminars in the field of acoustics and ecology held in St. Petersburg. A. Lubianchenko is the author of over 15 scientific publications and the co-author of textbooks.

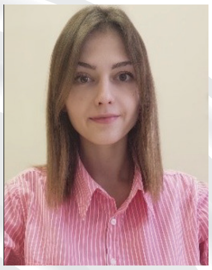

Viktoriia Vasilyeva *is Assistant of the Department of Ecology and Industrial Safety of the Baltic State Technical University "VOENMEH" named after D.F. Ustinov (St. Petersburg, Russia), Viktoriia Vasilyeva is engaged in research on the effects of noise on the human body. Development of methods for determining the individual body's response to noise with prevailing high and low frequencies. Author of scientific publications. Participant of scientific conferences on noise protection in St. Petersburg and Moscow.*

Paper No.3702021

SOUND PROPAGATION THROUGH STRUCTURAL COMPONENTS UNDER CONDITIONS OF NON-RIGID CONTACT AT THE BOUNDARIES BETWEEN THEM

[a] Konstantin Abbakumov, [b] Anton Vagin, [c] Alena Vjuginova

[a] St. Petersburg State Electrotechnical University 'LETI', St. Petersburg, Russia, KEAbbakumov@etu.ru
[b] St. Petersburg State Electrotechnical University 'LETI', St. Petersburg, Russia, AVVagin@etu.ru
[c] St.Petersburg State Electrotechnical University 'LETI', St. Petersburg, Russia, AAVyuginova@etu.ru

Abstract: *The report considers the problem statement, derivation and solution of the dispersion equation for sound propagation in a layered inhomogeneous medium with oriented fracturing, simulated by the presence of boundary conditions in the "linear slip" approximation. Numerical solutions are obtained and analyzed for the frequency range and values of the parameters of contact breaking, which is relevant in the problems of ultrasonic measurements*

Keywords: *acoustic contact, "linear slip", elastic displacements, incomplete transmission, layered inhomogeneous medium*

DOI: *: 10.36336/akustika202141155*

1. INTRODUCTION

The problems of elastic wave propagation in solids with internal deformations are of great importance in many applied fields: the seismic-acoustics, Geophysics, engineering, nondestructive testing, structure investigation etc. The problems of finding the physical characteristics of inhomogeneous elastic layered media have recently become significant [1]. First of all, this is due to the active use in practice of new functional-gradient and composite materials, the properties of which continuously change in thickness [2, 3]. Therefore, the determination of the material parameters and the geometric structure of the layered medium has become a task of primary importance. Finding the characteristics of layered materials allows modeling of the real behavior of objects with possible inhomogeneous properties, and expands the possibilities for creating and researching new materials. In order to obtain more information about the properties and parameters of the studied medium, it is necessary to conduct pre-measurement surveys to obtain the maximum possible number of elastic and mechanical characteristics.

Wave propagation in composite and inhomogeneous materials is the subject of many publications [4, 5, 6]. The analysis of longitudinal wave propagation in a layered medium with inhomogeneous boundary conditions at the boundaries at different directions of wave propagation is given in [7]. The works [8, 9] is also devoted to wave propagation in layered media, and they have a significant drawback in solving of dispersion equation for longitudinal and transverse waves propagating in a homogeneous and inhomogeneous layered medium. This drawback lies in the incorrect solution of the dispersion equation, and, consequently, in obtaining an incorrect value of the wave velocity, which is further related with a deviation of the elastic characteristics of the material from the true ones. This is confirmed by the graphical dependence of the velocity of the longitudinal and transverse waves on the relative thickness of the material layer. With an increase in the relative thickness of the material layer of the layered medium, the value of the wave velocity begins to decrease, which contradicts the physical concepts of the propagation of volume waves in inhomogeneous media. This contradiction is eliminated for the longitudinal wave propagating in an inhomogeneous medium by the authors in [7, 10].

Similarly to the above-mentioned case the derivation of the dispersion equation for longitudinal and transverse waves propagating in a layered homogeneous medium is given in [11, 12]. The solution of the dispersion equations in this case gives the correct graphical dependences of the velocities of the longitudinal and transverse waves on the relative thickness of the material layer.

Since these results are obtained for two extreme cases of contact between layers, it is of interest to compare them to evaluate the results for other types of contact. In the case of wave propagation in a homogeneous medium, the solution of the dispersion equation of this wave will give the true value of the effective velocity. In the presence of heterogeneity in layered medium the value of traveling wave velocity begins to decrease due to multiple reflections, absorption, attenuation, scattering of wave energy on the structural inhomogeneities in layered media.

In [13, 14] the propagation of a transverse wave in a layered inhomogeneous "steel-steel" structure with rough inteface is considered. The obtained results differ from the physical concepts of wave propagation in inhomogeneous medium, since the values of the found velocities are out of the correct graphical dependencies for the layer thickness.

In addition to inhomogeneities such as layerings, cracks, gas inclusions, etc., there are temperature effects [15], effects associated with filtration and focusing [16], which also affect the propagation velocity of elastic waves in the material.

In the case of a univalent analytical relationship between the wave parameters and the physical and mechanical properties of the material, the controlled elastic characteristics will be determined with a high accuracy. If one knows propagation velocities of longitudinal and transverse control waves, the Young's modulus, Poisson's ratio, and shear modulus are determined univalently [17].

The variety of constructional materials and media that are used in modern technology and production is extremely large, and has a long-term perspective in development. The expansion of the types of materials used in production relates with arising of new types of inhomogeneities, which detection should be based on the development of new means of ultrasonic testing and improvement of existing ones.

The aim of the present article is to derive the dispersion equation of a surface wave based on the solution of the dispersion equations for longitudinal and transverse waves for a layered inhomogeneous medium with oriented fracturing, simulated by the presence of boundary conditions in the "linear slip" approximation. Thus, it is necessary to consider the following cases of wave propagation geometry: a longitudinal wave propagating perpendicular to the layers, a transverse wave with vertical and horizontal polarization propagating perpendicular to the layers, and finally a surface wave propagating in a perpendicular direction. As an inhomogeneous medium used for the study we assume the layered-inhomogeneous structure "steel-graphite" with boundary conditions that determine the incomplete transfer of the components of elastic displacements while maintaining the transfer of elastic stresses [18].

A layered medium is a medium consisting of alternating layers of two homogeneous and isotropic materials. If a layered medium is consired "on average", that is, when the layers of the structure are sufficiently thin, and the condition of thinness of the layers means that their thicknesses are small compared to the compression and shear wavelengths in the materials of these media, it is considered as homogeneous, but anisotropic, and such a medium is called fine-layered [9, 19].

2. MODEL DESCRIPTION OF LAYERED-INHOMOGENEOUS MEDIUM WITH ORIENTED FRACTURING

Let us consider a model of a layered medium with alternating layers of thickness a and b, and parameters – for the first medium, and – for the second medium (fig. 1). As the first medium we consider steel, as the second – graphite. The total thickness of the layer is assumed to be 1 mm, and the frequency of ultrasound for modeling of the processes of wave velocity determining by acoustic measurements is 1 MHz.

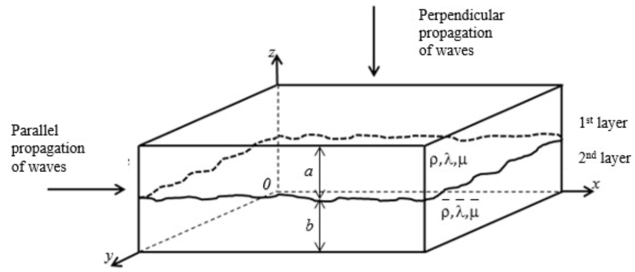

Fig. 1. Layered structure model

At Fig. 1: – medium density, – Lame constants. The similar parameters for the second medium are denoted with bar.

To describe the elastic behavior of the model of a layered medium presented at Fig. 1, it is necessary and sufficient to specify five elastic constants, that is, this model is an analog of a crystal of hexagonal symmetry. However, a medium with micro-cracks can be described using effective dynamic elastic modulus, the calculation of which is not an easy task and is achieved on the basis of statistical mechanics methods [20] and the self-consistent field method [21].

The wave equation for a longitudinal wave propagating in a layered structure has the following form:

$$\rho\frac{\partial^2\xi_l}{\partial t^2}-(\lambda+2\mu)\Delta\xi_l=0$$

where
ξ_l – vector of longitudinal displacement, $\Delta\xi_l = graddiv(\xi_l)$

The general solution of the wave equation for a longitudinal wave is determined through specially selected partial solutions, which are divided into two components relatively to the middle of the layers, namely, the cosine (symmetric) and sinusoidal (asymmetric) parts [9].

For the first layer of the layered medium model, we have the following form of longitudinal and transverse displacements in the direction of the axis ***x*** and ***z***:

$$P(z)=A\cos\alpha\left(z-\frac{a}{2}\right)+B\sin\alpha\left(z-\frac{a}{2}\right),\alpha^2=k_l^2-k^2 \tag{1}$$

where
ξ_{lx}, ξ_{lz} – longitudinal, and
ξ_{lx}, ξ_{lz} – transverse displacements in directions ***x*** and ***z*** respectively,
k – wave number. And also

$$P(z)=A\cos\alpha\left(z-\frac{a}{2}\right)+B\sin\alpha\left(z-\frac{a}{2}\right),\alpha^2=k_l^2-k^2$$
$$Q(z)=C\cos\beta\left(z-\frac{a}{2}\right)+D\sin\beta\left(z-\frac{a}{2}\right),\beta^2=k_t^2-k^2 \tag{2}$$

where
A, B, C, D – not yet defined constants,
k_l, k_t – wave numbers of longitudinal and transverse waves respectively.

The expressions for the components of the mechanical stress tensor for the first layer have the following form:

$$\sigma_{xz} = 2\mu\left(P'(z) + \frac{k^2 - \beta^2}{2ik}Q(z)\right)e^{-ikx}, \sigma_{yz} = 0$$

$$\sigma_{zz} = \left(\frac{\lambda k_l^2 + 2\mu\alpha^2}{ik}P(z) + 2\mu Q'(z)\right)e^{-ikx} \tag{3}$$

Similar parameters in the second environment for equations (1) – (3) are denoted with bar.

To describe the behavior of the studied waves at the boundaries of the layered model, we introduce boundary conditions for elastic displacements and mechanical stresses. Inhomogeneous boundary conditions describe the incomplete transfer of the elastic displacement components while maintaining the transfer of mechanical stresses for each boundary of the model, and are given as:

$$\xi_x(0) = \overline{\xi_x(0)} - \frac{\overline{\sigma_{xz}(0)}}{KGT}, \sigma_{xz}(0) = \overline{\sigma_{xz}(0)}$$

$$\xi_z(0) = \overline{\xi_z(0)} - \frac{\overline{\sigma_{zz}(0)}}{KGN}, \sigma_{zz}(0) = \overline{\sigma_{zz}(0)}, \tag{4}$$

where
KGT, KGN – tangential and normal stiffness coefficients.

It is assumed that in the general case, the inhomogeneous boundary of two elastic half-spaces was formed due to the combination of the interaction of peaks and valleys of the microrelief. Then the "gaps" in the transmission of elastic displacements arise due to the many micro-contacts between the two media under consideration. The peaks and valleys of the microrelief can be modeled by introducing the roughness value into the stiffness coefficients. Then the roughness introduced into the model will be determined by the average distance between neighboring inhomogeneities on the contacting surfaces. Thus, the degree of inhomogeneity for the layered medium model can be adjusted by changing the values of the stiffness coefficients.

The normal stiffness coefficient determines the transmission of the normal components of elastic displacements, and the tangential coefficient determines the transmission of tangential components. The stiffness coefficients depend on the perforation coefficient, which characterizes the degree of continuity between the adjoining media of the "steel-graphite" structure, as well as on roughness value.

A graphical representation of the normal and tangential stiffness coefficients is given by the authors in [7].

In the present paper the roughness value was assumed to be equal to $R_z = 40\ \mu m$, and the average distance between neighboring inhomogeneities on the contacting surfaces is equal to ***0,1 µm***.

Let us also introduce the boundary conditions of periodicity, which describe the continuous behavior of elastic displacements and mechanical stresses at the boundary of the layers:

$$\xi_x(a) = \overline{\xi_x(b)}, \sigma_{xz}(a) = \overline{\sigma_{xz}(b)}$$

$$\xi_z(a) = \overline{\xi_z(b)}, \sigma_{zz}(a) = \overline{\sigma_{zz}(b)} \tag{5}$$

that is, the specified values in the first layer under ***z=a*** are to be equal to the same values in the second layer under ***z=b***.

Substituting the components for elastic displacements (1) and mechanical stresses (3) in inhomogeneous boundary conditions (4), we obtain 8 equations for the constants $A, B, C, D, \overline{A}, \overline{B}, \overline{C}, \overline{D}$, which are dissociated to longitudinal and transverse wave [19].

3. PROPAGATION OF LONGITUDINAL WAVE PERPENDICULAR TO THE LAYERS OF INHOMOGENEOUS STRUCTURE

Let a longitudinal wave propagate in the direction of the x-axis. For such a wave coefficients ***B*** and ***C*** in the first and in the second medium are equal to 0. When the longitudinal wave propagates perpendicular to the layers, only the elastic displacement component is different from zero $P(z)e^{-ikx}$ [19]. For the case of a transverse wave in which the displacement is parallel to the layers, the non-zero component of the elastic displacement will be $\xi_{tz}^{\perp} = Q(z)e^{-ikx}$. With such a geometry of waves propagation, their propagation can be considered independently [20].

As it known from [22], if matrix-function ***A(t)*** is periodic, that is ***A(t) = A(t+T)***, so any its fundamental matrix ***Φ(t)*** has a form $\Phi(t) = \Psi(t)e^{Bt}$, where ***B*** – constant, a ***ψ(t)*** – continuously differentiable function. This statement describes Floquet's theorem.

Then, according to Floquet's theorem, in expressions describing the propagation of waves perpendicular to the layered structure (1), values ***P(z)*** and ***Q(z)*** are to be periodic functions with the period of structure ***h = a + b***. Inhomogeneous boundary conditions and periodicity conditions must be satisfied for the amplitudes $\xi_{lx}^{\perp}$ and $\sigma_{xz}^{\perp}$ in longitudinal wave, and for amplitudes $\xi_{tz}^{\perp}$ and $\sigma_{zz}^{\perp}$ in transverse wave.

Substituting the corresponding components for the case of perpendicular propagation of a longitudinal wave to inhomogeneous boundary conditions (4), we obtain the equations for the coefficients ***A*** and ***D*** in the first and second media:

$$Aik\cos\left(\alpha\frac{a}{2}\right)-D\beta\cos\left(\beta\frac{a}{2}\right)=$$
$$=\overline{A}\left[ik\cos\left(\overline{\alpha}\frac{b}{2}\right)+\frac{2ik\overline{\mu}\overline{\alpha}\sin\left(\overline{\alpha}\frac{b}{2}\right)}{KGT}\right]+\overline{D}\left[\frac{\overline{\mu}\left(k^2-\overline{\beta}^2\right)\sin\left(\overline{\beta}\frac{b}{2}\right)}{KGT}-\overline{\beta}\cos\left(\overline{\beta}\frac{b}{2}\right)\right],$$

$$A\cos\left(\alpha\frac{a}{2}\right)\left[1+\frac{1}{KGN}\left(\frac{\overline{\lambda}\overline{k}_l^2+2\overline{\mu}\overline{\alpha}^2}{ik}\right)\right]-D\sin\left(\beta\frac{a}{2}\right)=$$
$$=\overline{A}\cos\left(\overline{\alpha}\frac{b}{2}\right)-\overline{D}\left[\sin\left(\beta\frac{a}{2}\right)+2\overline{\mu}\overline{\beta}\cos\left(\overline{\beta}\frac{b}{2}\right)\right],$$

$$A4ik\mu\alpha\sin\left(\alpha\frac{a}{2}\right)-D(k^2-\beta^2)\sin\left(\beta\frac{a}{2}\right)=\overline{A}4ik\overline{\mu}\overline{\alpha}\sin\left(\overline{\alpha}\frac{b}{2}\right)-\overline{D}\left(k^2-\overline{\beta}^2\right)\sin\left(\overline{\beta}\frac{b}{2}\right),$$

$$A(\lambda k_l^2+2\mu\alpha^2)\cos\left(\alpha\frac{a}{2}\right)+D2\mu\beta ik\cos\left(\beta\frac{a}{2}\right)$$
$$=\overline{A}\left(\overline{\lambda}\overline{k}_l^2+2\overline{\mu}\overline{\alpha}^2\right)\cos\left(\overline{\alpha}\frac{b}{2}\right)+\overline{D}2\overline{\mu}\overline{\beta}ik\cos\left(\overline{\beta}\frac{b}{2}\right).$$

From the obtained equations for the coefficients ***A*** and ***D*** for the first and second media, we make a determinant and equate it to zero:

$$\begin{vmatrix} ik\cos\alpha\left(\frac{a}{2}\right) & -\beta\cos\beta\left(\frac{a}{2}\right) & ik\cos\overline{\alpha}\left(\frac{b}{2}\right)+\frac{2\overline{\mu}\overline{\alpha}ik\sin\overline{\alpha}\left(\frac{b}{2}\right)}{KGT} & \frac{\overline{\mu}\left(\overline{k}^2-\overline{\beta}^2\right)\sin\overline{\beta}\left(\frac{b}{2}\right)}{KGT}-\overline{\beta}\cos\overline{\beta}\left(\frac{b}{2}\right) \\ \cos\left(\alpha\frac{a}{2}\right)\left[1+\frac{1}{KGN}\left(\frac{\overline{\lambda}\overline{k}_l^2+2\overline{\mu}\overline{\alpha}^2}{ik}\right)\right] & -\sin\left(\beta\frac{a}{2}\right) & \cos\left(\overline{\alpha}\frac{b}{2}\right) & -\sin\left(\beta\frac{a}{2}\right)+2\overline{\mu}\overline{\beta}\cos\left(\overline{\beta}\frac{b}{2}\right) \\ 4ik\mu\alpha\sin\left(\alpha\frac{a}{2}\right) & -(k^2-\beta^2)\sin\left(\beta\frac{a}{2}\right) & 4ik\overline{\mu}\overline{\alpha}\sin\left(\overline{\alpha}\frac{b}{2}\right) & -\left(k^2-\overline{\beta}^2\right)\sin\left(\overline{\beta}\frac{b}{2}\right) \\ (\lambda k_l^2+2\mu\alpha^2)\cos\alpha\left(\frac{a}{2}\right) & 2\mu\beta ik\cos\beta\left(\frac{a}{2}\right) & \left(\overline{\lambda}\overline{k}_l^2+2\overline{\mu}\overline{\alpha}^2\right)\cos\overline{\alpha}\left(\frac{b}{2}\right) & 2\overline{\mu}\overline{\beta}ik\cos\overline{\beta}\left(\frac{b}{2}\right) \end{vmatrix}=0$$

Solving this determinant by decomposition along the first line, taking into account the boundary conditions of periodicity (5), we obtain the dispersion equation (6) for a longitudinal wave propagating perpendicular to the layers of the "steel--graphite" structure:

$$\cos(k_l a)\cos(\overline{k}_l b)\left[\frac{(\lambda+2\mu)k_l}{KGT}+1\right]+$$
$$+\frac{1-\chi_1^2}{2\chi_1}\sin(k_l a)\sin(\overline{k}_l b)\left[\frac{(\overline{\lambda}+2\overline{\mu})\overline{k}_l}{KGN}-1\right]-\cos[k(a+b)]=0 \tag{6}$$

where
$X_1=\frac{(\overline{\lambda}+2\overline{\mu})\overline{k}_l}{(\lambda+2\mu)k_l}$.

If in the given dispersion equation (6), the stiffness coefficients are directed to infinity ***KGT,KGN* –› ∞** what will correspond to wave propagation in a homogeneous medium, which is described by classical continuous boundary conditions, then we obtain the dispersion equation for a wave in a homogeneous medium, which is consistent with the results presented in [3].

Dispersion equation (6) defines the wave number for the longitudinal wave $k_l^{\perp}=\frac{\omega}{c_l^{\perp}}$, propagating perpendicular to the layers of the structure. Solving this equation with respect to the wave number, we can construct a graphical dependence of the velocity of the longitudinal wave $c_l^{\perp}$ from the relative thickness of the layer ***n*** (Fig. 2).

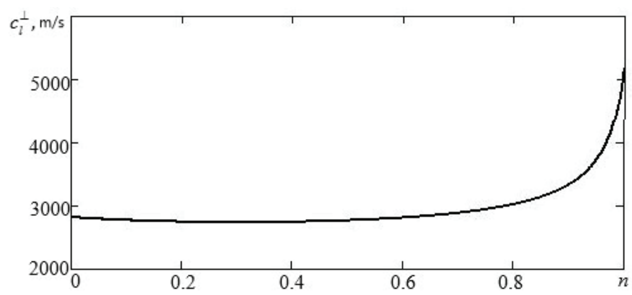

Fig. 2: Dependence of longitudinal wave velocity from relative thickness of layer when propagating perpendicular to the layers

As can be seen from this graphical dependence, the value of the velocity of longitudinal wave in case of propagation perpendicular to the layers begins to increase with an increase of relative thickness of the layer, which is consistent with the experimental data given in [18, 22]. In case of a homogeneous medium, the form of this graphical dependence is retained, but the value of longitudinal wave velocity is slightly higher than in an inhomogeneous medium, which is due to the presence of re-reflections of waves between the layers and scattering on the structural inhomogeneities of the medium [23].

4. PROPAGATION OF TRANSVERSE WAVE WITH VERTICAL AND HORIZONTAL POLARIZATION PERPENDICULAR TO THE LAYERS OF INHOMOGENEOUS STRUCTURE

Now consider the case of perpendicular propagation of transverse waves. Let a transverse wave propagate in the direction of the z-axis. As previously mentioned, for such a wave, the coefficients A and D in the first and second media are equal to 0. For the case of a transverse wave in which the displacement is parallel to the layers, it follows from (1) that only the elastic displacement component different from zero is $\xi_{tz}^{\perp}=Q(z)e^{-ikx}$. If the control of object is carried out together with longitudinal wave, then with such a propagation geometry, the transverse and longitudinal waves can be considered independently [23].

As it known from [24], if matrix-function ***A(t)*** is periodic, t h a t $A(t)\equiv A(t+T)$, is , so any its fundamental matrix $\Phi(t)$ has the form $\Phi(t)=\Psi(t)e^{Bt}$, where ***B*** – constant, a $\Psi(t)$ – continuously differentiable function. This statement describes Floquet's theorem.

Then by using of Floquet's theorem [24], in expressions, which describes propagation of waves perpendicular to layered structure (1), values ***P(z)*** and ***Q(z)*** are to be periodic functions with the period of structure ***h = a + b***. Inhomogeneous boundary conditions and periodicity conditions must be satisfied for amplitudes $\xi_{tz}^{\perp}$ and $\sigma_{zz}^{\perp}$ in transverse wave, and for amplitudes $\xi_{lx}^{\perp}$ and $\sigma_{xz}^{\perp}$ in longitudinal wave.

Substituting the corresponding components of elastic displacements and mechanical stresses for the perpendicular case of wave propagation, taking into account Floquet's theorem, into inhomogeneous boundary conditions (4), we obtain four equations for the coefficients A and D in the first and second media:

$$Bik\alpha\sin\left(\alpha\frac{a}{2}\right)=\bar{B}ik\left[1-\frac{\bar{\alpha}}{KGT}\right]\cos\left(\bar{\alpha}\frac{b}{2}\right)+\bar{C}\left[\bar{\beta}-\frac{\bar{k}^2-\bar{\beta}^2}{2KGT}\right]\sin\left(\bar{\beta}\frac{b}{2}\right),$$

$$B\alpha\cos\left(\alpha\frac{a}{2}\right)+Cik\cos\left(\beta\frac{a}{2}\right)=\bar{C}ik\left[\cos\left(\bar{\beta}\frac{a}{2}\right)-\frac{2\bar{\mu}\sin\left(\bar{\beta}\frac{b}{2}\right)}{KGN}\right],$$

$$C\mu(k^2-\beta^2)\sin\left(\beta\frac{a}{2}\right)=-\bar{B}\bar{\mu}\bar{\alpha}ik\sin\left(\bar{\alpha}\frac{b}{2}\right)+\bar{C}\bar{\mu}\left(\bar{k}^2-\bar{\beta}^2\right)\sin\left(\bar{\beta}\frac{b}{2}\right),$$

$$B(\lambda k_t^2+2\mu\alpha^2)\sin\left(\alpha\frac{a}{2}\right)=\bar{B}\left(\overline{\lambda k_t}^2+2\overline{\mu\alpha}^2\right)\sin\left(\bar{\alpha}\frac{b}{2}\right)+2\bar{C}\bar{\mu}\bar{\beta}ik\sin\left(\bar{\beta}\frac{b}{2}\right).$$

From the obtained equations for the coefficients A and D for the first and second media, we make a determinant and equate it to zero:

$$\begin{vmatrix} ik\alpha\sin\left(\alpha\frac{a}{2}\right) & 0 & ik\left[1-\frac{\bar{\alpha}}{KGT}\right]\cos\left(\bar{\alpha}\frac{b}{2}\right) & \left[\bar{\beta}-\frac{\bar{k}^2-\bar{\beta}^2}{2KGT}\right]\sin\left(\bar{\beta}\frac{b}{2}\right) \\ \alpha\cos\left(\alpha\frac{a}{2}\right) & ik\sin\left(\beta\frac{a}{2}\right) & 0 & ik\left[\cos\left(\bar{\beta}\frac{b}{2}\right)-\frac{2\bar{\mu}\cos\left(\bar{\beta}\frac{b}{2}\right)}{KGN}\right] \\ 0 & \mu(k^2-\beta^2)\sin\left(\beta\frac{a}{2}\right) & -\overline{\mu\alpha}ik\sin\left(\bar{\alpha}\frac{b}{2}\right) & \bar{\mu}\left(\bar{k}^2-\bar{\beta}^2\right)\sin\left(\bar{\beta}\frac{b}{2}\right) \\ (\lambda k_t^2+2\mu\alpha^2)\sin\left(\alpha\frac{a}{2}\right) & 0 & \left(\overline{\lambda k_t}^2+2\overline{\mu\alpha}^2\right)\sin\left(\bar{\alpha}\frac{b}{2}\right) & 2\bar{\mu}\bar{\beta}ik\sin\left(\bar{\beta}\frac{b}{2}\right) \end{vmatrix}=0$$

Similarly to already solved determinant, we decompose this determinant by the third line, taking into account the boundary conditions of periodicity (5), so we obtain the dispersion equation for a transverse wave propagating perpendicular to the layers of the inhomogeneous "steel-graphite" structure:

$$\cos(k_t a)\cos(\bar{k}_t b)\left(\frac{\mu k_t}{KGT}+1\right)+\frac{1-\chi_2^2}{2\chi_2}\sin(k_t a)\sin(\bar{k}_t b)\left(\frac{\bar{\mu}\bar{k}_t}{KGN}-1\right)-\cos[k(a+b)]=0 \tag{7}$$

where

$X_2=\frac{\bar{\mu}\bar{k}_t}{\mu k_t}$.

Solving this dispersion equation (7) with respect to wave number, we get graphical dependences of the velocity of transverse wave with horizontal (fig. 3) and vertical (fig. 4) polarization from the relative thickness of the layer n when propagating perpendicular to the layers of the structure.

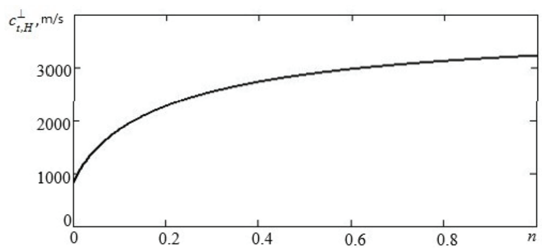

Fig. 3: Dependence of velocity of transverse wave with horizontal polarization from relative thickness of layer when propagating perpendicular to the layers

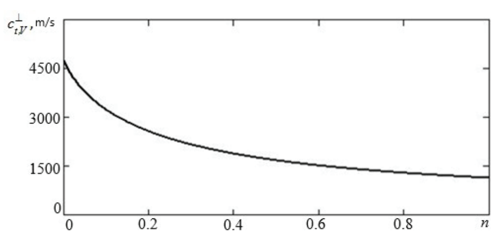

Fig. 4: Dependence of velocity of transverse wave with vertical polarization from relative thickness of layer when propagating perpendicular to the layers

As can be seen from these graphical dependences, the value of transverse wave velocity decreases with increasing of relative layer thickness, which is consistent with the experimental data [25]. In the case of wave propagation in a homogeneous medium, the appearance of these graphical dependencies does not change, however, the velocity values will be slightly higher than in the above case. The speed decrease in case of inhomogeneous medium is caused by possible re-reflections of the wave between the layers and scattering on the structural inhomogeneities of the medium.

5. DISPERSION EQUATION OF SURFACE WAVE IN CASE OF PERPENDICULAR PROPAGATION

After considering the propagation of a longitudinal and transverse wave in a layered inhomogeneous medium and obtaining the dispersion equations for these waves, we proceed with a problem of dispersion equation finding for a surface wave, and then will determine material parameters. The advantage of surface wave using compared with other wave types, mostly bulk waves, is certainly high. Without violating of problem solution generality while determining of physical and mechanical characteristics of material, it can be approached in two ways: if velocities of longitudinal and transverse waves are known, or at known velocity of the surface wave. Finding the parameters of the medium using the first case is based on substituting the velocities of the longitudinal and transverse waves into the dispersion equation for the surface wave, then solving this equation and finding the velocity of surface wave, and obtaining the necessary characteristics by substituting the found velocity in the known theoretical dependencies. The second method means measuring of surface wave velocity in the control sample and then substituting this velocity into expressions (1). The preference for the use of surface waves lies in the existing dependence of the parameters and physical and mechanical characteristics (Young's modulus, Poisson's ratio, shear modulus) of the medium in which the control wave propagates with its properties. This dependence is due to the localization of a large amount of wave energy in the near-surface layer of the control sample, which thickness is approximately two wavelengths. With such an existing dependence, the parameters found have sufficient accuracy to solve many practical problems of the theory of elasticity and propagation of acoustic waves in solids.

Solution of the inverse problem – finding elastic characteristics using a surface wave, also does not have any difficulties. Having a known velocity of surface wave, one can put it in the dispersion equation and solve it with respect to the wave numbers of the longitudinal and transverse waves, and substitute the resulting solution in the expressions (1) [26].

Consider an elastic half-space in which a surface wave propagates independently in two directions relating to position of layers system – parallel and perpendicular to the layers (Fig. 5).

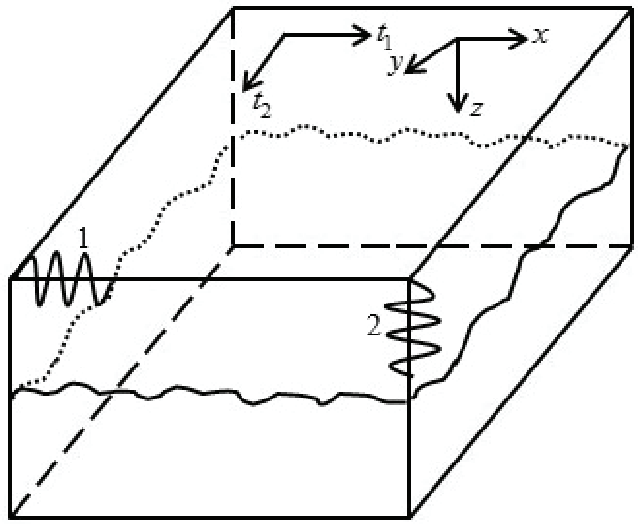

Fig. 5: Elastic half-space

At Fig.
5t$_1$ – vertical polarization of transverse wave,
t$_2$ – horizontal polarization of transverse wave,
1 – parallel propagation of surface wave,
2 – perpendicular propagation of surface wave.

Without taking into account the specific parameters (shape and size) of inhomogeneities present in inhomogeneous layered medium (elastic half-space), the present paper as it mentioned above, takes into account by formal means features of wave propagation in inhomogeneous medium, which is related with effective elastic parameters of medium for long-wave approximation: ***r, D*** « $\boldsymbol{\lambda}_{wave}$, where $\boldsymbol{\lambda}_{wave}$ – wavelength; ***r*** – distance between cracks; ***D*** – crack's diameter [27]. Based on this, the model of an elastic medium is described by the elastic characteristics represented by the expressions (1).

Let a surface wave propagate in the direction of the x-axis. The solutions of the wave equations are equations (1), which describe the decomposition of the elastic displacement into the solenoidal and potential parts. We will seek the solutions of these equations in the form of a plane surface wave in the following form:

$$\xi_{lx} = P_R(z)e^{-i(\omega t - kx)} \tag{8}$$

$$\xi_{tz} = Q_R(z)e^{-i(\omega t - kx)} \tag{9}$$

where
$P_R(z)$, $Q_R(z)$ are not yet defined functions.

By substituting of equations (8), (9) to wave equations solutions we get two equations for $P_R(z)$, $Q_R(z)$:

$$\frac{\partial^2 P_R(z)}{\partial z^2} - \left(k^2 - k_l^2\right)P_R(z) = 0$$
$$\frac{\partial^2 Q_R(z)}{\partial z^2} - \left(k^2 - k_t^2\right)Q_R(z) = 0$$

The solutions of the last two equations are functions $exp\left(\pm\sqrt{k^2 - k_l^2 z}\right)$ and $exp\left(\pm\sqrt{k^2 - k_t^2 z}\right)$. If $\boldsymbol{k^2 > k_t^2 > k_l^2}$, then solutions with positive radicals correspond to a propagating wave that increases with depth, and solutions with negative radicals correspond to a surface wave (a wave that decreases with depth). In accordance with this by introducing the following notation:

$$q = \sqrt{k^2 - k_l^2}, s = \sqrt{k^2 - k_t^2}$$

the expressions for the longitudinal and transverse displacements are written as:

$$\xi_{lx} = Ae^{[-qz - i(\omega t - kx)]}$$
$$\xi_{tx} = Be^{[-sz - i(\omega t - kx)]}$$

where
A,B – certain constants.

Then solving this system of equations and substituting the obtained solution in the boundary conditions, we obtain the dispersion equation for the surface wave (10).

$$4k^2\left[s(1+\gamma) + \frac{\gamma}{n}\right]\left[q(1+\delta) + \frac{\delta}{h}\right] - \left[(s^2 + k^2)(1+\gamma) + \frac{s\gamma}{h} + \frac{\gamma}{h^2}\right] \times$$
$$\times \left\{(s^2 + k^2)(1+\delta) + \frac{c_R^2}{c_t^2 c_l^2}\left[\frac{q\delta}{n} + \frac{\delta}{h^2}\right]\right\} = 0, \tag{10}$$

where

$$\delta = \left[1 - \frac{\rho\bar{k}_t^2 ctg\left(\frac{\bar{\alpha}a}{2}\right)}{KGT}\right], \gamma = \left[1 - \frac{\bar{\rho}\bar{k}_l^2 ctg\left(\frac{\bar{\beta}a}{2}\right)}{KGN}\right]$$

Substituting to the dispersion equation (10) the corresponding velocities for a longitudinal or transverse wave to obtain the velocity of propagation of surface wave in a certain direction and solving this dispersion equation with respect to the value of the velocity of surface wave, it is possible to obtain a graphical dependence for parallel or perpendicular wave propagation.

Calculations and graphical dependencies plotting were performed in the computer algebra environment Mathcad 15.

To obtain the velocity of surface wave with perpendicular propagation with respect to location of the layers in layered system, it is necessary to substitute the solutions of expressions (6) and (7) in the dispersion equation (10).

Let us plot a graphical dependence of the surface wave velocity from the relative thickness of material layer (Fig. 6).

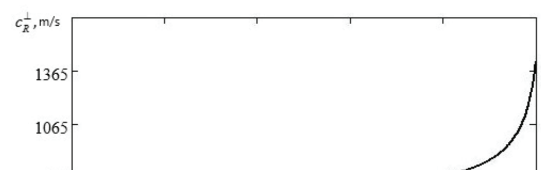

Fig. 6: Dependence of surface wave velocity from relative layer thickness under perpendicular propagation

Fig. 6 shows that as relative thickness of the layer increases, the dependence gradually increases from small velocity values to the velocity value in graphite, which is consistent with the theoretical results presented in [28].

The study of control sample by using of surface wave will be more optimal, since the energy of the surface wave is almost completely localized in the near-surface layer of the control sample in a thickness of about two wavelengths – this gives a significant dependence of the parameters of propagating surface wave on the properties of the layer in which it propagates.

6. CONCLUSION

1. The problem of finding the velocities of longitudinal waves and transverse waves of vertical and horizontal polarization with perpendicular to layers propagation relatively to layers of an inhomogeneous structure with volume fracturing is solved by solving the dispersion equation with respect to wave number.
2. The influence of the inhomogeneity of the layered model on the value of wave propagation velocity is shown. The influence of heterogeneity presence on the values of physical and mechanical characteristics of control object's material is evaluated.
3. Based on the obtained dispersion equations for a longitudinal wave, a transverse wave of vertical and horizontal polarization, the dispersion equation for a surface wave propagating in a layered inhomogeneous medium with oriented fracturing is derived and solved with respect to wave number.
4. The obtained dependences are used for tasks of defining the main physical and mechanical characteristics of material based on acoustic measurements, as well as the main material for realizing of pre-measurement surveys for obtaining of maximum information without using of ultrasonic testing.

REFERENCES

[1] Kurashkin A.V. Investigation of the acoustoelastic effect in an anisotropic plastically deformed material (in Russian) // Acoustical Physics, 2019. Vol. 65. No. 3. pp. 382-388.
[2] Zarembo L. K., Koshkina E. N., Chunchuzov I. P. Mutual transformation of longitudinal and shear waves in an inhomogeneous isotropic medium (in Russian) // Acoustical Physics. 1984. Vol. 30. No. 6. pp. 781-784.
[3] Vatulyan A. O., Yavruyan O. V., Bogachev I. V. Identification of inhomogeneous properties of an orthotropic elastic layer (in Russian) // Acoustical Physics. 2013. Vol. 59. No. 6. pp. 752-758.
[4] Brun M., Guenneau S., Movchan A.B., Begoni D. Dynamics of structural interfaces: Filtering and focusing effects for elastic waves // J. Mech. Physics Solids. 2010. Vol. 58. pp. 1212–1224.
[5] Khlybov, A.A. Studying the Effect of Microscopic Medium Inhomogeneity on the Propagation of Surface Waves // Russ. J. Nondestruct. Test. 2018. Vol. 54. pp. 385–393.
[6] Panasyuk O. N. Analysis of the influence of boundary conditions on wave propagation in layered composite materials (in Russian) // Applied Mechanics. 2014. Vol. 50. № 4. pp. 52–58.
[7] Abbakumov, K.E., Vagin, A.V. Dispersion Equation for Longitudinal Waves in a Layered Medium with Inhomogeneous Boundary Conditions in Different Propagation Directions // Russ. J. Nondestruct. Test. 2020. Vol. 56. pp. 20–27.
[8] Rytov S. M. Acoustic properties of a fine-layered medium (in Russian) // Acoustical Physics. 1956. Vol. 2. No. 1. pp. 71-83.
[9] Brekhovskikh L. M. Waves in layered media (in Russian). Moscow: Nauka, 1973. 340 p.
[10] Abbakumov K. E., Vagin A.V. Wave processes in a layered micro-homogeneous medium with inhomogeneous boundary conditions (in Russian) // Izvestia SPbGETU "LETI". 2019. No. 5. pp. 12-19.
[11] Abbakumov K. E., Vagin A.V. Wave processes in a layered medium (in Russian) // Izvestia SPbGETU "LETI". 2018. No. 8. pp. 87-91.
[12] Panasyk O.N. Propagation of Quasishear Waves in Prestressed Materials with Unbonded Layers // Int. Appl. Mech. 2011. Vol. 47. pp. 276–282.
[13] Jose M. Carcione anisotropic Q and velocity dispersion of finely layered media // Geophysical Prospecting. 1992. Vol. 40. pp. 761–783.
[14] Luk'yashko O.A., Saraikin V.A. Transient one-dimensional wave processes in a layered medium // Journal of Mining Science. 2007. Vol. 43. pp. 145–158.
[15] Gei M., Bigoni D., Franceschini G. Thermoelastic small-amplitude wave propagation in nonlinear elastic multilayers // Math. and Mech. of Solid. 2003. № 1. pp. 27–36.

[16] Brun M., Guenneau S., Movchan A.B., Bigoni D. Dynamics of structural interfaces: Filtering and focusing effects for elastic waves // J. Mech. Physics Solids. 2010. № 58. pp. 1212–1224.
[17] Shermergor T. D. Theory of elasticity of micro-homogeneous media (in Russian). Moscow: Nauka, 1977. 400 p.
[18] Dubinskii, S.V., Sevastyanov, F.S., Golubev, A.Y., Denisov, S. L., Kostenko, V. M., Zharenov I. A. A Computational and Experimental Study of the Effect of Vibroacoustic Loads on the Structural Performance of Composite Skin-Stringer Joint // Acoustical Physics. 2019. Vol. 65, pp. 359–368.
[19] Evel'son R.L A fine-layered medium of finite-thickness in an electromagnetic field // Journal of communications technology and electronics. 2015. Vol. 60. I. 6. pp. 552–559.
[20] Chaban I. A. Calculation of effective parameters of micro-homogeneous media by the self-consistent field method (in Russian) // Acoustical Physics. 1965. No. 1. pp. 102-109.
[21] Chaban I. A. The self-consistent field method in application to the calculation of effective parameters of micro-homogeneous media (in Russian) // Acoustical Physics. 1964. No. 3. pp. 351-358.
[22] Vavakin A. S., Salganik R. L. Effective elastic characteristics of bodies with isolated cracks, cavities and rigid inhomogeneities (in Russian) // Solid State Mechanics. 1978. No. 2. pp. 95-107.
[23] Floquet M.G. Sur les equations differentielles lineaires a coefficients periodiques // Annales scientifiques de l'Ecole Normale Superieure. 1983. vol. 12. pp. 47–88.
[24] Non-destructive testing. Volume 3. Ultrasonic control / ed. by V. V. Klyuev. Moscow: Mashinostroenie. 2004. 864 p.
[25] Tartarovsky B. D. On the transition of sound waves through the boundaries of solid and liquid media (in Russian) // Technical Physics. 1949. № 10. p. 1126.
[26] Abbakumov K. E., Golubev A. S. Evaluation of acoustic properties of thin stratifications and single-line nonmetallic inclusions in steel sheets (in Russian) // Russ. J. Nondestruct. Test. 1982. No. 9. pp. 22-31.
[27] Vorob'ev E. A. The theory of ultrasonic vibrations as a basis for the construction and application of technical means of information obtaining (in Russian) // St. Petersburg: Publishing House of SPbGUAP. 2002. 54 p.
[28] Kupradze V. D., Sobolev S. L. Elastic waves at the boundaries of two media (in Russian) // Trud. Seismic. Inst. AN USSR. 1930. No. 10. pp. 58-67.

Konstantin Abbakumov *is Doctor of Engineering Science, Professor, Head of Electroacoustic and Ultrasonic Engineering Department of St. Petersburg Electrotechnical University "LETI", Honored Scientist of Russian Federation.*
Konstantin Abbakumov has 45 years experience in scientific and educational work. Scientific areas of interest are acoustical methods of nondestructive testing, wave processes in nonhomogeneous media, diffraction of elastic waves at nontypical objects. Educational work: graduating of bachelors, masters and postgraduates by «Instrument Engineering» program and development of scientific-methodological documents in higher education field. He published over 200 scientific papers, including 5 monographs and 10 patents. Konstantin Abbakumov is Head of the scientific-methodological Counsel in Federal educational-methodological association "Photonics, instrument engineering, optical and bio-technical systems and technologies". He is 3rd grade specialist in acoustic methods of nondestructive testing.

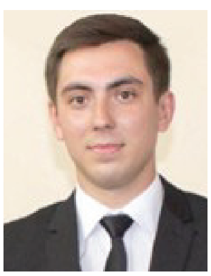

Anton Vagin *is Master student of Electroacoustic and Ultrasonic Engineering Department of St. Petersburg Electrotechnical University "LETI", design engineer of the 3rd category of «Concern «Okeanpribor» JSC.*
Anton Vagin is a specialist in the field of signals processing for acoustic sounders, sidescan sonars. He also studies wave propagation in layered and thin-layered media. Vagin Anton is the author of 8 scientific researchers on the subject of processing of hydroacoustic signals and theory of layered media.

Alena Vjuginova *is Ph. D. of Engineering Science, Assistant Professor of Electroacoustic and Ultrasonic Engineering Department of St. Petersburg Electrotechnical University "LETI", Deputy Head of Electroacoustic and Ultrasonic Engineering Department for scientific work.*
Alena Vjuginova is a specialist in the field of low frequency and resonance ultrasonic systems, ultrasonic transducers, power ultrasonic technologies, acoustical methods of nondestructive testing and others. Alena Vjuginova is the author of over 30 scientific works, she is author and co-author of 10 patents, co-author of teaching aids.

Paper No.371/2021

ATTENUATION OF THE INPUT SIGNAL BY PROTECTIVE AND FIXING TOOLS FOR HEARING AIDS AND COCHLEAR IMPLANTS

[a] Sergei Levin, [b] Gaziz Tufatulin [c] Inna Koroleva, [d] Viktoriia Vasilyeva, [e] Elena Levina

[a, b, c] Center of pediatric audiology, St. Petersburg, Russia
[b, c, e] St. Petersburg scientific research Institute of ear, throat, nose and speech, St. Petersburg, Russia
[a, b] North-Western State Medical University named after I.I. Mechnikov, St. Petersburg, Russia
[d] The department of Ecology and Industrial Safety, Baltic State Technical University 'VOENMEH' named after D.F. Ustinov, St. Petersburg, Russia
[a] dr.tufatulin@mail.ru, [b] megalor@gmail.com, [c] prof.inna.koroleva@mail.ru, [d] viktoria1107568@mail.ru, [e] xramoval@gmail.com

Abstract: *The aim was to study amount of attenuation of input signal at the hearing aid (HA) or cochlear implant sound processor (SP) microphone by different protective tools or clothes. Materials and methods. The acoustic measurements were conducted in the soundproof cabin using artificial head with HA/SP and different protective tools, which can influence on microphone function. Probe microphone was integrated in the microphone input of SP and connected with HA verification system. Results. The biggest amount of signal attenuation was observed using water-resistant cases for SP. Changes affect the speech spectrum, therefore using such protective tools can lead to decrease of speech intelligibility. Maximum attenuation was 9.36±0.33 dB at 4000 Hz. Non-hermetic membrane protective cases gave maximum attenuation 7.67±0.18 dB (5000 Hz). Clothes which cover head lead to significant change of signal at microphone up to 9.24±0.16 dB mostly at high-frequencies, which less influences on speech intelligibility. The results confirm that clothes and protective tools for HA of SP show significant attenuation of sounds.*

Keywords: *hearing loss and deafness, sensorineural hearing loss, cochlear implant, hearing aid, hearing aid's verification, speech intelligibility.*

DOI: *: 10.36336/akustika202141163*

1. INTRODUCTION

Hearing loss is a global problem of the modern world. According to the World Report on Hearing (WHO, 2021) more than 1.5 billion people worldwide have hearing problems and 430 million need special care [1]. Hearing receptor damage (neuroepitelium in the inner ear) occurs in the most cases of permanent hearing loss. There are hitherto no methods of drug therapy or surgery of sensorineural hearing loss, so technical devices – hearing aids (HA) and cochlear implants (CI) remain as a primary approaches of hearing correction. HAs are used for amplification in cases of mild, moderate and moderately-severe hearing loss, but severe and profound hearing loss is indication for cochlear implantation [2].

HA – is mostly digital amplification device, which includes a microphone (or several microphones in directional systems), analogue-digital and digital-analogue converters, processor, receiver, acoustic path, battery, manual volume control and/or program button. There are several types of HAs depending on placement at the body: behind-the-ear, in-the-ear, completely-in-the-canal. Behind-the-ear HA's mold is located behind the patient's pinna and amplified sound gets the ear canal through the tube and earmold. All parts of in-the-ear and completely-in-the-canal HA's are completely located in the individual mold, which is made according to the ear impression [3].

CI system consists of an external component (speech processor, SP) and an implant. The implanted part includes an electrode array, which is inserted in the tympanic duct, ground electrode and an implant itself. [4] Cochlear implantation is a surgical operation, which is held once in a lifetime and in the absence of some consequences implant replacement isn't supposed to occur. SP includes a microphone, an analogue-digital converter, a processor, a battery, and a magnet (stimulator). Data transferring to the implanted part is held transcutaneous through magnet fixation. SP could be behind-the-ear or like a round magnet, which is located on the patient's head [5] (Fig. 1).

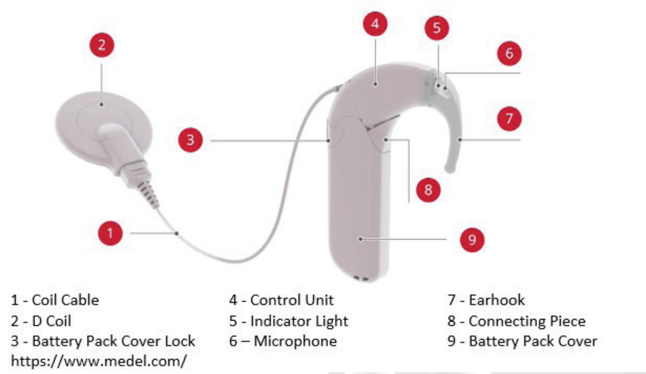

Fig. 1: Speech processor Medel "Opus 2"

Permanent and adequate sound stimulation of the auditory cortex is critically important for hearing impaired patients, especially for children. That's why, it's highly recommended to use HA and SP during all day [6]. Pedagogical and medical rehabilitation is no less important [7,8].

Accordingly, most time these devices are adjacent to a human body and expose to sweat, humidity and dirt. It's especially actual in paediatric practice. Changes in microphone quality will affect speech intelligibility. In childhood, this can cause impairment or delay in hearing and speech development [9]. Therefore, patients are recommended to use drying tools. Furthermore, most of the modern HAs and SPs have certain water resistance (IP 58/68 in HAs, IP 54/68 in SPs). Alas it doesn't solve this problem each time. Besides that, the above-mentioned water resistance doesn't allow a patient to swim with HA or SP. For these purposes manufacturers offer different cases for protection against a rain, sweat, for swimming or additional fixation (Fig. 2). In cool seasons the microphone of HA or SP can be covered with a knit cap, hoods or shawls [10].

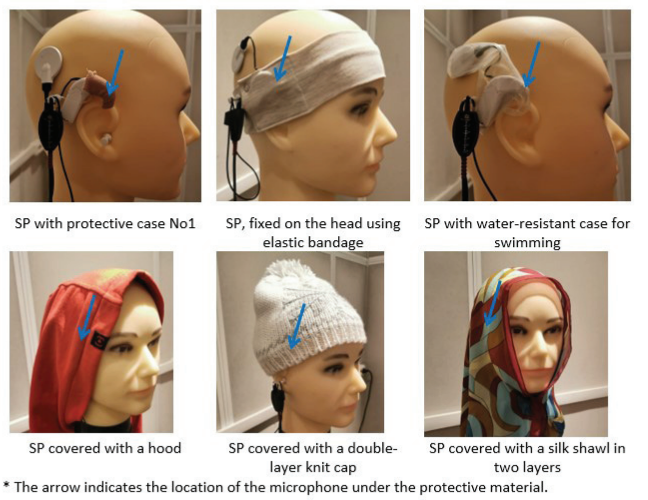

Fig. 2: Examples of protective devices

In clinical practice specialists often encounter with patients' or parents' questions about the amount of sound attenuation by cases or clothes and how it can influence on sound quality and speech intelligibility. We didn't find some studies on this topic in the literature or databases.

Goal: study the amount of attenuation input signal at the microphone of HA and SP using different cases and clothes.

2. MATERIALS AND METHODS

The study was conducted in soundproof cabin at Saint Petersburg Research Institute of Ear, Nose, Throat and Speech and Center of Paediatric Audiology (St Petersburg, Russia). Acoustic measurements were carried out using an artificial head and different objects, which can influence on microphone function of HA and SP. A probe microphone was integrated in the microphone input of behind-the-ear SP (the same shape with behind-the-ear HA) (Fig.3).

Fig. 3: Behind-the-ear SP with integrated probe microphone

The acoustic parameters measured by Interacoustics Affinity 2.0 verification system which was connected with a probe microphone. REAR (Real Ear Aided Response) protocol was used with free-field stimulation. As a stimulus International Speech Test Signal (ISTS) was chosen. ISTS – is a mixture of different phonemes of many languages, which makes it valid for HA verification all around the world [11]. Signal level - 65 dB SPL. Stimulus duration – 12 s. Frequency range – 200-8000 Hz. Recording method – 1/3 octave weighted.

Each measurement conducted with an artificial head to minimize influence of ambient and biological noise on test results. During the experiment SP was located on the right ear, the distance between loudspeaker and the center of artificial head 1 meter, azimuth 0^0. Sequential measurements were conducted in following conditions:

1. SP without any protective tools.
2. SP with protective case No 1.
3. SP with protective case No 2.
4. SP with protective case No 3.
5. SP with water-resistant case for swimming.
6. SP, fixed on the head using elastic bandage
7. SP covered with a hood.
8. SP covered with a double-layer knit cap.
9. SP covered with a silk shawl in two layers.

Several measurements were conducted for each condition. Total number of measurements is 99. After the data export, it was analyzed in notepad++, Excel and Statistica 12 for visual and digital differences representation. Statistical significance of the differences in sound pressure levels in different measurement conditions estimated for each frequency in 1/3 octave filters: 200, 250, 315, 400, 500, 630, 800, 1000, 1250, 1600, 2000, 2500, 3150, 4000, 5000, 6300, 8000 Hz. U-criteria of Mann-Whitney was used.

3. RESULTS

During the study the reference sound pressure level on the microphone of SP without any additional tools were compared with the sound pressure level measured with different tools. Results for tissue protective cases presented on Fig. 4.

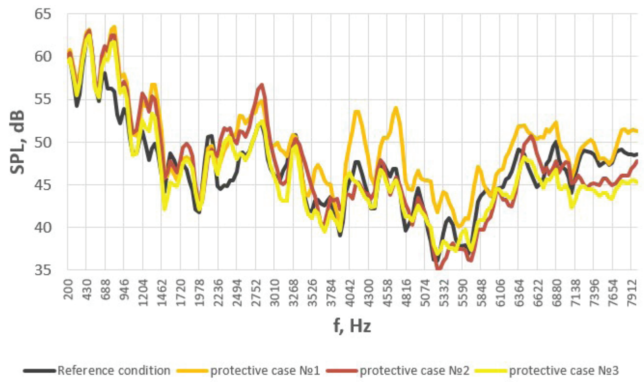

Fig. 4: Comparison of sound pressure level at the microphone in reference condition and with tissue protective cases

Comparison of frequency characteristics showed that most distortion brought protective tissue case No1. Sound pressure levels with and without case No1 significantly differ at 200, 800, 1250, 1600, 2500-3150 and >5000 Hz (***p***<0.05) (Tab. 1).

1/3 octave band, Hz *	200	800	1250	1600	2500	3150	5000	6300	8000
Maximum difference, dB	0,94	**7,57**	**7,42**	5,75	5,27	3,95	**7,67**	5,58	2,92
St Dev	0,23	0,36	0,73	0,47	0,64	0,34	0,18	0,35	0,43

** only **p** <0.05 frequencies shown*
Tab. 1: Differences in sound pressure level between reference condition and protective case No1

With protective case No2 the significant differences were found at 200, 800-1250, 2500 and 8000 Hz (***p***<0.05) (Tab. 2).

1/3 octave band, Hz *	200	800	1250	2500	8000
Maximum difference, dB	0,60	**6,58**	**6,05**	**6,67**	4,25
St Dev	0,22	0,25	0,66	0,29	0,08

** only **p** <0.05 frequencies shown*
Tab. 2: Differences in sound pressure level between reference condition and protective case No2

Protective case No3 leads to minimal influence on microphone effect. Differences were found at 800, 1250, 2500–3150 and >8000 Hz (***p***<0.05) (Tab. 3).

1/3 octave band, Hz *	800	1250	2500	3150	8000
Maximum difference, dB	**5,77**	4,09	**5,52**	4,28	4,45
St Dev	0,28	0,67	0,54	1,11	0,11

** only **p** <0.05 frequencies shown*
Tab. 3: Differences in sound pressure level between reference condition and protective case No3

The largest amount of signal changes was observed at near 817 Hz band with all the cases. Maximum signal absorbing by tissue case No3 was 5.77±0.28 dB in contrast with more thick tissue cases No2 (6.67±0.29 dB) and No1 (7.67±0.18 dB).

Influence of water-resistant swimming case (IP68) for SPs on microphone effect. Case for swimming is soft silicone tool with zip-lock. Water-resistant case leads to signal attenuation at the microphone at the most of 1/3 octave bands (12 out of 17; ***p***<0.05) (Tab. 4).

1/3 octave band, Hz *	200	315	400	500	800	1250	1600	2000	4000	5000	6300	8000
Maximum difference, dB	1,06	2,66	4,63	5,29	**6,54**	5,20	5,15	5,49	**9,36**	4,96	**8,09**	3,98
St Dev	0,27	0,21	0,20	0,29	0,27	0,55	0,51	0,82	0,33	0,18	0,52	0,80

** only **p** <0.05 frequencies shown*
Tab. 4: Differences in sound pressure level between reference condition and water-resistant case

Maximum signal attenuation was 9.36±0.33 dB (Fig. 5).

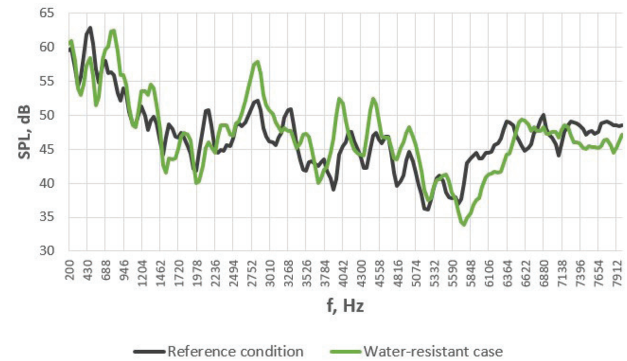

Fig. 5: Evaluation of water-resistant case effect on sound pressure level

On the next step signal distortions with elastic bandage were measured (Fig. 6).

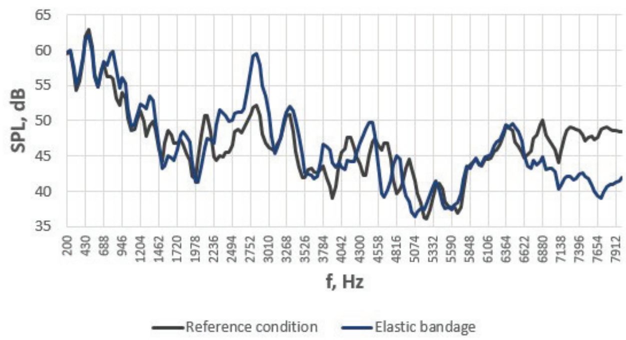

Fig. 6: Measurements of the elastic bandage effect on sound pressure level at the microphone

Maximum differences between an elastic bandage and reference condition were 9.73±0.35 dB (Tab. 5).

Tab. 5. Differences in sound pressure level between reference condition and elastic bandage.

1/3 octave band, Hz *	800	1250	1600	2500	5000	8000
Maximum difference, dB	3,93	4,26	3,67	**7,17**	**7,60**	**9,73**
St Dev	0,22	0,65	0,03	0,77	0,18	0,35

** only p <0.05 frequencies shown*

Maximum differences were observed in high frequency non-speech region 5000, 8000 Hz (***p***<0.05). It can be assumed that these differences might be related to resonance of bandage and sound field. At low and middle frequencies (speech spectrum) differences were minimal.

Different elements of clothes influence on signal level. It was shown that a hood leads to maximum signal attenuation if it fits to the body quite snugly (Fig. 7). A knit cap shows a small influence, and ashawl causes the smallest one. The most prominent changes in frequency characteristics with hood were observed at 4000-8000 Hz.

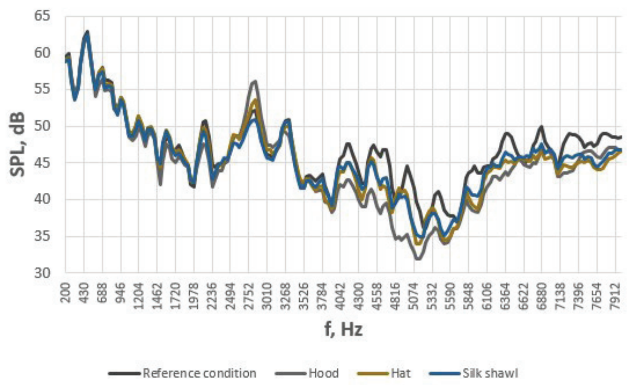

Fig. 7: Influence of different clothes on sound pressure level at the microphone of SP
** only p <0.05 frequencies shown*

1/3 octave band, Hz *	1600	3150	4000	5000	6300	8000
Hood*						
Maximum difference, dB	2,08	4,04	5,61	**9,24**	**6,09**	5,31
St Dev	0,63	0,43	0,45	0,16	0,06	0,17
Knit cap*						
Maximum difference, dB				**6,14**	5,47	4,67
St Dev				0,16	0,65	0,38
Silk shawl*						
Maximum difference, dB				**5,50**	3,87	3,83
St Dev				0,08	0,85	0,29

Tab. 6: Differences in sound pressure level between reference condition and SP covered with different clothes

A hood led to maximum attenuation 9.24±0.16 dB. Significant difference was detected at 1600, 3150-8000 Hz (***p***<0.05). The knit cap and the shawl demonstrated less changes. In case of a knit cap significant differences were confirmed at 5000, 6300, 8000 Hz. Maximum attenuation – 6.14±0.16 dB. A shawl caused minimal differences mostly at 5000, 6300, 8000 Hz, maximum 5.50±0.08 dB.

4. CONCLUSION

Hearing aids and cochlear implants are effective rehabilitation methods of hearing impaired patients. It's necessary to protect a microphone from humidity, cold and wind. For this purpose, different clothes and protective tools are used. The study of the microphone input signal attenuation by these objects was conducted. The most significant attenuation was observed in the water-resistant case for swimming. The changes were detected at the most 1/3 octave frequency bands (12 out of 17). The most of them are located at the speech spectrum, which can lead to a significant decrease of speech audibility, intelligibility and quality. Maximum attenuation by water-resistant case is 9.36±0.33 dB at 4000 Hz. The usage of membrane tissue protective cases helps to avoid penetration of sweat, humidity into HA or SP, as well as protects them from a wind noise, showed that they give 7.67±0.18 dB attenuation at 5000 Hz. The most amount of amplification was demonstrated with a membrane case, which has maximum sweat protection. In contrast, a textile case demonstrated less attenuation. Fixing bandage influences on sound pressure level as well, especially at middle-high frequency region. Different types of head covering clothes lead to a significant signal changing up to 9.24±0.16 dB, primarily on high frequencies, which less influence on speech intelligibility.

The results of the study confirm that using different tools to protect HA of SP leads to a significant change of input signal.

The acoustic input signal measurements, presented in this paper, could be used in the certification process of new protective tools for HA and SP, which might allow to control their quality and effects. Audiologists also should use real-ear measurements with protective cases during HA verification process in their clinical practice. The information about signal attenuation must be taken into account during HA fitting to make this case acoustically transparent.

REFERENCES

[1] World Report on Hearing [Electronic resource]. WHO. Available at: https://www.who.int/publications/i/item/world—report—on—hearing. Accessed May 1, 2021.
[2] Tavartkiladze GA. Rukovodstvo po klinicheskoi audiologii. M.: Meditsina; 2013. (In Russ.)
[3] Dillon H. Hearing aids. Second edition. Sydney : Boomerang Press ; New York : Thieme, 2012 ISBN: 9781604068115.
[4] Bilateral cochlear implantation / Kuzovkov V.E., Yanov Y.K., Megrelishvili S.M., Levin S.V. // Rossiyskaya otorinolaringologiya.-2010.-№1(44).-C.-50-57.
[5] Eisenberg. Clinical management of children with cochlear implants. 2nd edn L S Eisenberg Plural Publishing, 2016 ISBN 9781597567237
[6] Spoken language and everyday functioning in 5—year—old children using hearing aids or cochlear implants / L. Cupples, T.Y. Ching, L. Button [et al.] // Int. J. Audiol. – 2018. – Vol. 57, № 2. – P. 55—69.
[7] Koroleva IV. Reabilitatsiya glukhikh detey i vzroslykh posle kokhlearnoy i stvolomozgovoy implantatsii. SPb.: KARO; 2016.
[8] Long-term remote support of the patients with cochlear implants: the concept, methodology and experience / Kuzovkov V.E., Yanov Y.K., Vakhrushev S.G., Toropova L.A., [и др.] // Rossiyskaya otorinolaringologiya. – 2010. – № 6(49). – C. 31-39.
[9] Psychoacoustic tests for perceptual assessment of processor fitting in patients with cochlear implants / KOROLEVA I.V., OGORODNIKOVA E.A., LEVIN S.V., PAK S.P. // Vestnik of otorhinolaryngology.– 2021. – T. 86. – № 1. – C. 30-35. – DOI 10.17116/otorino20218601130.
[10] McCreery RW, Walker EA. Pediatric amplification. Enhancing Auditory Access. – San Diego, CA: Plural Publishing; 2017.
[11] Development and analysis of an international speech test signal (ISTS) / L. Holube, S. Fredelake, M. Vlaming, B. Kollmeier // Int. J. Audiol. – 2010. – Vol. 49, № 12. – P. 891—903.

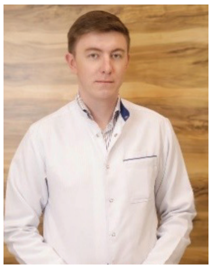

Gaziz Tufatulin *is PhD, ENT, audiologist. Head of Center of Paediatric Audiology, teaching assistant at the Department of Otorhinolaryngology, North-Western State Medical University named after I.I. Mechnikov (St Petersburg, Russia). Area of scientific interests – pediatric audiology, amplification and rehabilitation of hearing-impaired children. Author and co-author of more than 30 publications, 2 patents and 1 book. Creator of hydrovibrostimulation – an innovative method of rehabilitation deaf children before the cochlear implantation. Participant and moderator of many Russian and international conferences (St Petersburg, Moscow, Cape Town, Lisbon, Bucharest). He completed an internship on hearing aids and cochlear implants fitting in Austria and Turkey. A member of editorial board of "Pediatric pharmacology" journal. Author and host of "Conversations about hearing" TV - program.*

Sergey Levin *is Ph.D. of Medical Science, Assistant Professor of otorhinolaryngology chair of the Saint-Petersburg Research Institute of Ear, Throat, Nose and Speech Ministry of Healthcare in Russian Federation. At present, he is Senior Researcher of the electrophysiological laboratory of the department of diagnostics and rehabilitation of hearing impairments. Engaged in developments in the field of hearing research, cochlear implantation system, otoneurology. He is a member of the organization committees of conferences and seminars in the field of hearing loss in St. Petersburg and Moscow. Sergey Levin is the author of over 60 scientific publications, the author of 8 patents in the hearing loss. He presented the main results of scientific research at the international conferences in St. Petersburg, Moscow, Munich, Lisbon, Toulouse, Bucharest, Rome, Innsbruck, Istanbul, Chennai (India).*

Inna Koroleva *is PhD in physiology, DSc in psychology, Professor, Senior researcher of Department of Diagnostic and Rehabilitation of Hearing Disorders of Saint-Petersburg's Institute of ENT and Speech, Leader of Rehabilitation Department of Center of Pediatric Audiology, member of Presidium of Russian Audiological Society.*
Specialist in the field of speech perception, speech development, hearing impairment. The author of 700 publications in the fields- physiology of auditory system, speech perception, speech recognition, audiology, development of speech, speech and voice pathology, hearing disorders, rehabilitation of patients with cochlear implants. The author of 25 textbooks, handbooks, monographs, the co-author of 7 patents.
She presented the main results of scientific research at the international conferences in Austria, Belarus, Germany, France, India, Italy, Japan, Kazakhstan, Portugal, Russia, Turkey etc. Organize and lecture in the fields: rehabilitation of patients with cochlear implants, early intervention of hearing impaired children, diagnostic of hearing loss in Russia, Georgia, Belarus, Kazakhstan, etc.

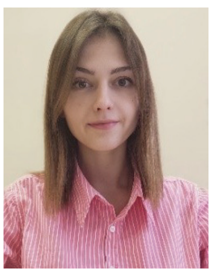

Viktoriia Vasilyeva *is Assistant of the Department of Ecology and Industrial Safety of the Baltic State Technical University "VOENMEH" named after D.F. Ustinov (St. Petersburg, Russia), Viktoriia Vasilyeva is engaged in research on the effects of noise on the human body. Development of methods for determining the individual body's response to noise with prevailing high and low frequencies. Author of scientific publications. Participant of scientific conferences on noise protection in St. Petersburg and Moscow.*

Elena Levina *is Ph.D. Sci., Associate Professor, Department of Otorhinolaryngology, St. Petersburg Research Institute of Ear, Throat, Nose and Speech, Ministry of Health of Russia. She is currently a Senior Research Fellow at the Department of Diagnostics and Rehabilitation of Hearing Disorders. Engaged in developments in the field of hearing research, cochlear implantation systems, otoneurology. She is the author of over 49 scientific publications, author of 6 patents on hearing loss. She presented the main results of scientific research at international conferences in Munich, Lisbon, Toulouse, Bucharest, Rome, Innsbruck, St. Petersburg, Moscow.*

Paper No.372/2021

THE SENSITIVITY ESTIMATION FOR THE ULTRASONIC ANGULAR VELOCITY SENSORS

[a] Nikolay Akhremenko, [b] Yasemin Durukan, [c] Ekaterina Popkova, [b] Mikhail Shevelko

[a, b, c, d] St. Petersburg Electrotechnical University "LETI",
Department of Electroacoustics and Ultrasonic Technology (UT), Saint-Petersburg, Russia
[a]naakhremenko@stud.etu.ru, [b] mmshevelko@etu.ru, [c] espopkova@etu.ru, [d] mmshevelko@etu.ru

***Abstract**: The paper discusses the principles of the occurrence of inherent noise of the sensitive element of the angular velocity sensor, the calculation of these noises and methods of their reduction. The principle of operation of the sensing element of the angular velocity sensor on bulk acoustic waves, which consists in detecting the rotation of the polarization vector of the emitted linearly polarized shear wave, is presented in the work. The results of calculations of the noise level for various materials and sizes of plate piezoelectric transducers and acoustic duct are presented in the work. It is shown that a sensitive element with plate piezoelectric transducers made of langasite and an acoustic duct made of glass, a heavy flint, has a minimum noise level. It is shown that with an increase in the operating frequency of a plate piezoelectric transducer, the noise level decreases. A program for calculating the noise characteristics of solid-state angular velocity sensors based on bulk acoustic waves has been developed. The element base of the receiving amplifier of the device has been selected. Recommendations for reducing the level of noise are formulated, such as: increasing the operating frequency and reducing the bandwidth of plate piezoelectric transducers, as well as the choice of optimal materials for both piezoelectric transducers and acoustic duct.*

***Keywords:** thermal noise, inherent noise, acoustic duct, piezo transducer noise.*

***DOI:** : 10.36336/akustika202141168*

1. INTRODUCTION

In recent years, interest has increased in the possibility of using solid-state gyro sensing elements based on the characteristics of acoustic wave propagation, since they are able to function quite well under high loads and strong vibration, unlike most other types of angular velocity sensors [1] - [2]. Therefore, it is a relevant and promising direction in the modern motion sensor development.

The receiving and amplifying path of acoustoelectronic devices operating on bulk acoustic waves (BAW) can be represented as a block diagram shown in Fig. 1.

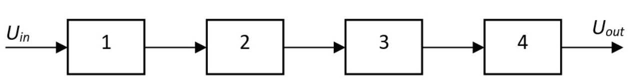

Fig. 1: Simplified block diagram of the receiving and amplifying path of acoustoelectronic devices
Uin – input voltage, 1 – emitting piezoelectric transducer, 2 – acoustic duct, 3 – receiving piezoelectric transducer, 4 – signal amplifier, Uout – output voltage.

The value of the informative signal of the sensing element of the angular velocity sensor on bulk acoustic waves lies in the range of fractions to tens of mV and is subject to interference and noise. Thus, the problem of assessing the level of the noise arising at the output of the sensitive element plays an important role in improving the parameters of the sensitive elements of angular velocity sensors on bulk acoustic waves, selecting the dimensions of the acoustic duct and transducer, as well as the materials of which they are composed.

2. SOLID STATE MOTION SENSORS ON BULK ACOUSTIC WAVES

Currently, there are a number of implementations of bulk acoustic wave motion sensors proposed by the authors of this paper [3]. The principle of operation of such sensors is based on the detection of secondary vibrations of the shear wave caused by the influence of the Coriolis force under rotation. The generation of secondary oscillations with frequency ω for a transverse wave propagating along the axis of rotation of the acoustic duct is shown in Fig. 2.

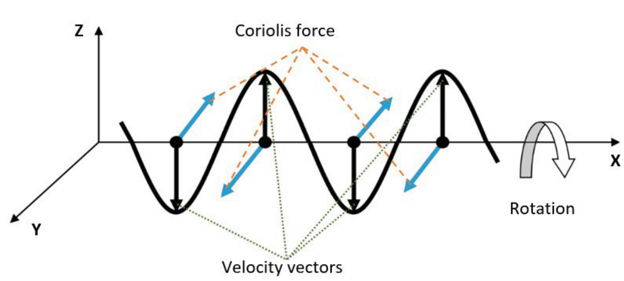

Fig. 2: The generation of secondary oscillations with frequency ω for a transverse wave propagating along the rotation axis of the acoustic duct under rotation

Physically, the formation of secondary oscillations can be considered as a rotation of the polarization vector of the emitted linearly polarized shear wave, which occurs as the wave propagates. The angle of rotation $\boldsymbol{\beta}$ is proportional to the angular velocity of rotation $\boldsymbol{\Omega}$ of the object and is determined by the following relation:

$$\boldsymbol{\beta = \tau\Omega} \qquad (1)$$

where
$\boldsymbol{\tau}$ is the propagation time of the acoustic wave along the acoustic duct.

In this case, the orthogonal component of the polarization vector arising from the displacement arising from the presence of rotation is determined by the following expression:

$$\boldsymbol{\xi_c = \xi_0 \sin(\tau\Omega) = \xi_0\tau\Omega} \qquad (2)$$

where
$\boldsymbol{\xi_0}$ is a displacement amplitude of the radiated BAW.

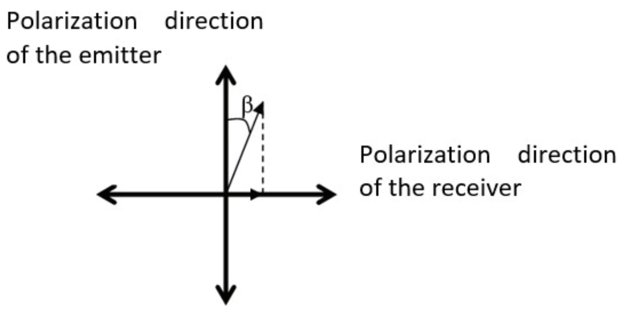

Fig. 3: The polarizations direction of the emitter and receiver

Fig. 4 shows a tract design for such a rotation sensor.

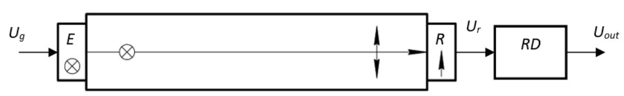

Fig. 4: The design of the tract of the angular velocity sensor on BAW

Where
U_g *is a generator voltage,*
E *– emitting piezoelectric transducer,*
R *– receiving piezoelectric transducer,*
RD *– receiving device,*
U_r *– receiving voltage,*
U_{out} *– output voltage.*

The sensing element of the angular velocity sensor on bulk acoustic waves is a solid-state acoustic conduit, which can be made in the form of a cylinder (the main condition is the presence of plane-parallel ends), on the opposite ends of which plate emitting and receiving piezoelectric transducers are located. In this case, the sound conductor must be made of an isotropic material, for example, glass, and the sensitivity axes of the piezoelectric transducers must be shifted by 90 degrees relative to each other.

The applied voltage to the emitter excites linearly polarized waves in the acoustic conductor, the polarization vector of which rotates as the wave propagates, due to the presence of rotation, the signal Ur received by the receiving transducer, proportional to the value $\boldsymbol{\xi_c}$, Goes to the receiving device PU, at the output of which a voltage is generated $\boldsymbol{U_{out}}$ proportional to the input signal level.

Thus,

$$\boldsymbol{U_{out} = U_g(K_{SE}\tau\Omega)K_{RD}} \qquad (3)$$

where
$\boldsymbol{U_g}$ is a generator voltage;
$\boldsymbol{K_{SE}}$ is a sensor transmission coefficient;
$\boldsymbol{K_{RD}}$ – receiver gain.

The sensitivity of the sensor built according to this scheme will be determined by the signal-to-noise ratio at the input of the receiving device and will not depend on $\boldsymbol{K_{RD}}$.

3. SENSITIVITY OF SENSORS ON BULK ACOUSTIC WAVES

As mentioned above, the ability of BAW solid-state motion sensors to detect an informative signal associated with rotation is determined by the level of noise at the input of the receiving device, the evaluation of the inherent noise is an important task in determining the sensitivity of the device. All the noises arising in devices of this type can be divided into:
- Acoustic duct noises caused by thermal vibrations of the crystal lattice of a solid;
- thermal noise of the piezoelectric receiver of acoustic waves;
- preamplifier noise.

The theory that describes the noise arising in the sound line and the piezoelectric receiver is described in the works [4-9].

In order to estimate the total noise level at the output of the sensitive element of the solid-state angular velocity sensor, it is necessary to carry out the energy addition of the thermal noise of the piezoelectric transducer and the noise of the crystal lattice of the acoustic duct, taken by the transducer according to the formula:

$$\boldsymbol{U_\Sigma = \sqrt{U_{n,p}^2 + U_{n,s}^2}} \qquad (4)$$

Fig. 5 shows the dependence of the thermal noise voltage of the piezoelectric transducer, the noise of the crystal lattice of the acoustic duct and the total noise at the output of the sensitive element on the antiresonant frequency of the piezoelectric transducer. In the calculation, a piezoelectric transducer with a radius of ***a = 4 mm***, made of piezoquartz, a sound conductor made of fused quartz, was used, the propagation time of an acoustic wave in acoustic duct is ***τ = 1 μs***.

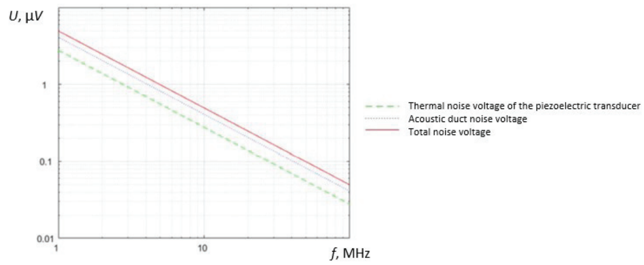

Fig. 5: Dependence of the noise voltage on the antiresonant frequency of the piezoelectric transducer

An important noise characteristic of a piezoelectric receiver is the signal-to-noise ratio at the output of the piezoelectric receiver:

$$\boldsymbol{N = 20\lg\frac{U_c}{U_\Sigma}} \qquad (5)$$

For reliable signal reception and its separation from the background noise, the signal-to-noise ratio should be at least 6 dB. Therefore, the value of the minimum received signal must be at least 2 times higher than the total noise signal.

4. CALCULATION SOFTWARE FOR SENSITIVE ELEMENT NOISE CHARACTERISTICS OF ANGULAR VELOCITY SENSOR

To ensure the calculation of the noise characteristics of the sensitive element of the angular velocity sensor, namely the thermal noise of the piezoelectric receiver and the noise of the crystal lattice of the acoustic duct, a special software program was developed that allows calculating all the necessary noise characteristics of the sensitive element with the specified parameters.

Figure 6 shows the block diagram of the developed algorithm. After entering the characteristics and choosing the materials for the acoustic duct and piezo transducers, the program calculates the parameters of the sensitive element, the noise voltage of the acoustic duct and the transducer, the total noise and the minimum voltage of the received signal.

The calculating result for all characteristics of the sensitive element is displayed in special fields. The program also allows to calculate and display a graph of the dependence of the noise voltage on the center frequency of the piezoelectric receiver on a logarithmic scale.

Thus, the program realizes a quick estimation of the optimal characteristics of the sensitive element of BAW gyro sensor.

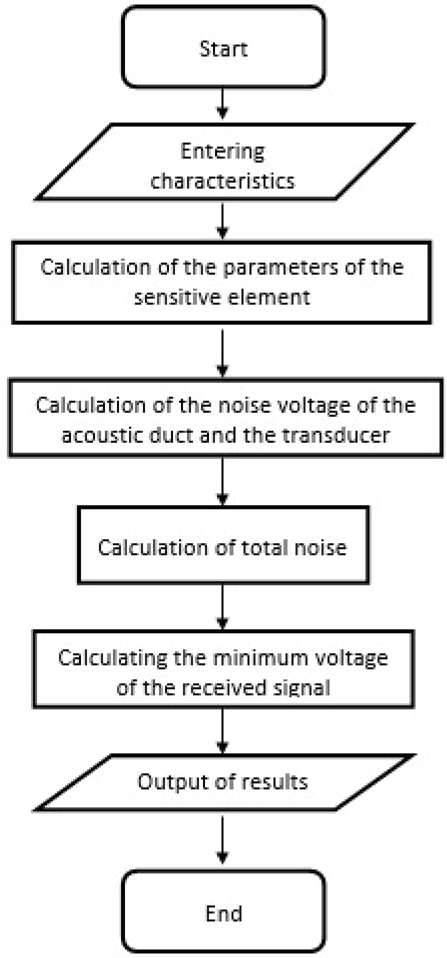

Fig. 6: Block diagram of the operation algorithm of the program for calculating the noise of the sensitive element of the angular velocity sensor

5. CALCULATIONS RESULTS

Tab. 1 shows the calculation results for total noise voltage of the sensing element for various materials of the acoustic duct and piezoelectric transducer.

Piezo receiver Acoustic duct	Piezoquartz	Lithium niobate	Lithium tantalate	Langasit
Fused quartz	0,492	3,135	1,656	0,326
Chalcogenide glass (HCG)	0,581	3,637	1,919	0,383
Heavy flint glass - 10 (HF-10)	0,436	2,801	1,481	0,291

*Tab. 1: Dependence of noise voltage (**U_Σ, µV**) on the materials of the sensitive element*

As can be seen, the least noise sensitive element is the one with the piezoelectric transducer made of langasite, and the acoustic duct made of a heavy flint glass.

Tab. 2 shows the calculation results for the voltage of the acoustic duct noise (TF-10), thermal noise of the piezoelectric transducer for a flat piezoelectric transverse wave receiver (LiNbO3), as well as the total noise of the sensitive element depending on the antiresonant frequency of the piezoelectric transducer and the wave propagation time in the acoustic duct.

Antiresonant Frequency [MHz]	Wave propagation time τ [μs]	Acoustic duct noise voltage $U_{n,a}$ [μV]	Noise voltage piezoelectric transducer $U_{n,r}$ [μV]	Total noise voltage U_{Σ} [μV]
10	0,5	3,159	2,125	3,807
	1	2,321	1,569	2,801
	1,5	1,906	1,293	2,303
50	0,5	0,659	0,449	0,805
	1	0,472	0,318	0,569
	1,5	0,384	0,262	0,464
100	0,5	0,335	0,225	0,404
	1	0,236	0,159	0,284
	1,5	0,192	0,131	0,233

Tab. 2: Sensing element noise characteristics

As can be seen from the table, the noise values of the acoustic duct and the transducer are of comparable orders.

6. RECEIVER NOISES

The noise properties of the receiving device are largely determined by the noise ratio of the receiving amplifier, which is determined at a given frequency of the input signal under the same temperature conditions at the input and output of the stage as the ratio of the total noise power at the output to the part created by their amplification. A state-of-the-art ultralow noise amplifier should be used to minimize noise. For example, a modern amplifier based on the MCP6286 microcircuit is capable of operating at high frequencies up to 100 MHz and has a gain of about 120 dB.

Currently, there are many ultra-low noise amplifiers operating at high frequencies. Tab. 3 lists examples of ultra-low noise amplifiers and their characteristics.

Manufacturer	Model	Frequency range [μs]	Gain [dB]	Noise voltage at 10 MHz, [μV]	Price[$]
Analog Devices	ADA4898-1	1-100	135	0,278	2,27
	LTC6229	0,1-100	103	0,285	1,56
Microchip Technology	MCP6286	1-100	120	1,707	0,96

Tab. 3: Main characteristics of modern ultra-low noise amplifiers

Its noise level is ***5.4 nV/√Hz***, that is, it is of the same order as the inherent noise of the sensing element. According to the comparison of the total level of thermal noise with the signal at the output of the sensitive element, the achievable sensitivity of the sensors of the considered type can reach tenths or even hundredths of a degree per second.

Thus, the correct approach to the selection of a preamplifier for a solid-state sensor based on BAW can minimize the noise of the receiving device. Then the intrinsic noise of the sensor will be determined to a greater extent by the noise of thermal vibrations of the piezoelectric transducer and the crystal lattice of the acoustic duct.

7. CONCLUSIONS

In this paper, the design of the sensing element of the angular velocity sensor based on bulk acoustic waves was presented, and the article also describes the main mechanisms of occurrence and types of noise that appear in the described sensing element of the angular velocity transducers based on BAW. To automate the determination of the noise characteristics of the sensors, a program was developed for calculating the noise characteristics of solid-state angular velocity sensors based on BAW.

Several methods have been identified to increase the sensitivity of a solid-state acoustic gyro by reducing the noise level at the input of the receiving-amplifying path of the device. This reduction can be achieved by:

- selection of a piezoelectric transducer operating at higher frequencies;
- reduction of the effective frequency band of the piezoelectric transducer;
- selection of optimal materials for the piezoelectric transducer and acoustic duct.

REFERENCES

[1] Gribkova, A. Peregudov and M. Shevelko Theoretical and experimental researches of the bulk acoustic waves' availability in angular motion sensors // Proceedings of the IEEE Russia –2011 –№1 –pp. 69 – 72.
[2] Durukan Y. The Effect of a Rotating Medium on Bulk Acoustic Wave Polarization: From Theoretical Considerations to Perspective Angular Motion Sensor Design/ Durukan Y., Shevelko M., Peregudov A., Popkova S. ,Shevchenko S. // Sensors – 2020 –vol. 20(9) – 2487. DOI : doi:10.3390/s20092487
[3] Gribkova E.S., Marusichenko V.A., Peregudov A.N., Shevelko M.M. Estimation of the limiting sensitivity of gyro sensors based on bulk acoustic waves // Izvestiya SPbGETU "LETI" –2012 - №7 - P. 84 - 89.
[4] J. Reisland. Physics of phonons. Moscow: Mir, 1975, 367 p.
[5] Buckingham M. Noises in electronic devices and systems. Moscow: Mir, 1986,399 p.
[6] Van der Ziel A. Fluctuations in radio engineering and physics. Moscow: Gosenergoizdat, 1958. 296p.
[7] Goncharov KV, Krasilnikov V.A. Thermal mechanical vibrations (fluctuations) of piezoelectric crystals // Izv. Academy of Sciences of the USSR. Ser. Phys. 1956. Vol. 20, No. 2. S.231-236.
[8] Domarkas V.I., Kazhis R.-I. Yu. Control and measuring piezoelectric transducers. Vilnius: MINTIS, 1975, 255 p.
[9] Domarkas V.I., Kazhis R.-I. Yu., Yaronis E.P. Thermal Noise at the Output of Piezoelectric Sound Receivers // Akust. Journal. 1971. Vol. 17, No. 1. S. 43-49.
[10] Domarkas V.I., Kazhis R.-I. Yu. Analysis of thermal noise of piezoelectric receivers // Tr. All-Union. interuniversity. conf. on ultrasonic spectroscopy. Kaunas, 1969.S. 56-57.

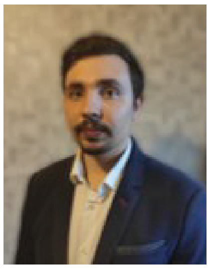

__Nikolay Akhremenko__ is a master's student at the St. Petersburg State Electrotechnical University "LETI". Graduate of the Department of Electroacoustics and Ultrasonic Technology (EUT).
Research interests - electroacoustics, electronics, circuitry.

__Durukan Yasemin__ completed her postgraduate studies in the direction of "Acoustics" at of the Department of Electroacoustics and Ultrasonic Technology (EUT) of the St. Petersburg State Electrotechnical University "LETI". She is the author of over 20 scientific papers and winner of the American Acoustic Society Prize.
Research interests - crystal acoustics, electronics.

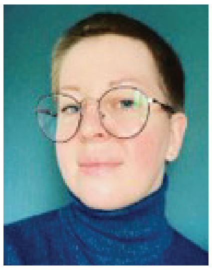

__Ekaterina Popkova__ is PhD in Technical Sciences, Associate Professor and Leading Lecturer of the Department of Electroacoustics and Ultrasonic Technology (EUT) of the St. Petersburg State Electrotechnical University "LETI". Author of over 30 scientific papers and patents.
Research interests - solid state acoustics, i.e. acoustic wave propagation under non-classical condition (deformation, rotation, etc.), methodological support of the educational process.

__Mikhail Shevelko__ is Candidate of Technical Sciences, Associate Professor and Leading Lecturer of the Department of Electroacoustics and Ultrasonic Technology (EUT) of the St. Petersburg State Electrotechnical University "LETI". Author of over 100 scientific papers, monographs and patents.
Research interests - solid state acoustics, methods and equipment for ultrasonic monitoring of the state and composition of media, electronics.

Paper No.373/2021

THEORETICAL ANALYSIS ON REGULARITIES OF THE PROCESS OF NOISE GENERATION OF PLANING, SLOTTING AND PLANING-MILLING MACHINES

[a)]Alexander Chukarin, [b)]Besarion Meskhi, [c)] David Shoniya

[a)] Rostov State Transport University, Rostov-on-Don, Russia, tan_fin@mail.ru
[b, c)] Don State Technical University, Rostov-on-Don, Russia

Abstract*: The acoustic characteristics of the planing machines, which are the most widespread and the most noisy metalworking equipment, are considered. The article presents the theoretical models of the process of noise generation of planing, slotting and planing-milling machines. Regularities of sound pressure levels and sound power are obtained for brittle materials (cast iron blanks) mounted on the machine table. The regularities of the vibration velocities of the cutting tool and the workpiece are derived. The system of second-order differential equations is obtained for the version of the cantilever fixing of the planing cutter, using the developed approaches to the calculating vibrations and noise of machine equipment.*

Keywords: *planing machines, noise sources, model, vibration, operating area, labor conditions, safety.*

DOI: *: 10.36336/akustika20214173*

1. INTRODUCTION

Metalworking industries can be classified as hazardous and harmful, since the machine equipment used there creates increased noise levels at workplaces that exceed the permissible values provided for by sanitary standards [1].

The article discusses machines, which belong to the planing group, since they are the most widespread and are the most noisy metalworking equipment. These include planing, planning- milling machines and slotting machines.

2. FORMULATION OF THE PROBLEM

The pronounced high-frequency noise that exceeds the permissible standards occurs during the technological process of planing parts made of brittle materials on the planing group machines. Its intensity depends on the design of the cutting tool, the number of turnovers of the knife shaft, feed rate and parameters of the material being processed. The noise level is high if the workpiece is thiner, the bluntness of the knives is higher and the cutting speed is higher. It also depends on the type of metal being processed, its fragility, hardness. The noise level is high if the material is harder.

The characteristic feature of the range of planing machines is that flat and shaped-ruled surfaces are processed with cutters. Therefore, the entire variety of cutting tools and workpieces can be reduced to rods and plates from the point of view of geometric configurations. The rods include the entire range of cutting tools and workpieces which length is much greater than the cross-sectional dimensions.

3. THEORETICAL STUDY ON ACOUSTIC DYNAMICS OF THE ROUGHING-GRINDING MACHINE

3.1 Models of noise sources of the research objects

The geometric parameters of the cutting tool and workpieces allow to use the models of beams and plates of limited dimensions. For beam-type sources (which include a cutting tool and long-length workpieces), according to the data of [3,4], the sound pressure (P) and the sound power (N) are determined according to the formulas:

for a cutting tool:

$$P = \frac{S\omega\rho_0 k_0 v_k}{\sqrt{2\pi k_0 r}} \tag{1}$$

$$N = \frac{\pi^2 \sqrt{\frac{S}{\pi}}\, l \rho_0 c_0 \left(k_0 \sqrt{\frac{S}{\pi}}\right)^3 v_k^2}{4} \tag{2}$$

for a beam-type workpiece:

$$P = \frac{\pi\sqrt{\frac{S}{\pi}}\,\omega\rho_0 k_0 v_k}{\sqrt{2\pi k_0 r}} \tag{3}$$

$$N = \frac{\pi^2 \sqrt{\frac{S}{\pi}}\, l \rho_0 c_0 \left(k_0 \sqrt{\frac{S}{\pi}}\right)^3 v_k^2}{2} \tag{4}$$

where

- S is the source surface area, m^2;
- ω is the circular vibration frequency, rad/s;
- p_0 is the air density, kg/m^3;
- k_0 is the wave number, m^{-1};
- v_k is the vibration speed at the corresponding natural vibration frequency, m/s;
- l is the source length, m;
- r is the distance from the cutting zone to the machine operator's workplace, m.

Taking into account the mechanical characteristics of the material and methods of fixing, these regularities are reduced to the following form:

for cutters as steel beams of rectangular section cantilevered:

$$P = 1,2 \cdot 10^4 \left(\frac{2k-1}{l}\right)^3 b^{1,5} v_k (hl + bl + bh) \quad (5)$$

$$L_p = 60\, lg \frac{2k-1}{l} + 20\, lg\, v_k\, (hl + bl + bh) + 30\, lg\, b - 10\, lg\, r + 136 \quad (6)$$

where
l is the source length, m;
b and h are cross-sectional dimensions, m;
k is a coefficient that determines the natural frequencies of the source.

$$N = 1,4 \cdot 10^5 v_k^2 l b^3 \left(\frac{2k-1}{l}\right)^6 (bh + bl + hl)^2 \quad (7)$$

$$L_N = 20\, lg\, v_k\, (bh + bl + hl) + 60\, lg \frac{2k-1}{l} + 30\, lg\, b + 10\, lg\, l + 170 \quad (8)$$

Since in this work the processes of working brittle materials are studied, the regularities of the levels of sound pressure and sound power are obtained for cast iron blanks mounted on the machine table.

$$P = 3,2 v_k \left[9,4 \cdot 10^{11} \left(\frac{k}{l}\right)^4 bh^3 + j_{pr}\right]^{0,25} \left(\frac{bh + bl + hl}{r}\right)^{0,5} \quad (9)$$

$$L_p = 20\, lg\, v_k + 5\, lg \left[9,4 \cdot 10^{11} \frac{k}{l} bh^3 + j_{pr}\right] + 10\, lg \frac{bh + bl + hl}{z} + 124 \quad (10)$$

$$N = 0,24 \left[9,4 \cdot 10^{11} \left(\frac{k}{l}\right) bh^3 + j_{pr}\right]^{0,5} (bh + bh + hl) l v_k \quad (11)$$

$$L_N = 10\, lg\, v_k\, l (bh + hb + hl) + 5\, lg \left[9,4 \cdot 10^{11} \left(\frac{k}{l}\right) bh^3 + j_{pr}\right] + 114 \quad (12)$$

The sound power, which is emitted by processed workpieces such as plates, significantly depends on the ratio of natural vibration frequencies and the critical frequency, which is determined for cast iron workpieces by the formula:

$$f_{cr} = \frac{15,5}{h_{pl}} \quad (13)$$

where
h_{pl} is the thickness of the plate, m.

The natural vibration frequencies of cast iron plates are defined as:

$$f_{mn} = 2 \cdot 10^3 h_{pl} \left(\frac{m^2}{l_1^2} + \frac{n^2}{l_2^2}\right) \quad (14)$$

where
l_1 and l_2 are the length and width of the workpiece, m;
m and *n* are coefficients that determine the natural frequencies of vibrations.

Then the sound power for frequencies $f_{mn} \leq f_{cr}$ is determined [3,4] as:

$$N = \frac{\rho_0 c_0 k_0^2 F^2}{4\pi (\omega m_{mn})^{-1}} \quad (15)$$

where
p_0 and c_0 are density (kg/m³) and speed of sound in air (m/s);
k_0 is wave number, m⁻¹;
ω is circular vibration frequency, rad/s;
m_{mn} is distributed plate mass, kg/m²;
F is cutting force, N.

For cast iron blanks this dependence has the form, W:

$$N = 5,6 \cdot 10^{-12} (Fh)^2 \quad (16)$$

and sound pressure levels, dB:

$$L_N = 20\, lg\, F\, h + 7,5 \quad (17)$$

For the ratio $f_{mn} > f_{cr}$ this dependence has the form:

$$N = \frac{F^2}{16\sqrt{\rho h_{pl} EJ}} \cdot \frac{\eta_{em}}{\eta_{em} + \eta} \quad (18)$$

where
n_{em} is the emissivity,

$$\eta = \frac{\rho_0 c_0}{2\pi f_{mn} \rho h \sqrt{1 - \left(\frac{f_{mn}}{f_{cr}}\right)^2}} \quad (19)$$

$$\eta = \frac{\rho_0 c_0}{2\pi f_{mn} \rho h \sqrt{1 - \left(\frac{f_{cr}}{f_{mn}}\right)^2}} \quad (20)$$

n is vibration energy loss factor.

For cast iron blanks this dependence has the form:

$$N = \frac{2 \cdot 10^{-9} F^2}{\sqrt{hJ}} \quad (21)$$

$$\eta_{em} = \frac{10^{-2}}{h\sqrt{f_{mn}^2 - f_{cr}^2}} \quad (22)$$

then the sound power levels are determined by the formula:

$$L_N = 20\, lg\, F - 5\, lg\, hJ - 10\, lg \left(1 + 10^2 \eta h \sqrt{f_{mn}^2 - f_{cr}^2}\right) + 33 \quad (23)$$

where
J is moment of inertia of the workpiece, m⁴.

3.2 Derivation on regularities of the vibration velocities of the cutting tool and the workpiece

The calculation of the planing cutters is based on the assumption that at the time ***t = 0*** the cutting force is applied to the cutter and remains constant during the stroke of the planer cutter. In addition, it is taken into account that both for planing cutters and during milling, the coordinate of the application of the cutting force is constant relative to the spindle bearings. In this case, according to the data of [3,4], the differential equation of bending vibrations of the cutting tool has the form:

$$\frac{\partial^2 z(y)}{\partial x^2} + \frac{EJ_{z,y}}{\rho bh} \cdot \frac{\partial^4 y}{\partial x^4} = \frac{F(t)_{z,y}}{\rho bh} \delta(x - x_0) \tag{24}$$

where

J $_{z,y}$ are moments of inertia of the planer tool relative to the axes ***Oz*** and ***Oy***, m^4;

F(t) $_{z,y}$ are components of the cutting force in the direction of the same axes, ***N***;

δ(x-x0) is delta function in the coordinate of application of the cutting force.

According to research [5], the cutting force is defined as:

$$\widetilde{P}_{y,z} = P_{y,z}(1 + \cos \omega t) \tag{25}$$

where

ω=2πf is chip formation frequency [5].

The amplitudes of the components of the cutting forces and cutting speed are determined by the standards of cutting modes [6]:

cutting speed (m/min)

$$v = \frac{c_v}{\tau^m t^{x*} S^{y*}} K_v \tag{26}$$

where

τ is tool life, min;

t is cutting depth, mm;

S is longitudinal feed, mm/min;

m, x*, y*, K $_v$ and ***c*** $_v$ are empirical coefficients determined from the corresponding tables [6]:

The amplitudes of the cutting forces:

$$P_{z,y} = 10 c_p t * S * v^{n*} K_p \cdot K_{yv} \tag{27}$$

where

c $_p$, ***K*** $_p$ and ***K*** $_v$ are coefficients that take into account the material of the cutter and the workpiece [6,7], the coefficient ***K*** $_{yv}$ takes into account the type of machine and is taken equal to: 1 – for planing machines; 0.8 – for cross planers and 0.6 for slotting machines.

The equation (24) in relation to the version of the cantilever fastening of the planer cutter is reduced to the following system, using the developed approaches to calculating vibrations and noise of machine tool equipment:

$$\begin{gathered}
\frac{d^2 z_1}{dt^2} + 1,2 \cdot 10^7 b^2 \left(\frac{10k-3}{l}\right)^4 z_1 = \frac{2,8 \cdot 10^{-4} F_z}{bhl}(1 + 0,3 \cos \omega t) \\
\frac{d^2 z_2}{dt^2} + 1,2 \cdot 10^7 b^2 \left(\frac{2k-3}{l}\right)^4 z_2 = \frac{2,8 \cdot 10^{-4} F_z}{bhl}(1 + 0,3 \cos \omega t) \\
\frac{d^2 z_3}{dt^2} + 1,6 \cdot 10^{10} b^2 \left(\frac{k}{l}\right)^4 z_3 = \frac{2,8 \cdot 10^{-4} P_z}{bhl}(1 + 0,3 \cos \omega t) \\
\frac{d^4 z_4}{dt^2} + 2 \cdot 10^9 b^2 \left(\frac{k}{l}\right)^4 z_4 = \frac{2,8 \cdot 10^{-4} P_z}{bhl}(1 + 0,3 \cos \omega t) \\
\frac{d^2 y_1}{dt^2} + 1,2 \cdot 10^7 h^2 \left(\frac{10k-3}{l}\right)^4 z_1 = \frac{2,8 \cdot 10^{-4} P_y}{bhl}(1 + 0,3 \cos \omega t) \\
\frac{d^2 y_2}{dt^2} + 1,2 \cdot 10^7 h^2 \left(\frac{2k-3}{l}\right)^4 y_2 = \frac{2,8 \cdot 10^{-4} P_y}{bhl}(1 + 0,3 \cos \omega t) \\
\frac{d^2 y_3}{dt^2} + 1,6 \cdot 10^{10} h^2 \left(\frac{k}{l}\right)^4 y_3 = \frac{2,8 \cdot 10^{4} P_y}{bhl}(1 + 0,3 \cos \omega t) \\
\frac{d^2 y_4}{dt^2} + 2 \cdot 10^9 h^2 \left(\frac{k}{l}\right)^4 y_4 = \frac{2,8 \cdot 10^{4} P_y}{bhl}(1 + 0,3 \cos \omega t)
\end{gathered} \tag{28}$$

The solutions of the equations are obtained in the following form:

$$\begin{gathered}
Re\{z_1\} = \sum_{k=1}^{k*} \frac{2 \cdot 10^{-11} F_z l^3}{b^3 h} \cos 3,5 \cdot 10^3 b \left(\frac{10k-3}{l}\right)^2 t + \frac{2,8 \cdot 10^{-4} F_z}{bhl} \times \\
\times \frac{\left[1,2 \cdot 10^7 b^2 \left(\frac{10k-3}{l}\right)^4 - \omega^2\right] \cos \omega t}{\left[1,2 \cdot 10^7 b^2 \left(\frac{10k-3}{l}\right)^4 - \omega^2\right]^2 + 1,44 \cdot 10^{14} b^4 \eta^2 \left(\frac{10k-3}{l}\right)^8} \\
|Re\{v_{z_1}\}| = \frac{\partial z_1}{\partial t_1} = \sum \frac{7 \cdot 10^{-8} F_z l^3 \left(\frac{10k-3}{l}\right)^2}{b^2 h} \sin 3,5 \cdot 10^3 b \left(\frac{10k-3}{l}\right)^2 t + \\
+ \frac{2,8 \cdot 10^{-4} F_z \omega}{bhl} \cdot \frac{\left[1,2 \cdot 10^7 b^2 \left(\frac{10k-3}{l}\right)^4 - \omega^2\right]^2 \sin \omega t}{\left[1,2 \cdot 10^7 b^2 \left(\frac{10k-3}{l}\right)^4 - \omega^2\right]^2 + 1,44 \cdot 10^{14} b^4 \eta^2 \left(\frac{10k-3}{l}\right)^8}
\end{gathered} \tag{29}$$

$$\begin{gathered}
|Re\{z_2\}| = \sum \frac{2,8 \cdot 10^{-4} F_z}{bhl} \sum \frac{\left[1,2 \cdot 10^7 b^2 \left(\frac{2k-3}{l}\right)^4 - \omega^2\right] \sin \omega t}{\left[1,2 \cdot 10^7 b^2 \left(\frac{2k-3}{l}\right)^4 - \omega^2\right]^2 + 1,44 \cdot 10^{14} b^2 \eta^2 \left(\frac{10k-3}{l}\right)^8} \\
+ + \frac{2 \cdot 10^{-11} F_z l^3}{b^3 h} \sum \cos 3,5 \cdot 10^3 b \left(\frac{2k-3}{l}\right)^2 t \\
Re\{z_3\} = \frac{2 \cdot 10^{-11} F_z l^3}{b^3 h} \sum \cos 1,3 \cdot 10^5 b \left(\frac{k}{l}\right)^2 t + \frac{2,8 \cdot 10^{-4} F_z}{bhl} \times \\
\times \sum \frac{\left[1,6 \cdot 10^{10} b^2 \left(\frac{k}{l}\right)^4 - \omega^2\right] \sin \omega t}{\left[1,6 \cdot 10^{10} b^2 \left(\frac{k}{l}\right)^4 - \omega^2\right]^2 + 2,56 \cdot 10^{20} b^4 \left(\frac{k}{l}\right)^8 \eta^2}
\end{gathered} \tag{30}$$

$$\begin{gathered}
Re\{z_4\} = \frac{2 \cdot 10^{-11} F_z l^3}{b^3 h} \sum \cos 4,5 \cdot 10^4 b \left(\frac{k}{l}\right)^2 t + \\
+ \frac{2,8 \cdot 10^{-4} F_z}{bhl} \sum \frac{\left[2 \cdot 10^9 b^2 \left(\frac{k}{l}\right)^4 - \omega^2\right] \cos \omega t}{\left[2 \cdot 10^9 b^2 \left(\frac{k}{l}\right)^4 - \omega^2\right] + 4 \cdot 10^{18} b^4 \eta^2 \left(\frac{k}{l}\right)^8} \\
Re\{v_{z_4}\} = \frac{d\, Re\{z_4\}}{dt}
\end{gathered} \tag{31}$$

The vibration velocities of the workpieces processed on planing machines are determined from the system of equations:

$$\begin{gathered}
\frac{d^2 z}{dt^2} + 1,6 \cdot 10^9 b^2 \left(\frac{k}{l}\right)^4 z = \frac{2,8 \cdot 10^{-4} F_z}{bhl}(1 + \cos \omega t) \sin \frac{\pi k S}{l} t = \\
= \frac{2,8 \cdot 10^{-4}}{bhl} F_z \sin \frac{\pi k S}{l} t + \frac{1,4 \cdot 10^{-4} F_z}{bhl} \left(\sin\left(\frac{\pi k S}{l} + \omega\right) t + \sin\left(\frac{\pi k S}{l}\right) - \omega\right) t
\end{gathered} \tag{32}$$

$$\begin{gathered}
\frac{d^2 y}{dt^2} + 1,6 \cdot 10^9 h^2 \left(\frac{k}{l}\right) y = \frac{2,8 \cdot 10^{-4} F_y}{bhl} \sin \frac{\pi k S}{l} t + \\
+ \frac{1,4 \cdot 10^{-4} F_z}{bhl} \left[\sin\left(\frac{\pi k S}{l} + \omega\right) t + \sin\left(\frac{\pi k v}{l} - \omega\right) t\right]
\end{gathered} \tag{33}$$

The solutions of the equations are obtained in the following form:

$$\begin{gathered}
Re\{v_z\} = \frac{9 \cdot 10^{-4} F_z S}{bhl^2} \sum \frac{k\left[1,6 \cdot 10^9 b^2 \left(\frac{k}{l}\right)^4 - \left(\frac{\pi k S}{l}\right)^2\right] \cos \frac{\pi k S}{l}}{\left[1,6 \cdot 10^9 b^2 \left(\frac{k}{l}\right)^4 - \left(\frac{\pi k S}{l}\right)^2\right]^2 + 2,56 \cdot 10^{18} b^4 \eta^2 \left(\frac{k}{l}\right)^8} + \\
+ \frac{1,4 \cdot 10^{-4} F_z}{bhl} \{ \frac{\left[1,6 \cdot 10^9 b^2 \left(\frac{k}{l}\right)^4 - \left(\frac{\pi k S}{l} + \omega\right)^2\right] \left(\frac{\pi k S}{l} + \omega\right) \cos\left(\frac{\pi k S}{l} + \omega\right) t}{\left[1,6 \cdot 10^9 b^2 \left(\frac{k}{l}\right)^4 - \left(\frac{\pi k S}{l} + \omega\right)^2\right]^2 + 2,56 \cdot 10^{18} b^4 \eta^2 \left(\frac{k}{l}\right)^8} + \\
+ \frac{\left[1,6 \cdot 10^9 b^2 \left(\frac{k}{l}\right)^4 - \left(\frac{\pi k S}{l} + \omega\right)^2\right] \left(\frac{\pi k S}{l} - \omega\right) \cos\left(\frac{\pi k S}{l} - \omega\right) t}{\left[1,6 \cdot 10^9 b^2 \left(\frac{k}{l}\right)^4 - \left(\frac{\pi k S}{l} + \omega\right)^2\right]^2 + 2,56 \cdot 10^{18} b^4 \eta^2 \left(\frac{k}{l}\right)^8} \} \\
Re\{v_y\} = \frac{9 \cdot 10^{-4} F_y S}{bhl^2} \sum \frac{k\left[1,6 \cdot 10^9 b^2 \left(\frac{k}{l}\right)^4 - \left(\frac{\pi k S}{l}\right)^2\right] \cos \frac{\pi k S}{l}}{\left[1,6 \cdot 10^9 b^2 \left(\frac{k}{l}\right)^4 - \left(\frac{\pi k S}{l}\right)^2\right]^2 + 2,56 \cdot 10^{18} b^4 \eta^2 \left(\frac{k}{l}\right)^8} + \\
+ \frac{1,4 \cdot 10^{-4} F_y}{bhl} \{ \frac{\left[1,6 \cdot 10^9 b^2 \left(\frac{k}{l}\right)^4 - \left(\frac{\pi k S}{l} + \omega\right)^2\right] \left(\frac{\pi k S}{l} + \omega\right) \cos\left(\frac{\pi k S}{l} + \omega\right) t}{\left[1,6 \cdot 10^9 b^2 \left(\frac{k}{l}\right)^4 - \left(\frac{\pi k S}{l} + \omega\right)^2\right]^2 + 2,56 \cdot 10^{18} b^4 \eta^2 \left(\frac{k}{l}\right)^8} + \\
+ \frac{\left[1,6 \cdot 10^9 b^2 \left(\frac{k}{l}\right)^4 - \left(\frac{\pi k S}{l} + \omega\right)^2\right] \left(\frac{\pi k S}{l} - \omega\right) \cos\left(\frac{\pi k S}{l} - \omega\right) t}{\left[1,6 \cdot 10^9 b^2 \left(\frac{k}{l}\right)^4 - \left(\frac{\pi k S}{l} + \omega\right)^2\right]^2 + 2,56 \cdot 10^{18} b^4 \eta^2 \left(\frac{k}{l}\right)^8} \} \\
v_k = \sqrt{Re\{v_z\}^2 + Re\{v_y\}^2}
\end{gathered} \tag{34}$$

The components of the cutting forces during milling according to the standards of cutting conditions [8,9] are determined by the regularities:

$$F_z = \frac{10c_p t * S_z^{y*} B^{n*} z *}{D^{\eta *} n^{\omega *}} K_m F_x \cos\left[0,1nz * t - (q-1)\frac{2\pi}{z *}\right] \tag{35}$$

where
S_z is feed per cutter tooth, mm/tooth;
n is rotation frequency, rpm;
D is cutter diameter, mm;
B is milling width, mm.

$$F_y = (0,4..0,6)F_z$$

The vibration speeds of the workpieces during milling are determined from the system of equations:

$$\begin{gathered}\frac{d^2z}{dt^2} + 1,6\cdot 10^9\left(\frac{k}{l}\right)^4 z^2 = \frac{P_z}{bhl}\cdot\cos\left[0,1nz * t - (q-1)\frac{2\pi}{z *}\right]\sin\frac{\pi k v}{l}t = \\ = \frac{0,5F_z}{bhl}\left\{\sin\left[\left(\frac{\pi kS}{l} + 0,1nz * t\right) - (q-1)\frac{2\pi}{z *}\right] + \sin\left[\left(\frac{\pi kS}{l} + 0,1nz *\right)t + (q-1)\frac{2\pi}{z *}\right]\right\}\end{gathered} \tag{36}$$

$$Re\, v_z = \frac{0,5F_z}{bhl} *$$

$$* \sum \frac{\left[1,6\cdot 10^9 b^2\left(\frac{k}{l}\right)^4 - \left(\frac{\pi kS}{l} + 0,1nz *\right)^2\right]\left(\frac{\pi kS}{l} + 0,1nz *\right)\cos\left[\left(\frac{\pi kS}{l} + 0,1nz *\right)t - (q-1)\frac{2\pi}{z*}\right]}{\left[1,6\cdot 10^9 b^2\left(\frac{k}{l}\right)^4 - \left(\frac{\pi kS}{l} + 0,1nz *\right)^2\right] + 2,56\cdot 10^{18} b^4\eta^2\left(\frac{k}{l}\right)^8} +$$

$$+ \frac{\left[1,6\cdot 10^9 b^2\left(\frac{k}{l}\right)^4 - \left(\frac{\pi kS}{l} - 0,1nz *\right)^2\right]\left(\frac{\pi kS}{l} - 0,1nz *\right)\cos\left[\left(\frac{\pi kS}{l} - 0,1nz *\right)t + (q-1)\frac{2\pi}{z*}\right]}{\left[1,6\cdot 10^9 b^2\left(\frac{k}{l}\right)^4 - \left(\frac{\pi kS}{l} - 0,1nz *\right)^2\right] + 2,56\cdot 10^{18} b^4\eta^2\left(\frac{k}{l}\right)^8}$$

4. CONCLUSION

1. Theoretical models of the process of noise generation of planing, slotting and planing-milling machines are presented.
2. Regularities of sound pressure levels and sound power are obtained for brittle materials (cast iron blanks) mounted on the machine table.
3. The regularities of the vibration velocities of the cutting tool and the workpiece are derived.
4. The system of second-order differential equations [9-11] is obtained in relation to the option of cantilever fixing of the planing cutter, using the developed approaches to calculating vibrations and noise of machine tool equipment.

REFERENCES

[1] SN 2.2.4/2.1.8.562-96 Noise in the workplace, in the premises of residential and public buildings and on the territory of residential development. Sanitary standards
[2] Life safety: studies. manual I.G. Pereverzev, T.A. Finochenko, I.A. Yaitskov [et al.]; FGBOU VO RSTU. 2nd ed., reprint. and additional. Rostov n/D. 2019 – 308 p.
[3] Chukarin A. N. Theory and methods of acoustic calculations and design of technological machines for mechanical processing. Rostov n/D: Publishing Center of DSTU. 2004. -152 p.
[4] Nikiforov A. S. Acoustic design of ship structures. L.: Shipbuilding. 1990. - 200 p.
[5] Klimov M. M. Influence of fluctuations in the parameters of the friction process on the wear of hard alloys: dis ... kand. tehn. nauk. - Rostov n/D. 1988 – 167 p.
[6] Handbook of technologist-machine-builder. - Vol. 2 Ed. by A.G. Kosilova and R.K. Meshcheryakov. - Moscow: Mashinostroenie. 1985. - 496 p.
[7] Strength calculations in mechanical engineering / Ed. by S.D. Ponomarev. M.: Mashgiz, 1959. – 884 p.
[8] Ryzhkov D. I. Vibrations in metal cutting and methods of their elimination. - M.: Mashinostroenie, 1961. - 172 p.
[9] Ivanov N. I. Engineering acoustics. Theory and practice of noise control / Moscow: Logos, 2010. 423 p.
[10] Theoretical research of noise and vibration spectra in cabins of locomotive and diesel shunting locomotive Yaitskov I.A., Chukarin A.N., Finochenko T.A. International Journal of Applied Engineering Research. 2017. Vol. 12. № 21. P. 10724-10730.
[11] The methodology and technical support for the experimental research of the definition of noise at work Finochenko T.A., Balanova M.V., Yaitskov I.A. Scientific and technical journal: "Proceedings of the RSUPS" № 1(46), 2019 from 5-7

Alexander Chukarin *is Doctor of Engineering Sciences, Professor, Head of the Chair «Fundamentals of Machine Design», Rostov State Transport University (RSTU) (Rostov-on-Don, Russia).*
The direction of the scientific research is the process of vibro acoustic dynamics of the technological machines in various functional purposes.
In 1985 he defended his thesis on the topic «Improving vibro acoustic characteristics of the bearing assemblies of the machine tools». In 1996 he defended his doctoral thesis in the specialty «Vibro acoustic bases for calculating machine tools at the design stage».
Under the leadership of Professor A.N. Chukarin, 3 doctoral and 19 master's theses were defended.
A.N. Chukarin published more than 220 scientific and educational works: 6 monographs.
He is the Deputy Chairman of the Doctoral Dissertation Council on the specialties «Labor Protection» (mechanical engineering) and «Machine engineering, Drive Systems and Machine Parts». He is a member of the editorial boards of a number of the abstract journals.

Besarion Meskhi *is a Russian scientist, Rector of the Don State Technical University (Rostov-on-Don, Russia), Doctor of Technical Sciences, Professor, Corresponding Member of the Russian Academy of Education.*
The area of scientific research is technology and industrial safety, theory and methods of comprehensive provision of occupational safety in machine-building industries and technological equipment during its design.
Prof. Meskhi has more than 30 monographs, 180 articles, 5 copyright certificates, diplomas, patents and licenses, 45 study guides approved by the Education and Methodics Association.
Besarion Meskhi actively participates in the training of academic teaching and research staff.

David Shonia *is currently pursuing a Master's degree at Don State Technical University (Rostov-on-Don, Russia).*
Research interests are as follows: ensuring safe working conditions of technological equipment for mechanical processing at the design stage, the causes of industrial accidents and occupational diseases in the production processes of large city enterprises and building.
David Shonia is a participant of international scientific and scientific-practical conferences.
Graduated with a Bachelor`s degree from the Don State Technical University (2020).

Paper No.374/2021

THEORETICAL RESEARCH OF THE SWITCHED RELUCTANCE MOTOR VIBROACOUSTIC ACTIVITY

[a] Natalya Yaitskova, [b] Maxim Tchavychalov, [c] Ivan Yaitskov

[a] Rostov State Transport University, Rostov-on-Don, Russia, yia11@bk.ru
[b] Rostov State Transport University, Rostov-on-Don, Russia, chavychalov-maxim@yandex.ru
[c] Rostov State Transport University, Rostov-on-Don, Russia, yia@rgups.ru

Abstract: *The article describes the features of the occurrence of vibroacoustic activity of a promising type of electric motors – switched reluctance. Explanations of the mechanism of occurrence of an increased level of vibrations and noise from the action of unbalanced radial forces of interaction between the stator and the rotor are given. The calculation of radial forces for a valve-inductor motor is given, on the basis of which recommendations are given to reduce the impact of vibrations and noise from a running motor on a human.*

Keywords: *switched reluctance motor, noise, vibration, radial force.*

DOI: *: 10.36336/akustika20214178*

1. INTRODUCTION

Switched reluctance electric motors (SRM) are considered a promising replacement for an induction motor for use both in general-purpose installations and in installations with heavy operating conditions. These motors are distinguished by high energy efficiency indicators, increased reliability indicators, simple and technological construction (Fig. 1).

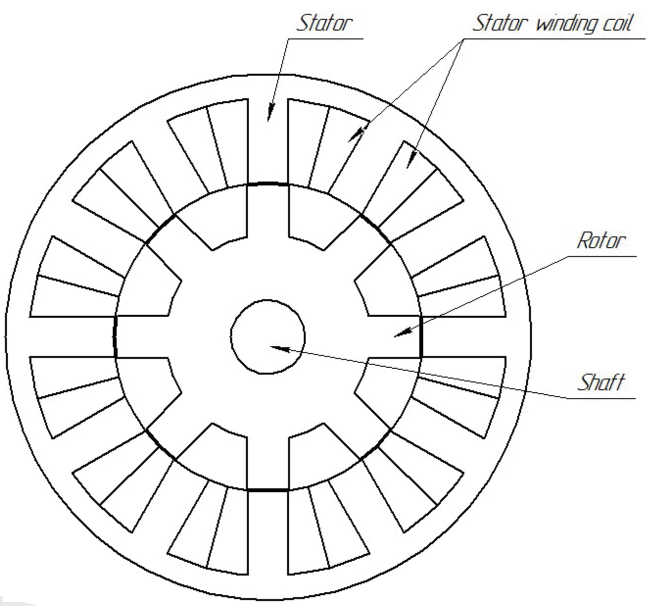

Fig. 1: Switched reluctance motor 12/8 (12 stator teeth, 8 rotor teeth)

Limiting factors for the SRM widespread use are the main disadvantages: an increased level of the electromagnetic torque ripple and an increased level of vibrations and noise.

Torque ripple on the motor shaft are typical also for a frequency-controlled induction motor, so this feature of the operation of SRM can not be considered the main limiting factor. In addition, there are many methods for significantly reducing the level of electromagnetic torque pulsations both by means of controls [1-3] and at the stage of the electric motor design.

2. PROBLEM DESCRIPTION

Acoustic noise, as well as vibrations during the operation of an electric machine, are notable not only for SRM [4]. The electric motor is an assembly unit, and the cause of the resulting noise and vibrations can be, among other things, rolling bearings, unreliable connections, etc. We will consider such cases as disadvantages of specific instances and do not consider them in this article. The main causes of noise and vibration in electric machines can be divided into three classes [5].

Aerodynamic noise is characteristic of absolutely all electric machines and is a consequence of the accelerated movement of air flows during rotation of the rotor. SRM are potentially more prone to an increased level of aerodynamic noise since the rotor has a toothed shape. In this case, the teeth are like lobes and when they move, air swirling occur, increasing the noise level. To reduce this noise, the rotor slots are filled with a polymer compound with the appropriate characteristics. Since the rotor does not contain conductors, the main requirement for the polymer compound will be to ensure the required mechanical strength. Thus, the rotor takes the form of a cylinder with anisotropic magnetic properties in the radial direction. This shape of the rotor will reduce the level of aerodynamic noise as much as possible. Among the disadvantages of the described solution, it is the relative complexity of the rotor design.

Another source of noise in electric machines is magnetostriction. The magnetic circuit of the vast majority of electric machines is made laminated, i.e. it consists of separate plates firmly tightened into a monolithic structure. Such a solution can significantly reduce the amount of eddy currents and thereby reduce the amount of power loss and heating of the magnetic circuit elements. The individual plates of the magnetic circuit change their shape during the magnetization process, rub against each other, resulting in acoustic noise. The magnetic field of SRM, unlike the other machines, has a pulsating character. In this case, the individual teeth of the rotor and stator are magnetized and demagnetized at certain moments. To reduce the noise arising from the influence of magnetostriction, magnetic core structures made of amorphous alloys can be used. In this case there is no need to make the magnetic core laminated, the anisotropy of the magnetic properties is provided by the properties of the amorphous material. Since the elements of the magnetic circuit are monolithic, under the influence of magnetostriction, there is no friction of individual plates and accompanying noise. As a disadvantage of such a solution, we can point out the fact that the magnetic properties of amorphous materials are slightly inferior to the traditional ones used in laminated structures.

In addition to those listed above, when any electric machine is operating, noise arises from mechanical reasons. The non-ideality of the construction of an electric machine is usually indicated as the main one. When developing any product, the design documents specifies the permissible dimensional deviation dictated by the size of the structural element and the capabilities of the equipment. Improving the accuracy of manufacturing a structural element will require the use of more advanced and expensive equipment. Therefore, when developing design documents, they proceed from the capabilities of available equipment. During the operation of an electric machine, tangential forces act on the rotor, producing a torque on the shaft and radial forces of attraction of the rotor to the stator (Fig. 2). In a perfectly executed SRM, the action of radial forces is compensated or negligible. However, if there are permissible dimensional deviation in the size of the elements of the electric machine, the radial forces can significantly increase, cause vibrations, noise and contribute to the accelerated failure of the electric machine. This article is devoted to the consideration of the described case and the process of the occurrence of vibrations during the operation of a SRM.

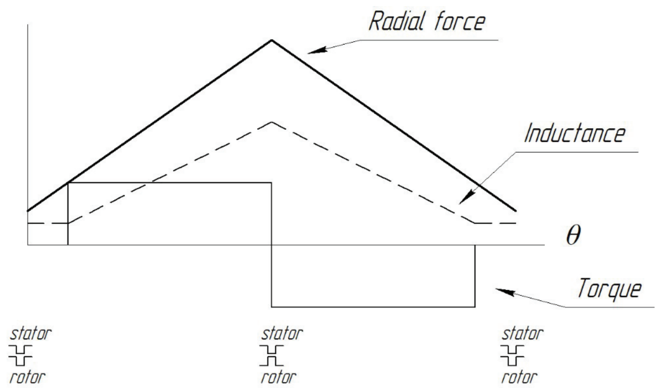

Fig.2: Dependences of inductance, radial force and torque from rotor position

3. MATHEMATICAL MODELLING

The SRM phase windings can be considered as completely independent. Thus the electric balance equation for the SRM phase in accordance with equivalent circuit [7-9] may be written as follows

$$\boldsymbol{u = i \cdot R + \frac{d\psi(\theta, i)}{dt}}$$

where
$\boldsymbol{u}$ – phase voltage,
$\boldsymbol{i}$ – phase current,
$\boldsymbol{R}$ – phase resistance,
$\boldsymbol{\psi}$ – flux linkage,
$\boldsymbol{\theta}$ – angular rotor position.

SRM electromagnetic shaft torque is the sum of the torques produced by the currents of the phases (phase torques).

Phase torques are determined by the equation

$$\boldsymbol{T_{ph}(\theta, i) = \left.\frac{\partial W_c(\theta, i)}{\partial \theta}\right|_{i=const}}$$

where
$\boldsymbol{W_c}$ – coenergy, determined as

$$\boldsymbol{W_c(\theta, i) = \left.\int \psi(\theta, i) di\right|_{\theta=const}}$$

Radial force is determined as

$$\boldsymbol{F_r(\theta, i) = \left.\frac{\partial W_c(\theta, i)}{\partial l_\delta}\right|_{i=const}}$$

where
$\boldsymbol{l_\delta}$ – air gap.

Mechanical part of SRM is described by equations

$$\boldsymbol{J\frac{d\omega}{dt} = \sum_{n=1}^{N_{ph}} T_{ph}(\theta, i_n) - T_L - B \cdot \omega}$$

$$\boldsymbol{\frac{d\theta}{dt} = \omega \cdot N_R \cdot 180/\pi}$$

where
$\boldsymbol{\omega}$ – rotary speed,
$\boldsymbol{J}$ – equivalent moment of inertia,
$\boldsymbol{N_{ph}}$ – SRM phase number,
$\boldsymbol{T_L}$ – load torque on the shaft,
$\boldsymbol{B}$ – friction ratio,
$\boldsymbol{N_r}$ – number of rotor teeth.

Considering the phase flux as a function of two variables, we open the derivative and obtain

$$u_{ph} = i_{ph} \cdot R + \frac{\partial\psi(\theta, i)}{\partial\theta} \cdot \frac{d\theta}{dt} + \frac{\partial\psi(\theta, i)}{\partial i} \cdot \frac{di}{dt} = i_{ph} \cdot R + \frac{\partial\psi(\theta, i)}{\partial\theta} \cdot \omega + L_d(\theta, i) \cdot \frac{di}{dt},$$

where
$\boldsymbol{L_d(\theta,i)}$ – incremental inductance,

$\boldsymbol{\frac{\partial\psi(\theta, i)}{\partial i}}$ – rotational emf ratio.

Using the equations described above to simulate SRM, initial information about the SRM in the form of 3 lookup tables will be required: $\boldsymbol{L_d(\theta,i)}$, and $\frac{\partial\psi(\theta,i)}{\partial i}$ $\boldsymbol{T_{ph}(\theta,i)}$. It reduces the speed of calculation and increases the probability of error calculations.

Let us consider the phase current as a function of the rotation angle of the rotor and the flux linkage. Then the electrical part of the SRM phase is described by the equations

$$\boldsymbol{\psi} = \int (\boldsymbol{u} - \boldsymbol{i} \cdot \boldsymbol{R})$$

$$\boldsymbol{i} = \boldsymbol{f}(\boldsymbol{\theta}, \boldsymbol{\psi})$$

This approach involves a significant reduction in the initial information about the VIEW because only need two lookup tables: $\boldsymbol{i(\theta,\psi)}$ and $\boldsymbol{T_{ph}(\theta,i)}$. At the same time, the use of this approach is associated with the calculation of algebraic loops. Modern modeling tools, such as MATLAB / Simulink, successfully solve such problems.

4. SIMULATION RESULTS

Simulation was made for 3-phase SRM 12/8. The dependence of the flux linkage on the current and the angle of rotor rotation is calculated by the finite element method using FEMM software [9]. The picture of the magnetic field for the aligned position of the rotor of the motor under study is shown in Fig. 3.

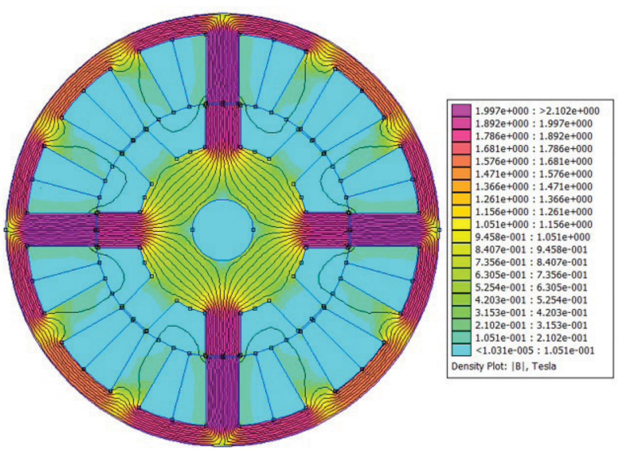

Fig. 3: SRM 12/8 magnetic field

Obtained dependence $\boldsymbol{\psi(I,\theta)}$ as a surface is shown on Fig.4.

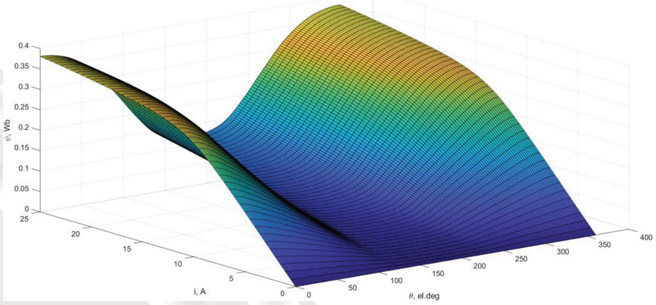

Fig. 4: Dependence $\boldsymbol{\psi(I,\theta)}$

Computer model is realized in MATLAB/Simulink and shown at Fig. 5. The model consists of 3 parts. The electrical part simulates the operation of the converter according to the scheme of an asymmetric bridge with ideal semiconductor elements and a power source. In the blocks Phase1, Phase2 and Phase 3, the above equations of the electric balance of the phase are solved using a single lookup table. In the mechanical part, the above equation of motion of the electric drive is solved, and the current angular position of the rotor is determined. In the control part, based on the angular position of the rotor and the value of the phase currents, signals are generated that are fed to the converter transistors.

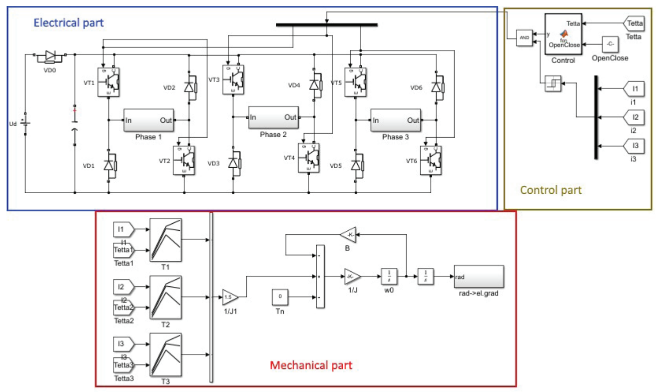

Fig. 5: Matlab/Simulink model

As a result of simulation the dependence $\boldsymbol{i(\theta)}$ was obtained for rotor speed 300 s^{-1} (Fig. 6)

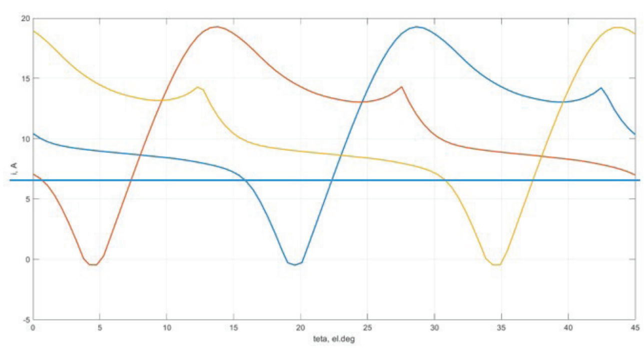

Fig. 6: Dependence $\boldsymbol{i(\theta)}$

When studying the radial interaction of the rotor and the stator, two cases are considered: the shift of the axis of rotor rotation (case 1) and the shift of the rotor relative to the axis of rotation (case 2). The value of the shift in both cases is assumed to be 10% of the value of the air gap along the $\boldsymbol{X}$ and $\boldsymbol{Y}$ axes. Since the coils of the phase windings are connected in series, a change in the magnetic resistance under the stator teeth in the case of a rotor shift will not affect the value of the phase current. The values of the phase currents and the angle of rotor rotation obtained above are used in the FEMM software to calculate radial forces from the Maxwell stress tensor. As a result, for each of the cases, the values of the radial force along the orthogonal axes are obtained. However, a more detailed picture is given by the hodograph of the vector of the total radial force acting on the rotor during motor operation [10] (Fig. 7).

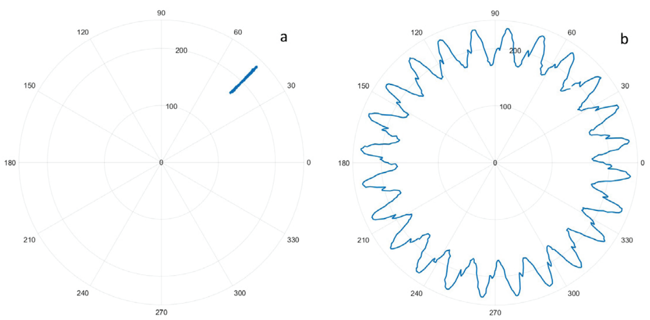

Fig. 7: Hodograph of the total radial force vector

5. CONCLUSION

The above results of computer modeling are valid for one mode of SRM operation. The magnitude of the radial force significantly depends not only on the inaccuracies allowed in the manufacture of the motor, but also on the phase windings current, the angles of opening and closing of the converter semiconductor switches, as well as the current limiting method in starting modes.

Fig. 7 shows that for the displacement of the rotor relative to the stator, the direction of the radial force will have the same direction as the displacement of the rotor. In this case, the increased vibration level will not only increase the noise level, but also lead to rapid wear of the bearing assemblies. For case 2 the direction of the radial force will have an angular displacement together with the rotor. In this case, the constant component of the radial force has a value of about 180 N, and the frequency of the first harmonic will be determined by the equation

$$f = \omega \cdot N_{ph} \cdot N_r.$$

Since it is fundamentally impossible to produce a motor with zero deviations in the dimensions of structural elements, based on the above equation, it is possible to predict the main harmonic frequency of noise and vibrations. At the speed of rotation of the rotor specified in the technical specification in the nominal mode, combined with the known dependence of the threshold of sensitivity of the human ear to sounds of different frequencies, it is possible at the design stage to choose such a value of the number of rotor teeth and the number of motor phases

REFERENCES

[1] Torque ripple minimization of axial laminations switched reluctance motor provided with digital lead controller / M. Hany, S.M. Muyeen, J.J. Tamura // Energy Conver Manage, Vol. 51, pp. 2402 – 2406, 2010.
[2] A New Control Method Based on DTC and MPC to Reduce Torque Ripple in SRM / A. Xu, C.Shang, J. Chen, J.Zhu, and L.Han // IEEE Access, pp.68584-68593, 2019
[3] Artificial Intelligence based Torque Ripple Minimization of Switched Reluctance Motor Drives / E.Gouda, M. Hamouda,and A. Amin // Proc. of the 18thInternational Middle East Power Systems Conference, 2016.
[4] Acoustic Noise Reduction of a High-Efficiency Switched Reluctance Motor for Hybrid Electric Vehicles With Novel Current Waveform / M. Kawa, K. Kiyota, J. Furqani, and A.Chiba // IEEE Transactions on Industry Applications, Vol. 55, No. 3, pp. 2519-2528, 2019.
[5] Noise in Electric Machines: A Review / Praveen Vijayraghavan, R. Krishnan // IEEE Transactions on industry applications, Vol. 35, No. 5, September/October, p. 1007, 1999.
[6] Switched Reluctance Motor and Their Control. / T.J.E. Miller. – Magna Physics Publishing and Oxford University Press, 1993. – 198 p.
[7] Switched reluctance motor drives: modeling, simulation, analysis, design, and applications. / R. Krishnan. – Magna Physics Publishing, 2001. – 416 p.
[8] SRM simulation with reduced amount of initial information / M.V. Tchavychalov, N.V. Grebennikov, D.V. Trinz // Proceedings - 2020 International Conference on Industrial Engineering, Applications and Manufacturing. – 2020. – P. 9112075.
[9] http://femm.info
[10] Influence of sensorless control on the noise of switched reluctance motor drive / Petrushin, A., Tchavychalov, M. // International Journal of Power Electronics and Drive Systems, 2015, 6(3), p. 433–438

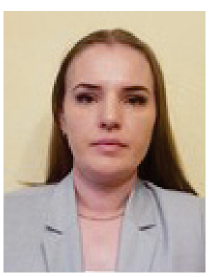

Natalya Yaitskova *is Leading Engineer Researcher at the Scientific and Production Center "Labor Protection" of the Rostov State Transport University (Rostov-on-Don, Russia).*
The field of the scientific research is the processes of the vibroacoustic dynamics of machines of the various industries. She is the participant of the international and national scientific conferences.
He has two higher educations: She graduated from the Rostov State Transport University (2008) and the Rostov State University of Economics (2011).

***Maxim Tchavychalov** is Engineering Sciences, Associate professor of the Department Tracktion Rolling Stock of the Rostov State Transport University (Rostov-on-Don, Russia). Author if over 40 scientific works. Tchavychalov M. conduct active research work in the field of electric drive, its control and vibroacuostic characteristics.*

***Ivan Yaitskov** is Doctor of Engineering Sciences, Professor, Dean of the Electromechanical Faculty of the Rostov State Transport University (RSTU), Leading Researcher at the Scientific and Production Center "Labor Protection" of the RSTU (Rostov-on-Don, Russia).*
He is the author of over 90 scientific papers, monographs, educational and methodical works for patent of reducing noise device. Yaitskov I.A. conducts the research work and made a significant contribution in the field of vibro acoustic safety of the railway transport and transport workers, engineering, improving the design of noise and vibration protection, automatic brakes of the railway rolling stock, ensuring the safety of train traffic and labor protection. He is the participant of the international and all-Russian exhibitions. He is a winner of an increased candidate grant from the Russian Ministry of Railways, a grant within the framework of the Federal Targeted Program "Scientific and Scientific-Pedagogical Personnel of Innovative Russia" and a number of others. Under the leadership of Yaitskov I.A. Research grants of the Russian Railways company are performed.He is a participant and organizer of the international conferences, exhibitions, forums and symposia held by the Transport Ministry of the Russian Federation, Russian Railways and the University in the field of transport, industry and life safety.He passed a foreign internship at the Berlin Technical University, Faculty of Transport and Machine Systems of the Institute of Land and Water Transport, Department of Railways and Operation of Railways "Functioning of Innovative Infrastructure Objects Based on the University" and a course in innovative management. Yaitskov I.A. has awards from the Transport Ministry of the Russian Federation, the Central Committee of the Russian Trade Union of Railway Workers and Transport Builders and Russian Railways.

Paper No.375/2021

THEORETICAL STUDY OF NOISE GENERATION DURING DRILLING OF WOOD WORKPIECES WITH REGARD TO THE DRILL FEED RATE

Dmitry Ruslyakov

Don State Technical University, Rostov-on-Don, Russia, ruslyakof@yandex.ru

***Abstract**: In contrast to metal-cutting machines, woodworking machines are characterized not only by sound pressure levels at the operators' workplaces that exceed the sanitary standards, but also by dust concentrations that also exceed the standards. At present, a set of theoretical and experimental studies has been carried out and engineering solutions have been proposed to bring vibroacoustic characteristics and dustiness to the sanitary standards for woodworking thickness-jointing machines, band and circular saw machines, model and contour-milling machines. Studies of this kind in relation to woodworking drilling machines have not been done. It should be noted that not only the layout of woodworking drilling machines, but also the dynamics of the drilling process has significant differences from the above mentioned machines.*

***Keywords:** woodworking drilling machine, noise pressure level, drill feed rate.*

***DOI:** : 10.36336/akustika20214183*

1. INTRODUCTION

Woodworking machines of the drilling group include single-and multi-spindle machines, the number of spindles of which is 3 – 12.

The cutting forces during drilling are less than during milling, and the sound and sound pressure levels are formed by the simultaneous action of an appropriate number of simultaneously operating spindle units. In addition, the characteristic features of multi-spindle drilling woodworking machines, which distinguish them from other types of machines, is that the spindle units can be re-installed on the corresponding base parts.

The analysis of the layout of the machines showed that it is possible to reduce noise generation in the sources of occurrence only for the bodies of the cutting units. The layout of the load-bearing system of the entire range of multi-spindle drilling woodworking machines provides a system to protect operators from the effects of noise.

2. MATERIALS AND METHODS OF RESEARCH

When drilling workpieces that are characterized by the ratio $\frac{h}{d} > 5$ (where h is the height of the workpiece; d is the diameter of the drill), the vibro – acoustic characteristics should be calculated for the shell model, fixed on the machine table and taking into account the fact that the cutting force moves along the height of the workpiece. The dependence for calculating the natural frequencies of vibrations taking into account the physical and mathematical characteristics of timber species (Table.1) and these papers [1-3] are given in the form.

Timber species	Elastic modulus, Pa	Density, g/m^3	Correlation, E/p
Birch	1,54*10^{11}	650	2,4*10^8
Spruce	1,1*10^{11}	520	2,1*10^8
Pine	1,26*10^{11}	520	2,2*10^3
Oak	1,54*10^{11}	690	2,2*10^8
Plywood	3,4*10^9	800	4,3*10^6
Chipboard	3*10^9	1000	3*10^6

Tab. 1: Mechanical characteristics of different timber species

$$f_k = \frac{9 \cdot 10^2}{\sqrt{F} h^2} \cdot \sqrt{k^4 J + 3 \cdot 10^{-8} \frac{j_{us}\, h^4}{p}}$$

where

- J_{us} is the reduced stiffness of the "workpiece– table" system, H/m;
- h is the height of the workpiece, m;
- F is the cross-sectional area of the workpiece, m^2;
- J is the moment of inertia, m^4;
- p is the density of wood, kg/m^3;
- k is the coefficient that determines the natural frequency of vibrations.

In this case, the dependences for calculating the sound pressure and sound pressure levels are determined according to the obtained dependences.

$$P = 5.3 \cdot 10^2 \frac{V_k}{h\sqrt{r}} \sqrt[4]{\left(k^4 J + 3 \cdot 10^{-8} \frac{j_{us}\, h^4}{p}\right) F}$$

$$L_p = 20lg \frac{V_k}{h} + 5lg \left(k^4 J + 3 \cdot 10^{-8} \frac{j_{us}\, h^4}{p}\right) F - 10lgr + 148$$

The output of the dependences of the oscillation rates is presented for a shell-type workpiece having different moments of inertia in the direction of the coordinate axes ***OZ*** and ***OY*** (the ***OX*** axis is aligned with the axis of the drill and, respectively, the hole). The differential equations of oscillations in this case have the form:

$$\begin{cases} 2,2\cdot 10^3 I_y\dfrac{\partial^4\xi}{\partial x^4}-I_y\dfrac{\partial^4\xi}{\partial x^2\partial t^2}+F\dfrac{\partial^2\xi}{\partial t^2}+\dfrac{j_{n\rho}}{\rho}\xi=P(t)V(t)\delta(x-x_\partial) \\ 2,2\cdot 10^3 I_z\dfrac{\partial^4\varepsilon}{\partial x^4}-I_z\dfrac{\partial^4\varepsilon}{\partial x^2\partial t^2}+F\dfrac{\partial^2\varepsilon}{\partial t^2}+\dfrac{j_{n\rho}}{\rho}\varepsilon=P(t)\delta(x-x_\partial). \end{cases}$$

After performing similar transformations, the following equations are obtained:

$$\begin{gathered}\left[F+6I_y\left(\frac{10k-1}{l}\right)^2\right]\frac{\partial^2\xi}{\partial t^2}+\left[1,34\cdot 10^9 I_y\left(\frac{10k-1}{l}\right)^4+\frac{j_{n\rho}}{\rho}\right]\xi_1=\frac{4\cdot 10^{-3}P}{\rho l}\times \\ \times\sum_{k=1}^{k^*}\sum_{1}^{k_{cd}}\cos^4\frac{\pi k x_i}{l}\cos\frac{2k-1}{l}\pi k x_i\Big\{\cos\Big(\frac{10k-1}{2l}\pi V+0,2n\Big)t+ \\ +\cos\Big(\frac{10k-1}{2l}\pi V-0,2n\Big)t+\cos\Big(\frac{6k+1}{2l}\pi V+0,2n\Big)t+ \\ +\cos\Big(\frac{6k+1}{2l}\pi V-0,2n\Big)t+4\Big[\cos\Big(\frac{6k-1}{2l}\pi V+0,2n\Big)t+ \\ +\cos\Big(\frac{6k-1}{2l}\pi V-0,2n\Big)t+\cos\Big(\frac{2k+1}{2l}\pi V+0,2n\Big)t+ \\ +\cos\Big(\frac{2k+1}{2l}\pi V-0,2n\Big)t\Big]+3\Big[\cos[\Big(\frac{2k-1}{2l}\pi V-0,2n\Big) \\ +\cos\Big(\frac{2k-1}{2l}\pi V+0,2n\Big)t\Big]\Big\},\end{gathered}$$

$$\begin{gathered}\left[F+6I_y\left(\frac{6k+1}{l}\right)^2\right]\frac{\partial^2\xi_2}{\partial t^2}+\left[1,34\cdot 10^9 I_y\left(\frac{6k+1}{l}\right)^4+\frac{j_{n\rho}}{\rho}\right]\xi_2=\frac{4\cdot 10^{-3}P}{\rho l}\times \\ \times\sum_{k=1}^{k^*}\sum_{1}^{k_{cd}}\cos^4\frac{\pi k x_i}{l}\cos\frac{2k-1}{l}\pi k x_i\Big\{\cos\Big(\frac{10k-1}{2l}\pi V+0,2n\Big)t+ \\ +\cos\Big(\frac{10k-1}{2l}\pi V-0,2n\Big)t+\cos\Big(\frac{6k+1}{2l}\pi V+0,2n\Big)t+ \\ +\cos\Big(\frac{6k+1}{2l}\pi V-0,2n\Big)t+4\Big[\cos\Big(\frac{6k-1}{2l}\pi V+0,2n\Big)t+ \\ +\cos\Big(\frac{6k-1}{2l}\pi V-0,2n\Big)t+\cos\Big(\frac{2k+1}{2l}\pi V+0,2n\Big)t+ \\ +\cos\Big(\frac{2k+1}{2l}\pi V-0,2n\Big)t\Big]+3\Big[\cos[\Big(\frac{2k-1}{2l}\pi V-0,2n\Big) \\ +\cos\Big(\frac{2k-1}{2l}\pi V+0,2n\Big)t\Big]\Big\},\end{gathered}$$

$$\begin{gathered}\left[F+6I_y\left(\frac{2k+1}{l}\right)^2\right]\frac{\partial^2\xi_4}{\partial t^2}+\left[1,34\cdot 10^9 I_y\left(\frac{2k+1}{l}\right)^4+\frac{j_{n\rho}}{\rho}\right]\xi_4=\frac{1,6\cdot 10^{-2}P}{\rho l}\times \\ \times\sum_{k=1}^{k^*}\sum_{1}^{k_{cd}}\cos^4\frac{\pi k x_i}{l}\cos\frac{2k-1}{l}\pi k x_i\Big\{\cos\Big(\frac{10k-1}{2l}\pi V+0,2n\Big)t+ \\ +\cos\Big(\frac{10k-1}{2l}\pi V-0,2n\Big)t+\cos\Big(\frac{6k+1}{2l}\pi V+0,2n\Big)t+ \\ +\cos\Big(\frac{6k+1}{2l}\pi V-0,2n\Big)t+4\Big[\cos\Big(\frac{6k-1}{2l}\pi V+0,2n\Big)t+ \\ +\cos\Big(\frac{6k-1}{2l}\pi V-0,2n\Big)t+\cos\Big(\frac{2k+1}{2l}\pi V+0,2n\Big)t+ \\ +\cos\Big(\frac{2k+1}{2l}\pi V-0,2n\Big)t\Big]+3\Big[\cos[\Big(\frac{2k-1}{2l}\pi V-0,2n\Big) \\ +\cos\Big(\frac{2k-1}{2l}\pi V+0,2n\Big)t\Big]\Big\},\end{gathered}$$

$$\begin{gathered}\left[F+6I_y\left(\frac{2k-1}{l}\right)^2\right]\frac{\partial^2\xi_5}{\partial t^2}+\left[1,34\cdot 10^9 I_y\left(\frac{2k-1}{l}\right)^4+\frac{j_{n\rho}}{\rho}\right]\xi_5=\frac{1,25\cdot 10^{-2}P}{\rho l}\times \\ \times\sum_{k=1}^{k^*}\sum_{1}^{k_{cd}}\cos^4\frac{\pi k x_i}{l}\cos\frac{2k-1}{l}\pi k x_i\Big\{\cos\Big(\frac{10k-1}{2l}\pi V+0,2n\Big)t+ \\ +\cos\Big(\frac{10k-1}{2l}\pi V-0,2n\Big)t+\cos\Big(\frac{6k+1}{2l}\pi V+0,2n\Big)t+\end{gathered}$$

where
V is the feed rate of the drill, m/s;
n is the rotation speed of the drill, round per minute;
P is the cutting force (H), determined according to the standards of cutting modes during timber processing.

The real parts of the vibration velocity modules due to their bulkiness are not given in this article.

Timber species	Cutting speed, m/s	Feed, mm/r
Softwood species	0,8 – 4	0,6 – 0,7
Hard-wooded species	0,2 – 0,5	0,1 – 0,5

Tab. 2: Drilling modes

The cutting power (W) is determined by the formula:

$$N_p=\frac{KPD^2u_0\,n}{4*60*102}=1,3*10^{-4}D^2u_0nK_Ta_na_b,$$

where
D is the drill diameter, mm;
n is the rotation speed, round per minute;
u_0 is the feed, mm / rev;
K_T is the specific cutting work, kg * m/cm³, set according to Table;
a_n is the coefficient that takes into account the timber species;
a_b is the coefficient that takes into account bluntness.

The average K_T values for drilling pine across the fibers are shown in the Tab. 3.

The values of the a_n coefficient for other timber species (higher a_n values for lower a_b):
Alder . . . . 0,9 Beech 1,8
Birch . . . . .1,2 – 1,5 Oak. 2,2

Drilled diameter, mm	K_T at the rate of drill feed u_0, mm/r					
	1	0,7	0,4	0,3	0,2	0,1
5	8	8,5	8,8	9,6	12,4	20
10	4	4,2	4,4	4,8	6,2	10
15	3	3,2	3,4	3,6	4,2	7,5
20	2,4	2,5	2,6	2,9	3,6	6
25	2	2,1	2,2	2,4	3,1	5

Tab. 3: Specific cutting work of KT (approximate) when drilling pine across the fibers with center drills with bit

The value of the legal coefficient for blunting the instrument (a_b):
Working time of the tool after sharpening in
h 1 2 3 4 5 6
a_b 1,2 1,3 1,35 1,4 1,45 1,5

The correction factor for the timber species is determined according to Tab. 4 (for pine).

Lime, Aspen	0,8	Birch	1,2 – 1,3
Spruce	0,9 – 1	Beech	1,3 – 1,5
Alder	1 – 1,05	Oak	1,5 – 1,6
Larch	1,1	Ash	1,5 – 2

Tab. 4: Correction factor for timber species

The specific cutting work is defined as the product of:

$$K=K_Ta_na_b$$

The cutting speed during drilling is determined by the dependence (m/s):

$$V_{cp}=\frac{\pi d_c n}{2*1000*60}$$

The amplitude of the cutting force during drilling is (H)

$$P=\frac{N}{V}=3,8\,K_Td_cu_0a_na_b$$

the cutting force in a function of time

$$P(t)=P\sin 0,2\,nt$$

3. CONCLUSION

The obtained theoretical dependences of the oscillation rates take into account all structural and technological parameters: geometric dimensions, timber species, physical and mechanical characteristics, and in particular, the coefficient of loss of vibrational energy ŋ, technological modes of processing, methods of fixing workpieces. These data allow us to perform engineering calculations of both noise levels and vibration levels at the design stages of both the equipment itself and technological processes, which in fact makes it possible to justify noise and vibration reduction systems at the same stages.

REFERENCES

[1] Afanasyev P. S. Constructions and calculations of woodworking equipment - Moscow: Machine manufacturing, 1970. - 400 p.
[2] Chukarin A. N. Theory and methods of acoustic calculations and design of technological machines for mechanical processing. Rostov on Don, Publishing Center of DSTU, 2004. 152 p.
[3] Ivanov N. I., Nikoforov A. S. Fundamentals of vibroacoustics. - St. Petersburg: Politechnika, 2000. - 482 p.
[4] Strength calculations in mechanical engineering / Ed. by S. D. Ponomarev. - M.: Mashgiz, 1959 – - 884 p.
[5] Analysis of acoustic characteristics when grinding rails by means of small mechanization and noise reduction of drive systems of rail-grinding machines / A. N. Chukarin, A. A.
[6] Nazaretov, I. A. Yaitskov / / Bulletin of the Rostov State University of Railway Transport. 2020. № 1 (77). pp. 34-40.
[7] Noise protection system of the vibration shock hardening stand / Chukarin A. N., Shamshura A. S., Finochenko T. A. - The International Technical and Economic Journal No. 4, 2018, pp. 110-116.
[8] Balanova M.V., Finochenko T.A., Yaitskov I.A.: Methodology and technical support for experimental studies of determining noise at workplaces, Scientific and technical journal: "Proceedings of the RGUPS", №1 (46), pp. 5-7, 2019
[9] Morozov S. A., Finochenko T. A., Chukarin A. N. Experimental studies of noise and vibration during local hardening of parts with a ball-rod hardener // Russian scientific and technical journal "Monitoring. Science and Technology". 2019. № 1. pp. 56-62.
[10] Finochenko, T., Yaitskov, I, Dergacheva, L.: Risk Management in Transportation Safety System. IOP Conference Series: Earth and Environmental Science Volume 2, c. 144-145 (2021). doi:10.1088/1755-1315/666/2/022050
[11] The Derivation of the Noise Level Dependences and Vibration Velocities of Elements and Units of the Drive System of the Rail Grinding Machines / A. N. Chukarin, A. A. Nazaretov, I. A. Yaitskov // IOP Conference Series: Earth and Environmental Science: Earth and Environmental Science 720 (2021) 012014. IOP Publishing doi:10.1088/1755-1315/720/1/012014
[12] Borisova, A.V., Finochenko, T.A., Finochenko, V.A.: The Use of the Expert Method in Solving the Issues of Choosing the Instrumentation of the Procedure for Controlling Production Factors. IOP Conference Series: Earth and Environmental Science; IOP Publishing ([Bristol, UK], England), Volume 666 № 2, 2021, doi:10.1088/1755-1315/666/2/ 022022. doi:10.1088/1755-1315/666/2/ 022022
[13] Chukarin A.N., Beskopylny A.N., Isaev A.G. Studies of vibroacoustic characteristics in the operator's work area during abrasive treatment of welds // Work safety in industry. 2019. 11. pp. 7-12. DOI: 10.24000/0409-2961-2019-11-7-12
[14] Balanova M.V., Finochenko T.A., Pereverzev I.G. Physical factors affecting the reliability of rail crane operators. Dependability. 2019; 19 (1): 36-39. https://doi.org/10.21683/1729-2646-2019-19-1-36-39
[15] Chukarin A.N., Solod S.A., Novikov V.V., Litvinov A.E. Structuring information on the state of labor safety at mechanical engineering enterprises. IOP Conference Series: Materials Science and Engineering, 1001 (2020) 012112. doi:10.1088/1757--899X/1001/1/012112

Dmitry Ruslyakov *is Candidate of Technical Sciences, Associate Professor, Dean of the Faculty of Engineering and Technology, Associate Professor of the Department of Automobile Transport and Technological Equipment of the Institute of Service and Business (branch) of the Don State Technical University in Shakhty, the Rostov region. Dmitry Ruslyakov is a specialist in the field of noise generation and dustiness in the woodworking industry, calculation and design of noise barriers of woodworking machines, noise and dust absorption in working areas of production facilities. He is a member of the Association of Engineering Education of Russia, as well as a member of the organizing committees of conferences and seminars on topical issues of engineering and technology. Dmitry Ruslyakov is the author of more than 70 scientific papers, the co-author of textbooks and patents. He presented the main results of his research at international conferences in Moscow, Rostov-on-Don, Tula, Novocherkassk, Sofia (Bulgaria).*

Paper No.376/2021

TRAFFIC CONTROL AT THE AIRPORT BASED ON ACOUSTIC SCANNING

a, b) Alexey Shvetsov, b) Viktor Gromov

a) North-Eastern Federal University, Yakutsk, Russia
a) Vladivostok State University of Economics and Service, Vladivostok, Russia, transport-safety@mail.ru
b) Peter the Great St. Petersburg Polytechnic University (SPbPU), St. Petersburg, vgromov2021@list.ru

***Abstract**: The round-the-clock vehicles operation at the airports, including in low visibility conditions with fog, snowfall, etc., requires the development of new methods for monitoring their traffic, including those that do not require direct visual contact between the dispatcher and the vehicles. In this study, a method for monitoring airport traffic based on acoustic scanning of the territory has been developed. The method allows you to control traffic remotely, including in conditions of 'zero' visibility. Controlled vehicles include ground vehicles that ensure airport operation, including tractors, tankers, buses for delivering passengers and the crew to the aircraft, snow plows, cars, etc. The method provides equipping the airport territory where vehicle traffic is possible with a network of acoustic sensors configured to detect noise generated by vehicle traffic, which allows you to receive traffic data on the airport territory. The structure of the airport traffic control system based on acoustic scanning and the algorithm of its operation is developed in the study for practical implementation of the method. To configure the acoustic sensors, which are the main element of the system, the noise generated by various types of airport vehicles was measured. The proposed method and the system implementing it can be used to prevent emergencies, as well as to ensure aviation security at airports.*

***Keywords:** airport, traffic, acoustic scanning.*

***DOI:** : 10.36336/akustika20214186*

1. INTRODUCTION

A modern airport as a complex system imposes strict requirements to the operational reliability of its constituent elements. Malfunctioning of one of the elements can lead to a shutdown of the entire airport, and in some cases to an aviation accident.

The main structural elements of a modern airport include ground vehicles that ensure its functioning [1-3].

In the process of the ground vehicles operation at the airport, they constantly interact with the aircraft serviced by the airport. Such interaction includes refueling, baggage transportation, delivery and boarding of passengers and crew on board of the aircraft, etc. At the same time, emergency situations connected with a collision of ground vehicles and aircraft (Fig. 1) often arise, the consequence of which is both damage to the vehicles and injury and in some cases death of people [4-7].

Fig. 1: Accident at Hong Kong airport (https://www.telegraph.co.uk/travel/news/watch-van-crash-into-plane-as-it-prepares-for-take-off/)

Such accidents explain the need for continuous monitoring of the ground vehicles traffic on the airport territory.

Analyzing the modes of airport ground vehicles operation, we see that their operation can occur both in normal mode and in the mode of extreme weather conditions, such as fog, snowfall, heavy rain, etc.

In such conditions, the dispatcher cannot control the vehicle traffic visually, monitoring is only performed using technical systems [8-11]. Accident statistics [1, 2] confirms that there is a need to develop additional methods for monitoring vehicle traffic, while their joint work with existing systems [7-13] will reduce the risk of emergencies at modern airports.

2. THE METHOD OF THE AIRPORT TRAFFIC CONTROL BASED ON ACOUSTIC SCANNING

To increase the controllability of the process of ground vehicle traffic, including in difficult weather conditions, the author has developed a method for monitoring the airport ground vehicle traffic based on acoustic scanning.

The method is implemented as follows. Acoustic sensors tuned to the noise range generated by vehicle traffic are installed throughout the entire territory of the airport where ground vehicles move. When a vehicle passes near the sensors, the sensors record the noise coming from it, then the signal from the sensors goes to the dispatcher's computer, which allows you to reflect the vehicle traffic situation on the airport territory.

The structure of the system that practically implements the developed method of airport traffic control based on acoustic scanning is shown in Fig. 2.

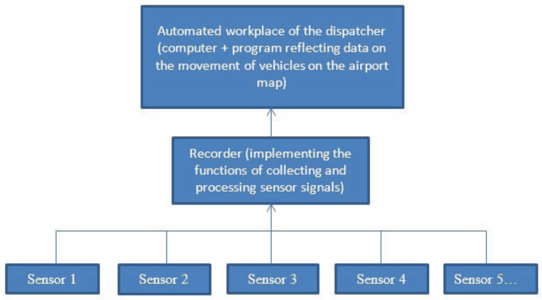

Fig. 2: Structure of the airport ground vehicle traffic control system based on acoustic scanning

When choosing the settings of the acoustic sensors included into the system, it is necessary to take into account the noise level generated by both ground vehicles and aircraft operating in the immediate vicinity of them.

In the aircraft service area, the noise level of aircraft engines is 90-120 dB, when the engines are operating in take-off mode, the total sound pressure levels can reach 160-165 dB, 160-168 dB during flow disruptions and 140-145 dB in the boundary layer [13].

To determine the noise range generated by moving airport ground vehicles, the level of the acoustic radiation intensity adjusted according to the 'A' scale of LA was measured by portable noise meters (in accordance with the regulation methodology – 'Regulation No. 51' of the UNECE [15]) (Fig. 3).

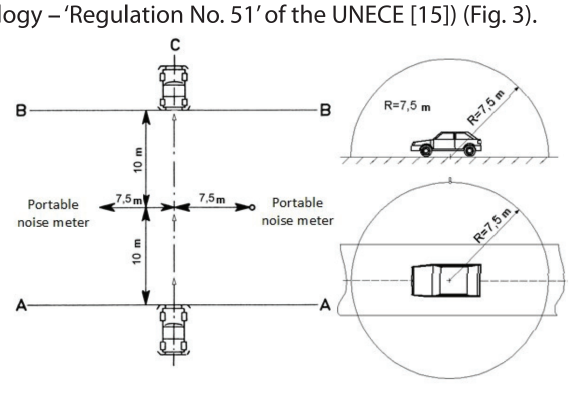

Fig. 3: Scheme for determining the vehicle noise
** When preparing the figure, the elements of the scheme for measuring the noise from the source were used [15]*

At the same time, the following conditions for determining LA were set: tests for evaluating LA are carried out on a measuring section of the road A-B with a length of 20 m; the vehicle in front of the measuring section (up to the A-A line) moves uniformly at a speed of ~50 km/h at an engine speed of n ~~ 3/4nnom; the measurement is made when the vehicle passes the middle of the measuring section with noise meters [14, 15] installed at a distance of 7.5 m from its axis; two measurements are made on each side of the vehicle. The maximum sound level, expressed in decibels (dB), is measured at the moment when the vehicle passes between lines A-A and B-B. The obtained value is the measurement result [15].

The obtained measurement results are shown in Tab. 1.
Tab. 1: Noise generated by airport ground vehicles

Analyzing the transport noise level of the monitored objects (Table 1), we can conclude that the settings of acoustic sensors

Vehicle	Generated noise level (dB)
Buses for the transportation of passengers	58
Aviation Security Service vehicles	45
Pushback tractors	78
Stair vehicles for passenger boarding	60
Fuel trucks	83
Vehicles for the transportation of luggage and cargo to the airplane	72
Catering service vehicles	48
Vehicles with warming-up and AC units	77
Fire tenders	80
Medical vehicles	58
Tank trucks for treating the airplane with anti-icing fluid	78
Mobile power supply units	73

should be in the range of 35-85 dB.

3. THE ALGORITHM OF THE AIRPORT TRAFFIC CONTROL SYSTEM OPERATION BASED ON ACOUSTIC SCANNING

Based on the goals of the acoustic scanning system, we can formulate an algorithm for its operation (Fig. 3).

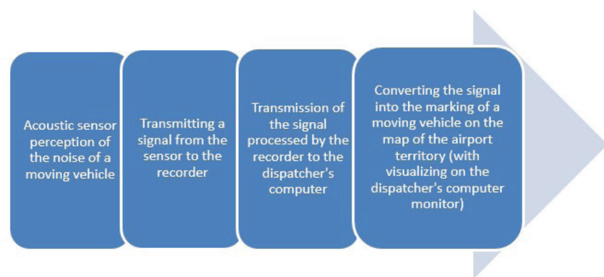

Fig. 4: The algorithm of the airport traffic control system operation based on acoustic scanning

4. CONCLUSION

In this study, a method for monitoring the airport ground vehicles traffic based on acoustic scanning and a system implementing it has been developed. The proposed development is aimed at reducing the number of emergencies that occur during the interaction of air and ground vehicles at the airport. It is established that the acoustic sensors included into the system must have a setting in the range of 35-85 dB. This setting will allow you to record the ground vehicles traffic and will not be triggered by the noise of aircraft engines. Equipping the airport territory with a network of sensors with appropriate settings will allow the dispatcher to receive information about the ground vehicles traffic even in conditions of 'zero' visibility. Taking into account the fact that traditional systems that allow monitoring airport traffic are quite complex technical systems, as a result of which there are frequent failures in their operation, the use of the proposed traffic control system will increase the reliability of such a complex system as a modern airport and reduce the risk of accidents involving air and ground vehicles.

REFERENCES

[1] ICAO Safety Report 2020. https://www.icao.int/safety/Documents/ICAO_SR_2020_final_web.pdf, (date of the application 01.09.2021)
[2] Boeing. Statistical summary of commercial jet airplane accidents: Worldwide operations 1959–2016. Technical Report. https://www.skybrary.aero/bookshelf/books/4239.pdf, (date of the application 01.07.2021)
[3] Shvetsova, S., Shvetsov, A.: Method for Managing the Route of an Unmanned Aerial Vehicle. Russian Aeronautics. VOLUME 64(1), pp. 142–145, 2021, doi: 10.3103/s1068799821010190
[4] The information from an investigation conducted by the Interstate Aviation Committee. https://www.mak-iac.org/rassledovaniya/, (date of the application 01.07.2021)
[5] Information on the state of safety of aircraft flights. Federal Air Transport Agency report. http://www.favt.ru/public/materials/6/8/8/6/1/688612206d6548462c1f2dac2aa1c161.pdf, (date of the application 01.09.2021).)
[6] Runway Safety Accident Analysis Report. Technical Report. International Air Transport Association. https://www.iata.org/en/publications/safety-report/, (date of the application 01.09.2021)
[7] Shvetsova, S., Shvetsov, A.: Ensuring safety and security in employing drones at airports, Journal of Transportation Security. VOLUME 14(1-2), pp. 41–53, 2021, doi: https://doi.org/10.1007/s12198-020-00225-z
[8] Alomar, I., Tolujevs, J.: Optimization of ground vehicles movement on the aerodrome. Transportation Research Procedia. VOLUME 24, pp. 58–64, 2017, doi:10.1016/j.trpro.2017.05.068
[9] Shvetsov, A. et al.: Transportation safety in an urban condition, E3S Web of Conferences, VOLUME 135, Article Num. 02004, 2019, doi: https://doi.org/10.1051/e3sconf/201913502004
[10] Shvetsova, S., Shvetsov, A.: Safety when Flying Unmanned Aerial Vehicles at Transport Infrastructure Facilities. Transportation Research Procedia. VOLUME 54, pp. 397–403, 2021, doi: http://dx.doi.org/10.1016/j.trpro.2021.02.086
[11] Lyovin B. A., et al.: Method for Remote Rapid Response to Transportation Security Threats on High Speed Rail Systems. International Journal of Critical Infrastructures. VOLUME 15(4), pp. 324–335, 2019, doi: 10.1504 / IJCIS.2019.103015
[12] D'yachenkova, M., et al.: Aircraft and vehicle motion path registering and analyzing system for conflicts prediction at the aerodrome movement area. Aerospace MAI Journal. VOLUME 27(3), pp. 209-2018, 2020, doi: 10.34759/vst-2020-3-209-218
[13] Shvetsov, A.: ASPECTS OF TRAFFIC NOISE REDUCTION. Akustika. VOLUME 39, p.25, 2021, doi: 10.36336/akustika20213925
[14] AVIATION ACOUSTICS. https://bigenc.ru/technology_and_technique/text/4424361, (date of the application 03.09.2021)
[15] M.G. Shatrov, A.L. Yakovenko, T.Y. Krichevskaya: The noise of automobile internal combustion engines [Shum avtomobil'nykh dvigateley vnutrennego sgoraniya : ucheb. Posobiye], MADI, p. 68, 2014

Alexey Shvetsov *is Ph.D. of Engineering Science, Associate Professor of Department of Automotive Transport and Car Service of the North-Eastern Federal University (Yakutsk, Russia), and Associate Professor of Department of Transport Processes of the Technologies of the Vladivostok State University of Economics and Service (Vladivostok, Russia). He obtained his PhD in 2018 from the Russian University of Transport, in the field of transportation safety. He current research interests are in the fields of to protection transportation critical infrastructure. He has published more than 75 books, papers in journals and international conferences, on transportation safety and about the protection of critical infrastructures.*

Viktor Gromov *is a DSc, Professor of the Higher School of Cyber-Physical Systems and Management of Peter the Great St. Petersburg Polytechnic University (SPbPU), Honored Worker of the Higher School of the Russian Federation, Author of more than 280 publications of scientific works in the field of information technologies and automated control systems of metro systems, 4 monographs, 3 textbooks, 25 copyright certificates and 4 patents, 38 educational and methodological works. The leader of the scientific school of development of methodology, theory and practice of using the general logical-probabilistic method of modeling complex systems. The main results of scientific research were presented at international conferences in St. Petersburg, FarEastCon, Minzu University of China and other countries*

Paper No.377/2021

THEORETICAL RESEARCH STUDIES OF REGULARITIES FORMATION OF ACOUSTIC CHARACTERISTICS FOR THREADING AND SPLINE SHAFT MILLING MACHINE

[a] Alexander Nabokov, [b] Ivan Yaitskov, [c] Alexander Chukarin

[a] *Rostov State Transport University, Rostov-on-Don, Russia, mr.nae@yandex.ru*
[b] *Rostov State Transport University, Rostov-on-Don, Russia, yia@rgups.ru*
[c] *Rostov State Transport University, Rostov-on-Don, Russia, fta09@bk.ru*

Abstract: *The research paper presents the theoretical studies results of noise generation during workpieces processing on threading and spline shaft milling machines. It is proposed the analytical dependence determining the sound pressure and sound power for various acoustic models of the noise sources with grounding conditions of the cutting tool, workpieces and their geometric dimensions.*

Keywords: *cutter, thread milling machine, spline shaft milling machine, noise source models, vibration frequencies, cutting force.*

DOI: *: 10.36336/akustika20214189*

1. INTRODUCTION

The milling process of external and internal threads is widely used in industry and it is mainly carried out by disc and group (comb) cutters. Nowadays, the theoretical and experimental studies have been carried out; the practical recommendations have been developed for improving the acoustic comfort during the process of the threading and spline shaft milling machines [1–8].

2. SUBJECT OF RESEARCH

It have been analyzed the configuration of thread-milling, turning, thread-cutting and spline shaft milling machines. Methods of installing cutting tools and workpieces use the design schemes of the acoustic characteristics of the main sources of noise generation.

The 5350A spline shaft milling machine in Fig. 1 is designed for milling straight-sided and involute splines on shafts as well as gear teeth used with the shaft.

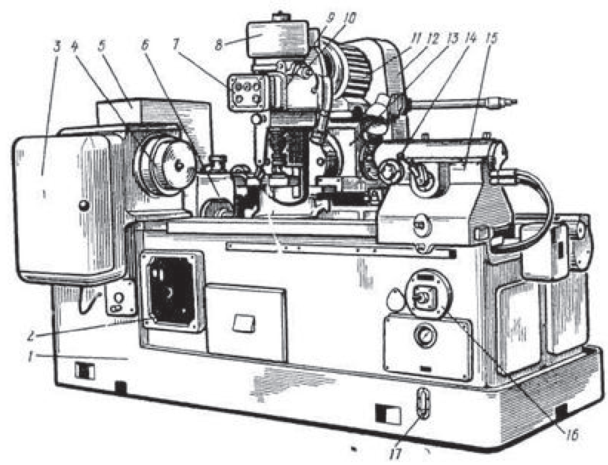

Fig. 1: Spline shaft milling machine 5350A: 1 - foundation slab, 2 - control panel, 3 - separating box, 4 - product spindle, 5 - electrical cabinet, 6 - feed gear box, 7 - upper control panel, 8 – balance - wheel, 9 - milling head, 10 - square of the cutter axial movement, 11 - main drive machine, 12 - casing of change wheel, 13 – tap carriage, 14 - handle for moving the quill, 15 - poppethead, 16 - hydraulic filter, 17 - hydraulic oil indicator

Milling of the splines and gear teeth is performed with a worm spline cutter using the rolling method that is similar to cutting teeth on hobbing machines.

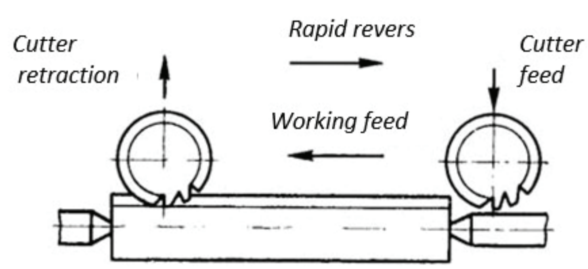

Fig. 2: Automatic cycle of spline shaft milling machine 5350A

3. DESCRIPTION OF THE MACHINE 5350A DESIGN

The milling head moves in the guides of the foundation slab, which can be fixed in the required position according to the component part dimensions. The milling head carries the spindle of the hob cutter. It can be rotated in the vertical plane for the corresponding adjustment of the hob cutter axis relative to the workpiece axis at the cutter helix angle. The milling head moves relative to the part along its axis with the dependence on the component part length and perpendicular to it with the dependence on the component part diameter.

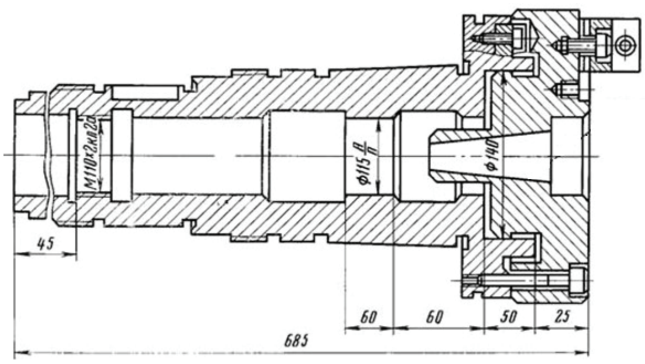

Fig. 3: The spindle workpiece schematic of the machine 5350A

Parameter title	5350
The largest diameter of the product installed over the foundation slab, mm	500
The smallest distance between the axes of the product and the cutter, mm	40..140
Distance between centers, mm	750, 1000, 1500, 2000
Maximum milling length, mm	675, 925, 1425, 1925
Number of splines (teeth) to be cut, mm	4..36
The largest diameter of the cutter, mm	140
Milling spindle speed limits	80..250
Number of electric motors installed on the machine	4
Main drive electric motor, kW	6,5
Overall dimensions of the machine (length x width x height), mm	2595 x 1550 x 1650
Machine weight with electrical equipment and cooling system, kg	3800

Tab. 1: Main parameters of the spline shaft milling machine

In mechanical engineering, threading is mainly carried out on thread processing machines according to classification referred to the fifth group. The main types of threading machines are thread-cutting, threading-milling, tapping, threading and worm grinding machines.

The engineering characteristics of the most common models of thread-cutting and thread-milling machines and semiautomatic devices are given in Tab. 2 and the threading and worm grinding machines are presented in Tab. 3.

Parameters	Machine model				
	5994 / 5994П	2054M	2056	2E056	5Б65
Diameter of the thread to be cut	M24…M76	(M6)	(M18)	(M18)	(M200)
Pitch of the cut thread, mm	3…6	0,4…1,25	1…3,5	0,5…3	-6
Tool spindle rotation frequency, s – 1	0,26…1,5	3,73…37,33	1,86…18,66	1,86…18,66	0,83…13,33
Tap carriage working speed, mm / min	250…450	—	—	5Б63	

Tab. 2: Threading and spline shaft milling machine and semiautomatic machines

Parameter	Machine model				
	5K822B / 5П822	5Д822B	5897	5K823B	MB139
The largest dimensions of the workpiece to be installed, mm:					
diameter	200	200	10…33	320	20
	160	160		280	
length	500	1500	80…280	1000	90
Diameter of threads to be ground in a circle, mm:					
Single-hreaded	3…150	20…150	—	30…320	—
	30…125	30…125		70…220	
Multithreaded	10…120	20…120	—	30…320	—
The pitch of the threads to be ground with a single-thread wheel: metric					
metric	0,25…24	1,5…24	0,5	1…75	0,2…2
	1…6	1…6	3,5	1…6	
inch (number of threads per 1)	28…3	14…3	—	24…3	—
modular	0,3п…14п	1п…14п	—	0,5п…25п	—

Tab. 3: Threading and worm grinding machines

Fig. 4 shows a design diagram of the milling external threading technological process used in the thread milling machine with a comb cutter.

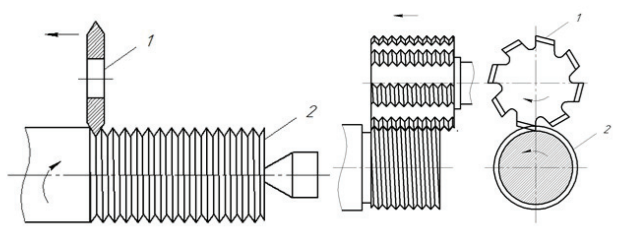

Fig. 4: Design diagram of external thread milling: 1 - comb cutter; 2 - workpiece

Fig. 5 shows the design diagram for milling the internal thread of a hollow workpiece with a comb cutter.

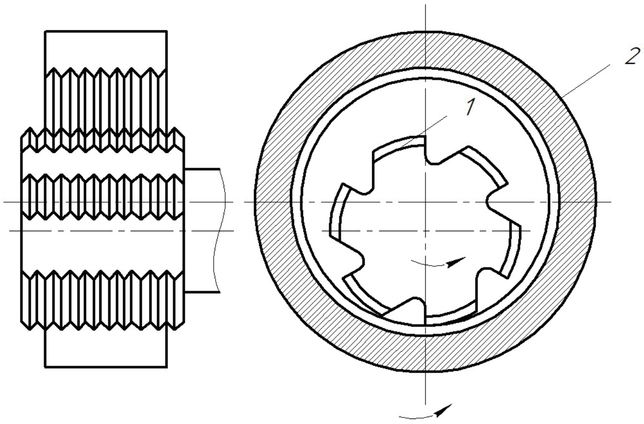

Fig. 5: Design scheme for milling internal: 1 - comb cutter; 2 – workpiece

The disc cutters are used for milling high-pitch threads and long workpiece threads. The diagram of the long workpieces thread milling is shown in Fig. 6.

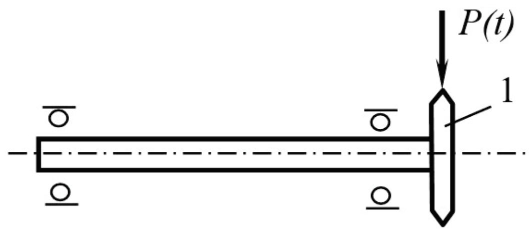

Fig. 6: Design scheme for long workpieces thread milling: 1 - disc cutter

It is used the carbide-reinforced cutter for high-speed threading. Fig. 7 shows a design diagram of a cutting tool used on thread-cutting machines.

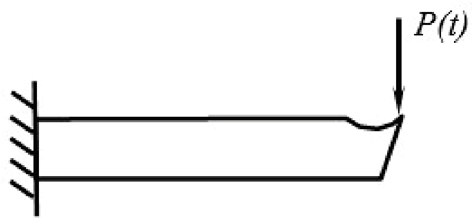

Fig. 7: Design diagram of the cutting tool: ***P(t)*** *- cutting force*

Fig. 8 shows a diagram used for the technological process for cutting splines, milling and turning threads on long workpieces.

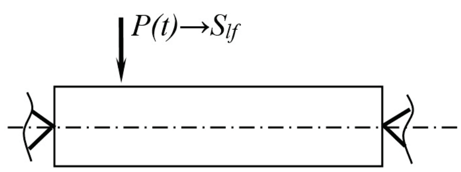

Fig. 8: Design scheme for processing a long workpiece for cutting splines, milling and thread turning: ***P(t)*** *- cutting force;* ***S_{lf}*** *- longitudinal feed*

The threads can be cut with a worm thread-milling with an appropriate profile and pitch. Fig. 9 shows the design diagram of the cutting unit of the spline shaft milling machine.

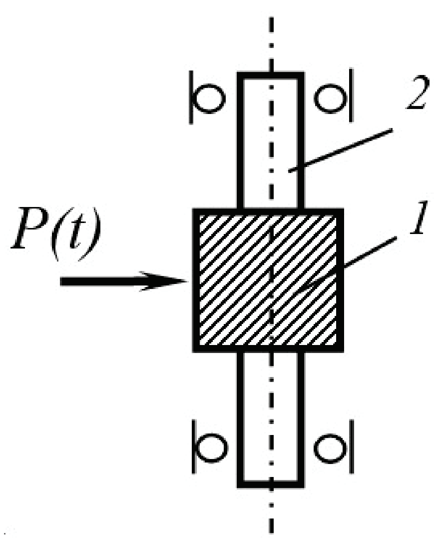

Fig. 9: Design diagram of the cutting unit for spline shaft milling machines: 1 - worm cutter; 2 – case

Based on the grounding conditions of the cutting tool, workpieces and their geometric dimensions, the following acoustic source models were adopted:

1. The point sources are worm and comb cutters, workpieces, machined comb cutters and threaded cutters.
2. Disc cutters for cutting long threads are round insert fixed in the center.
3. The hob cutters cases for milling splines as well as workpieces fixed in the centers are the limited length cylinders.

4. MATERIALS AND METHODS

The dependences determining the sound pressure (***P***), sound power (***N***) and their levels with the studies given in [1-15], are brought to the following formulas:

The worm, comb cutters, workpieces for thread cutting with comb cutters:

$$P = 4 \cdot 10^{-4} \frac{D^3 \omega^2 V_K \cos\theta}{r} \tag{1}$$

$$L_P = 20\, lg \frac{V_K \cos\theta}{r} + 40\, lg\, f_c + 60\, lg\, D + 60 \tag{2}$$

$$N = 1{,}2 \cdot 10^{-10} D^6 f_C^4 V_K^2 \cdot L_N = 60\, lg\, D + 40\, lg\, f_C + 40\, lg\, V_K + 52 \tag{3}$$

where
D is source diameter, m;
f_c is a natural frequency of the sources` oscillations, Hz;
V_K is a vibration speed, m / s;
r is distance from the source to the calculated point, m;
θ is a radiation angle.

There are the threaded cutters:

$$P = 7{,}6 \cdot \frac{S_{ca} f_C V_K}{r} \tag{4}$$

$$L = 20\, lg \frac{S_{ca} f_C V_K}{r} + 112 \tag{5}$$

where
S_{ca} is cross-sectional cutter area, m^2.

$$N = 20\, lg\, S_{ca} f_C^2 V_K^2 + 118 \tag{6}$$

The natural frequencies of the sources` oscillations are determined by the following dependencies:
- the comb cutters and workpieces for thread cutting with comb cutters:

$$f_C = \sqrt{\frac{c}{m + \left(\frac{l}{l_1}\right)^3 \rho F}} \tag{7}$$

$$c = \frac{EJ_X}{l^3} \tag{8}$$

Where

m is the mass of the cantilever part (kg), that is a workpiece or comb cutter, kg;

p and ***F*** are a density and cross-sectional area of the spindle, (kg / m^3) and (m^2), respectively;

l is a spindle length, m;

l_1 is the length of the cutter or the cantilever part of the tool, m;

E and ***I_x*** is a modulus of elasticity and moment of inertia, Pa and m^4, respectively.

It is the worm cutter case for milling splines:

$$f_C = \frac{1}{2\pi}\sqrt{\frac{c}{m + 0,25\rho_0 F_0}} \tag{9}$$

$$c = \frac{40EJ_X}{l_c^3} \tag{10}$$

where

l_c is cutter length, m.

It is the threaded cutter:

$$f_C = \frac{1}{2\pi}\sqrt{\frac{c}{m + 0,23\rho S_{ca}}} \tag{11}$$

$$c = \frac{3EJ_X}{l_{tc}^3} \tag{12}$$

where

l_{tc} is cutter length, m.

It is a disc cutter:

$$f_C = \frac{3 \cdot 10^3 \cdot k \cdot h}{D} \tag{13}$$

where

h is a cutter thickness, m;

k is a coefficient that determines the natural vibrations` frequencies;

$$P = 3 \cdot 10^3 \frac{D \cdot h \cdot V_K \cdot k}{r} \tag{14}$$

$$L_P = 20\,lg\frac{D \cdot h \cdot V_K \cdot k}{r} + 164 \tag{15}$$

$$N = 0,1(D \cdot h \cdot V_K \cdot k)^2 \tag{16}$$

$$L_N = 20\,lg\,D\,hV_K k + 110 \tag{17}$$

There are the workpieces clamping in centers for threading and milling splines:

$$P = 35 \cdot V_K \cdot D\sqrt{\frac{f_C}{r}} \tag{18}$$

$$L_P = 20\,lg\,V_K \cdot D + 10\,lg\frac{f_C}{r} + 125 \tag{19}$$

$$N = 9,4(D \cdot V_K)^2 l \cdot f_C \tag{20}$$

$$L_N = 20\,lg\,D\,V_K + 10\,lg\,l\,f_C + 130. \tag{21}$$

Two options are considered depending on the ratios of the bending stiffness of the workpieces and the stiffness of the supports:

1. a hinged-supported workpiece and on elastically dissipative supports, in which:

$$f_C = 1,5\left(\frac{k}{l}\right)^2\sqrt{\frac{EJ}{\rho F}} \tag{22}$$

2. for steel workpieces:

$$f_C = 8 \cdot 10^3 d\left(\frac{k}{l}\right)^2\sqrt{\frac{J}{F}} \tag{23}$$

According to the standards [10] of cutting rate for threading with cutters, the force and cutting speed, cutting power are determined by the following dependencies:

$$P_Z(t) = P_P(1 + 0,3\,sin\,\omega\,t) \tag{24}$$

$$P_P = \frac{10C_P p^{y^*}}{i^{n*}} k_P \tag{25}$$

where

C_p, y*, n*, k_p are the coefficients given according to [10];

p is a thread pitch, mm;

ω is a frequency of chip formation, r / s;

i is the number of working cutting strokes.

For cutting with rotating heads, it is used:

- the trapeziform cutters:

$$N = \frac{28 \cdot S^{1,2} \cdot S_Z^{0,6} \cdot z^{0,3} \cdot V_P^{0,8}}{d^{0,7}} \tag{26}$$

- the triangular thread:

$$N = \frac{100 \cdot S^{0,5} \cdot S_Z^{0,4} \cdot z^{0,5} \cdot V_P^{0,3}}{d^{0,7}} \tag{27}$$

$$V_P = \frac{C_V \cdot k_V \cdot 1,7 \cdot 10^{-2}}{T^m \cdot S_Z^{x*} \cdot S_z^{y*}} \tag{28}$$

where

T is a durability period, min;

c_v, k_c, m, x*, y*, n*, k_p are coefficients set according to the standards of cutting conditions [10];

S is a longitudinal feed, mm / min;

S_Z is a case per cutter tooth, mm / tooth;

d is a cutter diameter, mm.

For thread and spline shaft milling, the cutting force is given by the formula [2-4]:

$$P_{z,y}(t) = P_P\,cos\left[0,1nz^* t - (q-1)\frac{2\pi}{z^*}\right] \tag{29}$$

$$P_P = \frac{10 \cdot C_P \cdot t_P^{x*} \cdot S_z^{y*} \cdot B^{n*} \cdot z^*}{D^{q*} \cdot n^{w*}} k_{mP} \tag{30}$$

Where

c_p, x*, y*, n*, q*, w* are the elliptical coefficients;

t_p is a cutting depth, mm;

S_z is case per tooth, mm / tooth;

B is a milling width, mm;

z* is a number of teeth;

n is a frequency of the cutter rotation, rpm.

5. CONCLUSION

Consequently, the calculation of the noise spectra is reduced to determining the vibration velocities at the natural source frequencies and summing the corresponding levels by octaves.

The calculation diagrams of the vibroacoustic characteristics during threading with a cutter, thread milling and spline milling are practically identical and use all possible alternative versions of processing conditions and parameters of the technological process.

REFERENCES

[1] The influence of cutting processes on the noise of milling machines / I.A. Balykov, A.N. Chukarin, D.Z. Evseev // New in safety and life and ecology: St. Petersburg, 1996, pp. 222-223

[2] Balykov, I.A. On the calculation of the noise emitted by the workpiece during milling / DSTU, Rostov-n / D, 1996, Dep. in VINITI 08.16.96, № 2687-B96

[3] Experimental studies of noise and vibration of milling machines / I.A. Balykov, A.N. Chukarin // DSTU, Rostov-n / D, 1996, Dep. in VINITI 08.16.96, № 2687-B96

[4] Balykov, I.A. Acoustic model of the cutting tool during milling // Reliability and efficiency of machine and tool systems: Rostov n / a, 1996, pp. 116-122

[5] Gergert, V.A. Mathematical modeling of the noise generation of the tool-workpiece system during milling and grinding. Construction-2003: RSSU. - Rostov n / a, 2003

[6] Kalashnikova, O.A. Calculation of vibration velocities when milling spars // Bulletin of DSTU, 2009, V9, № 1, pp.102-110

[7] Calculation of the required sound insulation of soundproofing systems for long-length parts with hardening technologies and dynamic tests / S.A. Shamshura, O.A. Kalashnikov // Perspective directions of development of mechanical engineering and metalworking technology: Rostov n / a, 2008, V II, pp. 190-194

[8] Experimental studies of noise in the section of spar pipe milling / T.A. Finchenko, A.N. Chukarin, A.S. Shamshura, O.A. Kalashnikov // International technical and economic journal, 2018, № 5, pp.73-79

[9] Chukarin, A.N. Theory and methods of acoustic calculations and design of technological machines for mechanical processing // Rostov n / A: Publishing Center of DSTU, 2004, 152 p.

[10] Handbook of a technologist-mechanical engineer. - T.2 / Ed. A.G. Kosilova and R.K. Meshcheryakov. - M .: Mashinostroenie, 1985, 496 p.

[11] Kucherenko, A.P. Theoretical substantiation of measures to reduce the noise of wheel-turning and wheel-milling machines // Vestnik RGUPS, 2010, № 3, pp. 19-24

[12] Goguadze M.G.: Experimental studies on the noise and vibration of a special boring machine due to the formation of the operator`s workplace sound field / M. Goguadze, A. Shashurin, A. Lubianchenko // AKUSTIKA, Vol. 34, pp. 100-104, 2019

[13] Dosov, V.E. Assessment of noise levels generated by milling cutters when processing wheelsets // Bulletin of DSTU, 2013, № 5/6 (74), pp. 91–96

[14] Dosov, V.E. Vibroacoustic characteristics of a wheel milling machine // Izvestiya IUI AP, 2011, V3-4 (25-26), pp. 131-137

[15] Dosov, V.E. Substantiation of sound-absorbing cladding of sections of special wheel milling machines // Izvestiya IUI AP, 2012, V1-2 (27-28), pp. 10-15

Alexander Nabokov *Deputy Dean for Academic Education Processing of the Department «Electromechanical», Senior Lecturer of the Chair «Structural Mechanics», Senior Researcher of the SPC «Labor Protection», the Rostov State Transport University (Rostov-on-Don, Russia).*
The field of scientific research is the processes of the vibroacoustic dynamics of the threading and spline shaft milling machines in various industries. He is participant of the international scientific and practical conferences. He graduated from Rostov State Transport University in 2001. He is awarded from the Ministry of Transport of the Russian Federation.

Ivan Yaitskov *is Doctor of Engineering Sciences, Professor, Dean of the Electromechanical Faculty of the Rostov State Transport University (RSTU), Leading Researcher at the Scientific and Production Center "Labor Protection" of the RSTU (Rostov-on-Don, Russia).*
He is the author of over 90 scientific papers, monographs, educational and methodical works for patent of reducing noise device. Yaitskov I.A. conducts the research work and made a significant contribution in the field of vibro acoustic safety of the railway transport and transport workers, engineering, improving the design of noise and vibration protection, automatic brakes of the railway rolling stock, ensuring the safety of train traffic and labor protection. He is the participant of the international and all-Russian exhibitions. He is a winner of an increased candidate grant from the Russian Ministry of Railways, a grant within the framework of the Federal Targeted Program "Scientific and Scientific-Pedagogical Personnel of Innovative Russia" and a number of others. Under the leadership of Yaitskov I.A. Research grants of the Russian Railways company are performed.He is a participant and organizer of the international conferences, exhibitions, forums and symposia held by the Transport Ministry of the Russian Federation, Russian Railways and the University in the field of transport, industry and life safety.He passed a foreign internship at the Berlin Technical University, Faculty of Transport and Machine Systems of the Institute of Land and Water Transport, Department of Railways and Operation of Railways "Functioning of Innovative Infrastructure Objects Based on the University" and a course in innovative management. Yaitskov I.A. has awards from the Transport Ministry of the Russian Federation, the Central Committee of the Russian Trade Union of Railway Workers and Transport Builders and Russian Railways.

Alexander Chukarin *is Doctor of Engineering Sciences, Professor, Head of the Chair «Fundamentals of Machine Design», Rostov State Transport University (RSTU) (Rostov-on-Don, Russia).*
The direction of the scientific research is the process of vibro acoustic dynamics of the technological machines in various functional purposes.
In 1985 he defended his thesis on the topic «Improving vibro acoustic characteristics of the bearing assemblies of the machine tools». In 1996 he defended his doctoral thesis in the specialty «Vibro acoustic bases for calculating machine tools at the design stage».
Under the leadership of Professor A.N. Chukarin, 3 doctoral and 19 master's theses were defended.
A.N. Chukarin published more than 220 scientific and educational works: 6 monographs.
He is the Deputy Chairman of the Doctoral Dissertation Council on the specialties «Labor Protection» (mechanical engineering) and «Machine engineering, Drive Systems and Machine Parts». He is a member of the editorial boards of a number of the abstract journals.

Paper No.378/2021

TRAFFIC NOISE ANALYSIS IN THE URBAN ENVIRONMENT

[a)]Yuri Kholopov, [a)]Elena Lukeniuk, [b)]Bela Musatkina, [b)]Inna Denisova

[a)]*Samara State Transport University, Samara, Russia, kholopov@bk.ru*
[b)]*Omsk State Transport University, Omsk, Russia, iovv@mail.ru, mig161704@gmail.com*

Abstract*: The article notes the negative impact of traffic noise on human health. The principles of noise pollution control are considered in the article. The article introduces the measurement results of traffic noise near the academic buildings of the railway transport universities in Omsk and Samara as well as the railway noise measurement results obtained near the Oktyabrsk station. Conclusions and suggestions based on the research results are presented in the article.*

Keywords: *traffic noise, noise control regulation, noise mapping*

DOI: *: 10.36336/akustika20214195*

1. INTRODUCTION

The growth of traffic noise in the urban environment is due to increasing car traffic intensity, railways running across residential areas and nearby runways. All this leads to noise exposure on people as well as on the inhabitants of the natural and urban ecosystems. Recently the difference between the traffic noise actual level in the daytime and at night has been rapidly decreasing.

The State Report "On the state and protection of the environment of the Russian Federation in 2018" [1, p.338] notes the hygienic value of acoustic noise. Its excessive levels are more often recorded in the close city development. Traffic noise (road traffic noise, railway noise, air traffic noise) still dominates in the inhabited locality. According to the Federal Service for Surveillance on Consumer Rights Protection and Human Wellbeing (Russian: Rospotrebnadzor) the number of public complaints related to excessive noise levels was 16,000 or as 58% of the total number in 2018.

The excessive noise level causes hearing impairment, cardiovascular disorders and nervous system depression. Noise poses a risk to health of employed population and people in general. The international standard ISO 1999: 1975 (1975) determined the permissible risk of developing hearing loss: at the noise level of 90 dBA for 5 years the risk was 4%, for 15 years - 14%, for 35 years - 20%; and at the noise level of 85 dBA - 1; 5 and 9% respectively. The socially acceptable criterion is recognized as the noise level of 90 dBA (although there is the category of people who suffer from hearing loss at the level of 75 dBA). The ISO 1999: 1990 standard recommends the noise exposure limit (NEL) of 85 dBA and gives a forecast of hearing loss depending on the frequency and duration of noise exposure, on the gender and age of people.

According to the World Health Organization (WHO) the risk of heart disease among people living in vibrant environment (noise level 65-75 dBA) increases by 20%. The report of European Parliament "Noise strategy" notes that every year in the EU 50 thousand people die prematurely from heart attacks and 200 thousand people suffer from heart diseases caused by traffic noise [2, p.14]. According to Russian physicians the percentage of diseases caused by noise is 3.3% among the additional (above average) deaths in industrial centers [3, p.43].

Deterioration of work and leisure conditions at the excessive traffic noise level slows down productivity and work quality, causes hearing impairment, nervous system depression, cardiovascular disorders and other health disorders [1-3]. Therefore, the population protection against traffic noise is becoming not only socially, but also economically significant right across-the-board.

2. THE PECULIARITIES OF TRAFFIC NOISE LEVELS REGULATION

Russian standards establish stricter requirements for a noise exposure limit (NEL) than WHO recommends. NEL for residential areas in the Russian Federation is presented in the sanitary standards SN 2.2.4 / 2.1.8.562-96. For areas directly adjoining to dwellings, buildings and educational institutions the A-weighted equivalent sound level LAeq should not exceed 55 dBA in the daytime (from 7 a.m. to 11 p.m.) and 45 dBA at night (from 11 p.m. to 7 a.m.), and the maximum noise level LAmax should not exceed 70dBA in the daytime and 60dBA at night [4, p.16]. The maximum allowable road traffic and railways noise levels for some enterprises are 10 dBA higher.

In 2017 the sanitary requirements SanPiN 2.2.4.3359-16 [5, p.14] introduced a new noise index - the peak C-weighted sound level, dBC (measured using a standard frequency weighting of a sound level meter). Thus, international principles for sound intensity and noise evaluation (typical for transport) were introduced in Russia as at the excessive sound levels the frequency response of human hearing corresponds in a great measure with C-weighting.

The most important aspect in evaluating and regulating the traffic noise impact is environmental, primarily in terms of Specially Protected Areas (SPAs) and Biological Diversity.

The noise impact levels on SPAs in the Russian Federation are currently regulated by the Industry-Specific Construction Standards (ISCS) 8-89 "Environment protection regulation in construction, repair and maintenance of highways" where the standards for equivalent sound levels are set: up to 35 dBA in the daytime, up to 30 dBA at night. Developing and affirming scientifically based standards of the noise impact on ecosystems would contribute to the design and widespread implementing noise protection technologies that minimize damage to the environment [6, p.716].

3. NOISE MAPPING

Russian Branch road guidelines ODM 218.2.013-2011 specify that protecting the areas directly adjoining to roads from traffic noise involves functional zoning taking into account the allowable sound levels in the daytime or at night and taking passive and active measures for reducing traffic noise [7, p.10]. The reliable data on noise levels in residential areas is essential for a justified choice of protective measures. In global practice, traffic noise monitoring is more often based on forecast calculations as measuring noise levels at all estimated points is time-consuming. Russian State Standard GOST R 53187 [8, p.4] recommends using computational approach while noise mapping [9]. The EU countries stand by the same principles (Directive 2002/49 / EC of the European Parliament and of the Council of 25 June 2002). Using European calculated methods in Russia demands significant adaptation to the current standards, the noise characteristics of domestic cars, road surfaces, etc.

A number of works [10, p.273, 11, p.299] are devoted to the noise safety in an urban setting. To characterize the acoustic load there were used the maps of the university campus in a number of studies [12, p.90, 13, p.15]; the method of city noise mapping based on a two-parameter model of the acoustic noise spectrum is presented in [14, p.765].

Omsk and Samara with the population of over 1 million people each experience the negative impact of intensive traffic flows, besides these cities are also large railway hubs with higher-density housing near the railway tracks. The problems of studying the traffic noise intensity and hearing protection are quite acute.

The authors measured the noise of traffic flows in the area adjoining to Omsk State Transport University (OSTU), which is situated in the historical center of Omsk, and the noise that penetrates into the classrooms and employees' workplaces through the windows which are located on the southern and western facades of buildings 1 and 3 (the noisiest areas). The measurements were taken with a class 1 sound level meter SVAN-912M; data processing and the evaluation of the results were performed in accordance with the requirements of regulatory documents [4, 5, 8]. The calculation of the expanded uncertainty was carried out in accordance with Russian State Standard GOST 23337-2014 paragraph 9 [15]. The expanded uncertainty U (95%) for the 95% confidence level was 1.95 dBA. The highest sound levels are recorded in the frequency range of 125 to 1000 Hz (mid-frequency noise) [16, p.304]. The results of traffic noise mapping in the area adjoining to the university are shown in Fig. 1.

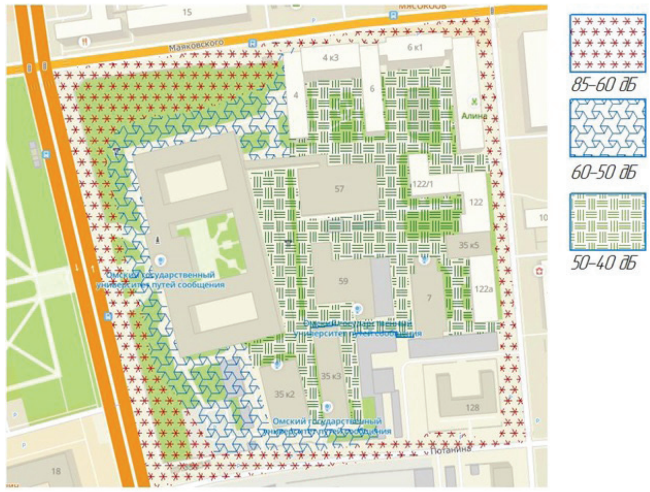

Fig. 1: The results of traffic noise mapping (Omsk)

The measurement results and the evaluation of penetrating noise are shown below. It should be noted that according to [4, p.16] the allowable noise levels from external sources in the premises are established on the assumption of ensuring the ventilation of the premises (with open window leaves, vents, narrow window sashes). In the classrooms on the 5th floor (OSTU building 3, the western facade, the distance from K. Marks prospect is 125 m, from Potanina St. - 40 m), the equivalent and maximum levels of penetrating traffic noise were the following: with the window open - 45.4 dBA and 61.1 dBA; with the window closed - 36.0 dBA and 53.2 dBA respectively. This complies with Russian sanitary standards [4, p.16].

In classroom 1-161 (the western facade, the distance from K. Marks prospect is 40 m, sound absorbing green planting) the equivalent and maximum levels of penetrating traffic noise were the following: with the window open - 49.2 dBA and 68.0 dBA; with the window closed - 45.6 dBA and 63.0 dBA respectively. This complies with Russian sanitary standards [5, p.81].

In classroom 1-156 (the southern facade, the distance from K. Marks prospect is 60 m, from Potanina St. - 80 m, no green planting) the equivalent and maximum levels of penetrating traffic noise were the following: with the window open - 64.1 dBA and 73.7 dBA ; with the window closed - 62.3 dBA and 69.0 dBA respectively. This does not comply with Russian sanitary standards [5, p.81], the excess of the equivalent noise exposure limit (NEL) for workstations equipped with a personal computer was from 2.3 to 4.1 dBA. At the same time a survey of employees did not reveal any subjective complaints about noise [16, p.305].

Earlier an assessment of noise pollution was made in the campus of Samara State Transport University (SSTU) situated on Litvinova Street. Measurements were taken outdoors using the electronic sound level meter Testo 815 (accuracy class 2, the error of measurement is 1 dB) during rush hours on working days [17, p.182]. The significant noise sources are road and railway transport which also have a vibration effect on buildings and structures. Motor vehicles are only operated outside the area under study (except for single vehicles and special vehicles for cleaning snow or pumping water).

The results are presented in Table 1 for the road and in Tab. 2 for the railway.

The name of the area	Traffic intensity (the number of traffic units per hour)	Noise level, dBA
Litvinova Street	2110	74
Litvinova Street and Dnepropetrovskij proezd Intersection	2950	79
Litvinova Street and Magistral'naya Street intersection	1530	73

Tab.1. Road traffic noise load

Types of rolling stock	Traffic intensity (the number of traffic units per hour)	Noise level, dBA
Freight rolling stock	10	84
Passenger rolling stock	7	83
Specialized rolling stock (for transporting containers, vehicles, etc)	3	83

Table 2. Railway traffic noise load

The influence of railway traffic noise is much greater than of the road traffic noise as the distance from the "L" building and the hangar to the railway is only 15 m. The length of the rail track along the training ground (including "Volga Region Museum of Railway Technology" located on the territory of SSTU on Litvinova Street) is 520 m. During classes students and academic staff feel discomfort from the railway traffic noise coming from the railway passing along the academic buildings. So, for example, the railway traffic noise level in classrooms with the window open is 83 dBA on average [17, p.182].

Noise impact monitoring and noise mapping are promising areas of the environmental program of Joint Stock Company "Russian Railways" (JSCo "RZD"). The main purpose of monitoring is to develop measures to reduce the negative impact of railway transport on people and residential buildings. As an example, there is a pilot project of a noise impact mapping on residential buildings in Oktyabrsk, Samara Region, developed by specialists from the Environmental Safety Center of SSTU. The measurements were taken in connection with residents' appeals to JSCo "RZD". They requested to reduce the noise impact on residential buildings from passing freight trains as there is the railway track directly near apartment buildings and private houses [18].

Authorized equipment such as sound level meter, vibration meter, spectrum analyzer EKOFIZIKA-110A, laser range finder "LeicaDistoD8" and acoustic calibrator AK-1000 was used to measure the noise impact on residential buildings. The measurements were taken at the distance of 10 m from the railway track in various areas near residential buildings in the daytime when freight and passenger trains passed at different speeds along the first and second tracks, as well as when two trains were running simultaneously. The noise measurement at Oktyabrsk station (Kuibyshev railway) are shown in Fig. 2.

Fig. 2: The noise measurement at Oktyabrsk station (Kuibyshev railway)

Studies have shown that the railway traffic noise level changes in the ranges of 62-93 dBA. It can have a negative impact of noise on people and residential buildings. Noise impact maps which were made with the help of the software "Ecologist. Noise "will allow JSCo "RZD" to determine the areas where it is necessary to implement measures for reducing noise exposure and avoiding penalties as a result.

4. PREVENTION OF TRAFFIC NOISE

The Branch road guidelines ODM 218.2.013-2011 determine measures to protect the adjoining territory from traffic noise by the category of the road, traffic intensity, the type of the territory and its development [7, p.27]. For city streets and roads with the close city development and multi-storey buildings the following measures are proposed:

- organizing the heavy trucks traffic outside residential areas (freight traffic assignment);
- full or partial (in time) restriction or prohibition of the heavy trucks traffic;
- organizing traffic with limited speed (up to 30 km / h);
- developing public transport;
- noise protective screens of medium (2-6 m) and large (over 6 m) heights provided that the normative insolation of residential buildings is ensured;
- full or partial isolation of the roadway (tunnels, galleries);
- soundproof glazing of building facades near the roads;
- screen planting;
- a combination of the above activities.

Active measures include those to eliminate or minimize the generation of noise due to the significant modernization of vehicle structures, roadways, logistics solutions and the introduction of urban electric transport [19, p.35, 20, p.77]. The most effective is replacing the noise exposure source, the implementing the priority development of quiet city transport (for example, monorail and subway) [21, p.14, 22, p.176].

The comparative analysis of the noise characteristics of ground railway transport and the effectiveness of noise protection measures were considered earlier [23, p.301]. Among the measures which reduce the noise impact from railway transport there can also be the following:

- continuous welded track laying;
- rail grinding;
- using noise-absorbing pads.

5. CONCLUSIONS

Noise mapping makes it possible to evaluate the spread of the negative impact of roads and railways on a residential area. The adjacency of academic buildings of railway transport universities in Omsk and Samara to roads and railways can cause increased noise exposure (when opening windows for ventilation). To minimize the acoustic load it is necessary to plant trees in the areas adjoining to the roadways, arrange noise protection screens and install air conditioners to minimize the window opening. To evaluate the impact of noise on ecosystems and establish man-made noise standards for biological objects it is necessary to do additional research.

REFERENCES

[1] Ministry of Natural Resources of Russia: State report "On the state and protection of the environment of the Russian Federation in 2018", Publishing NPP "Cadastre", Moscow, 844 p., 2019
[2] Ivanov, N.I.: The concept of noise reduction in the Russian Federation, in the reports of the V All-Russian scientific and practical conference with international participation: Protection from increased noise and vibration. ISBN 978-5-91753-100-7, Publishing House "Icing", St. Petersburg, P. 12-23, 2015
[3] Blagodareva, M. S., Kornilkov, A. S., Yarushin S. V., Malykh O. L.: On methodological approaches to the assessment of multifactorial risks for the health of the population exposed to the adverse effects of the human environment // Occupational medicine and industrial ecology, ISSN: 1026-9428, Moscow, No. 11. P. 41-45, 2018 DOI: 10.31089/1026-9428-2018-11-41-45
[4] Ministry of Health of Russia: Sanitary norms of SN 2.2.4/2.1.8.562-96 "Noise in the workplace, in the premises of residential, public buildings and on the territory of residential development", Information and Publishing Center of the Ministry of Health of Russia, Moscow, 28 p., 1997
[5] Ministry of Health of Russia: Sanitary rules and norms of SanPiN 2.2.4.3359-16 "Sanitary and epidemiological requirements for physical factors in the workplace", Information and Publishing Center of the Ministry of Health of Russia, Moscow, 106 p., 2016
[6] Kholopov, Yu.A., Khmelnitsky, Yu.N., Musatkina, B.V.: Analysis of the effectiveness of noise protection measures on railway transport, in the collection of reports of the All-Russian Scientific and practical conference with international participation: Protection from increased noise and vibration. ISBN 978-5-6042448-7-6, Publishing Institute of Acoustic Structures, LLC, Saint-Petersburg, P. 710-717, 2019
[7] Ministry of Health of Russia: Branch road methodological document of the ODM 218.2.013-2011 "Methodological recommendations for the protection of territories adjacent to highways from traffic noise", Publishing Federal Road Agency (Rosavtodor), Moscow, 160 p., 2012
[8] National standard of the Russian Federation GOST R 53187-2008. Acoustics. Noise monitoring of urban areas, Publishing Standartinform, Moscow, 34 p., 2009
[9] Ministry of Regional Development of the Russian Federation: Code of Rules SP 51.13330-11. Protection against noise. Updated version of SNiP 23-03-2003, Publishing Ministry of Regional Development of the Russian Federation, Moscow, 89 p., 2011
[10] Vasiliev A.V.: Analysis and approbation of modern methods of monitoring and mapping of physical pollution on the example of the Samara region // Izvestiya Samara scientific center of the Russian Academy of Sciences. ISSN 1990-5378, Samara scientific center of RAS. Vol. 15. No. 3. P. 272-277, 2013.
[11] Vasiliev A.V.: Noise safety of urban areas // Izvestiya Samara scientific center of the Russian Academy of Sciences. ISSN 1990-5378, Samara scientific center RAS. Vol. 16. No. 1. P. 299-305, 2014.
[12] Batrakova, G.M., Balandina, A.V., Zamarayeva, O.A.: Assessment of the traffic flow intensity and noise load on the territory of the PNRPU campus // Bulletin of the Perm National Research Polytechnic University. Applied ecology. Urban studies. 2016. № 4 (24). P. 88-100. DOI 10.15593/240975125/2016.04.07
[13] Balandina, A.V., Zamarayeva, O.A., Batrakova, G.M.: Analysis of the noise load on the sections of the road network near the educational buildings of the university // Transport. Transport facilities. Ecology. 2018. № 1. P. 13-20. DOI: 10.15593/24111678/2018.01.02
[14] Bocharov, A.A., Kolesnik, A.G., Soloviev, A.V.: Two-parametric model of the spectrum of traffic noise in Tomsk // Acoustical Physics. T. 58. № 6, P. 718-724, 2012. DOI: 10.1134/S1063771012060024
[15] National standard of the Russian Federation GOST 23337-2014 Noise. Methods for measuring noise in the residential area and in the premises of residential and public buildings, Publishing Standartinform, Moscow, 26 p., 2014
[16] Musatkina, B.V., Koobar, A.A.: Noise mapping as a tool for monitoring and assessing environmental quality, in the collection of works of the IV All-Russian scientific and practical conference with international participation: Instruments and methods of measurement, quality control and diagnostics in industry and transport. ISBN 978-5-949-41267-1, Publishing Omsk State Transport University, Omsk, P. 300-307, 2020
[17] Lysov, S.I., Kholopov, Yu.A.: On the effect of traffic flow on noise load in the urban environment, SCIENCE AND EDUCATION FOR TRANSPORT, Publishing Samara State Transport University, Samara, № 1, p. 182-183, 2015.
[18] SamGUPS scientists investigate the noise impact of rail transport // https://www.samgups.ru/news/uchenye_samgups_issleduyut_shumovoe_vozdeystvie_2020zheleznodorozhnogo_transporta/ Date accessed: 14.02.2021
[19] Basharkin, M.V., Kholopov, Yu.A.: Some approaches to creating a comfortable urban environment based on ecological and logistics solutions // Environmental systems and devices. ISSN 2072-9952. № 2, p. 33-40, 2019.
[20] Basharkin, M.V., Kholopov, Yu.A.: Ecological and logistical advantages of urban electric transport development in Samara, VOLGA TRANSPORT BULLETIN, ISSN 1997-0722, Publishing Samara State Transport University, Samara, № 3 (63), p. 73–77, 2017.
[21] Anfilofiev, B.A., Privalov, S.A., Kholopov, Yu.A.: Monorail - a promising solution to the transport problems of the city of Samara, ELPIT-2013. Ecology and life safety of industrial and transport complexes: a collection of works of the IV International Ecological Congress (VI International Scientific and Technical Conference), Publishing Togliatti state University, Togliatti, p. 10-15, 2013.
[22] Kalugina Yu.V., Kholopov Yu.A. Trends in the development of transport and the creation of a comfortable urban environment, ELPIT-2015. Ecology and life safety of industrial and transport complexes: a collection of works of the V International

Ecological Congress (VII International Scientific and Technical Conference), Publishing Togliatti state University, Togliatti, p. 173-177, 2015.
[23] Kholopov, Yu., Musatkina, B., Denisova, I.: The comparative analysis of the noise characteristics of land rail transport and the efficiency of noise protection measures // Akustika. ISSN 1801-9064. T. 32, p. 299-304. 2019

__Yurij Kholopov__ is Ph. D in Agricultural Science, Associate Professor, the Department of Biomedical Traffic Safety, Samara State Transport University; the member of the Social Council at the Ministry of Forestry, Environmental protection and Environmental Management of Samara Region.
Yurij Kholopov is a specialist in the field of transport and environmental issues, environmental monitoring and education, safety assessment and urban environment assessment. He participated in the international environmental educational project TEMPUS RECOAUD, EACEA, 2013-2016.
Yurij Kholopov is the author and co-author of more than 120 scientific publications He presented the main results of scientific research at international conferences in Moscow, St. Petersburg, Novosibirsk, Samara, Omsk, Yekaterinburg, Minsk, etc.

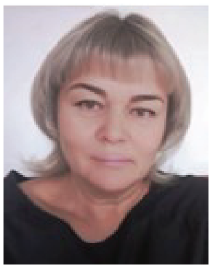

__Elena Lukenyuk__ is Ph. D in Technical Science, Associate Professor, the Department of Biomedical Traffic Safety, Samara State Transport University.
Elena Lukenyuk is a specialist in the field of transport and environmental issues, environmental monitoring and education, safety assessment and assessment of urban environment. She participated in the international environmental educational project TEMPUS RECOAUD, EACEA, 2013-2016.
Elena Lukenyuk is the author and co-author of more than 60 scientific publications, she presented the main results of scientific research at international conferences in St. Petersburg, Novosibirsk, Samara, Penza, Orenburg, Ryazan, etc.

__Bela Musatkina__ is a senior lecturer, the Department of Life Safety and Ecology, Omsk State Transport University (OSTU).
Bela Musatkina is a specialist in the field of employment protection and environmental protection in transport, assessing and reducing the negative impact of monorail transport on the environment, improving the quality and environmental friendliness of current collection devices, environmental education. She participated in the international environmental educational project TEMPUS RECOAUD, EACEA, 2013-2016.
Bela Musatkina is the author and co-author of more than 100 scientific publications and methodological guidelines, 4 monographs and 3 patents. She presented the main results of scientific research at international conferences in Moscow, St. Petersburg, Omsk, Samara, Yekaterinburg, Irkutsk, Rostov-on-Don, Seattle (the USA) etc.

__Inna Denisova__ is a senior lecturer, the Department of Russian and Foreign Languages, Omsk State Transport University (OSTU).
Inna Denisova is a specialist in the field of linguistics and has qualifications in railway car engineering and linguistics. She participated in Erasmus Mundus Programme «MULTIC» and took the internship at Sapienza University, Rome, in the Civil, Constructional and Environmental Engineering Department, 2015.
The subject of her scientific research is the multicomponent term formation in the field of railway cars and car maintenance.
Inna Denisova is the author of more than 20 scientific publications and methodological guidelines. She is the author of an English-Russian Dictionary of railway terms in the field of railway cars and car maintenance. She presented the main results of scientific research at international conferences in St. Petersburg, Samara, Bryansk, Omsk, Bishkek (Kyrgyzstan), Prague (the Czech Republic), Seattle (the USA) etc.

Paper No.379/2021

ANALYSIS OF METHODS AND PRESENTATION OF RESULTS OF EXPERIMENTAL RESEARCH OF LOW FREQUENCY GAS DYNAMIC PULSATIONS IN PIPELINES OF POWER PLANTS

Andrey Vasilyev

Samara State Technical University, Samara, Russia, avassi62@mail.ru

Abstract: *The results of analysis of Russian approaches and of experience of development of methods and of results of experimental research of low-frequency gas dynamic pressure pulsations in pipelines of power plants are described. Peculiarities of Russian standards and of the sanitary norms are considered. According to results of experimental researches is possible to conclude that the maximal vibration levels are observed on the frequencies 31,5 Hz and 40 Hz. The same results were obtained during the measurements of sound pressure level on the same experimental compressor mount. Earlier during the experiments on the same mount it was achieved that the maximal values of low frequency gas pressure pulsations are observed on the frequency 35 Hz. Thus, it was experimentally shown that gas pressure pulsations are making the main contribution into forming of low frequency sound and vibration of compressor mount.*

Keywords: *low frequency, pulsations, pipelines, power plants*

DOI: *: 10.36336/akustika20214200*

1. INTRODUCTION

Low frequency gas dynamic pressure oscillations (pulsations) generating during power plants operation are presently considered as a serious problem and may cause increased noise and vibration leading to the human health problems and for operational characteristic of power plants and joining pipeline systems [1-3, 7, 9-12]. Low-frequency gas dynamic pressure pulsations are spreading along pipeline main and appearing during alternating gas suction into the cylinder due to the pressure drop between cylinder recess and abutting pipeline [5, 6, 8].

This paper is devoted to discussion of results of analysis of Russian approaches and of experience of development of methods and of results of experimental research of low-frequency gas dynamic pressure pulsations in pipelines of power plants.

2. ANALYSIS OF THE RUSSIAN APPROACHES TO RESEARCH OF LOW FREQUENCY GAS DYNAMIC PLSATIONS IN PIPELINES OF POWER PLANTS

In Russia standards in the field of vibration safety are subdivided on the three main types.

1. Standards of type A. This type is including basic standards on vibration safety which are determining general terms and rules of provision of vibration safety; measured values; general methods of measurement and estimation of vibration taking to account different condition of impact of vibration to the man. In this type of standards the following Russian standards are included: 12.1.012, 31191.1, 31192.1 etc. Russian State Standard 12.1.012-2004 "Occupational safety standards system. Vibration safety. General requirements" determines general requirements to provision of vibration safety in industry, transport, construction, mining and other works connected with negative impact of vibration to the man. This standard is also determines the structure of complex of standards in the field of vibration safety and requirements to these standards.

2. Standards of type B (standards of group questions of vibration safety) are determining methods of measurement and estimation of vibration in concrete conditions of it impact or for large groups of products as well as separate private aspects of vibration safety. This type of standards is including Russian standards 31192.2, 31319, 31191.4, 16519, 31193, ISO 10326-1 etc.

2. Standards of type C are the standards on vibration safety connected with separate objects and separate products. Standards of this type may include vibration testing description, methods of reduction of vibration of machines, means of protection from vibration etc.

Concerning research of vibration of machines of separate kinds it should be noted that the standards in this field may be completely devoted to the questions of vibration safety or include some separate questions of vibration safety.

Vibration of machines may be measured in points where vibration is transmitted to support or connecting structures.

Noise of automobile internal combustion engines is measured according to the Russian State Standard R 53838-2010

"Automobile engines. Noise exposure limits and measurement techniques". This standard is determining the following noise characteristic of automobile engines: sound pressure level corrected on frequency characteristics of sound level meter, dBA; sound pressure levels in octave or 1/3 octave frequency bands, dB; sound power levels in octave bands of frequencies with average geometric frequencies from 125 up to 8000 Hz, dB; corrected for frequency response A of sound level meter sound power level, dBA.

During measurement of noise the microphone in the point of measurement must be oriented in direction of testing engine. Between the microphone and the engine should not be the objects that distort the sound field. The distance between microphone and observer should be at least 0,5 m. The switcher of time characteristic of sound level meter should be installed in position "slow".

Sound pressure levels should be measured in every of measurement points on the measuring surface with full fuel supply and at the speed of the crankshaft rotation corresponding to gross capacity (external speed characteristic).

In the point with maximal sound pressure level should be measured sound pressure levels in all operating range of crankshaft rotation frequencies. The number of measurements in the given point should be sufficient for determination of regime with maximal noise level.

Russian State Standard R 52231-2004 "External noise of motor vehicles. Permissible levels and methods of measurement" determines methods of automobile external noise measurement. As external noise indicator when checking the technical condition of the car the level of the automobile exhaust system is used. Measuring microphone is installed above the platform surface at the height of the location of exhaust pipe of muffler, but not lower than 0,2 m. Microphone is displaced at the distance (0,5±0,05) m from exhaust pipe cross section. The main axis of the microphone should be parallel to the surface of the platform with the deviation of no more than ±15° and make up the angle 45°±15° with vertical plane passing through the axis of flow of exhaust gases coming out of the exhaust pipe of the muffler. For the automobile with vertical location of the exhaust pipe the microphone is installed at the height of the exhaust pipe cutoff at the distance (0,5±0,05) m in direction of the nearest side of the automobile. Microphone axis is directed vertically, the membrane is oriented upwards.

Noise levels in industry in Russia are evaluated according to hygiene requirements, stated by valid sanitary norms, Russian state standards and building norms and rules. Normative parameters for unstable noise are equivalent sound levels and maximal sound levels , dBA. There are different noise values norms for different operational processes, but in any case noise levels must be lower than 80 dBA.

Vibration levels in industry in Russia are evaluated according to hygiene requirements, stated by valid sanitary norms, Russian state standards and building norms and rules. Hygienic vibration estimation parameters are vibration velocity and it logarithm levels and vibration accelerations in octave and 1/3 octave frequency bands. It is also admitted integral vibration estimation for all frequency range of vibration and estimation of vibration dose according to the time of vibration impact. For estimation of vibration levels of technological equipment also vibration displacements and its amplitudes are using as normative parameters.

In paper [4] the results of vibroacoustic characteristic research of the gas pipeline with discrete throttle valve are described. The levels of vibration acceleration in different parts of the main gas pipeline were measured. On the basis of experimental data, the possible causes of the acoustic-induced vibration are described, the measures of reduction of vibration loading of a gas pipeline were proposed.

Analysis is showing that existing methods and recommendation on research of vibration characteristic of gas guides of power plants are not allowing take into consideration characteristic and specific features of low frequency pulsations impact, e.g. measurements range, vibration load of the elements of power plants etc. Therefore, it is necessary to develop the methods of research of vibration characteristic of gas guides of power plants, including specific of low frequency gas dynamic pulsations impact.

3. EXPERIMENTAL SET-UP AND RESULTS OF EXPERIMENTAL RESEARCH OF LOW FREQUENCY GAS DYNAMIC PULSATIONS IN PIPELINES OF POWER PLANTS

Experimental research of characteristic of low-frequency gas dynamic pressure pulsations and caused by it noise and vibration were carried out by using of compressor mount installed in department of chemicals technology and industrial ecology of Samara State Technical University of Russia. The scheme of compressor mount is shown in Fig. 1. For measurements of gas dynamic pressure pulsations portable 4-40 channels analyzer of vibration, acoustic and tensor signals LMS SCADAS Mobile of production of "LMS International" company together with pulsations sensor of "PCB" company. For measurements of compressor noise and vibration sound level meter, vibration meter, spectrum analyzer ASSISTANT TOTAL was used.

Main frequency of compressor operation is frequency 35 Hz. Discharge pressure was fixed by pressure gauges.

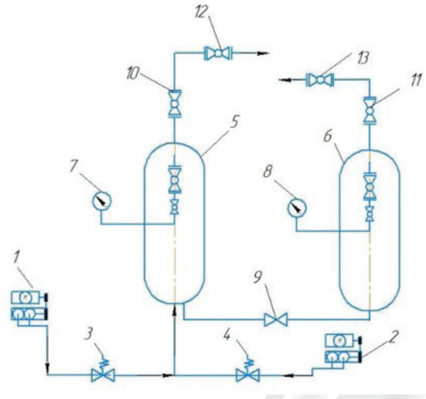

Fig. 1. The scheme of compressor mount for research of characteristic of low-frequency gas dynamic pressure pulsations: 1, 2 – compressors, 3, 4 – safety valves, 5, 6 - receivers, 7, 8 – pressure gauges, 9 – vent, 10, 11, 12, 13 – flanged connections

In Fig. 2 spectral characteristic of low-frequency gas pressure pulsations measured on experimental compressor mount during discharge pressure value 2 atmospheres is shown.

In Fig. 3 dependencies of levels of low frequency gas pressure pulsations measured on the main frequency of compressor mount operation from discharge pressure are shown.

Also, measurements of noise and vibration levels were carried out on experimental compressor mount. In Fig. 4 third-octave spectrum of sound pressure level during compressor mount operation is shown. In Fig. 5 octave spectrum of vibration acceleration level on pipeline of experimental compressor mount (direction X) is shown.

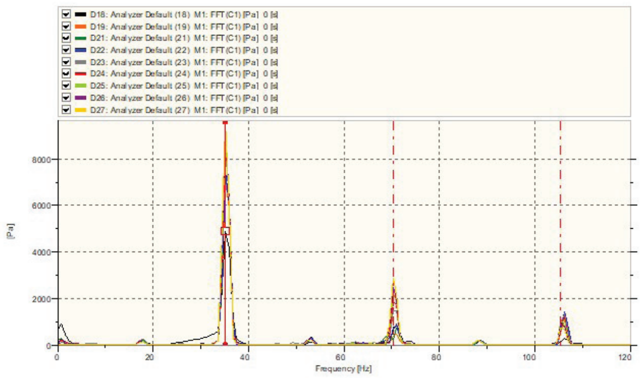

Fig. 2. Spectral characteristic of low-frequency gas pressure pulsations measured on experimental compressor mount during discharge pressure value 2 atmospheres

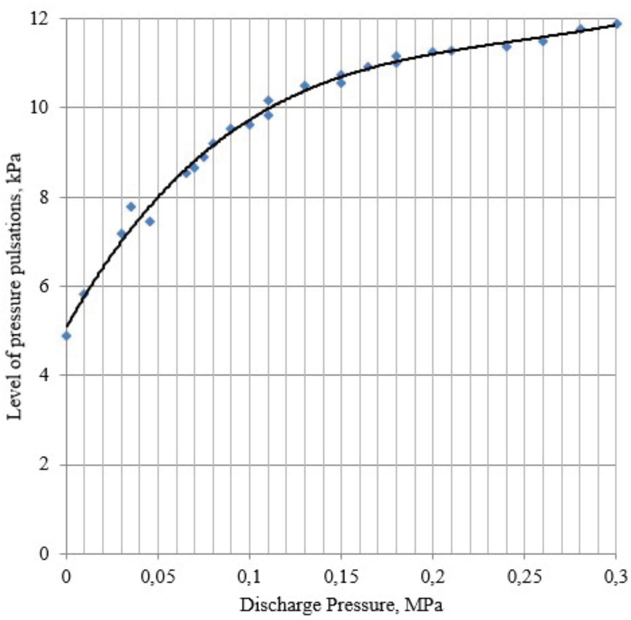

Fig. 3. Dependencies of levels of low frequency gas pressure pulsations measured on the main frequency of compressor mount operation from discharge pressure, MPa

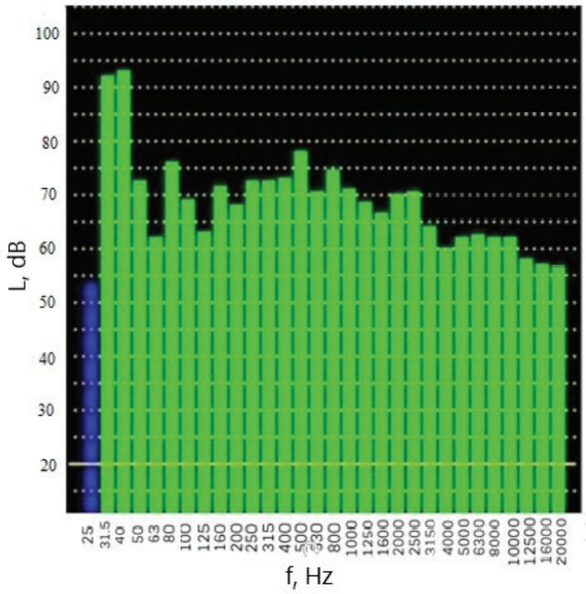

Fig. 4. Third-octave spectrum of sound pressure level during compressor mount operation

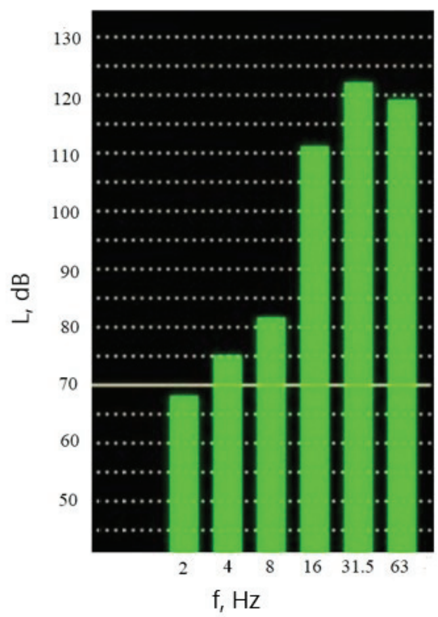

Fig. 5. Octave spectrum of vibration acceleration level on pipeline of experimental compressor mount (direction X)

In real industrial conditions in shop N4 of "KuibyshevAzot" public joint stock company (chemical enterprise of Russian Federation) acoustical and vibration characteristic of opposed piston compressor "Mannesmann – Meer" were done. Third-octave spectrum of sound pressure level measured during operation of opposed compressor mount is shown in Fig. 6.

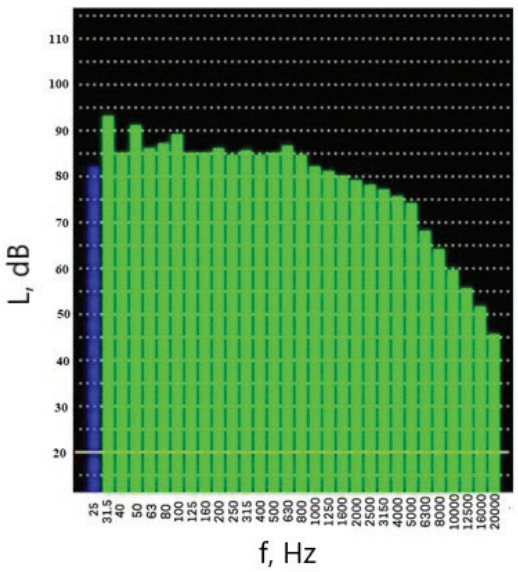

Fig. 6. Third-octave spectrum of sound pressure level measured during operation of opposed compressor mount of in shop N4 of "KuibyshevAzot" public joint stock company:

Analysis of results of experimental researches was carried out. According to results of experimental researches it is possible to conclude that:

- The main frequency of compressor operation is 31,5 Hz;
- For compressor mount for all measurements the maximal values of gas pressure pulsations were observed on the main frequency of compressor operation;
- Intensity of discrete components of gas pressure pulsations in depending on discharge pressure. The more high discharge pressure, the more amplitude of pulsations;
- The characteristic of pulsations is harmonic, amplitude of pulsations is increasing with increasing of discharge pressure.
- Analysis of octave and third octave spectra of vibration acceleration measured on pipeline of experimental compressor mount is showing that the maximal vibration levels are observed on the frequencies 31,5 Hz and 40 Hz. The same results were obtained during the measurements of sound pressure level on the same experimental compressor mount.

Earlier during the experiments on the same mount it was achieved that the maximal values of low frequency gas pressure pulsations are observed on the frequency 35 Hz. Thus, it was experimentally shown that gas pressure pulsations are making the main contribution into forming of low frequency sound and vibration of compressor mount.

According to results of experimental researches of acoustical characteristic of opposed piston compressor "Mannesmann – Meer" of "KuibyshevAzot" public joint stock company it is possible to conclude, that maximal values of sound pressure level were measured in low frequency range. On the main frequency of compressor operation 125 Hz sound pressure level is maximal which is in correspondence with measurement results on the laboratory compressor mount.

4. CONCLUSIONS

Russian approaches of power plants low frequency noise and vibration characteristic estimation are described. Russian standards, sanitary norms as well as personal author's methods are considered. Experimental set-up for research of characteristic of low-frequency gas dynamic pressure pulsations and caused by it noise and vibration was developed. Experiments were carried out by using of compressor mount installed in department of chemicals technology and industrial ecology of Samara State Technical University of Russia and in real industrial conditions in shop N4 of "KuibyshevAzot" public joint stock company.

In result of experiments it was shown that gas pressure pulsations are making the main contribution into forming of low frequency sound and vibration of power plant on the example of compressor mount.

Using of results of this paper may be useful for analyzing and selecting optimal decisions for power plants low-frequency noise and vibration reduction and for further development and application of constructions of power plants with reduced vibration levels.

ACKNOWLEDGEMENT

The research described in this paper was supported by the grant of Russian Scientific Foundation, project number: 20-19-00222.

REFERENCES

[1] A.A. Igolkin, A.N. Kovartsev, D.M. Stadnik. A research on acoustic characteristics of gas pressure regulator with silencer. International Journal of Acoustics and vibrations. 2017. Vol. 22. N4. Pp. 507-510.
[2] N.I. Ivanov, I.S. Rassoshenko, V.V. Krylov. The problem of estimating the vibrational fields produced by surface Rayleigh waves by high-speed railways. Noise Theory and Practice. 2018; 2 (4), pp.21-29.
[3] P R. Kirby, K. Amott, P.T. Williams, W.Duan. On the acoustic performance of rectangular splitter silencers in the presence of mean flow. Journal of Sound and Vibration, Volume 333, Issue 24, 2014, pp. 6295-6311.
[4] L.F. Musaakhunova, A.A. Igolkin and, K.Y. Shabanov, The vibroacoustic characteristics research of the gas pipeline. Procedia Engineering. 2015. Vol. 106, pp. 316-324.
[5] A.A. Ogarkov, A.V. Vassiliev, V.I. Voltchonkov. About the experience of low-rotated piston compressor units vibration reduction. Proc. of the 29 International Congress on Noise Control Engineering "Inter-noise 2000", Nice, France, 2000 August 27-30, Volume 6, pp.3932-3936.
[6] R.N. Starobinsky, A.V. Vassiliev, V.N. Krokhin, V.I. Voltchonkov, A.M. Desyatkin. Pressure oscillations damper for the suction system of piston machine. Invention certificate 1789748, Russia, 1993.
[7] Tan Y., Guan R., Zhang Z. Performance of accelerated oscillator dampers under seismic loading. Advances in Mechanical Engineering, 2018, 10 (4).
[8] A.V. Vasilyev. Development and approbation of methods and technical solutions of reduction of vibration of power plants and joining mechanical systems. Procedia Engineering. 2015. Vol. 106. pp. 354-362.
[9] A.V. Vasilyev. New methods and approaches to acoustic monitoring and noise mapping of urban territories and experience of it approbation in conditions of Samara region of Russia. Procedia Engineering. 2017. Volume 176. pp. 669-674.
[10] A.V. Vasilyev. Approaches to the estimation of ecological risk during the impact of acoustical pollutions. "Ecology and Industry of Russia", Moscow, 2018, Vol. 22, N3, pp. 25-27.
[11] A.V. Vasilyev, V.A. Sannikov and N.V. Tyurina Experience of estimation and reduction of noise and vibration of industrial enterprises of Russia. Journal "Akustika", Czech Republic, Volume 32, March 2019, pp. 247-250.
[12] V.M. Zinkin, S.K. Soldatov, A.V. Bogomolov, S.P. Dragan. Relevant problems of protection of population from low frequency noise and infrasound. Technologies of civil security. 2015. Vol. 12, No. 1(43), pp. 90-96.

Andrey Vasilyev *is Doctor of Technical Science, Professor, honorary worker of higher education of Russia. Presently he is director of the Institute of Ecology of Volga Basin of Russian Academy of Science – Branch of Samara Federal Research Center of Russian Academy of Science and professor of Department of Chemical Technology and Industrial Ecology of Samara State Technical University, head of Povolzhsky Resources Center of Industrial Ecology and Chemical Technology of Samara State Technical University. Author of over 15 books (ecology, environmental protection, acoustics), over 900 scientific papers. Main organizer and scientific manager of ELPIT congresses since 2003 (http://elpit-congress.ru). Editorial and scientific member of a number of famous Russian and foreign scientific journals and editions. Expert of Russian Academy of Science, of Russian scientific fund, of scientific-technical field of Ministry of education and science of Russia etc., grant-holder of DAAD (Germany), Open world program (USA) etc.*

Paper No.380/2021

ANALYSIS OF THE FACTORS DECREASING THE EFFICIENCY OF OPERATION OF ACTIVE NOISE AND VIBRATION CONTROL SYSTEMS IN DUCTS AND THE WAYS OF IMPROVEMENT OF PROTECTION

Andrey Vasilyev

Samara State Technical University, Samara, Russia, avassi62@mail.ru

Abstract*: The factors influencing on the active noise and vibration control system efficiency of operation and the ways of the system protection improvement are discussed. Analysis of factors decreasing the efficiency of operation of active noise and vibration control systems in ducts is showing that there are such factors as physical characteristics of operating medium (temperature, pressure, moisture, vibrations, dust), masking acoustic and vibrating interferences of other sources of noise and vibration etc., which may significantly reduce the efficiency, reliability and durability of active systems operation. The ways of improvement of protection of the elements of the active noise and vibration control system are discussed. Further improvement of active noise control and vibration system elements protection allows the system to operate with higher efficiency and reliability. Widely, achieving of good results in the solution of this problem helps us to extend the possibilities of active noise and vibration control systems practical application.*

Keywords: *active control, low frequency, noise, vibration, ducts, protection*

DOI: *: 10.36336/akustika20214205*

1. INTRODUCTION

Active noise and vibration control technique is especially efficient in low frequency range of sound and vibration [1, 2, 7, 11, 28, 29, 32]. Recent years have brought a significant progress in active noise and vibration control systems developments for different kinds of transport noise reduction. It is brightly illustrated by a huge and continuously increasing number of patents in active noise & vibration control. Presently the world-wide companies – automobile manufacturers ("General Motors", "Ford", "Lotus Engineering", "Volkswagen", "BMW", "AUDI", "Peugeot", "Nissan" etc. [4, 9, 17, 19, 24, 34 etc.]), specialized consulting companies ("Sound Attenuators Ltd.", "Nelson Industries", "Topexpress Ltd", "Noise Cancellation Technologies, Inc.", "Active Noise and Vibration Technologies, Inc" etc., [5, 8, 21, 26 etc.]), research & development institutions and universities (National Research Development (Great Britain), Müller BBM GmbH (Germany), Fraunhofer-Gesellschaft (Germany), Acoustic Institute named by N. N. Andreev of Russian Academy of Science, Samara State Technical University etc. [3, 12, 16, 30, 31, 33 etc.]), and also such well-known companies as Matsushita, Hitachi, Toshiba, Philips, Sharp, Lockheed etc. [5, 6, 10, 18, 22, 25, 26]) have developed a numerous number of active noise and vibration control elements and devices.

Now active noise and vibration control technique is using in a variety of fields of practical application, see e.g. [20], and every year brings us the new possibilities for this principal realization. One of specific fields is active noise and vibration control in ducts. But even here we may point out many branches of application, e.g. intake and exhaust noise of internal combustion engines, vibration of pipelines of power plants, fan noise in ducts, noise of fluid distribution systems etc.

There are many publications on this topic devoted to theoretical and experimental data analysis. For the purposes of practical usage of active noise and vibration control technique the problem of elements protection from external interferences arises. External interferences may change the system frequency response, directional characteristics, impedance, sensitivity etc. The improvement of active noise control system elements protection allows the system to operate with higher efficiency and reliability. Widely, achieving good results in the solution of this problem helps us to extend the possibilities of active noise control systems practical application.

This paper is devoted to analysis of factors decreasing the efficiency of operation of active noise and vibration control systems in ducts and to discussion of the ways of improvement of protection.

2. ANALYSIS OF FACTORS DECREASING THE EFFICIENCY OF OPERATION OF ACTIVE NOISE AND VIBRATION CONTROL SYSTEMS IN DUCTS

For the purpose of active noise and vibration control systems in duct practical usage, despite on the different fields of application we may find some common factors which affect the system operation efficiency, durability and reliability. Let us point out and briefly analyse the main factors here.

1. Physical characteristics of operating medium.

1.1. High pressure and velocity of gas flow

This problem seems to be one of the main for the active noise and vibration control technique application to reduce fan or compressor noise in flow ducts, especially for high flow pressure and velocity values. It should be noted that not only the absolute value of high-pressure level causes the problems of protection, but also rapid pressure increasing.

1.2. High temperature

The problem of high temperature is well known in exhaust noise mufflers development. There are also the problems for other active noise and vibration control applications: noise and vibration control of combustion turbines, boiling systems, waste gas incinerators etc. High temperatures could significantly influence the loudspeaker protection, especially to membrane elasticity, damage the steaky connection between different membrane elements, may also cause the plastic deformation of membrane parts etc. Also changing in duct acoustics, e.g., for system resonators development, and active noise and vibration control microphone damage under high temperatures are the practical problems that often occur.

1.3. Moisture variations

This factor could be very significant for some cases of active noise and vibration control systems practical application where the operating medium contains liquid adding in the gas flow. The problem of active noise and vibration control system protection for the medium with high moisture level is a field for the serious investigations carrying out. A special problem of moisture is that it increases the mass of the loudspeaker´s membrane, which could change its characteristics.

1.4. Dust or environmental dirties

ANC system elements pollution by dust and environmental dirties could change systems characteristics, reduce system operation efficiency. Especially low-dispersed dust is undesirable. The interaction of moisture and dirt storing in the inert fibres is to provide a breeding ground for micro-organisms.

2. Masking interferences of other noise and vibration sources.

Masking interferences could affect active system turn-in and to decrease the value of noise level reduction. For example, when we use an active noise and vibration control system for automobile internal combustion engine intake noise reduction such interferences are caused by exhaust noise, engine body noise etc.

3. External vibration sources.

Vibration influence on the active system elements causes the system frequency characteristics variation, mechanical damage, alteration of the loudspeakers sound radiation value and directivity.

4. Affecting of active noise and vibration control system elements by active chemical components in flow.

In some cases of active noise and vibration control system practical usage for cancellation of flow noise in ducts there are aggressive chemical components in the flow (e.g. chlorine, ammonia etc.) which could damage active noise and vibration control system elements. Especially rubber and plastic elements of the loudspeaker membrane tend to be damaged by aggressive contaminations.

5. "Weak links" of active system elements.

Here we are using the term "weak links" for describing of the elements of active noise and vibration control systems in ducts which are most sensitive to the influence of external factors. Usually such "weak links" are actuators (e.g. loudspeakers) and sensors (e.g. microphones).

Especially steaky connections between loudspeaker´s membrane elements disturbance is dangerous.

3. THE WAYS OF IMPROVEMENT OF PROTECTION OF ACTIVE NOISE AND VIBRATION CONTROL SYSTEMS IN DUCTS

Let us consider the main ways of improvement of protection of

1. Mechanical protection.

Despite on the variety of different approaches to solve the problem of protection for active noise and vibration control systems, the method of mechanical protection still remains one of the most reliable (but not always the cheapest). For the purpose of active noise and vibration control system elements protection under high pressure, dust or other pollutions in ducts the mechanical protection is especially convenient to use.

2. Using of alternative sound energy sources and sensors.

S. Akishita suggested using of piezoelectric elements as actuators and sensors [1, 2]. Besides of the problem of active system elements protection (disturbances exciting vibration in the structure system control), this approach allows to significantly reduce sound power mainly at natural mode frequencies.

Using of flow energy as the source for flow noise reduction may be considered as a promising solution for alternative sources using. This approach is relatively new, but some interesting results were achieved.

A good solution, especially for attenuation of low-frequency periodic noise in pipe reduction is using of oscillating valve as a sound generator [11]. The main advantages of this type of actuator using are its small size and durability. But there are also some problems of such actuator using: back pressure forming, restricted possibilities for high frequencies etc.

In order to avoid active noise and vibration control system elements contamination with dust and dirt and further growth of microorganisms as well as to prevent migration of fibres in the air stream H.Leventhall et al are suggesting an alternative non-fibrous low-air resistance method of noise reduction in ducts [14]. It was shown, that the low frequency noise attenuation of an active silencer is similar to, or better than, that of passive silencer of the same length and is free of fibres and pressure loss.

One of the approaches is using of alternative sources for high sound pressures and low frequencies. There are also some other patents for alternative actuators (e.g. hollow piezoceramic cylinders).

3. Active noise and vibration control system elements construction improvement.

There are well known many publications on the subject of active noise and vibration control system elements constructive parameters improvement, especially for loudspeaker construction design [11, 13, 15 etc.]. In Fraunhofer Institute of Building Physics a number of theoretical and experimental investigations were undertaken for the new active noise and vibration control systems constructions development for the different fields of application. In paper [12] a new active absorbing silencers construction is suggested to use for noise reduction in large ducts new active absorbing silencers construction consisted of cascaded autonomous cassettes with analogue feedback which are able to provide the desired wall impedances and at the same time to avoid the complexity of systems based on digital signal processors.

There is specific problem of automobile intake system low-frequency noise reduction because of additional hydraulic resistances in the intake noise mufflers could cause significant air flow pressure losses in the intake system. Specific problems of automobile intake noise reduction using active noise and vibration control systems and new system constructions with improved protection are discussed and suggested by the author in [23, 28, 31].

4. CONCLUSIONS

The analysis of different external factors affecting the efficiency, reliability and durability of active noise and vibration control systems in ducts is showing that industrial application of active noise and vibration control units is restricted by the number of factors. Among of them are:

1. Insufficient active systems protection from the influence of interferences, such as physical characteristics of operating medium (temperature, pressure, moisture, vibrations, dust), masking acoustic and vibrating interferences of other sources of noise and vibration, etc., which may significantly reduce the efficiency, reliability and durability of active systems operation.
2. Rather expensive construction of active noise and vibration control units.
3. Significant power consumption for creation of required active sound characteristics etc.

Further improvement of active noise control and vibration system elements protection allows the system to operate with higher efficiency and reliability. Widely, achieving of good results in the solution of this problem helps us to extend the possibilities of active noise and vibration control systems practical application. Thus, it is necessary to develop active noise and vibration control systems with improved protection from external and internal factors impact, including active noise and vibration control systems elements protection, especially "weak links" - the elements of an active noise control system for ducts which are most sensitive to the influence of external factors. Usually such "weak links" are actuators (loudspeakers) and sensors (microphones).

The next tasks are reducing of energy consumption during active noise and vibration control systems operation (for example, by using of alternative sound energy sources and sensors), increasing of durability and reliability of active noise and vibration control systems, decreasing of the cost of active noise and vibration control systems etc. It is necessary also to develop the methods for further investigations of power plants noise and vibration reduction using active noise and vibration control technique, including the investigations for capsulated and partially capsulated noise sources; evaluation of the influence of designed active noise and vibration suppressors on the operative characteristic of power plants, temperature regime etc.

Using of results of this paper may be useful for analyzing and selecting of optimal decisions for power plants low-frequency noise and vibration reduction using active noise and vibration control approaches.

ACKNOWLEDGEMENT

The research described in this paper was supported by the grant of Russian Scientific Foundation, project number: 20-19-00222.

REFERENCES

[1] S. Akishita, T. Okamoto, Y. Mitani. Power optimal control of sound transmission through plate by use of piezoelectric elements: Proc. of "Inter-Noise 96" Congress, pp.1207-1210, England, 1996.
[2] S. Akishita, K. Matsuo, Y. Mitani. Adaptive disturbance cancelling control for sound transmission through plate by using piesoelectric sensors and actuators: Proc. of ACTIVE 97 Symposium, Budapest, Hungary, 1997.
[3] V.D. Belov, A.I. Orlov, D.A. Smagin. Devices of active cancellation of vibration. Patent of Russian Federation N RU 2572664 C2. Filed: June 04 2014. Patented: January 20 2016.
[4] Chen Min-Te, Li Min-Ran, Krishnasvami Ramasunder (Ford Global Technologies, USA): Active noise reduction and suppression system. Patent of Russian Federation N RU 2709700 C2. Filed: April 07 2016. Patented: December 19 2019.
[5] A.R.D. Curtis (ANVC, USA): Active Noise Cancellation. International Patent Application WO 93/15501 A1. Priority (GB): January 28, 1992. Published: August 5, 1993.
[6] M. Eguchi, H. Iida (Sharp, Japan): Active Silencer with Improved Method of Selecting Coefficient Sequence. European Patent Application No. 0 530 523 A2. Priority (J): August 6, 1991. Published: March 10, 1993.
[7] S. Elliott. Active Control of Noise and Vibration - State of the Art and Future Prospects. - NAM'94, Aarhus, Denmark, 1994 - pp.13-24.
[8] L.J. Eriksson, M.C. Allie, R.H. Hoops (Nelson Ind., USA): Hybrid Active Silencer. US Patent No. 4,665,549. Filed: Dec. 18, 1985. Patented: May 12, 1987.
[9] E.R. Geddes (Ford, USA): An Active Noise Cancellation Apparatus. European Patent Application No. 0 454 341 B1. Priority (USA): April 25, 1990. Patented: August 23, 1995.
[10] H. Hamada et al. (Hitachi, J): Electronic Noise Attenuation System. US Patent No. 4,783,817. Patented: Nov. 8, 1988. Priority (Japan): Jan. 14, 1986.
[11] C.H. Hansen, S.D. Snyder. Active Control of Noise and Vibration. 1997, Cambridge University Press UK. P:1267.
[12] J. Krüger, Ph. Leistner. Calculation of actively absorbing duct linings. Proc. of ACTIVE 97 Symposium, Budapest, Hungary, 1997.
[13] H.G. Leventhall. Loudspeaker in active attenuation. NOISE-93, St. Petersburg, Russia, 1993.
[14] H.G. Leventhall, S. Dineen, J. Walker, S. Wise. Active noise attenuation as a route to quiet duct systems without using fibrous material. INTER NOISE 96, Liverpool, England, 1996.
[15] A.M. McDonald et al. (Lotus, GB): Attenuation of Dynamic Pressure Fluctuations in Ducts. International Patent Application WO 91/09214 A1. Priority (GB): December 12, 1989. Published: June 27, 1991.
[16] F.P. Mechel. Hybrider Schalldämpfer. German Patent Application No. 40 27 511 C1. Filed: August 30, 1990. Patented: October 2, 1991.
[17] Y. Nakaji (Nissan, J): System for Reducing Noise in Vehicular Cabin. European Patent Application No. 0 410 685 A2. Priority (J): July 24, 1989. Published: January 30, 1991.
[18] J.A.M. Nieuwendijk et al. (Philips, NL): Silencer Arrangement for Combustion Engines. European Patent Application No. 0 589 516 A2. Priority (EP): September 23, 1992. Published: March 30, 1994.
[19] D.P. Pfaff et al. (General Motors, USA): Method and Apparatus for Attenuating Engine Generated Noise. European Patent No. 0 479 367 B1. Priority (USA): October 4, 1990. Patented: August 9, 1995.
[20] S. Renault, P. Micheau, J. Tartarin, M. Besombe. Industrial Applications of Active Control of Pulsed Flow. "Inter Noise 96", Liverpool, pp. 1061-1066.
[21] C. F. Ross, G.P. Eatwell (ANVT, USA): Active Sound and/or Vibration Control. US Patent No. 5,365,594. Patented: November 15, 1994. Priority (GB): August 17, 1988.
[22] S. Suzuki (Toshiba, J): Active Noise Control Apparatus. US Patent No. 5,377,275. Priority (J): July 29, 1992. Patented: December 27, 1994.
[23] R.N. Starobinsky, A.V. Vasilyev, V.N. Gordeev, V.V. Vasilyev. System of active noise suppression of internal combustion engine. Patent of Russian Federation 2096651, Russia, 1997.
[24] I. Stothers et al. (Lotus Cars Ltd., GB): Adaptive Control System. International Patent Application WO 94/09480 A3. Priority (GB): October 21, 1992. Published: April 28, 1994.
[25] S. Suzuki (Toshiba, J): Active Noise Control Apparatus. US Patent No. 5,377,275. Priority (J): July 29, 1992. Patented: December 27, 1994.
[26] Swinbanks, M.A. (National Research Development, GB): Active Control of Sound Waves. US Patent No 4,044,203. Priority (GB): Nov. 24, 1972. Patented: August 23, 1977.
[27] H. Takeyama et al. (Matsushita, J): Acoustic Conductance and Silencer Utilizing Same. European Patent Application No. 0 483 921 A1. Priority (J): October 31, 1990. Published: May 6, 1992.
[28] A.V. Vassiliev. Compact active noise control units for automobile intake low-frequency noise attenuation. Proc. of "ACTIVE 97" International Symp., Budapest, Hungary, August 21-23 1997, p.587-594.
[29] A.V. Vassiliev. Automobile engine low frequency noise reduction by complex using of active noise control method: Proc. of "ISMA 25" the International Noise and Vibration Conference, Leuven, Belgium, September 13-15 2000, Vol.1, pp.37-44.
[30] A.V. Vasilyev. Development and approbation of methods and technical solutions of reduction of vibration of power plants and joining mechanical systems. Procedia Engineering. 2015. Vol. 106. pp. 354-362.
[31] A.V. Vasilyev A.V. Automobile internal combustion engine low frequency noise reduction using active noise control solutions. Journal "Akustika", Czech Republic, Volume 34, November 2019, pp. 113-117.

[32] A.V. Vasilyev. Approaches to the estimation of ecological risk during the impact of acoustical pollutions. "Ecology and Industry of Russia", Moscow, 2018, Vol. 22, N3, pp. 25-27.
[33] A.I. Vyalyshev, A.M. Gavrilov, G.S. Lyubashevsky, Yu.S. Choni. Synthesis of system of compensation of vibration and sound fields. Acoustical Journal. 1977, Vol. 23, N2, pp. 467-475.
[34] Y. Yuan (General Motors, USA): Active Noise Control System for Attenuating Engine Generated Noise. US Patent No. 5,222,148. Filed: April 29, 1992. Patented: June 22, 1993. and: US Patent No. 5,321,759. Filed: April 29, 1992. Patented: June 14, 1994.
[35] S. Wise, G. Leventhall. Active Noise Control As a Solution to Low Frequency Noise Problems Journal of Low Frequency Noise, Vibration and Active Control. Vol. 29, N.3, pp. 19-137. 2010.

Andrey Vasilyev *is Doctor of Technical Science, Professor, honorary worker of higher education of Russia. Presently he is director of the Institute of Ecology of Volga Basin of Russian Academy of Science – Branch of Samara Federal Research Center of Russian Academy of Science and professor of Department of Chemical Technology and Industrial Ecology of Samara State Technical University, head of Povolzhsky Resources Center of Industrial Ecology and Chemical Technology of Samara State Technical University. Author of over 15 books (ecology, environmental protection, acoustics), over 900 scientific papers. Main organizer and scientific manager of ELPIT congresses since 2003 (http://elpit-congress.ru). Editorial and scientific member of a number of famous Russian and foreign scientific journals and editions. Expert of Russian Academy of Science, of Russian scientific fund, of scientific-technical field of Ministry of education and science of Russia etc., grant-holder of DAAD (Germany), Open world program (USA) etc.*

Paper No.381/2021

DETERMINATION OF THE INFLUENCE OF STRUCTURAL ELEMENTS ON ACOUSTIC EFFICIENCY AND BACK PRESSURE IN EXHAUST AND SUCTION NOISE SILENCERS

[a] Nickolay Ivanov, [b]Aleksandr Shashurin, [c]Aleksandr Burakov

[a, b] Samara State Technical University, Samara, Russia, [a] 7596890@mail.ru
[c] Baltic State Technical University «VOENMEH» named after D.F. Ustinov, St. Petersburg, Russia

***Abstract**: The features of noise generation processes in exhaust and suction noise silencers are shown. A method for testing silencers has been developed. The classification of the main structural elements of exhaust and suction noise silencers, depending on the purpose, is proposed. Experimental studies of the relationship between the acoustic efficiency and the back pressure of silencers from the structural design of the elements are performed. The factors influencing the efficiency in the low-frequency and high-frequency regions of the spectrum are determined: the volume of silencers, the number of chambers, perforation, sound absorption, flow ejection, etc. Recommendations for the design of noise silencers are proposed.*

***Keywords:** noise, silencers, noise generation processes, structural elements, volume of silencers, ejection elements, perforation, sound absorption, flow rotation, design of silencers, recommendations.*

***DOI:** : 10.36336/akustika20214210*

1. INTRODUCTION

The outstanding Russian scientist Professor E. Ya. Yudin called the design of silencers to a considerable extent an art [1], because there were no reliable engineering methods for calculating silencers. And currently there are no engineering methods for calculating them. There are no answers to important questions about how to link the acoustic efficiency of a silencer, for example, with its volume, the area of perforation of internal elements, or a change in the direction of movement of the gas flow, etc., despite many publications considering various acoustic processes in silencers [2-5, 10]. For the sake of objectivity, we note the presence of a number of software products that are widely used in practice for the design of silencers, but the accuracy of these results requires additional consideration.

It seems useful to study these dependencies experimentally. For this purpose, more than 100 models of silencers were developed and manufactured, which were tested on a special stand. The experimental stand was created on the basis of a mobile compressor station equipped with an internal combustion engine with a capacity of 60 kW. The engine develops 2200 rpm. The load on the engine is carried out by a compressor with the last compressed air produced diverted to the side. The engine and compressor are located under the soundproof hood. The exhaust was brought to the roof, the tested silencers were sequentially located at the end of the exhaust pipe.

Tests of silencers were carried out in accordance with the documentation [6]. The acoustic efficiency of the silencers was determined as the difference between the average values of the exhaust noise with a measuring pipe (a pipe whose length is equal to the length of the silencer, and the diameter is proportional to the diameter of the silencer inlet pipe). The location of the measuring points on the cut of the tube or outlet pipe of the muffler is shown in Fig. 1.

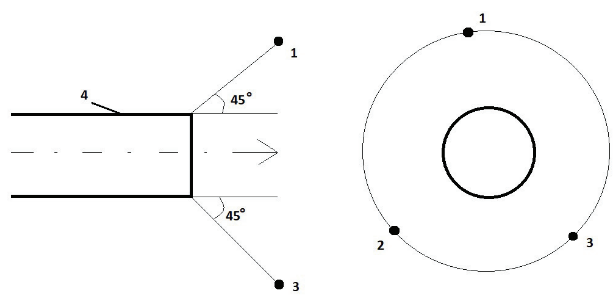

Fig. 1. Measurement scheme: 1-3 – measurement points, 4 – pipe (muffler outlet pipe), –› – flow direction

Additionally, the back pressure created by the experimental muffler was measured, as well as the temperature of the exhaust gases at the inlet to the muffler and in the outlet pipes of the muffler.

2. THE MAIN DESIGN SCHEMES OF THE TESTED SILENCERS

The physical processes in silencers are quite complex. With some degree of simplification, all the processes associated with the occurrence of noise on the exhaust pipe section can be reduced to two main ones [7]. The low-frequency and partly medium-frequency regions of the noise spectrum (Fig.2) are formed by processes occurring in the combustion chamber, where sound levels can reach 130-140 dB. This noise exits through the exhaust valves, passes through the exhaust pipe, and its levels at the measured points reach 110-120 dB in the specified frequency ranges. Note that these components are predominant in the spectrum. The components in the high--frequency part of the spectrum in the frequency range of 1000-8000 Hz are characterized by sound pressure levels of 100-115 dB (Fig.2). The noise in the high-frequency region and partly at medium frequencies owes its origin to a gas jet that generates turbulent flows at the outlet of the pipe. The intensity of turbulent noise is primarily related to the speed of the gas flow and the phenomena of pulsations in it [8]. Noise maxima are observed in both the left and right parts of the spectrum, respectively, at frequencies of 63 and 2000 Hz.

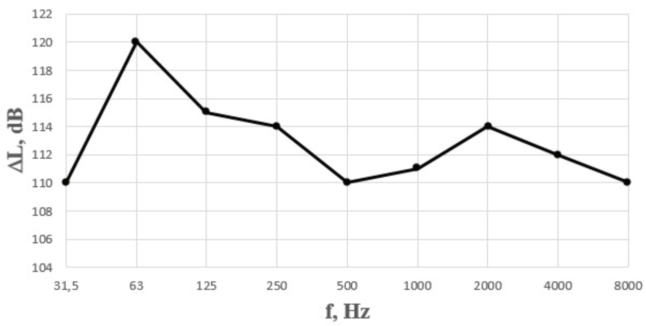

Fig. 2. The noise spectrum of the free exhaust of the internal combustion engine

Experimental models of silencers were developed in accordance with their classification [7, 9]. The main structural elements that affect the acoustic efficiency of mufflers: expansion chambers, perforated and blind tubes and partitions, elements of ejection and conversion of the gas flow, etc.

The task was set: to find out the degree of influence of the main structural elements of silencers on their acoustic efficiency and the amount of back pressure, as well as to identify the mechanisms of noise suppression. The design schemes of the experimental silencers were designed to identify the impact on the studied parameters:

- the volume of the silencer chamber,
- the number of chambers,
- the presence of perforation,
- the presence of a Venturi tube,
- the presence of sound absorption,
- the presence of a resonant chamber,
- the location of the inlet and outlet pipes in the silencer,
- the presence of devices that change the flow direction in the silencer.

The main design schemes of the tested silencers are shown in Tab. 1.

№	Design scheme, name	Symbols on the diagram	Efficiency, dBA
01	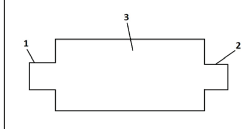 Single-chamber	1 – inlet pipe, 2 – outlet pipe, 3 – hollow chamber	5
02	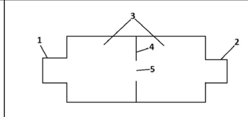 Two-chamber	1 – inlet pipe, 2 – outlet pipe, 3 – hollow chamber, 4 – partition, 5 – hole	6
03	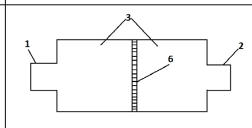 Two-chamber	1 – inlet pipe, 2 – outlet pipe, 3 – hollow chamber, 6 – partition with perforation	8
04	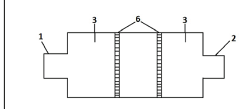 Three-chamber	1 – inlet pipe, 2 – outlet pipe, 3 – hollow chamber, 6 – partition with perforation	11
	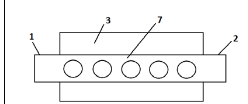 Single-chamber	1 – inlet pipe, 2 – outlet pipe, 3 – hollow chamber, 7 – perforated pipe	8
05	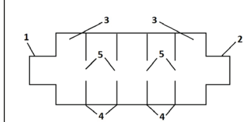 Five-chamber	1 – inlet pipe, 2 – outlet pipe, 3 – hollow chamber, 4 – partition, 5 – hole	12
06	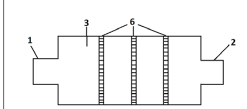 Four-chamber	1 – inlet pipe, 2 – outlet pipe, 3 – hollow chamber, 6 – partition with perforation	14
07	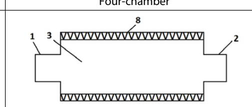 Single-chamber with sound-absorbing material	1 – inlet pipe, 2 – outlet pipe, 3 – hollow chamber, 8 – sound-absorbing material	13
08	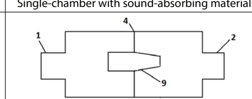 Silencer with Venturi tube	1 – inlet pipe, 2 – outlet pipe, 4 – partition, 9 – Venturi tube	9
09	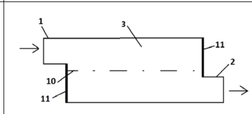 Silencer with an end asymmetric arrangement of the pipes	1 – inlet pipe, 2 – outlet pipe, 3 – hollow chamber, 10 – central axis of the silencer, 11 – end walls	8
10	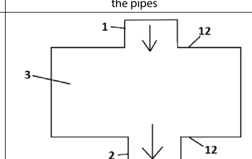 Silencer with a side symmetrical arrangement of pipes	1 – inlet pipe, 2 – outlet pipe, 3 – hollow chamber, 12 – side wall (shell)	6
11	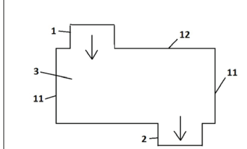 Silencer with a side asymmetric arrangement of	1 – inlet pipe, 2 – outlet pipe, 3 – hollow chamber, 11 – end walls, 12 – side wall (shell)	7

	pipes		
12	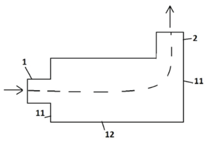 Silencer with flow rotation at the outlet	1 – inlet pipe, 2 – outlet pipe, 11 – end walls, 12 – side wall (shell)	10
13	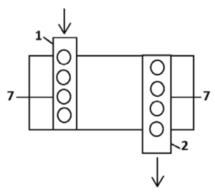 Silencer with a side asymmetric arrangement of pipes with perforated tubes	1 – inlet pipe, 2 – outlet pipe, 7 – perforated pipe	9
14	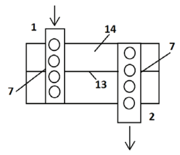 Two-chamber silencer with a resonant chamber	1 – inlet pipe, 2 – outlet pipe, 7 – perforated pipe, 13 – blind partition, 14 – resonant chamber	10

Tab. 1: The main design schemes of the tested silencers

3. INFLUENCE OF STRUCTURAL ELEMENTS ON ACOUSTIC EFFICIENCY AND BACK PRESSURE

3.1 Influence of the expansion chamber volume

The expansion chamber is the main structural element of any noise muffler. The tests were carried out on hollow chambers, the volume of which was selected in the ratio of 0.5:1:4. The results are shown in Fig. 3. An increase in the volume of the expansion chamber significantly affects the acoustic efficiency of the muffler, mainly in the low-frequency range (31.5-250 Hz). There is a certain pattern: with each doubling of the chamber volume, the efficiency at individual frequencies increases by 3-5 dB. With an increase in volume of almost 10 times, the effectiveness of the muffler at low frequencies increases by 5-14 dB.

Fig. 3. Acoustic efficiency of the expansion chamber of the silencer

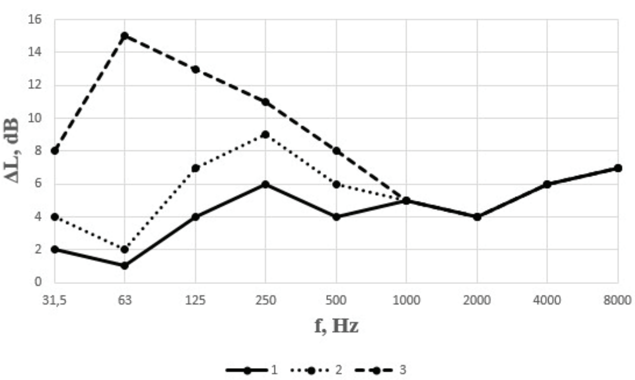

with a volume of: 1 – 0,05 m3, 2 – 0,1 m3, 3 – 0,4 m³

Returning once again to the processes of noise formation of the free exhaust (Fig. 1), we note that the volume change affects mainly the processes associated with noise formation in the engine cylinders. But, at the same time, the volume also has a certain effect on the gas jet, slowing down its speed. This reduces the sound pressure levels by 4-7 dB in the high-frequency range (1000-8000 Hz).

3.2 Influence of the number of silencer chambers

In practice, silencers generally have from one to four chambers separated by a partition. Partitions can be either with single holes or with perforation. The test results of one -, two-and three-chamber, etc. silencers of various types are shown in Tab. 2.

Number of cameras	Type of partition	Acoustic efficiency, dB, in octave bands with average geometric frequencies, Hz									Acoustic efficiency, dBA
		31,5	63	125	250	500	1000	2000	4000	8000	
1	-	4	2	7	9	6	5	4	6	7	5
2	Single hole	4	1	7	8	7	6	7	7	10	6
2	Perforation in the partition	5	2	9	8	10	7	9	10	12	8
3	Perforation in the partitions	5	3	8	10	14	9	12	14	15	11
5	Single holes	4	2	9	9	15	11	14	17	17	12
4	Perforation in the partitions	3	4	10	11	18	15	16	20	19	14

Tab. 2: Acoustic efficiency of silencers with different number of chambers

When comparing the test results, we note that partitions with single holes are less effective than partitions with perforations. A two-chamber silencer with a partition with a single hole is only 1-3 dB more efficient than a hollow chamber. The same muffler with a perforated partition is more effective than a hollow chamber by 4-5 dB. The influence of partitions affects the high-frequency range (1000-8000 Hz). The greater the number of partitions, the more effective the silencer is. Thus, a four-chamber silencer with perforated partitions is more effective than a hollow chamber by 10-14 dB in the medium-high frequency ranges (500-8000 Hz). A five-chamber silencer, where single holes are located in the partitions, is more effective than a hollow chamber by 6-10 dB in the high-frequency range. Approximately, the presence of each partition with a perforation, and, consequently, an increase in the number of chambers in the silencer, increases its efficiency by 2-3 dBA. The mechanism of action of partitions, both with perforation and with a single hole, is the effect on the jet of escaping gases, so they are effective in the high-frequency range.

The relative values of the back pressure of the silencers, where the back pressure in the hollow chamber is assumed to be 100%, are shown in Tab. 3.

Number of cameras	Type of opening in the partition	Relative back pressure, %
1	-	100
2	Hole	175
2	Perforation	225
3	Perforation	300
4	Perforation	350
4	Hole	300
5	Hole	350

Tab. 3: Relative values of the back pressure of one -, two- and multi-chamber silencers

There is a certain regularity in the back pressure values: starting with two-chamber silencers, the introduction of each partition increases the back pressure by 50-75%. Partitions with perforations have approximately 50% more resistance to flow movement than with a single hole.

In silencers, along with perforated partitions, perforated tubes are also widely used. Comparative tests of such silencers were performed (Tab. 4).

Number of cameras	Type of perforation element	Acoustic efficiency, dB, in octave bands with average geometric frequencies, Hz									Acoustic efficiency, dBA
		31,5	63	125	250	500	1000	2000	4000	8000	
1	-	4	2	7	9	6	5	4	6	7	5
2	Partition wall	5	2	9	8	10	7	9	10	12	8
1	A tube	4	3	6	10	11	7	8	9	13	8

Tab. 4: Comparative results of acoustic efficiency of mufflers with perforation of internal elements

It should be noted that the efficiency of perforated structures almost does not differ from each other (with approximately equal perforation area). At the same time, the back pressure of a single-chamber silencer with a perforated tube is almost 50% higher than that of a two-chamber design. This is due to the irrational organization of the gas flow movement in a single-chamber muffler with a perforated tube. The organization of the gas flow movement in the muffler is a significant factor affecting the acoustic efficiency and back pressure.

3.3 The effect of sound absorption

Sound absorption is often used in mufflers. Fig. 4 shows the effect of sound absorption on the acoustic efficiency of the muffler. Noise reduction is observed in a wide frequency range from 125 to 8000 Hz, i.e. in the low -, medium-and high--frequency ranges from 2 to 7 dB. Especially effective sound absorption in the high-frequency range (5-7 dB). When using sound absorption in silencers, there is no increase in back pressure, which makes this measure one of the most effective, reducing sound levels to 8 dBA.

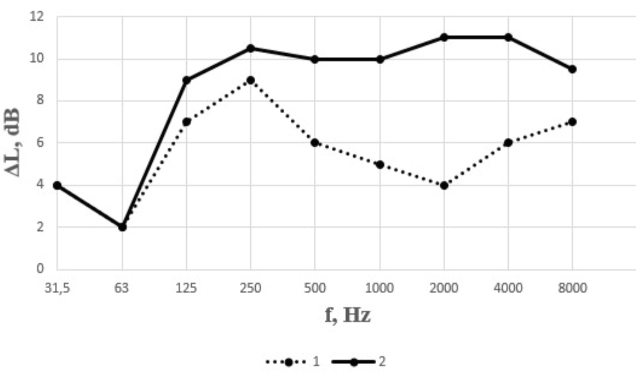

Fig. 4. The effect of sound absorption on the acoustic efficiency of the muffler: 1-a hollow chamber, 2-a chamber with sound absorption

3.4 Venturi Tube Effect

The diagram of this device is shown in Fig. 5. The device affects the flow: the flow rate changes, causing a change in pressure. In this case, a pressure drop occurs, which can be considered as a certain damping of the jet. Figure 6 shows the efficiency values of a silencer with a Venturi tube mounted in a partition. The highest efficiency is noted in the low-frequency range of 63-125 Hz, which is 6-8 dB, in the range of 250-8000 Hz, the efficiency of the device is 2-3 dB. The Venturi tube is one of the few devices that reduce sound pressure levels in the low-frequency range. At the same time, a slight increase in the back pressure of the silencer with a Venturi tube was recorded (150%).

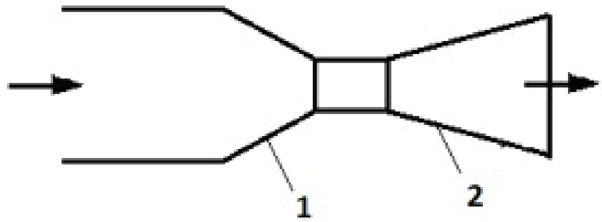

Fig. 5. Venturi tube: 1 – nozzle, 2 – diffuser

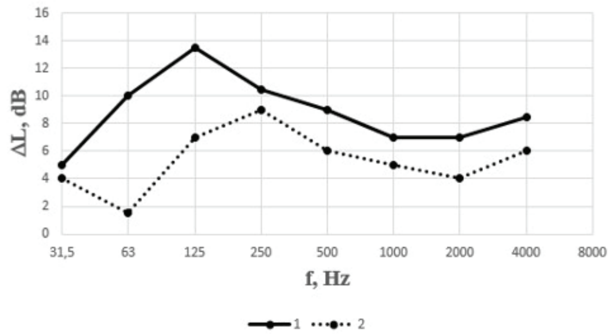

Fig. 6. Acoustic efficiency of a silencer with a Venturi tube (1) compared to a hollow chamber (2)

3.5 Influence the location of the inlet and outlet pipes

In most silencer designs, the inlet and outlet pipes are located in the end walls of the silencer on the same axis. Other types of arrangement can also be used to slow down the gas jet:

- unsymmetrically to the central axis;
- on the side walls of the silencer;
- on the front end wall (inlet pipe) and on the side wall (outlet pipe).

The results of comparative tests of silencers are presented in Table 5 and shown in Fig. 7.

Location of the inlet and outlet pipes	Acoustic efficiency, dB, in octave bands with average geometric frequencies, Hz									Sound level reduction, dBA	Back pressure, %
	31,5	63	125	250	500	1000	2000	4000	8000		
In the end walls on the central axis	4	2	7	9	6	5	4	6	7	5	100
In the end walls, asymmetrically	4	2	9	12	9	7	8	10	12	8	200
In the side walls, symmetrically	4	2	10	14	9	4	5	8	8	6	125
In the side walls, asymmetrically	5	2	9	13	10	8	9	14	14	9	200
The inlet pipe is in the end wall, the outlet pipe is in the side (at the maximum distance)	4	2	9	11	10	9	10	15	15	10	200

Tab. 5: Results of comparative tests of silencers with different positions of inlet and (or) outlet pipes

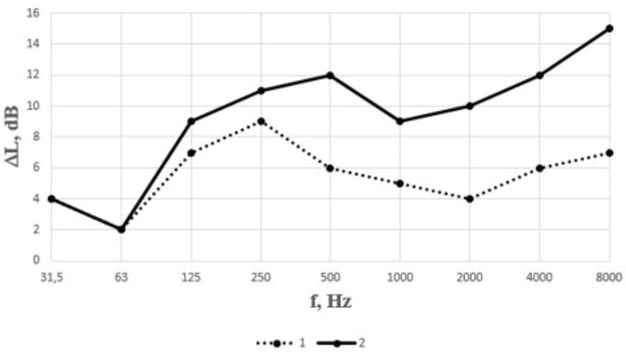

Fig. 7. Comparative data on the acoustic efficiency of silencers: 1 – direct-flow, 2 – with the flow turning to 90°

With an asymmetric arrangement of the inlet and outlet pipes, additional transformations of the jet movement occur, at first it hits the wall, which further reduces its energy. In all these cases, there is an increase in the effectiveness of the muffler in the medium and high-frequency ranges on average from 3 to 6 dB. The greatest effect is observed when the input is located in the end, and the output is located in the side parts of the muffler, i.e. the flow additionally turns by 90°. Increase in acoustic efficiency in the medium-high frequency ranges (500-8000 Hz) from 4 to 8 dB. (fig. 7). The efficiency according to the integral indicator is 10 dBA. In all the cases considered, the back pressure of the muffler increases approximately twice.

We also note an increase in the muffler efficiency by 3-5 dB in the low-medium frequency ranges (125-500 Hz), when the ratio m (m=D/d, D is the diameter of the muffler, d is the diameter of the inlet pipe) increases sharply, i.e. the inlet and outlet pipes are located in the side walls of the muffler shell.

3.6 Influence of the resonant chamber

A considerable number of silencers use resonant chambers that increase efficiency at certain frequencies. One of these silencers, in which the inlet and side pipes are located on the muffler shell, and also perforated tubes are used, was tested. The test results are shown in Tab. 6.

Description of an experienced silencer	Efficiency, dB, in octave bands with average geometric frequencies, Hz									Efficiency, dBA
	31,5	63	125	250	500	1000	2000	4000	8000	
Hollow chamber with side entrance and exit	4	2	9	13	11	6	6	9	10	7
A hollow chamber with a side entrance and exit with the presence of perforated tubes	4	1	8	13	12	8	10	11	13	9
With the presence of a resonant chamber	5	1	9	13	12	9	16	13	14	10

Tab. 6: Comparative test results of mufflers with perforated tubes and a resonant chamber

The experiment confirms the correctness of some of the previous conclusions:

- an increase in the number m increases the efficiency of the silencer (compared to a hollow chamber with end-mounted nozzles) at certain frequencies of the low-frequency range;
- the asymmetric movement of the jet in the silencer increases its efficiency at high frequencies;
- the effect of perforation is noticeable at high frequencies.

The presence of a resonant chamber in the silencer increased its efficiency to 5 dB at a frequency with an average geometric value of 2000 Hz.

4. DESIGN OF SILENCERS

There are two main noise reduction mechanisms in engine silencers, one of which is associated with the reduction of internal noise generated outside the silencer, which manifests itself mainly in the low-frequency and partly in the mid-frequency ranges. The second mechanism is associated with a decrease in the noise formation of the jet by reducing, first of all, its speed, which manifests itself mainly in the high-frequency range.

When creating silencers, the results obtained by the research can be used, the main ones of which include:

- changing the volume of the silencer has the greatest effect on its efficiency in the low-frequency range (the first noise reduction mechanism), so when the volume is increased by 8 times, an increase in efficiency to 6 -13 dB is recorded at certain frequencies. Increasing the volume of the silencer is the most effective way to increase its efficiency in the low-frequency range. We note a slight decrease in the hollow chamber and high-frequency noise (up to 5 dBA), i.e. the sudden expansion and narrowing of the flow reduces its speed (the second noise reduction mechanism also works);
- an increase in the number of silencer chambers leads to an increase in its efficiency in the high-frequency range (the second noise reduction mechanism), while perforated partitions are the most effective. Each hollow chamber with this type of partition increases the muffler efficiency by about 4 dBA, while there is an increase in back pressure by about 50-75% for each new chamber;
- the use of sound absorption in the design of a muffler is one of the most effective measures to increase its efficiency in a wide frequency range (125-8000 Hz), where both mechanisms operate, the greatest reduction to 8 dBA at high frequencies (in accordance with the acoustic characteristic of the sound-absorbing material). Sound absorption is one of the few elements, the use of which does not increase the back pressure of the muffler;
- The use of a Venturi tube in the design of a muffler is a reliable method of increasing its efficiency in a wide frequency range (63-8000 Hz), where both noise-muffling mechanisms operate. The efficiency of such a device reaches 7-8 dB in the low-frequency range (63-125 Hz), but does not exceed 4-6 dB in the high-frequency range (4 dBA);
- the effectiveness of silencers is significantly related to the location of the input and output pipes; with their symmetrical arrangement (on the same axis) on the side covers of the silencer, the resistance is minimal, but the efficiency is also low (about 5-6 dBA). If they are not symmetrical, the second noise reduction mechanism operates, the jet speed is further reduced when interacting with the back cover, and an additional increase in efficiency is up to 2-3 dBA. When the pipes are arranged symmetrically on the side walls (shell), an additional increase in efficiency is

observed at individual frequencies in the low-frequency range (up to 5 dB at a frequency of 125 Hz) – the action of the first mechanism due to an increase in the number of m. When the inlet pipe is located in the end cap, and the outlet is located in the side (on the opposite side), there is a maximum increase in efficiency (up to 10 dBA), the action of the second mechanism with an additional rotation of the gases at the outlet of the muffler. In all cases of an asymmetric arrangement of the pipes, the back pressure increases noticeably (up to 200%).

Thus, the creation of highly efficient silencers follows the path of increasing their volume, the use of sound absorption and elements with Venturi tubes, the asymmetric arrangement of the inlet and outlet pipes, the organization of multiple turns of the gas flow in the silencers. An example of a silencer design, in which the listed principles are most fully implemented, is shown in Figure 8, and the results of its tests are shown in Table 7. The silencer is multi-chamber with perforation, the presence of sound absorption, with a rotation of the gas flow at the outlet. The muffler efficiency reaches 23-34 dB at low frequencies and 36-52 dB in the medium-high frequency ranges (40 dBA). The back pressure does not exceed 1000 mm of the water column. The silencer is recommended for serial use.

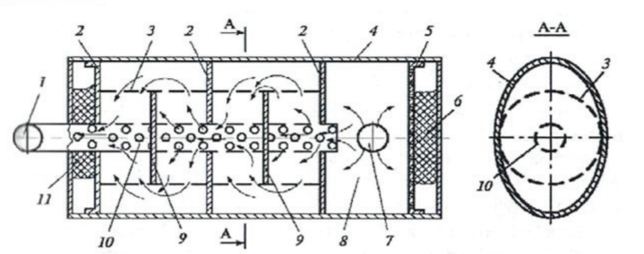

Fig. 8. Silencer of the release of the internal combustion engine that is installed on mobile compressor stations: 1— the outlet; 2 — elliptical partition; 3 — a cylindrical glass; 4 — exhaust silencer; 5 — perforated partition; 6 — vibration damping material; 7 — inlet; 8 — input camera; 9 — partition; 10 — Central perforated tube; 11 – absorbing material

Characteristic	Sound pressure levels, dB, in octave bands with average geometric frequencies, Hz							
	63	125	250	500	1000	2000	4000	8000
Release noise:								
without a silencer	129	124	128	125	122	121	129	123
with a silencer	106	98	94	84	86	84	81	71
Muffler efficiency	23	26	34	41	36	37	48	52

Tab. 7: Efficiency of the muffler of the internal combustion engine exhaust noise

5. CONCLUSION

The description of two main mechanisms of operation of silencers is proposed. The first one is associated with the low – frequency range (partly with the mid-frequency), the second one describes the noise reduction at high frequencies. To develop the basic design principles of silencers, more than 100 models of prototypes were tested on a special stand. The characteristics of acoustic efficiency, dB, in the normalized sound range (31.5-8000 Hz), as well as dBA were measured.

The relationship of the studied characteristics was revealed depending on the following design parameters:

- the volume of the silencer chamber
- the number of chambers
- the presence of perforation
- the presence of a Venturi tube
- the presence of sound absorption
- the presence of a resonant chamber
- the location of the inlet and outlet pipes in the silencer
- the presence of devices that change the flow direction in the silencer.

A recommendation has been developed for the design of silencers, with the use of which a silencer design has been created that provides high (about 40 dBA) acoustic efficiency and acceptable (about 1000 mm of water column) back pressure.

ACKNOWLEDGEMENT

The research described in this paper was supported by the grant of Russian Scientific Foundation, project number: 20-19-00222.

REFERENCES

[1] Yudin E.Ya.. Rassadina I. D.. Nikolskiy V.N. Spravochnik proyektirovshchika. Zashchita ot shuma. Pod red. E. Ya. Yudina. M.: Stroyizdat., 1974. – 134 p.
[2] Agrafonova A.A.. Smirnov S.G.. Tupov V.V. Issledovaniye akusticheskoy effektivnosti glushiteley shuma // Izvestiya vysshikh uchebnykh zavedeniy. Mashinostroyeniye. №9 [666] 2015, p. 75-82
[3] Komkin A.I.. Tupov V.V. Osnovy proyektirovaniya glushiteley shuma transportnykh sredstv // Bezopasnost zhiznedeyatelnosti. – 2003. – №1. – C. 15–20.
[4] Lubianchenko A.A., The approximate physical and mathematical models of gas-dynamic and aero-acoustic processes in the exhaust mufflers of ICE, Noise Theory and Practice. 2015. Vol. 1. № 2., P. 72-83
[5] Munjal M.L., Rao K.N., Sahasrabudhe A.D. Aeroacoustic analysis of perforated muffler components // Journal of Sound and Vibration. – 1987. – V. 114, № 2. – P. 173–188.
[6] Lubianchenko A.A., Improvement of vibroacoustic characteristics of high-power internal combustion engine exhaust noise mufflers. Abstract of the dissertation for the degree of Candidate of Technical Sciences. St. Petersburg, 2016. - 23 p.
[7] Ivanov N.I. Inzhenernaya akustika. Teoriya i praktika borby s shumom: uchebnik – 4-e izd. pererab. i dop. – M.: Logos. 2015. – 432p.
[8] Lighthill M.J. On sound generated aerodynamically. Part 1: General theory. Proc. Roy. Soc. Lond., 1952. – P. 564-587.
[9] Ivanov. N. I. Zashchita ot shuma i vibratsii: uchebnoye posobiye / N. I. Ivanov. A. E. Shashurin. - 2-e izd.. pererab. i dop. - SPb.: Pechatnyy Tsekh. 2019. – 282 p.
[10] Vasilyev A.V. Automobile internal combustion engine low frequency noise reduction using active noise control solutions. Journal “Akustika”, Czech Republic, Volume 34, November 2019, pp. 113-117.

__Nickolay Ivanov__ is Doctor of Engineering Science, Professor of Department of Ecology and Industrial Safety of the Baltic State Technical University ‘VOENMEH’ named after D.F. Ustinov (Saint-Petersburg, Russia), Honored Scientist of the Russian Federation.
Nickolay Ivanov is the creator of the transport acoustics scientific school. He developed the theory of the transportation vehicles acoustics, proposed the solution to the problems of generating the sound field in low volume, diffraction on complex obstacles, methods of calculation of the sound fields of spatial emitters. Nickolay Ivanov has published over 400 scientific papers, including about 10 textbooks, manuals and monographs. He presented the main results of scientific research on the international conferences in Australia, Austria, Hungary, Germany, Denmark, Italy, Canada, China, the Netherlands, Poland, Portugal, the USA, Finland, Switzerland, Sweden and other countries.

__Aleksandr Shashurin__ is Doctor of Engineering Science, Professor, Head of Department of Environment and Safety of the Baltic State Technical University ‘VOENMEH’ named after D.F. Ustinov (Saint-Petersburg, Russia), CEO of the LLC (OOO) ‘Acoustic Design Institute’.
Aleksandr Shashurin is a specialist in calculation and design of noise barriers, noise reduction at production facilities, soundproof booths design and others. He is a member of the organizing committees of conferences and seminars in the field of acoustics and ecology held in St. Petersburg and Moscow. Aleksandr Shashurin is the author of over 40 scientific publications and the co-author of textbooks and teaching aids, the author of 6 patents for noise control devices. He presented the main results of scientific research at the international conferences in St. Petersburg, Moscow, Samara, Hiroshima (Japan).

__Aleksandr Burakov__, job seeker for the position of engineer at the Baltic State Technical University ‘VOENMEH’ named after D.F. Ustinov (Saint-Petersburg, Russia), is a specialist in design of low noise compressor, compressor unit with low vibration activity, low noise power equipment, installations for the production and preparation of industrial gases and others.
Aleksandr Burakov is the co-author of over 30 scientific publications and co-author of over 50 patents for compressor equipment. He presented the main results of scientific research at the international conferences in St. Petersburg, Omsk.

Paper No.382/2021

FEATURES OF NOISE REDUCTION IN GAS PATHS OF BOILERS DURING CONDENSATION OF WATER VAPOR FROM FLUE GASES

[a)] **Evgenii Zhuravlev,** [b)] **Dmitry Chugunkov,** [c)] **Galina Seyfelmlyukova**

[a, b, c)] *National Research University 'Moscow Power Engineering Institute', Moscow, Russia*
[a)] *ZhuravlevYA@mpei.ru,* [b)] *ChugunkovDV@mpei.ru,* [c)] *SeyfelmliukGA@mpei.ru*

***Abstract**: An important characteristic of noise silencers, which determines the effectiveness of their use, in addition to reducing the noise level and the pressure losses they create, is the operational resource. Short-term unfavorable operating modes of boilers are possible, in which condensation of water vapor on the walls of flues through which flue gases are evacuated to the environment is possible. Condensation in the gas path leads to corrosion of the metal of the flues, as well as noise silencers. The article lists recommendations for the design of noise silencers installed in the gas paths of boilers operating under conditions of possible condensation of water vapor from flue gases. The introduced silencers of noise of gas paths of boilers which not only reduce noise highly effectively, but also allow to work in difficult operational conditions are given.*

***Keywords:** noise silencers, condensation of water vapor, corrosion, gas paths of boilers, fuel combustion products, reliability.*

***DOI:** : 10.36336/akustika20214217*

1. INTRODUCTION

To produce water vapor and hot water, organic fuel is burned in the furnaces of power and hot water boilers. In Russia, gaseous fuel has become the most widespread in power complexes for the operation of boilers due to its relatively low cost, high environmental and energy indicators. Fuel combustion is the process of exothermic oxidation of a combustible substance. Gaseous fuel is a mixture of combustible gases and impurities. The admixtures of gaseous fuels include water vapor, dispersed moisture, non-flammable gases, resins and dust. The most common gaseous fuel is natural gas. Natural gas contains methane CH4 (75...98%), heavy hydrocarbons (ethane, propane, butane and others), hydrogen, hydrogen sulfide, oxygen, nitrogen, carbon dioxide and water vapor. When 1 m3 of methane is completely oxidized, carbon dioxide, water vapor and 36 MJ of heat are formed.

If the flue gas temperature corresponding to the dew point is reached, condensation of water vapor occurs inside the gas paths. The dew point temperature is determined by the partial pressure of water vapor and depends on the sulfur content for liquid fuel and ash content for solid fuel.

When burning fuel oil in the condensate falling out on the walls of the flue, the sulfur dioxide formed during burning sulfur contained in the fuel oil is dissolved. The result of the dissolution of sulfur dioxide in water is the formation of sulfuric and sulfurous acids. The contact of sulfuric and sulfurous acids with the metal surfaces of the flue leads to the intensive development of low-temperature corrosion and damage to the surface of the flue up to its complete destruction. Therefore, it is important to prevent condensation of water vapor of flue gases, and to minimize the duration of unfavorable modes of operation of the gas path.

In Russia, boiler flues are often made of carbon steel and condensation on their internal surfaces can significantly reduce the service life of the flue, as well as noise silencers, due to the intensification of low-temperature corrosion. The optimal value of the exhaust flue gas temperature for various fuels and boiler steam parameters are established on the basis of technical and economic calculations. Table 1 shows the ranges of optimal leaving flue gas temperatures for the most common types of fuels [1].

Item number	Types of fuels	Leaving flue gas temperatures, °C
1.	Natural gas	120-140
2.	Fuel oil	150-160
3.	Coal	120-150

Tab. 1: Leaving flue gas temperatures for various types of fuels

The table (Tab.1) shows that for natural gas and coal, the temperature of leaving flue gases at stations should not fall below 120°C, and for fuel oil - not below 150°C. Ensuring this condition will guarantee not only the exclusion of condensation of water vapor, but also the preservation of the natural thrust of the gas path.

However, in some cases, short-term unfavorable modes of operation of the gas path may occur when the temperature of the outgoing flue gases decreases below the dew point temperature, especially near the walls of the flues as a result of heat exchange with the environment. Figure 1 shows the result of corrosion on the perforated plate wall of a dissipative noise silencer installed in the flue of an energy boiler of one of the combined heat and power plant, as well as on the wall of the gas path.

Fig. 1: Corrosion of the metal of the gas path of the boiler under the influence of condensate from flue gases

Ensuring the reliable operation of silencers, their long service life, as well as the preservation of acoustic properties throughout the entire service life is the most important task. Reliability is understood as the property of an object not to reach the limit state for some time or operating time with an established system of maintenance and repair. At the same time, the condition of the object will be considered marginal when its operation is unacceptable due to exceeding the established noise standards in the area of operation of the equipment due to a decrease in the effectiveness of noise reduction [2].

A large amount of energy is used to transport flue gases from the boiler furnace to the environment. The reliability of energy complexes depends on the operation of gas paths, and its construction is associated with significant labor and material costs [3]. The temperature of the flue gases has a decisive influence on the efficiency of the boiler, since the heat losses with the outgoing gases in the structure of the total losses are the greatest in value and can reach 12% of the available heat of combustion of fuel. For example, reducing the temperature of the exhaust gases by 12-16°C will lead to an increase in boiler efficiency by about 1%. The cooling of gases requires an increase in the size of convective heating surfaces or an intensification of heat exchange.

2. RECOMMENDATIONS FOR IMPROVING THE DURABILITY OF GAS PATHS AND SILENCERS

To prevent condensation of water vapor from flue gases in the boiler paths, the following technical solutions can be used:
- increase in the temperature of combustion products at the outlet of the boiler;
- thermal insulation of flues;
- increasing the speed of movement of combustion products in flues;
- flue gas drying.

In order to increase the operational life of noise silencers, it is recommended to develop them in accordance with the following recommendations:
- silencers must be made of corrosion-resistant steels (various stainless steels, for example, AISI 430, AISI 304);
- the sound-permeable shell and the sound-absorbing material must have non-hygroscopic properties;
- the elements of dissipative noise silencers must be positioned vertically without lining the lower walls of the gas paths with sound-absorbing material;
- at the lower points of the housing of noise silencers or flues in which noise silencers are installed, it is necessary to provide drainage connections for the discharge of accumulated condensate.

3. EXPERIENCE IN IMPLEMENTING EFFECTIVE AND LONG-LASTING NOISE SILENCERS

At one of the large thermal power plants in Moscow, an efficient and durable sound attenuation system of the gas path of the TGMP-314 power boiler was installed behind the axial smoke pumps DOD-31.5 FGM in front of the flue with a height of 250 m [4]. The noise reduction system included (Fig. 2) the installation in the gas path of a dissipative silencer made of seven plates with volumetric elements [5] 4 m long and 200 mm thick, sound-absorbing lining of the turn and the wall of the flue made of plates with volumetric elements [6] 100 mm thick and installation of guide concentric blades in order to compensate for the pressure losses formed by plate silencers.

The relative cross-section of the plate silencers of the boiler gas path silencing system was 71%.

Fig. 2: The noise reduction complex in the flue behind the smoke pumps DOD-31.5FGM in front of the flue of the TGMP-314 power boiler

The use of plates with volumetric elements in the noise reduction system was justified by the insufficient acoustic characteristics of plates with flat side walls at the average geometric frequencies of octave bands[7]. In order to extend the service life of the silencing system, the rigid boxes of the silencer plates and linings were made of stainless steel AISI 430 and AISI 304. Non-combustible and non-hygroscopic mats made of basalt fiber with a density of 40 kg/m3 were used as the sound-absorbing material of the plates[8]. Stitched mats allow not to be covered with sound-absorbing material, thus preserving acoustic properties for a longer time. The results of the implementation of the sound attenuation system showed that the introduced difference in sound pressure levels was 5.5-30.3 dB in the spectrum of octave bands with frequencies of 31.5-8000 Hz and sound level of 24.9 dBA without reducing boiler performance [9].

In many cases, on existing power complexes, the gas paths of boilers do not have rectilinear sections of sufficient length where it is possible to install a silencer [10]. In such cases, sound-absorbing turn linings are used, but its effectiveness may be insufficient. To solve this problem, a new noise reduction device was proposed. Figure 3 shows the device of a compact dissipative silencer for turning boiler flues, which can be used in the absence of rectilinear sections of gas paths when condensate falls out of flue gases [11,12].

Fig. 3: Noise silencer for turning the boiler flue

The noise silencer is a 90° stainless steel elbow of rectangular cross-section with inlet and outlet sockets. Inside the case of the noise silencer there is a sound-absorbing element having a curvature in the longitudinal direction, a sound-absorbing lining and a hole for the removal of flue gas condensate. A feature of the silencer is the presence of a streamlined sound-absorbing element, which, in addition to sound absorption, shields sound waves back into the channel. The internal surfaces of the sound-absorbing element and the lining are perforated, and the element and the lining are filled with sound-absorbing material. To prevent the sound-absorbing material from blowing out, the perforated sheets are covered with fiberglass[13]. The housing, inlet and outlet sockets, perforated cladding sheets are made of AISI 430 stainless steel. As a sound-absorbing material, a material with a density of 60 kg / m^3 of basalt fiberglass is used, which has fire-resistant and non-hygroscopic properties. According to the results of field tests, the effectiveness of noise reduction with a silencer was up to 30 dB in octave bands at high geometric frequencies. The proposed device was implemented on several hot water boilers. The operation of these silencers has shown that such devices introduce low aerodynamic drag at flue gas flow rates up to 10 m/s[14].

4. CONCLUSION

The durability of silencers should be given special attention due to their critical impact on the reliability of power supply and heat supply of the entire system. The article provides recommendations for designing highly efficient noise silencers for gas paths of boilers with a long service life, as well as examples of implemented noise silencers made in accordance with these recommendations.

ACKNOWLEDGEMENT

The study was carried out within the framework of the state task of the Ministry of Education and Science of the Russian Federation (FSFW-2020-0021).

REFERENCES

[1] Komponovka i teplovoj raschet parovogo kotla (rus)/ Y.M. Lipov, D.F. Samoilov, T.V. Vilenskii. - M.: Energoatomizdat, 1988. – 208 p.
[2] Yablonik L.R. Shumozashchitnye konstrukcii turbinnogo i kotel'nogo oborudovaniya: teoriya i praktika (rus): Dis. DSc: 05.14.12. – Moscow, 2006. – P. 427
[3] Gazovozdushnye trakty teplovyh elektrostancii (rus)/ L. A. Rihter. – 2. vydání přepracované a rozšířené – M.: Energoatomizdat, 1984 . – 264 s.
[4] Zhuravlev E.A., Chugunkov D.V. Razrabotka sistemy shumoglusheniya originalnoi konstrukcii dlya gazovogo trakta kotla TEC (rus) // Conference «Prioritetnye napravleniya innovacionnoi deyatelnosti v promyshlennosti (November 29-30, 2020, Kazan): Collection of scientific articles on the results of the eleventh International Scientific Conference. Part 1. Kazan: Publishing house of LLC "Envelope", 2020. – pp. 114-116
[5] Kasseta zvukopogloshchayushchaya dlya glushitelei shuma gazo-vozdushnyh traktov (rus): pat. 187890 Russia, MPK F01N 1/10/ D.V. Chugunkov, G.A. Seyfelmlyukova, E.A. Zhuravlev, K.S. Fomenko, A.D. Skurihina, A.E. Bogdanova
[6] Kasseta zvukopogloshchayushchaya dlya glushitelei shuma gazo-vozdushnyh traktov (rus): pat. 188650 Russia, MPK F01N» 1/10/ D.V. Chugunkov, G.A. Seyfelmlyukova, E.A. Zhuravlev, K.S. Fomenko, A.D. Skurihina, A.E. Bogdanova
[7] F. E/ Grigorian E A Pertsovskii Raschet i proektirovanie glushitelei shuma energoustanovok L Energiia 1980. - 120 p.
[8] Borba s shumom na proizvodstve Spravochnik Pod obshch red E IA IUdina - M Mashinostroenie 1985. - 400 p.
[9] Zhuravlev E.A., Chugunkov D.V., Seyfelmlyukova G.A. Improving the acoustic efficiency of laminated dissipative noise silencers for boiler gas-air paths // E3S Web of Conferences 140, 02005 (2019). - pp. 1–5
[10] Zhuravlev E.A., Chugunkov D.V., Seyfelmlyukova G.A. Study of acoustic and aerodynamic characteristics of a silencer gas paths boilers // Proceedings of the VII All-Russian research to practice conference with international participation «Protection against excessive noise and vibration». – St.-Petersburg, 19-21 March 2019 – pp. 301-311
[11] Zhuravlev E.A., Chugunkov D.V., Seyfelmlyukova G.A., Fomenko K.S. / Snizhenie shuma v gazohode kotla maloi teploproiz voditelnosti (rus) // International Scientific Conference «NEDELYA NAUKI SPbPU»: materials of the scientific conference with international participation. Institute of Energy and Transport Systems of SPbPU. CH.1. SPb: pub.h. POLITEKH-PRESS, 2018. – pp. 6-8
[12] Chugunkov D.V., Seyfelmlyukova G.A., Zhuravlev E.A. Study on silencer acoustic efficiency in gas-air flow duct bends // AKUSTIKA Vol. 32. № 270/2019. – 2019 - P. 141–143
[13] Ivanov N.I/ Inzhenernaia akustika Teoriia i praktika borby s shumom// textbook N.I. Ivanov M Universitetskaia kniga, 2016.- 424 p
[14] Idelchik I.E. Spravochnik po gidravlicheskim soprotivleniiam (rus)// M.O. SHteinberga, 3-d edition revised and expanded, M Mashinostroenie, 1992.- 672 p

***Evgenii Zhuravlev** is Postgraduate and Junior researcher of Department 'Thermal Power Plants' of the National Research University 'Moscow Power Engineering Institute'. Author of 10 patents for noise reduction devices. Zhuravlev Evgenii is the author of 18 scientific publications. He presented the main results of his research at many international conferences.*

***Dmitry Chugunkov** is Ph.D. of Engineering Science, Assistant Professor of Department 'Thermal power plants' of the National Research University 'Moscow Power Engineering Institute'. Laureate of the Russian Federation Government Prize. He has many years of experience in the field of noise reduction from power equipment. Dmitry Chugunkov is the author of more than 40 scientific publications and co-author of a number of textbooks. Author of 10 patents for noise reduction design. He presented the main results of his research at several international conferences.*

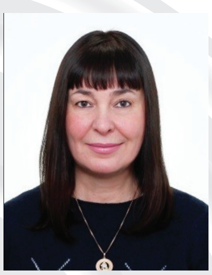

***Galina Seyfelmlyukova** is Researcher of Department 'Thermal power plants' of the National Research University 'Moscow Power Engineering Institute'. He has many years of experience in the field of noise reduction from power equipment. Galina Seyfelmlyukova high - class specialist in the design and calculation of structures, the reduction in the energy facility. Author of 6 patents for noise reduction devices. She presented the main results of her research at several international conferences.*

Akustika, odborný časopis o akustice a vibracích
Šéfredaktorka: Ing. Jana Dolejší (Studio D-akustika s.r.o., České Budějovice, Česká republika)

Redakce a administrace: Studio D- akustika s.r.o., U Sirkárny 467/2a, 370 04 České Budějovice
Adresa webové schránky: www.akustikad.com, e-mailová adresa: akustikad@akustikad.com, Vydává: Studio D-akustika s.r.o., České Budějovice, tisk: HERBIA spol. s r. o. Distribuce v ČR, předplatné: Studio D-akustika s.r.o., U Sirkárny 467/2a, 370 04 České Budějovice, Česká republika, tel.: +420 737 705 636, akustikad@akustikad.com, Distribuce v SR, předplatné: Magnet Press, Slovakia s.r.o., Šustekova 8, 851 04 Bratislava, Slovenská republika, tel.: +421 2 67201921, vojackova@press.sk,
Registrace: ISSN 1801-9064, MK ČR E 18950